Final Report

Applied Coastal Research and Engineering

Evaluation of Channel Dredging on Shoreline Response at and Adjacent to Mobile Pass, Alabama

Mark R. Byrnes, Sarah F. Griffee, and Mark S. Osler

Applied Coastal Research and Engineering
Mashpee, MA

January 2008

January 10, 2008

Evaluation of Channel Dredging on Shoreline Response at and Adjacent to Mobile Pass, Alabama

Mark R. Byrnes, Sarah F. Griffee, and Mark S. Osler

Applied Coastal Research and Engineering
766 Falmouth Road, Suite A-1
Mashpee, MA 02649

Final Report

Prepared for U.S. Army Corps of Engineers, Mobile District
Planning and Environmental Division
Coastal Environmental Team
109 St. Joseph Street
Mobile, AL 36602

TABLE OF CONTENTS

LIST OF FIGURES

LIST OF TABLES

Unit Conversion Factors

Multiply	By	To Obtain
cubic feet	0.02831685	cubic meters
cubic yards	0.7645549	cubic meters
degrees (angle)	0.01745329	radians
feet	0.3048	meters
hectares	1.0 E+04	square meters
knots	0.5144444	meters per second
miles (nautical)	1,852	meters
miles (U.S. statute)	1,609.347	meters
miles per hour	0.44704	meters per second
square feet	0.09290304	square meters
square inches	6.4516 E-04	square meters
square miles	2.589998 E+06	square meters
square yards	0.8361274	square meters
yards	0.9144	meters

1 Introduction

This report was prepared under the Litigation Settlement Agreement signed 15 July 2005 by The United States of America (Department of Justice), The State of Alabama (Office of the Attorney General), and The Dauphin Island Property Owners' Association (represented by Blackburn & Conner, PC). The settlement agreement was established in response to a lawsuit filed by Plaintiffs in the United States Court of Federal Claims (Dauphin Island Property Owner's Association, et al. vs. United States, No. 00-115-L) alleging that "the United States' (acting by and through the Corps of Engineers) dredging practices have caused significant shoreline erosion of Plaintiffs' property on Dauphin Island, Alabama resulting in an uncompensated taking of their property in contravention of the Fifth Amendment of the Constitution". The Litigation Settlement Agreement resulted in the following impacts study and anticipates eventual dismissal of the lawsuit based on study results.

As stated in the settlement agreement, "The United States will conduct an Impacts Study pursuant to Section 111 … the process will begin with Dr. Mark Byrnes of Applied Coastal Research and Engineering (the Principal Investigator ("PI")) and will include meaningful participation by an Independent Technical Review Team ("ITRT")". The ITRT consisted of Dr. Robert Dean, University of Florida (Plaintiffs); Dr. Nicholas Kraus, U.S. Army Corps of Engineers, Engineer Research and Development Center; and Mr. Robert Mink, Geological Survey of Alabama (State). A contract between the U.S. Army Corps of Engineers District, Mobile, and Applied Coastal Research and Engineering, Inc. (Applied Coastal) to conduct the study was signed on 26 September 2006.

The report is organized into eight chapters. Chapter 1 provides an overview of the project purpose and physical setting of the study area. Chapter 2 discusses historical shoreline change trends along Dauphin Island and the Morgan Peninsula relative to storm and normal conditions, and dredging activities in the Mobile Outer Bar Channel. Chapter 3 describes inlet and nearshore morphology at and adjacent to Main Pass based on sequence of historical bathymetric surveys. Chapter 4 documents historical sediment transport pathways throughout the study area based on a detailed comparison of sequential shoreline and bathymetric surveys to quantify sand volume changes. Chapter 5 describes numerical simulations of waves, wave-induced and tidal currents, and sediment transport pathways at and adjacent to Main Pass. Chapter 6 develops a sediment budget for the study area, and Chapter 7 evaluates the potential impact of construction and maintenance dredging at the

Mobile Outer Bar Channel on erosion at Dauphin Island, landward and west of the northwestern extent of Pelican Island. Chapter 8 provides conclusions and recommendations for future dredging and placement practice associated with the Mobile Outer Bar Channel.

Purpose and Scope

The purpose of this study was to evaluate the impact of construction and maintenance dredging activities for the Federal navigation project in Mobile Outer Bar Channel on shoreline response along Dauphin Island, Alabama. Since at least the 1970s, science and engineering studies have suggested that construction and maintenance dredging in the outer bar channel of Main Pass has produced a deficit of sand in the littoral drift system west of the channel, including the western lobe of the ebb-tidal delta (e.g., Hardin et al., 1976; USACE, 1978; Douglass, 1994; Otvos, 2006; Morton, 2007). Although none of these studies relied on a detailed evaluation of historical dredging records for the outer bar channel or a quantitative comparison of historical shoreline and bathymetry surveys for documenting historical sediment transport pathways and net rates of change across the ebb shoal and along the shoreline of Dauphin Island, qualitative connections continue to be made between channel dredging and beach erosion along Dauphin Island.

In the present study, the working hypothesis was that historical construction and channel maintenance dredging in the Mobile Outer Bar Channel have resulted in adverse changes to the western lobe of the ebb-tidal delta and the beach along Dauphin Island west of Pelican Island. Ebb-shoal changes and shoreline response relative to storm and normal forces, and dredging in the outer bar channel, were evaluated to determine the extent to which beach erosion along Dauphin Island could be attributed to U.S. Army Corps of Engineers (USACE) channel construction and maintenance dredging operations.

Based on historical shoreline and bathymetry surveys, two distinct periods were evaluated; one representing conditions prior to significant construction and maintenance dredging activities to determine natural changes (1847/48 to 1917/20), and the other representing conditions after significant changes to the outer bar channel had been imposed (1917/20 to 2002) to quantify beach response along Dauphin Island. A time series of shoreline and bathymetry surveys was available for quantifying change throughout the study area for each time period, and the history of dredging from the outer bar channel was well documented using annual reports of the Corps of Engineers and operations and maintenance data provided by Mobile District personnel. Pre- and post-dredging morphologic response on the ebb shoals

and along the shoreline of Dauphin Island were compared to document changes imposed as a result of construction and maintenance dredging in the Mobile Outer Bar Channel. Finally, a sediment budget was developed for the period 1917/20 to 2002 to document sediment transport pathways and quantify sediment volume changes and fluxes throughout the study area relative to maintenance dredging in the outer bar channel.

Physical Setting

Coastal Alabama extends approximately 90 km from about 87°30' longitude at Perdido Pass to about 88°25' longitude at Petit Bois Pass. About 75 km of sandy shoreline along the open Gulf at about 30°15' latitude (Chermock et al., 1974) encompasses the southern portions of Mobile and Baldwin Counties (Figure 1-1). The entrance to Mobile Bay, between Mobile Point on the western end of the Morgan Peninsula and Pelican Point on the eastern end of Dauphin Island, is an extensive natural inlet that has been improved by channel dredging activities since 1904, primarily through the outer bar at the seaward extent of the ebb-tidal delta (Figure 1-2). The entrance is commonly referred to as Main Pass or Mobile Pass and is the

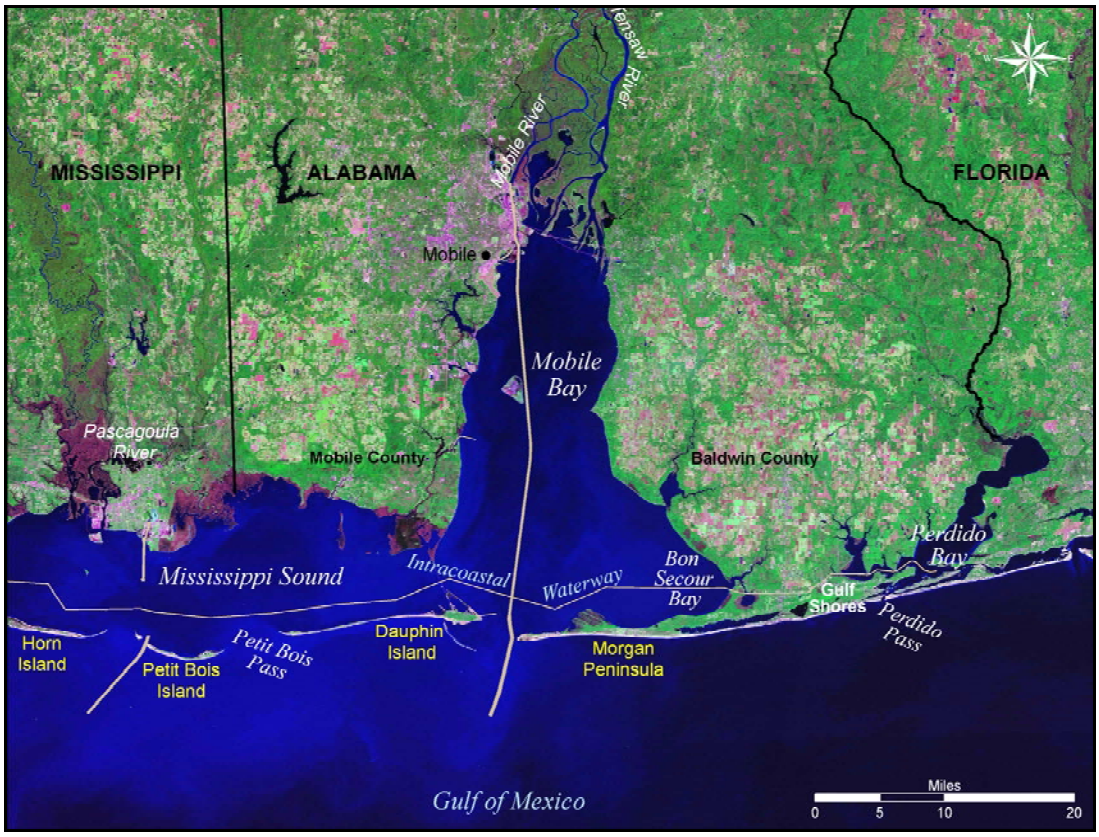

Figure 1-1. Map of coastal Alabama.

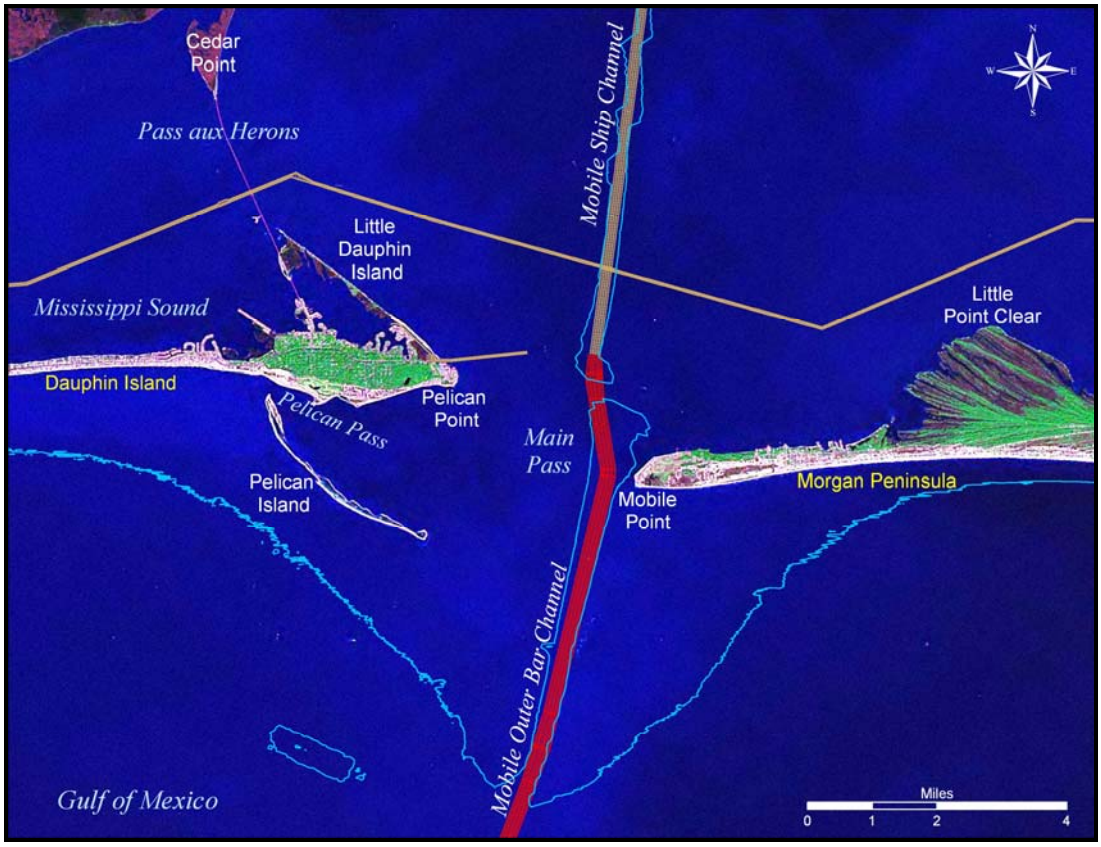

Figure 1-2. Main Pass and adjacent environments, including Mobile Outer Bar Channel and the 30-ft depth contour defining the seaward extent of the ebb–tidal delta and the Mobil Outer Mound disposal site.

primary point of access between Mobile Bay (via the north-south Mobile Ship Channel) and the Gulf of Mexico. The entrance is about 3 miles wide. The east-west Intracoastal Waterway intersects the Mobile Ship Channel just inside the entrance to the bay. The waterway connects Mississippi Sound with Mobile Bay via Pass aux Herons on the west, and eventually heads to Perdido Bay via Bon Secour Bay.

Mobile Bay Estuary. Mobile Bay estuary is a bell-shaped, submerged river valley system approximately 31 miles long between the estuary mouth and the Mobile River delta, and 23 miles wide between Mississippi Sound and Bon Secour Bay (Hummell, 1996). It receives water and sediment from the Mobile-Tensaw River system, the nation's fourth largest river system relative to discharge and sixth largest in term of total drainage area (Isphording and Flowers, 1987), and it has an average width of 13 miles. The bay encompasses about 413 square miles of open water (Isphording et al., 1996) and has an average depth of about 9.7 ft at mean high water (Chermock et al., 1974).

The watershed that supplies Mobile Bay with water and sediment encompasses about 43,200 square miles and has an average discharge through the Mobile-Tensaw River system of about 62,000 cubic feet per second (Isphording et al., 1996). On an annual basis, this water carries approximately 3.58 million tons of suspended sediment from the Mobile River delta into Mobile Bay, composed almost entirely of silt and clay (Isphording and Imsand, 1991). About 0.61 million tons/year of sand and coarser fluvial sediment are retained at the head of the Mobile River Delta and in the main river channels. Two outlets from Mobile Bay provide discharge points for fluvial water and sediment from the watershed: 1) Mobile Pass discharges about 84 percent of the outflow, and 2) Pass aux Herons discharges about 16 percent of flow into Mississippi Sound (Isphording et al., 1996). Of the sediment not retained in the Bay, Isphording et al. (1996) estimates that 0.94 million tons/year is transported to the Gulf of Mexico and 0.18 million tons/year to Mississippi Sound.

Gulf Beaches. Dauphin Island is the westernmost beach environment in coastal Alabama. The island is approximately 15 miles long and extends from Main Pass at the Mobile Bay entrance to Petit Bois Pass, a 4-mile-wide tidal inlet separating western Dauphin Island, Alabama and eastern Petit Bois Island, Mississippi (see Figure 1-1). The western two-thirds of Dauphin Island is a low-relief, washover barrier that is subject to overwash by Gulf of Mexico waters during tropical storms and hurricanes (Nummedal et al., 1980; Byrnes et al., 1991; Hummell, 1996; Morton, 2007). Maximum relief along this portion of the island is about 7 ft relative to mean water level (MWL), except for dune features that may reach 10 ft MWL in elevation. Island width varies between about 800 and 2,600 ft. Currently, the main channel at Petit Bois Pass is located adjacent to Dauphin Island and extends to about 23 ft below MWL (McBride et al., 1991). The eastern end of Dauphin Island has an average elevation near the beach of about 10 ft MWL; however, an extensive interior dune system that reaches an elevation of approximately 45 ft MWL exists north of beach deposits on top of existing Pleistocene coastal deposits (Otvos, 1979; Otvos and Giardino, 2004).

Seaward of the beach along eastern Dauphin Island, an ephemeral, subaerial sand deposit called Pelican Island is associated with the Mobile Pass ebb-tidal delta. This feature is prominent in its impact on shoreline response along eastern Dauphin Island (Byrnes et al., 1999; Parker et al., 1997). The island has continuously changed its shape, size, and location throughout the historical record in response to storms and normal wave and current processes (Hummell, 1996).

Along the eastern Alabama coast in Baldwin County, the shoreline extends approximately 30 miles from Mobile Point, at the eastern margin of Main Pass, along

the Morgan Peninsula east to Perdido Pass (Figure 1-1). The Morgan Peninsula forms the southeastern terminus of Mobile Bay and consists of an extensive beach backed by parallel dunes and numerous sub-parallel beach ridges, formed as a result of net longshore sediment transport processes (Bearden and Hummell, 1990; Stone et al., 1992).

Offshore Sedimentary Environment. Seafloor topography and Holocene sediment distribution on the Alabama shelf reflect a combination of processes, including regression during the late-Pleistocene and reworking of the exposed shelf surface by ancient fluvial systems, and reworking of the exposed shelf surface by coastal processes during the subsequent Holocene rise in sea level (Ludwick, 1964; Parker et al., 1997; Bentley et al, 2002). Redistribution of sediment by waves and currents during transgression partially or totally destroyed geomorphic features associated with Pleistocene fluvial environments. Concurrently, these same processes formed modern shelf deposits as subaerial coastal features became submerged and reworked during relative rising sea level. As such, much of the shelf offshore Alabama is sand (Figure 1-3) (Ludwick, 1964; Doyle and Sparks, 1980; Parker et al., 1997). On the

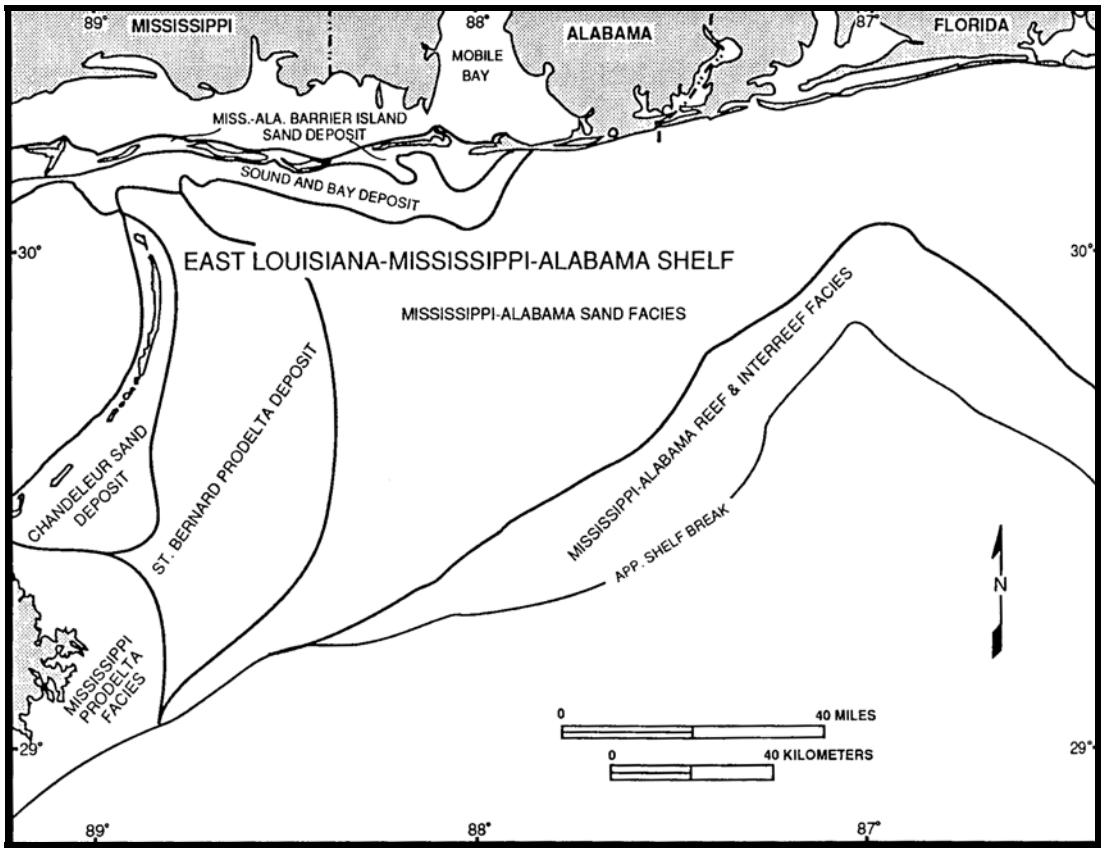

Figure 1-3. Sedimentary facies on the east Louisiana-Mississippi-Alabama shelf (after Ludwick, 1964; from Parker et al., 1997).

inner shelf offshore Dauphin Island, an extensive deposit of sandy mud occurs as a result of sediment discharge from Mobile Bay through Main Pass (Figure 1-4; Hummell, 1996; Parker et al., 1997). Parker et al. (1992) indicate that sediment type can change from sand to mud over a distance of several meters within the large Mississippi-Alabama sand facies.

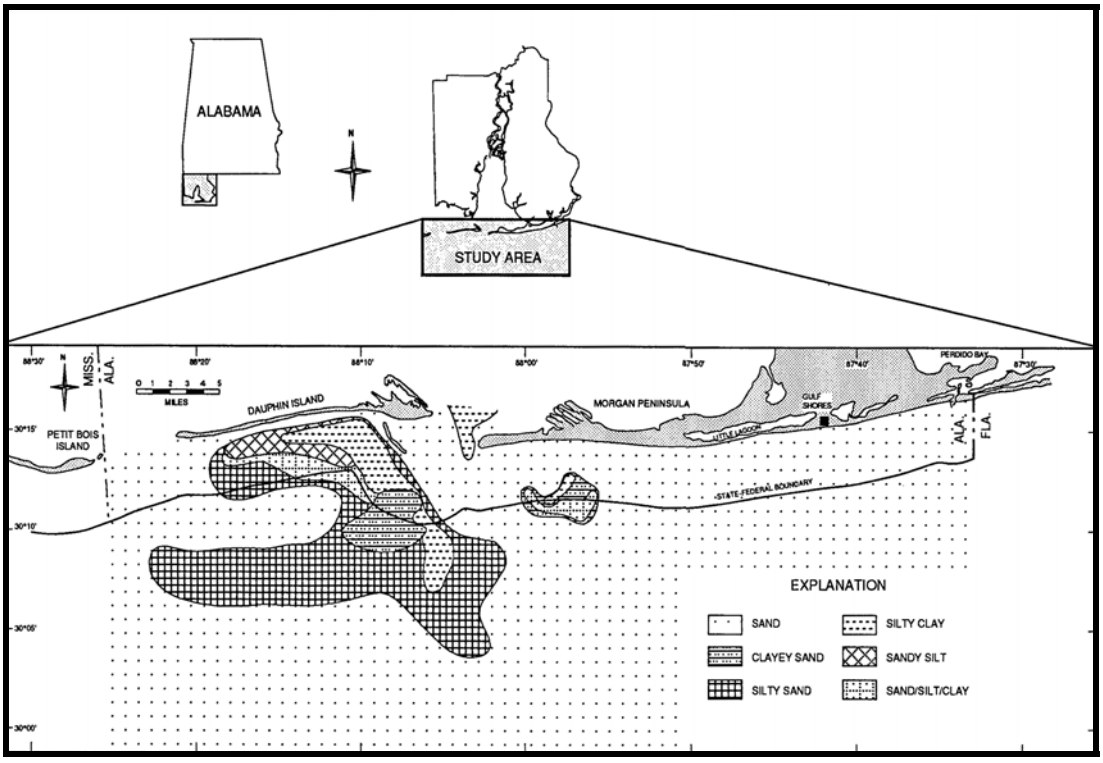

Figure 1-4. Surface sediment texture map (from USACE, 1984).

Parker et al. (1992) suggest that much of the variation is due to changes in bathymetry. Large ridges on the eastern part of the Alabama shelf extend for several hundred yards in length, a couple of hundred yards in width, and are composed of sand. Shell gravel is common on the landward flanks of the ridges with mud occasionally depositing in the troughs between ridges (Parker et al., 1992; McBride and Byrnes, 1995; Parker et al., 1997).

Seabed Morphology. The Alabama continental shelf can be divided into two regions based on regional geomorphology and hydrology (Parker et al., 1997). The eastern shelf extends from the Alabama-Florida state boundary near Perdido Pass to Main Pass (see Figure 1-1). The western shelf extends from Main Pass to the Alabama-Mississippi state boundary at Petit Bois Pass. The large ebb-tidal delta at Main Pass is approximately 10 miles wide, extends about 6 miles offshore (Hummell, 1990), and separates the two regions (Figure 1-5). The subaerial portion of the ebb-

tidal delta consists of Pelican Island, and occasionally Sand Island (an ephemeral shoal southeast of Pelican Island), both of which lie in the western shelf region.

The eastern portion of the study area is dominated by numerous shelf and shoreface sand ridges and swales that trend northwest to southeast (McBride and Byrnes, 1995; Parker et al., 1997). The ridges are considered shoreface-attached and detached (Parker et al., 1992), and they form an oblique angle to the shoreline that opens to the east. Some of the ridges were identified by Parker et al. (1997) as pre-Holocene paleotopography draped with Holocene sand, rather than modern deposits resulting from marine hydrodynamic processes. The ridges average about 3.6 miles in length and range from 0.5 to 7 miles long. Ridge widths range from 0.25 to 2.5 miles with spacing between ridges varying between 0.5 and 4.5 miles. Ridge side slopes average about 1°, and relief above the surrounding seafloor ranges from about 3 to 16 ft (McBride and Byrnes, 1995). The ridges recognized as shoreface-attached or shoreface-detached generally form opening angles with the east-west trending shoreline of 30 to 60°. Ridges formed as pre-Holocene topographic highs generally are oriented nearly perpendicular to the shoreline, reflecting their fluvial origin.

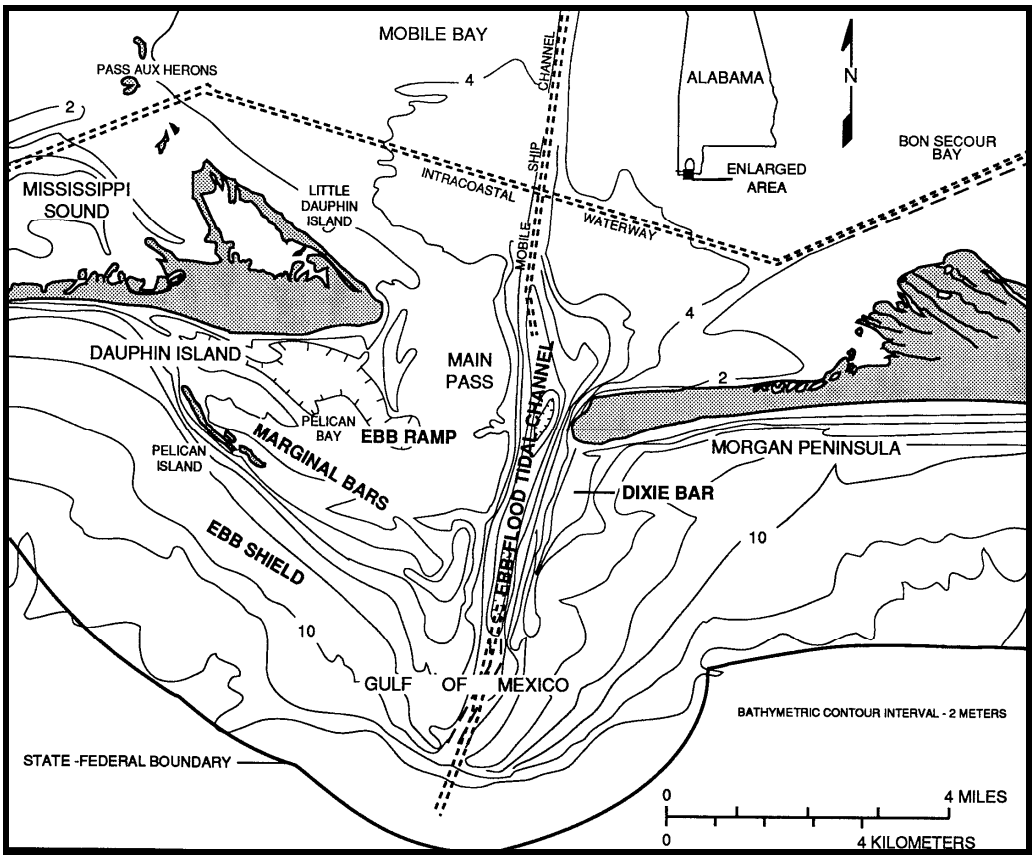

Figure 1-5. Geomorphology of the ebb-tidal delta seaward of Mobile Bay entrance (from Hummell, 1996).

A large southwest-trending shoal, located approximately 10 miles east of Mobile Point, is prominent in the eastern part of the study area. Although its origin is not known, evidence from Parker et al. (1997) suggests that it may be a drowned sand spit during the early Holocene as the western end of Morgan Peninsula evolved. Alternatively, it could be the remnants of a large ebb-tidal delta formed when an inlet was present through Morgan Peninsula. The sand shoal extends about 9 miles offshore and has almost 20 ft topographic relief. The occurrence and character of ridges on the eastern Alabama shelf are described by McBride and Byrnes (1995).

The upper shoreface of the eastern shelf region is steeper than the western shelf region, and gradients range from 30 to 40 ft/mile (McBride and Byrnes, 1995; Parker et al., 1997). However, the eastern shelf surface from the shoreline to the shelf break averages approximately 5 ft/mile.

The western half of the study area, from Main Pass west to Petit Bois Pass, has relatively few geomorphic features compared with the eastern part of the study area. Shoals associated with deposition near the entrances to Main Pass and Petit Bois Pass are prominent; however, the shelf seaward of Dauphin Island is smooth and concave. Marginal shoals of the ebb-tidal delta are quite shallow to the west of Main Pass (see Figure 1-5; Pelican Island is subaerial and Sand Island is intermittently subaerial). Hummell (1990) discusses the importance of these features to sediment transport patterns along the shoreline of eastern Dauphin Island.

Surface Sediments. Surface sediments throughout the study area are composed of two primary facies. The Mississippi-Alabama Sand Facies dominates the eastern portion of the study area (Figure 1-6; Ludwick, 1964). It consists predominantly of well-sorted clean quartz sand, with shelly sands occurring locally (Figure 1-7). McBride and Byrnes (1995) and Sawyer et al. (2001) characterize samples taken from this area as >90% sand and <3% mud. Median grain size ranges from 0.14 to 0.46 mm or fine-to-medium sand. Ludwick (1964) characterized the sand as 93% terrigenous and 7% carbonate, with a median grain diameter of 0.18 mm. Doyle and Sparks (1980) found the same general trend and named the facies the Mississippi-Alabama-Florida (MAFLA) sand sheet.

Parker et al. (1997) collected bottom sediment samples throughout the study area to characterize surface sediment distribution. Besides the sand facies described above, east of Main Pass, another large-scale pattern is the presence of a muddier facies near the Main Pass of Mobile Bay. Sediment from Mobile Bay contributes fine-grained material to the shelf, particularly during times of heavy flow. Much of the fine-grained sediment is carried as a sediment plume offshore and to the west of

Main Pass, due primarily to dominant wind, wave, and tidal currents between the Bay and the Gulf (Wiseman et al., 1988; Stumpf and Gelfenbaum, 1990).

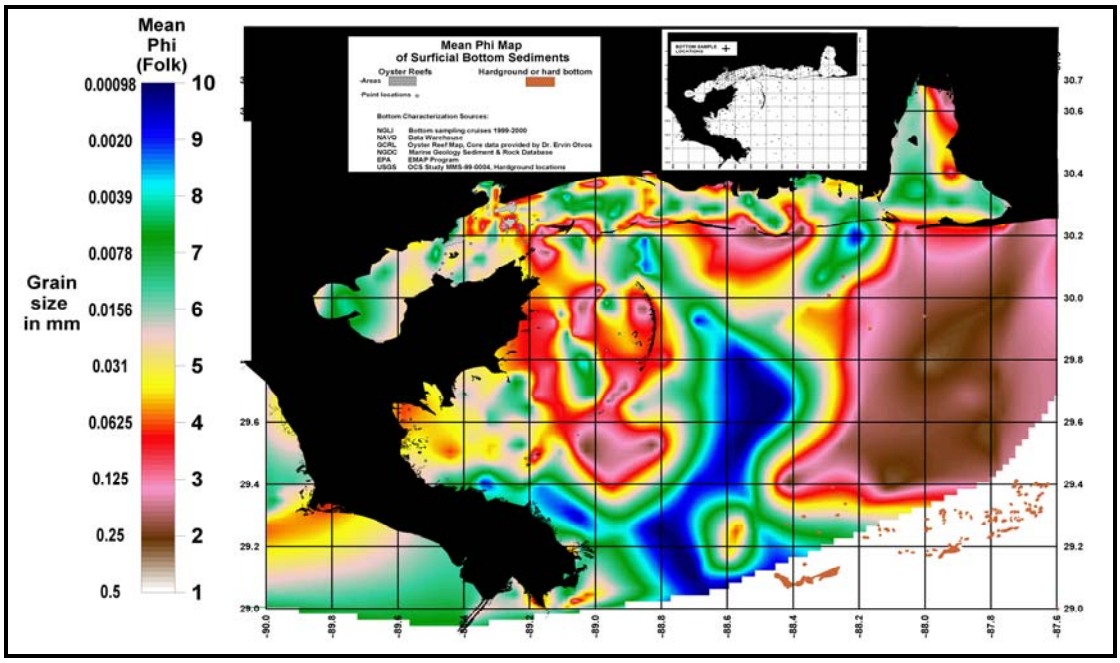

Figure 1-6. Map of sediment mean grain size in the Mississippi Bight (from Sawyer et al., 2001).

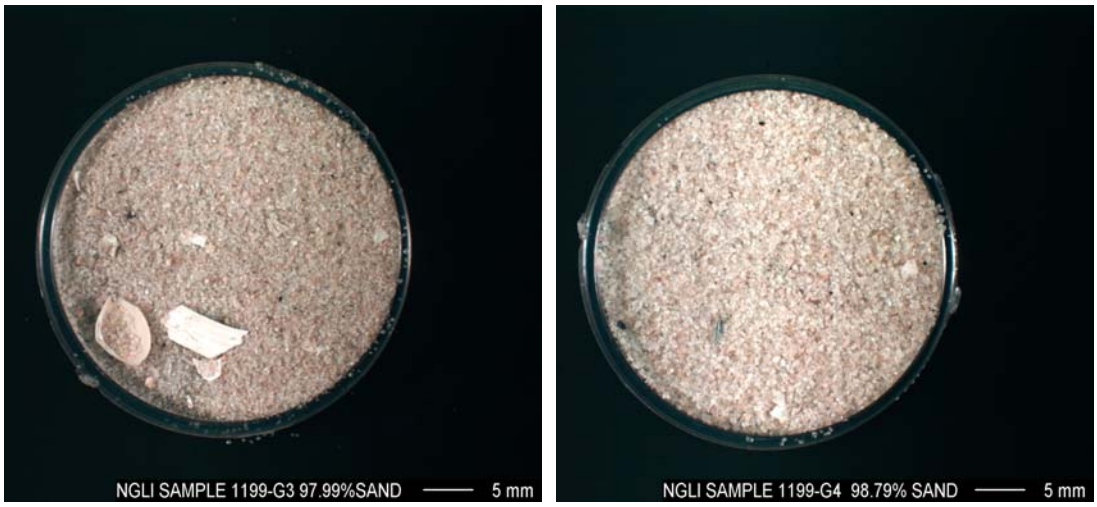

Figure 1-7. Shelf sediment texture east of Mobile Pass (from Sawyer et al., 2001).

Parker et al. (1997) illustrated the distribution of fine-grained sediment in the western portion of the study area based on limited samples, whereas Hummell and Smith (1995, 1996) used USACE data to summarize the distribution of bottom sediment seaward of and adjacent to Main Pass and Dauphin Island (USACE, 1984).

Figure 1-8 illustrates the distribution of bottom sediment in the western portion of the study area where the influence of fine-grained sediment from Mobile Bay is recognized as areas of silty clay, silty sand, and sandy silt on an otherwise sandy shelf surface.

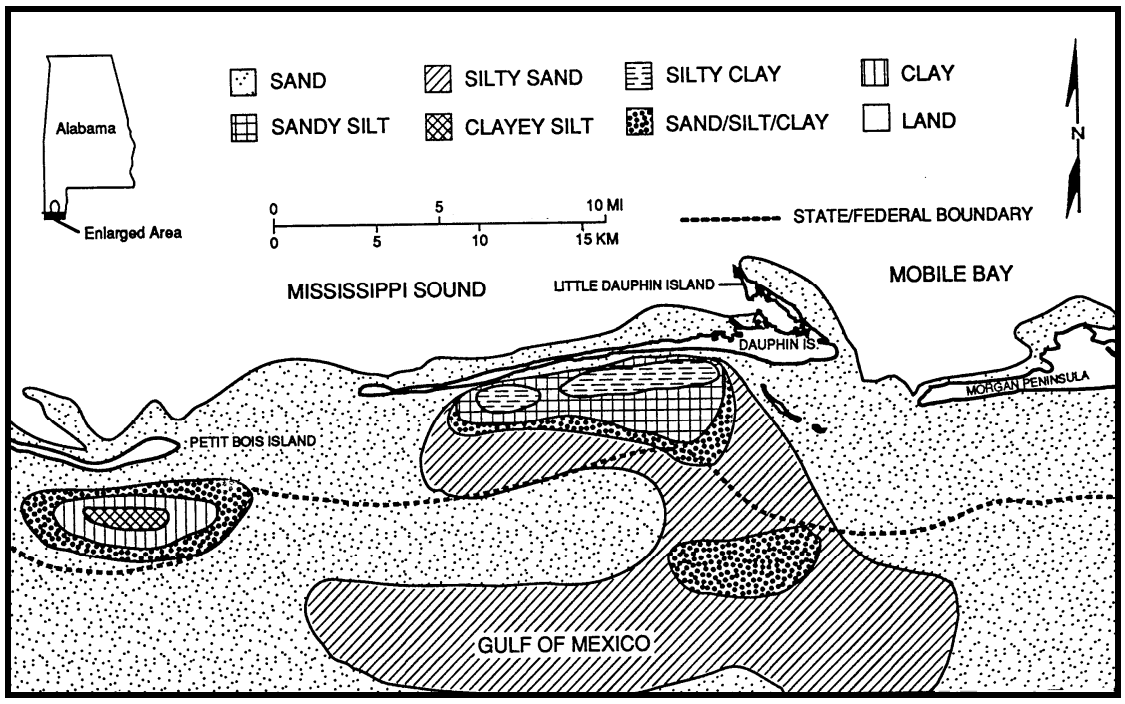

Figure 1-8. Surface sediment distribution in the west Alabama inner continental shelf (from Hummell, 1996).

Subsurface Deposits. The Holocene geologic framework of nearshore Alabama has been documented by Parker et al. (1993, 1997), Hummell (1996), and Hummell and Smith (1996). Parker et al. (1997) obtained vibracores from throughout the study area to illustrate the history of sediment deposition on the continental shelf within the study area. Based on core data analysis, five primary Holocene lithofacies were identified for the study area. They included a clean sand lithofacies, a graded shelly sand lithofacies, a dirty sand lithofacies, a biogenic sediment lithofacies, and a muddy sediment lithofacies. The sedimentologic characteristics of these facies are detailed in Parker et al. (1997; p. 33-71). As a summary, Figure 1-9 provides a generalized composite stratigraphic sequence of sedimentary facies in the study area. Overall, much of the inner shelf is composed of a shelf sand sheet depositional environment formed during Holocene transgression. It is a deposit that grades into other sand depositional environments that have been reworked by high-energy storm events, as well as non-storm currents and bioturbation (Parker et al., 1997). On the eastern shelf, numerous sand ridges have

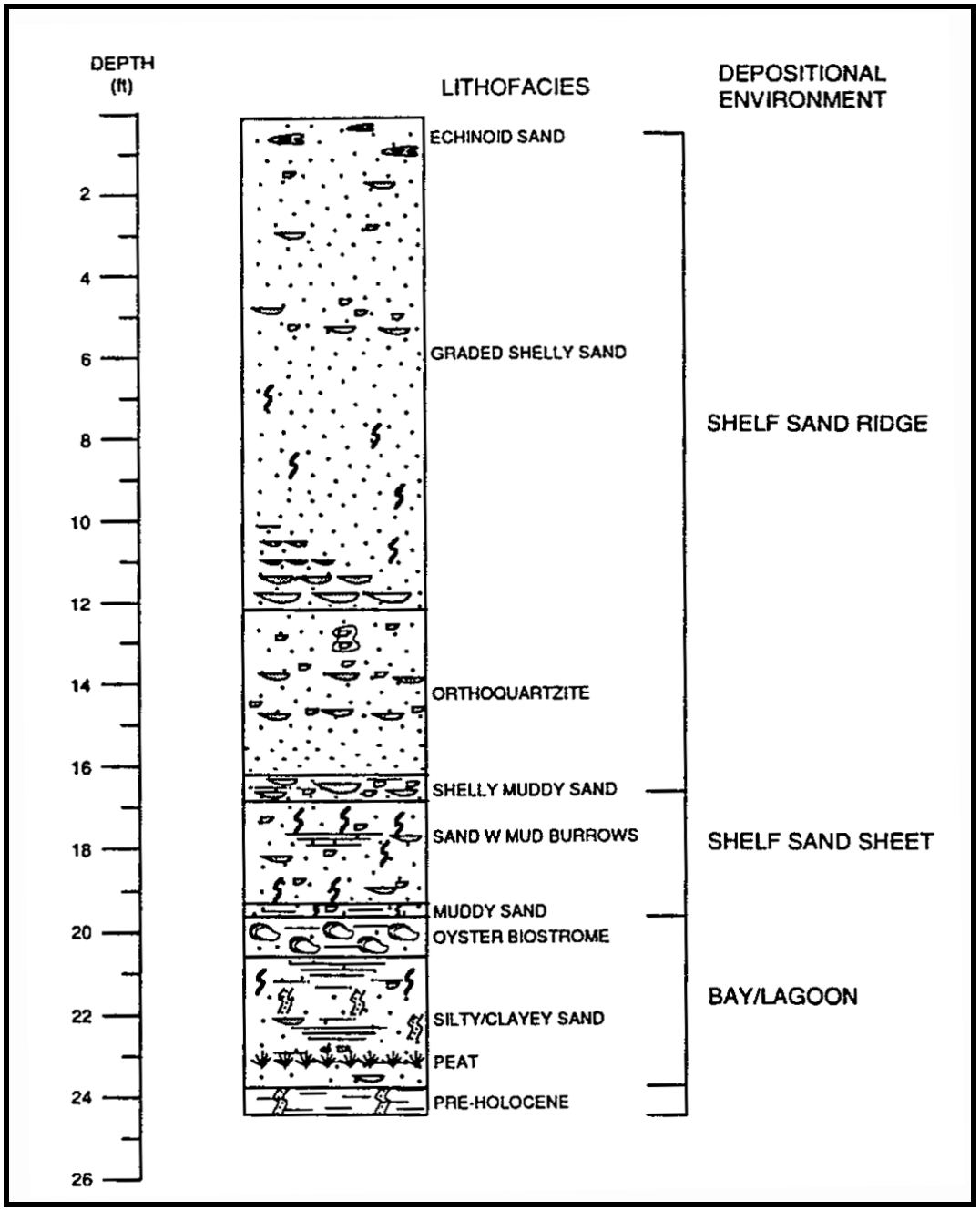

Figure 1-9. Generalized stratigraphic sequence of the Alabama EEZ study area (from Parker et al., 1997).

formed on top of the sand sheet in response to local and regional hydrodynamics (Swift and Niedoroda, 1985; Byrnes and McBride, 1996; McBride, 1997).

The western portion of the study area contains greater variability in depositional characteristics due to the influence of fine-grained sediment from Mobile Bay. The muddy sand lithofacies is common on the shelf west of Main Pass and seaward of

Dauphin Island. Hummell and Smith (1996) used the classification criteria of Parker et al. (1993, 1997) to describe the lithology of deposits adjacent to and west of Main Pass. Overall, sand deposits on the western shelf are finer-grained relative to shelf deposits to the east.

Coastal Circulation and Waves. Review of previously-published literature indicates that circulation patterns in the offshore result primarily from three dominant processes. These processes are wind-driven flow, tidal flow, and buoyancy (or density)-driven flow. Nearshore currents in the study area display significant spatial and temporal variability, resulting from the relative strength of each forcing mechanism.

Winds and Wind-Generated Currents. The meteorological climate for the northeastern Gulf of Mexico (NEGOM) can be separated into two distinct seasonal periods: summer and winter (Clarke, 1994; Schroeder et al., 1994). Each period is dominated by different types of air masses. The summer period is defined as May (late spring) through early fall (October), and is characterized by stable high pressure air resulting from the more-northerly position of the Atlantic high pressure zone ('Bermuda High'). During this time, high pressure off the Atlantic coast brings relatively mild tropical air into the region, resulting in typically weak southerly winds. During the winter period, defined typically as December through April, the southern migration of the Atlantic high pressure zone allows polar air to intrude into the region, bringing with it Arctic frontal systems of cold, dry air. Northerly winds are more common during this period.

A meteorological station has been operational on eastern Dauphin Island since the mid-1970s. Schroeder and Wiseman (1985) summarized data for the period 1974 to 1985, illustrating that the most common wind direction is from the north, the direction from which strongest winds blow. Using U.S. Weather Bureau data for Mobile between 1872 and 1930, Chermock et al. (1974) documented that prevailing winds in coastal Alabama tend to be variable, but from March through August, winds blow from the south to southwest, and from September through February, they blow from the north and northwest. Winds generating waves along south facing beaches of the Morgan Peninsula and Dauphin Island are much more common from the east and south than from the west and south (Douglass, 1991). As such, locally-generated sea waves move sand predominantly from east to west.

Polar air intrusions occur at time scales of 3 to 10 days, and result in more energetic air-sea disturbances from December through January. The effect of these winds on nearshore currents can be exaggerated due to the presence of the shoreline, which

creates an impermeable flow boundary, blocking typical Ekman response of the water column to wind forcing (Clarke, 1994). The result can be stronger response of the water column to wind forcing in nearshore zones than would be expected in deeper water. Lewis and Reid (1985) described the along-shelf flow to be correlated with along-shelf winds. Reid (1994) stated that the longshore reversals in near-shore current directions (on subtidal time scales of order 3 to 10 days) observed during the Louisiana-Texas Shelf Physical Oceanography Program resulted from similar reversals in the longshore wind component. For coastal Alabama, this suggests that wind-driven currents are likely strongest between October and April, when currents are oriented approximately in the direction of the longshore wind component. Wind-driven currents in the summer months would be expected to be weaker.

Storms, typically hurricanes, passing the region can generate anomalous currents in the nearshore. Murray (1970) presented current observations obtained along the inner shelf (approximately 20-ft water depth) offshore Pensacola during the passage of Hurricane *Camille*. The eye of *Camille* passed approximately 100 miles to the west of the mooring. The current meter collected readings exceeding 5.25 ft/sec (wave orbital velocities had been removed from the record) before malfunctioning. Winds had not yet reached peak speed at the time of malfunction; extrapolating the current signal suggests the current speeds during the storm may have exceeded 6.5 ft/sec. These high speed flow responses to storm winds were oriented in the direction of the wind stress vector; at that time, the wind was blowing from the east. Further information on historical tropical cyclones is presented below.

Waves and Wave-Generated Currents. The interaction of wind with the water surface generates waves. Waves are usually present at the shoreline because the sea surface is vast, winds are prevalent, and waves can travel long distances. Waves are primarily responsible for sediment transport in the nearshore zone and for subsequent shoreline and seafloor change; therefore, waves are of fundamental interest when evaluating the potential effects of channel dredging on beach erosion.

As waves enter the nearshore zone, varying seafloor morphology causes the characteristics of waves (e.g., height and direction of travel) to change. As waves enter shallow water, their height increases (shoaling), and the direction of travel bends toward the coast so that wave crests become more parallel to the shoreline (refraction). As waves approach shore, shoaling and wavelength modifications overcome dissipation effects and cause wave height to increase and waves to steepen. Eventually wave steepness causes waves to become unstable and break, which dissipates wave energy. Energy also is distributed along a wave crest by a process called wave diffraction. Together, wave shoaling, refraction, diffraction, and

breaking can focus wave energy on particular areas, depending upon the characteristics of nearshore bathymetry.

Generally, there are seasonal variations in wave climate governed by seasonal characteristics of wind. Summer months (typically considered May through October) are characterized by relatively calm winds and low-energy waves, while winter months (typically considered December through April) are characterized by a more energetic wind and wave climate. Sporadic storms, such as hurricanes and cold fronts, generate the largest waves that impact the Alabama Coast.

More specific information about the waves along the Alabama Coast is provided in the published literature (although existing literature discussing waves and wave-generated currents is limited). For instance, Bedford and Lee (1994) collected short-term wave data in August and September 1989, approximately 2,500-ft offshore of Dauphin Island and west of the Mobile ship channel. These authors deployed a pressure and current (PUV) sensor at a water depth of approximately 20 ft. Spectral analysis showed that wave periods ranged from 3 to 10 sec, with maximum wave energy associated with a peak wave period of 5.8 sec. Significant wave heights were approximately 2.6 ft. Although wave direction was not resolved well, it was determined that waves were directed almost due north.

Another set of wave and current data in this region was collected by the USACE using wave gauges and near-bottom electromagnetic current meters as part of a monitoring program of nearshore dredged material disposal sites off the Alabama Coast. McGehee et al. (1994) provide details on the gauges and data collection procedures. Two wave gauges were installed 0.8 and 1.6 miles offshore by the National Data Buoy Center (NDBC) for that study between 1987 and 1990.

Douglass et al. (1995) evaluated these long-term wave measurements and concluded that waves in this region provide the dominant mechanism responsible for moving Alabama berms persistently landward. Wave-driven sediment transport is due to faster landward current speeds under wave crests that are characteristic of shallow water, nonlinear waves. It was concluded that wave processes dominate other potential sediment transport processes, such as mean currents and short-term storms.

Tides and Tide-Generated Currents. Tidal currents in the Northeast Gulf of Mexico are strongly diurnal, dominated by the O1 (period of 25.82 hours) and K1 (period of 23.93 hours) tidal constituents (Clarke, 1994). Water elevation variations due to the tides average about 1.5 to 2 ft, although the maximum range (tropic tides)

can approach 2.6 ft while the minimum (equatorial tides) can be near-zero (Schroeder et al., 1994). As Gulf of Mexico water floods lower Mobile Bay, water entering the Bay is deflected to the east and propagates north along the eastern side of the estuary. Figure 1-10 provides a summary of average annual surface currents during flood and ebb tide. Except for the Mobile Ship Channel, bottom currents generally mimic surface currents throughout the Bay (Hummell, 1990). During ebb tide, southward flow is fairly uniform throughout the Bay.

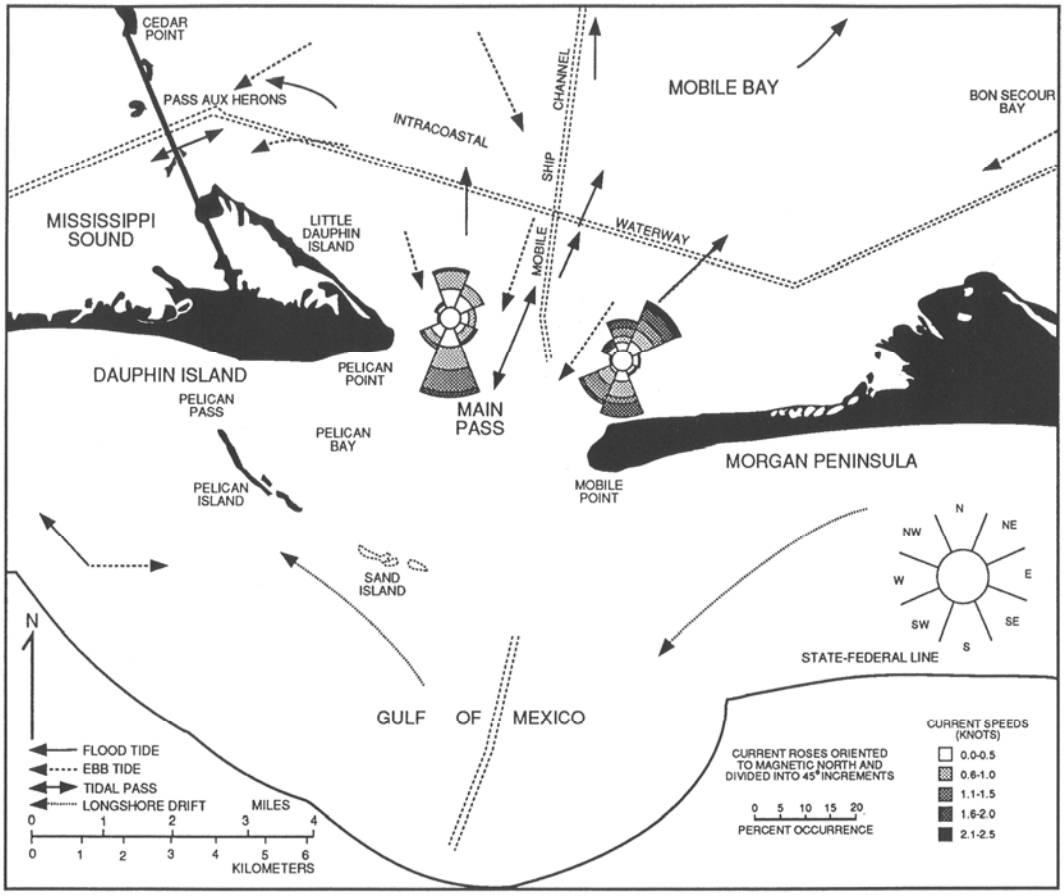

Figure 1-10. Average surface current during flood and ebb tide near Main Pass (from Hummell, 1990).

Seim et al. (1987) found that tides on the Alabama-Mississippi inner shelf have a major axis oriented perpendicular to the shoreline with a shore-normal mean amplitude of approximately 0.2 to 0.3 ft/sec and a minor axis in the alongshore direction with a mean amplitude of 0.1 ft/sec. The tidal ellipses rotate in a clockwise sense on the shelf (Kinoshita and Noble, 1995).

Tidal currents on the inner shelf near the entrance to Mobile Bay are influenced by the ebb-tidal jet and, hence, dominated by the southward ebb flow from the Bay. However, measurements of the current made just west of the lighthouse at the entrance show that the dominant tidal component is in the alongshore direction (Douglass et al., 1995), with a relatively weaker cross-shore component.

Density-Driven Currents. Density-driven (baroclinic) currents on the continental shelf can be important in determining spatial variability of flow. Fresh water discharged from Mobile Bay is significant. This input of low density water creates a density gradient in the cross-shore direction. This gradient can result in an alongshore movement where the direction of flow will be to the right of the pressure gradient (Blanton, 1994). For Alabama, this suggests a baroclinic flow to the west when nearshore density gradients are present.

The structure of the nearshore density field can vary seasonally. In summer, a strong vertical stratification develops due to surface heating, as well as decreased vertical mixing (winds are milder). In winter, reduced heating and more vigorous vertical mixing tend to weaken the vertical stratification and produce a horizontal gradient (Clarke, 1994). Hence, the strength of the alongshore flow due to cross-shore density gradients is assumed to vary on a seasonal basis, with baroclinic flows likely strongest in winter.

Schroeder et al. (1994) describes the plume from Mobile Bay as advecting to the east; however, no physical explanation of why this occurs was given. Other studies (Stumpf et al., 1993; Gelfenbaum and Stumpf, 1993) suggest the plume responds rapidly to local wind stress, hence the direction of the plume upon exit from the Bay likely depends on the direction of the alongshore wind stress component.

Gelfenbaum and Stumpf (1993) presented observations of currents and waves collected on both sides of a well-developed buoyant plume front near the mouth of Mobile Bay. Measurements collected in ambient water were compared to those collected within the plume. Results indicated flow within the buoyant plume was largely decoupled from the ambient flow; the ambient flow moved around and beneath the plume. In addition, the plume created a buffer above the ambient water; this buffer retarded vertical mixing as well as attenuated surface waves. Surface wave heights within the plume were lower than those measured outside the plume. Also, wave periods within the plume were shorter than those detected outside the plume. This implies that the plume modifies the local wave field, and may modify sediment transport processes beneath it.

Nearshore Sediment Transport. Nearshore sediment transport is a complex process, which governs erosion and accretion of beaches. Sediment is moved alongshore and cross-shore (on and offshore) by physical coastal processes, such as wind, waves, tides, currents, and sea-level rise. The time scales of sediment movement and shoreline change vary from the initial formation of headlands and coasts on geologic time scales (thousands of years) to severe coastal erosion over a few days or hours during tropical storms and hurricanes.

In addition to physical coastal processes, sediment transport patterns are dependent upon the characteristics and supply of sediment. Grain size is the most important characteristic of the sediment. The quantity of sediment moved under constant wave and current processes is inversely proportional to its grain size. Sediment transport rates decrease with increasing grain size, because heavier sediment requires more time and energy to be transported. Sediment density, durability, and shape also affect transport rates. In addition, the supply of sediment governs sediment transport rates; transport rates are reduced where sediment is in short supply.

When waves break at an angle to the beach, alongshore-directed currents are generated, capable of lifting and moving sediment along the coast. For example, waves approaching the Gulf Shores shoreline from the east tend to move sand alongshore from east-to-west toward Main Pass. Because wave direction changes frequently, sand is moved back-and-forth along the beach. On an annual basis, however, there typically is a dominant wave direction that occurs most frequently on seasonal time scales. In the case of coastal Alabama, the dominant direction of littoral sand transport on an annual basis is from east to west.

Past work regarding longshore transport rates for Dauphin Island and the Morgan Peninsula is limited. According to Parker (1990), wave-generated longshore currents have the most apparent effect on sediment transport. Although it is generally accepted that the typical east-to-west currents dominate beach transport processes, the amount of sediment entrained in the littoral system along Alabama barrier beaches is not known with confidence.

Walton (1974) used visual estimates of wave height, period, and direction from shipboard observations in the Gulf of Mexico to estimate net potential littoral drift along Dauphin Island. West of Pelican Island along the open ocean beach, Walton estimated west-directed transport at about of 600,000 cy/year and east-directed transport at about 140,000 cy/year, resulting in net west-direct transport of about 460,000 cy/year. Garcia (1977) determined that net potential longshore sediment transport at Dauphin Island was approximately 196,000 cy/year to the west, and the

USACE (1955) estimated about 200,000 cy/year of net potential littoral transport at Perdido Pass. More recently, Cipriani and Stone (2001) calculated maximum net potential transport to the west along central Dauphin Island of 81,000 cy/year.

Tropical Cyclones

Recent damage caused by tropical cyclones over the past decade, particularly related to the 2005 season, has generated additional interest in recurring climatological hazards as a dominant mechanism for change in coastal settings. Numerous studies have documented the impact of tropical cyclones on the redistribution of sediment in coastal environments (e.g., Nichols and Marston, 1939; Hayes, 1967; Scott et al., 1969; Dolan and Godfrey, 1973; Fisher and Stauble, 1977; Nummedal et al., 1980; Schramm et al., 1980; Byrnes and Gingerich, 1987; Froede, 2006b; Guidroz et al., 2007). These high-energy, short-duration events are particularly devastating in the northern Gulf of Mexico where storm frequency is high and ground elevation is low (USACE, 1978; Nummedal et al., 1980; Sallenger et al., 2005). Along the coast, raised water level and wave height, and extreme winds, create destructive forces that often alter the landscape by orders of magnitude greater than average conditions (Graumann et al., 2005; Sallenger et al., 2005). A comparative understanding of the occurrence of tropical cyclones (i.e., tropical storms and hurricanes) in relation to shoreline and bathymetry data sources used for quantifying long-term change is essential for documenting natural variations in beach and nearshore morphology relative to potential changes induced by engineering activities. Table 1-1 provides a summary of tropical cyclones causing beach changes in the study area between 1852 and 2005, the approximate time period covered by shoreline and bathymetry data sources.

Available historical data on tropical cyclones were derived from three primary sources. Blake et al. (2007) provided an update to the original publications by Jarvinen et al. (1984) and Jarrell et al. (1992) that created a tropical cyclone data base for the Atlantic and Gulf coasts of the US. The so called 'best-track' data set covers the period 1851 to 2005. Appendix A illustrates a decadal breakdown of Category 3 or stronger hurricanes for the Gulf and Atlantic coasts based on the best-track database.

Although accurate records of tropical cyclones impacting the Alabama coast are generally incomplete prior to 1851, recent storm compilations by Bossak (2003) and Bossak and Elsner (2004) used historical accounts from Ludlum (1963) to include additional tropical cyclones for the period 1800 to 1850. Furthermore, publications by Tannehill (1956), Dunn and Miller (1964), and USACE (1978) document colonial

events for the period 1711 to 1799. The following is a summary of primary storms for each of the major geomorphic change time periods.

Table 1-1. Chronology of Tropical Cyclones that Affected the Alabama Coast: 1852 to 2005 (updated from Jarrell et al. [1992] and reflecting official HURDAT reanalysis changes).

Year	Date	Landfall	Category at Landfall	Central Pressure (mb)	Wind Speed (kt)	Name
1852	Aug 26	Horn Island, MS	3	961	100	"Great Mobile"
1855	Sept 16	Bay St. Louis, MS	3	950	110	“Middle Gulf Shore”
1859	Sept 15	Dauphin Island, AL	1	985	70	-----
1860	Aug 12	Biloxi, MS	3	950	100	-----
1860	Sept 15	Bay St. Louis, MS	2	969	90	-----
1870	Jul 30	Mobile, AL	1	985	70	"Mobile"
1872	Jul 11	Ship Island, MS	TS	-----	50	-----
1877	Sept 19	Pensacola, FL	1	985	70	-----
1879	Oct 7	Waveland, MS	TS	-----	50	-----
1881	Aug 3	Petit Bois Island, MS	TS	-----	50	-----
1882	Sept 10	Pensacola, FL	3	949	100	-----
1885	Sept 27	Ship Island, MS	TS	-----	60	-----
1887	Jun 14	Horn Island, MS	TS	-----	35	-----
1887	Jul 27	Pensacola, FL	1	981	75	-----
1887	Oct 19	Cat Island, MS	1	981	65	-----
1889	Sept 23	Gulf Shores, AL	1	985	70	-----
1893	Oct 2	Ship Island, MS	2	948	95	-----
1894	Aug 7	Gulf Shores, AL	TS	-----	50	-----
1895	Aug 16	Horn Island, MS	TS	-----	50	-----
1900	Sept 13	Horn Island, MS	TS	-----	40	-----
1901	Aug 15	Ship Island, MS	1	973	80	-----
1902	Oct 10	Gulf Shores, AL	TS	-----	55	-----
1906	Sept 27	Horn Island, MS	2	958	95	-----
1907	Sept 21	Ship Island, MS	TS	-----	40	-----
1911	Aug 11	Gulf Shores, AL	1	985	70	-----
1912	Sept 14	Petit Bois Island, MS	1	988	65	-----
1914	Sept 18	Horn Island, MS	TS	-----	35	-----
1916	Jul 5	Ship Island, MS	3	979	105	-----
1916	Oct 18	Perdido Key, FL	3	974	100	-----
1917	Sept 28	Pensacola, FL	2	966	85	-----

Table 1-1. Continued.

Year	Date	Landfall	Category at Landfall	Central Pressure (mb)	Wind Speed (kt)	Name
1922	Oct 17	Gulf Shores, AL	TS	-----	40	-----
1923	Oct 17	Ship Island, MS	TS	-----	45	-----
1926	Sept 21	Dauphin Island, AL	2	955	95	-----
1932	Sept 1	Fort Morgan, AL	1	979	70	-----
1934	Oct 6	Dauphin Island, AL	TS	-----	40	-----
1939	Jun 16	Morgan Peninsula, AL	TS	-----	35	-----
1944	Sept 10	Bay St. Louis, MS	TS	-----	40	-----
1947	Sept 8	Petit Bois Island, MS	TS	-----	40	-----
1947	Sept 19	Chandeleur Islands, LA	1	966	80	-----
1950	Aug 31	Morgan Peninsula, AL	1	980	75	Baker
1955	Aug 1	Chandeleur Islands, LA	TS	-----	60	Brenda
1955	Aug 27	Chandeleur Islands, LA	TS	-----	40	-----
1956	Sept 24	Pensacola, FL	1	980	80	Flossy
1959	Oct 8	Gulf Shores, AL	TS	1001	50	Irene
1960	Sept 15	Ship Island, MS	TS	981	60	Ethel
1964	Oct 4	MS/AL Coast	ES	-----	60	Hilda
1969	Aug 18	Bay St. Louis, MS	5	909	165	Camille
1975	Sept 23	Pensacola, FL	3	955	110	Eloise
1979	Sept 13	Dauphin Island, AL	4	946	115	Frederic
1985	Sept 2	Ship Island, MS	3	957	105	Elena
1985	Oct 31	Orange Beach, AL	TS	978	60	Juan
1994	Jul 3	Pensacola, FL	TS	993	55	Alberto
1995	Aug 3	Gulf Shores, AL	1	974	80	Erin
1995	Oct 4	Perdido Key, FL	3	938	110	Opal
1997	Jul 19	Mobile Pass, AL	1	987	65	Danny
1998	Sept 28	Ship Island, MS	2	964	90	Georges
2002	Sept 14	Horn Island, MS	TS	1003	50	Hanna
2004	Sept 16	Morgan Peninsula, AL	3	943	105	Ivan
2005	Jun 11	Gulf Shores, AL	TS	990	55	Arlene
2005	Jul 6	Bay St. Louis, MS	TS	994	50	Cindy
2005	Jul 10	Perdido Key, AL	3	942	110	Dennis
2005	Aug 29	Waveland, MS	3	923	110	Katrina

1847 to 1918. During this 71-year time interval, 30 tropical cyclones, 19 of which were hurricanes, directly affected the coastline in the study area (Table 1-1). United States Coast and Geodetic Survey (USC&GS; currently the National Ocean Survey [NOS] of the National Oceanic and Atmospheric Administration [NOAA]) topographic sheet (T-sheet) 240, dated April 1853, illustrates that the central portion of Dauphin Island was breached (Figure 1-11), likely during the August 1852 hurricane. The USACE (1978) reported significant storm surges associated with the hurricanes of 1893, 1901, 1909, 1915, and 1916 at Mobile where erosion due to wave action on the mainland and outer coast shorelines was particularly severe. The hurricane of July 5, 1916 produced a surge of 7.7 ft above mean sea level (MSL) at Dauphin Island and 11.3 ft above MSL at Gulf Shores, with a maximum wind speed of 107 miles per hour from the east at Fort Morgan (USACE, 1978; Morton, 2007). Erosion and overtopping of barrier beaches and dunes resulted in substantial geomorphic change along the beaches, particularly along the western sand spit where breaching by storm waves was common (Figure 1-12).

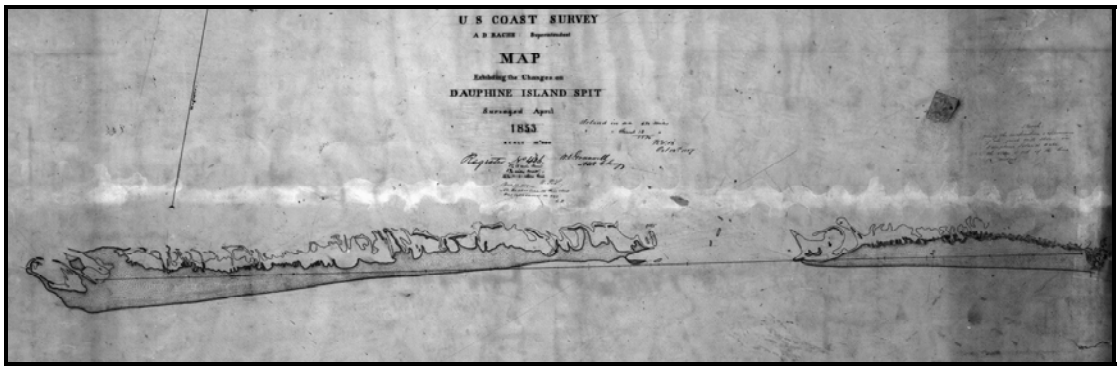

Figure 1-11. First recorded breach along central Dauphin Island by the US Coast and Geodetic Survey, likely resulting from the hurricane of August 26, 1852.

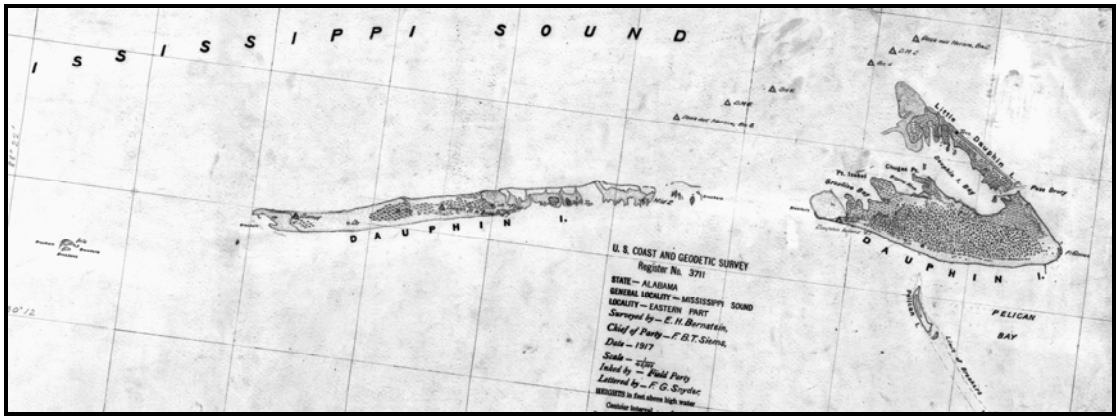

Figure 1-12. Island breaching along Dauphin Island in response to the 1916 hurricane.

1919 to 1957. Thirteen tropical cyclones, five of which were hurricanes, influenced beach and nearshore sedimentation processes during this 38-year period. Most storms produced minimal damage along the coast; however, the hurricanes of September 20-21, 1926 and September 18-19, 1947 were very destructive storms for the Alabama and Mississippi Gulf coastlines. The 1926 hurricane passed directly over eastern Dauphin Island as a Category 2 storm with sustained winds of about 95 knots from the north and a central pressure of about 955 mb. Storm surge at Mobile was about 4.5 ft above MSL. The 1947 hurricane tracked east to west, south of the Alabama coastline, creating a storm surge at Gulf Shores of about 7.9 ft MSL (Chermock et al, 1974; USACE, 1978). It eventually made landfall near New Orleans, resulting in extensive overwash along the Mississippi Sound barrier islands, including a breach along central Dauphin Island that was visible on March 23, 1950 aerial photography (Hardin et al., 1976). In Mississippi, a considerable portion of what is now US Highway 90 was destroyed. In addition, all piers along the Harrison County shore were destroyed along with numerous homes and other structures (Escoffier, 1958). The central portion of Ship Island also was breached during this event.

1958 to 1982. During this 24-year period, only six tropical cyclones (three hurricanes) caused changes throughout the study area. However, Hurricanes *Camille* (August 17-18, 1969) and *Fredric* (September 13, 1979) resulted in substantial overwash along Dauphin Island and substantial sand movement on the ebb shoal at Mobile Pass. During *Camille*, storm surge on Dauphin Island was recorded at 9.2 ft MSL. Schramm et al. (1980) and Nummedal et al. (1980) provide detailed discussions of the geomorphic response of Dauphin Island to Hurricane *Fredric*, with particular attention to storm overwash and washover fan development along central and western Dauphin Island (Morton, 2007).

1983 to 2005. The most recent 22-year period has experienced 13 tropical cyclones, eight of which were hurricanes. Hurricane *Katrina* (August 29, 2005) is now considered the storm of record in the study area, resulting in complete overwash of the western two-thirds of Dauphin Island and exacerbating the breach along the central portion of the island that resulted from waves and storm surge during Hurricane *Ivan* (September 16, 2004) (Froede, 2006b; Otvos, 2006). However, the hurricane of July 5, 1916 had far greater impact on the western Dauphin Island sand spit, as illustrated on USC&GS T-sheet 3711 (see Figure 1-12).

Inlet History at Main Pass

Historical maps from 1851 to present document the dynamic nature of shoals and channels on the ebb-tidal delta at Main Pass. According to Hubbard et al. (1979), the inlet system associated with Main Pass would be classified as tide-dominated because it has a well-developed ebb-tidal delta, poorly developed flood shoals, and a deep central channel with channel margin bars. A sequence of USC&GS navigation charts will be used to qualitatively illustrate the evolution of inlet shoals and the main channel since 1847. A detailed analysis of bathymetric change from historical survey data is presented in Chapter 4.

The first survey-quality data of nearshore and entrance areas to lower Mobile Bay were collected by the USC&GS in 1847/48. These data were used to create the navigation chart dated 1851 (labeled BiC-14; Figure 1-13). Because it is common for

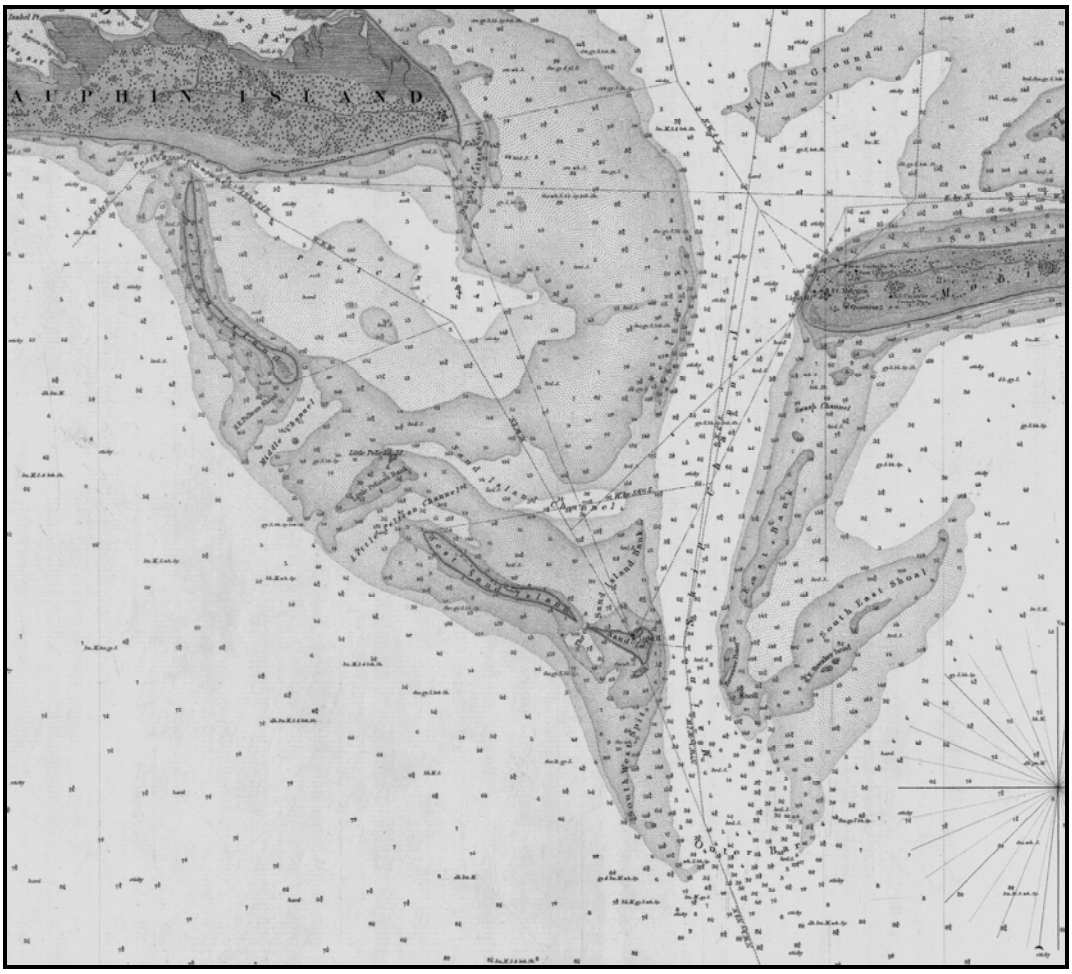

Figure 1-13. 1851 nautical chart of the entrance to Mobile Bay illustrating 1847/48 topographic and hydrographic survey data.

the date on navigation charts to be different than the date all bathymetric survey data were collected, these charts should never be used for quantifying surface changes between survey dates. Furthermore, the data points recorded on charts represent only a subsection of the total number of points collected as part of original hydrographic surveys (referred to as H-Sheets). Chart dates reflect a publication date for a given map, which may be reprinted because a buoy marker was added or moved in a channel since the last publication date, or that only a small number of the bathymetry data points were replaced by new survey data. In other words, any small update to the chart requires a new publication date.

At the time of the first systematic and accurate survey of the Pass, the deepest point in the inlet channel was about 57 ft relative to mean low water (MLW). The shallowest depth over the outer bar channel was about 21-ft MLW (Figure 1-14). Overall, the ebb-tidal delta at Main Pass consisted of east and west bars separated by a deep channel. East of the channel, East Bank and South East Shoal were extensive subaqueous sand deposits fed by west-directed littoral sand being diverted offshore along the east margin of the channel. Eventually, sand deposited along the southeast extent of the east bar was transported to the west across the outer bar, supplying sand to shoal deposits and subaerial islands west of the main channel. Sand from ebb-tidal shoals slowly makes its way to Dauphin Island via littoral transport processes. This is best illustrated in 1868 where shoreline surveys document a large depositional cusp on the shoreline just north of the location of Pelican Island in 1847 (see Chapter 2), indicating that Pelican Island had attached to Dauphin Island between 1847 and 1868. The western side of the ebb-tidal delta is at least two times larger in extent and volume than the shoal complex east of Main Pass.

Although numerous versions of 1851 chart were published under different dates over the following 40 years, only depths in and adjacent to Main Pass channel were updated as those data became available. It was not until Chart 188 was published in 1894 that depths over the east and west lobes of the ebb shoal were updated with data from the 1892 hydrographic and topographic surveys (Figure 1-15). The 1892 survey documented a number of interesting changes relative to the 1847/48 surveys. First, an island east of the channel (Dixie Island) had formed on the old Main Bank as an ephemeral feature that was never present on subsequent maps of this area. Second, the orientation of the outer bar channel had shifted west in response to sand deposition along the east side of the channel; however, minimum channel depth over the outer bar had not changed. Third, Pelican Island was no longer present west of the channel, apparently due to storm processes forcing this feature onshore, producing a large accretion cusp on the beach in 1868. Sand Island and West Sand

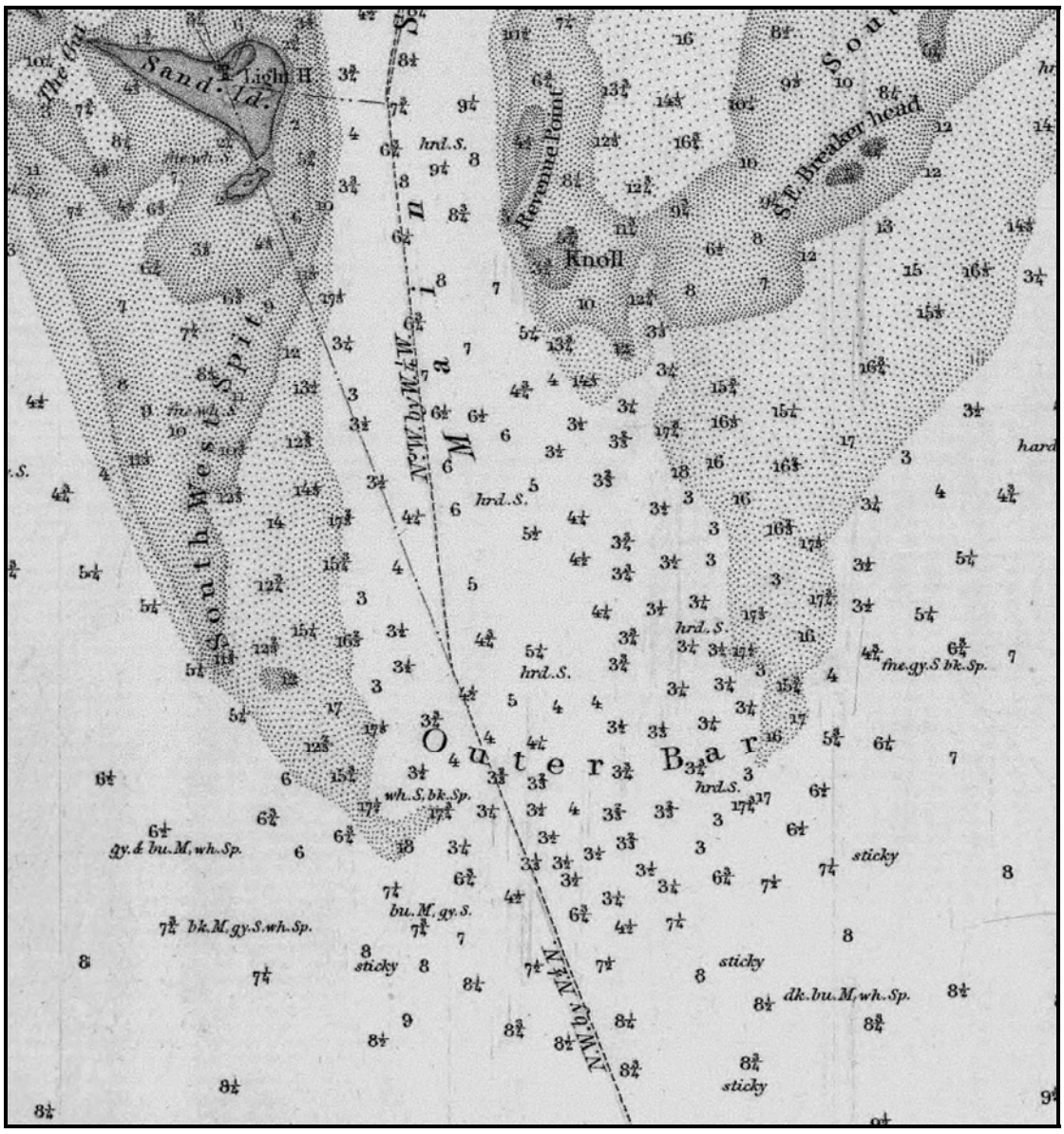

Figure 1-14. Depths across the Mobile Outer Bar in 1847/48. Sand bypassing from east to west around the outer bar was occurring at approximately the 18- to 21-ft depth contour.

Island remained viable in 1892, but as the main channel migrated to the west toward Sand Island Light, sand transport to the west left this portion of the ebb-tidal shoal more vulnerable to chronic erosion and change (Lee, 1998). Although beach erosion along Sand Island was first noticed in 1848, the 1899 annual report from the Lighthouse Board stated that the island was quickly washing away after years of repeated efforts to construct shore protection structures to protect Sand Island Lighthouse. Lee (1998) provides a detailed chronology of erosion at Sand Island Lighthouse as recorded in historical documents of the Lighthouse Board.

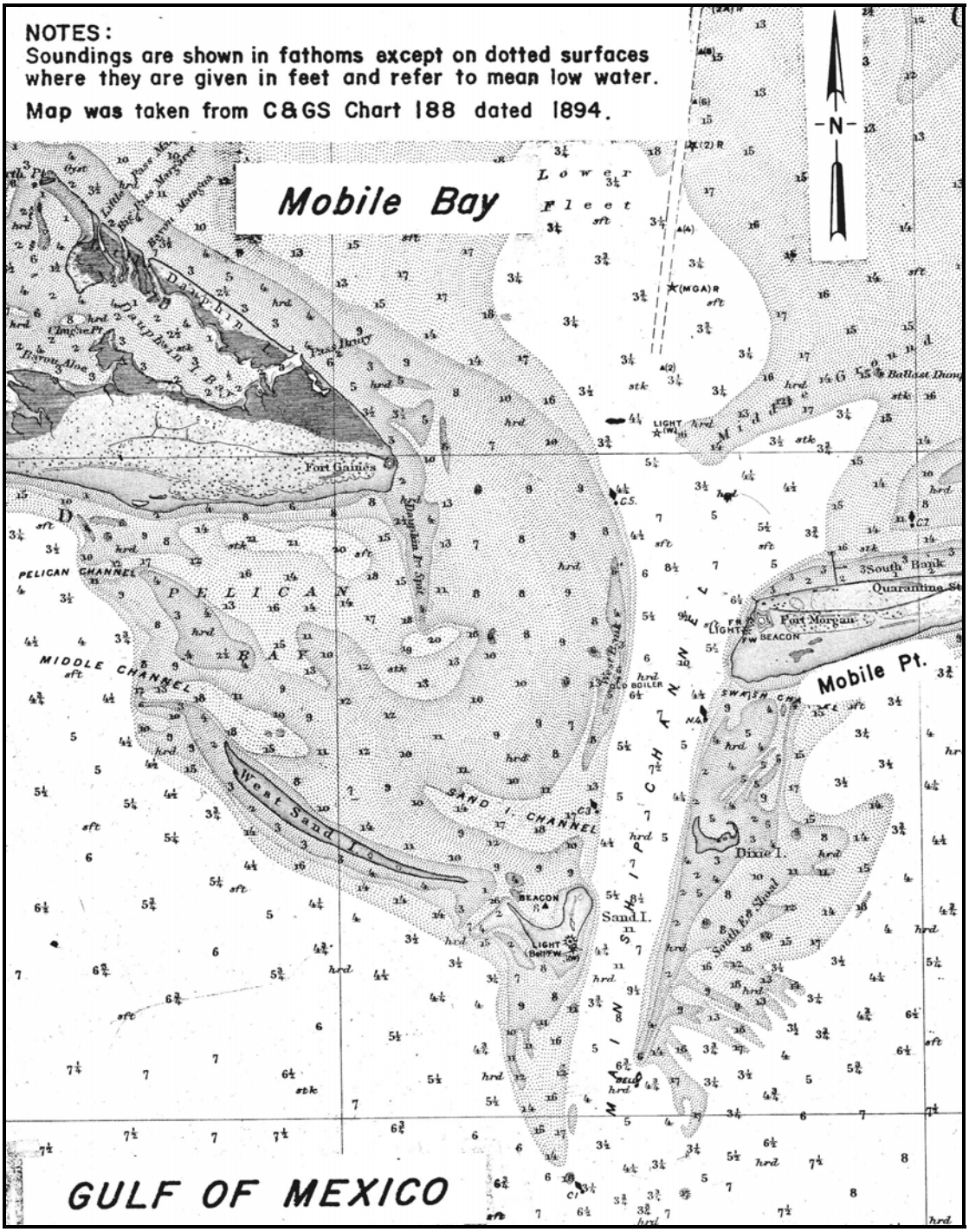

Figure 1-15. 1894 nautical chart #188 of the entrance to Mobile Bay illustrating 1892 topographic and hydrographic survey data (from USACE, 1978).

By 1908, maximum depth in the gorge of the main ship channel was still about 57 ft MLW, and minimum channel depth over the outer bar was still about 21 ft, even though the outer bar channel continued to migrate to the west (Figure 1-16). Dixie

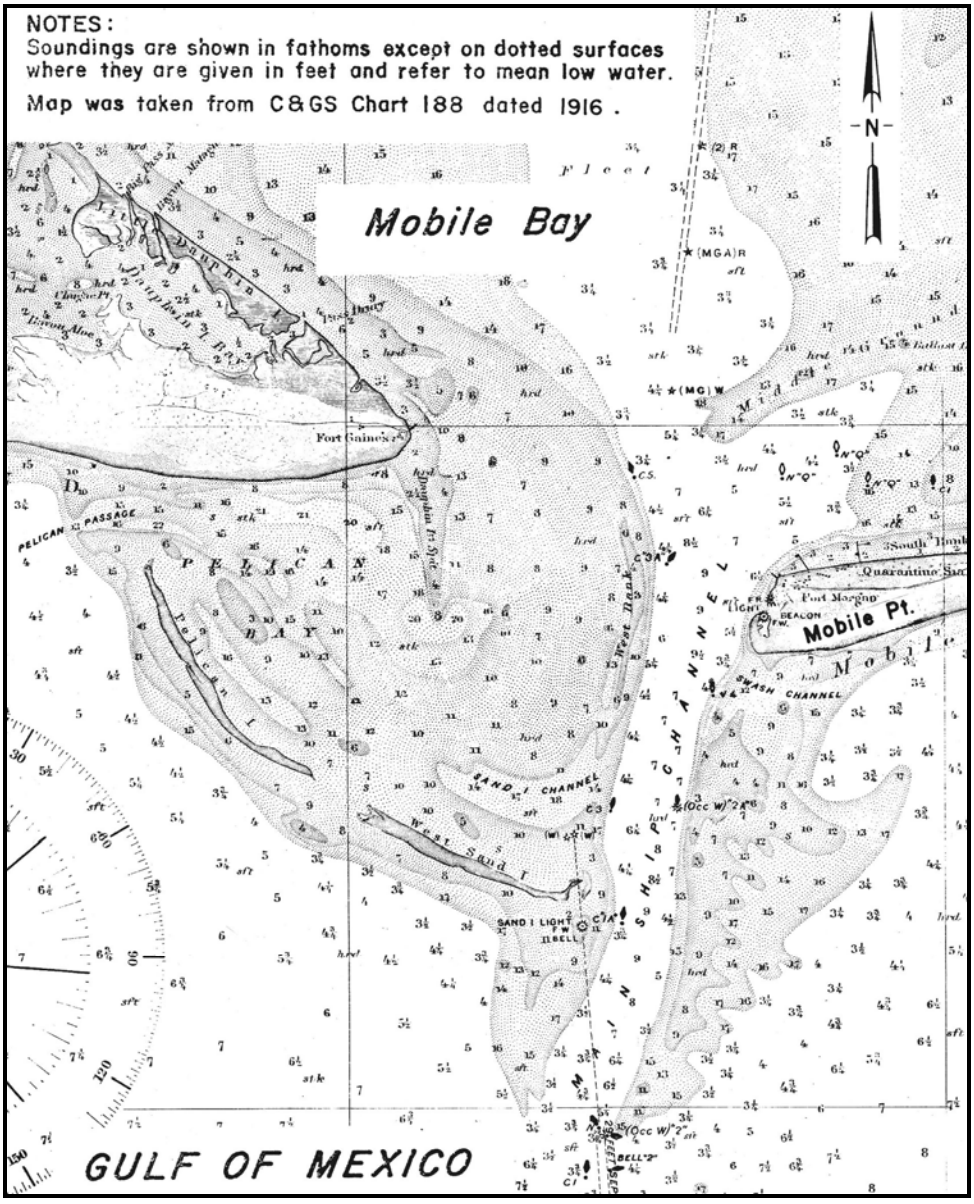

Figure 1-16. 1916 nautical chart # 188 of the entrance to Mobile Bay illustrating 1908 topographic and hydrographic survey data (from USACE, 1978).

Island was no longer present east of the channel, and Sand Island Lighthouse was surrounded by water (Sand Island was gone). West Sand Island remained vigorous, and Pelican Island had reformed northwest of West Sand Island since 1892. The main channel east of West Sand Island developed a slight eastward deflection as channel sections north and south of this point naturally migrated to the west at rates greater than the shoal east of Sand Island Light. Although channel dredging through the outer bar was completed to a depth of 30 ft and a width of 225 ft by June 1908, authorized channel boundaries were not marked on the 1916 chart.

Figure 1-17 documents ebb shoal morphology after the hurricane of 1916, perhaps the most devastating storm to strike this area since the mid-1800s. Although Chart 1266 was dated 1921, shoreline and bathymetry survey data from 1917/18 were used to create the map. As a result of the 1916 hurricane, only a remnant of West Sand Island remained, and Pelican Island was reduced to about 50% of its previous size. Channel depth remained about the same except a marked channel was now present across the outer bar that was maintained to a depth of about 30 ft. Shoals on the east and west lobes of the ebb-tidal delta were generally reduced in size as the brunt of hurricane energy was dissipated along the shoreline and on the ebb-tidal delta.

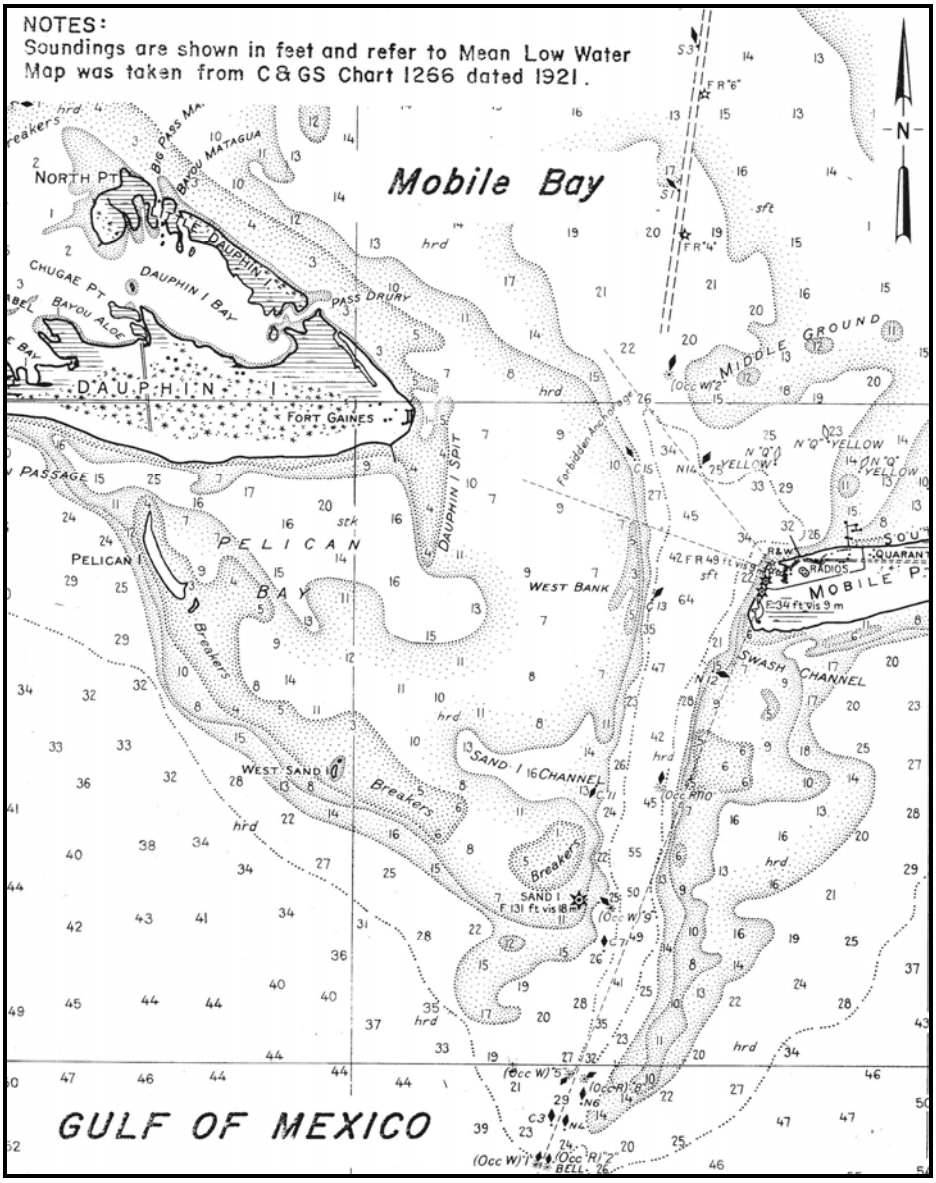

Figure 1-17. 1921 nautical chart # 1266 of the entrance to Mobile Bay illustrating 1917/18 topographic and hydrographic survey data (from USACE, 1978).

By 1933, channel depth over the Mobile Outer Bar was authorized at 33-ft MLW, and channel width was 450 ft at the bottom. This is shown on Chart 1266 (Figure 1-18), but besides the channel boundaries and some updated channel markers, bathymetry and shoreline data reflect conditions recorded in 1917/18 immediately after the 1916 hurricane. As such, ebb shoal morphology as described for the 1921 map has not changed, except the channel is now maintained to a depth of 33 ft MLW.

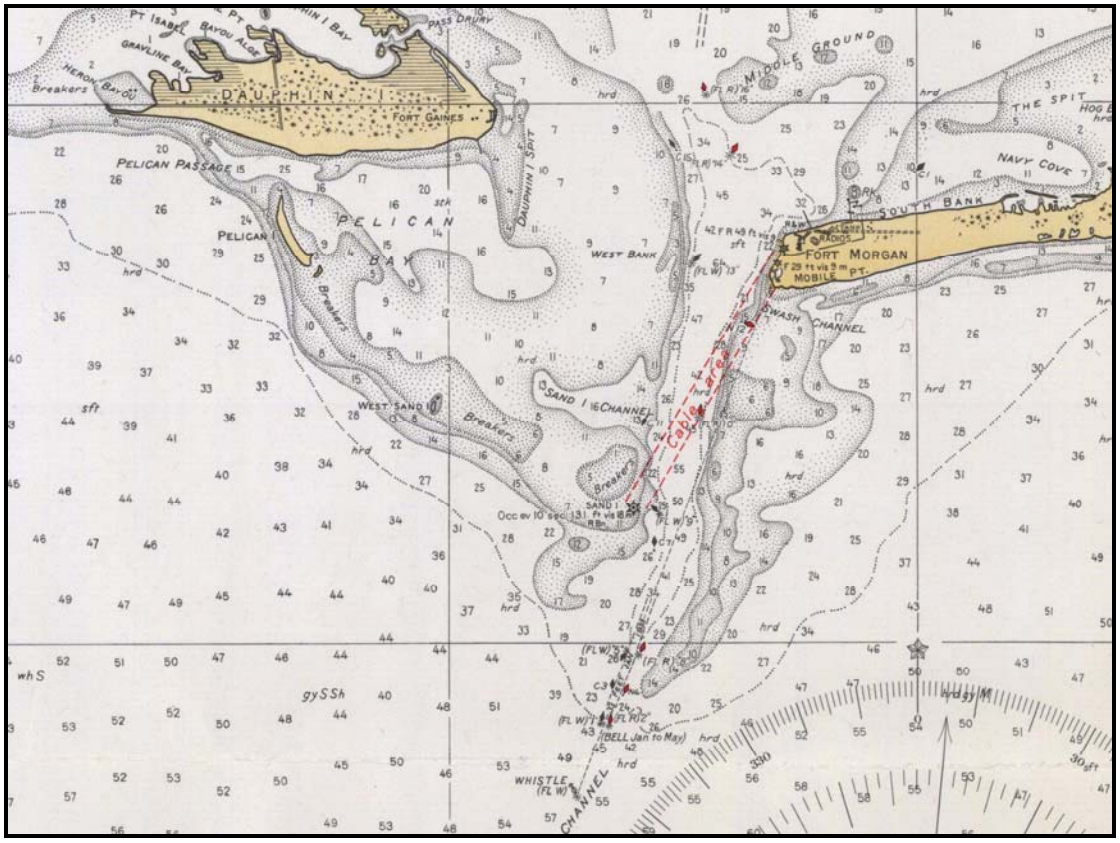

Figure 1-18. 1933 nautical chart # 1266 of the entrance to Mobile Bay illustrating the location of the outer bar channel on the 1917/18 topographic and hydrographic survey data.

Chart 1266 printed in 1958 combines shoreline data from 1934 with bathymetry data from 1941, and channel dimensions in 1956 (36-ft MLW and 400-ft wide; Figure 1-19). Maximum water depth in the natural channel throat is 60 ft, shoaling to about 40 ft just north of where it meets the dredged channel through the outer bar. Relatively low storm activity between 1916 and 1941 (with the exception of the 1926 hurricane) allowed Sand Island to reform just south of Sand Island Channel. Shallow shoals continue to develop between Sand Island and Pelican Island, and the channel between Pelican Island and Dauphin Island continues to persist. Shoals on the eastern side of the channel continued to erode as sand from these features migrated west to fill the relict channel as the entire system migrated to the west.

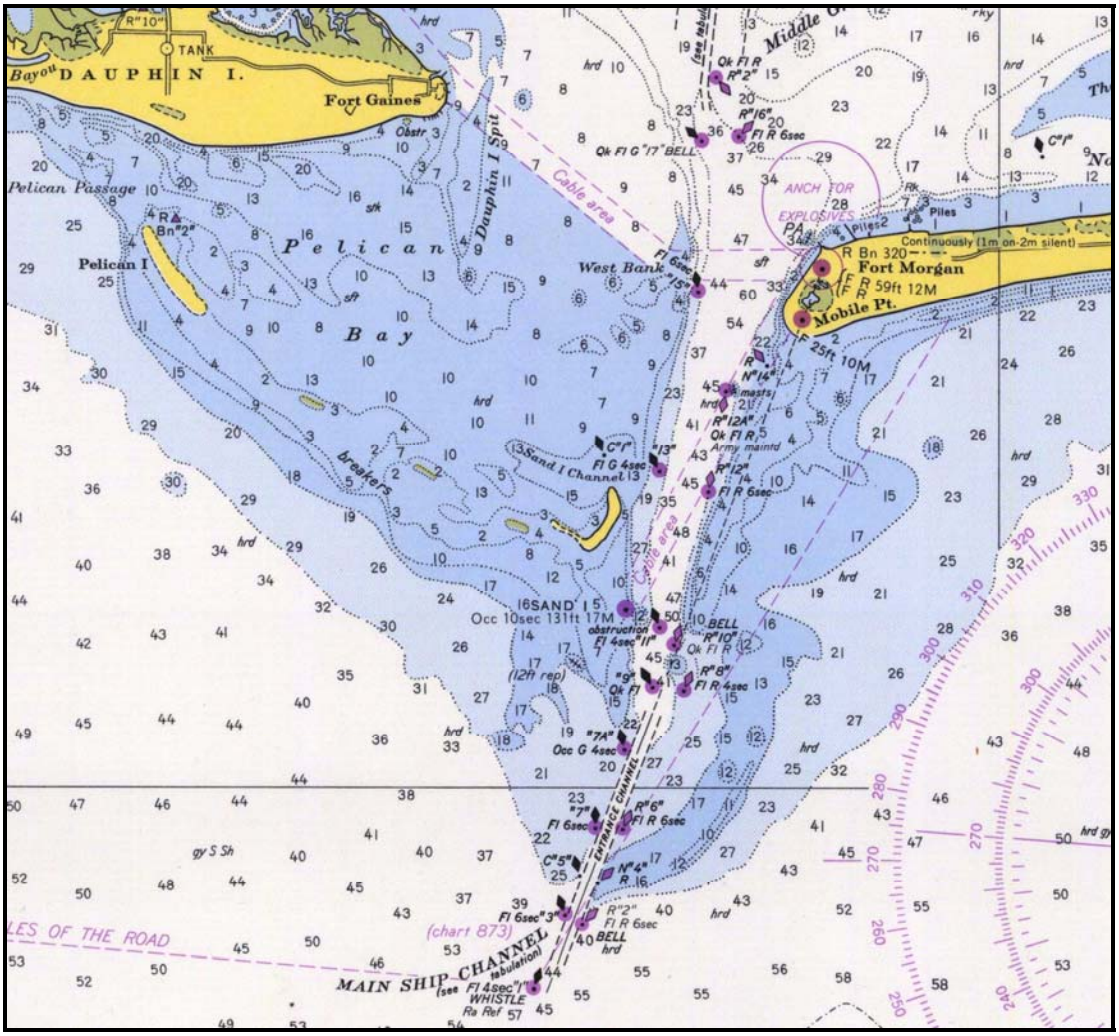

Figure 1-19. 1958 nautical chart # 1266 of the entrance to Mobile Bay illustrating the location of the outer bar channel relative to 1934 shoreline data and 1941 hydrographic survey data.

By 1966, the ebb shoal on Chart 1266 was represented by 1960 survey data and the 1957 shoreline. Sand Island had grown substantially since 1941, but Pelican Island was reduced. Natural channel dimensions remained relatively unchanged; bar channel authorized dimensions of 42 ft MLW and 600-ft wide were maintained by dredging (Figure 1-20).

Between 1966 and 1985, authorized channel dimensions through the outer bar channel were unchanged; however, shoals and islands west of the channel on the ebb shoal continued to form, disburse, and reform in response to tropical cyclones and winter cold fronts (Stone and Wang, 1999). Whereas Sand Island was the dominant island on the ebb shoal in 1966, as sand continued to move from southeast to northwest on the west lobe of the ebb-tidal delta, the primary depocenter shifted

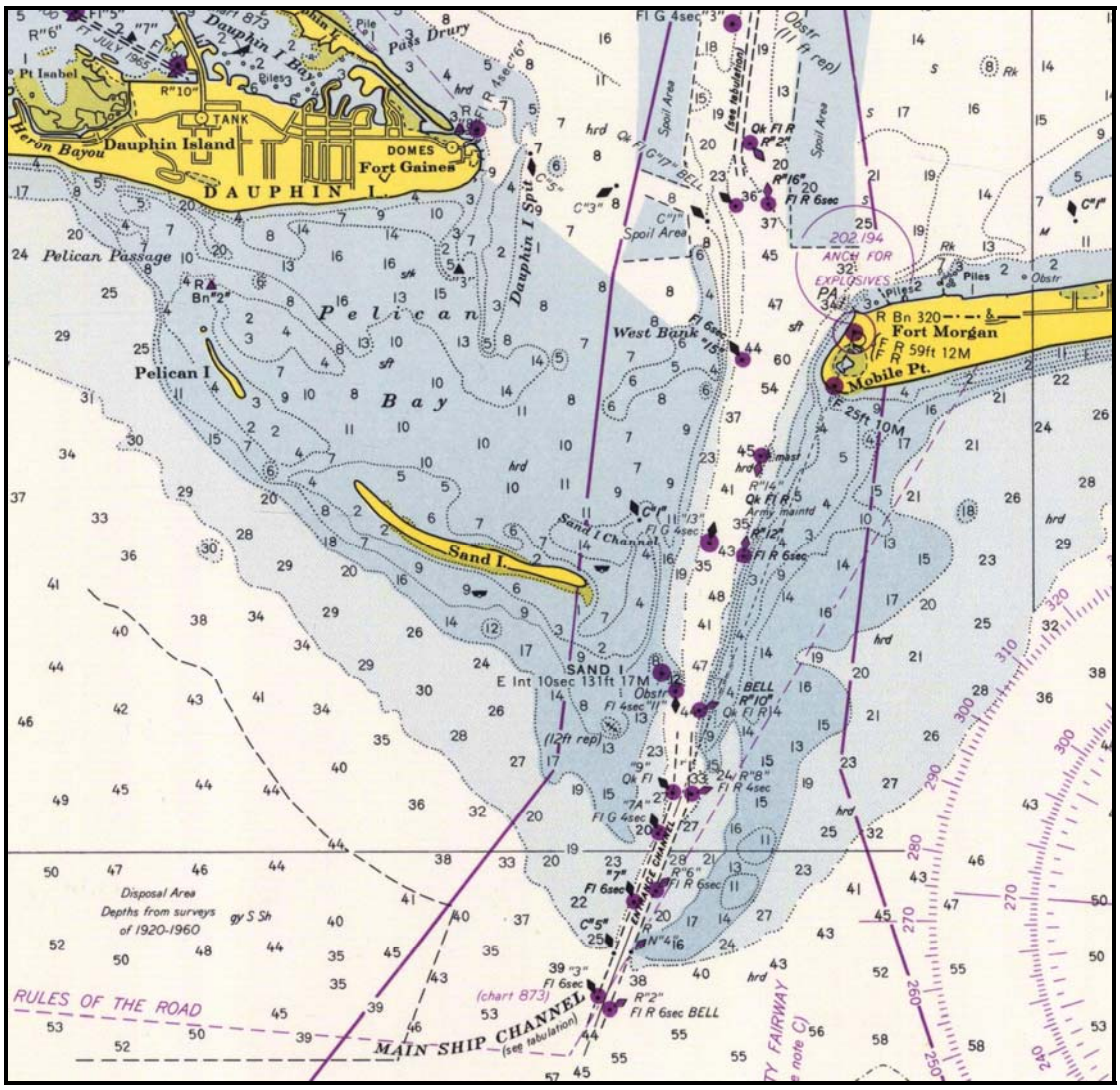

Figure 1-20. 1966 nautical chart # 1266 of the entrance to Mobile Bay illustrating the location of the outer bar channel relative to 1957 shoreline data and 1960 hydrographic survey data.

from Sand Island in 1966 to Pelican Island in 1985 (mislabeled as Sand Island on the 1985 chart; Figure 1-21). This trend of northwest-directed sand transport by littoral processes along the western margin of the ebb shoal documents the dominant mechanism by which sand is transferred from the ebb shoal to Dauphin Island and downdrift beaches.

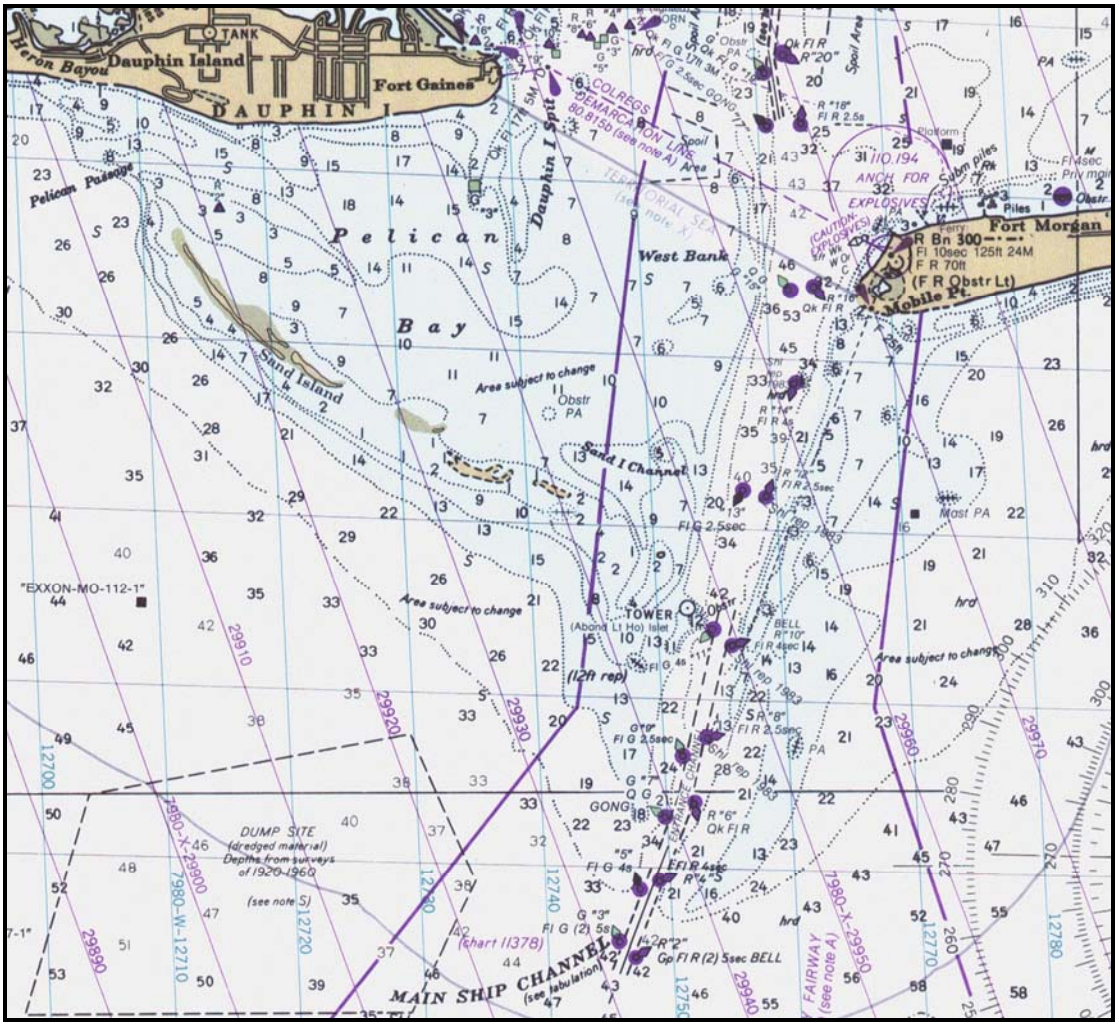

Figure 1-21. 1985 nautical chart # 11376 of the entrance to Mobile Bay illustrating the location of the outer bar channel relative to 1981 shoreline data and 1981/82 hydrographic survey data.

On the 1997 chart, Pelican Island had become a much more extensive subaerial feature as sand continues to be supplied from the shelf and shoreline east of Main Pass channel (Figure 1-22). According to information from the chart, bathymetry describing morphology on the ebb shoal is from surveys compiled from 1983 to 1986. Shoreline data were compiled from photography in the 1990s. Channel dimensions were similar to those depicted on the 1985 chart. In fact, the general shape of the shoal is relatively unchanged compared with the 1985 chart except for the growth and migration of Pelican Island to the northwest. The result of island growth and migration has been to constrict Pelican Channel between Dauphin Island and Pelican Island, potentially creating localized beach erosion where flows have accelerated due to a narrower channel (Figure 1-22; Hardin et al., 1976; Douglass, 1994).

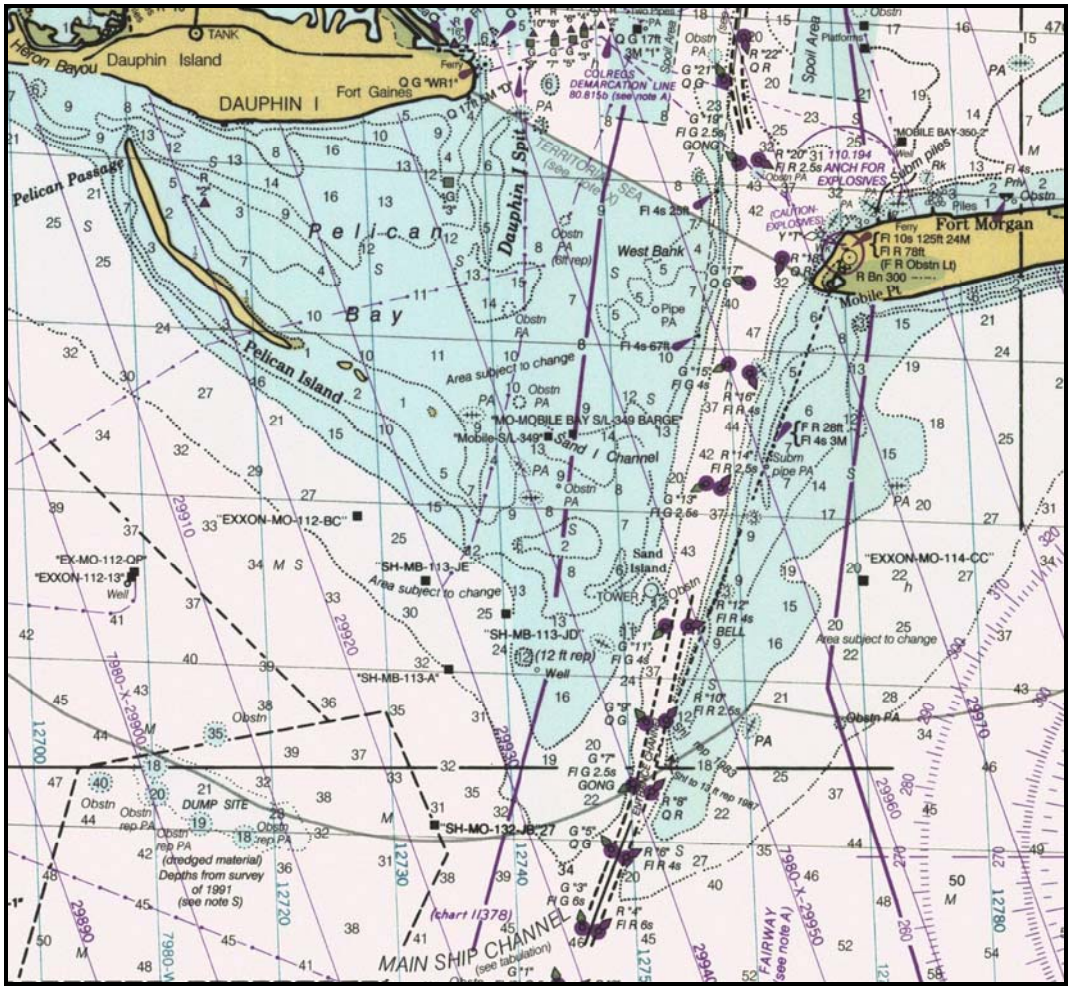

Figure 1-22. 1997 nautical chart # 11376 of the entrance to Mobile Bay illustrating the location of the outer bar channel relative to 1981 shoreline data and 1981/82 hydrographic survey data.

To summarize, the ebb-tidal delta at Main Pass has always been a very dynamic feature since the first shoreline and hydrographic surveys were collected. Islands and shoals on both sides of the channel have developed, eroded, and migrated based on supply of sand to the shoals and the frequency and magnitude of storm events. Although tropical cyclones are destructive events that generally produce erosion and breaching on ebb shoal islands and along Dauphin Island, the morphologic record suggests that the quantity of sand supplied from the east to ebb-tidal shoals and beaches west of the channel is sufficient to grow ebb-shoal islands and fill breaches over a period of years to decades.

Dredging and Placement History

Although Mobile Bay was first visited by Europeans in 1500, and the first settlement in the area by Mexico dates to 1559, it was not until Pierre Le Moyne d'Iberville and his brother Jean Baptiste Le Moyne de Bienville explored Mobile Point and Dauphin Island in 1696 and developed strong alliances with the Choctaw Tribe that permanent development of the area began. Mobile was formally incorporated as part of the United States in 1813 when General Wilkinson captured the area from the British (Sherrill, 1913). In the early 1800s, Mobile grew rapidly as a cotton port, and by May 1826, the first appropriation by Congress was made to dredge a channel from Mobile to the Gulf of Mexico. By 1857, a channel 10 ft deep was dredged from Mobile through Mobile Bay to the entrance at the Gulf. In June 1902, the River and Harbor Act was amended to include a channel through the outer bar as part of the original Mobile Harbor project (ARCE, 1902).

As early as 1702, d'Iberville found a controlling depth of 20 ft over the outer bar (ARCE, 1896). As tonnage and vessel size increased in relation to product demand, the need for a consistent controlling depth greater than 20 ft was required. Dredging commenced on May 16, 1904 to create a channel 25-ft deep through the outer bar, and dredged material was to be placed in "deep water". All indications are that "deep water" meant any location seaward and west of the channel. By March 1905, Congress made a separate project of the Mobile Bar dredging project, and by 1908, most of the outer bar channel was deepened to 30 ft with a width of 250 to 275 ft (ARCE, 1908). The total amount of sand dredged from the channel between 1904 and 1908 to create a 30-ft deep by 250-ft wide channel was 474,225 cy (see Appendix B for a detailed listing of dredging activities and quantities from the Mobile Outer Bar Channel).

New work in the outer bar channel was completed in 1913 to relocate the channel 700 ft west of its existing location because "the channel was naturally shifting in this direction and shoals were forming from the east more rapidly than the dredge could remove them". After completing the work on October 13, 1913, the channel was 30 ft deep and 300 ft wide between the 30-ft depth contours in the channel and offshore the outer bar. Maintenance dredging accounted for 529,727 cy of sand, and new work required removal of 787,304 cy of sand (Table 1-2).

Project dimensions were authorized to 33 ft deep and 450 ft wide in 1917, but construction was not completed until 1924. At that time, new work accounted for 1,865,730 cy of the 3,046,693 cy of sand dredged from the channel. In July 1930, the Rivers and Harbors Act provided for a channel 36 ft deep, 450 ft wide, and about

Table 1-2. Summary of dredging history for Mobile Outer Bar Channel.

Date (Authorized Dimensions)	New Work (cy)	Maintenance Dredging (cy)
May 1904 to October 1913 (30 ft deep, 300 ft wide)	787,304	529,727 (58,900 cy/yr)
October 1913 to June 1924 (33 ft deep, 450 ft wide)	1,078,426	651,236 (59,200 cy/yr)
June 1924 to August 1934 (36 ft deep, 450 ft wide)	685,171	2,012,611 (201,300 cy/yr)
August 1934 to July 1965 (42 ft deep, 600 ft wide)	3,510,878	5,944,787 (191,800 cy/yr)
July 1965 to April 1990 (47 ft deep, 600 ft wide)	6,755,352	11,422,278 (456,900 cy/yr)
April 1990 to September 1999 (49 ft deep, 600 ft wide)	3,061,598	3,204,170 (356,000 cy/yr)
September 1999 to June 2006	None	4,562,767 (651,800 cy/yr)
Total (SIBUA)	15,878,729 (3,061,598)	28,327,576 (4,515,176)

1 mile long connecting the 36-ft depth contours north and south of the outer bar. Although new work was started in 1931, the project was not completed until August 3, 1934. As such, depth values for the channel on the 1933 chart (see Figure 1-18) indicate a controlling depth of 33 ft.

In July 1952, the Chief of Engineers recommended modification of the existing project to enlarge the Mobile Outer Bar Channel to -42 ft MLW and 600 ft wide (ARCE, 1953). In June 1953, a survey of the outer bar channel indicated that controlling depths were between 35 and 36 ft, except the eastern section of the outer channel, which had a controlling depth of 29 ft MLW. This sedimentation trend is consistent with shoaling patterns recorded in 1913. That is, transport of littoral sand from the east and into the channel often overwhelms maintenance dredging activities in the outer bar channel. This pattern persists with the modern channel as well. By July 1965, channel dimensions authorized in 1954 were completed. Of the 15,200,140 cy of sand extracted from the channel since dredging commenced in 1904, 6,061,779 cy was new work and 9,138,361 cy was maintenance work. As such, annualized sand dredging rates from the channel averaged about 171,000 cy/year.

No new work was conducted in the outer bar channel between 1965 and 1988, but in 1989, the controlling channel depth was increased to 47 ft MLW and the bottom width was maintained at 600 ft. Between February 1989 and April 1990,

6,755,352 cy of sand was extracted from 1.5 miles of channel across the Mobile Outer Bar to attain a 47-ft deep channel that was 600 ft wide. In 1999, the channel was again deepened to 49 ft MLW, the channel depth maintained in 2006.

Figure 1-23 illustrates maintenance dredging volumes from the outer bar channel between 1909 and 2006. Changes in average maintenance dredging rates were evaluated for time periods when primary changes in channel dimensions occurred. Linear regression analysis was used to determine average maintenance dredging rates for each of these periods. Between 1956 and 1965, major changes were made to channel width and depth (36 ft deep by 450 ft wide prior to 1956 and 42 ft deep by 600 ft wide after 1965), resulting in a 2.5 to 3 fold increase in maintenance dredging quantities. During this same period, deposition on the west lobe of the ebb-tidal delta and growth of Pelican Island was unprecedented, suggesting that greater volumes of sand were being transported to the ebb shoals, possibly the result of increased frequency and magnitude of storms.

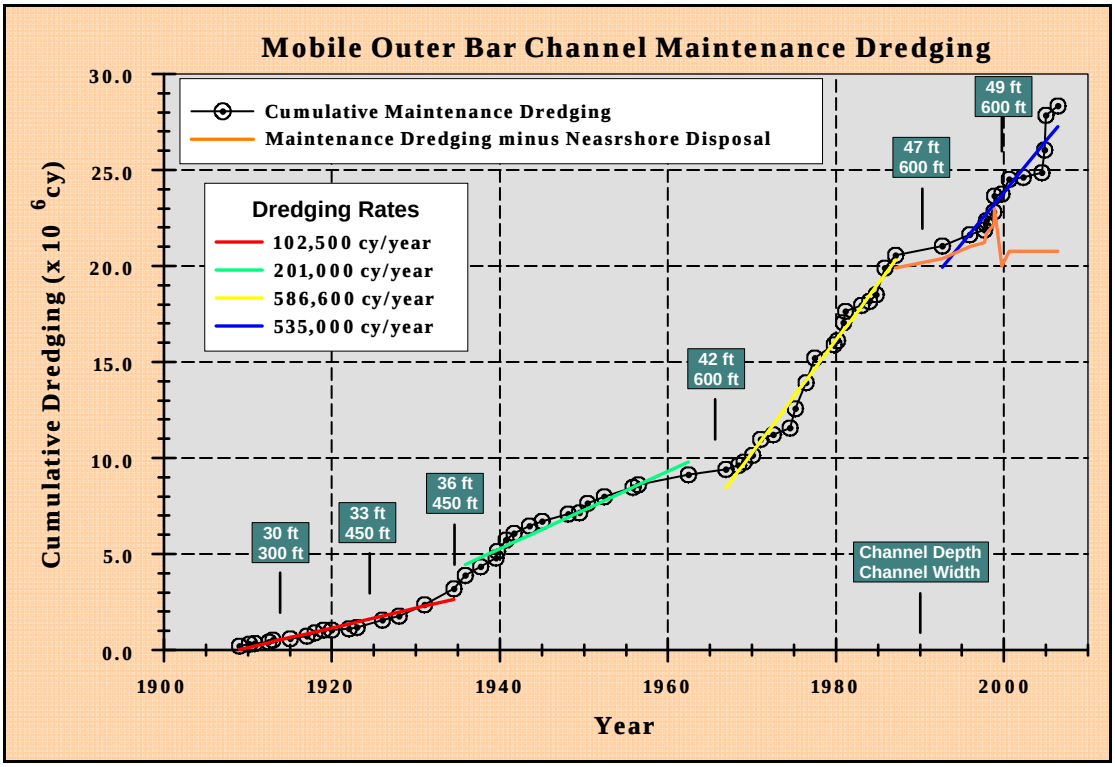

Figure 1-23. Maintenance dredging volumes extracted from the Mobile Outer Bar Channel between 1909 and 2006. Sand extraction rates were determined using linear regression analysis on segments of the curve reflecting changes in channel dimensions with time (data available in Appendix B).

In addition, starting in 1987, 54% of all maintenance dredging and 31% of new work dredging had been placed in beneficial use sites west of the channel in about 20-ft water depth. Since 1999, 82% of maintenance dredging and 100% of new work dredging has been placed at beneficial use sites (Green areas west of the outer bar channel in Figure 1-24). As such, net disposal of maintenance material at offshore sites has decreased to less than 1 million cubic yards since 1986. This practice of beneficial dredged material disposal has contributed to net increases in sedimentation on the west lobe of the ebb-tidal shoal since the mid-1980s.

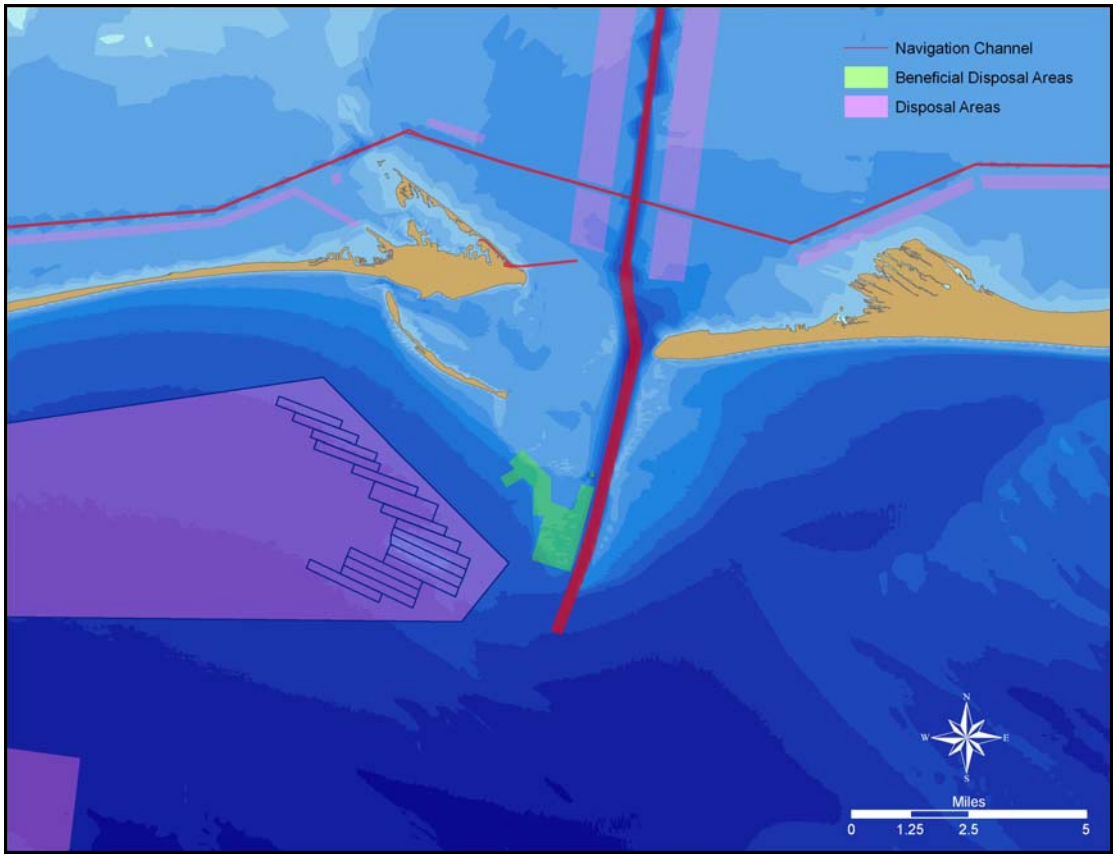

Figure 1-24. Location of dredged material disposal areas relative to channels near Mobile Bay Entrance. Green sites west of the channel are designated for beneficial disposal of sand from the Mobile Outer Bar Channel.

2 Shoreline Dynamics

Shoreline migration along the Alabama outer coastline reflects the imbalance between sand supply and energy (waves, currents, and wind) required to move sand throughout the system. Natural perturbations to sand transport throughout the study area result from variations in high energy storms and normal transport processes relative to the sand availability. Human-induced perturbations in shoreline change may be direct (e.g., erosion directly downdrift of a structure) or indirect (e.g., increased beach erosion due to altered wave propagation resulting from offshore sand extraction). Either way, historical shorelines document natural and human-induced changes depending on the frequency of data collection relative to the frequency of events resulting in change.

Although metric-quality maps of shoreline position were not available prior to 1847, historical depictions of shoreline shape in the study area suggest that the Main Pass ebb-tidal delta and eastern Dauphin Island were the primary sources of sand to downdrift barrier islands fronting Mississippi Sound. Prior to becoming part of the United States, a map of coastal Alabama, created by D'Anville in 1732, indicated that Dauphin Island and Petit Bois Island may have been one continuous feature. Figure 2-1 indicates that Dauphin Island was an extremely long, continuous feature in 1732, with an inlet at its western end, adjacent to Isle aux Corne (Horn Island). Based on this map, Otvos (1979) and Otvos and Giardino (2004) stated that Dauphin and Petit Bois Islands formed a single unit in the early 18th century.

However, in 1814, Mathew Carey published a map of the Alabama coast indicating that Dauphin and Petit Bois Islands were separated by a pass, although Ship Island was named Wood Island at that time (Figure 2-2). In 1837, John LaTourrette produced a map entitled "An Accurate Map of the State of Alabama and West Florida" that captured the position of Petit Bois Pass separating Dauphin and Petit Bois Islands (Figure 2-3). The map also marked the general position of the ebb-tidal delta and the location of Pelican Island on the northwestern side of the ebb shoal. Although this map was published two years prior to constructing the first Sand Island Lighthouse (Lee, 1998), an unlighted iron spindle was placed on the outer bar in 1830 that can be recognized as the small dot on "Little Pelican Island". LaTourrette's map is consistent with original metric maps published by the U.S. Coast Survey between 1847 and 1852, the starting point for which quantitative analysis of shoreline and bathymetric change throughout the study area is based.

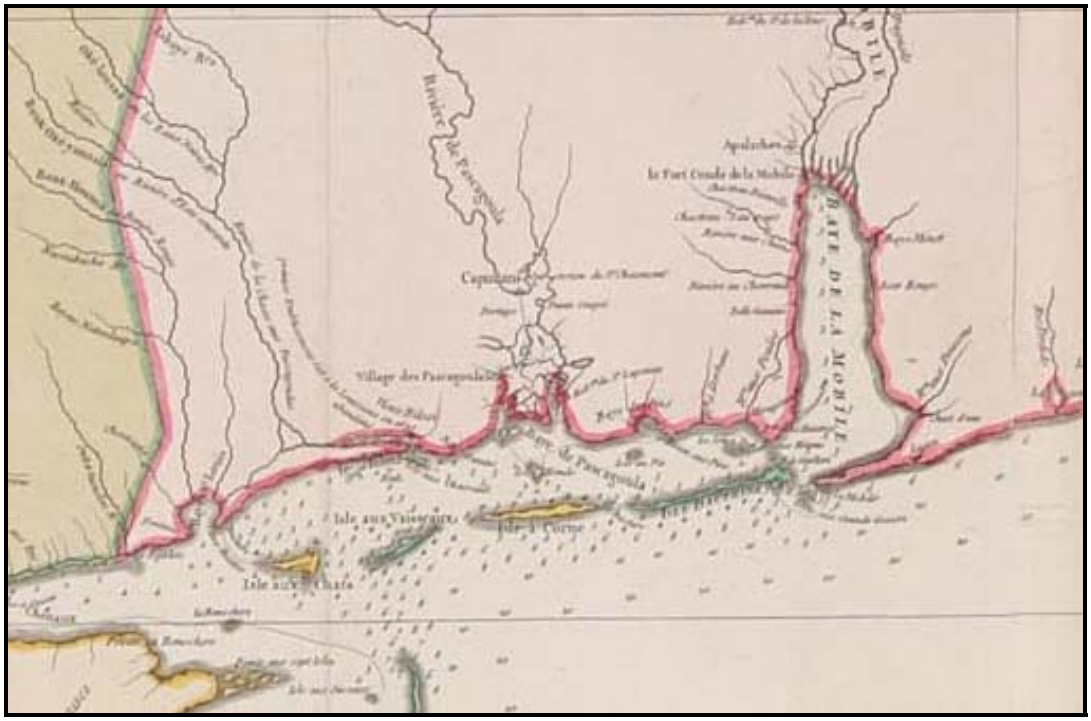

Figure 2-1. 1732 map of coastal Alabama and Mississippi (D'Anville "Carte de la Louisiane") illustrating an elongated Dauphin Island that may have encompassed Petit Bois Island at the time (from David Rumsey Map Collection).

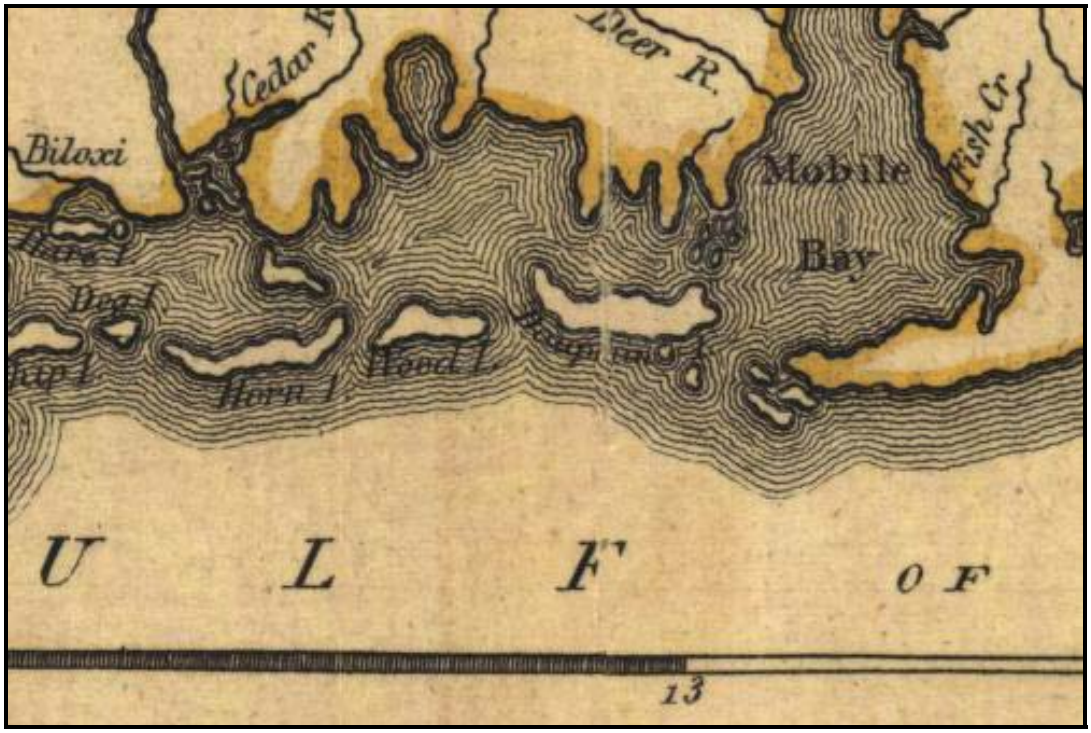

Figure 2-2. 1814 map of coastal Alabama illustrating the presence of a pass between Dauphin and Wood (Petit Bois) Islands (from W.S. Poole Special Collection Library).

Figure 2-3. 1837 map by John LaTourrette illustrating separate Dauphin and Petit Bois Islands, the general shape of the ebb-tidal delta, and the presence of Pelican Island along the northwest margin of the shoal (from the Alabama Department of Archives and History).

Data Sources

Seven regional outer coast shoreline surveys were used to quantify historical shoreline change between Petit Bois Pass, MS (west) and Perdido Pass, AL (east) during the time interval 1847/67 to 2006. The first five surveys were conducted by the USC&GS in 1847/67, 1917/18, 1934, 1957, and 1978/82, the sixth survey was conducted by Applied Coastal in June 2001, and the seventh survey was acquired by the USACE, Mobile District, in May 2006 (Table 2-1). The 1847/67 and 1917/18 surveys were completed as field surveys using standard planetable techniques; the 1934, 1957, and 1978/81 shoreline surveys were interpreted from aerial photography; the 2001 shoreline survey was conducted using a Trimble Pro/XR differential GPS; and the 2006 shoreline was interpreted from orthorectified aerial imagery with a pixel resolution of 1 ft. Furthermore, five additional shorelines were compiled (1853, 1868, 1892, 1908, and 1970) to document changes at the entrance to Mobile Bay where gaps in the regional data exist.

Table 2-1. Shoreline Source Data Characteristics		
Date	**Data Source**	**Comments and Map Numbers**
1847/67	USC&GS Topographic Maps; 1:10,000 (T-1042); 1:20,000 (T-240, T-277)	First regional shoreline survey throughout study area using standard planetable surveying techniques; May and June, **1847** - western end of Dauphin Island to entrance to Mobile Bay (T-240); June and July, **1849** - outer coastline south of Bon Secour Bay (T-277); June and July, **1867** - shoreline south of Shelby Lakes east to Perdido Pass (T-1042).
April 1853	USC&GS Topographic Map; 1:10,000 (T-406)	Shoreline survey of western Dauphin Island illustrating an island breach, likely occurring as a result of the August 1852 hurricane.
1868	USC&GS Topographic Map; 1:20,000 (T-1066)	Shoreline survey of the Entrance to Mobile Bay illustrating the attachment of Pelican Island to eastern Dauphin Island.
Feb-March 1892	USC&GS Topographic Map; 1:10,000 (T-2086)	Shoreline survey of the Entrance to Mobile Bay.
May 12 – June 30, 1908	USC&GS Topographic Map; 1:20,000 (T-2865)	Last shoreline survey of the Entrance to Mobile Bay before maintenance dredging in the Mobile Outer Bar Channel commenced.
1917/18	USC&GS Topographic Maps; 1:40,000 (T-3711, T-3714)	Second regional shoreline survey along the seaward coast of the study area using standard planetable surveying techniques (regional-scale reconnaissance survey); Oct – Dec, **1917** - Dauphin Island (T-3711); **1918** - Mobile Point east to Perdido Pass (T-3714).
June/July 1934	USC&GS Topographic Maps; 1:10,000	First regional shoreline survey completed using aerial photography; central Dauphin Island (T-5537); shoreline adjacent to Mobile Bay Entrance (T-5536); outer shoreline south of Bon Secour Bay (T-5535); shoreline south of Little Lagoon (T-5534); Gulf Shores (T-5497); shoreline south of Shelby Lakes (T-5498); Perdido Pass (T-5495).
November 1957	USC&GS Topographic Maps; 1:10,000	All maps produced from interpreted aerial photography; Dauphin Island (T-Sheets 10761, 10762, 10770, 10771, 10772); Morgan Peninsula east to shoreline south of Shelby Lakes (T-Sheets 10773, 10774, 10775, 10776, 10993, 10994, 10996).
May 1970	USACE Rectified Aerial Photography (1:24,000)	Western end of Morgan Peninsula and all of Dauphin Island.
April 1978, Feb-March 1981/82	USC&GS Topographic Maps 1:20,000	All maps produced from interpreted aerial photography; **1978** - shoreline south of Little Lagoon east to Perdido Pass (TP-sheets 00542, 00543); **1981/82** - Mobile Bay east to shoreline south of Bon Secour Bay (TP-sheets 00931, 00932); Dauphin Island (TP-sheets 00929, 00930).
June 2001	Differential GPS Survey (1:1)	Outer coast of Dauphin Island and western side of Morgan Peninsula from Mobile Bay east to shoreline south of Shelby Lakes.
February 2002	USACE Rectified Aerial Photography (1:12,000)	All of Dauphin Island and the Morgan Peninsula east to Perdido Pass.
May 19, 2006	Orthorectified Digital Imagery (1:3,500)	Outer coast of Mobile and Baldwin Counties; 1-ft pixel resolution.

Digital shoreline data for 1847/67, 1853, 1868, 1892, 1908, 1917/18, 1934, 1957, and 1978/81 were compiled at Applied Coastal from scanned topographic sheets using techniques described in Byrnes and Baker (2003) and Baker and Byrnes (2004).

Digital shoreline data for 2001 were developed from GPS survey points collected at 15-ft intervals along the outer coast of Dauphin Island and the beaches east of Fort Morgan to Gulf Shores. The 1970 and 2002 shorelines for Dauphin Island were interpreted by Applied Coastal personnel from rectified aerial photography supplied by the USACE Mobile District. Using May 2006 digital orthophotography, high-water shoreline position was interpreted via on-screen digitizing using GIS.

The horizontal position of the GPS high-water shoreline was determined visually using a hierarchy of criteria dependent on morphologic features present on the subaerial beach. The primary criterion was a well-marked limit of uprush by waves associated with high tide. This generally was recognized on the beach as the berm crest (Figure 2-4). If the berm crest did not exist, a debris line could usually be identified, above which aeolian processes dominated sediment transport and below which wave and current processes created a relatively smooth foreshore. The criteria adopted are consistent with those used by field topographers and photo interpreters in developing NOS T-sheet shorelines (Shalowitz, 1964). All high-water shoreline data were converted to shapefile format and projected into a common horizontal coordinate system and datum, in this case Universal Transverse Mercator (UTM) Zone 16 (meters), North American Datum of 1983 (NAD83).

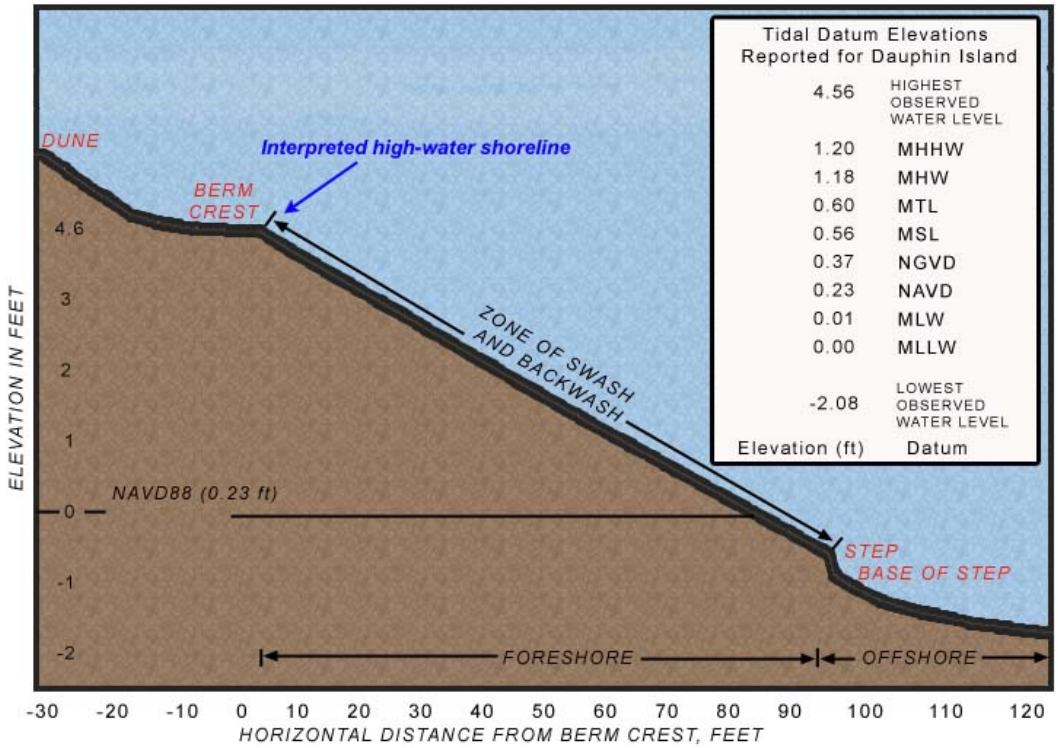

Figure 2-4. High-water shoreline position classification referenced to the beach berm crest.

Measurement Uncertainty

In determining shoreline position change, all data contain inherent uncertainties associated with data acquisition and compilation procedures. It is important to quantify limitations in survey measurements and document potential systematic errors that can be eliminated during quality control procedures (Anders and Byrnes, 1991; Crowell et al., 1991; Byrnes and Hiland, 1995; Baker and Byrnes, 2004). Substantial effort was spent ensuring that any systematic errors were eliminated prior to change analysis. Therefore, measurement errors associated with present and past shoreline surveys are considered random. However, data compilation uncertainties should be quantified to gauge the significance of measurements used for research/engineering applications and management decisions. Table 2-2 summarizes estimates of potential uncertainties at any given point along the outer coast of Alabama for shoreline data sets illustrating temporal and spatial changes. Because individual uncertainties are considered to represent standard deviations, root-mean square estimates are calculated as a realistic assessment of combined

Table 2-2. Estimates of potential random error associated with shoreline surveys.

Traditional Engineering Field Surveys (1847/67, 1853, 1868, 1908, and 1917/18)			
Location of rodded points	±3 ft		
Location of plane table	±7 to 10 ft		
Interpretation of high-water shoreline position at rodded points	±10 to 13 ft		
Error due to sketching between rodded points	up to ±16 ft		
Cartographic Uncertainties (1847/67, 1853, 1868, 1908, 1917/18, 1934, 1957, and 1978/82)	**Map Scale**		
	1:10,000	**1:20,000**	**1:40,000**
Inaccurate location of control points on map relative to true field location	up to ±10 ft	up to ±20 ft	up to ±40 ft
Placement of shoreline on map	±16 ft	±33ft	±66 ft
Line width for representing shoreline	±10 ft	±20ft	±40 ft
Digitizer error	±3 ft	±6ft	±12 ft
Operator error	±3 ft	±6ft	±12 ft
Historical Aerial Surveys (1934, 1957, 1970,1978/82, and 2002)	**Map Scale**		
	1:10,000	**1:20,000**	**1:40,000**
Delineating high-water shoreline position	±16 ft	±33 ft	±66 ft
2006 Orthophotography (delineating shoreline position)	±6 ft		
GPS Surveys (2001 shoreline)			
Delineating high-water shoreline	±3 to 10 ft		
Position of measured points	±6 to 16 ft (specified) ±3 to 10 ft (field tests)		

Sources: Shalowitz, 1964; Ellis 1978; Anders and Byrnes, 1991; Crowell et al., 1991.

potential uncertainty. Positional random errors for each shoreline can be calculated using the information in Table 2-2; however, change analysis requires comparing two shorelines from the same geographic area, but different time periods. Table 2-3 presents a summary of potential random errors associated with change analyses computed for specific time periods. As expected, maximum positional uncertainties are associated with the oldest shorelines (1847/67 and 1917/18) at smallest scale (1:40,000). However, most change estimates for the study area document shoreline advance or recession greater than these values. Overall, because random errors are considered equally distributed, they can be neglected relative to change calculations.

Table 2-3. Maximum root-mean-square potential uncertainty for shoreline change data from western Dauphin Island to Perdido Pass, Alabama.

	1917/18	1934	1957	1978/82	2001	2006
1847/67	±104[1]	±56.8	±56.8	±74.5	±53.4	±50.3
	(±1.7)[2]	(±0.7)	(±0.6)	(±0.6)	(±0.4)	(±0.3)
1917/18		±95.4	±95.4	±106.9	±93.5	±91.7
		(±5.6)	(±2.4)	(±1.7)	(±1.1)	(±1.0)
1934			±38.2	±61.5	±28.8	±25.8
			(±1.7)	(±1.3)	(±0.4)	(±0.3)
1957				±61.5	±28.8	±25.8
				(±2.7)	(±0.7)	(±0.5)
1978/81					±57.0	±55.5
					(±2.7)	(±2.1)
2001						±15.4
						(±3.1)

[1] Magnitude of potential uncertainty associated with high-water shoreline position change (ft); [2] Rate of potential uncertainty associated with high-water shoreline position change (ft/yr).

Lateral Island Growth

Waves and wave-generated currents are the primary processes causing shore erosion and accretion in the study area. The dominant direction of littoral transport is from east to west, resulting in sand deposition along the eastern margin of Main Pass and Petit Bois Pass. Although Main Pass occupies the location of the ancient Mobile River valley (Mars et al., 1992; Davies and Hummell, 1994) and illustrates relatively minor changes in position during historical times, western Dauphin Island and Petit Bois Pass have migrated at least 5 miles to the west since 1847 (Byrnes et al., 1991). Furthermore, Sand Island and Pelican Island on the west lobe of the ebb-tidal delta have experienced significant changes in location and extent as sand shifts from southeast to northwest along the seaward margin of the ebb-tidal delta in response to wave-induced sand transport under storm and normal conditions. Northwest-

directed sand transport on the shoal eventually makes its way to Dauphin Island, supplying sediment to lengthen the island to the west, fill island breaches that occur during major storm events, and nourish Gulf beaches along Dauphin Island as the western two-thirds of the island migrates landward in response to storm overwash and sea-level rise. The following sequence of changes records the destructive influence of storms on island development and the resilience of beaches and offshore islands sourced by sand from the ebb-tidal delta (see Otvos, 2006).

1847 to 1917. In 1847, more than half of Petit Bois Island was located east of the western Alabama state line (Harden et al., 1976). Seventy years later in 1917, much of the eastern half of Petit Bois Island eroded in response to the 30+ tropical cyclones that traversed the region since 1847 (particularly the 1916 hurricane; see Table 1-1) and the westward migration of Petit Bois Pass as Dauphin Island rapidly expanded to the west. Figure 2-5 illustrates significant geomorphic changes along central Dauphin Island resulting from the July 1916 hurricane. The central 5 miles of the island was breached during the storm, creating a temporary gap between east and west Dauphin Island. Pelican and Sand Islands on the ebb-tidal delta eroded substantially during this period, resulting in an island configuration that was most vulnerable to continued erosion than at any other time during the historical record. Although shoreline position was not mapped for the entire island between 1847 and

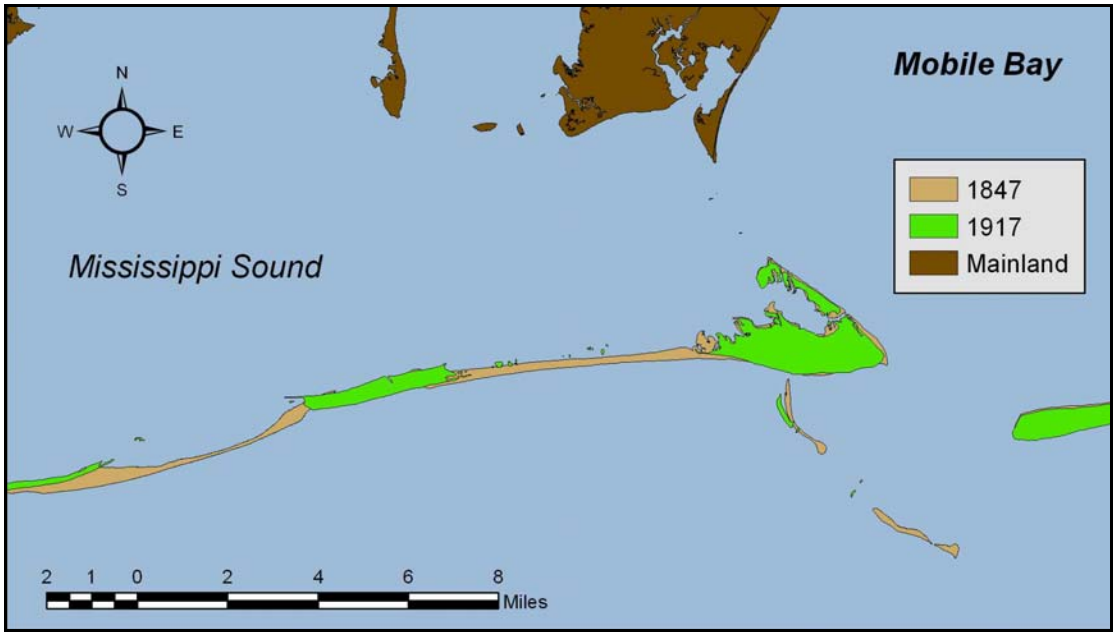

Figure 2-5. 1917 shoreline superimposed on the 1847 shoreline illustrating westward growth of Dauphin Island, forcing Petit Bois Pass and Island to the west. The large breach between east and west Dauphin Island in 1917 is the result of the July 1916 hurricane.

1917, interim surveys were completed along eastern Dauphin Island that document changes on Sand and Pelican Islands influencing the development of Dauphin Island.

Between 1847 and 1868, at least five tropical cyclones controlled erosion and accretion processes in the area. Sand and Pelican Islands on the western lobe of the ebb shoal were extensive features in 1847, but by 1868, both islands experienced erosion, and Pelican Island attached to the shoreline along eastern Dauphin Island, creating an extensive shoreline protuberance (Figure 2-6). Over the following 50 years, the large volume of sand that migrated onshore as Pelican Island steadily dispersed to the west provided for westward island growth. This is the only occurrence of mass sand migration from the subaerial portion of the ebb shoal to the beaches of Dauphin Island in the historical shoreline survey record.

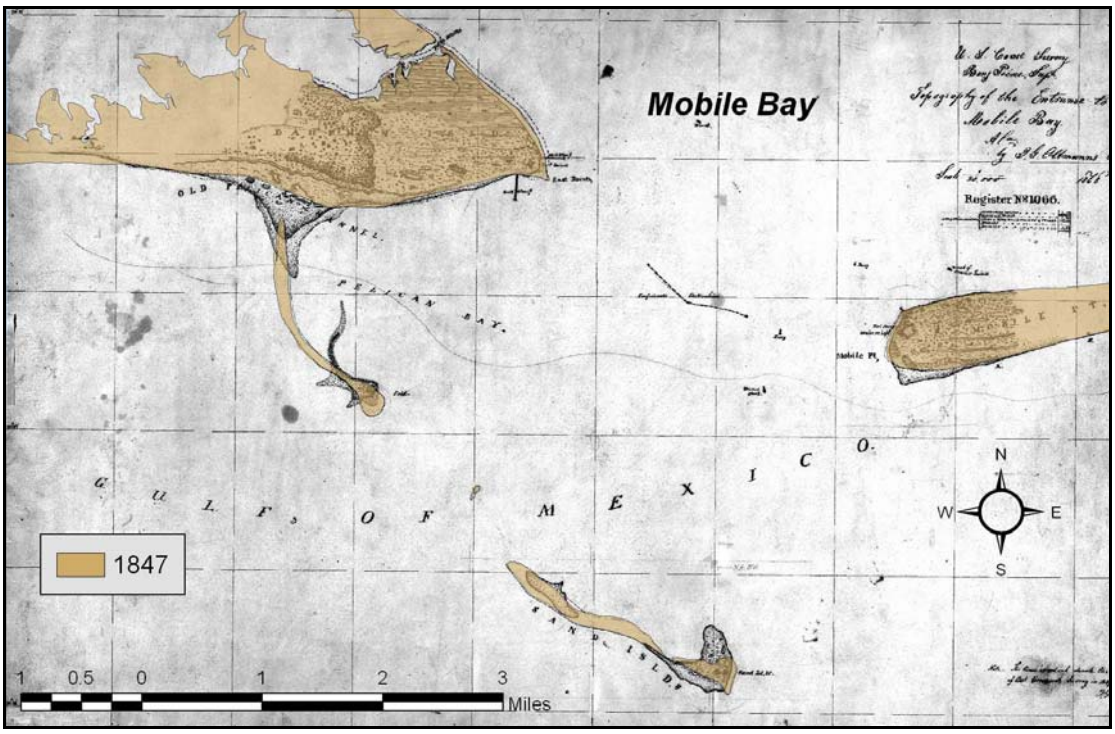

Figure 2-6. 1847 shoreline superimposed on the 1868 registered T-sheet illustrating mass migration of sand from Pelican Island to eastern Dauphin Island.

Between 1868 and 1892, Sand Island began to reform and migrate to the northwest toward the previous location of Pelican Island. Similarly, sand deposited on the shoreline in 1868 from Pelican Island dispersed to the west, and the beach at Mobile Point continued to accrete to the south and west as littoral sediment was supplied from the east (Figure 2-7A). In fact, sand transport from the east was so plentiful at this time that Dixie Island (normally mapped as East Bank shoal) was present on the 1892 map for the first time since accurate surveys were recorded. Natural westward

migration of Mobile Pass after this time trapped substantial littoral sand from the east, limiting the chances of recording this subaerial feature on future surveys.

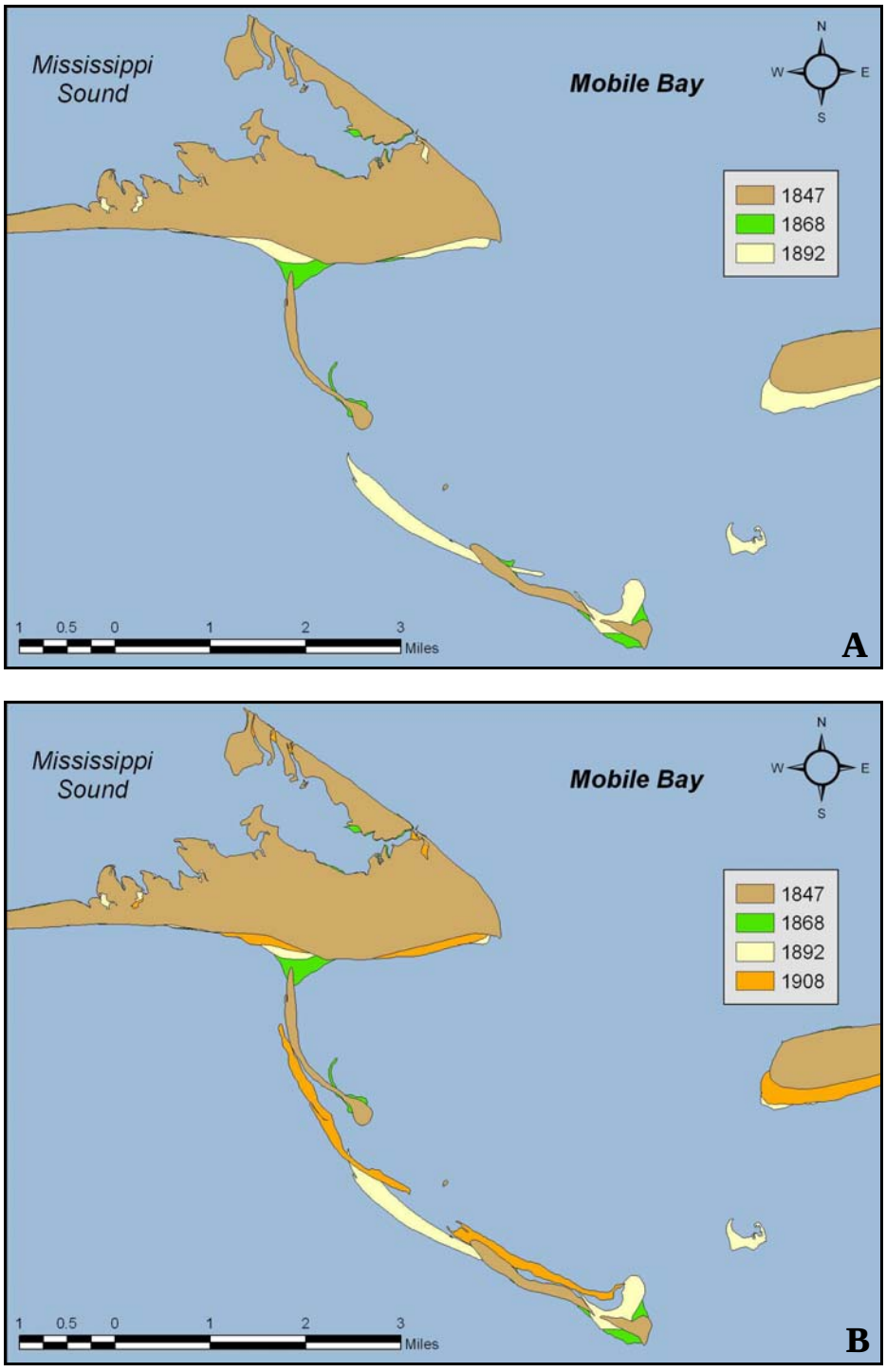

Figure 2-7. Shoreline and shoal evolution at and adjacent to eastern Dauphin Island and the west lobe of the ebb-tidal delta from 1847 to 1908.

By 1908, sand deposited on eastern Dauphin Island 40 years earlier continued to disperse to the west supporting westward growth of the island (Figure 2-7B). Sand was deposited along the eastern end of the island as well, as sand eroded from the northeast-facing bay beaches of Dauphin Island was transported around Pelican Point and to the west (Figure 2-8). After 60 years of island growth and decay on the western lobe of the ebb-tidal delta, Pelican and Sand Islands were again subaerial features similar to those surveyed in 1847.

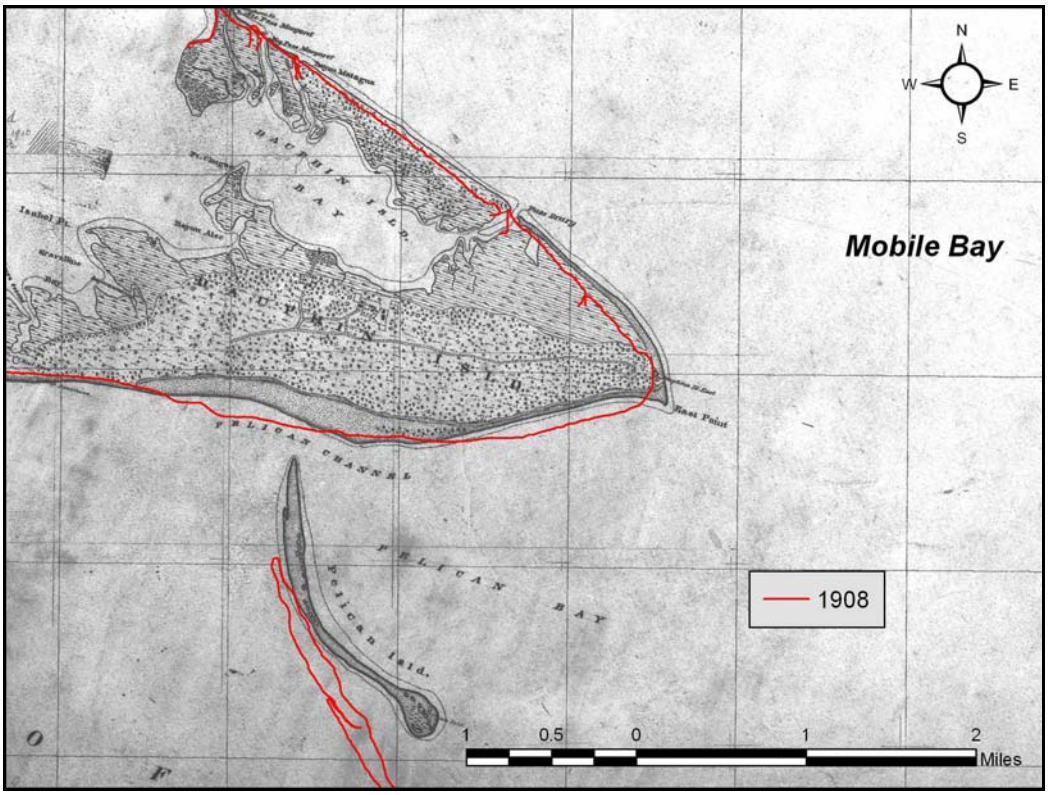

Figure 2-8. 1908 shoreline superimposed on T-sheet 240 (1847) illustrating shoreline erosion on the northeast-facing bay beaches of Dauphin Island and deposition along the south-facing beaches north of Pelican Island.

Although storm activity was not particularly intense between 1908 and 1917, the hurricane of July 5, 1916 produced a surge of 7.7 ft above MSL at Dauphin Island, with a maximum wind speed of 107 miles per hour from the east at Fort Morgan (USACE, 1978). This hurricane made landfall between Ship and Horn Islands as a Category 3 storm with a shelf duration of about 36 hours (Morton, 2007). The geomorphic changes it imposed on Dauphin Island and the islands and shoals of the ebb-tidal delta were larger than any others recorded with historical survey data. Basically, it was the storm of record for Dauphin Island. Figure 2-9 documents minor changes in shoreline position along eastern Dauphin Island and adjacent to

Mobile Point resulting from the hurricane, and major losses that occurred to Pelican and Sand Islands from 1847 to 1908 to 1917. Figure 2-5 illustrates the area of greatest impact; a 5-mile wide island breach separating east and west sections of the barrier. Because the ebb-tidal delta and shoreline/shelf source areas to the east are so sand rich, the island began recovering soon after the storm, and by 1934 (at the latest), the island was again continuous and expanding rapidly to the west.

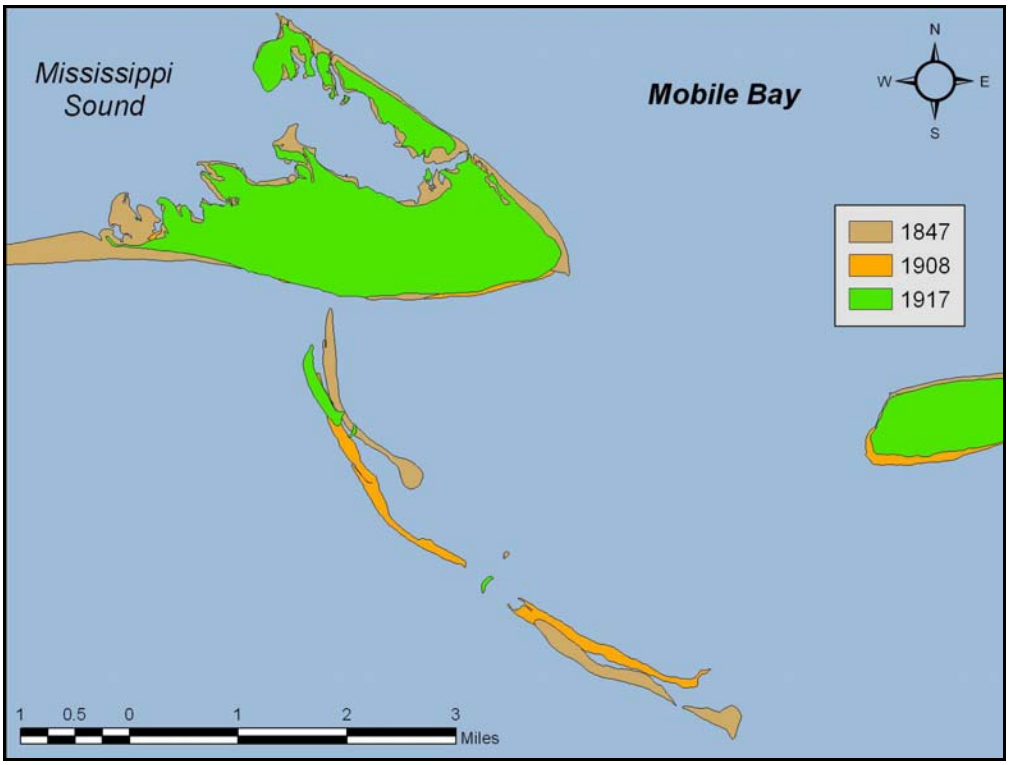

Figure 2-9. 1917 shoreline superimposed on 1847 and 1908 shorelines illustrating impact of the July 1916 hurricane on island evolution. Near-complete removal of subaerial sand from Pelican and Sand Islands and the eastern extent of island breaching are well documented.

1917 to 1957. Although the 1934 shoreline was not mapped west of the western breach boundary in 1917, changes recorded near Mobile Point and to the west demonstrate the resilience of this barrier island system in recovering from major storms. In a relatively short period of time (at most 18 years), the 5-mile breach formed during the 1916 hurricane had filled with sand transported from the ebb-tidal delta (Figure 2-10), even though another major hurricane made landfall at Dauphin Island in September 1926. Apparently, the great abundance of sand available for breach closing and lateral island growth reflects dominant westward sand movement from the western lobe of the ebb-tidal delta (Otvos, 2006). Furthermore, beach accretion south and west of Mobile Point and subaerial growth of Sand Island west of

the ship channel indicates a continuous supply of sand from the east to replenish losses due to storms.

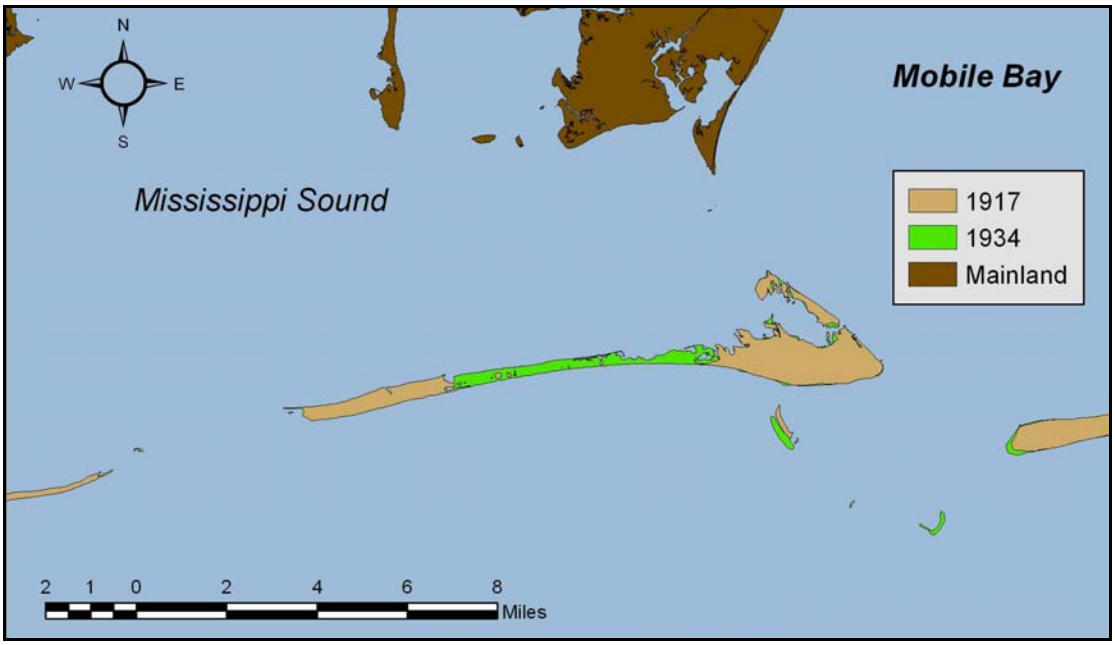

Figure 2-10. 1917 shoreline superimposed on 1934 shoreline illustrating complete infilling of the hurricane breach formed in 1916. Partial recovery of subaerial deposits on the ebb shoal is illustrated by the re-emergence of Sand Island by 1934.

As shown in Appendix B, channel dredging of the Mobile Outer Bar began in May 1904. By August 1934, the channel was maintained to a depth of 36 ft (MLW) and a bottom width of 450 ft. This required 2,551,000 cy of new work and 3,194,000 cy of maintenance dredging, a relatively minor amount of maintenance dredging compared with the estimated minimum volume of sand required to fill the island breach to the average dimensions of the 1934 shoreline (31,000 ft long by 1,200 ft wide by 5 ft thick = 6.9 million cy). Regardless, both dredging and recovery occurred, and Sand Island emerged during the same period. However, most dredging in the channel of the outer bar took place after 1934 (see Figure 1-23).

Between 1934 and 1957, only one significant storm event was energetic enough to cause overtopping of Dauphin Island. The hurricane of September 1947 originated in the Atlantic and reached Category 5 intensity before weakening to a Category 1 storm in the southeastern Gulf of Mexico (Morton, 2007). The storm passed south of the Alabama coast, creating a storm surge of 7.9 ft (MSL) at Gulf Shores (USACE, 1978) on its way to landfall along the northern Chandeleur Islands. Harden et al. (1976) reported that aerial photographs taken on March 23, 1950 documented a breach in Dauphin Island that was about 1,400 ft wide as a result of the September 1947

hurricane (misidentified as the September 1948 hurricane, which was only a tropical storm when it crossed eastern Louisiana in a northeasterly direction). The breach was located about 4,000 ft west of eastern margin of the 1917 breach, the location of narrowest beach width on the 1934 shoreline (Figure 2-10).

A comparison of 1917, 1934, and 1957 island configuration illustrated continuous beach recovery in the area of the hurricane breach and growth of the western end of Dauphin Island by about 1.6 miles relative to 1917 (Figure 2-11). Furthermore, Sand Island had grown to the northwest since 1934, although Pelican Island is no longer present. Growth of Sand Island suggests that the western lobe of the shoal continued to be supplied with sand from the east, regardless of dredging activities in the outer bar channel. By 1957, an additional 1,204,000 cy of new work and 5,411,000 cy of maintenance material had been dredged from the channel, apparently having no discernible impact on island recovery and growth on the western lobe of the ebb-tidal delta, or westward lateral expansion of Dauphin Island. Total dredging quantities as of 1957 were approximately 3,755,000 cy of new work and 8,604,000 cy of maintenance work, or about 29% and 38%, respectively, of total dredged material from the outer bar channel placed in the offshore disposal site.

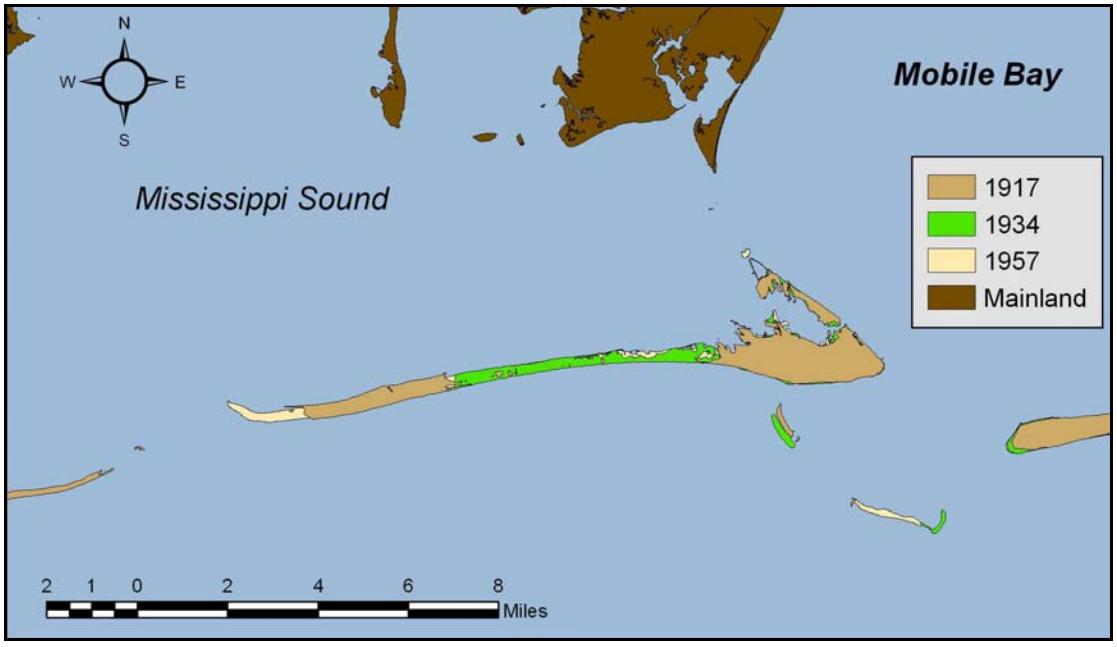

Figure 2-11. 1917 shoreline superimposed on 1934 and 1957 shorelines illustrating island recovery and growth on the ebb-tidal delta and on Dauphin Island after the 1916 hurricane and during the first 50 years of dredging in the outer bar channel.

1957 to 1982. During this 25-year period, the rate of westward island growth slowed, even though the number of tropical cyclones traversing the area was

relatively small. However, two of the three hurricanes causing significant geomorphic change during this period were *Camille* (1969) and *Fredric* (1979). Figure 2-12 provides post-hurricane photographs of a section of Dauphin Island after each of these storms, illustrating island overtopping, numerous surge channels, and washover deposits. Furthermore, islands on the western lobe of the ebb shoal

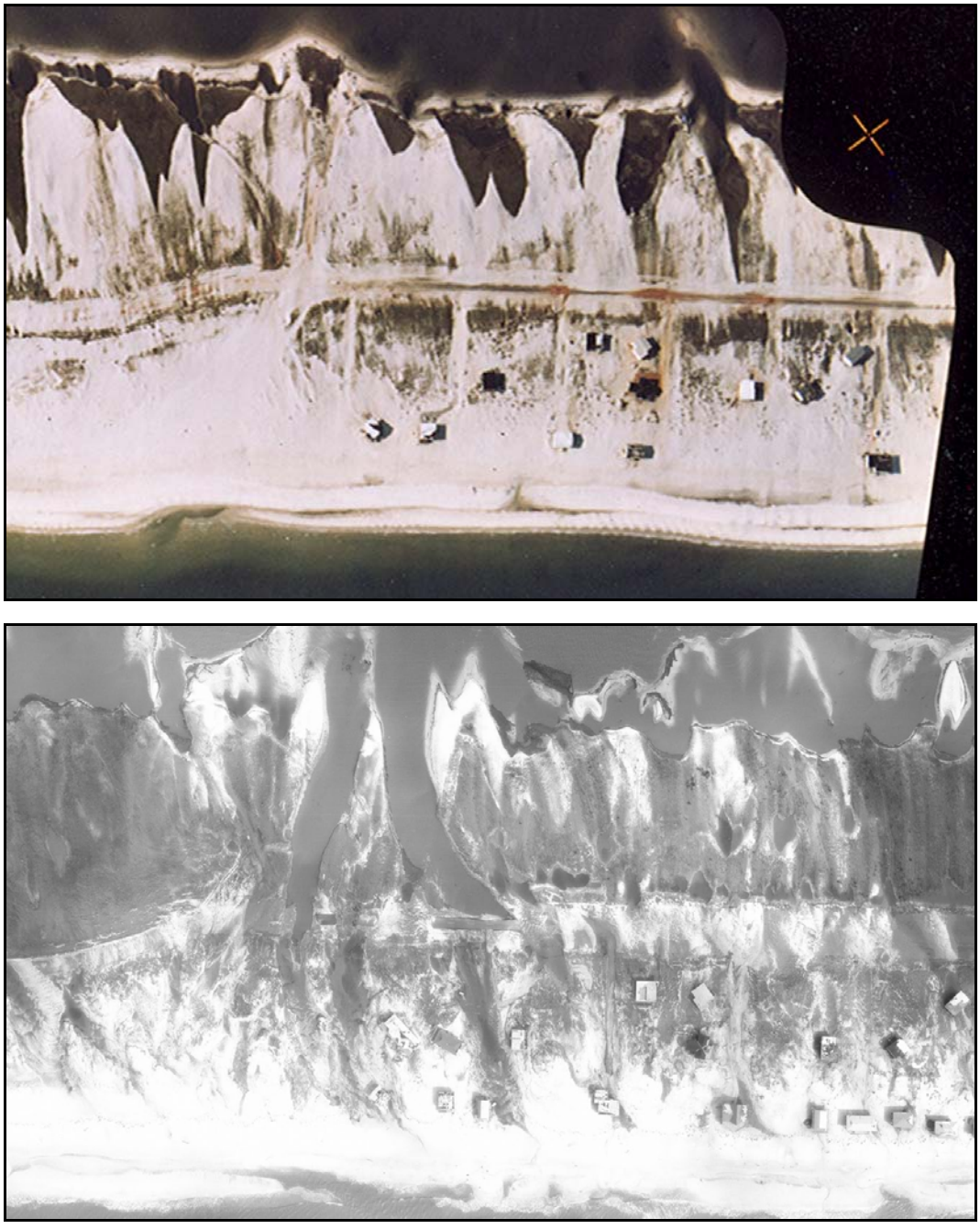

Figure 2-12. Surge channels and washover deposits on Dauphin Island follow Hurricanes *Camille* (A) and *Fredric* (B) (from Morton, 2007).

remained relatively small as they migrated from southeast to northwest (Figure 2-13), suggesting that a recovery period of 10 years between major storms may not be sufficient for sustained sand accumulation above the high-water line. Regardless, island growth to the west did continue between 1957 and 1981/82, even though a large portion of sediment transported to Dauphin Island from the ebb-tidal delta likely deposited in surge channels and on washover sediment as the island recovered from storm events.

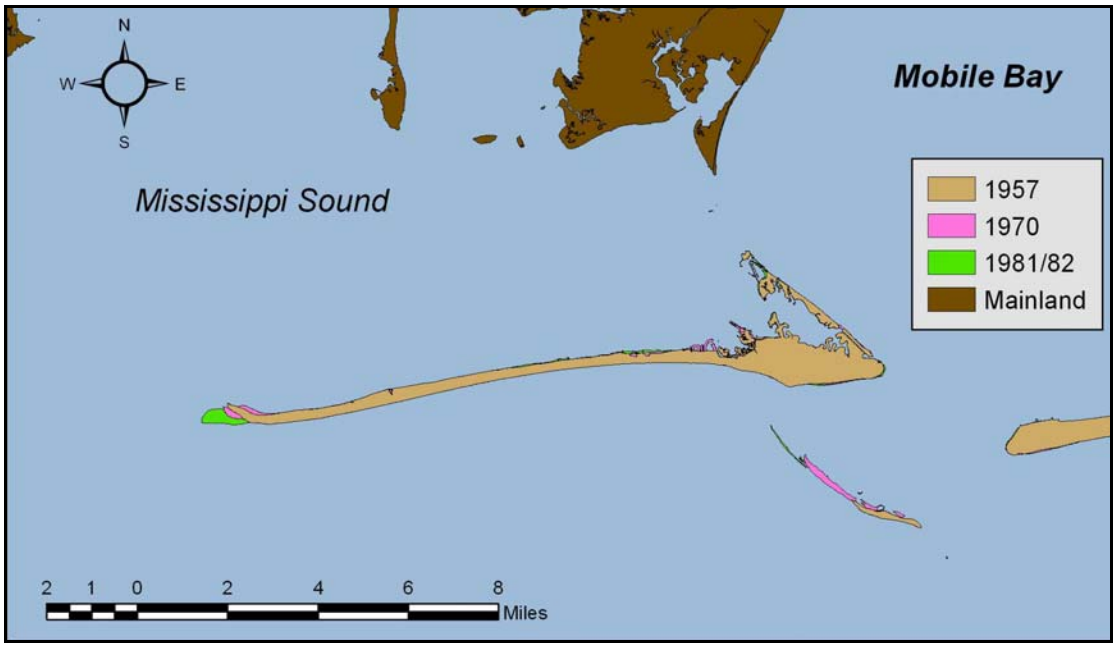

Figure 2-13. 1957 shoreline superimposed on 1970 and 1981/82 shorelines illustrating island movement on the ebb shoal to the northwest and lateral growth on western Dauphin Island.

Channel bar dredging between 1957 and 1982 accounted for 2,306,000 cy of new work and 9,042,000 cy of maintenance work, for total volumes of 6,062,000 cy and 17,646,000 cy, respectively, since 1904. These quantities represent about 47% and 74% of dredged material placed offshore since the project was authorized, and island growth on the ebb shoal, infilling of surge channels and low-lying washover flats caused by storms, and westward growth of the island continued.

1982 to 2006. Over the most recent 24-year period, 13 tropical cyclones traversed the study area (see Table 1-1), but five hurricanes had the greatest impact on geomorphic change along Dauphin Island. Storm surge and strong winds from Hurricanes *Elena* (1985), *Danny* (1997), *Georges* (1998), *Ivan* (2004), and *Katrina* (2005) caused overtopping across many portions of the island west of Pelican Island, creating extensive washover fans and terraces (Morton, 2007). Storm surge and

waves associated with *Ivan* resulted in the western three-fourths of the island being overwashed and an island breach forming west of the developed area. When *Katrina* crossed the Mississippi coast in 2005, western Dauphin Island was particularly vulnerable to overwash, and the breach initiated during *Ivan* widened substantially.

Figure 2-14 illustrates that Pelican Island widened and lengthened between 1982 and 2001/02, resulting in the most extensive island on the ebb-tidal delta since 1908. Dauphin Island also reached its greatest length in 2001/02; however, the island was slightly narrower than it was in 1982 (primarily from bayside erosion). By 2006, two major hurricanes had flattened many of the dunes, resulting in extensive washover deposits on the backside of the island and into the Sound, and a breach just west of the developed area (Figure 2-14). Pelican Island was reduced in length by storm processes, but the northwestern tip of the island was within about 200 ft of Dauphin Island in 2006. Not since 1868 has an island on the ebb-tidal delta been in such close proximity to the Dauphin Island, providing a near direct conduit for sand transfer from ebb shoals to the island.

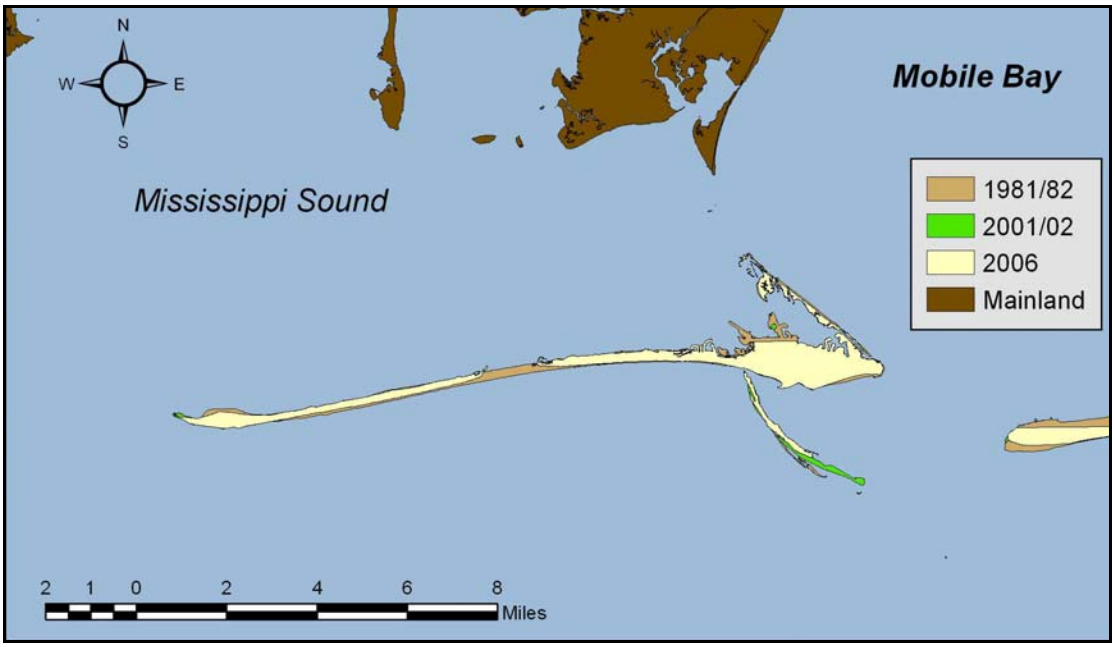

Figure 2-14. 2006 shoreline superimposed on 1981/82 and 2001/02 shorelines illustrating island growth on the ebb-tidal delta to the northwest and breaching on Dauphin Island after Hurricanes *Ivan* (2004) and *Katrina* (2005).

Between 1982 and 2006, channel dredging across the outer bar was extensive; however, since 1999, all new work and maintenance material have been placed in the Sand Island Beneficial Use Area (SIBUA) or on a feeder berm on the western lobe of the ebb shoal (initial placement on a feeder berm was completed in 1987). Although

9,817,000 cy of new work dredging was completed during this time, 3,062,000 cy was placed in the SIBUA. Maintenance dredging between1982 and 2006 totaled 10,682,000 cy, but 4,515,000 cy was placed in the SIBUA. Regardless of channel dredging across the outer bar, by 2002, Pelican Island was the longest it had been since dredging started, and it was at its closest point to Dauphin Island since 1868. Furthermore, Dauphin Island was longer than at any point since accurate shoreline surveys were initiated in 1847.

Island Length, Width, and Area Changes. Previous sections of this chapter have described the sequence of geomorphic changes that occurred on Dauphin Island and the western lobe of the ebb-tidal delta (Pelican and Sand Island) between 1847 and 2006. Figure 2-15 illustrates net changes for the period of record. Island length, width, and surface area changes were quantified for Dauphin Island to document variability in geomorphic response (Table 2-4). Boundaries for quantifying island area, width, and lateral movement are illustrated in Figure 2-16.

Net westward littoral transport has resulted in island expansion to the west by about 5.2 miles since 1847 (Figure 2-15). About 77% of this lateral movement occurred by 1957, but the island continued to lengthen through 2006. Figure 2-17 documents an increase in island width between 1847 and 1934 (note that island width was greatest after the 1916 hurricane due to extensive washover deposition), but after 1934, island

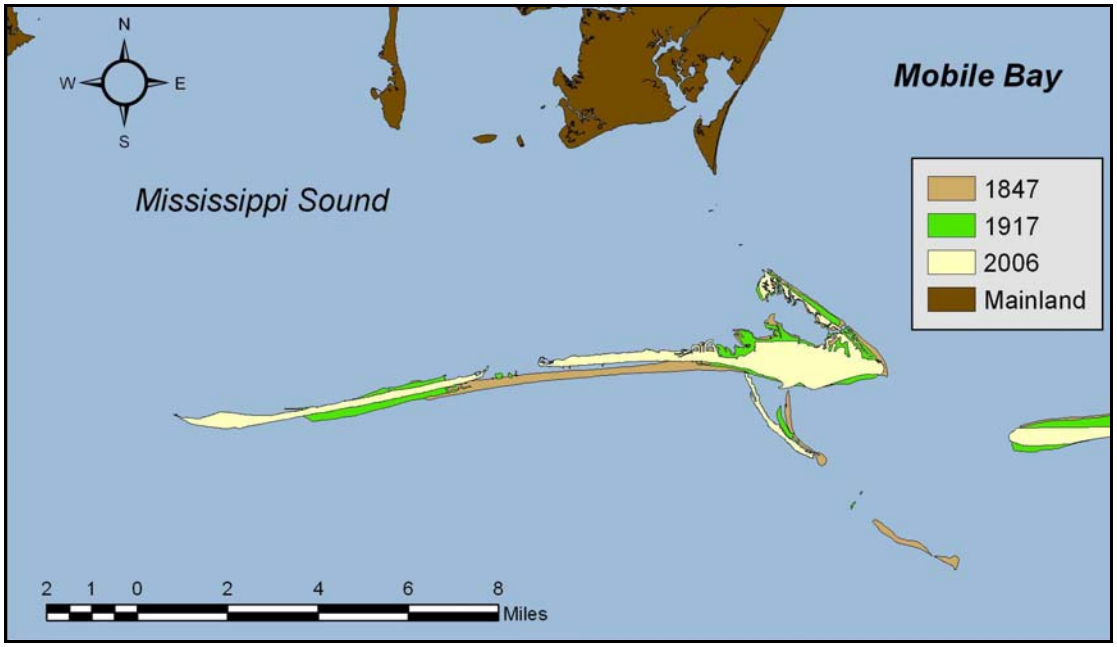

Figure 2-15. 2006 shoreline superimposed on 1981/82 and 2001/02 shorelines illustrating island growth on the ebb-tidal delta to the northwest and breaching on Dauphin Island after Hurricane Katrina in 2004.

Table 2-4. Historical changes in island length, width, and area.

Year	Lateral Growth (ft)[1]	Average Width (ft)[2]	Island Area (acres)[3]
1847	start	1,109	782
1917	12,085	1,898	780
1934	-----	1,154	-----
1957	21,084	1,184	1,445
1970	21,642	1,073	1,309
1981	24,165	1,081	1,347
1993	25,642	909	1,180
2001/02	27,387	850	1,135
2006	27,526	931	1,114

Note: [1] Lateral growth is measured relative to the western end of the 1847 island (see Figure 2-16A).
[2] Average island width is calculated from distance measurements between the front and back sides of the island.
[3] Island area is calculated for the western portion of the island as illustrated in Figure 2-16B.

width began to decrease. Except for an area of prominent island breaching, as shown on the 1917 shoreline map, island width in 1934 was greater than all subsequent periods (Figures 2-18, 2-19, 2-20). By 2006, island width began to increase again, primarily east of the breach related to hurricane washover deposition during Hurricanes *Ivan* and *Katrina* (Figure 2-20). Overall, island width decreased by about 330 ft between 1957 and 2001/02, resulting in a loss of about 310 acres of island area (Table 2-4). Although average island width increased by about 80 ft between 2001/02 and 2006, island area continued to decrease to a low of 1,114 acres since 1957. Historical records prior to 1934 indicate that island area was significantly lower than present island area, suggesting that large volumes of sand must have been supplied to the island from the Mobile ebb-tidal delta after 1917. Sediment supplied from the shoal created a continuous island that was badly breached during the 1916 hurricane, and a westward-migrating island that was 2.8 mi longer in 2006 than in 1917.

To summarize, Dauphin Island has continued to grow to the west since 1847, but island width and surface area began to decrease from historical maximums in 1957. Island width measurements in 1934 illustrate a slightly wider feature than present in 1957, except for a narrow zone along the eastern margin of the breach present in 1917. Because only a portion of the 1934 island was mapped by USC&GS, surface area was not computed for this date. However, we can estimate island area and length with chart information compiled by Hardin et al. (1976) indicating the position of the "1942" shoreline relative to 1917 USC&GS shoreline survey data (Figure 2-21). Because USC&GS data do not exist for 1942, the shoreline shown in

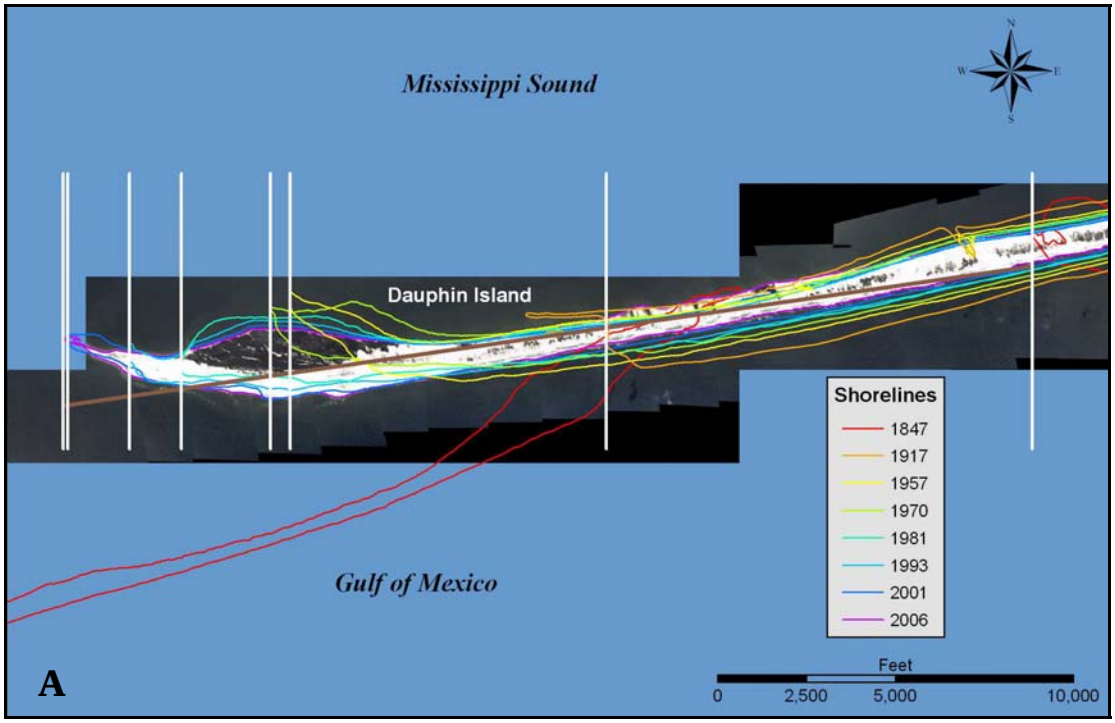

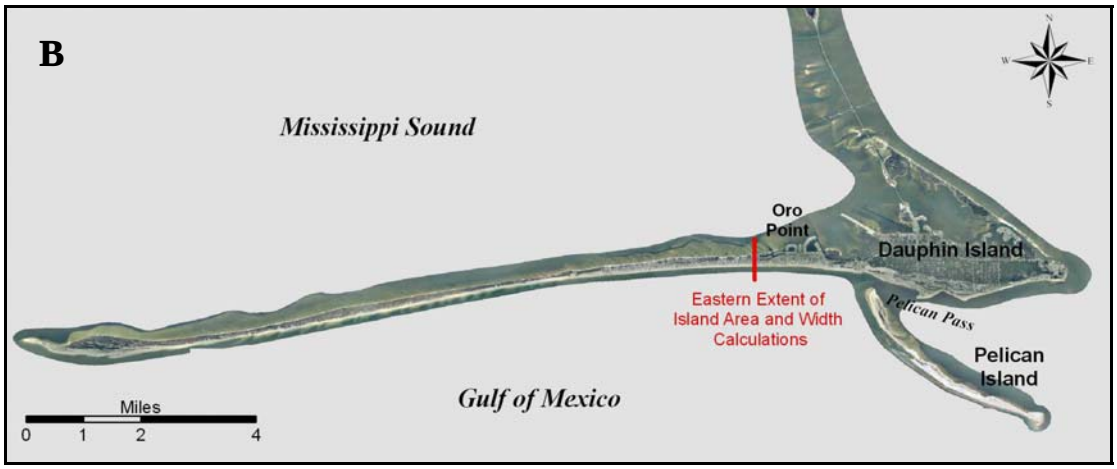

Figure 2-16. Measurement boundaries for quantifying island dimension changes relative to 2006 (A) and 2002 (B) orthophotography: A) lateral island growth calculations, and B) island width and area calculations.

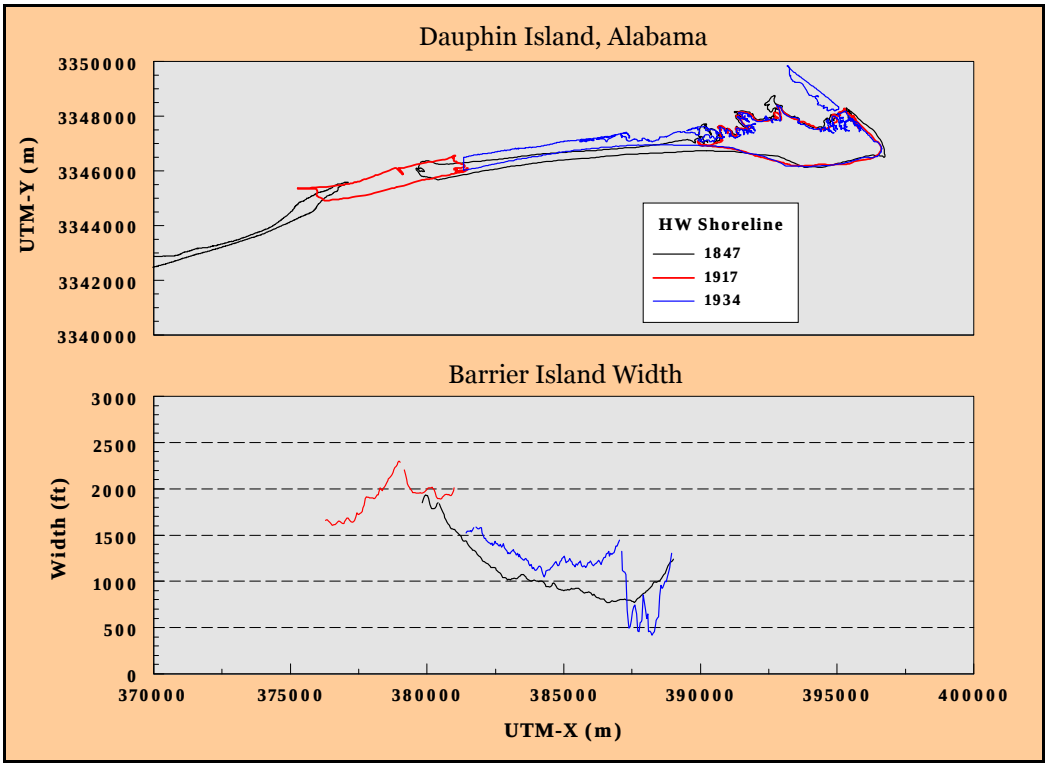

Figure 2-17. Changes in barrier island width between 1847 and 1934, Dauphin Island, AL.

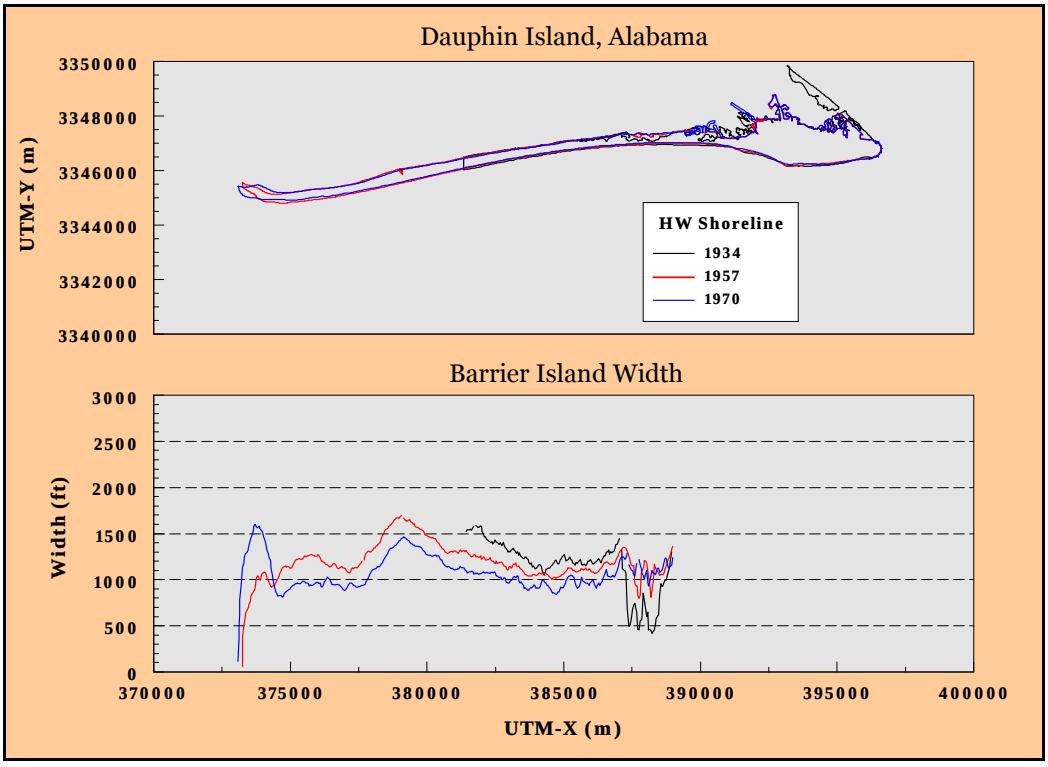

Figure 2-18. Changes in barrier island width between 1934 and 1970, Dauphin Island, AL.

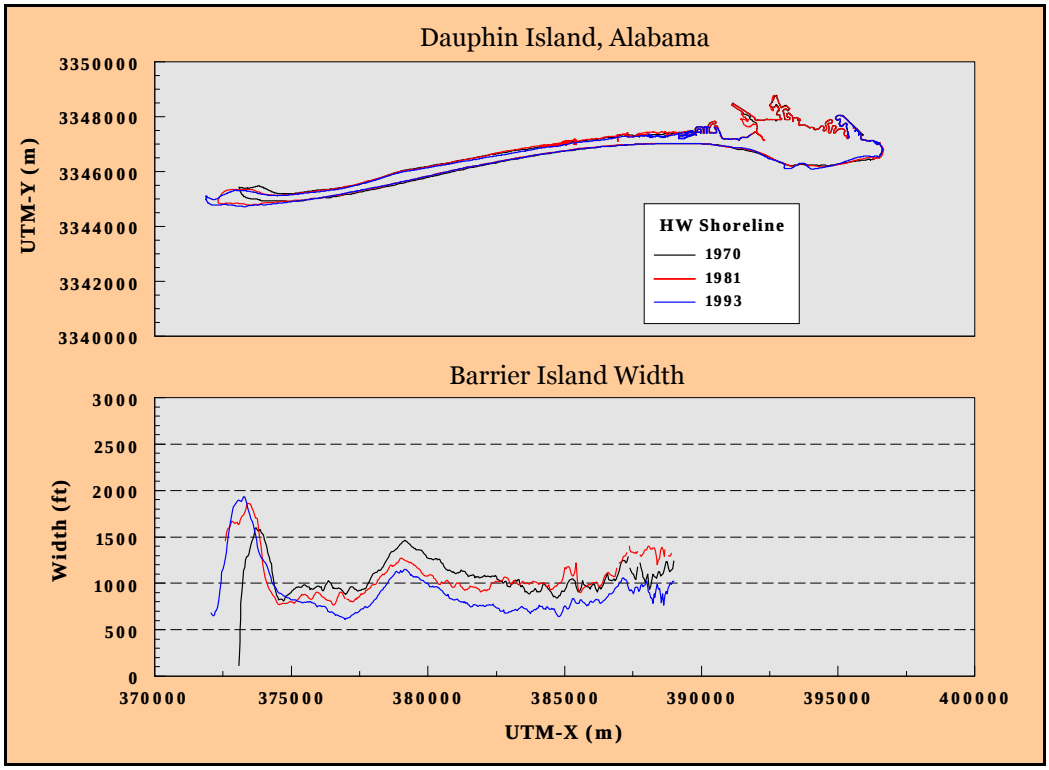

Figure 2-19. Changes in barrier island width between 1970 and 1993, Dauphin Island, AL.

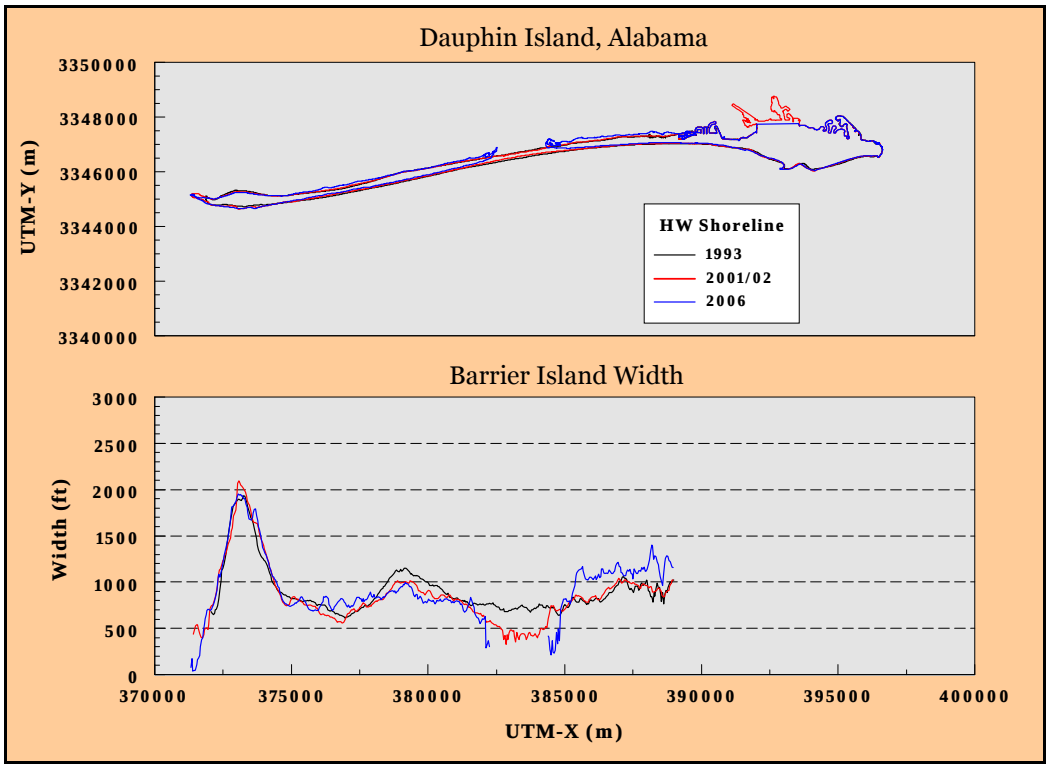

Figure 2-20. Changes in barrier island width between 1993 and 2006, Dauphin Island, AL.

Figure 2-21 might reflect a partial update to NOAA Charts 1266 and 1267 produced in 1943 and 1944, respectively. Using these data, island growth between 1847 and "1942" is about 19,100 ft, and island area is estimated to be about 1,590 acres. By 2006, the western portion of the island is about 5.2 miles longer than in 1847, its average width is about 178 ft narrower, and surface area is approximately 332 acres larger.

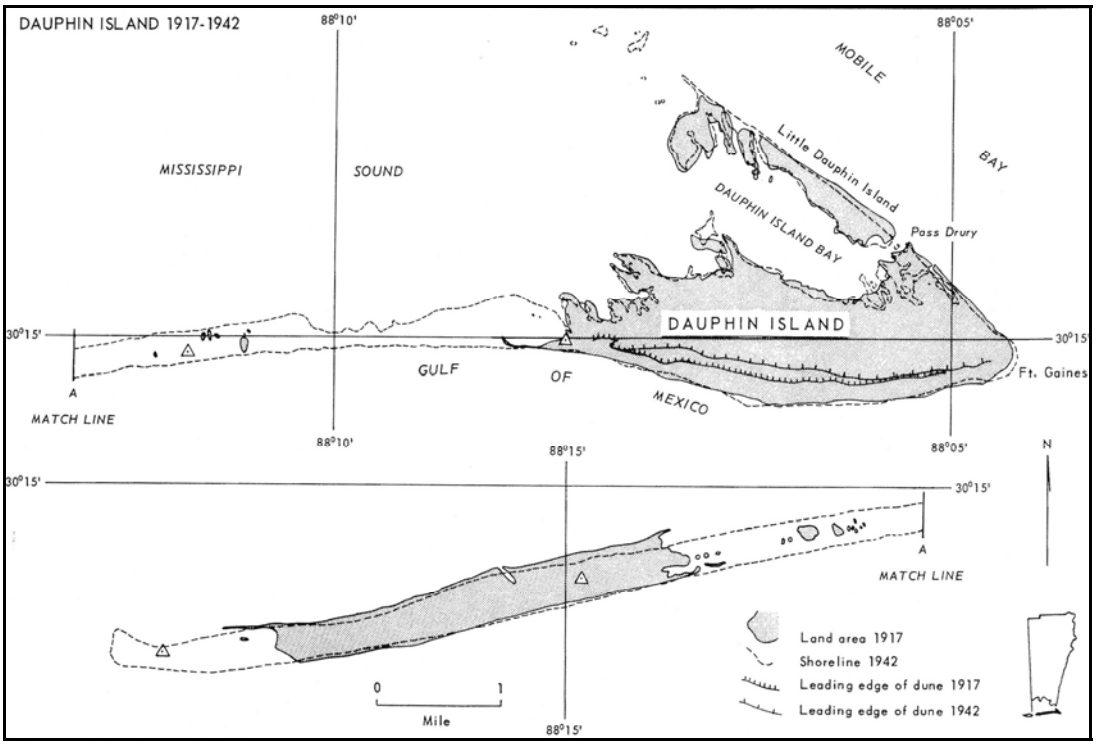

Figure 2-21. Shoreline change plot illustrating 1942 shoreline relative to the USC&GS 1917 high-water shoreline (from Hardin et al., 1976).

Breaching and Washover

Storm-related processes are the primary cause of geomorphic change on Dauphin Island. Island breaching and overwash processes promote northward-directed transport of sand from ocean beaches, across the island and into Mississippi Sound. Lateral movement of Dauphin Island due to the dominant east-to-west gradient in littoral transport produces rapid island growth, whereas sporadic events like hurricanes and tropical cyclones produce cross-shore movement of sand into the sound resulting in long-term landward migration of the island. This process of island migration is termed rollover. Washover deposition is the geomorphic response to overwash and inlet formation can result from island breaching.

The first survey of storm-induced changes along western Dauphin Island occurred just 6 years after the 1847 survey. The hurricane of 1852 produced a large breach in the central portion of the island and washover deposition in the sound along most of the western sand spit. Figure 2-22 illustrates the location of the breach relative to the 1847 shoreline, a common location for breaching during most large storms. Geomorphic response to extreme storms is rapid displacement of the island shoreline by erosion of the Gulf facing beach and deposition on the backside of the island and in the Sound. This rapid but sporadic beach response results in long-term net northward movement of the island, not necessarily permanent beach erosion.

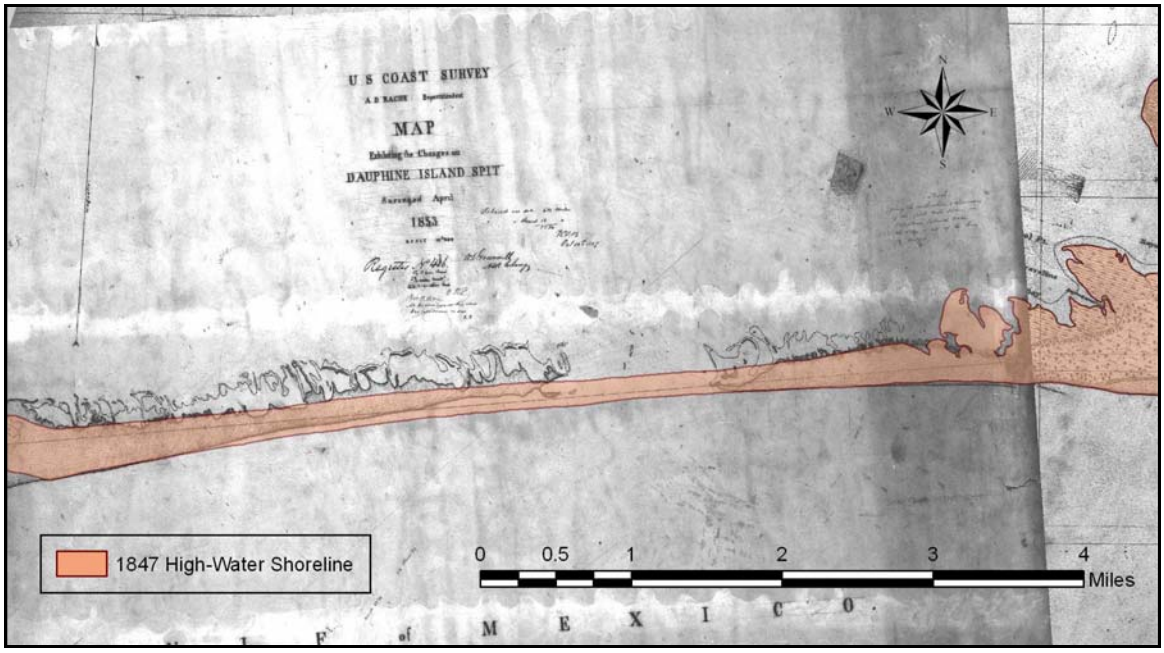

Figure 2-22. First-recorded breaching along the central portion of western Dauphin Island in response to the hurricane of 1852.

The July 1916 hurricane produced a much wider gap in the island than that mapped in 1853 (Figure 2-23). In fact, much of the central portion of the island was washed into Mississippi Sound. Island remnants were present throughout the western two-thirds of the breach, indicating that the deepest part of the breach was likely near the eastern margin of the feature, adjacent to the small sand spit protruding west from the island core. By 1934, the breach was closed by westward-directed sand transport from the western lobe of the ebb-tidal delta. In about 17 years, the central 3 miles of Dauphin Island went from being completely awash at low water to a continuous subaerial feature (Figure 2-24). Although an island breach was reported in the same general location as previous breaches in March 1950 (Hardin et al., 1976), the island in 1957 was continuous and wide, growing steadily to the west.

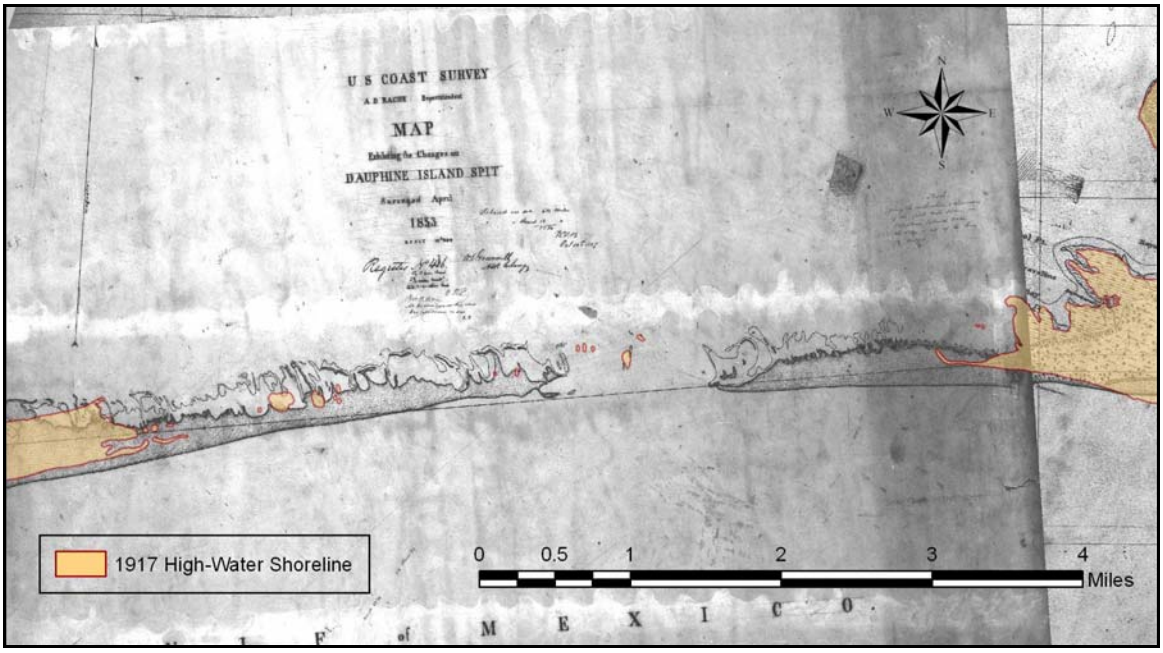

Figure 2-23. Large island breach formed by the July 1916 hurricane in the same general location as the 1853 breach.

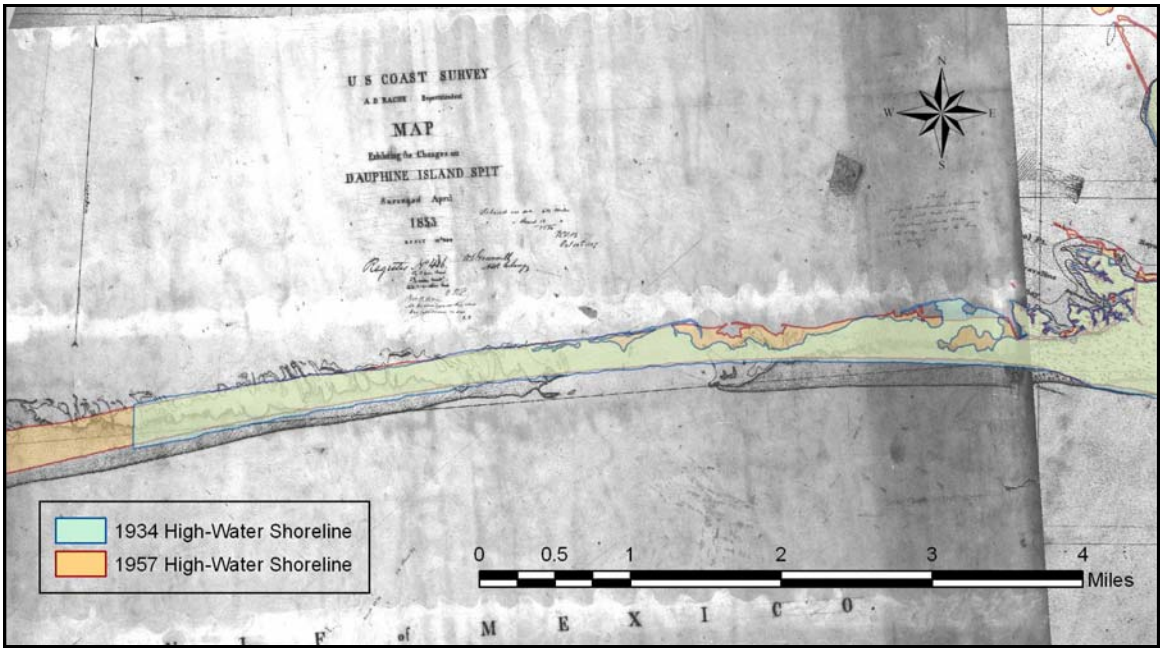

Figure 2-24. Location of the 1934 and 1957 shorelines relative to the 1853 island breach.

Multiple breaching and overwash produced a rapidly migrating island that moved landward its entire island width by 1934. It continued to migrate landward as tropical cyclones traversing the area produced waves and surge that promoted overtopping of the island. By 2006, the island was again breached by storm forces

produced by Hurricanes *Ivan* and *Katrina* (Figure 2-25). This dynamic cycle of destruction and reformation illustrates the balance that is required between sediment supply and energy to sustain a viable barrier island system. If sand supply from the east were disrupted for a long period, one would expect major changes in the way post-storm recovery occurred.

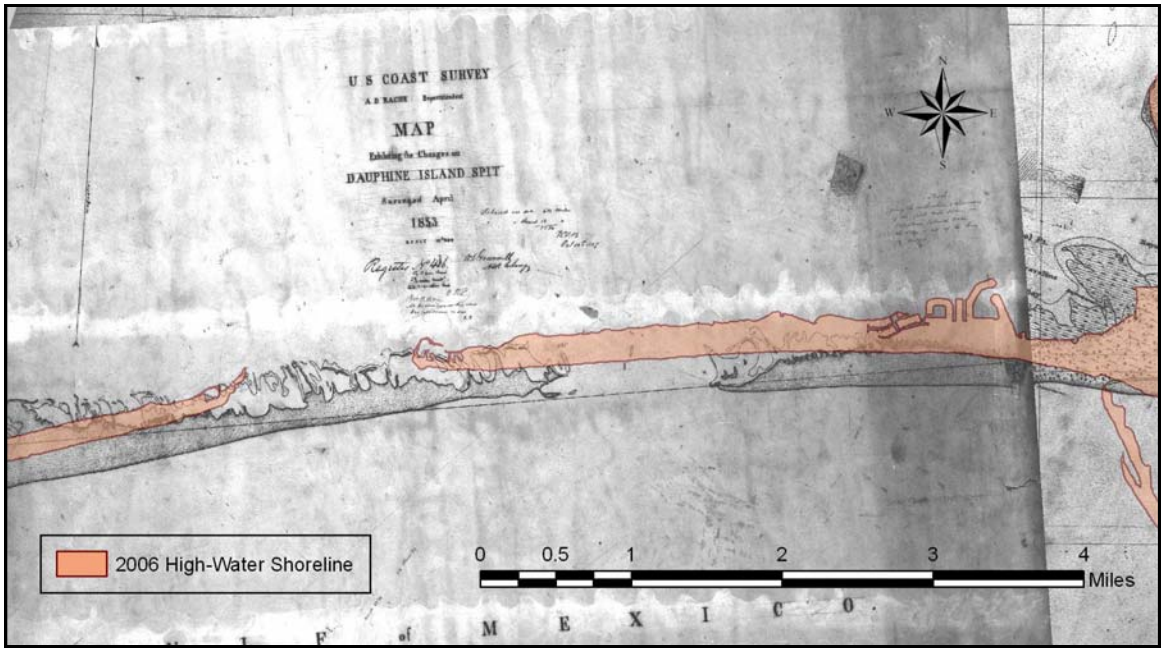

Figure 2-25. 2006 shoreline overlying the breached area in 1853, illustrating the same general location for storm breach vulnerability in 2006 as in 1853.

Figure 2-26 documents net changes in shoreline position in the area of active breaching on Dauphin Island. For the 160-year period, island width has increased slightly to the east of the 2006 breach, but the island has rolled landward approximately 1.5 times its original island width. The island west of the breach is narrower than the original island, but it is also longer than the original island, and past breaches have always filled. Recent orthophotography (May 2007) illustrates the same trend, as the modern breach has narrowed since 2006.

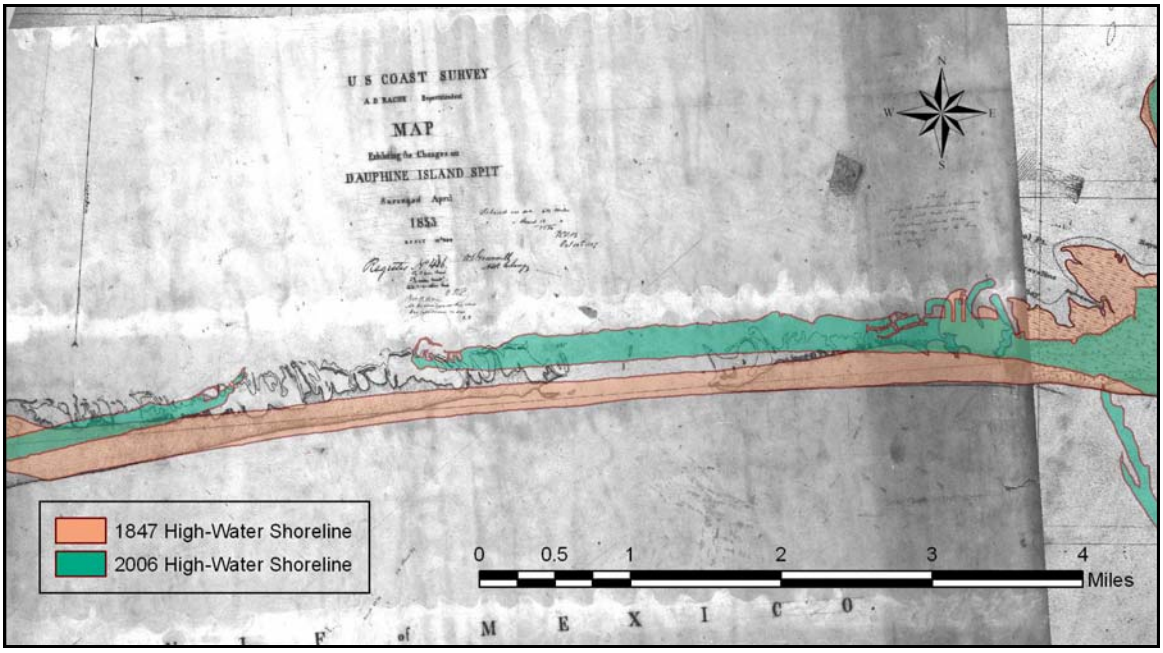

Figure 2-26. 2006 shoreline overlying the 1847 shoreline and the breached area in 1853, illustrating barrier rollover and breaching on central Dauphin Island.

Spatial and Temporal Trends

Sapp et al. (1975) and Hardin et al. (1976) first documented regional changes in shoreline position for all of coastal Alabama. Results from these reports were used by the USACE in a feasibility report on beach erosion control and hurricane protection for Mobile County, Alabama (including Dauphin Island) to summarize historical trends in shoreline position change (USACE, 1978). Lamb (1987) evaluated the complex interaction of waves and currents downdrift of tidal passes in Alabama and their impact on shoreline response. Smith (1990) used the Hardin et al. (1976) data set to discuss the progressive loss of shoreline and wetlands in coastal Alabama. Byrnes et al. (1991) analyzed the lateral growth of Dauphin Island as measured from compiled historical shorelines from maps and aerial photographs. Sanchez and Douglass (1994) used a sequence of aerial photography between 1970 and 1993 to document changes in beach width at 95 locations along the outer coast of Alabama.

More recently, Byrnes et al. (1999) quantified historical changes in shoreline position for the entire outer coast of Alabama in a study evaluating the potential impacts of offshore sand mining on coastal change. Overall, many authors discuss the effect of hurricanes on geomorphic change along Dauphin Island (e.g., Schramm et al., 1980; Froede, 2006b; Otvos, 2006; Morton, 2007), but a detailed analysis of spatial and temporal variability in shoreline position generally is lacking for coastal Alabama.

This section documents trends in shoreline response to waves and currents for the period 1847 to 2006. Change calculations were made every 60 ft along the outer coast of Mobile and Baldwin Counties using the Automated Shoreline Analysis Program under ArcGIS (ArcASAP).

Dauphin Island. The eastern end of Dauphin Island is the core of the island from which westward growth of an extensive barrier spit evolved under slowly rising sea level (Otvos and Giardino, 2004). Historical shoreline survey data have been collected along the Alabama coast by the USC&GS since 1847. Modern shoreline positions, extracted from registered aerial photography and a GPS survey, supplemented existing map data to produce a 159-year period of change (see Table 2-1). Appendix C illustrates incremental and cumulative changes for the period of record.

During the first 70 years of shoreline surveys (1847 to 1917), the island lengthened to the west substantially, but the hurricane of July 1916 produced a breach in the central portion of the island just west of Oro Point (Figure 2-27). As such, change between these two surveys could not be computed for the breached area, but the rate

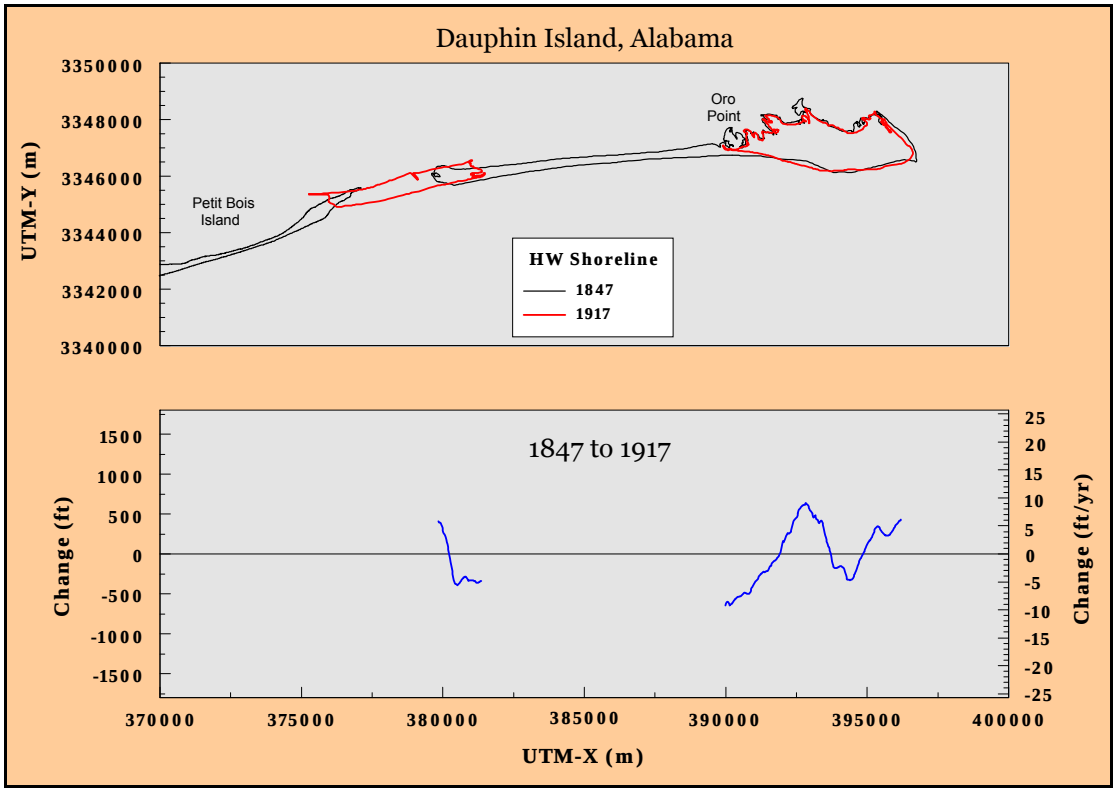

Figure 2-27. Gulf shoreline position change between 1847 and 1917, Dauphin Island, AL.

of shoreline recession at the eastern margin of the breach was about 9.3 ft/yr (650 ft). At either end of the island, net Gulf shoreline advance was indicated, and the deposition area formed by landward migration of Pelican Island onto the beach in 1868 (see Figure 2-6) remained prevalent through 1917.

By 1934 (17 years later), the island breach had filled with sand transported to the breach from the Mobile ebb-tidal delta. Shoreline change along the eastern end of the island was relatively minor, but net change since 1847 continued to illustrate primarily deposition along the beach east of Pelican Island. Although the breach filled between 1917 and 1934, the high-water shoreline was now 1,100 ft landward of its location in 1847, almost coincident with the Sound shoreline at that time (Figure 2-28). The island was approximately the same width in 1934 as it was in 1847, but it had been displaced to the north via barrier rollover its entire island width due to storm processes.

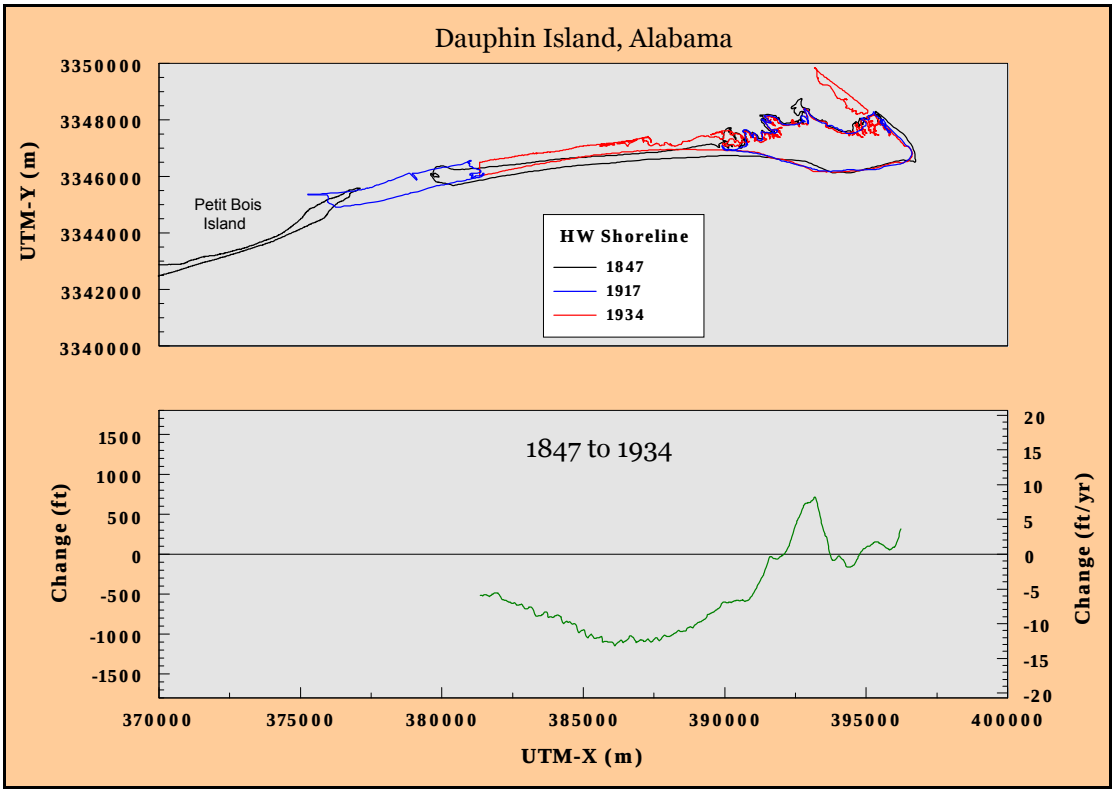

Figure 2-28. Breach infilling by 1934 created a continuous island that was displaced landward by about 1,100 ft of its position in 1847.

Shoreline change between 1934 and 1957 was reduced compared with long-term trends. However, shoreline recession remained pervasive in the area where breaching was mapped in 1917. West of the general location of Pelican Island,

average shoreline recession was approximately 120 ft (about 5 ft/year) compared with about 9 ft/year between 1847 and 1957. This recession trend continued between 1957 and 1970 at about 6 to 7 ft/yr. Between 1970 and 1981, shoreline advance began to occur north and west of Pelican Island, suggesting that the ebb-tidal delta was supplying the beach with a greater quantity of sand than incident energy could transport away from this location (Figure 2-29). In addition, the western end of the island was again accreting to the south and growing to the west.

Between 1981 and 1993, a period of weak tropical cyclone activity, most of the island showed net shoreline advance as Pelican Island began to expand and feed sand to island beaches (Figure 2-30; see Figure 2-14). By 2002, Pelican Island was at its greatest subaerial extent since 1908. However, increased storm activity between 1994 and 1998 resulted in a slight increase in shoreline recession along the central portion of Dauphin Island. In fact, this was the period when storm overwash and shoreline recession at the present location of the breach from Hurricanes *Ivan* and *Katrina* began to develop. Figure 2-30 illustrates increased recession between 1993 and 2001 coincident with the location of the breach present in 2006.

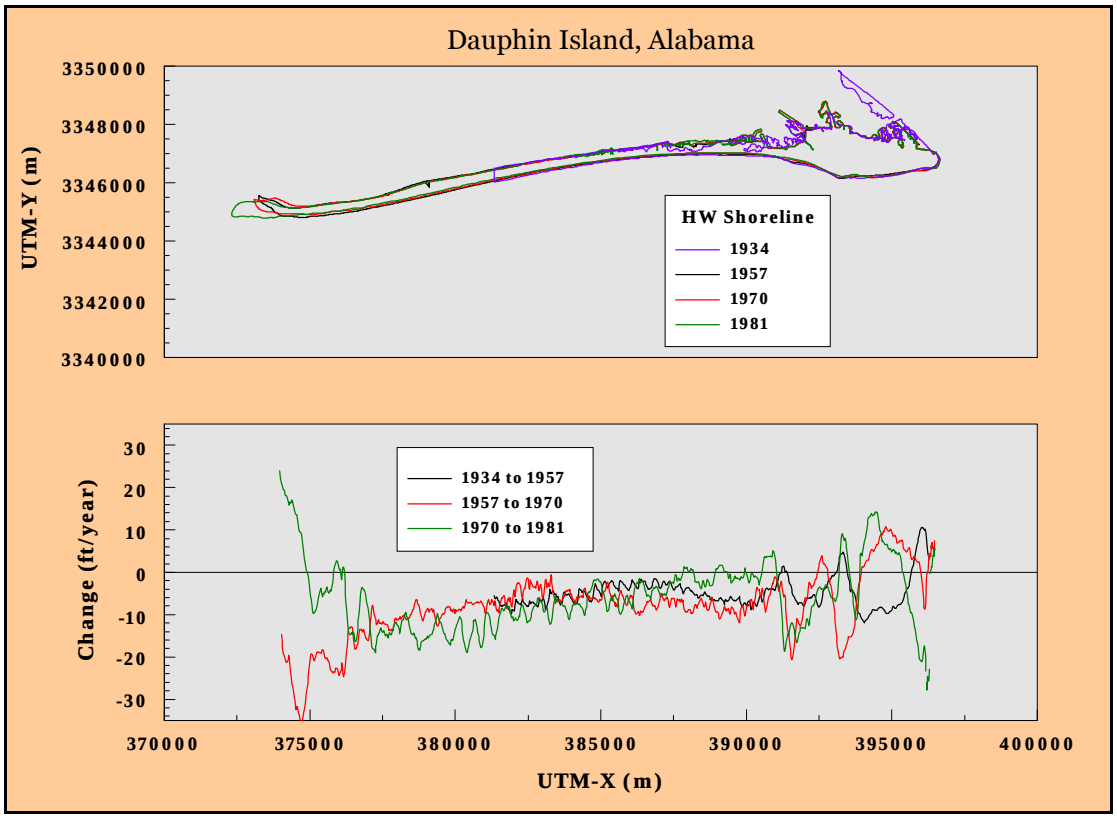

Figure 2-29. Gulf shoreline change between 1934 and 1981 illustrating net recession along the central portion of the island most vulnerable to overtopping during storms.

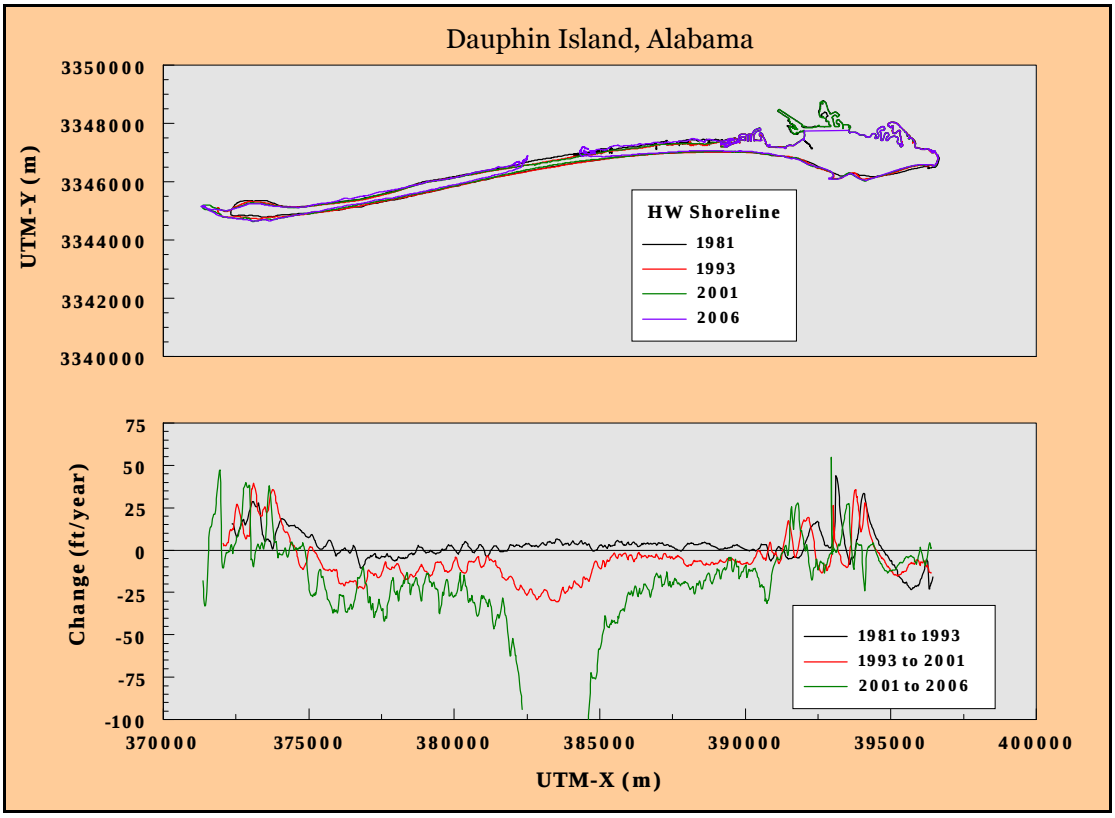

Figure 2-30. Shoreline change between 1981 and 2006, illustrating the progressive impact of increased storminess on shoreline recession and breaching along central Dauphin Island.

Between 2001 and 2006, tropical cyclone activity was even more intense than the previous period, resulting in increased recession along central Dauphin Island, massive overwash during *Ivan* and *Katrina*, and island breaching at the location weakened by storms during the 1990s. Through this 25-year period of change, both ends of Dauphin Island experienced large fluctuations in shoreline advance and retreat that on average illustrated net accretion (Figure 2-30). The island has weathered a very active period of storms and is in relatively good condition. Pelican Island remains wide and long and continues to supply sand to the island. If storm frequency and magnitude remain low over the coming years, island beaches may respond as occurred during the 1980s, when shoreline advance and stability were the norm.

Morgan Peninsula. The outer shoreline between Mobile Point (east side of Mobile Pass) and Perdido Pass spans about 31 miles and is composed of white sand beaches backed by low dunes. In 1847, the shoreline west of Perdido Pass was continuous; however, by 1918, one small inlet had formed south of the eastern pond of Shelby Lakes, and a slightly larger inlet formed south of the eastern end of Little Lagoon. Both features likely formed during the hurricane of July 1916. Despite the apparent

storm response, the shoreline illustrated net advance between 1847 and 1918 at an average rate of about 2.1 ft/year or about 139 ft (Figure 2-31). Average shoreline change away from entrances was about 1.2 ft/year (80 ft). The quantity of littoral sand available to these beaches from the east appears far greater than the energy necessary to transport excess sediment farther to the west. Appendix D illustrates incremental and cumulative changes for the period of record.

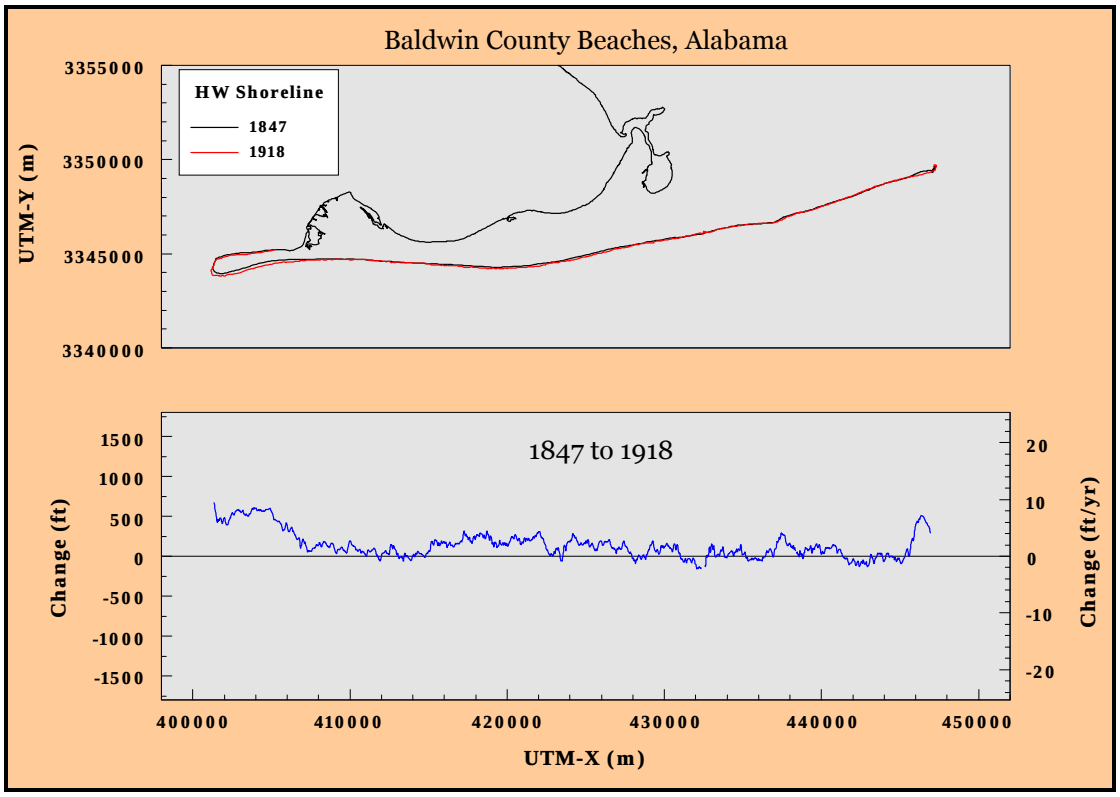

Figure 2-31. Variations in shoreline position change between Perdido Pass and Mobile Pass, Alabama, 1847 to 1918.

Even though inlets west of Perdido observed in 1918 had filled by 1934, average shoreline position change between 1918 and 1934 illustrated recession of approximately 130 ft, resulting in net recession of about 63 ft away from entrances between 1847 and 1934. Overall, the long-term (1847 to 1934) relationship between sediment supply and littoral energy needed to transport sand along beaches between Perdido Pass and Mobile Point results in net recession. Between 1934 and 1957, net shoreline advance resulted in an overall accreting beach between 1847 and 1957, particularly at the terminal end to littoral transport near Mobile Point (Figure 2-32). Unlike Dauphin Island, beaches along the Morgan Peninsula are able to better withstand the impact of tropical cyclones due to the width and elevation of their backshore environments. Furthermore, the source of littoral sand is from the east of

both sites, and because Baldwin County beaches are in the easternmost part of Alabama, they are closer to the ultimate source of sand from the Grayton Beach headland along the Florida panhandle (Stone et al., 1992).

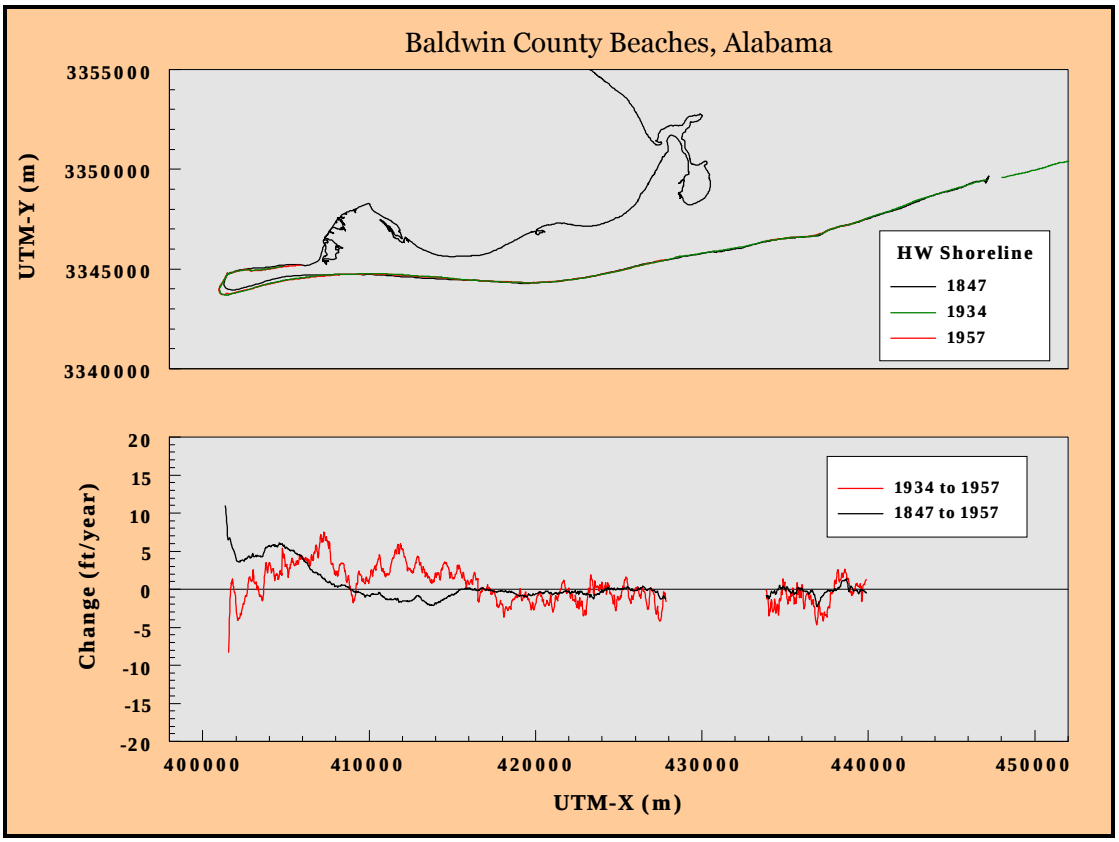

Figure 2-32. Gulf shoreline change between 1934 and 1957 relative to long-term trends between Perdido Pass and Mobile Point, Alabama.

Because the extent of the 1957 shoreline was limited relative to 1934 (due to missing map data), shoreline positions between 1934 and 1981/82 were used to document change after the jetties at Perdido Pass were constructed in 1968/69. Twin converging jetties were constructed at Perdido Pass as part of a weir-jetty system to stabilize the inlet (Sargent, 1988). Placement of a weir on the east jetty was based on the predominantly westward littoral drift. A deposition basin with 400,000 cy capacity was filled two years after jetty construction, and encroachment of additional sand into the channel suggested the need for prompt dredging of the basin on a regular basis. Assuming the channel is a total littoral barrier, westward littoral transport rates along this section of coast are at least 200,000 cy/year. A comparison of 1934 to 1981/82 and1981/82 to 2001/02 shoreline change illustrates significant shoreline advance at Perdido Pass on either side of the entrance, indicating that basin accumulation volumes only represent a portion of the littoral

transport rate (Figure 2-33). On average, only minor changes in average shoreline position occurred between 1934 and 1981/82 (-28 ft) except at the entrances on either end of the shoreline segment. Between 1981/82 and 2001/02, average shoreline advance was dominant away from the entrances, producing an average change of 49 ft for this 20-year period. The trend of shoreline recession at Mobile Point that started between 1934 and 1957 continued through 2001/02, even though the rest of the beach west to Perdido Pass is net depositional.

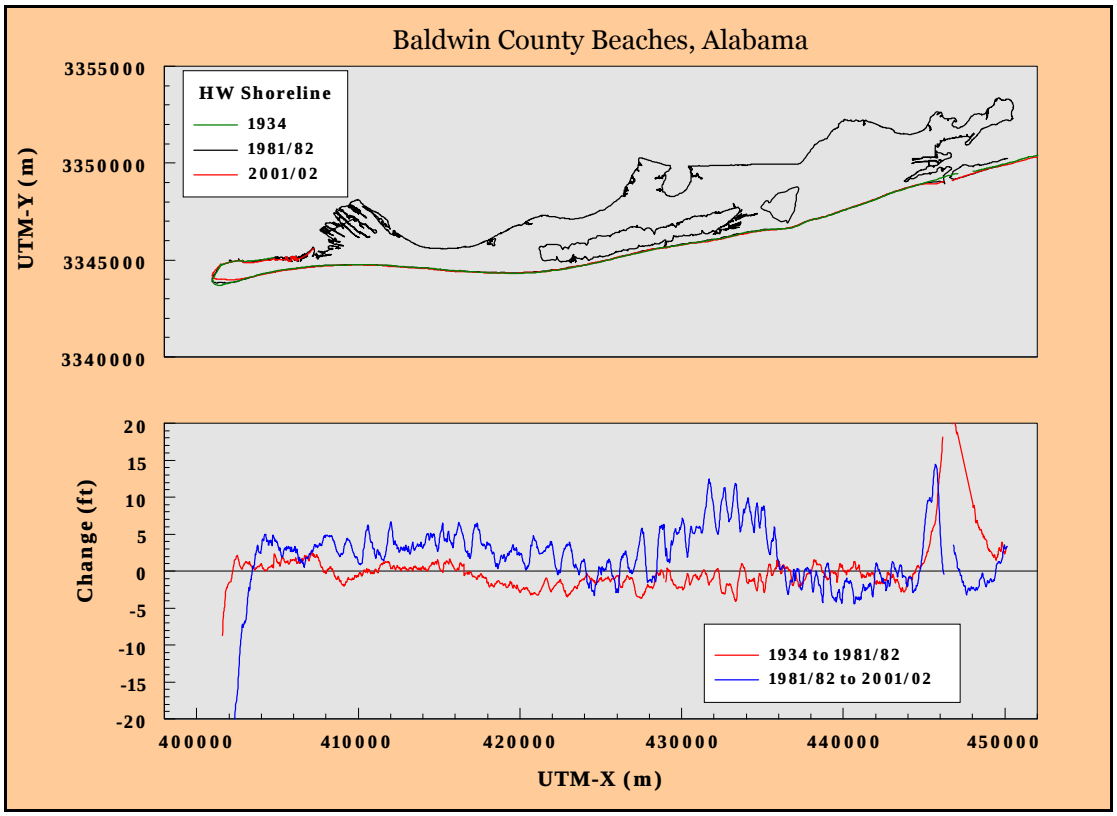

Figure 2-33. Shoreline change between 1934 and 2001/02 illustrating sand accumulation at the jetties at Perdido Pass and net shoreline advance west of this point until Mobile Point.

This trend in shoreline response persisted through 2006, producing average shoreline advance away from the passes of 73 ft relative to the 1981/82 shoreline, regardless of the increased frequency and magnitude of tropical cyclones impacting coastal Alabama between 1994 and 2005. Apparently, littoral sand in this area is so abundant that beaches have been able to withstand all potential erosional processes and engineering activities that under different circumstances may have altered shoreline response. For the 159-year period of record, shoreline change varied considerably near entrances at both ends of this coastal segment (Figure 2-34); however, average change over most of the coast showed little variation, recording average recession of about 0.2 ft/yr (26 ft).

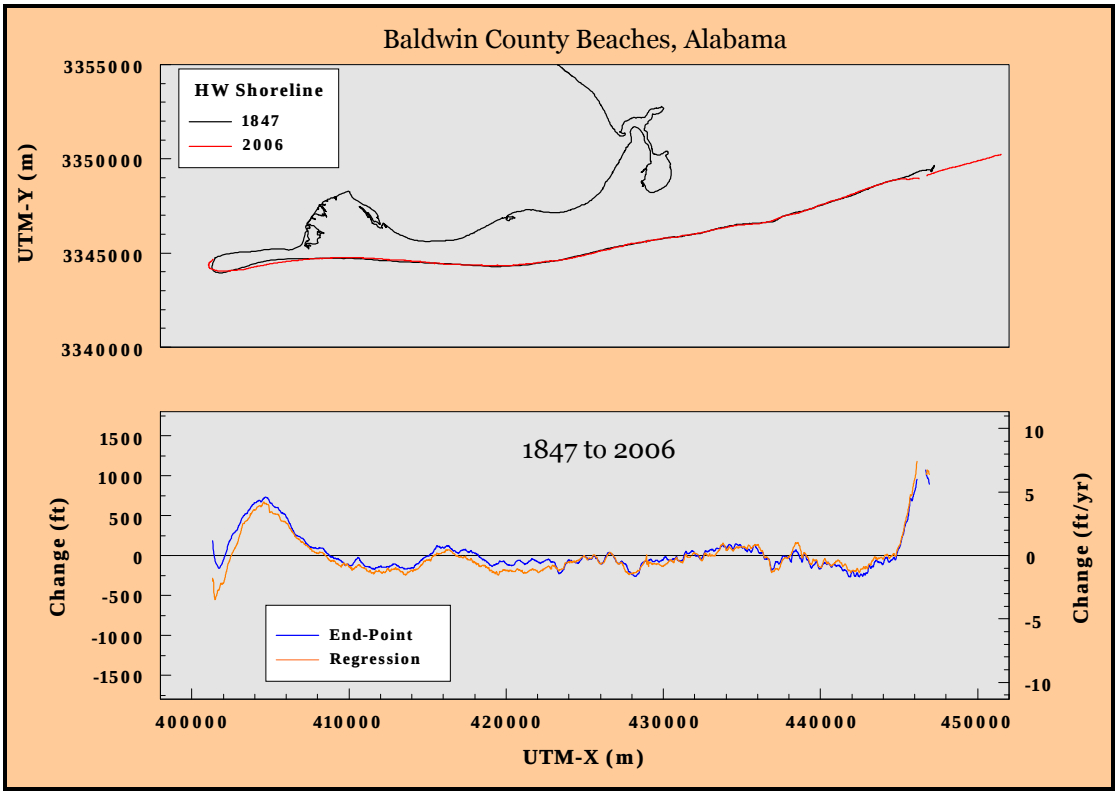

Figure 2-34. Net shoreline change between 1847 and 2006 for beaches between Perdido Pass and Mobile Point, Alabama.

Summary. Geomorphic characteristics are the primary difference between Gulf beaches in Baldwin County and Mobile County. Beaches along Morgan Peninsula are backed by wide and elevated backshore deposits. Backshore deposits on eastern Dauphin Island have the same general characteristics, and beaches are on average accreting in this area. However, the western two-thirds of Dauphin Island has always been a narrow and low barrier sand spit subjected to extreme storm waves and water levels, often resulting in island breaches and overwash that cause major geomorphic changes. Remarkably, island breaches and destruction of dunes have always been followed by natural island reconstruction. That is, breaches have filled, dunes have reformed, and the island continues to grow to the west due to a continuous supply of sand from the Mobile ebb-tidal delta, regardless of dredging in the Mobile Outer Bar Channel. The island west of Oro Point has migrated north due to breaching and washover, but infilling and deposition are the dominant processes maintaining this island, not erosion. Overall, sand supply from the east to Gulf beaches in coastal Alabama is capable of supplying potential transport quantities required throughout the historical, if not geological, record. There is no reason to expect this trend to change in the near future.

Change Contribution Due to Relative Sea-Level Rise

In addition to storm and typical wave and current processes, relative sea-level variations (rise and fall of water level relative to a fixed vertical reference plane) can cause permanent change in shoreline position. However, unlike change induced by waves and currents, those associated with rising or falling sea level typically require much longer periods of time before noticeable shoreline changes are recorded. In fact, short-term response of beaches to wave and current processes is often so large (particularly during storms) that long-term sea level change becomes background noise that may appear to have little influence on geomorphic change. From a geological timeframe, sea-level rise (or fall) is a dominant mechanism causing shoreline movement and coastal change. On a decadal to century scale, waves and currents are dominant processes causing coastal erosion, deposition, and shoreline migration. These time scales of change were described by Larson and Kraus (1995) for sediment transport and beach morphology.

Beaches adjacent to Main Pass (Mobile Bay Entrance) erode, accrete, and migrate primarily in response to variations in wave energy. However, sea-level rise over the past century may have contributed to morphologic change recorded by historical shoreline positions mapped since the mid-1800s. To estimate the contribution of change associated with sea-level rise, the Bruun Rule of erosion (Bruun, 1962) was applied for Dauphin Island west of Pelican Pass and along the Morgan Peninsula. The underlying assumption of the two-dimensional geometric rule is that a closed material balance system exists between the beach and nearshore bottom profile (Figure 2-35). Assuming an equilibrium profile shape, under long-term sea level rise (S), shoreline recession (R) and beach erosion must be associated with an equal amount of offshore deposition and seafloor rise to a maximum depth (h_d) and distance (L) of exchange of sand between the beach and offshore (Bruun, 1983).

The validity of applying the Bruun Rule to predict three-dimensional natural beach systems has been discussed for years (e.g., Bruun, 1988; Pilkey et al., 1993). Despite its simplicity and assumptions, the concept works well in many settings (Morang and Parson, 2002). In this study, the intent is not to predict where the shoreline may be at some time in the future under current rising sea level. Instead, we are interested in estimating the percentage change in historical shoreline position that may be associated with rising sea level during the change period. Implicit in this analysis is that sediment supplied to a section of beach from outside sources does not exist. Because beaches along the Alabama coast are in a sand-rich setting, estimates of shoreline change associated with long-term rising sea level rise may overstate the contribution to measured historical trends.

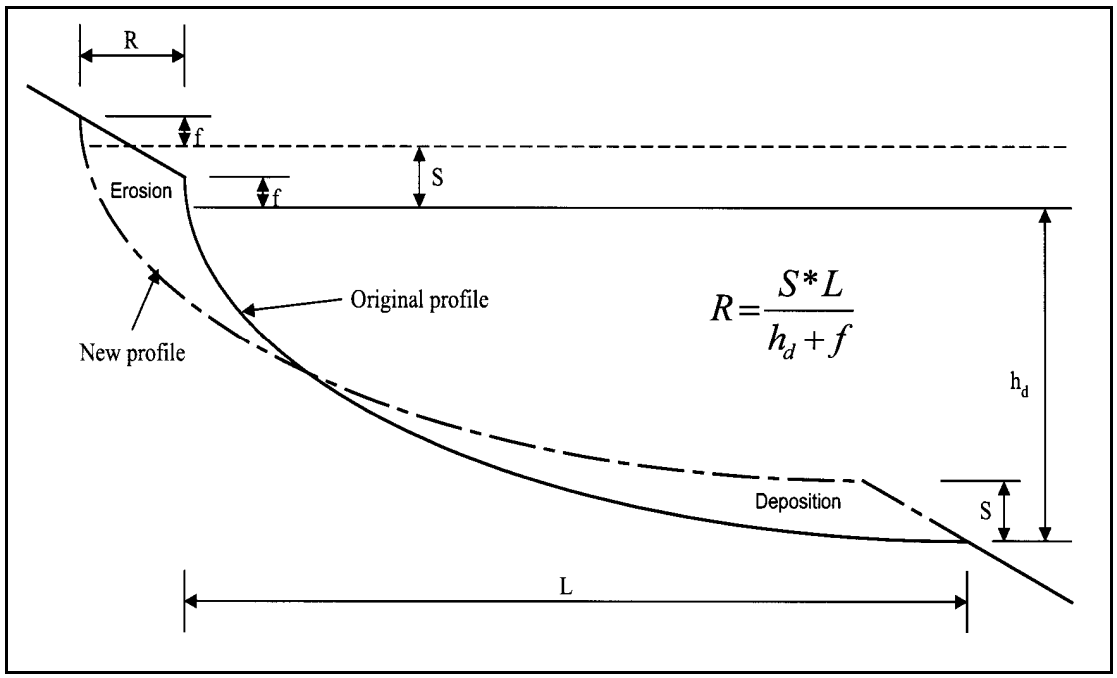

Figure 2-35. Translation of a beach profile under rising sea level in a two-dimensional closed material balance system (after Bruun, 1962).

Tide Gauge Records. Three long-term water level gauges were used to document sea-level change along the Alabama coast. For the western portion of the study area, mean annual and monthly data collected at a water level gauge maintained by the USACE in Biloxi Bay (#02480350; Figure 2-36) for the period 1896 to 2000 produced a rise rate of about 0.11 inches/year (Figure 2-37). Prior to 1928, all data were provided as annual averages, but since this date, monthly averages documented seasonal and long-term variability in water surface elevation (relative to the National Geodetic Vertical Datum [NGVD]) under storm and normal conditions.

NOAA tide gauge 8735180 at Dauphin Island, AL collected water level data for a shorter period of time (41 years), but the average rate of sea-level rise (0.114 inches/year; Figure 2-38) is similar to that recorded at the Biloxi gage. The closest NOAA gauge east of Mobile Bay is located in Pensacola Bay (#8729840), and the period of coverage is 1923 to 2007. Figure 2-39 documents changes in monthly mean water level for two distinct time periods based on observed trends. For the period 1923 to 1950, mean water elevation (relative to mean sea level) increased by about 0.2 inches/year, or approximately twice the rate of rise compared with the 1951 to 2007 change trend (0.08 inches/year). If both periods are analyzed as a continuous record, the average rate of sea-level rise is about 0.08 inches/year (Figure 2-40), nearly the same trend as that identified for the 1951 to 2007 period. This result suggests that the higher rate of change identified between 1923 and 1950 may

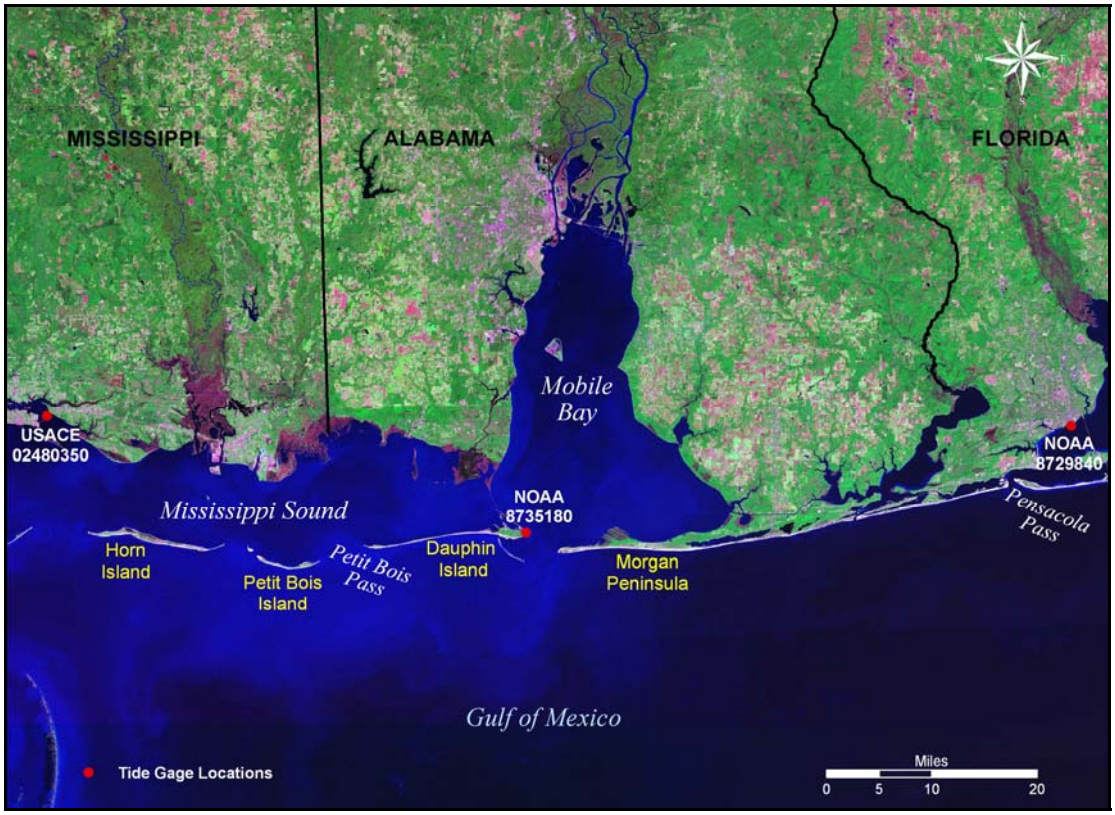

Figure 2-36. USACE (Biloxi) and NOAA (Dauphin Island, Pensacola) tide gauge locations.

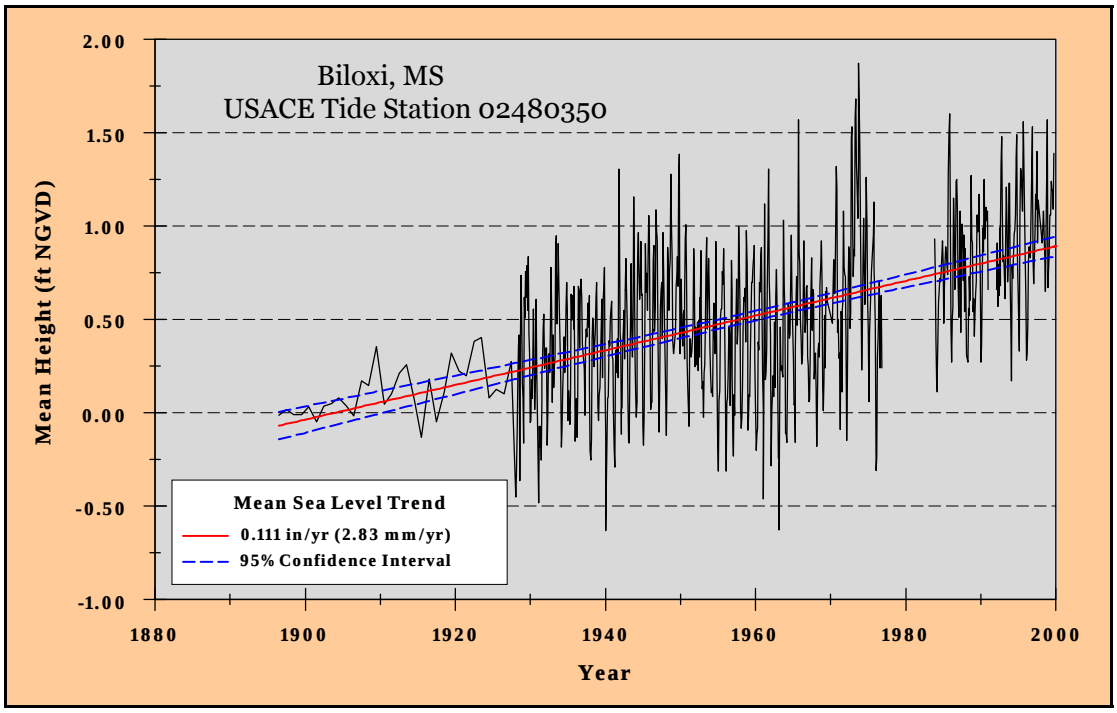

Figure 2-37. Mean annual and monthly water level measurements and sea-level rise trend at Biloxi, MS gauge 02480350, 1896 to 2000.

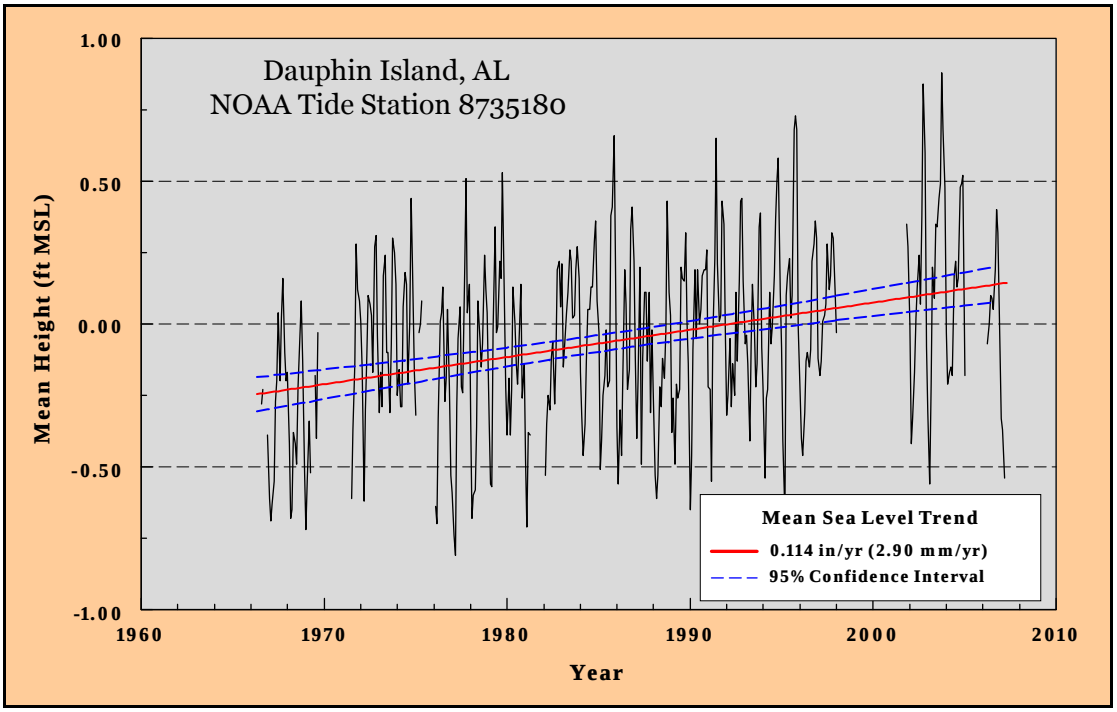

Figure 2-38. Monthly mean water level measurements and sea-level rise trend at Dauphin Island, AL gauge 8735180, 1966 to 2007.

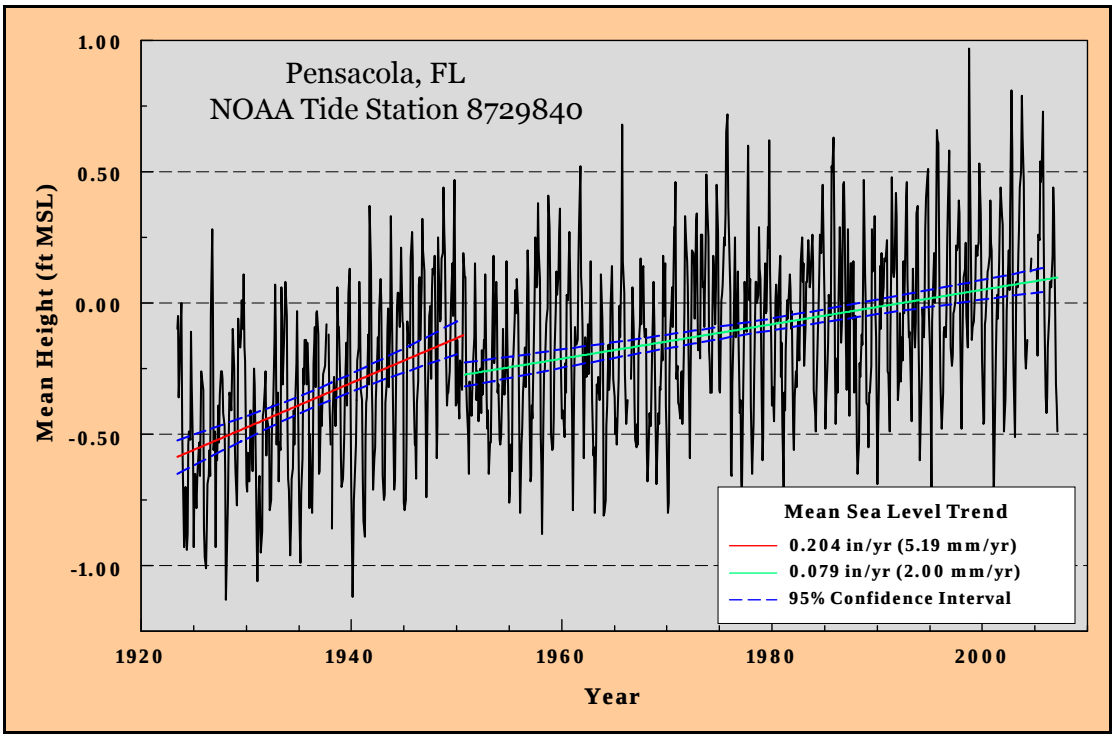

Figure 2-39. Monthly mean water level measurements and sea-level rise trends at Pensacola, FL gauge 8729840, 1923 to 1950 and 1951 to 2007.

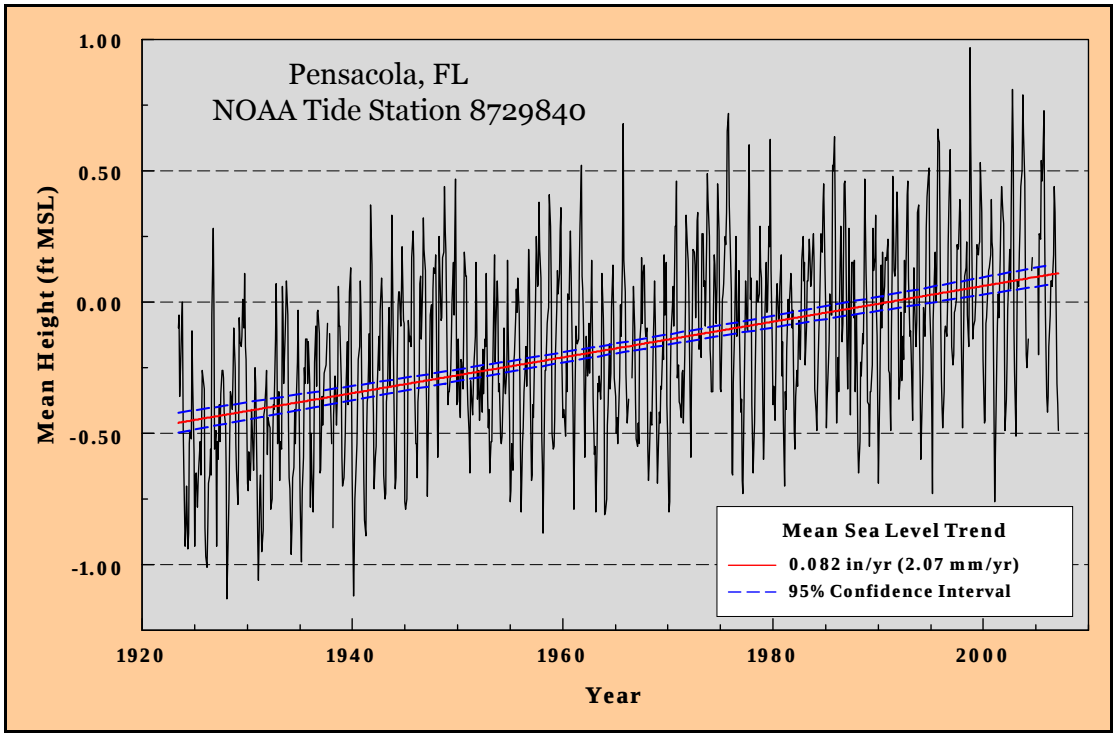

Figure 2-40. Monthly mean water level measurements at Pensacola, FL gauge 8729840, 1923 to 2007.

be controlled by anomalously high water level recorded between 1948 and 1950. Although subtle changes exist in sea-level rise rates at these sites, average rate of change is about 0.11 inches/year. This trend was used for estimating the magnitude of shoreline change associated with sea-level change throughout the study area.

Bruun Rule Calculation. Under a long-term sediment supply deficit, Bruun argues that as sea level rises, sediment must be deposited offshore equal to the amount of sea level rise to maintain a profile of equilibrium. If sediment is not available from elsewhere, it will be eroded from the adjacent beach face (see Figure 2-35). Using the equation

$$R*(h_d + f) = S*L \qquad 2.1$$

shoreline recession (R) resulting from long-term rising sea level (S) can be estimated by defining the maximum depth of exchange of littoral sediment between the nearshore and offshore (h_d) and the berm crest (f), and associated distance offshore from the berm crest (L). Based on a comparison of bathymetry data offshore central Dauphin Island and Gulf Shores, it was determined that h_d was equal to about 24 ft relative to the North American Vertical Datum (NAVD). Based on lidar and beach profile data for coastal Alabama, height of the berm crest (f) was estimated at 4.6 ft

(NAVD). Distance offshore to the 24-ft depth contour was 2,300 ft for central Dauphin Island and 1,200 ft offshore Gulf Shores. Based on the tide gauge data presented above, average sea level rise for coastal Alabama is estimated at 0.11 inches/year.

Applying appropriate values, shoreline recession on Dauphin Island that could be associated with long-term sea level rise is about 0.74 ft/yr. Based on shoreline change calculations for central Dauphin Island between 1847 and 2006, average rate of change is about 8 to 9 ft/yr, implying that sea level may be associated with about 8 to 9% of the total change signal. For the Gulf Shores area, net shoreline recession between 1847 and 2001/02 was relatively small due to a net sediment surplus in coastal Alabama, implying that that calculation may not be appropriate. Either way, sea-level rise contribution to short-term shoreline change anywhere along the Gulf shoreline is minor relative to the impact of storm waves and currents.

3 Inlet and Nearshore Morphology

The most direct method for evaluating regional sediment transport pathways and quantifying long-term net transport rates at and adjacent to an inlet is to quantify historical change in inlet and nearshore morphology with a time series of shoreline and bathymetric surveys. Shoreline data were presented in Chapter 2; this chapter focuses on evaluating bathymetry data collected between 1847 and 2002. At many entrances, survey data are lacking for drawing detailed and confident conclusions regarding the evolution of inlet systems relative to channel shoaling and adjacent beach changes. However, Mobile Pass, AL was surveyed many times over a 155-year period, providing an ample record for documenting shoal evolution, net transport quantities, and the exchange of sediment between the ebb-tidal delta and adjacent shorelines (transport pathways).

Although shoreline response adjacent to entrances contains a record of the influence of coastal processes on beach response, regional patterns of inlet and nearshore morphology better reveal dominant processes controlling the magnitude and direction of sediment transport throughout the inlet system. Analysis of long-term change in seafloor morphology provides a method of identifying net sediment transport pathways, quantifying volume change, and evaluating sediment budgets for assessing large-scale evolution of the Mobile Pass coastal depositional system.

Data Sources

Seafloor elevation measurements, compiled from historical hydrographic surveys, were used to identify seafloor morphology and change to quantify sediment transport pathways and rates relative to natural processes and engineering activities. Nine bathymetry data sets were compiled to document seafloor changes between 1847/51 and 2002. Eight of these data sets were compiled from hydrographic surveys completed by the USC&GS in 1847/51, 1892, 1908, 1917/20, 1941, 1960/61, 1970, and 1982/92, and one was compiled from digital beach profile and hydrographic survey data collected between April and July 2002 by the USACE, Mobile District (Table 3-1). Regional comparisons were made between 1847/51, 1917/20, and 1982/2002 to observe historical seafloor change; recent bathymetric changes were documented by comparing the 1982/92 and 2002 surfaces.

Furthermore, bathymetric comparisons were made for the ebb-tidal delta and adjacent shores for time periods where survey coverage was limited (1847/48 to 1892, 1892 to 1908, 1908 to 1917/20, 1917/20 to 1941, 1941 to 1960/61, 1960/61 to 1970, 1970 to 1986, and 1986 to 2002). Regional data extend from the east side of

Table 3-1. Bathymetry Source Data Characteristics

Date	Data Source	Comments and Map Numbers
1847/51	USC&GS Hydrographic Sheets 1:20,000 (H-192, H-193, H-261-1, H-261-2)	First regional bathymetric survey within the study area. 1847/48 - Offshore Mobile Bay Entrance, east side of Dauphin Island, and east of Fort Morgan (H-192). 1848 - Mobile Bay (H-193). 1851 – East of Fort Morgan to Gulf Shores (H-261-1 and H-261-2).
1892	USC&GS Hydrographic Sheets 1:20,000 (H-2124)	Bathymetric survey completed directly offshore Mobile Bay Entrance area between 5 March and 21 May 1892.
1908	USC&GS Hydrographic Sheets 1:20,000 (H-2939)	Bathymetric survey completed immediately offshore Mobile Bay Entrance area between 10-25 June 1908
1917/20	USC&GS Hydrographic Sheets 1:40,000 (H-4020, H-4023, H-4023a) 1:80,000 (H-4171)	Second regional bathymetric survey in the study area. First survey covering entire study region. May 1917 to January 1918 – Dauphin Island to Gulf Shores (H-4020, H-4023, H-4023a); 10 June to 9 November 1920 - Offshore Mobile Bay Entrance and Dauphin Island (H-4171)
1941	USC&GS Hydrographic Sheets 1:20,000 (H-6685, H-6686)	Mobile Bay Entrance (H-6685) and Offshore Mobile Bay Entrance (H-6686); 19 Sept to 28 Nov 1941.
1960/62	USC&GS Hydrographic Sheets 1:10,000 (H-8524, H-8525, H-8526, H-08560, H-8561, H-8562, H-8563, H-8573, H-8574, H-8575, H-8584, H-8587, H-8588, H-8633, H-8634, H-8635, H-8636, H-8642, H-8643, H-8644) 1:20,000 (H-8647, H-8648)	Bathymetric survey completed primarily inside Mobile Bay. 26 Jan 1960 to 21 July 1961 - Inside Mobile Bay and directly offshore entrance area (H-8524, H-8525, H-8526, H-8560, H-8561, H-8562, H-8563, H-8573, H-8574, H-8575, H-8584, H-8587, H-8588,). 24 April 1961 to 23 May 1962 - Mobile Bay (H-8633, H-8634, H-8635, H-8636, H-8642, H-8643, H-8644, H-8647, H-8648)
1970	USC&GS Hydrographic Sheets 1:20,000 (H-9109)	Bathymetric survey completed directly offshore Mobile Bay Entrance area; 10 Feb to 7 May 1970
1982/92	USC&GS Hydrographic Sheets 1:10,000 (H-10393, H-10394, H-10403, H-10423, H-10418) 1:20,000 (H-10041, H-10114, H-10151A, H-10151B, H-10179, H-10208, H-10226, H-10247, H-10261) 1:40,000 (H-10053, H-10180, H-10206, D-00078)	Third regional survey of entire study area; 8 Aug 1982 to 11 Sept 1984 - Perdido Pass and offshore (H-10041, H-10053); 1 Sept 1983 to 29 April 1985 - Gulf Shores to Perdido Pass and Offshore (H-10114); 6 Aug 1984 to 24 March 1986 - Seaward of Little Lagoon (H-10151A, H-10151B) and inside Mobile Bay (D-00078); 24 May1985 to 3 June 1987 – East of Fort Morgan and offshore (H-10179, H-10180) and offshore Petit Bois Pass (H-10206, H-10208); 17 Sept 1986 to 7 Jan 1987 - offshore Mobile Bay entrance and eastern Dauphin Island (H-10226); 18 June to 22 Dec 1987 - Offshore Dauphin Island and Petit Bois Pass (H-10247, H-10261); 13 Aug to 11 Oct 1991 - offshore Mobile Bay entrance (H-10393, H-10394, H-10403); 13 April to 11 May 1992 - offshore Mobile Bay entrance (H-10418, H-10423)
19 April to 3 July 2002	USACE, Mobile District beach profile and hydrographic channel survey data.	Beach profile data collected at 1,000 ft intervals from the western end of Dauphin Island to Perdido Pass. Data extend approximately 3 miles offshore. Hydrographic data collected in Mobile Bay Entrance area and in Mobile Bay channel.

Petit Bois Island to about 5 miles east of Perdido Pass and offshore to about the 70-ft depth contour (about 15 miles) for 1847/51, 1917/20, and 1982/92; 2002 bathymetry data extend offshore to about the 30-ft contour (about 2.5 to 4 miles).

In addition to digital hydrographic and beach profile data compiled by the National Geophysical Data Center (NGDC) and the USACE Mobile District, digital survey data were developed from scanned hydrographic survey sheets that were digitized at Applied Coastal using standardized digitizing and registration procedures (see Baker and Byrnes, 2004). All bathymetry data sets were combined with concurrent shoreline data to produce bathymetric surfaces that extend offshore from the high-water shoreline. An elevation of 4.6 ft (NAVD) was assigned to the high-water shoreline based on berm crest elevations identified in 2004 lidar data and 2002 beach profiles plotted for Dauphin Island and beaches east of Mobile Point. Ten beach profiles, spaced at equal intervals along the outer coast, were used to make the elevation determination. Comparisons with beach profile data published by University of South Alabama (http://www.southalabama.edu/cesrp/albeach.htm) documented similar elevations for the berm crest between 1992 and 2001.

Coverage. The first USC&GS bathymetric surveys for the study area were conducted between 1847 and 1851. Data extend from the east side of Petit Bois Island (about 17 miles west of Pelican Point) to about 17 miles east of Mobile Point. Longshore survey line spacing ranged from about 1,000 to 3,000 ft. The 1847/51 bathymetric data were compiled in-house from scanned USC&GS hydrographic sheets using standard digitizing procedures (Baker and Byrnes, 2004). Data coverage for each time period is illustrated in Appendix E.

Hydrographic surveys conducted by USC&GS in 1892 and 1908 were limited in extent to directly offshore Mobile Bay entrance, with data coverage extending into the bay and offshore along the ebb-tidal delta at Mobile Pass. Data density for the 1892 survey was good (Figure 3-1); however, data coverage and density in 1908 was sufficient to encompass the ebb-tidal delta for comparison with surveys from other time periods (Figure 3-2). Line and point spacing varied from 300 to 1,000 ft. These surveys provided the coverage necessary for evaluating net change on the ebb-tidal delta and seafloor adjacent to Mobile Bay entrance, and for observing channel migration patterns.

The 1917/20 survey was the second regional bathymetry data set completed for the study area. Depth measurements were compiled at Applied Coastal from scanned USC&GS hydrographic sheets. Survey map scales (1:40,000 and 1:80,000) suggested that they were primarily reconnaissance surveys used to provide a regional

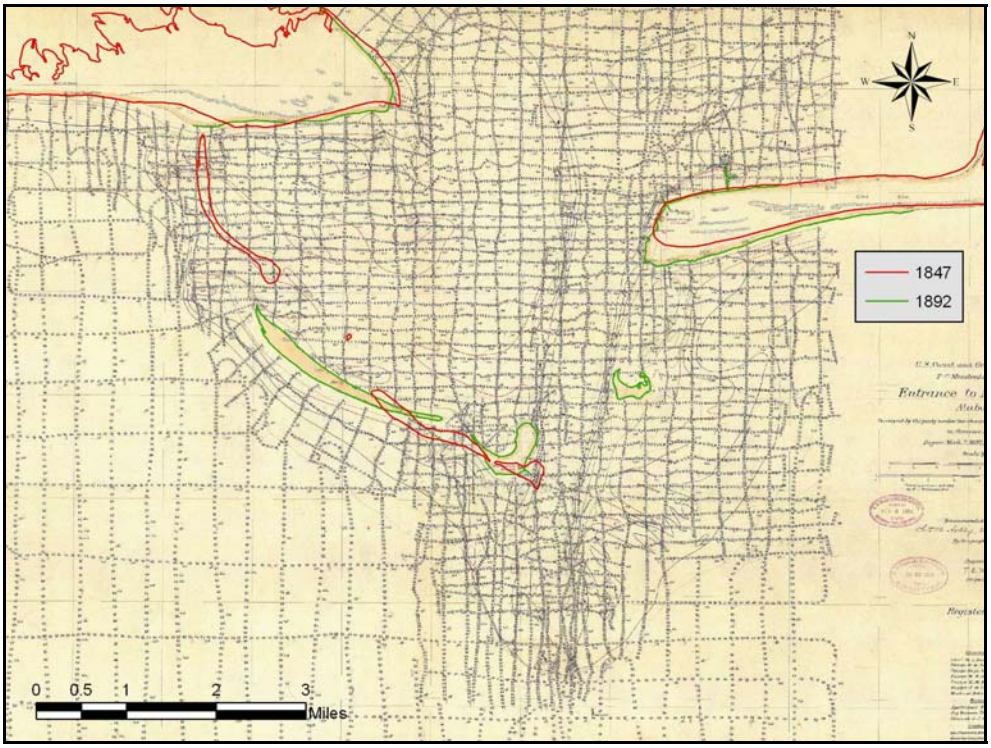

Figure 3-1. USC&GS bathymetry data coverage for the 1892 survey with overlays of the 1847 and 1892 high-water shorelines.

Figure 3-2. USC&GS bathymetry data coverage for the 1908 survey including the 1908 high-water shoreline.

overview of bathymetry. Offshore spacing of survey lines averaged about 3,000 ft, with along-line survey point spacing at about 500 feet. Line spacing within the nearshore zone and across the ebb-tidal shoals and channel at Mobile Pass ranged from about 1,000 to 2,000 ft. Depth values appear reasonable for describing bathymetric features, and the shape and location of features compared well with other surveys.

The 1941, 1960/61, and 1970 bathymetry data sets were available as digital data from the National Geophysical Data Center (NGDC). Data are limited in extent to regions directly offshore Mobile Bay entrance, with data coverage extending into the bay and offshore along the ebb-tidal delta at Mobile Pass. Data density for these data sets was quite good, with line and point spacing varying from 100 to 700 ft. Bathymetry data for these three time periods provided coverage necessary for evaluating net change on the ebb-tidal delta and seafloor adjacent to Mobile Bay entrance, and for documenting channel migration patterns.

The 1982/2002 hydrographic surveys were compiled to form the third regional data set for the study area. Data were available in digital format from the NGDC for the 1982/92 USC&GS surveys. Survey line spacing for these data was good, with lines spaced about 400 to 600 ft apart and points along survey lines collected at about 200 to 400 foot intervals. The 2002 bathymetry data were compiled from digital beach profile and hydrographic data provided by the USACE, Mobile District. Beach profile spacing was 1,000 ft along the outer coast of Dauphin Island and beaches east of Fort Morgan. Profile lines extended offshore to about the 30-ft depth contour. Hydrographic data also were collected within Mobile Bay at lines running parallel to the Mobile Ship Channel and spaced approximately 500 ft from Mobile Bay entrance north to Choctaw Point. The 2002 bathymetry data provided a good characterization of present-day conditions on the seafloor directly adjacent to Dauphin Island, east of Fort Morgan, and at the Mobile Bay entrance. The time between this survey and the 1917/20 data set (about 85 years) and the spatial extent of both surveys allow direct comparison for evaluating regional seafloor changes.

Vertical Adjustments. Because seafloor elevations are temporally inconsistent for the entire data set (i.e., reference tidal datums change with time), adjustments to depth measurements were made to bring all data to a common plane of reference (NOAA, 2003). These adjustments included changes in tidal datums due to relative sea level change and differences in reference vertical tidal datums. Vertical adjustments were made to each data set based on the time of data collection and the original vertical reference datum.

USC&GS hydrographic survey data were obtained online from the NOS hydrographic survey viewer, and all data were compiled relative to the mean low water (MLW) vertical tidal datum, the average of all the low water heights for each tidal day observed at a specific tidal station over the National Tidal Datum Epoch (NTDE; 18.6-year tidal epoch, rounded to a full year cycle, over which tide observations are recorded and reduced to establish mean values for tidal datums; NOAA, 2001). Reference tidal datum epochs are necessary for measurement standardization because of periodic and secular trends in relative sea level. The MLW tidal datum, therefore, varies with changes in sea level over time depending on the 19-year cycle referenced for measurement (Marmer, 1951; Harris, 1981; Hess, 2003; Foxgrover et al., 2004; Meyer et al., 2004). Because relative sea level changes, tidal datums at a specific site become out of date and must be updated to account for long-term vertical adjustments, such as global sea level change, subsidence, and glacial rebound (Hicks, 1981; NOAA, 2003). As such, all bathymetric data were adjusted to a common vertical reference plane (relative to 2002) to account for changing tidal datums accompanying fluctuations in relative sea level for the period of record. In addition, all depths were referenced to the North American Vertical Datum of 1988 (NAVD88) before surface modeling and change calculations commenced (Table 3-2).

Table 3-2. Vertical datum adjustments to bathymetry data for accurate comparison of surface change between 1847/51 and 2002.

Survey Date	Datum Adjustment MLW to NAVD88 (ft)	Sea Level Rise Adjustment (ft)	Total Depth Adjustment (ft)
1847/51	-0.22	-1.46	-1.68
1892	-0.22	-1.05	-1.27
1908	-0.22	-0.89	-1.11
1917/18	-0.22	-0.80	-1.02
1941	-0.22	-0.58	-0.80
1960/61	-0.22	-0.39	-0.61
1970	-0.22	-0.30	-0.52
1986	-0.22	-0.15	-0.37
1991	-0.22	-0.11	-0.33
2002*	0.00	0.00	0.00

* USACE 2002 bathymetric data were provided in digital format relative to NAVD88.

Vertical tidal datum adjustments were based on NOAA tidal benchmark #8735180 (Dauphin Island, Mobile Bay; Figure 3-3). Although sea-level observations at NOAA tidal benchmark #8729840 (Pensacola Bay; 1924 to 2002) were longer than changes recorded at the Dauphin Island gauge, USC&GS and USACE bathymetric surveys referenced the Dauphin Island gauge for tidal corrections during surveys. In addition, the USACE Biloxi gauge recorded water levels since about 1900 and

indicated a sea-level rise trend consistent with that recorded at Dauphin Island (0.11 inches/year; see Figure 2-37). Finally, the Dauphin Island gauge was closest to offshore survey data in the Gulf of Mexico and centered within the study area. Table 3-2 documents vertical adjustments used to bring historical bathymetric surfaces to the same vertical reference datum used for the 2002 bathymetric survey. The unit of measure for all surfaces is feet, and final values were rounded to tenths of feet before cut and fill computations were completed.

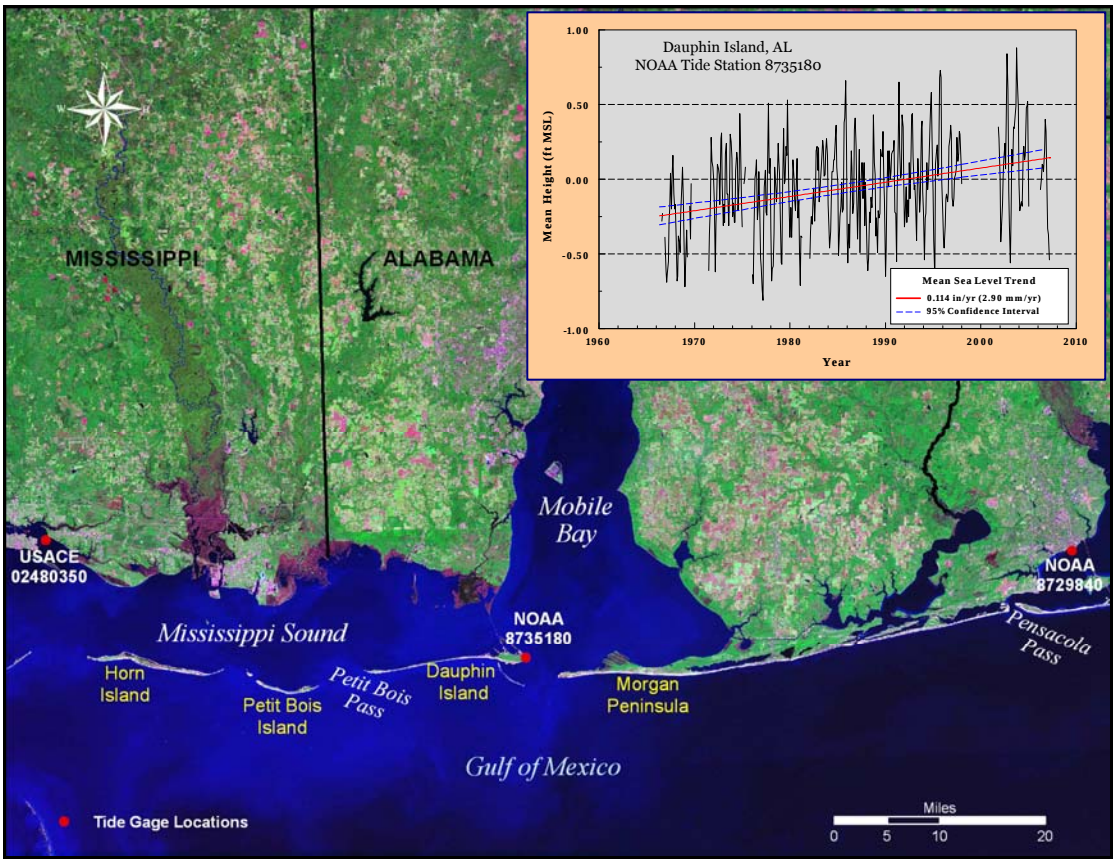

Figure 3-3. Locations of tidal benchmarks used for vertical adjustment determination.

NAVD Reference Elevation. From the shoreline to a distance offshore of about 500 to 800 ft, bathymetry data do not exist for most surveys. To better estimate beach and nearshore profile shape for change comparisons, the position of the 0 NAVD88 line was determined using documented distances between the position of NAVD88 and the position of the high-water line (HWL) on recent USACE lidar and beach profile surveys. The average horizontal position of the 0 NAVD88 line (0.23 ft MLLW) was approximately 100 ft seaward of the HWL. To verify the accuracy of this relationship, an NAVD88 line was established about 100 ft seaward of the HWL for the 2002 survey. Two surfaces were created; one included beach and nearshore

elevations from the original survey, and the other used the HWL, estimated 0 NAVD88 line, and offshore data deeper than 8 ft from the 2002 survey. Cross-sections were plotted for each surface to compare beach shape obtained using each method. Figure 3-4 illustrates a representative profile showing the similarity between estimated profile shape and measurements. After completing many similar comparisons, it was determined that the described technique for estimating profile shape between the HWL and offshore bathymetry data provided a good estimate of profile shape in the absence of survey data.

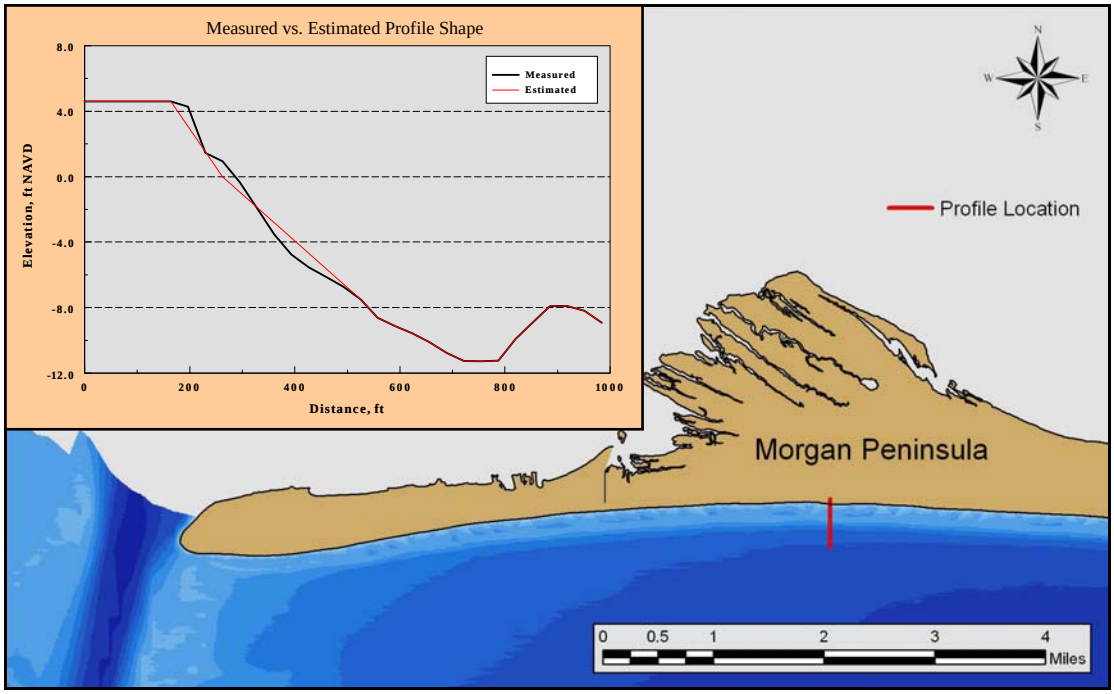

Figure 3-4. Comparison of measured profile elevations versus estimated profile shape using HWL to NAVD distance relationship derived from lidar and beach profile data.

Measurement Uncertainty

As with shoreline data, measurements of seafloor elevation contain inherent uncertainties associated with data acquisition and compilation. It is important to quantify limitations in survey measurements and document potential systematic errors that can be eliminated during quality control procedures (Byrnes et al., 2002). Most measurement errors associated with present and past surveys are considered random over the survey area. As such, random errors cancel relative to change calculations derived from two surfaces. A method for determining limits of reliability for erosion and accretion is to quantify measurement uncertainty associated with bathymetric surfaces. Interpolation between measured points includes a degree of uncertainty associated with terrain irregularity and data density. The density of

bathymetry data, survey line orientation, and the magnitude and frequency of terrain irregularities are the most important factors influencing uncertainties in volume change calculations between two bathymetric surfaces (Byrnes et al., 2002). Volume uncertainty relative to terrain irregularities and data density can be determined by comparing surface characteristics at adjacent survey lines. Large variations in depth between survey lines (i.e., few data points describing variable bathymetry) will result in large uncertainty calculations between lines. Additionally, surveys with track lines oriented parallel to major geomorphic features can result in large uncertainty calculations between lines. This computation provides the best estimate of uncertainty for gauging the significance of volume change calculations between two surfaces.

Uncertainty estimates were calculated for the all bathymetric surfaces using the methods outlined in Byrnes et al. (2002). Multiple sets of line pairs were compared for each time period to represent terrain variability. Line pairs were chosen that would accurately represent track line spacing for each survey and the irregularity of prominent geomorphic features in the region. Lines were established for each time period to overlay survey lines for that year. Bathymetry data were extracted along each line to calculate variations in elevation between line pairs. Depths were extracted at 10-ft intervals and the absolute value of the differences was averaged to calculate potential uncertainty for each pair.

Results of uncertainty calculations are summarized in Tables 3-3 and 3-4. Estimates were generated for each bathymetric surface, with particular emphasis on the ebb shoal/channel region. As expected, areas with greatest uncertainty were located along the channel and ebb-tidal delta at Mobile Pass. To identify potential uncertainty associated with sediment transport calculations, a separate calculation was made for the channel/ebb shoal areas. In general, potential depth uncertainty ranged from ±0.54 to 1.30 ft for calculations made across the entire surface, and from ±1.43 to 2.69 ft for the ebb shoal/channel area specifically (Table 3-3). Combining this information to gauge the impact of potential uncertainties associated with volume change calculations derived from these surfaces resulted in a root-mean-square variation of ±1.22 ft (entire surface) and ±2.59 ft (ebb-tidal delta) for the 1847/51 to 1917/20, ±0.8 ft (entire surface) and ±3.1 ft (ebb-tidal delta) for the 1917/20 to 1982/92 change surface, and ±1.6 ft (entire area) and ±2.9 ft (ebb–tidal delta) for the 1982/92 to 2002 change surface (Table 3-4). Based on the results of this uncertainty analysis, ±2 ft was used to delineate areas considered to represent no determinable change.

Table 3-3. Potential uncertainty for bathymetry surfaces from western Dauphin Island to Perdido Pass, AL.

	Entire Surface (ft)	Ebb Shoal/Channel (ft)
1847/51	±0.89	±1.78
1892	Ebb-shoal survey	±2.24
1908	Ebb-shoal survey	±2.60
1917/20	±0.84	±1.88
1941	Ebb-shoal survey	±2.69
1960/61	Ebb-shoal survey	±2.30
1970	Ebb-shoal survey	±2.50
1982/92	±0.54	±1.43
2002	±1.30	±2.59

Table 3-4. Maximum root-mean-square potential uncertainty for bathymetric change data from western Dauphin Island to Perdido Pass, AL (units in feet).

	1892	1908	1917/20	1941	1960/61	1970	1982/92	2002
1847/51	n/a [1] ±2.86 [2]	n/a ±3.15	±1.22 ±2.59	n/a ±3.22	n/a ±3.22	n/a ±3.07	±1.04 ±2.28	±1.58 ±3.14
1892		n/a ±3.43	n/a ±2.92	n/a ±3.50	n/a ±3.21	n/a ±3.36	n/a ±2.66	n/a ±3.42
1908			n/a ±3.21	n/a ±3.74	n/a ±3.47	n/a ±3.61	n/a ±2.97	n/a ±3.67
1917/20				n/a ±3.28	n/a ±2.97	n/a ±3.13	±1.00 ±2.36	±1.55 ±3.20
1941					n/a ±3.54	n/a ±3.67	n/a ±3.05	n/a ±3.73
1960/61						n/a ±3.40	n/a ±2.71	n/a ±3.46
1970							n/a ±2.22	n/a ±3.60
1982/92								±1.41 ±2.96

[1]Entire Surface, [2]Ebb Shoal/Channel

Surface Modeling

Digitized soundings and shorelines were used to create digital elevation models of the seafloor for the period 1847/51 to 1982/2002. The Triangulated Irregular Network (TIN) method was used in this study to form a surface of continuous connected triangular planes based on irregular points (Petrie, 1991). The elevation of each point in the model is determined by solving equations for its horizontal location on the triangulated surface. Therefore, only points existing in the original data sources are used to create the surface model, as opposed to grid models which interpolate evenly spaced points from original data. TIN model surfaces were used

for all calculations of bathymetric volumes and change; however, grid surfaces were generated for graphic display purposes.

TIN polygon volume is determined by summing calculated volumes for each triangle, or portion thereof, relative to a specified reference height and polygon boundary. Triangle volumes above and/or below the reference height are calculated for a defined polygon to compute net differences between surfaces. To calculate volume differences across two TIN surfaces, every data point from the primary surface is projected onto the secondary surface and the *z*-value of the secondary surface is subtracted from the *z*-value of the original point (Petrie, 1991). Likewise, every data point from the secondary surface is projected onto the primary surface and the *z*-values subtracted. The resultant difference TIN contains zero contours that represent the intersection between the two original TIN surfaces. The zero contours are added as breaklines to the difference TIN, and the resulting triangles are classified as above, below, or equal to zero. Volume change is calculated by summing the volume of each triangle region.

Regional Morphology

Nearshore sediment transport processes influence the evolution of shelf sedimentary environments to varying degrees depending on temporal and spatial response scales. Although micro-scale processes, such as turbulence and individual wave orbital velocities, determine the magnitude and direction of individual grain motion, variations in micro-scale processes are considered noise at regional-scale and only contribute to coastal response in an average way. By definition, regional-scale geomorphic change refers to the evolution of depositional environments for large coastal reaches (10 km or greater) over extended time periods (decades or greater) (Larson and Kraus 1995). An underlying premise for modeling long-term morphologic change is that a state of dynamic equilibrium is approached as a final stage of coastal evolution. However, the interaction between the scale of response and forces causing change often results in a net sediment deficit or surplus within a system, creating disequilibrium. This process defines the evolution of coastal depositional systems.

Three regional bathymetric surfaces were established for the Alabama coastal zone for the periods 1847/51, 1917/20, and 1982/2002 to describe large-scale variations in coastal and nearshore morphology. Sediment transport patterns and processes in the vicinity of the Mobile Pass ebb-tidal delta and outer bar channel are of primary interest; however, regional morphology and change provide insight regarding dominant transport pathways relative to sediment sources and sinks.

1847/51 Bathymetric Surface. Bathymetry data for the period 1847/51 were combined with 1847/48 shoreline data to create a continuous surface from the shoreline seaward to about the 60-ft depth contour (NAVD). The most prominent geomorphic feature throughout the study area is the ebb-tidal delta associated with Main Pass at Mobile Bay entrance (Figure 3-5A). A series of well-defined ebb shoals (primarily on the western side of the entrance) and a prominent channel dominate the entrance area to a distance approximately 6 to 7 miles offshore. The main orientation of the channel is north-south; however, the distal portion of the channel through the outer bar exits the coast in a northwest-southeast direction. Overall deposition on the ebb-tidal delta is skewed to the west. This observation is consistent with other geomorphic evidence documenting net westward sediment transport along the shelf and shoreline in coastal Alabama.

The linear sand shoal east of Main Pass and parallel to the channel (locally called Dixie Bar) represents a zone of net deposition supplied by longshore sand transport from the east. Channel currents create a dynamic diversion to east-west transport (Todd, 1968), resulting in a shoal that parallels the channel to the seaward margin of the ebb-tidal delta (Figure 3-5A). Extensive subaerial and subaqueous islands and shoals have formed and dissipated during the evolution of the ebb-tidal shoal (Hummell, 1990). All but one of these deposits resides west of Main Pass, supporting the hypothesis of a dominant direction of net transport to the west. Petit Bois Pass, at the western end of Dauphin Island, illustrates the same pattern of deposition, where the ebb shoals and channel are oriented to the west. Between the passes, offshore contours appear relatively straight and parallel to shoreline orientation.

East of Mobile Pass, shelf bathymetry is dominated by a large shore-oblique sand shoal (northeast-southwest orientation) just west of Little Lagoon, a relatively steep shoreface west of this deposit, and numerous northwest-southeast trending sand ridges to the east (McBride and Byrnes, 1995; McBride et al., 1999). The prominent sand shoal extending southwest from Little Lagoon reaches approximately 6 miles offshore and has topographic relief of about 20 ft. The steep shoreface and deep trough west of this sand ridge may be the remnant of a Pleistocene paleochannel for Mobile Bay (Hummell and Parker, 1995). However, Parker et al. (1997) show with vibracore data that the extensive sand shoal east of this bathymetric low contains Holocene sediment, indicating a depositional process of formation during modern sea level rise.

1917/20 Bathymetric Surface. Bathymetry data for the period 1917/20 were combined with the 1917/18 shoreline data to create a continuous surface from the shoreline seaward to about the 100-ft depth contour (NAVD). Most characteristics of

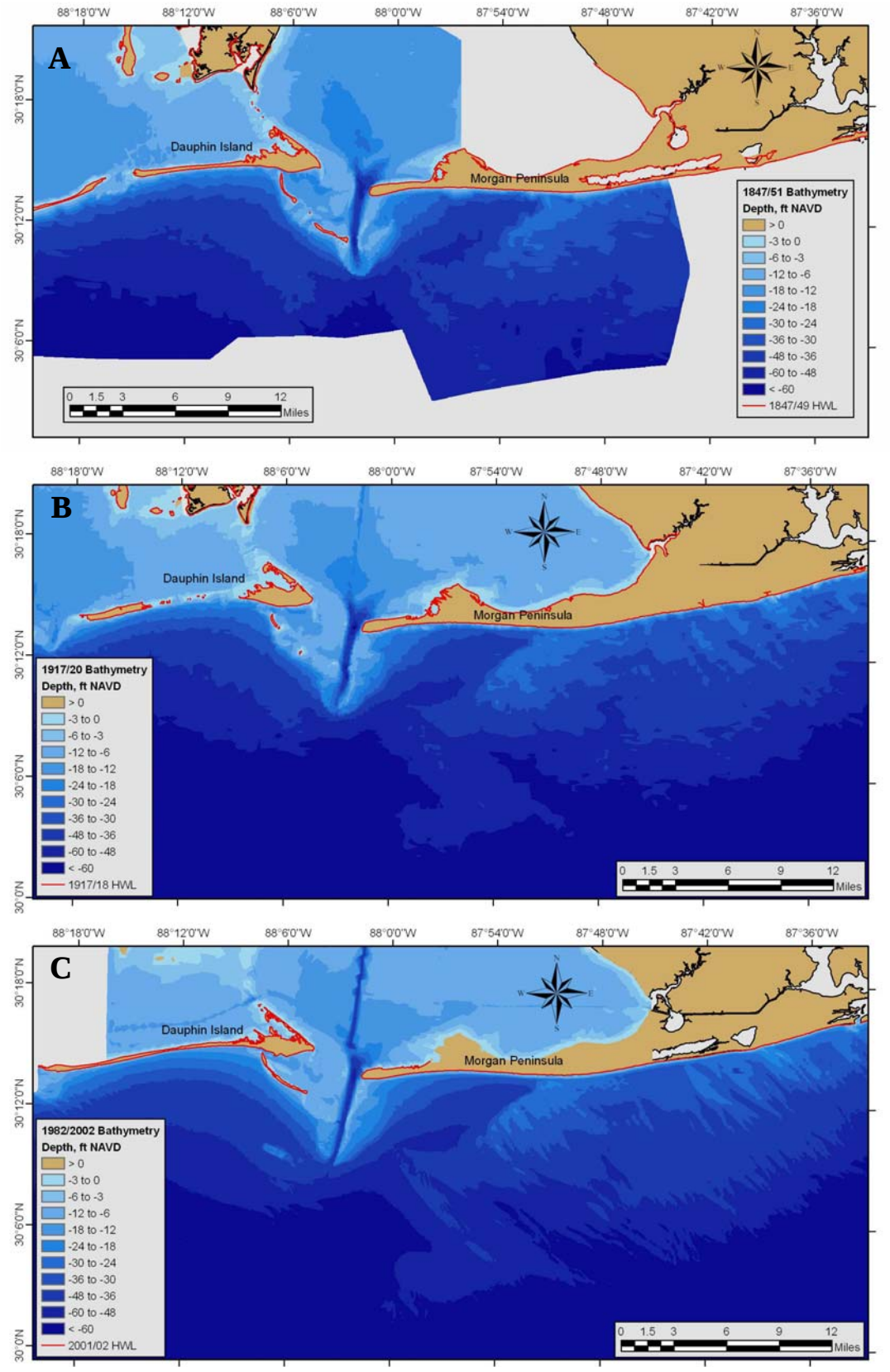

Figure 3-5. Regional bathymetric surfaces: A) 1847/51, B) 1917/20, C) 1982/2002.

the shelf surface are similar to those identified from the 1847/51 bathymetry. There are three notable exceptions: 1) Sand and Pelican Islands, and central Dauphin Island, were decimated by the July 1916 hurricane; 2) the channel crossing the outer bar at Mobile Pass shifted west and was oriented north-south; and 3) the ebb-tidal delta at Petit Bois Pass was much better defined than in the mid-1800s (Figure 3-5B). Channel dredging across the outer bar was initiated in 1904, so by 1917, a 30-ft deep by 300-ft wide channel was evident in the lower Bay and across the outer bar.

Dixie Bar, on the east side of Main Pass and parallel to the channel, documented changes by 1917/20 as well. Natural channel migration to the west was forced by large quantities of littoral sand being transported from the east and down the east margin of the channel, filling the old channel location as sand was diverted south by swift ebbing currents. As described previously, channel currents create a dynamic diversion to east-west transport (Todd, 1968), resulting in a shoal that parallels the channel to the seaward extent of the ebb-tidal delta. The large shore-oblique sand shoal on the shelf just west of Little Lagoon is better defined than that illustrated in 1847/51, but the same general characteristics prevail.

1982/2002 Bathymetric Surface. Bathymetric surface characteristics for the period 1982/2002 are similar to the 1917/20 surface with a few exceptions (Figure 3-5C). First, geomorphic features are better defined because the number of data points is larger for the most recent time period. The general shape and position of shoals is consistent for all three regional surfaces, although significant changes have occurred since 1917/20. Second, deposition along the western end of Dauphin Island has caused rapid growth of the beach to the west for the entire period of record (see Byrnes et al., 1991; Morton, 2007). Third, an elongated sediment shoal was deposited to the southwest of the ebb-tidal delta by the USACE between 1988 and 1990. Approximately 17 million cy of sediment was deposited about 6 miles southwest of the Mobile Bay entrance in about 45-ft water depth as an experimental berm for dissipating wave energy (Hands, 1991; Hands and Allison, 1991; Kraus et al., 1991; Hands, 1994). Known as the Mobile Outer Mound, sediment accumulation thickness was about 20 ft. Lastly, as the ebb-tidal delta evolved in response to natural processes and dredging activities, the subaerial extent of Pelican Island has increased, accompanied with a general decrease in water depth over the west lobe of the ebb-tidal delta. Island expansion, breach closure, and ebb-tidal delta growth since 1847/51 attest to the large supply of sand from the east, even though channel dredging across the outer bar commenced in 1904.

Although the Mobile Outer Bar Channel has been on a relatively routine maintenance dredging schedule since 1917/20, the outer margin of the ebb shoal was not displaced

seaward of the 1847/48 position by 1982/2002, suggesting that channel deepening may not have had a significant impact on shoal evolution or channel hydraulics during this 80-year period. This finding is in contrast to the impact of jetty construction on ebb-shoal evolution at structured entrances (e.g., Dean and Perlin, 1977; Kraus, 2000; Byrnes and Baker, 2003; Byrnes et al., 2007). The channel-margin shoal east of the pass remains prominent in 1982/2002, and sand deposits on the dominant western portion of the ebb shoal have become more extensive. Pelican Island is well-defined and appears to be bypassing sand to the beach along eastern Dauphin Island. Continued sand deposition along western Dauphin Island indicates predominant east to west sediment transport (Figure 3-5C).

Shelf morphology between Perdido Pass and Mobile Pass is well-defined for the modern surface by three prominent features: 1) a large northeast-southwest shoal trending seaward from the Little Lagoon area; 2) a substantial nearshore bathymetric low and shoreface steepening west of the shoal; and 3) a well-defined sand ridge field (northwest-southeast trending) on and east of the large sand shoal, extending seaward to about 65-ft water depth. The entire shelf surface in this area is composed of clean, medium-to-fine sand, the primary source of sand for beaches to the west and the ebb-tidal delta at Mobile Bay Entrance.

Shoal and Channel Evolution

As described in the previous chapter on shoreline dynamics, islands on the Mobile Pass ebb-tidal delta have experienced a sequence of changes since 1847/51, primarily driven by storms. This included the presence of Pelican and Sand Islands in 1847/51 through a destructive phase in 1917/20, when only a small portion of Pelican Island was present, to the extensive island that was mapped in 2002 and still exists in 2007. The addition of bathymetry data to shoreline positions provides a three-dimensional view of system evolution. The following discussion describes a series of surveys at and adjacent to Mobile Pass that document changes recorded during the past 159 years. As detailed in Chapter 1, channel dredging across the outer bar (southern end of the ebb-tidal delta) has been active since 1904. Most new work and maintenance dredging material has been placed slightly south and west of the offshore extent of the ebb-tidal delta.

1847/48. The initial bathymetric survey for the Mobile Pass ebb-tidal delta illustrates a deep and well-developed channel (Figure 3-6). Maximum depth across the outer bar was about 21 ft; however, natural depths in the rest of the channel were as great as 60 ft. At this time, flow from the channel exited to the Gulf in a south-southeast direction. Sand deposits on the east lobe of the ebb-tidal delta included a

channel margin bar referred to as East Bank (presently referred to as Dixie Bar) and South East Shoal near the distal end of the channel (see Figure 1-13). Sand bypassing from east to west across the outer bar was active at an average depth of about 20 ft.

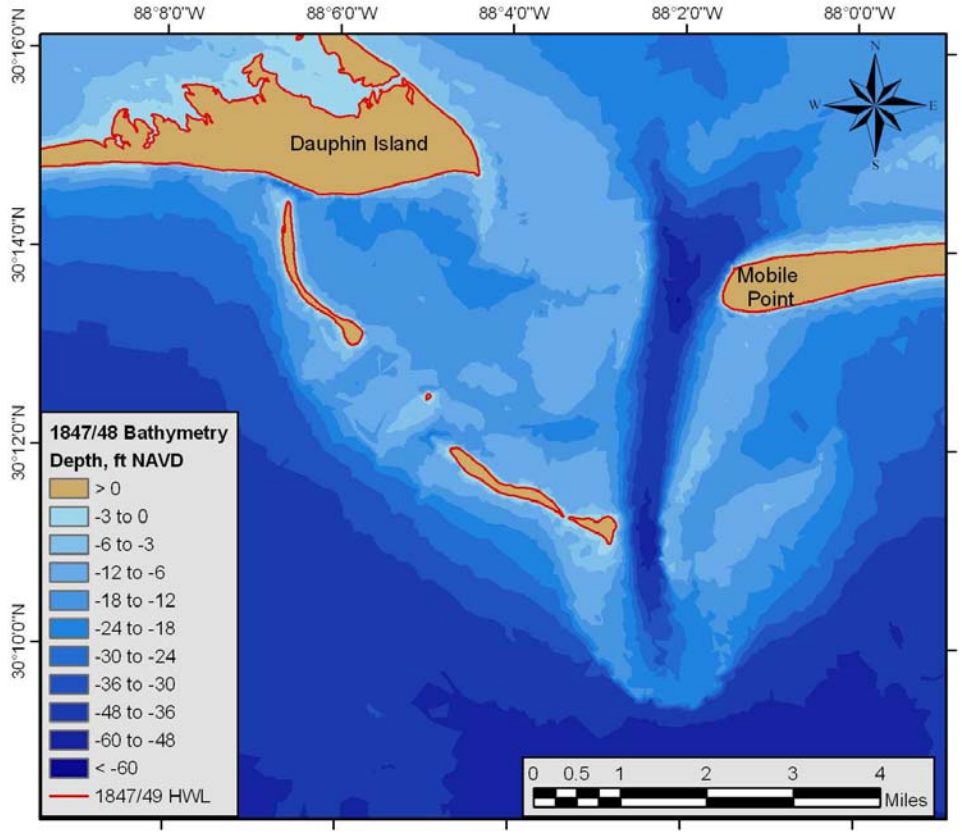

Figure 3-6. Bathymetric surface for Mobile Pass ebb-tidal delta and adjacent shores, 1847/48.

Sand deposits on the west lobe of the ebb-tidal delta were extensive, including Pelican and Sand Islands, but it appears that storm processes around this time may have created a pair of surge channels on the southeast and northwest ends of these islands, respectively. A small channel was located between Pelican and Dauphin Islands, and the presence of shoals off the northwestern end of Pelican Island and just west of this point along Dauphin Island indicates that sand bypassing from the ebb-tidal delta to the island was active.

1892. By 1868, shoreline data indicated that Pelican Island had migrated onto eastern Dauphin Island, creating a large sand protuberance that was reworked by littoral processes over the next few decades (see Figure 2-6). The 1892 bathymetric surface recorded the remnant of mass sand deposition landward of the location of Pelican Island in 1847/48, and the absence of Pelican Island on the ebb-tidal delta. However, Sand Island was once again extensive, indicating the effectiveness of sand

transfer from east-to-west across the navigation channel (Figure 3-7). Furthermore, an island formed on the east lobe of the ebb-tidal delta on the channel margin bar, referred to as Dixie Island. West- and south-directed transport east of the channel created this island and had naturally forced the channel to the west of its location in 1847/48. Southward transport of littoral material along the eastern channel margin also forced the outer bar channel to reorient to a more southward direction. Depths across the outer bar remained approximately 20 to 25 ft deep, and sand bypassing appeared active.

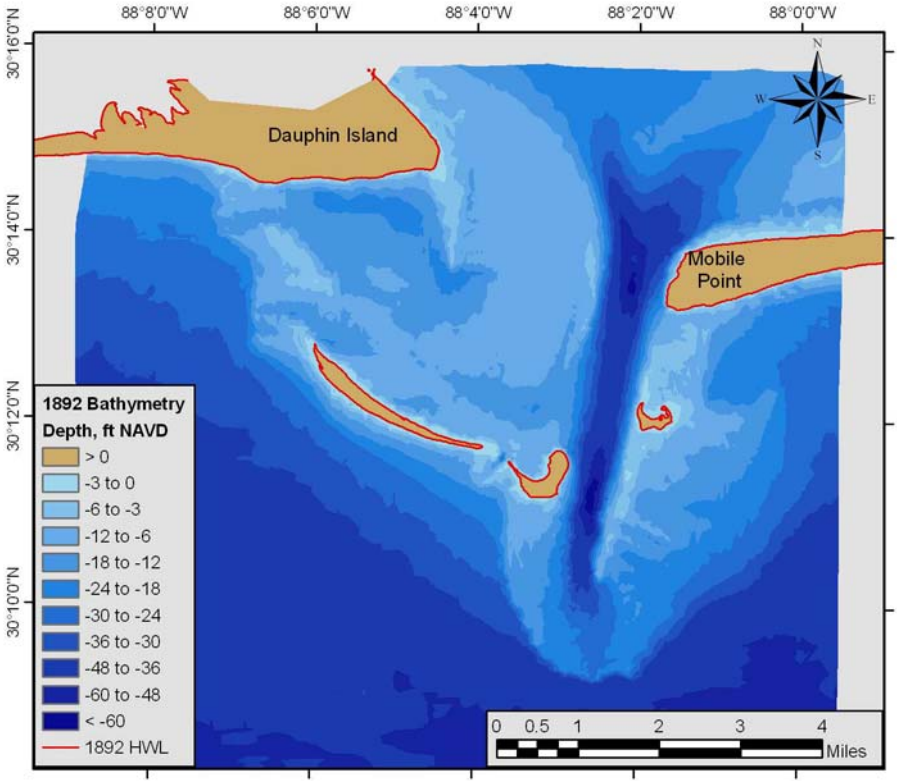

Figure 3-7. Bathymetric surface for Mobile Pass ebb-tidal delta and adjacent shores, 1892.

1908. The 1908 bathymetric surface was the first surveyed after channel dredging was initiated in 1904. A 30-ft deep channel was constructed across the outer bar as shown in Figure 3-8. This illustrates the general location where dredging has been required since 1904; most of the remaining channel naturally scours. Channel margin sedimentation along the east lobe of the ebb-tidal delta continued to extend to the south as the channel gorge naturally migrated to the west. Dixie Island eroded between 1892 and 1908, leaving behind what is now known as Dixie Bar.

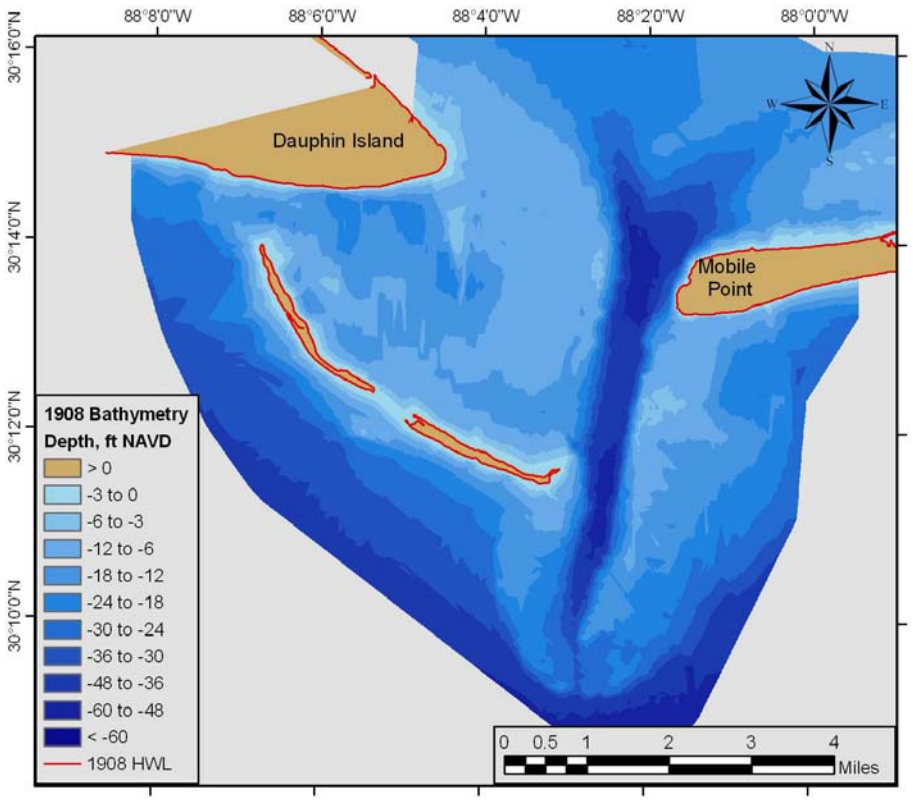

Figure 3-8. Bathymetric surface for Mobile Pass ebb-tidal delta and adjacent shores, 1908.

To the west of the channel, Pelican and Sand Islands developed into prominent subaerial features that are products of net movement of sand from east to west across the channel. Pelican Island remains a fair distance from Dauphin Island, separated by Pelican Pass, but net migration and growth of the island to the northwest emphasizes the direction of net transport throughout this system that provides a continuous source of sand to Dauphin Island.

1917/20. On July 5, 1916, a Category 3 hurricane crossed Ship Island with sustained winds of 105 knots. Mobile Pass and Dauphin Island bore the brunt of storm winds and waves from the northeast quadrant. The storm was particularly devastating to southwestern Alabama, resulting in large-scale breaching of Dauphin Island (see Figure 3-5) and nearly complete erosion and dispersal of sand on Pelican and Sand Islands (Figure 3-9). Only the northwestern portion of Pelican Island remained intact; however, the entire platform upon which both islands developed was largely unchanged.

Sand from the eastern lobe of the ebb-tidal delta was pushed to the west during the storm, creating a scalloped pattern along the eastern margin of the channel where sand cascaded into the channel. The channel margin shoal also extended to the

south filling what appears to be the location of the 1913 channel. As early as 1912, the USACE was aware of natural channel migration at Mobile Pass, and the channel was relocated 700 ft to the west across the outer mouth bar in 1913 because " shoals were forming from the east more rapidly than the dredge could remove them" (see Appendix B). In August, 1917, new project dimensions were authorized for the channel, and by 1924, a channel 33-ft deep and 450-ft wide was built to accommodate commercial vessel needs.

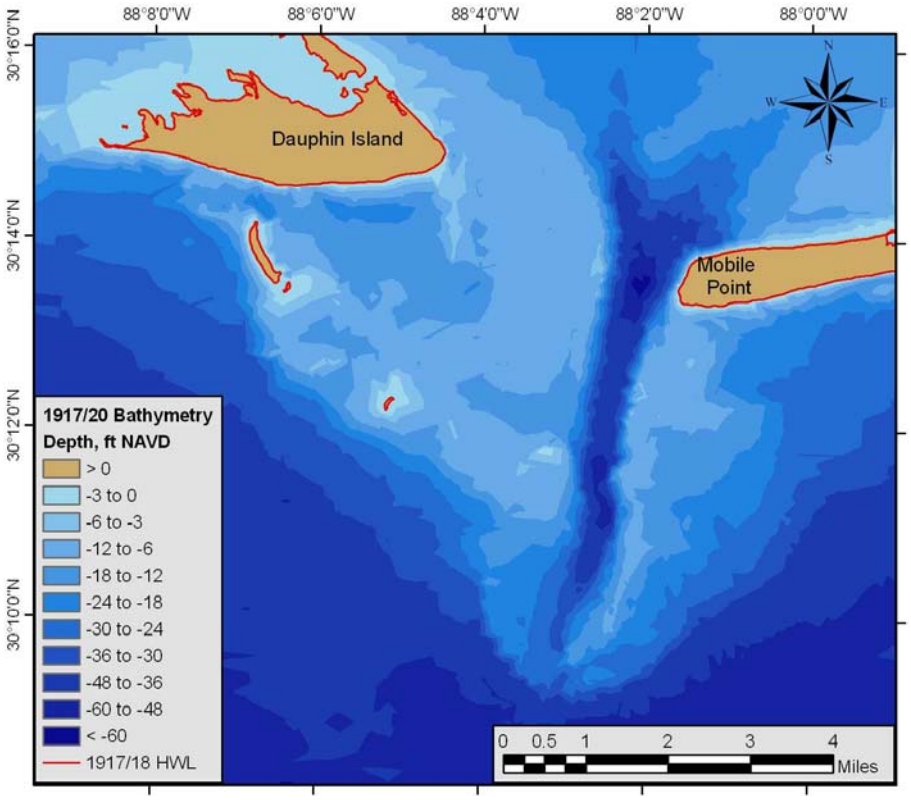

Figure 3-9. Bathymetric surface for Mobile Pass ebb-tidal delta and adjacent shores, 1917/20.

1941. By 1941, a channel 36-ft deep and 450-ft wide was well-maintained for a distance of about 1.7 miles across the outer bar (Figure 3-10). An area of deeper water existed east of the northern extent of the dredged channel as littoral sand transport from Mobile Point south along the channel margin bar continued to fill the eastern margin of the westward migrating channel. It appears that natural channel migration to the west created this offset in channel orientation relative to the position of the dredged channel. Maintenance dredging may have intercepted sand transported from the channel margin bar to this area, preventing channel infilling to occur. Alternately, channel overdredging along the northeastern margin of the maintained channel may have been imposed to manage high rates of shoaling from

the channel margin bar. However, dredging records do not indicate any overdredging measures.

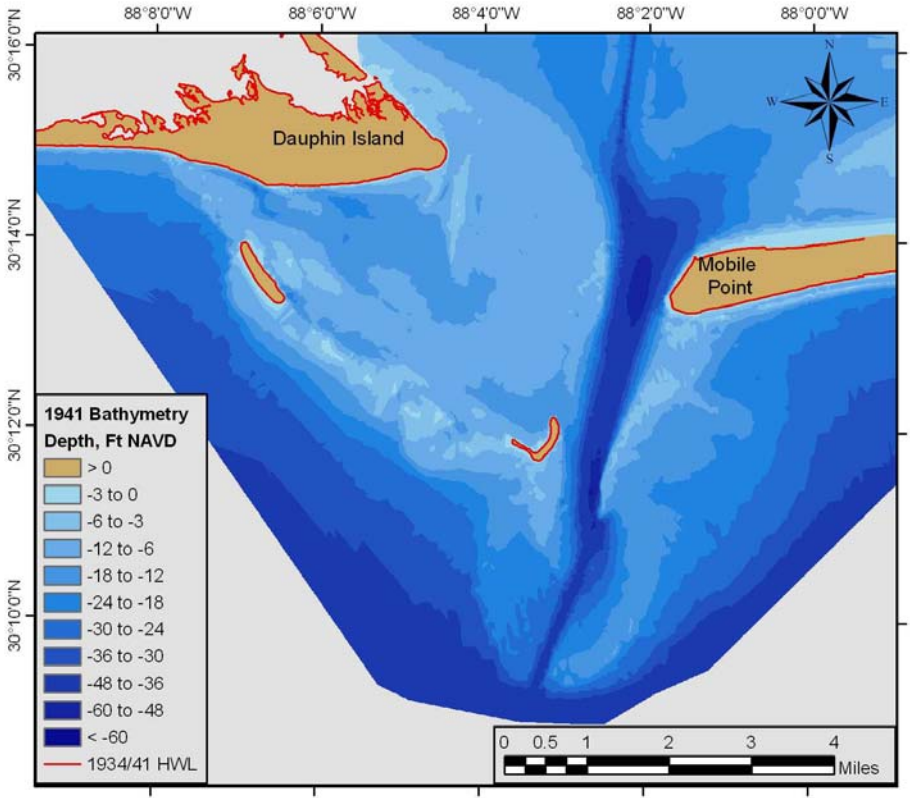

Figure 3-10. Bathymetric surface for Mobile Pass ebb-tidal delta and adjacent shores, 1941.

Although this apparent barrier to littoral transport from the east was well established, islands and shoals on the west lobe of the ebb-tidal delta illustrated growth between 1917/20 and 1941. Sand Island reformed just west of the point on the channel margin bar to the east where rapid sedimentation was occurring. The channel offset at this point may have provided an opportunity for bypassing sand where the northern extent of the east shoal overlaps the southern extent of the west shoal (Figure 3-10). Sand shoals between Sand and Pelican Islands are shallow compared with 1917/20. Furthermore, the shoal between Pelican Island and Dauphin Island has nearly sealed Pelican Pass, creating a conduit for sand transport between Pelican and Dauphin Islands. Regardless of dredging activities, sand from the east is being supplied to shoal and island deposits west of the channel.

1960/61. This survey did not include the western portion of the ebb-tidal delta where sand is transported from the shoal to Dauphin Island. However, the remaining portion of the delta is well-represented (Figure 3-11). The general shape

of the channel is similar to 1941 with a prominent offset just south of Sand Island Lighthouse. By 1961, the outer bar channel was maintained at a width of 450 ft and a controlling depth of 38 ft.

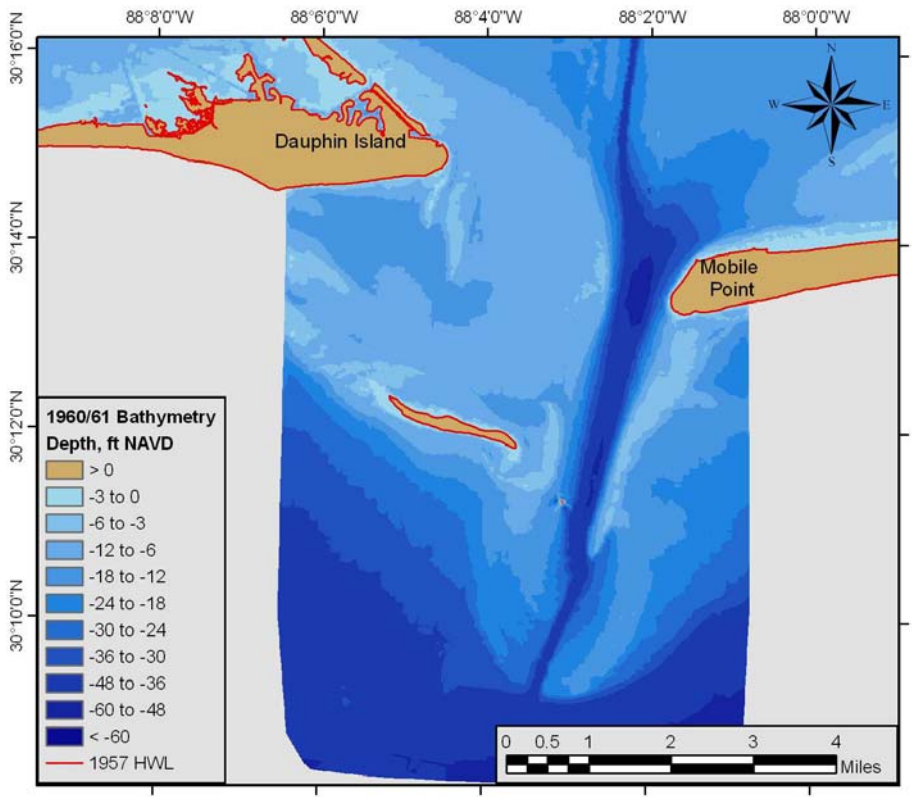

Figure 3-11. Bathymetric surface for Mobile Pass ebb-tidal delta, 1960/61.

Two major morphologic differences exist between the 1941 and 1960/61 surfaces. First, Sand Island and the shoals surrounding Sand Island are larger and shallower than in 1941. In a strongly net west-directed sand transport system, growth of Sand Island and surrounding shoals requires sand bypassing from the east. Second, the channel margin shoal east of the channel expanded to the south supplied by net littoral transport from Mobile Point. The offset between east and west lobes of the ebb-tidal delta remains in tact in 1960/61, providing a potential sand bypassing mechanism. The deeper area east of the maintained channel has filled slightly since 1941. A third observation is the westward deflection of the 35-ft depth contour due west of the maintained channel entrance to the Gulf. Deposition in this area likely is related to disposal of new and maintenance dredging material from the outer bar channel. Sediment from this disposal area may be a source of sand to islands and shoals on the west lobe as well.

1970. By 1965, the channel had been deepened to 42 ft and widened to 600 ft. An increase in channel width is illustrated on the 1970 surface (Figure 3-12). Channel shape remains similar to that depicted on the 1960/61 surface. However, the channel margin bar on the east side of the channel continues to expand to the south as littoral sand from Mobile Point supplies bar growth and bypassing to the west. Alignment of the channel margin bar along the east side of the natural channel with the western margin of the dredged navigation channel across the outer bar continues to be a location for shoal growth and migration on the west lobe of the ebb-tidal delta.

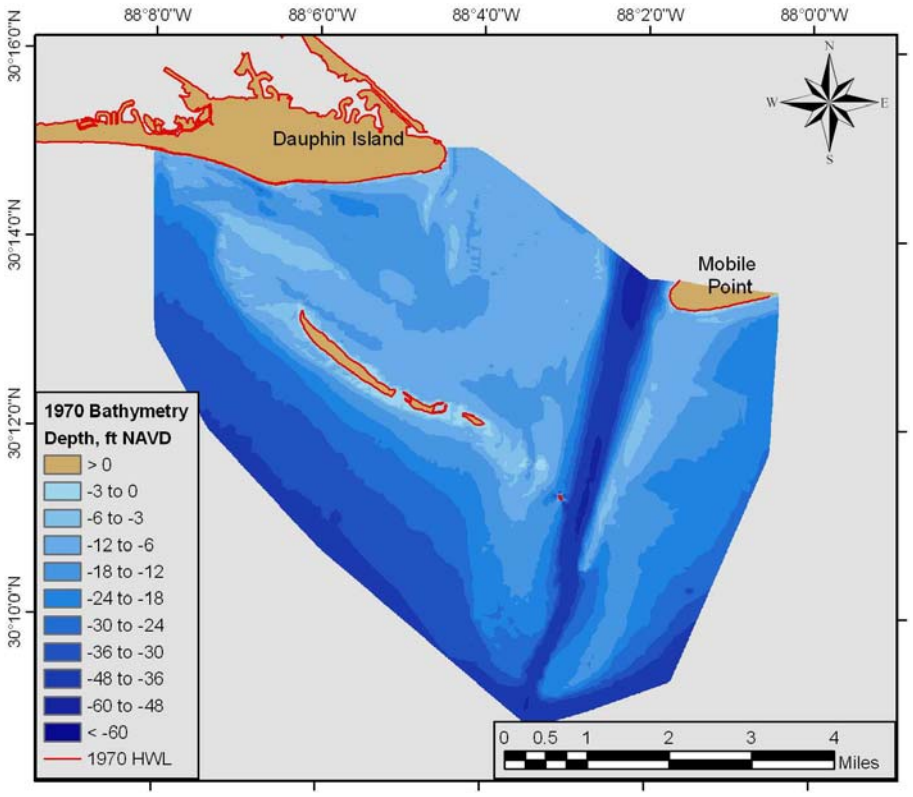

Figure 3-12. Bathymetric surface for Mobile Pass ebb-tidal delta and adjacent shores, 1970.

Sand Island expanded and migrated to the northwest, and shoals surrounding the island grew as well. Pelican Pass reformed since 1941, but sand shoals northwest of Sand Island continue to feed sand to Dauphin Island (Figure 3-12). This is illustrated by the presence of an attachment bar between Pelican Pass and Dauphin Island near the western extent of data coverage. The western lobe of the ebb-tidal delta continued to grow with sand supplied from east of the channel.

1986/87. Ebb-shoal morphology for the 1986/87 period illustrates substantial changes relative to the 1970 surface. Two major hurricanes (*Fredric* [1979] and *Elena* [1985]), and Tropical Storm *Juan* (1985), produced major changes along the

southeastern Alabama coast (Schramm et al., 1980; Froede, 2006a; Morton, 2007). In fact, channel shoaling was so extensive during Hurricane *Elena* that emergency dredging was authorized between August and October, 1985 to remove 1.39 million cy of sand from the outer bar channel. The channel offset that existed at the juncture of the natural channel and the maintained channel in 1970 was filled with sand from the east lobe of the ebb shoal and littoral sand transported south along the channel margin bar (Figure 3-13). The 18- and 24-ft depth contours on both sides of the maintained channel were skewed to the west as a result of dominant southeast to northwest storm waves and currents.

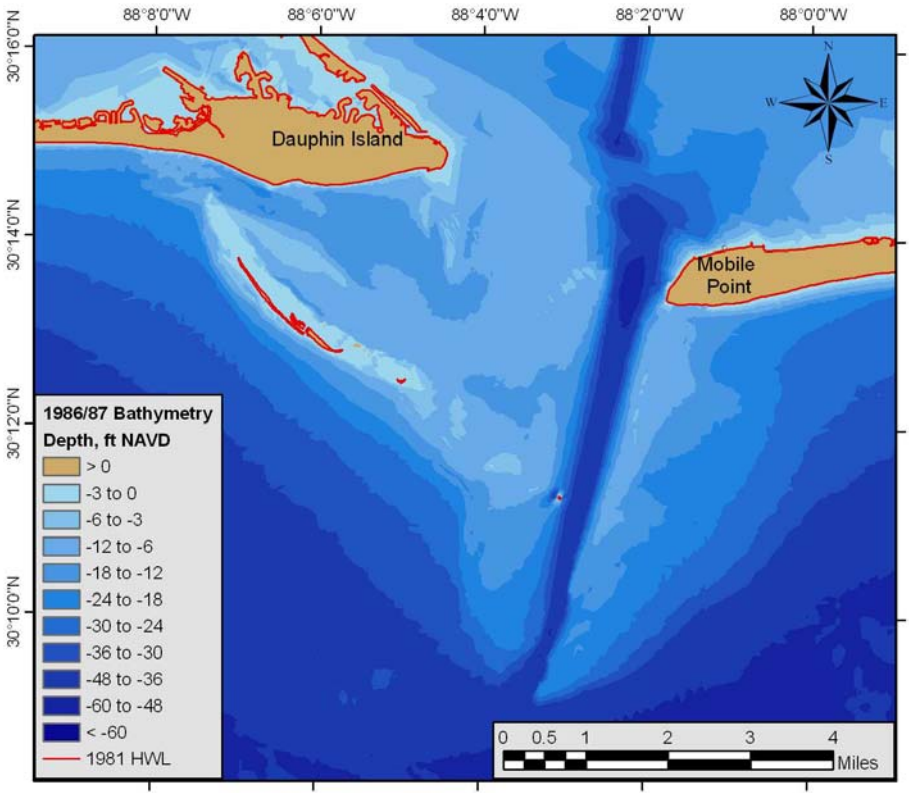

Figure 3-13. Bathymetric surface for Mobile Pass ebb-tidal delta and adjacent shores, 1986/87.

Water depth over the channel margin bar increased as sand was transported into the channel and south along the eastern channel margin. Conversely, water depths over the western lobe of the ebb-tidal delta decreased as sand transported from east to west continued to accumulate. Pelican Island shoal, as defined by the 3-ft depth contour, more than doubled by 1986/87, even though island area was relatively small (Figure 3-13). Furthermore, the shoal was within about 0.5 mi of the Dauphin Island shoreline, and transport to the beach was indicated by bar morphology between

Pelican and Dauphin Islands. The sequence of storms apparently increased sand transport from east to west during this period.

2002. The period from 1986 to 2002 contained six tropical cyclones, four of which made landfall east of Mobile Pass. Littoral sand transported south from Mobile Point along the channel margin bar continued to fill portions of the outer bar channel as it slowly migrated to the west. By 2002, the offset that existed between the natural and maintained channels in 1970 was no longer present, resulting in a straight, south-southwest oriented channel to the Gulf (Figure 3-14).

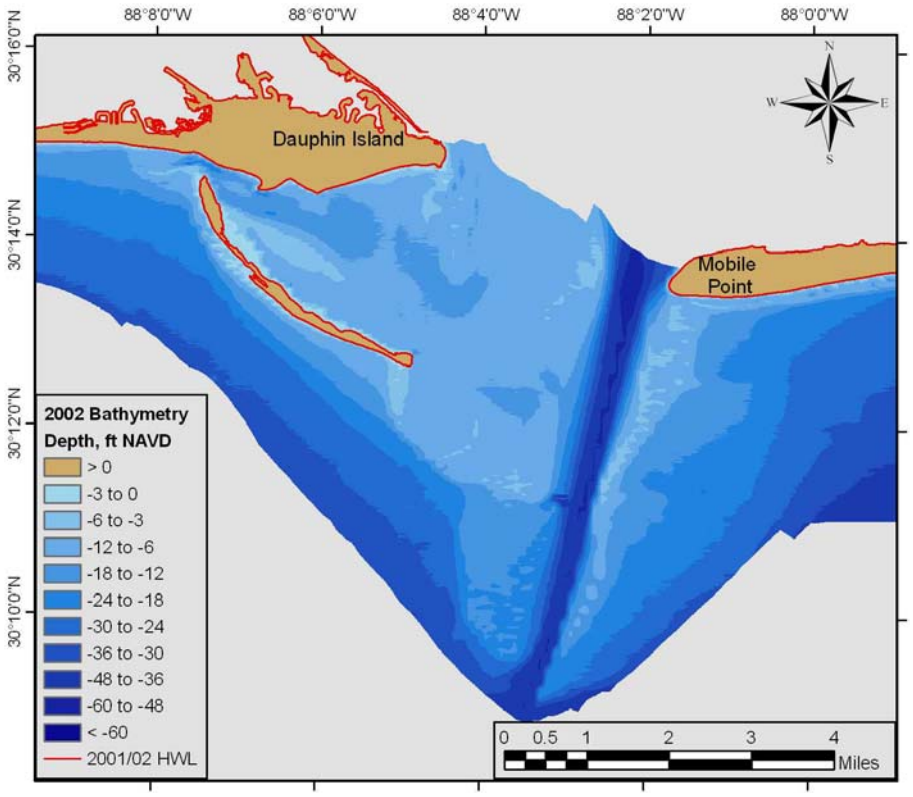

Figure 3-14. Bathymetric surface for Mobile Pass ebb-tidal delta and adjacent shores, 2002.

Three primary differences exist between the 1986/87 and 2002 bathymetric surfaces. First, although the shoreline receded at Mobile Point between 1981 and 2001, deposition on the channel margin bar east of the channel resulted in a shallow, elongated bar that extends almost the full length of the channel (Figure 3-14). Second, the west lobe of the ebb-tidal delta indicates net deposition between 1986/87 and 2002, a trend similar to that documented for the period 1970 to 1986/87. Third, Pelican Island expanded to its largest extent since 1908. Furthermore, the northwestern end of the island is at its closest position to Dauphin Island since 1868. By May 2006, the shoreline of Pelican Island was within 300 ft of the beach just east

of the Dauphin Island fishing pier. Sand transport from Pelican Island to Dauphin Island is illustrated via morphology on the 2002 bathymetric surface, and by a line of breaking waves between the two islands on May 2007 orthophotography.

Channel Migration. Evolution of the Mobile Pass channel has been controlled by net westward migration and southward growth of the sand bar east of the channel. Dredging engineers recognized the natural westward shift of the channel as early as 1912 and decided to accommodate natural channel migration by relocating the maintained channel 700 ft to the west of its originally authorized location. Figure 3-15 documents natural channel migration to the west between 1847/48 and 1908. In 1847/48, a connection did not exist across the outer bar for the 24- or 30-ft depth contours, and flow through the channel exited to the Gulf in a south-southeast direction. By 1892, the channel through the outer bar had migrated approximately 2,000 ft to the west and a narrow 24-ft deep channel naturally formed across the outer bar (Figure 3-15). The channel continued to migrate westward, and by 1908, a 2,100-ft wide gap existed between the 24-ft depth contours defining east and west lobes of the ebb-tidal delta. Initial dredging to a depth of 30 ft was completed in 1908, and this narrow channel is recorded by the 1908 30-ft depth contour (Figure 3-15). Natural migration of the channel to the west appears to have deepened the channel across the outer bar between 1847/48 and 1908, but dredging was required to establish a connection between the interior channel and the Gulf in 1908 to a depth of at least 30 ft.

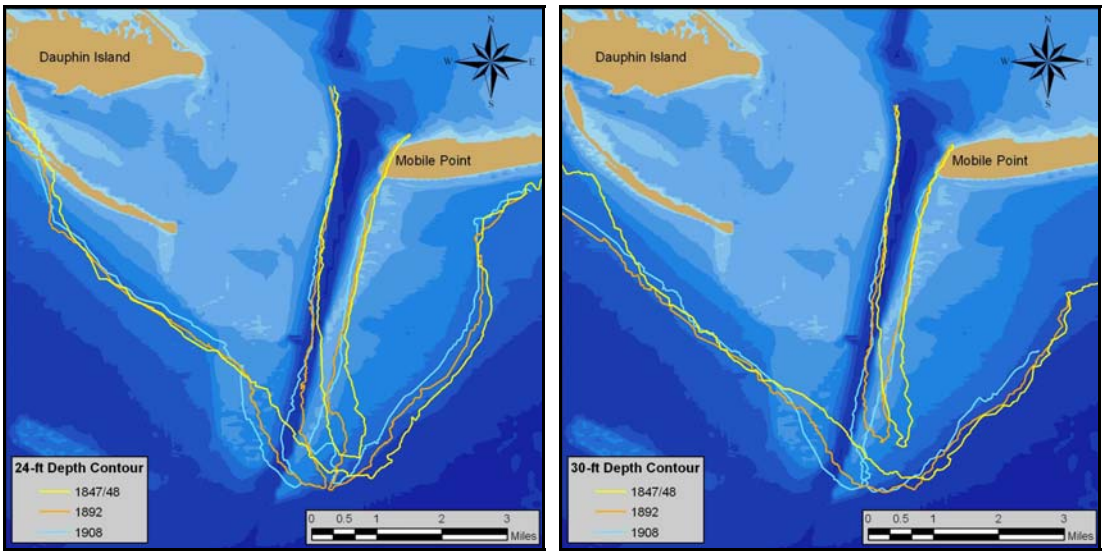

Figure 3-15. Variations in location of the 24- and 30-ft depth contours, 1847/48, 1892, and 1908.

Between 1908 and 1917/20, the channel across the outer bar continued to migrate westward, and channel width at the 24-ft depth contour was maintained at about 2,400 ft (Figure 3-16). The channel offset that developed during migration of the bar and channel was initiated in 1908, but it was not until 1941, when southward-directed littoral sand deposition along the southern extent of Dixie Bar exaggerated the offset (Figure 3-16). In 1917/20, a 30-ft deep channel no longer existed across the outer bar, likely related to channel infilling from the July 1916 hurricane. However, 24 years later, a well-maintained channel at least 36 ft deep was recorded in the bathymetry data.

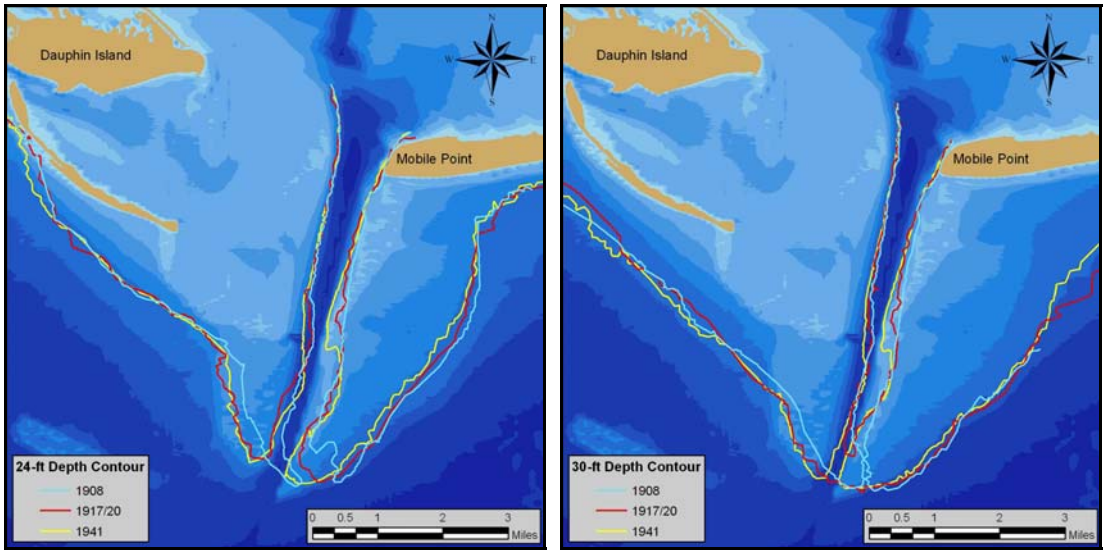

Figure 3-16. Variations in location of the 24- and 30-ft depth contours, 1908, 1917/20, and 1941.

General location of the navigation channel across the outer bar was relatively unchanged between 1941 and 2002. Channel dimensions increased from 36 ft deep and 450 ft wide in 1941 to 49 ft deep and 600 ft wide in 2002. Greatest change occurred along the eastern margin of the natural channel where sand transported from the east and north filled the historical channel south of the offset best recognized in 1941. Figure 3-17 best illustrates this progression of deposition along the east lobe of the ebb-tidal delta. Concurrently, sand along the western margin of the natural channel was eroded and transported to shoals on the west lobe of the ebb-tidal delta. Lack of channel migration on the outer bar was controlled by maintenance dredging.

Between 1970 and 2002, infilling along the eastern margin of the channel and erosion along the western margin continued through 1986/87, but the channel was relatively stable after this time (Figure 3-18). The primary change recorded between

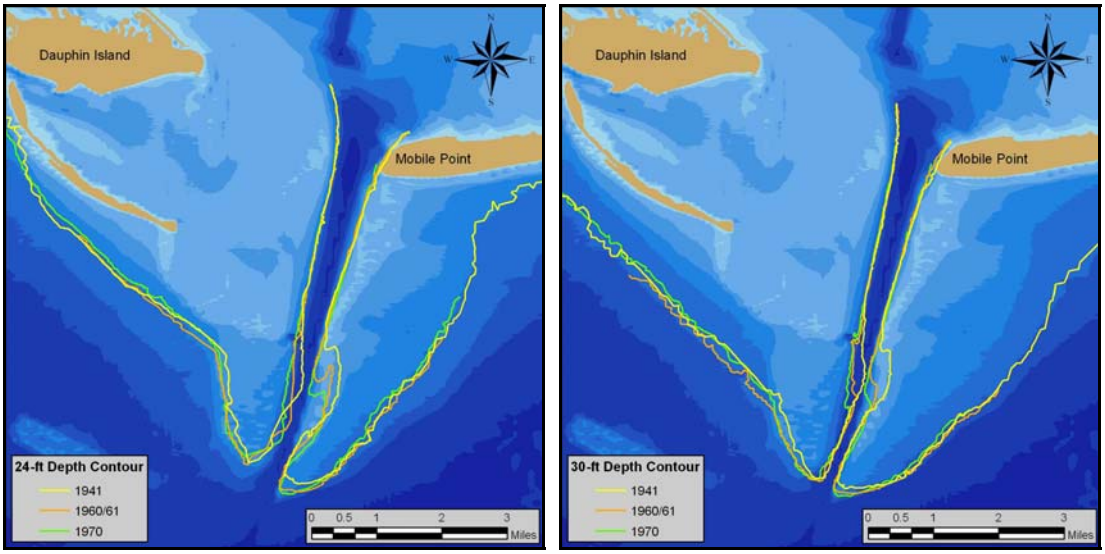

Figure 3-17. Variations in location of the 24- and 30-ft depth contours, 1941, 1960/61, and 1970.

1986/87 and 2002 is growth of the western lobe of the ebb-tidal delta. This growth is documented by seaward expansion of the 24- and 30-ft depth contours just west of the outer bar channel. Shoal growth in this area may in part be the result of dredged material disposal on the shoal; however, the beneficial use disposal site (SIUBA) is located north of the 24- and 30-ft contours in approximately 20-ft water depth.

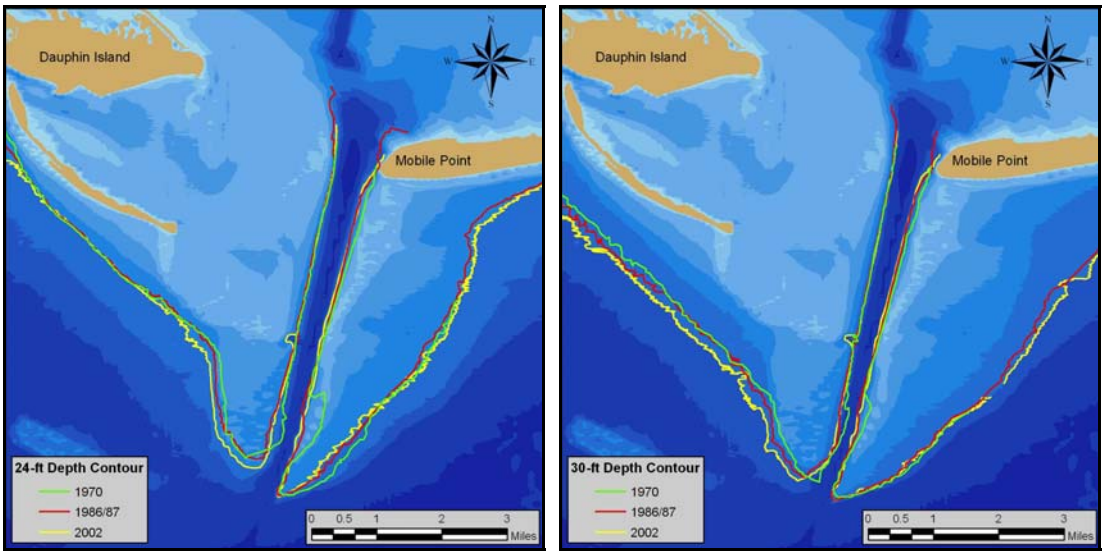

Figure 3-18. Variations in location of the 24- and 30-ft depth contours, 1970, 1986/87, and 2002.

Ebb-Tidal Delta Cross-Sections. Temporal variations in seafloor elevation were compiled at six representative profiles on the ebb-tidal delta to capture two-

dimensional changes for all depth contours at specific locations (Figure 3-19). Three channel cross-sections (Transects 1 through 3) document the westward migration of the eastern channel margin bar and the navigation channel. Transects 4 through 6 record changes in islands and shoals as they migrate, erode, and reform on the western lobe of the ebb-tidal delta.

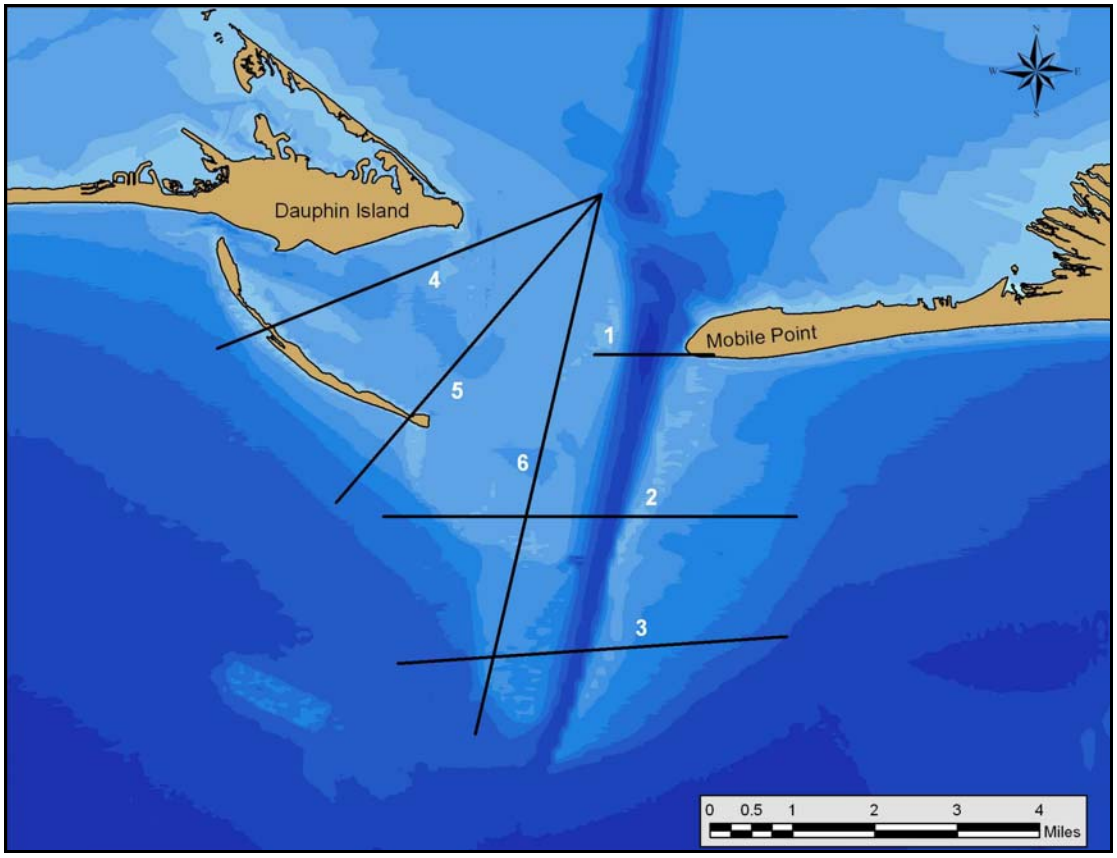

Figure 3-19. Transect locations on the Mobile ebb-tidal delta.

Transect 1. Between 1847 and 1941, the beach and shoreline at Mobile Point expanded to the west approximately 1,200 ft as large quantities of littoral sand were transported west from beaches to the east. Figure 3-20 indicates that greatest deposition occurred above the 35-ft depth contour. However, from 1941 to 1981/82, position of the high-water line at Mobile Point was relatively stable, and between 1981/82 and 2002, the shoreline showed net recession. During this 61-year period, channel deposition occurred primarily below the 30-ft depth contour, and the channel thalweg began to migrated to the west and shoal. Consequently, the western margin of the channel migrated to the west, but the rate of channel migration was less than deposition present along the eastern channel margin, creating a slightly narrower channel by 2002.

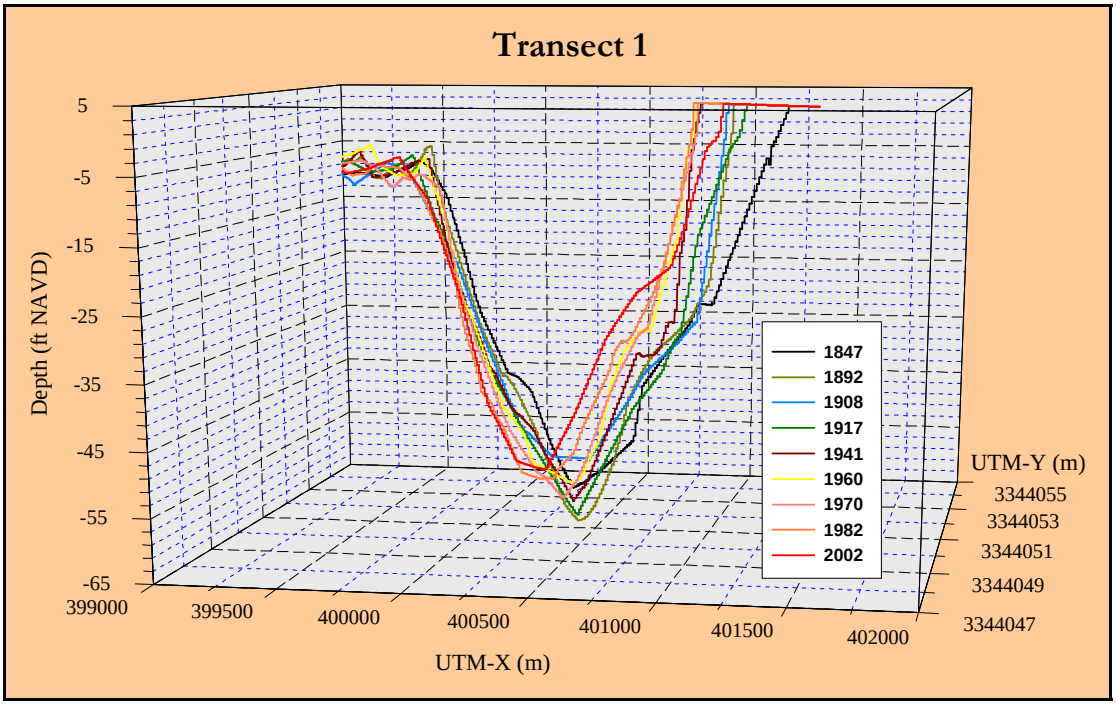

Figure 3-20. Channel movement at Transect 1 as sand deposited along the eastern channel margin and scour by tidal currents resulted in erosion along the west bank of the channel. Mobile Point is on the right side of the transects.

Transect 2. Elevation change along this transect illustrates net erosion of shoals on the eastern lobe of the ebb-tidal delta and deposition along the eastern margin of the channel (Figure 3-21). Greatest deposition occurred between 1917 and 1941, and only minor adjustments were indicated between 1941 and 2002. Deposition along the east side of the channel was associated with an equal amount of scour along the western margin, resulting in net movement of about 1,500 ft. The western lobe of the ebb-tidal delta was very active along Transect 2 as Sand Island migrated, eroded, and reformed in response to storm activity. Overall, the shoreface long the western side of the transect eroded from 1847 to 2002, but net deposition since 1960 formed a subaqueous sand bar at the 1847 location of Sand Island.

Transect 3. This transect is located along the southern end of the ebb-tidal delta and crosses the outer bar where the navigation channel has been maintained since 1904. The most notable change is the location of the channel in 1847 relative to 2002. Greatest channel migration occurred between 1847 and 1892, but this part of the channel continued migrating west through 2002 (Figure 3-22). From 1892 to 1917, the base of the channel migrated west, but the highest point on the eastern margin of the shoal was eroding. This trend continued through 1941, but between 1970 and 1982, rapid deposition along the eastern margin of the channel created a shoal about 16 ft deep at the channel margin and a steep side slope (Figure 3-22). By

2002, the channel margin shoal was about 13 ft deep and the channel depth was dredged to about 49 ft.

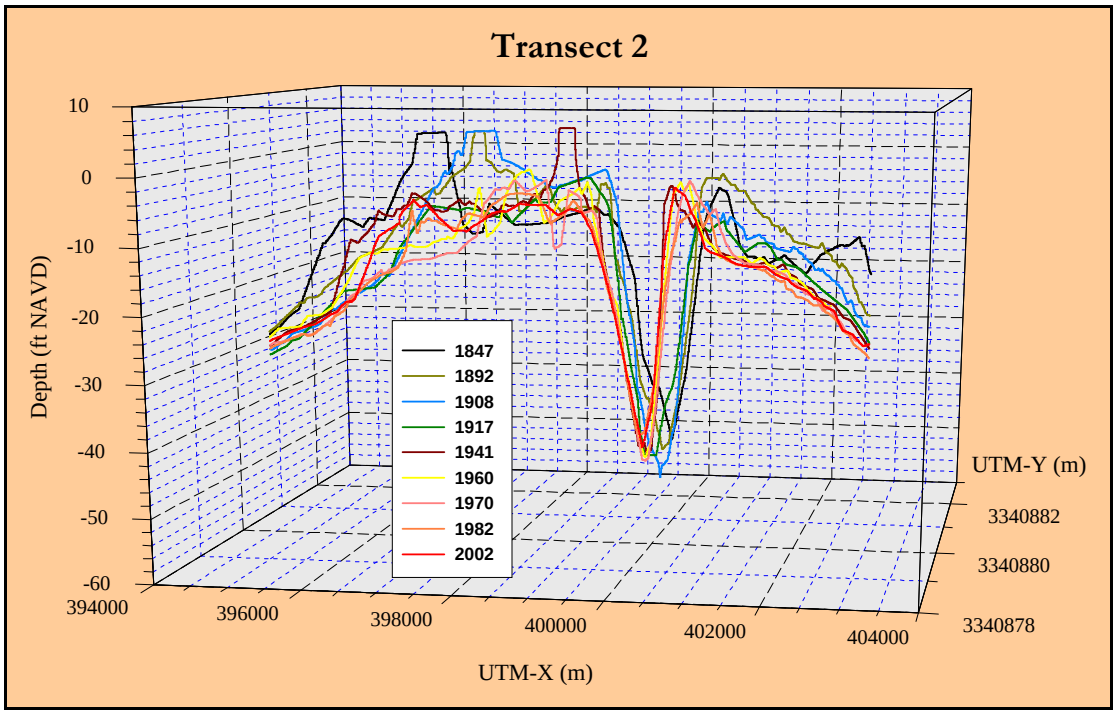

Figure 3-21. Elevation changes along Transect 2, 1847 to 2002.

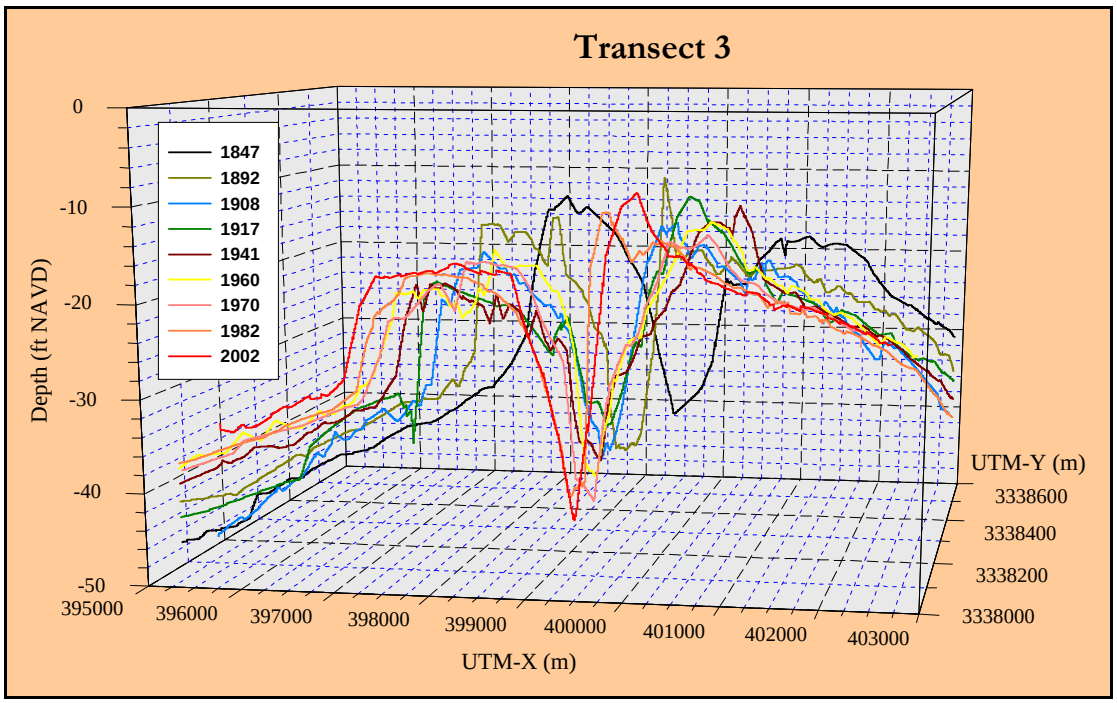

Figure 3-22. Elevation changes along Transect 3, 1847 to 2002.

The western channel margin migrated to the west in step with changes to the east. Between 1847 and 1917, the western lobe of the outer bar decreased in elevation and was forced to the west by natural channel migration (Figure 3-22). This trend continued through 1941, but the shoal has increased in height and width since 1941 as sand transport seaward of this transect continues to deposit sediment on the shoal as it moves to the northwest toward Dauphin Island.

Transect 4. Elevation changes along Transect 4 document the growth and movement of Pelican Island, deposition in Pelican Bay, evolution of the subaqueous spit south of Pelican Point (easternmost Dauphin Island), and stability of the interior portion of the ebb-tidal delta at the entrance to Mobile Bay (Figure 3-23). When present, Pelican Island consistently migrated to the west-northwest between 1847 and 2002. The shallow bar that formed to the northeast of Pelican Island is a result of storm overwash and breaching. The feature was present in 1892 and grew in height and width through 2002. Sand transport from Pelican Point to the south appears to be contributing to deposition within Pelican Bay (shallowest depths were recorded in 2002). Only minor changes were recorded on the northeast shoal, indicating the high quality of data compiled for each of the bathymetric surfaces. Greatest changes were recorded on the western side of the transect where deposition on the beach fronting Pelican Island since 1917 has added large quantities of sand to the transport system that nourishes Dauphin Island.

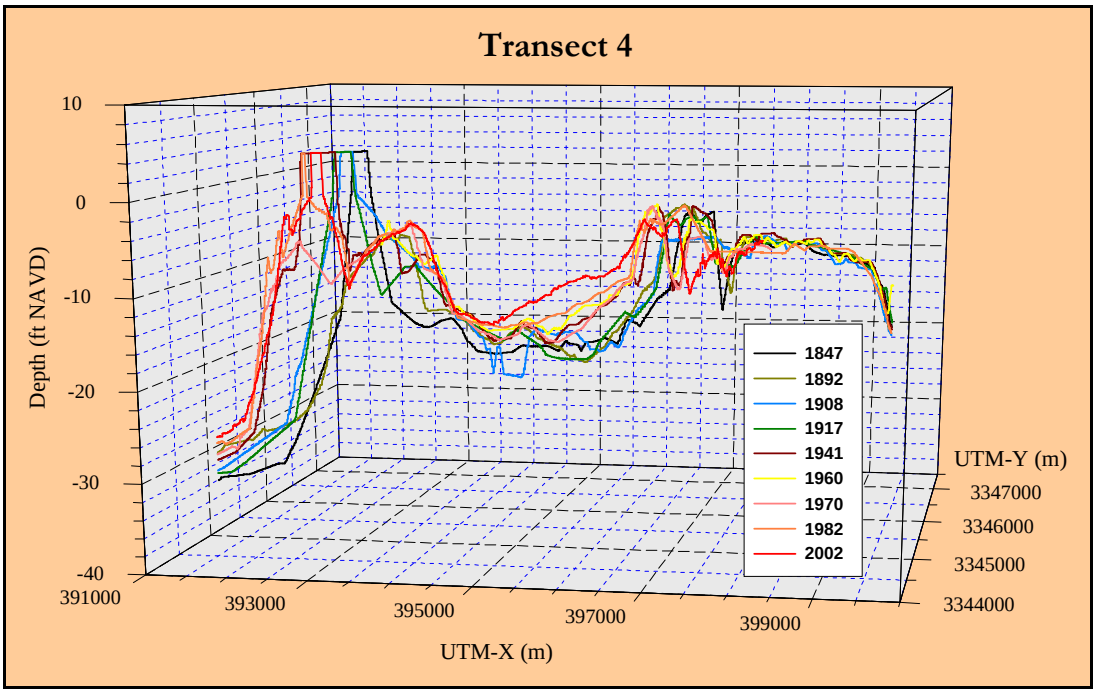

Figure 3-23. Elevation changes along Transect 4, 1847 to 2002. Transect extends from the entrance to Mobile Bay, southwest and across Pelican Island (see Figure 3-18).

Transect 5. This transect begins at the same location as Transect 4 but traverses southwest over southern Pelican Island. Greatest change exists along the southwestern end of the transect where Pelican Island evolves from a 12-ft deep shoal in 1847 to an island in 1892 as Sand Island expands and migrates to the northwest (Figure 3-24). Since 1892, the island and shoreface have migrated to the northeast, including when the island was reduced to a 6-ft deep shoal in 1982. By 2002, Pelican Island was located at its most northeast position since 1847. Transect 4 recorded just the opposite trend where the 2002 island was located southeast of most other time periods, meaning the entire island is rotating counterclockwise as it evolves. Northeast of the island, Pelican Bay has been filling since 1847 as sand is transported through breaches and over the island during storm and normal conditions. Most changes in the bay occurred by 1941, and only minor adjustment have been recorded since this time.

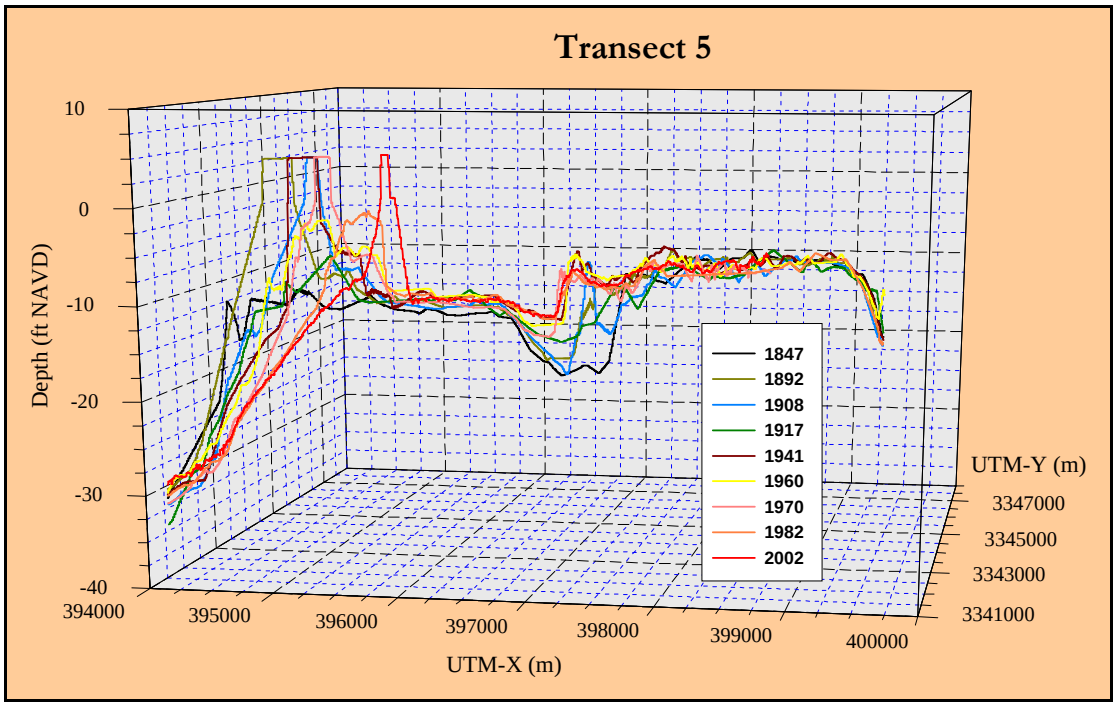

Figure 3-24. Elevation changes along Transect 5, 1847 to 2002.

Transect 6. This transect is located along the eastern margin of the west lobe of the ebb-tidal delta. Its orientation is similar to the orientation of the modern navigation channel. Greatest change along this transect is associated with the migration and erosion of Sand Island Figure (3-25). Although Sand Island existed along this transect at various times between 1847 and 1960, it has only existed as an 8- to 10-ft deep shoal since 1960. However, the shoreface south of Sand Island in 1847 illustrated net deposition throughout the historical record. This is particularly

evident since 1908 when the first authorized navigation channel was completed through the outer bar. Sand Island was not present in 1917 due to the hurricane of July 1916, but the island had reformed by 1941 and still existed in 1960. Only a shoal has existed in this area since Hurricane Camille traversed the Gulf Coast in 1969.

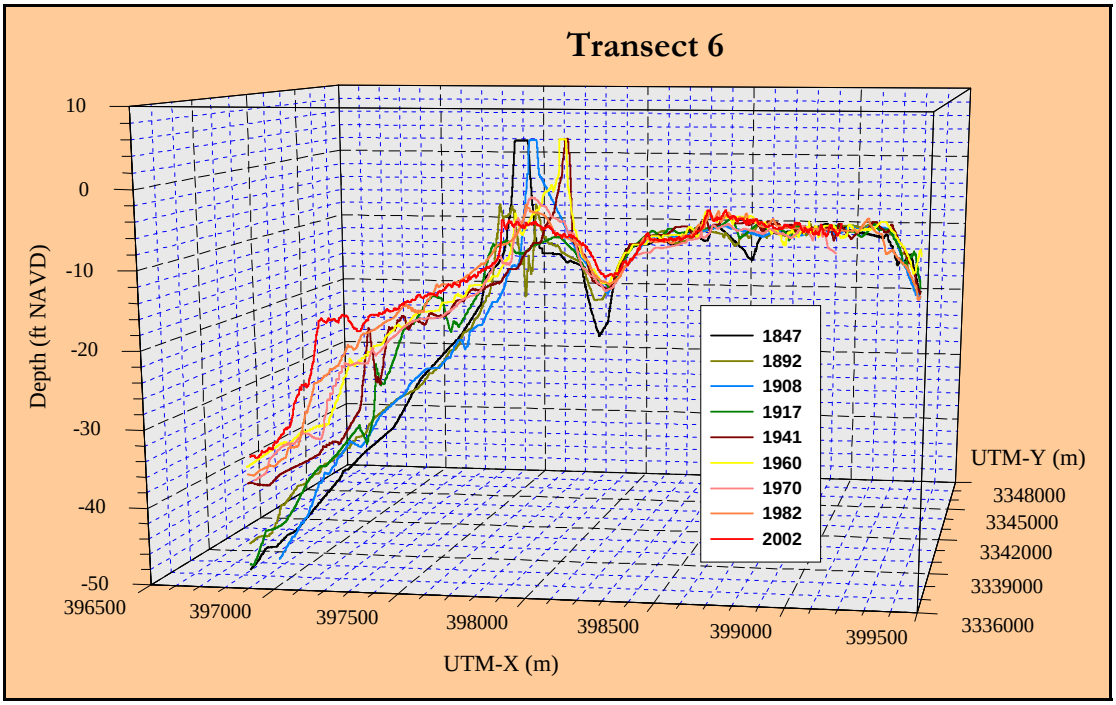

Figure 3-25. Elevation changes along the eastern margin of the west lobe of the ebb-tidal delta (Transect 6), 1847 to 2002.

Deposition on the western lobe of the outer bar has persisted since 1917. The southernmost section of Profile 6 extends through a portion of the historical dredged material disposal area for sediment from the outer bar channel (see Chapter 4). Apparently, a portion of this material may be supplying sand to the transport system that provided for expansion of Pelican Island and infilling of breaches and storm surge channels on Dauphin Island since 1941.

Ebb-Tidal Delta Sand Volumes. As the channel and shoals on the ebb-tidal delta evolved under varying wave and current processes and dredging conditions between 1847/48 and 2002, net erosion and net deposition were recorded in shoal volumes. Comparison of contour changes away from the main channel indicates that the 30-ft depth contour is approximately the seaward limit at which most sand is mobilized and supplied to shoals on the ebb-tidal delta and to Dauphin Island. As such, sand volume above the 30-ft depth contour was computed for each bathymetric surface for east and west lobes of the ebb-tidal delta. However, sand deposition and erosion

below the 30-ft depth contour associated with channel migration is a significant component of sand volume change on the ebb-tidal delta. As such, volume changes below the 300-ft depth contour within and adjacent to the channel were computed as well. Appendix F documents polygon boundaries for each time period. Figure 3-26 is a composite of polygon boundaries for each surface, showing the envelope of movement of the channel and shorelines for the period of record.

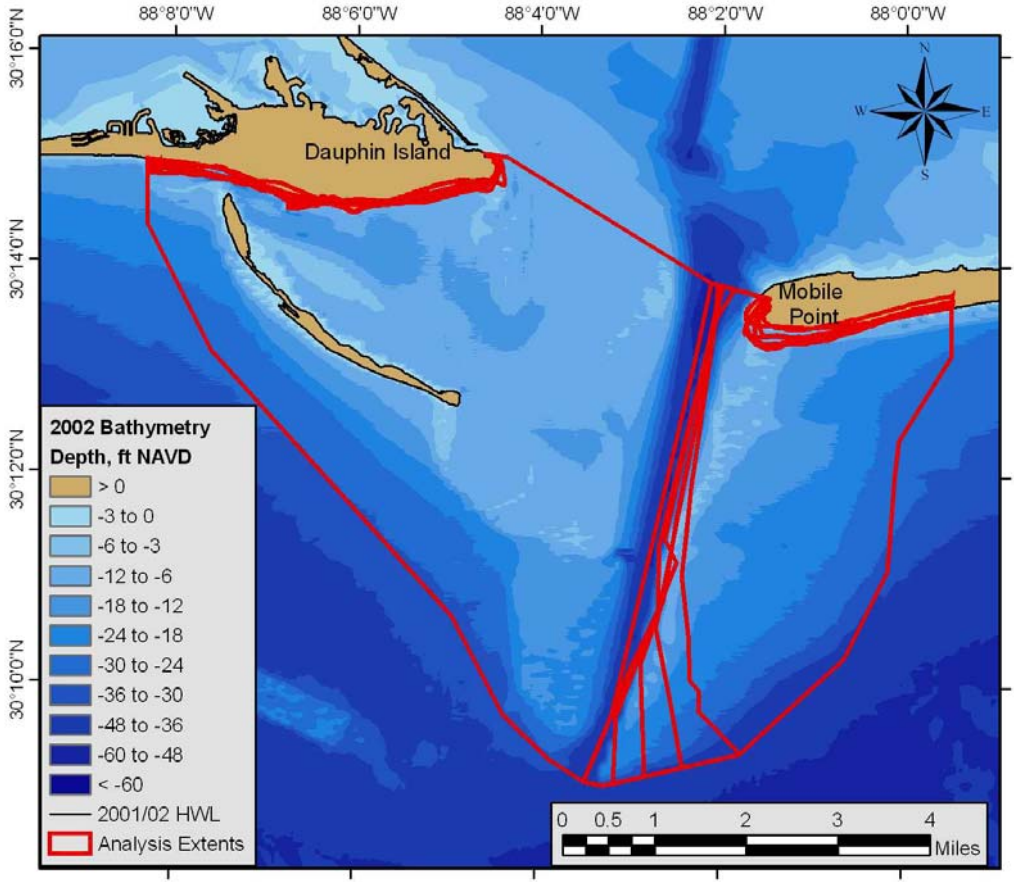

Figure 3-26. Area extents for calculating sand volume for east and west lobes of the ebb-tidal delta above the 30-ft depth contour, 1847/48 to 2002.

The computed time series of volumes west of the dredged navigation channel should document the impact of dredging on long-term sand accumulation and transport to Dauphin Island. In other words, if channel dredging and offshore disposal are removing sand from the littoral transport system that bypasses sand from east to west and on to Dauphin Island, sand volumes on the west lobe of the ebb-tidal delta should decrease in proportion to maintenance dredging volumes disposed offshore. A one-to-one correlation may not exist, but a long-term reduction in sand volume relative to pre-dredging volumes should be expected.

Sand volumes above the 20-, 25-, 30-, and 65-ft depth contours were computed to compare trends in sand volume change (the 65-ft depth contour is the reference depth for the base of the natural channel, above which cumulative net sand volume changes were recorded). Table 3-5 summarizes sand volumes above each reference depth contour. A major finding is that the volume of sand available for transport on the west lobe of the shoal (above the 30-ft depth contour) is on the order of 300 to 350 million cy. East of the channel, shoal deposits above the 30-ft depth contour contain another 104 to 117 million cy, or about 35% of the quantity that exists west of the channel. Both quantities are large compared with estimated net littoral transport

Table 3-5. Sand volume within defined polygons above the 20-, 25-, 30-, and 65-ft depth contours on east and west lobes of the ebb-tidal delta.

Year	Reference Contour (ft)	West Lobe Sand Volume (cy)	East Lobe Sand Volume (cy)	Cumulative Volume Change (cy)	
				West	East
1847/48	-20	120,143,000	33,582,000	0	0
	-25	204,467,000	65,366,000	0	0
	-30	299,153,000	106,679,000	0	0
	-65	865,649,000	435,964,000	0	0
1892	-20	135,366,000	40,848,000	15,223,000	7,266,000
	-25	220,666,000	72,876,000	16,199,000	7,510,000
	-30	318,002,000	115,403,000	18,849,000	8,724,000
	-65	885,100,000	449,623,000	19,451,000	13,659,000
1908	-20	136,700,000	32,307,000	16,557,000	-1,275,000
	-25	219,370,000	62,254,000	14,903,000	-3,112,000
	-30	313,349,000	104,378,000	14,196,000	-2,301,000
	-65	880,708,000	436,734,000	15,059,000	770,000
1917/20	-20	130,373,000	33,031,000	10,230,000	-551,000
	-25	212,618,000	63,561,000	8,151,000	-1,805,000
	-30	306,178,000	106,999,000	7,025,000	320,000
	-65	877,499,000	441,679,000	11,850,000	5,715,000
1941	-20	142,995,000	29,788,000	22,852,000	-3,794,000
	-25	226,155,000	60,589,000	21,688,000	-4,777,000
	-30	321,173,000	103,867,000	22,020,000	-2,812,000
	-65	890,417,000	441,160,000	24,768,000	5,196,000
1986/87	-20	148,522,000	27,827,000	28,379,000	-5,755,000
	-25	233,270,000	59,300,000	28,803,000	-6,066,000
	-30	329,367,000	104,067,000	30,214,000	-2,612,000
	-65	895,641,000	447,623,000	29,992,000	11,659,000
2002	-20	163,862,000	34,314,000	43,449,000	732,000
	-25	252,691,000	69,252,000	48,224,000	3,886,000
	-30	353,547,000	116,812,000	54,394,000	10,133,000
	-65	919,672,000	461,882,000	54,023,000	25,918,000

rates and maintenance dredging quantities deposited offshore since 1904. If one assumes that only sand above the 20-ft depth contour on the west lobe of the ebb-tidal delta is available for transport to Dauphin Island, upwards of 164 million cy of sand exists.

Although the absolute volume of sand in the active shoal is important for understanding the capability of the shoal as a sand source for withstanding potential impacts due to engineering activities, the primary question is whether trends in sand bypassing prior to channel construction have been disrupted by dredging. One way to evaluate potential changes is to compare volumes for each of the surveys to the initial survey (1847/48). Figure 3-27 illustrates volume changes on the east and west lobes of the ebb-tidal delta relative to the 1847/48 bathymetric survey. Overall, approximately 54 million cy of sand has accumulated above the 30-ft depth contour west of the channel since 1847/48. Greater than 80% of that material was deposited above the 20-ft depth contour. Primary sand losses resulting from the July 1916 hurricane created a net reduction in sand deposition relative to the 30-ft depth contour for the 1917/20 survey. It took approximately 20 years for shoal and shoreline deposits to recover from this major natural disaster. Since 1917/20, net deposition on the western lobe of the ebb shoal has been continuous.

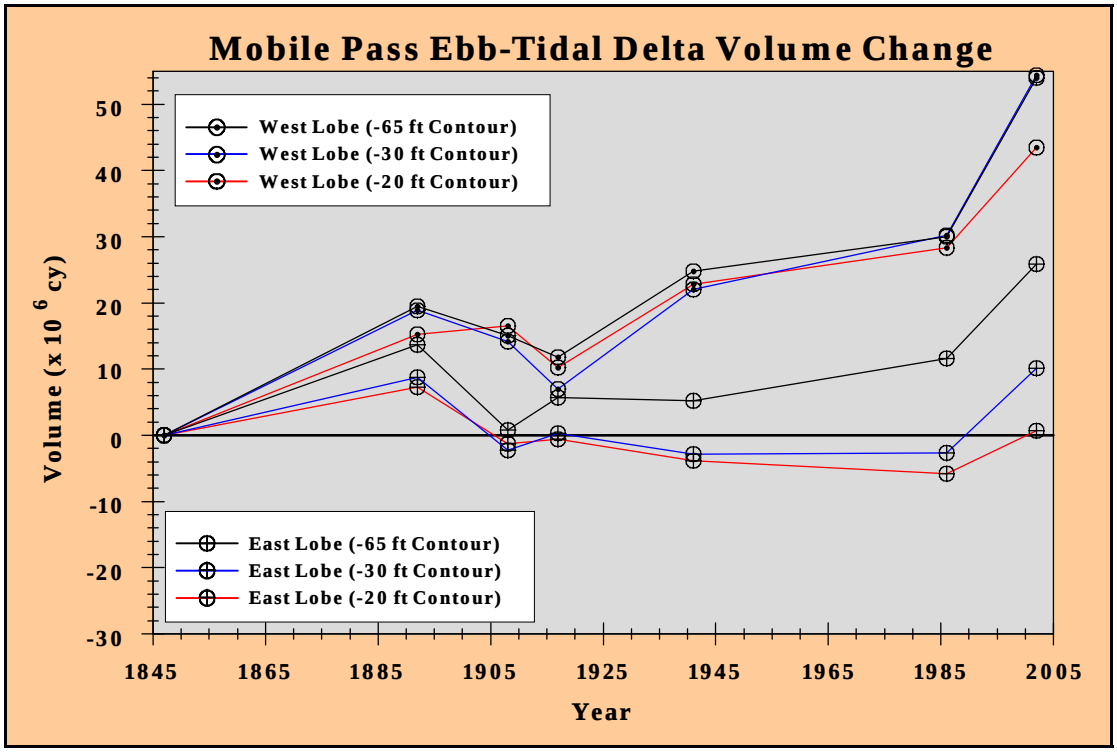

Figure 3-27. Plot of sediment volume change east and west of the channel for the Mobile Pass ebb-tidal delta, 1847/48 to 2002.

East of the channel, sand volume above the 30-ft depth contour fluctuated between deposition and erosion relative to the 1847/48 bathymetric survey. The principal cause of apparent shoal depletion east of the channel is related to the large quantity of sand eroded from the eastern portion of the shoal above the 30-ft depth contour and captured by the naturally deep channel (as deep as 60 ft) that migrated west during the period of record. As shown in Figure 3-27, significant sand deposition below the 30-ft depth contour and above the 65-ft depth contour along the channel margin bar resulted in net increases in total sand volume throughout the period of record. Cumulative volume change above the 30-ft depth contour illustrated relatively small net losses through 1986/87. However, net deposition above the 30-ft depth contour since 1986/87 has increased at a rate faster than anytime in the past. Sand deposited below the 30-ft depth contour during channel infilling may be permanently removed as a source of sand to the west. The volume of sand naturally removed from bypassing to the west was determined to be approximately 16 million cy since 1847/48.

4 Historical Sediment Transport Pathways

Comparison of bathymetric surfaces for the same geographic area but different time periods documents erosion and deposition patterns that reveal net sediment transport pathways. Erosion and deposition volumes define the magnitude of sediment exchange associated with these transport pathways. Together, these data describe the sediment budget for an area, constrained by import and export estimates (e.g., longshore transport) at the boundaries. Regional changes in seafloor topography were documented for the periods 1847/51 to 1917/20 (prior to major dredging operations) and 1917/20 to 1982/2002 (during major channel dredging operations over the outer mouth bar). These data provide a regional context under which specific changes at the Mobile Pass ebb-tidal delta were evaluated.

Regional Sediment Transport Dynamics

The natural movement of sediment within the Alabama coastal zone is controlled predominantly by east-to-west directed waves and currents, hydraulics associated with Mobile Pass, and the large source of sand from the shelf and shoreline east of Mobile Pass. Although major differences exist between the 1847/51 and 1917/20 bathymetric surfaces in specific areas, both shelf surfaces appear similar upon initial inspection. An analytical comparison of bathymetry data yields a difference plot that isolates areas of erosion and deposition for documenting sediment transport patterns and quantifying trends (Figure 4-1). The most significant changes occurring during this 70-yr interval were associated with deposition (and erosion) at and seaward of the Mobile Bay entrance, erosion along Dauphin Island, alternating erosion and deposition along the Morgan Peninsula shoreline, and net deposition on the shelf surface east of Mobile Pass ebb-tidal delta.

Fluid flow and sediment transport at and seaward of the entrance to Mobile Bay result in relatively predictable seafloor changes. Spring runoff and storm water outflow from Mobile Bay export substantial quantities of fine-grained sediment to the shelf surface seaward and west of the entrance through suspended sediment transport (Stumpf and Gelfenbaum, 1990; Isphording et al., 1996). Polygons of yellow to red (erosion) and green to blue (deposition) in the navigation channel and on the shoals of the ebb-tidal delta illustrate the dynamic nature of these features as waves and currents transport and redistribute sediment from east of the channel to the west (Figure 4-1).

North-to-south oriented deposition and erosion areas are a consequence of natural westward movement of the navigation channel. The red zone represents scouring of

the western margin of the channel during westward migration, and the elongated blue zone reflects historical channel infilling with littoral and shelf sand east of the entrance (Figure 4-1). The large blue lens on the southwestern margin of the channel indicates net deposition of sand transported from westward channel migration and east-to-west transport at about the 30- to 35-ft depth contours. Sand eroded during westward channel migration and through west-directed bypassing in the area eventually supplies sand to shoals on the western lobe of the ebb-tidal delta, which in turn provides sand to Dauphin Island beaches west of Pelican Island.

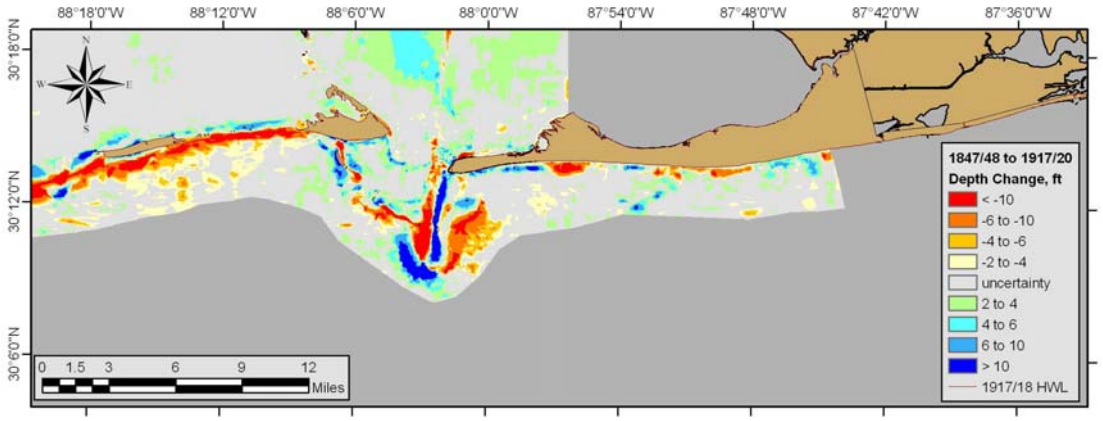

Figure 4-1. Bathymetric change between 1847/51 and 1917/20 for the Alabama coastal zone. Hot colors represent erosion (yellow to red) and cool colors represent deposition (green to blue).

Net erosion on the nearshore shelf seaward and west of central Dauphin Island illustrates significant changes that resulted from the July 1916 hurricane. Shoreline data documented widespread washover and breaching, but bathymetry data provided a comprehensive view of the magnitude and extent of nearshore erosion as well.

Between 1917/20 and 1982/2002, similar patterns of erosion and deposition occurred throughout the study area. As the navigation channel continued to migrate to the west, scour again supplied sand to the seaward extent of the ebb-tidal delta while littoral sand from the east continued to fill the historical location of the channel (Figure 4-2). Two prominent deposits formed offshore due to disposal of dredged material. The elongated deposit west of the ebb-tidal delta contains approximately 17 million cy of sand and mud dredged as part of the Mobile Harbor Deepening Program (Hands, 1992). This stable berm was originally placed near the 45-ft depth contour and is called the Mobile Outer Mound. The irregular shaped blue deposit just west of the channel as it exits the outer bar is likely the offshore disposal site used by dredgers over the past 90 years to dispose of sand from the outer bar channel. By 2002, it contained about 20.9 million cy of material. A substantial

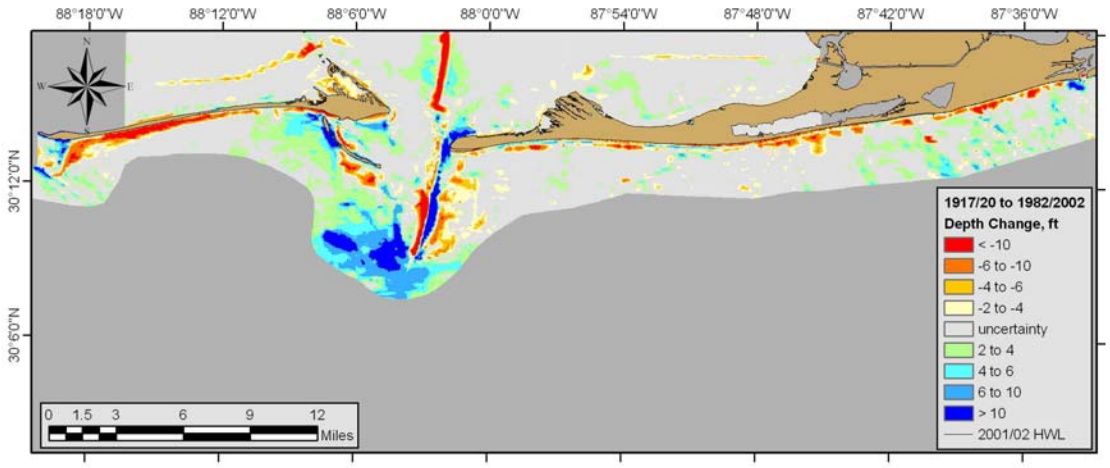

Figure 4-2. Bathymetric change between 1917/20 and 1982/2002 for the Alabama coastal zone. Hot colors represent erosion (yellow to red), and cool colors represent deposition (green to blue).

quantity of sand has deposited just south of eastern Dauphin Island in conjunction with the formation of northwestern Pelican Island. This feature continues to supply sand to beaches along western Dauphin Island, filling storm breaches and contributing to westward expansion of the island.

The red area seaward of Dauphin Island suggests that beach erosion is dominant during this period. However, Dauphin Island grew approximately 2.9 miles to the west during this time and migrated landward via storm overwash at least one island width. Much of the sand from this zone of erosion supplied material needed to create the island present in 2002 (natural sand recycling, not permanent erosion).

The trend in erosion and deposition along beaches between Mobile Point and Perdido Pass is similar to that identified for 1847/51 to 1917/20. In the Gulf Shores area, alternating patterns of erosion and deposition on the shelf surface are associated with an extensive northwest-southeast-trending sand ridge field, indicating an active nearshore shelf surface east of Mobile Pass (Figure 4-2). Because the shelf in this area is composed of sand, it is a known source to beaches and shoals west of this area.

Erosion and Deposition on the Mobile Pass Ebb-Tidal Delta

As illustrated above, greatest bathymetric changes occur on and adjacent to the Mobile Pass ebb-tidal delta, where dominant littoral transport processes interact with hydraulic processes controlled by the exchange of fluid and sediment between Mobile Bay and the Gulf of Mexico. This dynamic environment provides for long-

term bypassing of littoral sand in the dominant direction of transport (east-to-west). Over long time periods, net movement of shoals and channels reflect pathways of transport as sand moves through the inlet system.

1847/48 to 1892. Bathymetric change during this 45-year period documents active channel migration to the west, as littoral and nearshore shelf processes transport large quantities of sand to the eastern margin of the channel. Widespread deposition where the historical channel was once located is shown as a blue north-south deposit east of the erosion (red) area where the channel migrated (Figure 4-3). The natural process of channel migration caused some of the greatest changes recorded during all time periods. Deposition on the outer margin of the ebb-tidal delta to the south and west of the channel is the direct result of erosion and transport of sand from the ebb shoal south of Sand Island Light as the channel migrated westward. The shape and orientation of the shoal as it points to the northwest indicates the dominant direction of transport in this area.

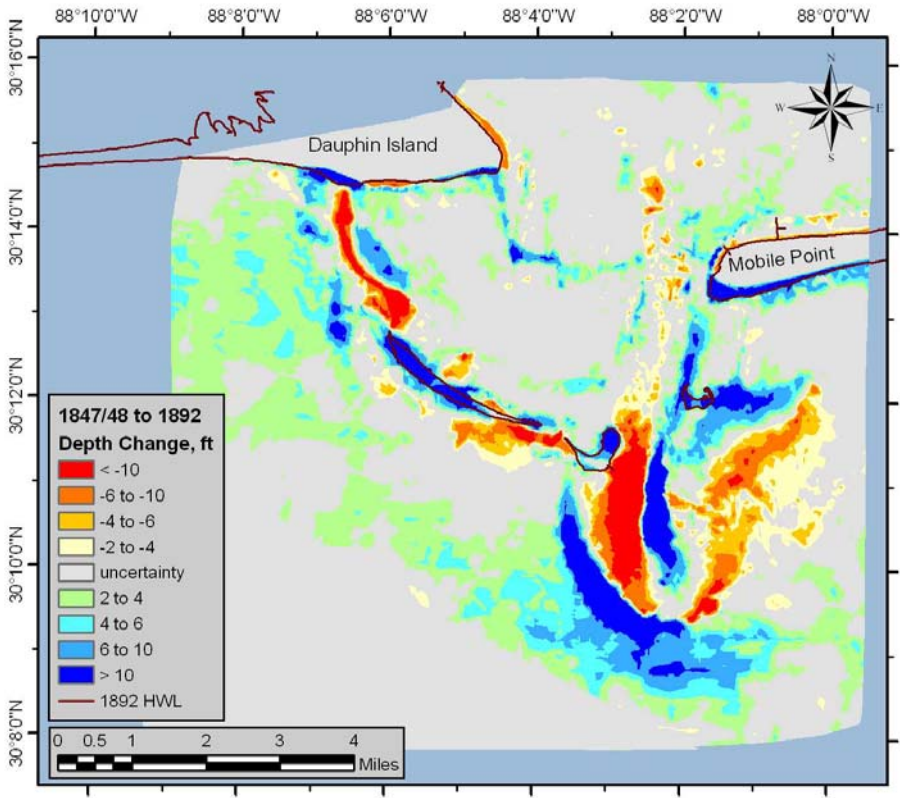

Figure 4-3. Areas of erosion and deposition on the Mobile Pass ebb-tidal delta illustrating net movement of the channel and shoals from east to west, 1847/48 to 1892.

Shoreline data in 1868 document mass movement of sand from Pelican Island, as mapped in 1847/48, to the eastern portion of Dauphin Island (see Figure 2-6).

Erosion of Pelican Island, as illustrated on Figure 4-3, is associated with onshore deposition north of the erosion zone. The blue area of deposition northeast of the original location of Pelican Island is the result of storm processes, possibly the Category 3 hurricane of 1860 or the Category 1 hurricane of 1859. Net migration of Sand Island from southeast to northwest is consistent with all morphologic changes recorded between 1847/48 and 1892.

1892 to 1908. Between 1892 and 1908, only a 16-year period, the same general trends of erosion and deposition were recorded (Figure 4-4). Erosion on the eastern flank of the shoal supplied sediment for channel infilling west and south of this area, and channel migration continued to redistribute sediment on the western lobe of the ebb-tidal delta. Active sand bypassing was indicated along the seaward margin of the outer bar, and a consistent, lens-shaped area of deposition had emerged again west of the navigation channel.

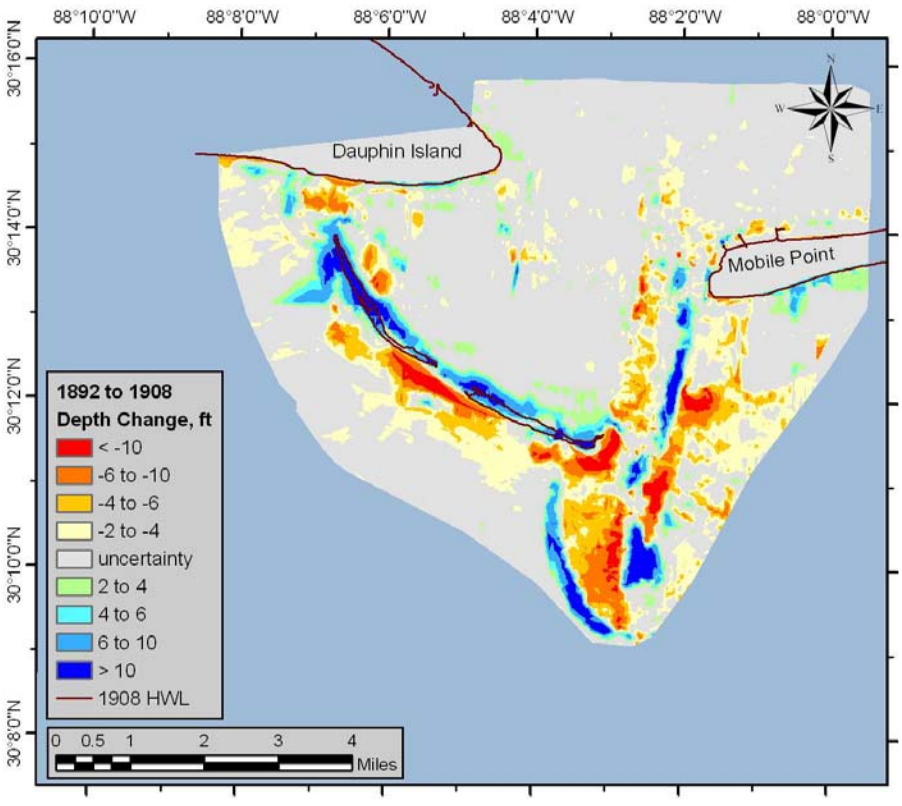

Figure 4-4. Bathymetric changes recorded on the Mobile Pass ebb-tidal delta for the period 1892 to 1908.

Re-emergence of Pelican Island and the growth of Sand Island slightly north and west of the position of Sand Island in 1892 indicates the transport mechanism by which sand is redistributed throughout the ebb-tidal delta (Figure 4-4). Further-

more, expansion of these islands and shoals suggests that sand supplied from east of the channel is critical to shoal development and the transport system along Dauphin Island. Erosion on and seaward of Dauphin Island, northwest of Pelican Island, provided sand to downdrift beaches as Pelican Island expanded to the northwest.

1908 to 1917/20. By 1917/20, islands on the western lobe of the ebb-tidal delta were nearly gone. In fact, few well-defined shoals existed as well (Figure 4-5). The shoreline and beach at and east of Mobile Point was net erosional, and the beach and nearshore west of what was left of Pelican Island was decimated (see Figure 2-23). The hurricane of July 1916 had the same effect on the western lobe of the ebb-tidal delta as it did on the shoreline of Dauphin Island.

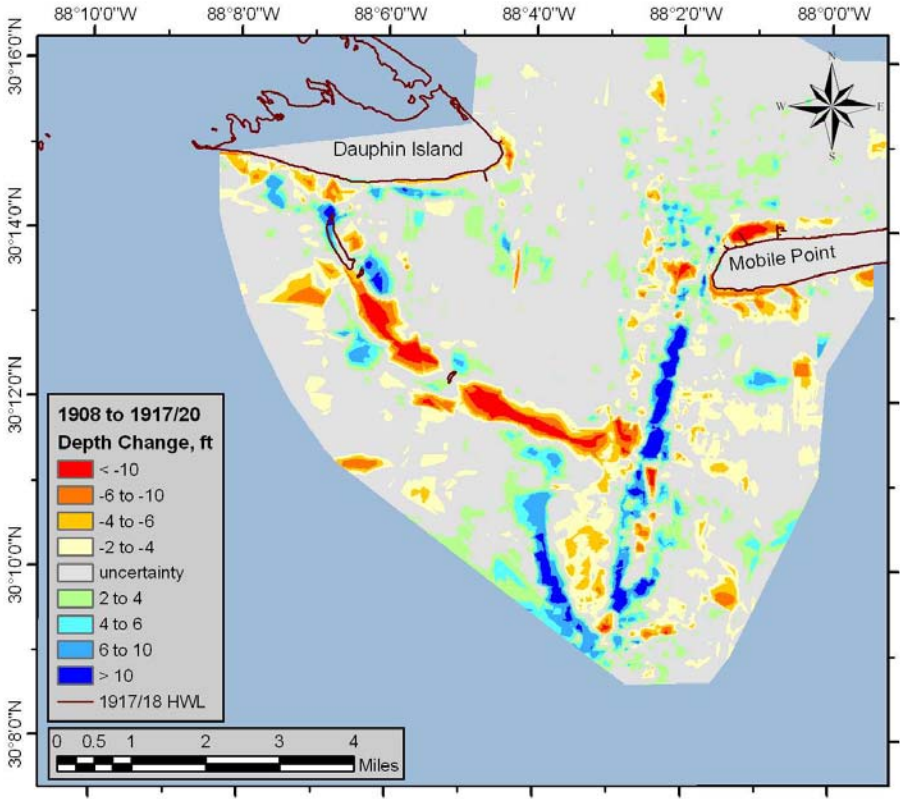

Figure 4-5. Channel infilling along the eastern margin of the navigation channel and deposition west of the channel continued even though erosion and sediment dispersal was dominant as a result of the July 1916 hurricane.

However, deposition along the eastern margin of the navigation channel and west of the channel as it exited the outer bar continued. Transport of littoral sand from Mobile Point south along the channel margin continued to supply sand shoals west of the channel as part of an active bypassing system. Water depths in this area were between 25 and 30 ft NAVD. At this time, the navigation channel was dredged to

about 30 ft deep and 300 ft wide, and maintenance dredging was minimal (see Figure 1-23). Reformation of Sand and Pelican Islands, and the reconstruction of central Dauphin Island, would depend solely on the effectiveness of sand transport from east-to-west across the navigation channel.

1917/20 to 1941. After the July 1916 storm of record for Dauphin Island, sand continued to be supplied to Dauphin Island via the western lobe of the ebb-tidal delta, even though significant dredging through the outer bar continued during this time. Maintenance dredging by 1941 accounted for about 6 million cy of sand to the offshore, and new work contributed about 2.5 million cy (see Appendix B). The channel was 36 ft deep and 450 ft wide, and new work in the outer bar channel can be recognized as a red linear feature through the outer part of the ebb-tidal delta (Figure 4-6). A lens-shaped zone of deposition east of the channel seems opposite of previous change surfaces, but a thin lens of deposition is present west of the channel as well.

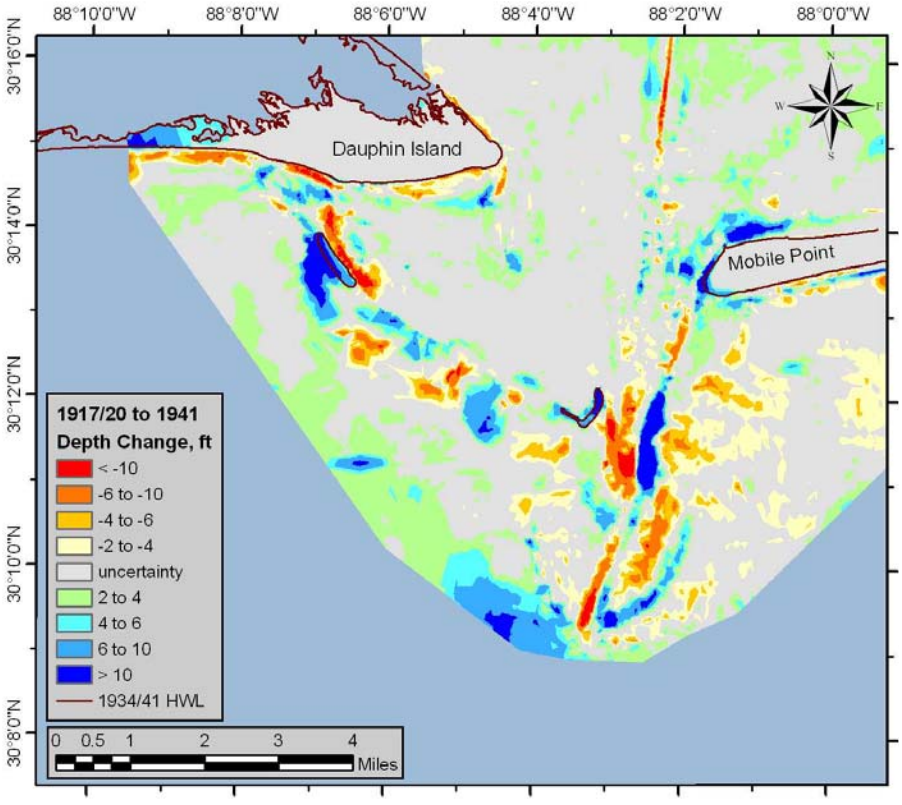

Figure 4-6. Bathymetric change after the July 1916 hurricane illustrating deposition along the eastern margin of the channel, minor island and shoal formation to the west of the channel, and deposition west of the outer mouth bar channel illustrating the offshore dredged material disposal site.

Beach and nearshore changes at Mobile Point once again recorded an excess of sediment that was common to this area prior to the 1916 hurricane. Furthermore, the eastern margin of the channel continued to fill with sand from the north as the channel continued to migrate west. A large sand deposit formed midway along the channel near the juncture of the natural channel and the dredged navigation channel (Figure 4-6). This deposition pattern appears to have created the north-south channel offset discussed in Chapter 3. Interestingly, an area of deposition formed west and downdrift of this offset where the eastern margin of the natural channel aligns with the western margin of the dredged channel, suggesting that sand maybe bypassing the channel at this location and time period.

Although deposition on the western lobe of the ebb-tidal delta was relatively minor, Sand and Pelican Islands were reforming, and sand continued to deposit northwest of Pelican Island on its way to Dauphin Island. Shoreline data indicate that breaches formed along most of the central portion of Dauphin Island during the July 1916 hurricane were filled by 1934, implying that sand transported from the ebb-tidal delta was adequate to recreate a continuous island by this time. Even though new work and maintenance dredging were quite active between 1917/20 and 1941, and the September 1926 hurricane passed directly over Dauphin Island, sand transport from the east, across the channel, and on to Dauphin Island was sufficient to produce an uninterrupted barrier island that continued expanding to the west.

1941 to 1960/61. Bathymetric changes recorded between 1941 and 1960/61 indicate that east-to-west sand bypassing across the outer bar channel was active even though the channel was maintained at 38-ft deep and 450-ft wide. Greatest deposition on the east side of the channel occurred just north of the maintained channel where an east-west offset existed with the natural channel (Figure 4-7). Dominant flow conditions at this offset appear ideal for transporting sand south and west across the channel on to the western lobe of the ebb-tidal delta. This deposition area is illustrated as a large northwest trending feature west of the channel that supplied sediment to Sand Island as it expanded to the northwest.

West-directed sand transport from beaches and shoals east of the navigation channel continued to supply sediment to Sand Island and other shoals on the western lobe of the ebb-tidal delta. Shoal deposition northwest of Sand Island signifies the transport pathway existing throughout the historical record (Figure 4-7). The presence of two sand bypassing locations is new since 1941, and bypassing appears to be operating efficiently.

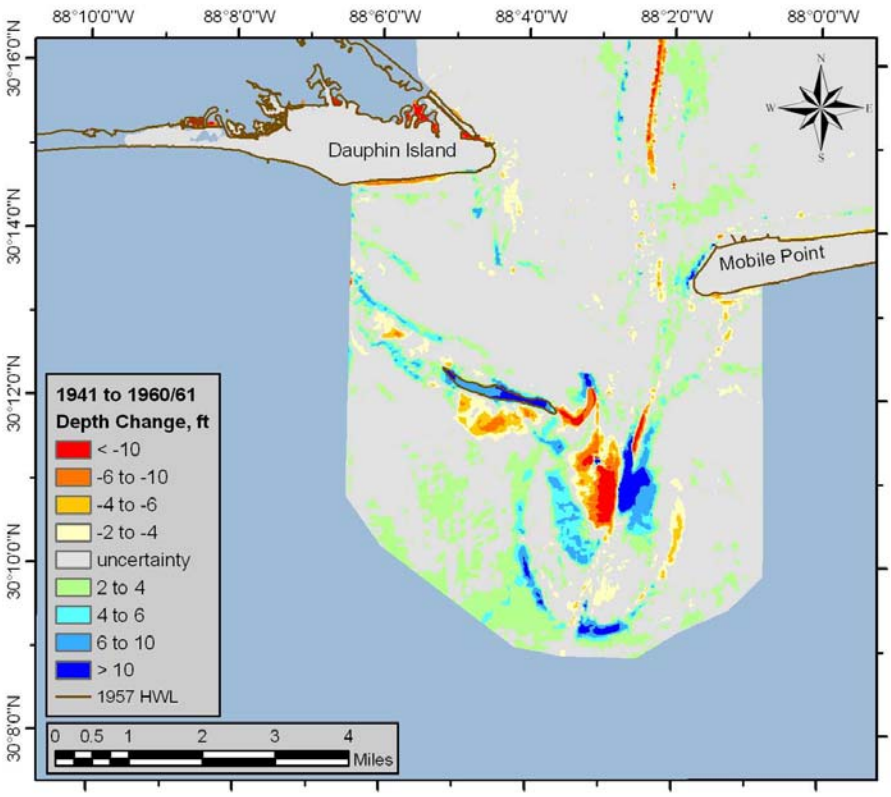

Figure 4-7. Bathymetric changes on the Mobile ebb-tidal delta, 1941 to 1960/61.

1960/61 to 1970. Sand Island continued to migrate and grow to the northwest during this 10-year period. Natural channel infilling continued north of the maintained navigation channel, and sand bypassing to the west at this point persisted (Figure 4-8). Sand bypassing of the outer bar channel is not as obvious, but new work was completed in 1965 that resulted in a 42-ft deep and 600-ft wide channel. The length of time between surveys makes it difficult to identify any changes in trend that may have evolved as a result of channel dredging. Overall, the general pattern of erosion and deposition on the ebb-tidal delta is consistent with previous time periods.

1970 to 1986. Deposition along the eastern margin of the channel from littoral transport at Mobile Point continued to infill the westward migrating navigation channel. Strong ebb-tidal currents maintained flow of sand south along the channel to infill bathymetrically low areas along the southeast margin of the channel. Sand bypassing persisted at two location; one along the southern margin of the outer bar and the other at the southern extent of deposition along the east channel margin bar (Figure 4-9). The two north-northwest oriented deposition zones (relatively thin blue to green curves) denote the regions of bypass deposition on the western lobe of

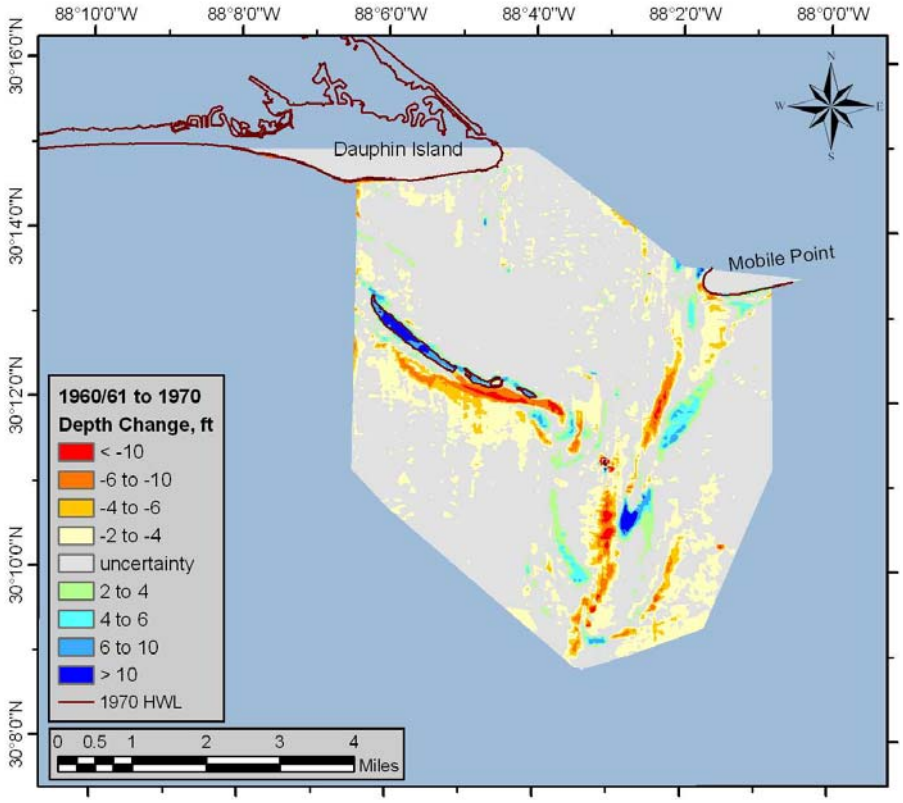

Figure 4-8. Bathymetric changes on the Mobile ebb-tidal delta, 1960/61 to 1970.

the ebb-tidal delta. Both features appear to supply sand to shoals northwest of this area, which eventually provides sand to Dauphin Island.

Subaqueous deposition associated with Pelican Island continued during this period. Pelican Island was not extensive, but the shoals surrounding the island appeared to be increasing in size (Figure 4-9). Erosion southeast of Pelican Island can be linked with deposition north of this zone, likely related to the hurricanes of 1985 (*Elena* and *Juan*). Sand deposition to the northwest of Pelican Island supplied sediment to Dauphin Island as wave-generated currents transport sand past Pelican Pass and to the beach.

1986 to 2002. By 2002, sand deposition associated with Pelican Island had created the most extensive island on the ebb-tidal delta since 1908. It extended approximately 3.4 miles from southeast to northwest (Figure 4-10). The southeastern portion of the island had migrated northeast in response to storm overwash processes, but the island was intact. The deposition pattern at the northwest end of the island provided a continuous pathway for sand transport from Pelican to Dauphin Island. Bypassing toward the southern end of the outer bar

appeared active, but a portion of the horseshoe-shaped bar on the western lobe of the ebb-tidal delta contained sand dredged from the channel that was placed in the SIBUA. Regardless, the pattern of deposition is similar to that identified for the previous time period when sand had not been placed in the SIBUA.

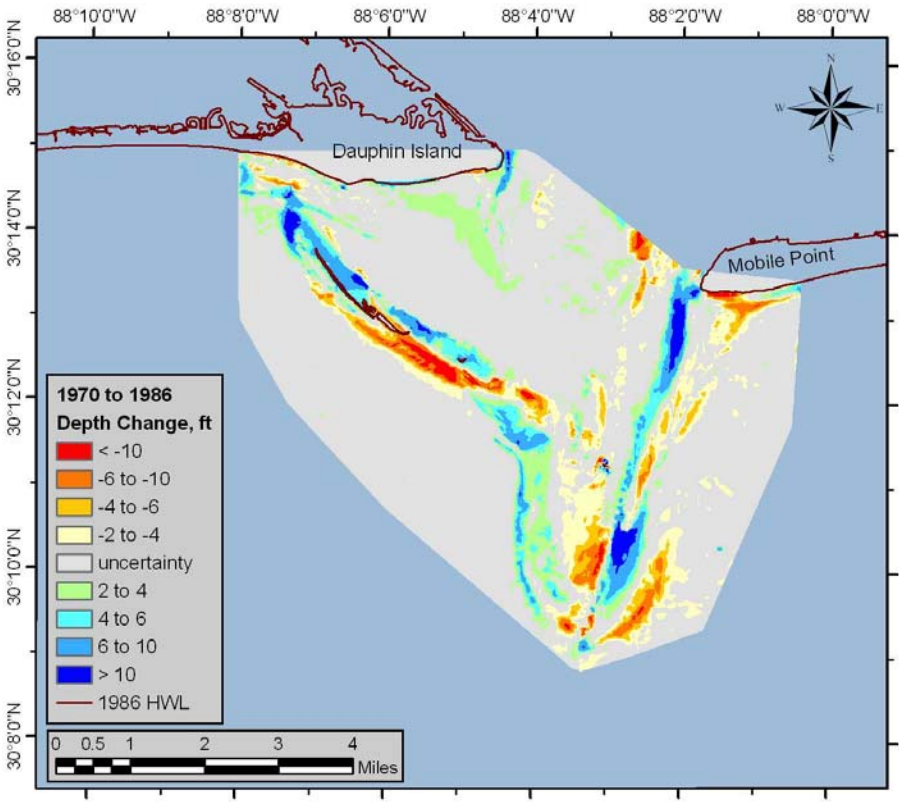

Figure 4-9. Bathymetric changes on the Mobile ebb-tidal delta, 1970 to 1986.

Sand deposition north and west of Sand Island Lighthouse likely originated from dredged material disposal in the Sand Island feeder berms (Hands, 1992). The pattern of deposition west and north of this area is consistent with historical transport pathways. It is likely that sand bypassing south of the feeder berms supplies sediment to the shoal. In turn, sand from the shoal supplies sediment to Pelican Island, which then supplies sand to Dauphin Island. This long-term sand transfer process appears to persist through most time periods, only to be disrupted temporarily by energy associated with major storms.

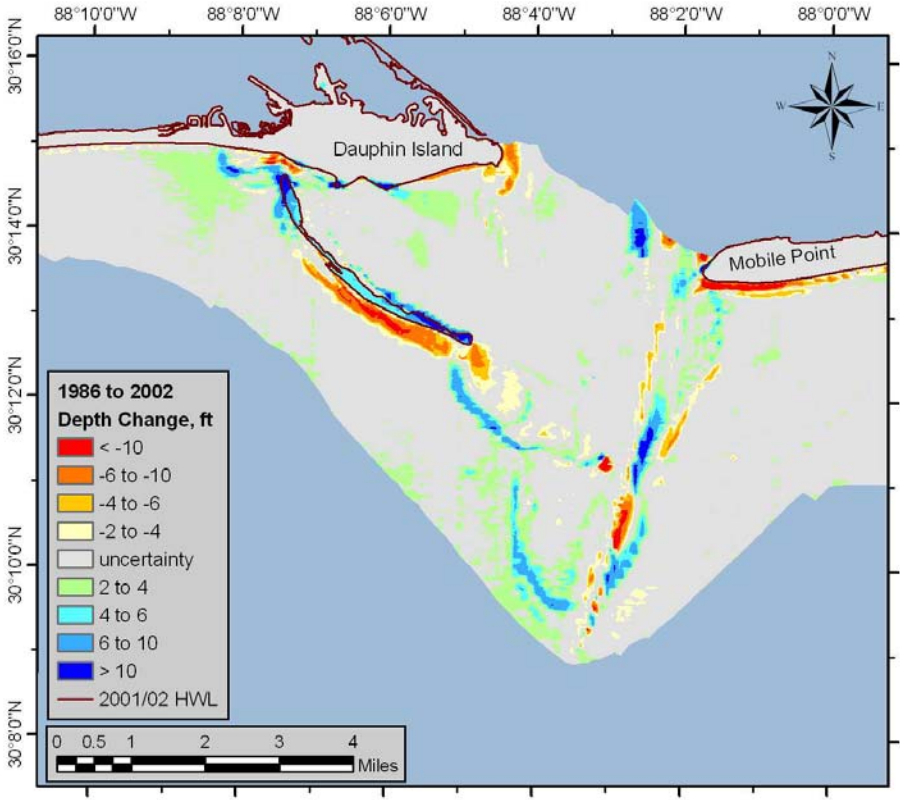

Figure 4-10. Bathymetric changes on the Mobile ebb-tidal delta, 1986 to 2002.

Volumetric Changes

Changes in erosion and deposition on the ebb-tidal delta were quantified to isolate trends that may have evolved as the result of channel dredging through the outer bar. Similar to the sand volume analysis completed for the east and west lobes of the ebb-tidal delta (see Table 3-4), bathymetric change results for pre- and post-dredging time periods were quantified for both areas as well. However, polygon boundaries for defining calculation limits were based on erosion and accretion boundaries in the channel, the approximate location of the 30-ft depth contour for the most recent surface where deposition occurred and the older surface where erosion was identified, and the landward boundary where sand deposition or erosion is associated with shoal migration or sand bypassing to the beach. As such, a portion of the ebb-tidal delta south of Pelican Point, where sand from little Dauphin Island and the shoreface fronting the eastern end of Dauphin Island have supplied sand to Pelican Bay, has been excluded from this analysis. Polygon boundaries for each change surface are provided in Appendix G.

Prior to Major Dredging Operations. Four change surfaces were evaluated to quantify sand volume adjustments on the east and west lobes of the Mobile ebb-tidal

delta. The goal was to document natural variations in deposition and erosion to gauge the significance of changes recorded once major channel dredging operations commenced. As shown on Figure 4-3, substantial changes in erosion and deposition occurred between 1847/48 and 1892, but deposition exceed erosion on either side of the channel as the channel migrated west. Net addition of approximately 21.9 million cy of sand to the east side of the ebb-tidal delta was indicated, and net deposition was documented west of the channel as well (about 13.6 million cy; Table 4-1). Although the same general trend was illustrated for the period 1847/48 to 1908, the magnitude of net changes was reduced. The entire ebb-tidal delta showed net deposition (about 17.9 million cy), but shoals west of the channel illustrated greater net deposition (10.2 million cy) than those to the east (7.7 million cy). By 1908, sand bypassing from the east had created extensive islands on the ebb-tidal delta west of the channel.

Between 1908 and 1917/20, the July 1916 hurricane, which made landfall as a Category 3 storm near Ship Island (MS), breached most of central Dauphin Island and reduced islands on the west lobe of the ebb-tidal delta to low-relief shoals. These changes were recorded as a net loss of sand west of the channel (about 9.9 million cy), but deposition on the east lobe continued during this period. Overall, net changes in shoal volume recorded between 1847/48 and 1917/20 illustrated net deposition on the order of 10.3 million cy. Considering the frequency and magnitude of tropical cyclones traversing coastal Alabama during this time, coastal and nearshore deposits demonstrated remarkable resilience, likely due to the large source of sand from beach and nearshore environments east of the channel.

After Major Dredging Operations Commenced. Between 1917/20 and 1941, east and west lobes of the ebb-tidal delta began recovering from the July 1916 hurricane. A well-maintained navigation channel had been established through the outer bar by 1941, but net deposition was dominant on both delta lobes. Net deposition for the entire ebb-tidal delta between 1917/20 and 1941 was about 16 million cy, of which 7.7 million cy were deposited west of the channel. During this same period, channel maintenance dredging accounted for about 214,000 cy/year, and infilling of breaches and lateral growth of Dauphin Island required at least an additional 200,000 cy/year. Again, sand supply east of the channel controlled sand transport magnitudes, and it appeared plentiful.

Net deposition on the eastern lobe of the ebb-tidal delta between 1941 and 1986 was consistent with the previous analysis (about 8.5 million cy). However, shoals west of the channel recorded net erosion of about 3.3 million cy, likely the result of a series of tropical cyclones that caused erosion on islands west of the navigation channel,

including Hurricanes *Ethel* (1960), *Camille* (1969), *Fredric* (1979), and the 1985 hurricanes (*Elena* and *Juan*). The hurricanes of 1985 likely had the greatest impact on change because they were closest in time to the 1986 survey.

Table 4-1. Deposition and erosion on the east and west lobes of the ebb-tidal delta, 1847 to 2002.

Analysis Period	Deposition (cu yd)	Erosion (cu yd)	Net Change (cu yd)
1847/48 to 1892 East	38,340,000	16,450,000	21,890,000
1847/48 to 1892 West	50,510,000	36,890,000	13,620,000
1847/48 to 1908 East	34,710,000	26,960,000	7,750,000
1847/48 to 1908 West	56,640,000	46,450,000	10,190,000
1908 to 1917/20 East	21,120,000	16,490,000	4,630,000
1908 to 1917/20 West	16,880,000	26,750,000	-9,870,000
1847/48 to 1917/20 East	42,050,000	37,680,000	4,370,000
1847/48 to 1917/20 West	54,140,000	48,230,000	5,910,000
1917/20 to 1941 East	23,700,000	15,400,000	8,300,000
1917/20 to 1941 West	26,510,000	18,820,000	7,690,000
1941 to 1986 East	27,320,000	18,800,000	8,520,000
1941 to 1986 West	29,270,000	32,590,000	-3,320,000
1917/20 to 1986 East	38,820,000	24,690,000	14,130,000
1917/20 to 1986 West	38,490,000	32,720,000	5,770,000
1917/20 to 2002 East	46,540,000	20,170,000	26,370,000
1917/20 to 2002 West	52,880,000	28,210,000	24,670,000
1941 to 2002 East	33,060,000	14,180,000	18,880,000
1941 to 2002 West	42,300,000	27,580,000	14,720,000
1908 to 2002 East	54,280,000	23,530,000	30,750,000
1908 to 2002 West	57,010,000	40,550,000	16,460,000
1847/48 to 2002 East	74,680,000	43,970,000	30,710,000
1847/48 to 2002 West	83,350,000	52,370,000	30,980,000

Between 1986 and 2002, net sedimentation trends changed significantly as deposition on the ebb-tidal delta was dominant, producing a net increase in sand volume east of the channel between 1917/20 and 2002 of about 26.4 million cy. The western lobe of the ebb-tidal delta recovered well from tropical cyclone impact between 1960 and 1985. Sand deposition between 1917/20 and 2002 west of the channel was slightly less than to the east at 24.7 million cy. As stated earlier, by 2002, Pelican Island was a dominant feature west of the navigation channel, supplying large quantities of littoral sand to Dauphin Island. The capacity of this area to recover from large storm-related losses in a relatively short time period

indicates how vigorous the east-to-west sand transport system is at and adjacent to Mobile Pass.

Summary. Although significant quantities of littoral sand were dredged from the channel across the Mobile Outer Bar, only two of the 11 time periods illustrated a net loss of sediment from the ebb-tidal delta since dredging commenced in 1904. Both were directly related to one or more major storms in close proximity to the ending survey date. Under natural conditions (1847/48 and 1917/20), relatively small quantities of net deposition were documented due to the impact of the July 1916 hurricane. Under major channel dredging operation between 1917/20 and 2002, substantial deposition was indicated across the entire ebb-tidal delta (Figure 4-11). Although maintenance dredging removed about 268,000 cy of littoral material annually from the channel during this period, net deposition on the west lobe of the ebb-tidal delta resulted in the greatest subaerial extent of Pelican Island since 1908. In addition, breach closure and lateral island growth along central and western Dauphin Island required approximately 160,000 cy of deposition annually.

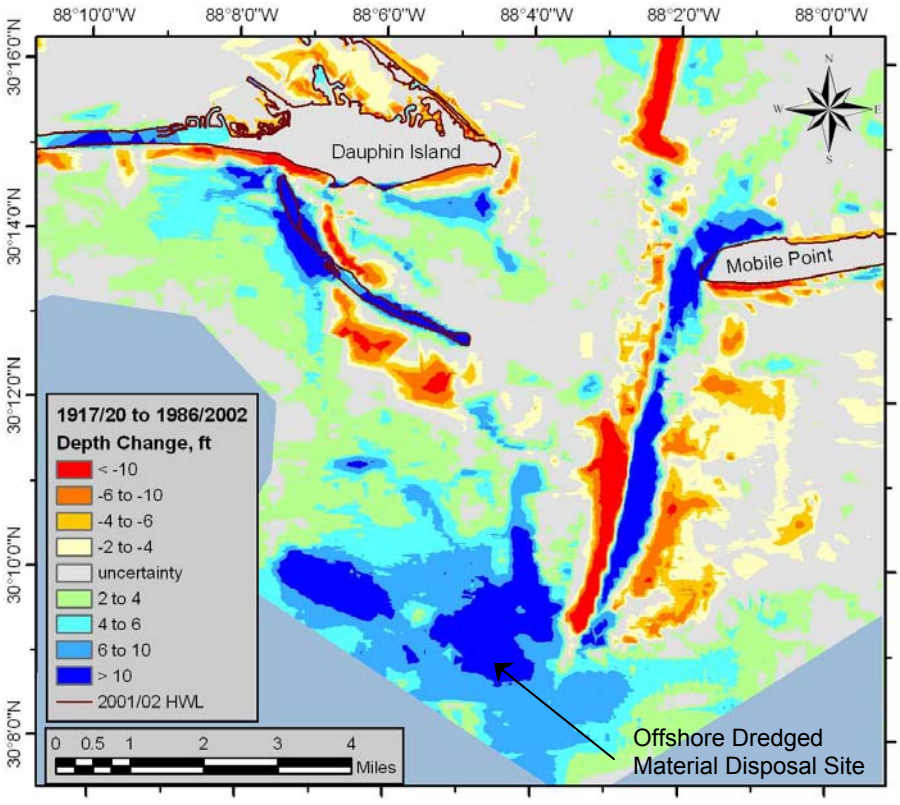

Figure 4-11. Bathymetric change on the Mobile ebb-tidal delta, 1917/20 to 1986/2002. Deposition zones seaward and west of the navigation channel were last surveyed in 1991. The deposition area farthest to the west is the Mobile Outer Mound. The irregular polygon just west of the outer mouth bar channel is believed to mark the historical location of dredged material disposal from the outer bar channel.

Sand transport from east of the ebb-tidal delta provided about 475,000 cy of sand per year to the Mobile Pass shoal system during the time of channel dredging, a quantity similar to the amount supplied to shoals prior to dredging. There is evidence of sand bypassing from east-to-west across the maintained navigation channel, and onshore transport of sand from the historical offshore disposal area appears to be supplying sand to the active transport system on the west lobe of the ebb-tidal delta that eventually nourishes beaches on Dauphin Island (Figure 4-11).

5 Wave Propagation, Sediment Transport, and Hydrodynamic Simulations

Nearshore Wave Modeling

Nearshore wave heights and directions along Dauphin Island and the Fort Morgan peninsula were estimated using the USACE STeady-state spectral WAVE model (STWAVE) to simulate the propagation of offshore waves to the shoreline. Offshore wave data available from the USACE Wave Information Study (WIS) provided input wave conditions for STWAVE. Wave modeling results were used to estimate longshore sediment transport potential as input for estimating morphology changes on the ebb shoal complex, as well as to gain a general understanding of the nearshore forcing under various process conditions.

Regional Wave Conditions. The interaction of wind with the water surface generates waves. Once wind waves are generated, the forces of gravity, and to a lesser extent surface tension, allow waves to travel long distances across the sea surface. Waves are usually present at the coast because the sea surface is vast, winds are prevalent, and waves can travel long distances. Waves are primarily responsible for sediment transport in the nearshore zone and for subsequent shoreline change; therefore, waves are of fundamental interest to determine potential longshore sand transport rates within the study area.

As waves enter the nearshore zone, varying seafloor morphology causes waves (height and direction) to change. As waves enter shallow water, their height increases (shoaling), and the direction of travel bends toward the coast so that wave crests become more parallel to the shoreline (refraction). As waves approach shore, shoaling and wavelength modifications overcome dissipation effects and cause wave height to increase and waves to steepen. Eventually wave steepness causes the wave to become unstable and break, which dissipates wave energy. Energy also is distributed along a wave crest by a process called wave diffraction. Together, wave shoaling, refraction, diffraction, and breaking can focus wave energy on particular areas, depending upon the characteristics of nearshore bathymetry.

In general, waves that move sand along and across the shore of coastal Alabama are generated by winds in the Gulf of Mexico. Seasonal variations in wave climate occur and are governed by overall seasonal characteristics of wind. Summer months (typically considered May through October) are characterized by relatively calm winds and low-energy waves, while winter months (typically considered December

through April) are characterized by a more energetic wind and wave climate. Sporadic storms, such as hurricanes and cold fronts, generate the largest waves that impact the Alabama coast.

Availability of Wave Data. The USACE Wave Information Study (WIS) has met a critical need for wave information in coastal engineering studies since the 1980s. WIS contains a time series information of spectrally-based, significant wave height, peak period, peak direction, and wind speed and direction produced from a computer hindcast model. The hindcast wave model, WISWAVE (Resio and Tracy, 1983), is run using wind data (speed and direction) at selected coastal locations around the United States. The model provides wave climate based on local and regional wind conditions. Because the data are numerically generated, consistent and long-term wave data are available at most coastal locations.

WIS Offshore Boundary Conditions. Figure 5-1 illustrates WIS stations (yellow markers) located within in the project study area. It is desirable for the offshore boundary of the wave model to fall at the same latitude as the WIS Stations, so that no wave transformation need be performed to apply WIS data to the offshore boundary of the model. This concern, together with an effort to minimize the model domain for computational reasons, led this work to focus on the closest inshore WIS Stations in the study area.

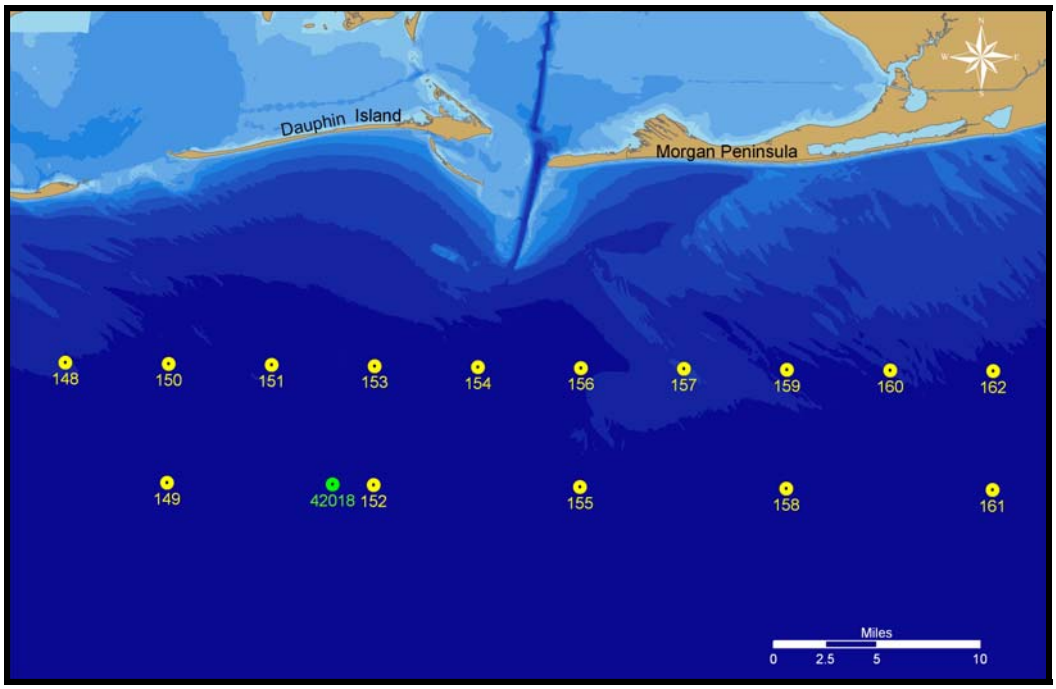

Figure 5-1. WIS stations in the study region are shown with yellow markers. NDBC Buoy 42018 is shown in green.

A comparison of wave roses for WIS Stations 148, 156, and 162 is shown in Figure 5-2. These plots confirm that a majority of the wave energy offshore Mobile Bay is incident from the SSE and the SE. Given the 45-mile distance spanned by these data, the uniformity of the wave conditions is striking. Moving from west to east there is a slight reduction in the percent occurrence of waves from the east and south, but these differences are quite small. For the given latitude, it is accurate to say that the offshore wave climate is spatially constant. As a result, it was decided to operate the wave model with data from a single WIS Station rather than impose a spatially varying offshore wave condition. WIS Station 156 provided offshore boundary conditions for the coarse wave grid. For the 20-yr hindcast, average wave height was 2.8 ft, with a peak wave period of 4.6 sec from the southeast (154 deg). In addition to the physical argument for simplifying boundary condition in this way, a single source for the boundary conditions greatly simplifies the estimation of longshore sediment transport potential, which is calculated from the wave model solution. Using a single WIS record for the boundary condition allows the direct calculation of percent occurrence for each wave case and hence the percent contribution to the total sediment transport.

Verification of WIS Data. Wave measurements made by NOAA during the 1980s made verification of WIS results possible by comparing the statistics and distributions of wave heights and periods from different time periods (Hubertz et al., 1993). Improvements have been made through subsequent modeling efforts to increase the accuracy of WIS relative to NOAA measurements. Second Generation (2G) WIS data, which accounts for weak nonlinear wave-wave interaction, equilibrium spectral functions, refraction, shoaling and dissipation, were used in the present study. The 2G WIS data provide wave parameter results every hour. A detailed comparison between the 2G WIS data, the Third Generation (3G) wave models WAM and WAVEWATCH III and the relevant National Data Buoy Center (NDBC) stations are reported in Tracy and Cialone (2004) as follows:

> *The 2G WIS results are consistent with results from the more complex calculations done in the 3G models. No one model is the clear winner in these comparisons. The 3G models tend to have slightly better directional results. WIS tends to slightly over-predict wave height and the 3G models tend to under-predict. WIS captures storms and hurricane events quite well and is a good tool for the quick frontal changes in the Gulf of Mexico.*

Analysis of wave periods showed that all models tested could be improved in their predictions in this regard.

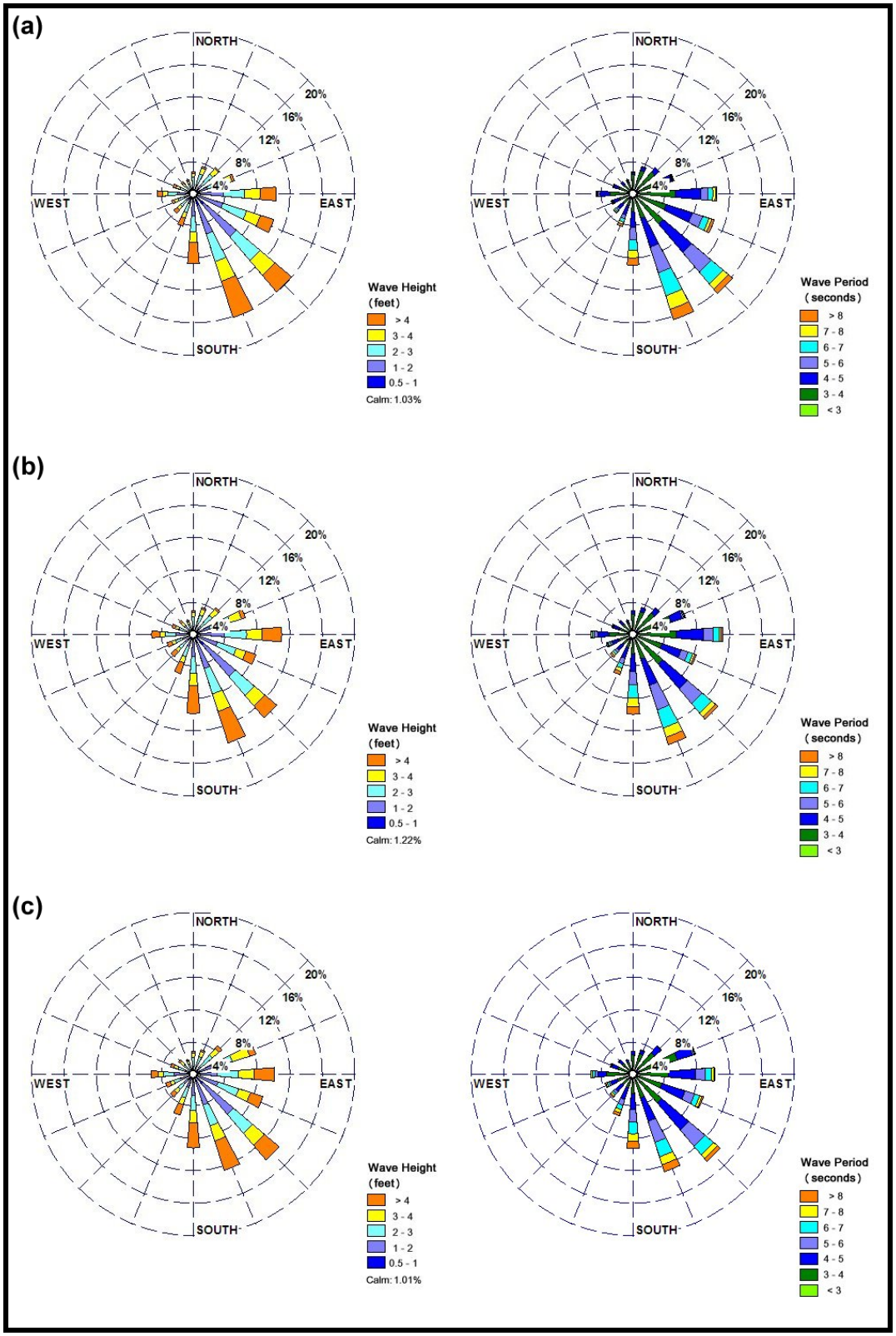

Figure 5-2. Wave height and period roses for (a) WIS station148, (b) WIS station156, and (c) WIS station162.

To supplement the regional-scale verification referenced above, the current work also compared 2G WIS data with an inshore NDBC location nearby the area of interest. WIS Station 152 and NDBC station 42018 are located less than 2 miles from each other, and both are approximately 16 miles offshore Dauphin Island (Figure 5-1).

Unfortunately, NDBC Station 42018 was only active for 45 days, from 6 February 1990 to 22 March 1990. However, this short time period still provides useful information with which to assess the accuracy of WIS data in this region. Comparison of wave heights for this period is shown in Figure 5-3. Both data sources reported wave heights at one hour intervals.

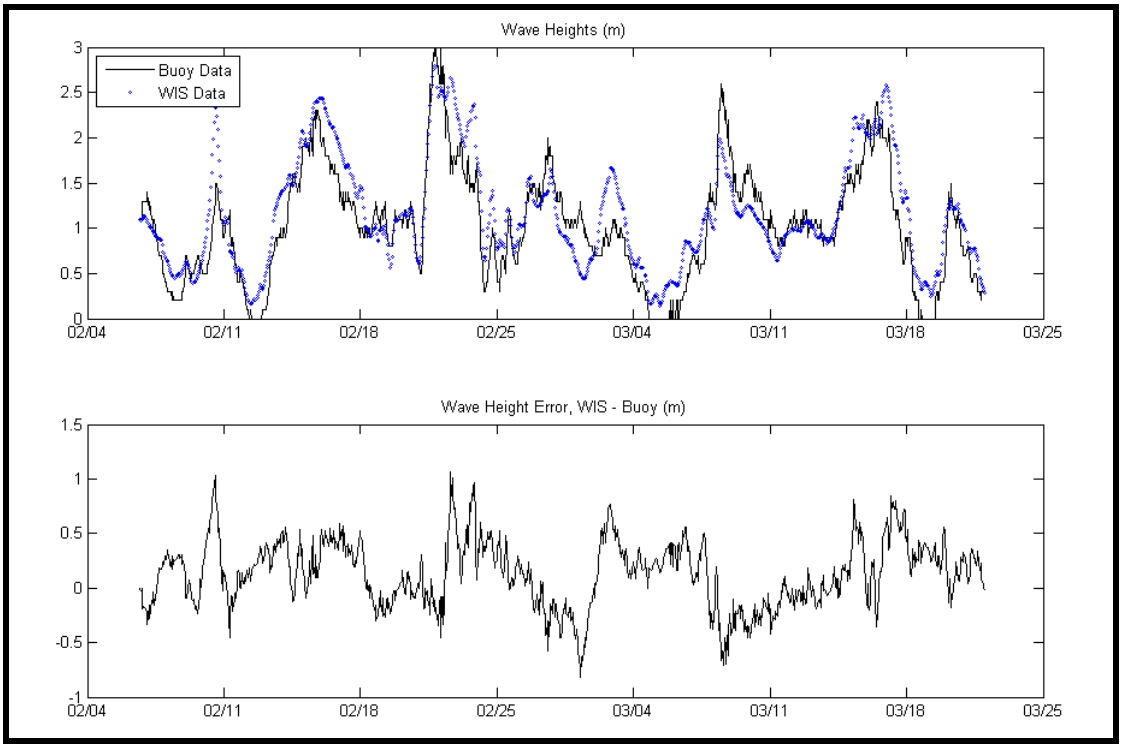

Figure 5-3. Wave height comparison between WIS Station 152 and NDBC Station 41018. The top panel illustrates WIS and NDBC wave height time series, and the bottom panel shows the error in WIS data reported as WIS prediction - Buoy measurement.

As the figure shows, WIS data reproduces the trend of measured data fairly well, but reveals a bias in wave height. WIS data generally over predicted wave height by about 1.2 ft. This finding is in agreement with the work by Tracy and Cialone (2004).

Data reported from NDBC Station 41018 did not include wave direction, so no direct comparison of wave direction could be made for this location. Work described in Tracy (1999) did compare wave directions predicted by WIS to those from relevant buoy data. Of specific interest to the present work is the comparison between the

Level 3 WIS solution (1/12 deg solution grid) and the data recorded at NDBC buoy 42007 for 9 months during 1997. NDBC Station 42007 lies offshore of Biloxi, MS in 44 ft of water, approximately 44 miles southwest of Mobile Pass. Tracy (1999) illustrates a bias in the WIS solution such that, on average, the predicted wave directions are less clockwise than the measured direction from the buoy. Three of the 9 months analyzed show an opposite trend, however, where WIS wave directions are more clockwise than the buoy data. Perhaps most important is that ±95% confidence bounds were calculated for the WIS solution. The average range of the ±95% confidence interval was found to be approximately 8 deg. Although this can be considered good agreement for a regional wave model, the discussion of the sediment transport modeling will show that a range of ±8 deg is quite significant.

Despite the bias toward over predicting wave height and the uncertainty in wave direction, the availability and continuity of WIS hindcast data make it an attractive choice when considering different sources for regional wave conditions. Because data are widespread and continuous, absent accurate field data from very near the site, the 2G WIS data are the best option for the development of spectral boundary conditions.

STWAVE. Developed by the USACE Waterways Experiment Station (WES), STWAVE v4.0 is a steady-state, spectral wave transformation model (Smith et al., 1999). Two-dimensional (frequency and direction versus energy) spectra were used as input to the model. STWAVE can simulate wave refraction and shoaling induced by changes in bathymetry and by wave interactions with currents. The model includes a wave breaking model based on water depth and wave steepness. Model output includes significant wave height (H_s), peak wave period (T_p), and mean wave direction ($\bar{\theta}$).

STWAVE is an efficient program that requires minimal computing resources to run well. The model is implemented using a finite-difference scheme on a regular Cartesian grid (grid increments in the x and y directions are equal). During a model run, the solution is computed starting from the offshore open boundary and is propagated onshore in a single pass of the model domain. As such, STWAVE can propagate waves only in directions within the ±87.5 deg half plane. A benefit of applying this single pass approach is that it uses minimal computer memory because the only memory-resident spectral data are for two grid columns. Accordingly, changing wave spectra across each grid column are computed with information solely from the previous grid column.

STWAVE is based on a form of the wave action balance equation. The wave action density spectrum, which includes the effects of currents, is conserved along wave rays. In the absence of currents, wave rays correspond to wave orthogonals, and the action density spectrum is equivalent to the wave energy density spectrum. A diagram showing the relationship of wave orthogonal, wave ray, and current directions is shown in Figure 5-4. The governing equation of wave transformation, using the action balance spectrum, in tensor notation is written as (Smith et al., 1999)

$$\left(C_{ga}\right)_i \frac{\partial}{\partial x_i} \frac{C_a C_{ga} \cos(\mu - \alpha) E}{\omega_r} = \sum \frac{S}{\omega_r} \tag{5.1}$$

where

$E = E(f,\theta)$ wave energy density spectrum,
S = energy source and sink terms (e.g., white capping, breaking, wind input),
α = wave orthogonal direction,
μ = wave ray direction (direction of energy propagation),
ω_r = relative angular frequency ($2\pi f_r$),
C_a, C_{ga} = absolute wave celerity and group celerity, respectively.

The breaking model in STWAVE is based on a form of the Miche criterion as discussed by Battjes and Janssen (1978). It sets a maximum limit on the zero-moment wave height (H_{mo}), the wave height based on the distribution of energy in the wave spectrum. The formulation of this model is

$$H_{mo(max)} = 0.1L \tanh(kd) \tag{5.2}$$

where L is the wavelength, k is the wave number ($k = 2\pi/L$), and d is the depth at the point where the breaking limit is being evaluated. This equation is used with a simpler breaking model, which was used alone in earlier versions of STWAVE, where the maximum H_{mo} wave height is always expressed as a constant ratio of water depth

$$H_{mo(max)} = 0.64\, d \tag{5.3}$$

An advantage of using Equation 5.2 over Equation 5.3 is that it accounts for wave breaking resulting from wave steepening caused by wave-current interactions. Once model wave heights exceed $H_{mo(max)}$, STWAVE uses a simple method to reduce the energy spectrum to set the value of $H_{mo} = H_{mo(max)}$. Energy at each frequency and direction is reduced by the same percentage. As a result, non-linear transfers of energy to high frequencies during breaking are not included in STWAVE.

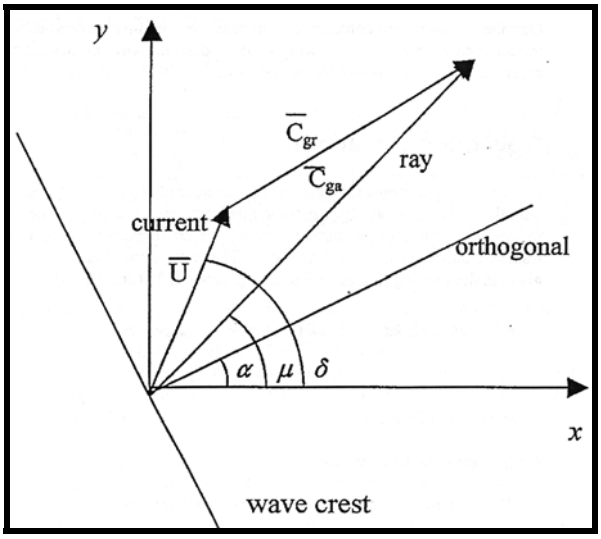

Figure 5-4. Wave and current vectors used in STWAVE. Subscript *a* denotes values in the *absolute* frame of reference, and subscript *r* denotes values in the *relative* frame of reference (with currents).

Model Domain and Bathymetry. Wave modeling consists of a regional coarse model grid (200 m x 200 m grid cells) as well as three fine grids (25 m x 25 m grid cells), which provide a detailed solution in areas of interest. The solution from the coarse wave model is mapped onto the offshore boundary of each of the fine grid, providing a detailed and spatially varying boundary condition for each of the fine grid runs.

Limits of the coarse grid (the largest rectangle in Figure 5-5) were chosen so the offshore boundary falls at the same latitude as WIS Station 156, which was chosen to supply the boundary conditions for wave runs. Lateral extents of the coarse grid are taken far from the fine grids to ensure the solution at the boundary of the fine grids is free of any edge effects. The inshore extent of the coarse grid is somewhat immaterial, provided it passes beyond the outer boundaries of the fine grids. The solution from the coarse wave grid was used only to formulate the boundary conditions for fine wave grids.

Three different fine grid domains were chosen so each area of interest could be examined with the required amount of detail. The two fine grids located along Dauphin Island and Morgan Peninsula were developed to achieve a detailed view of wave refraction and breaking in the nearshore region. Both these grids are comprised of 25 m x 25 m grid cells. The central fine grid encompasses the ebb shoal complex, Pelican Island, and Mobile pass, as well as a portion of the adjacent beaches. It also extends into Mobile Bay, so this same grid can be used for CMS-

M2D model runs as well. Because of the larger size of this grid, cell sizes were increased to 50 m x 50 m to keep model run times reasonable. A summary of the properties for each grid is given in Table 5-1.

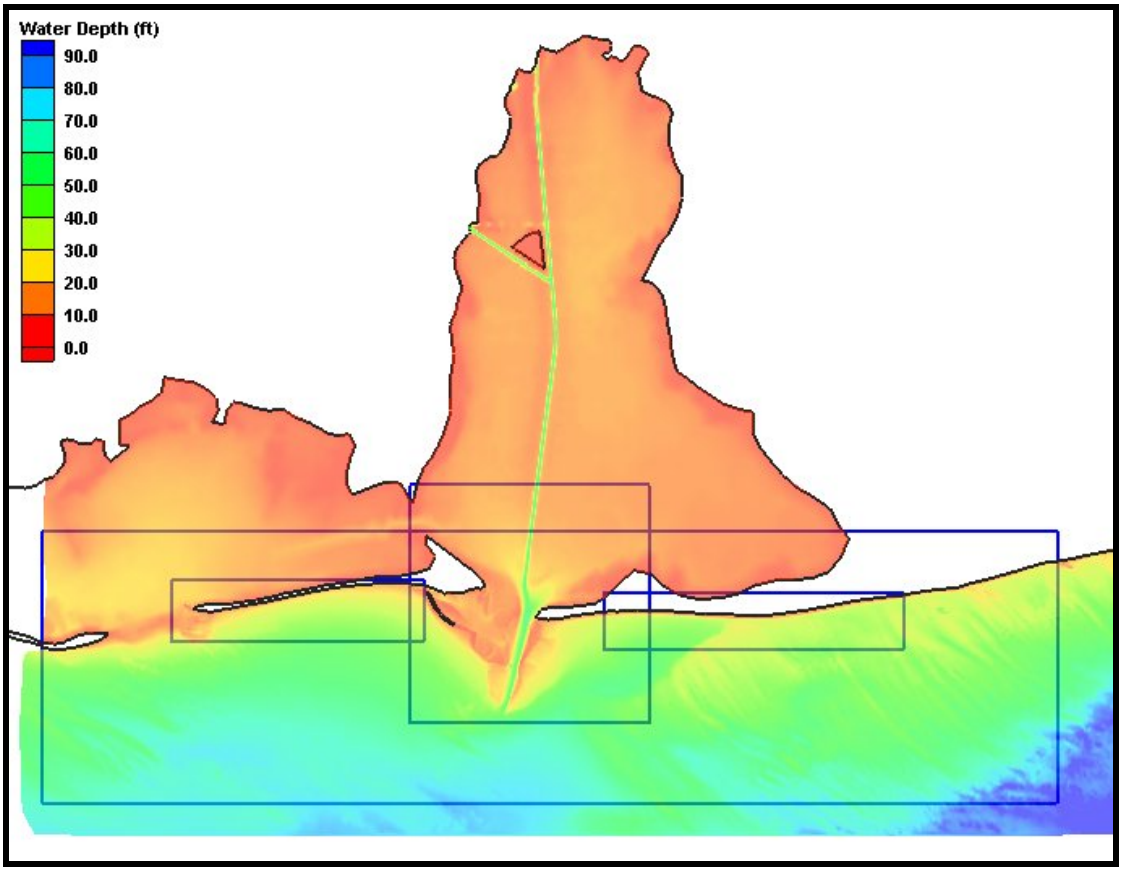

Figure 5-5. STWAVE bathymetry and model grid domains.

Table 5-1. Grid dimensions for offshore (coarse) and nearshore (fine) wave grids

	Cell Size	Grid Dimensions	Number of Water Cells	Typical Run Time (10 Wave Cases)
Coarse Grid	200 m x 200 m	430 rows x 115 columns	37,220	~11 min
West Fine Grid	25 m x 25 m	814 rows x 153 columns	88,888	~13 min
Center Fine Grid	50 m x 50 m	436 rows x 416 columns	167,970	~25 min
East Fine Grid	25 m x 25 m	1016 rows x 192 columns	138,182	~21 min

Bathymetry data were gathered from several sources and combined to provide a single data set which covered the study area. The offshore bathymetry is comprised of data collected in 1982/1988. All bathymetry along the ebb-tidal delta and within 3 miles of the Dauphin Island and Fort Morgan Peninsula shorelines was surveyed in 2002. Mississippi Sound and Mobile Bay bathymetry was taken from a 1960/1962 data set. Despite its age, this data set represents the most recent bathymetry covering Mobile Bay and Mississippi Sound. A detailed description of these data, including their original sources, datum adjustments applied, and other details can be found in Chapter 3.

Boundary Conditions. STWAVE input spectra were developed using a numerical routine that recreates a two dimensional spectrum for each individual wave condition in the WIS record, from 1980 to 1999. The program computes the frequency and directional spread of a wave energy spectrum based on significant wave parameters (i.e., wave height, peak period, and peak direction) and wind speed (Goda, 1985). The frequency spectrum $S(f)$ is computed using the relationship

$$S(f) = 0.257 H_{1/3}^2 T_{1/3} (T_{1/3} f)^{-5} \exp\left[-1.03 (T_{1/3} f)^{-4}\right] \tag{5.4}$$

known as the Bretschneider-Mitsuyasu spectrum, where $H_{1/3}$ is the significant wave height, f is the discrete frequency where $S(f)$ is evaluated, and $T_{1/3}$ is the significant period, estimated from the peak wave frequency (f_p) by

$$T_{1/3} = 1/\left(1.05 f_p\right). \tag{5.5}$$

To compute the two-dimensional energy spectrum, a directional spreading function $G(f,\theta)$ must be applied to the frequency spectrum such that

$$S(f,\theta) = S(f) G(f,\theta). \tag{5.6}$$

In this method, the directional spreading function is computed using the relationship

$$G(f,\theta) = G_o \cos^{2s}\left(\frac{\theta}{2}\right) \tag{5.7}$$

where s is a spreading parameter related to wind speed and frequency, θ is the azimuth angle relative to the principle direction of wave travel, and G_o is a constant dependent on θ and s. The spreading parameter s is evaluated using the expression

$$s = \begin{cases} s_{max} \cdot (f / f_p)^5 : f \le f_p \\ s_{max} \cdot (f / f_p)^{-2.5} : f \ge f_p \end{cases} \quad (5.8)$$

where $s_{max} = 11.5(2\pi f_p U / g)^{-2.5}$. Wind speed U therefore to controls the directional spread of the spectrum by increasing the directional spread with increasing wind speed. Finally, the constant G_o is computed by evaluating the integral

$$G_o = \left[\int_{\theta_{min}}^{\theta_{max}} \cos^{2s}\left(\frac{\theta}{2}\right) d\theta \right]^{-1} \quad (5.9)$$

The result is a wave energy spectrum that is based on parameters from the WIS record, and that distributes spectral energy based on wave peak frequency and wind speed. An example of a two-dimensional spectrum generated by this method is presented in Figure 5-6.

After recreating a two-dimensional spectrum from the parameters given in the WIS record, each individual spectrum is sorted, or "binned", by peak direction and peak period. Wave spectra computed from wave parameters that occur within the limits of individual direction and period bins are added, and a mean spectrum for all waves in each bin is computed based on total number of wave events in the bin. In total, ten direction bins and one period bin were used to characterize wave data. These ten bins were selected based on percent occurrence and percent energy for conditions in each bin.

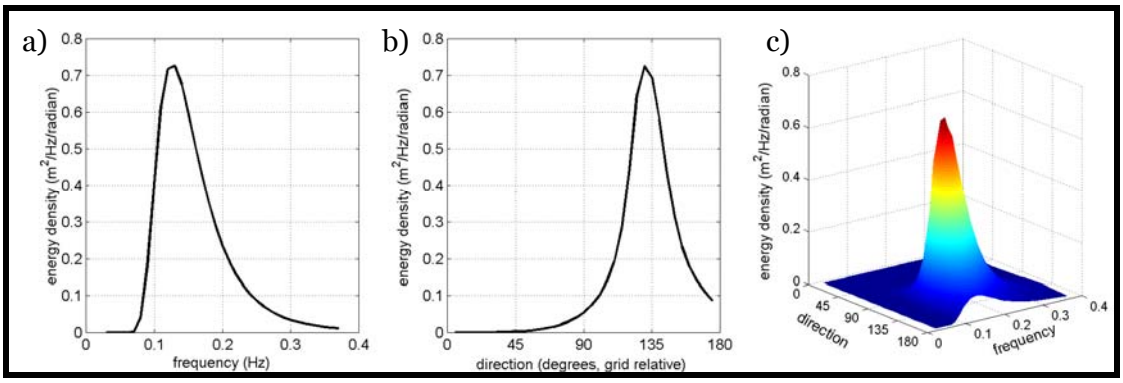

Figure 5-6. STWAVE input spectrum developed using WIS 20-year hindcast data with Goda (1985) method of computing frequency and direction spectrum. Plots show a) frequency distribution of energy at peak direction, b) directional distribution of energy at peak frequency, and c) surface plot of two-dimensional energy spectrum (H_{mo} = 0.9 m, θ_{mean} = 130 deg).

Selected conditions have a percent occurrence greater than 1%, and also contain more than 1% of the energy of the entire wave record. Conditions selected for the base model run are shown in Table 5-2, with the significant parameters of each input spectrum. The percent occurrence values do not add up to 100% as the WIS record reports waves which are traveling offshore. The waves accounted for in this work are only those which contribute energy to shorelines in the study area.

Table 5-2. Input wave spectra parameters used for 20-year average cases, WIS Station 156.

STWAVE Model Input Case	Percent Occurrence	H_{mo} Wave Height (ft)	Peak Wave Period, T_p (sec)	Peak Wave Direction, θ_p (deg true north)
1	10.81	3.2	5.9	105
2	4.75	3.2	5.9	130
3	10.72	2.9	5.9	145
4	12.49	4.1	6.7	160
5	9.27	4.9	7.7	170
6	4.53	4.2	6.7	185
7	3.30	3.4	6.7	200
8	2.17	2.9	5.3	215
9	1.76	3.1	5.9	230
10	5.18	3.2	5.3	260

Model Results. Results for the coarse grid were used to provide offshore boundary conditions for each of the 3 nested fine grids. However, a review of coarse wave results can provide an overview of the wave processes in the area and provide some guidance for what to look for in the nested grid results. Color contour and vector plots for Cases 5 and 10 are shown below in Figures 5-7 and 5-8 respectively. All wave modeling results are illustrated in Appendix H.

A larger energy event simulated in Case 5 (Figure 5-7) reveals significant wave breaking across the ebb shoal complex on both sides of the navigational channel at Mobile Pass. There is a significant sheltering effect provided by Pelican Island as well, where wave heights are reduced shoreward of the island. Some amount of shoaling can be seen across Dixie Bar while wave breaking again is seen across Petit Bois Pass to the west.

For the milder Case 10 results, there was a reduction of wave heights within Mobile Pass, but the strong gradient in wave heights denoting breaking is not seen here (Figure 5-8). There was a significant reduction in wave height between Pelican

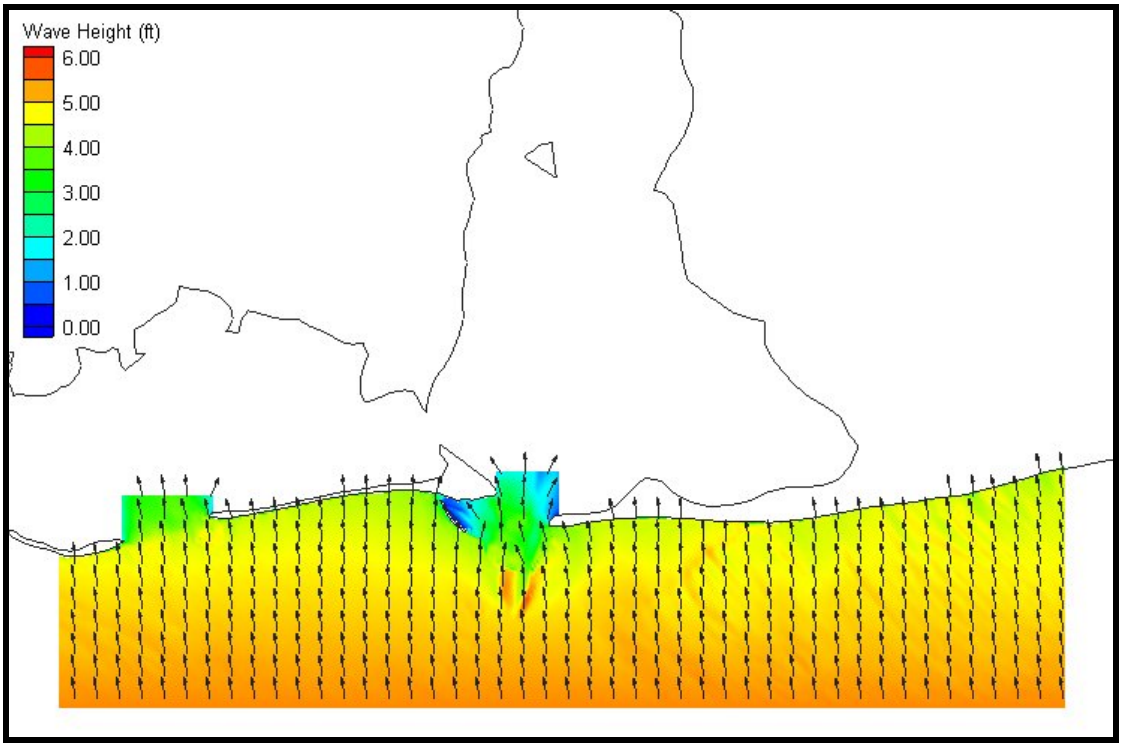

Figure 5-7. Coarse grid (200 m x 200 m) wave results for Case 5. Wave heights are shown by color while wave direction is indicated by the arrow direction.

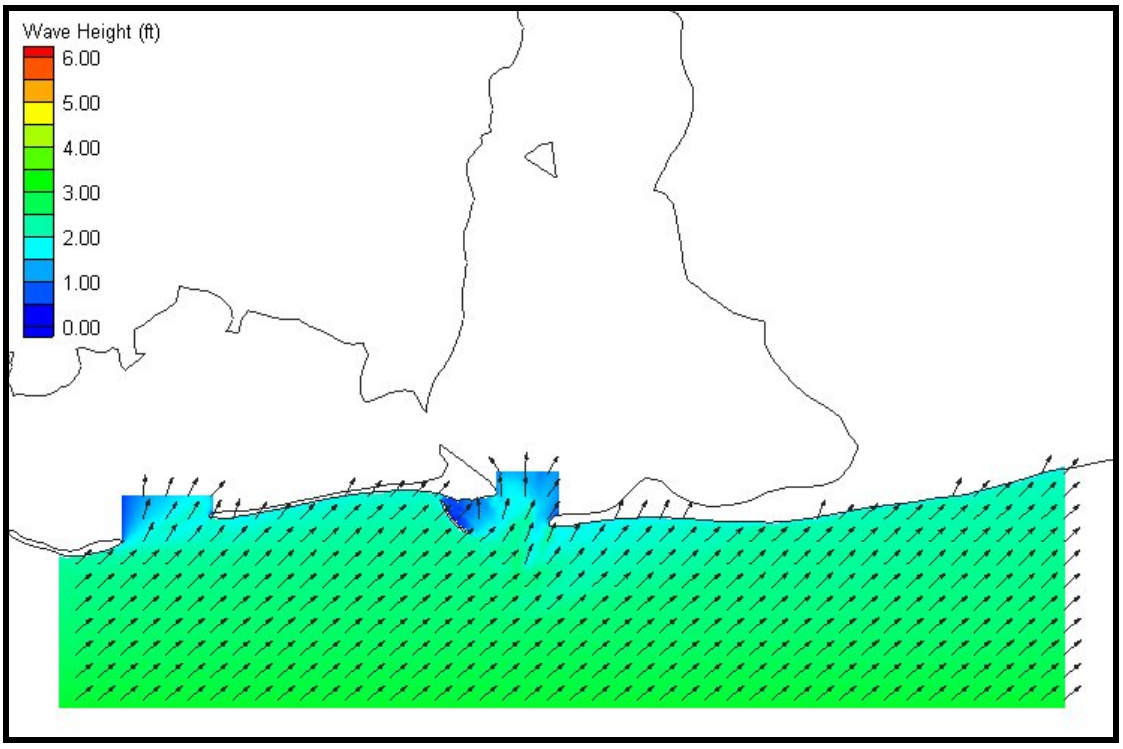

Figure 5-8. Coarse grid (200 m x 200 m) wave results for Case 10. Wave heights are shown by color while wave direction is indicated by the arrow direction.

Island and Dauphin Island. Wave propagation over the ebb-shoal complex and Dixie Bar appear to refract wave energy away from the western end of the Fort Morgan Peninsula, resulting in an area of somewhat reduced wave heights immediately east of Mobile Pass. There is little to no wave breaking at Petit Bois Pass for these smaller waves incident from the southwest.

In both cases it was observed that nearshore wave heights and directions along open coastal areas, such as central Dauphin Island and Fort Morgan Peninsula, were refracted normally as they approach the shoreline. In the absence of significant bathymetric features, these regions of the wave solution showed no drastic changes in wave height or direction.

Fine grid model results for Dauphin Island are shown for Cases 5 and 10 in Figures 5-9 and 5-10, respectively. The results for Case 5 show wave breaking at both ends of the grid. At the western end of the island, the shoal extending into Petit Bois Pass has a strong influence on wave heights and directions. At the east end of the model grid, the shoal extending between Pelican Island and Dauphin Island also causes these larger waves to break. Throughout the center portion of Dauphin Island, there is normal wave refraction, as expected. It is notable that along this section of the shoreline, waves from Case 5 are almost shore-normal adjacent to the shoreline. This fact serves to illustrate that shoreline orientation of the central portion of the island has adjusted to become perpendicular to the most significant direction of wave energy. As such, sediment transport predictions based on these results will be sensitive to wave angle for these high-energy contributions.

Wave results for Case 10 along Dauphin Island show little variation. Again the shoal at the west end of the island is causing wave refraction, but breaking observed in the higher energy waves from the southeast is absent (Figure 5-10). For the majority of the model domain, waves are seen to continue their refraction as they approach the shoreline, with breaking observed immediately adjacent to the beach.

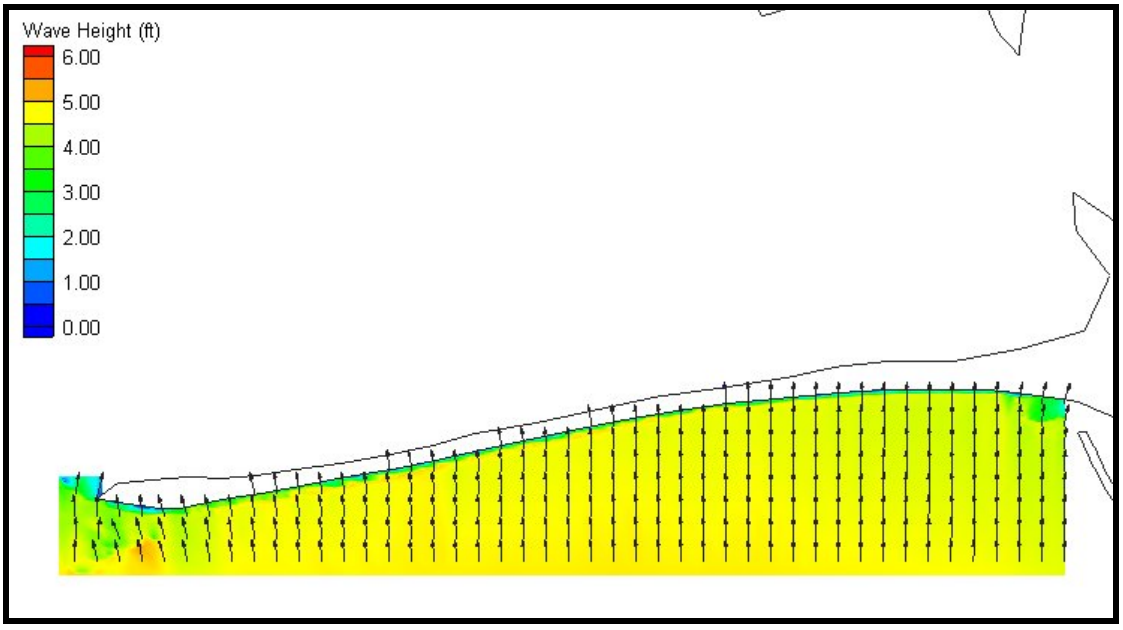

Figure 5-9. Fine grid (25 m x 25 m) wave results for Case 5, Dauphin Island. Wave heights are shown by color while wave direction is indicated by arrow direction.

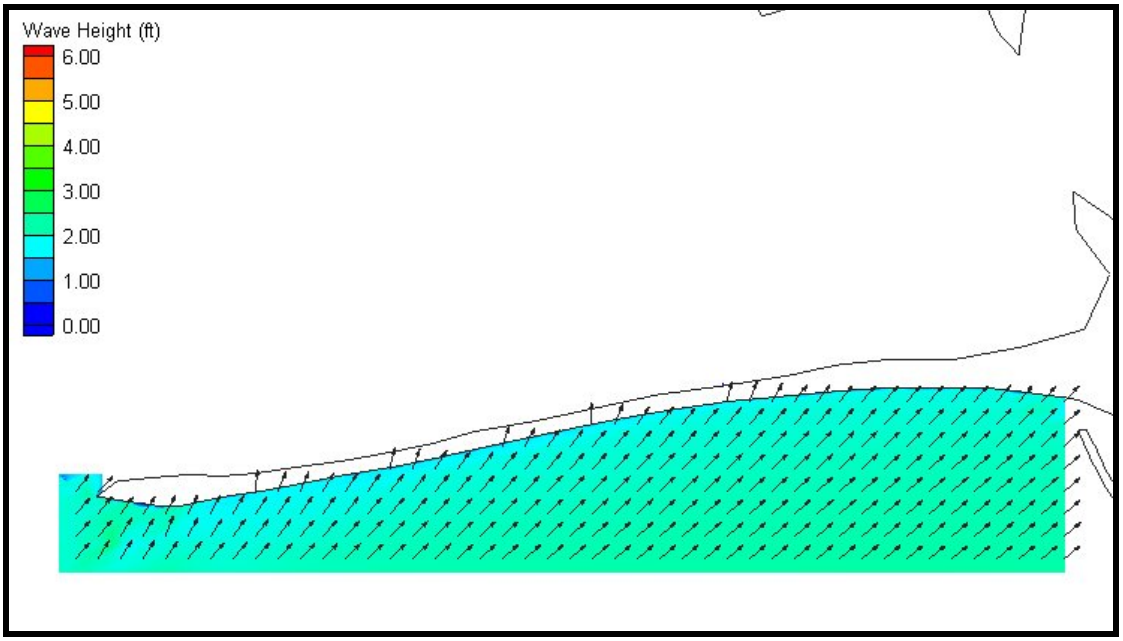

Figure 5-10. Fine grid (25 m x 25 m) wave results for Case 10, Dauphin Island. Wave heights are shown by color while wave direction is indicated by arrow direction.

Detailed wave results for Mobile Pass are shown in Figures 5-11 and 5-12. For Case 5 (Figure 5-11), the ebb-shoal complex dominates wave transformation seaward of the inlet. Wave steepening and breaking are observed along the outer edge of the ebb-tidal delta on either side of the navigation channel. The sheltering effect of Pelican

Island is apparent while there is strong refraction in the lee of the island, with waves traveling to the west. Inside the inlet, there is diffraction of wave energy as expected. The navigational channel within Mobile Bay promotes wave refraction to the east slightly, resulting in a decrease in wave height along the main channel.

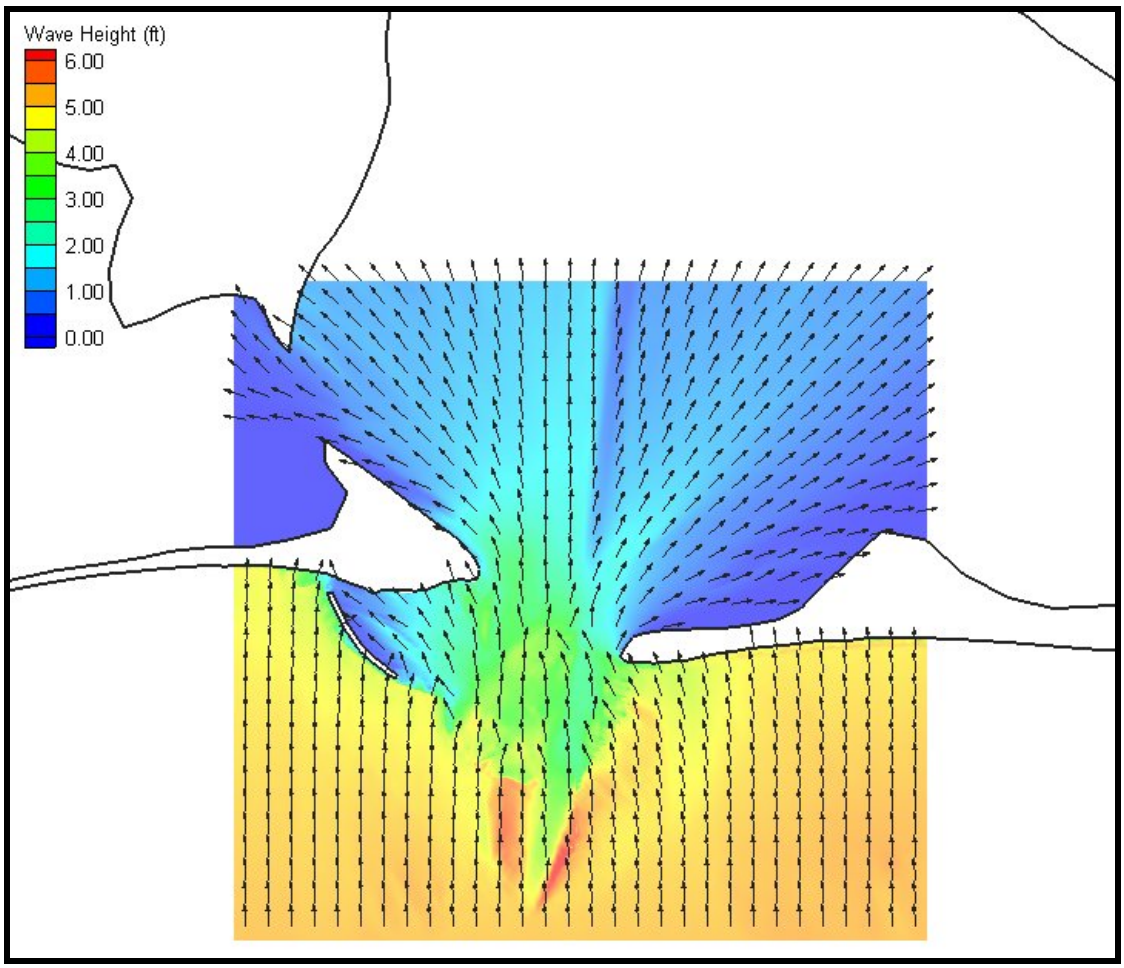

Figure 5-11. Fine grid (50 m x 50 m) wave results for Case 5, Mobile Pass. Wave heights are shown by color while wave direction is indicated by the arrow direction.

The smaller energy event modeled in Case 10 (Figure 5-12) shows some wave steepening over the ebb shoal but there is not the strong breaking that was illustrated in Case 5. Wave sheltering of Pelican Island is broader for these waves from the southwest, while refraction behind the island again orients the waves strongly to the west. The similarity of wave directions in the lee of Pelican Island for two different incident wave conditions serves to highlight the major influence the ebb-shoal complex has on wave transformation in the area, regardless of offshore conditions. Within the inlet itself, normal diffraction is observed. The influence of the

navigational channel is still evident, although the difference in wave height caused by wave refraction at the channel is smaller than in Case 5.

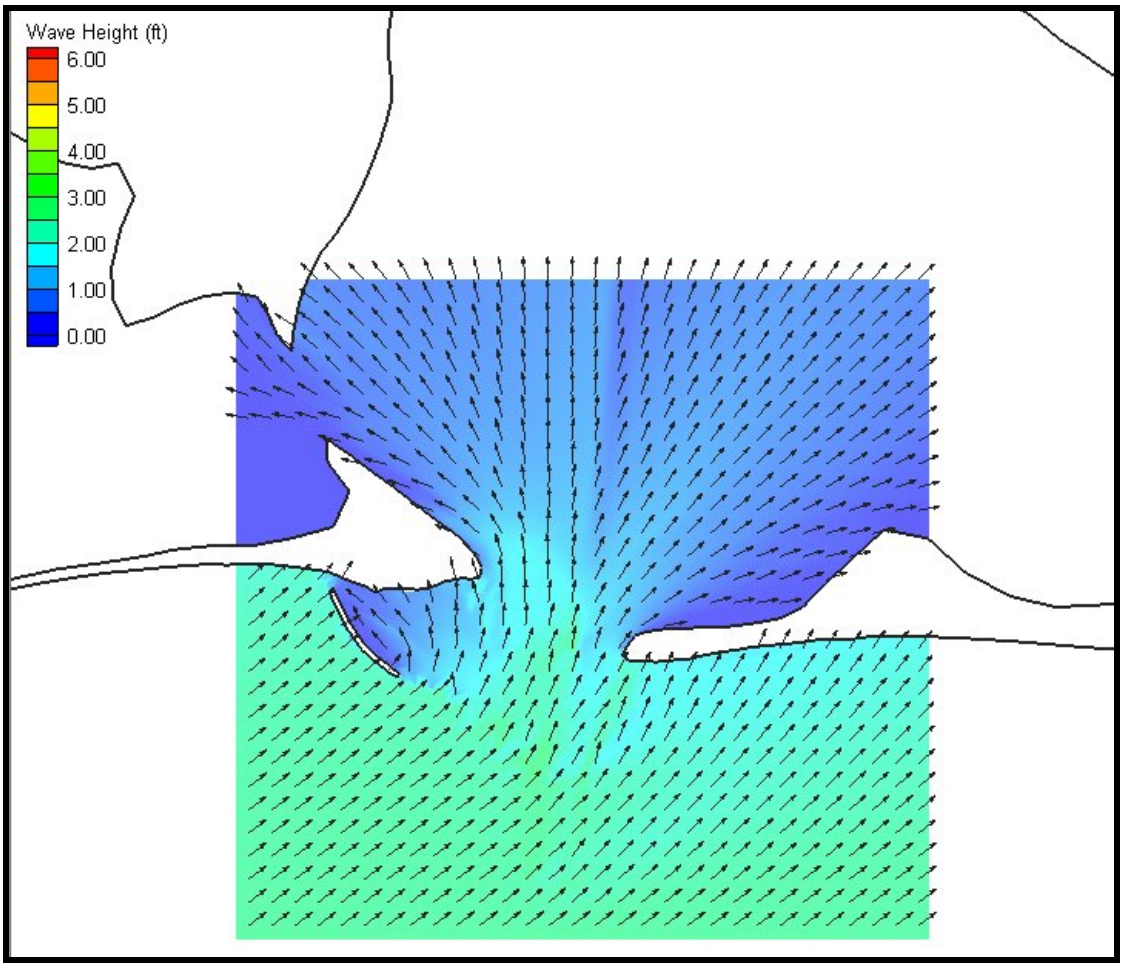

Figure 5-12. Fine grid (50 m x 50 m) wave results for Case 10, Mobile Pass. Wave heights are shown by color while wave direction is indicated by the arrow direction.

Figure 5-13 shows the results for Case 5 along Morgan Peninsula. Waves at the edge of the grid are almost shore normal, and there is little change in direction as the waves propagate towards the shoreline. The influence of Dixie Bar is seen in more detail here, with some wave steepening evident across the shoal. There is little wave refraction associated with the shoal in this case as the waves are essentially perpendicular to shoal orientation.

For waves from the southwest (Figure 5-14), Dixie Bar can be seen to have some influence on wave directions. There is a small gradient in wave height along the edge of the shoal, where waves traveling along the shoal are refracted to the east, whereas those waves which pass to the west of the shoal continue to the shoreline unaffected.

Aside from this slight focusing of wave energy, wave transformation along this stretch of open coast is typical of what is expected.

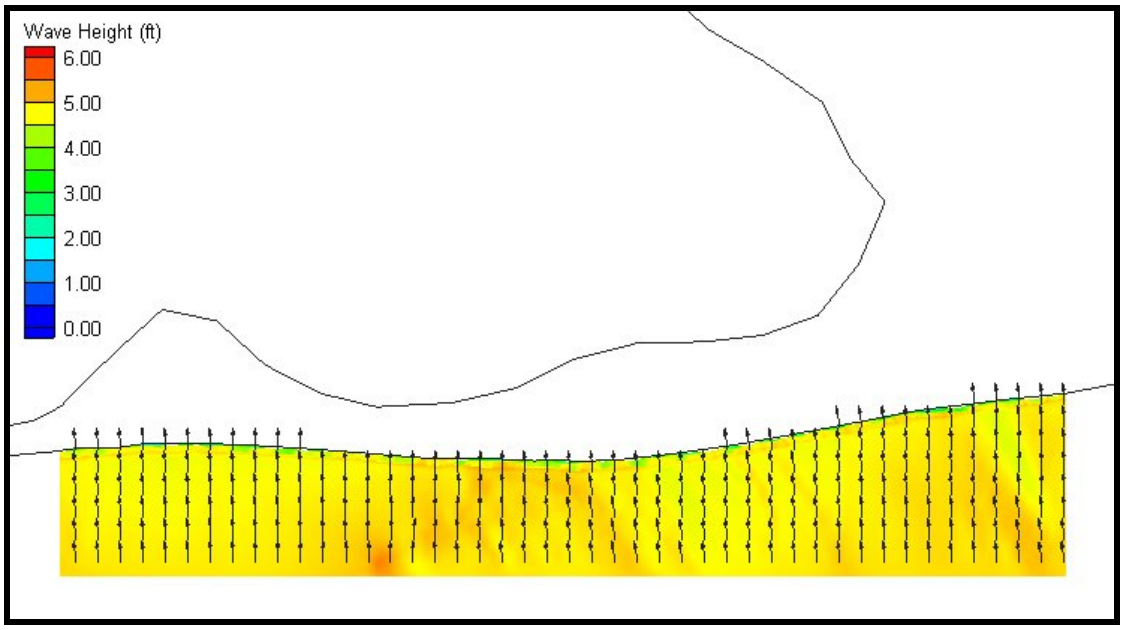

Figure 5-13. Fine grid (25 m x 25 m) wave results for Case 5, Morgan Peninsula. Wave heights are shown by color while wave direction is indicated by the arrow direction.

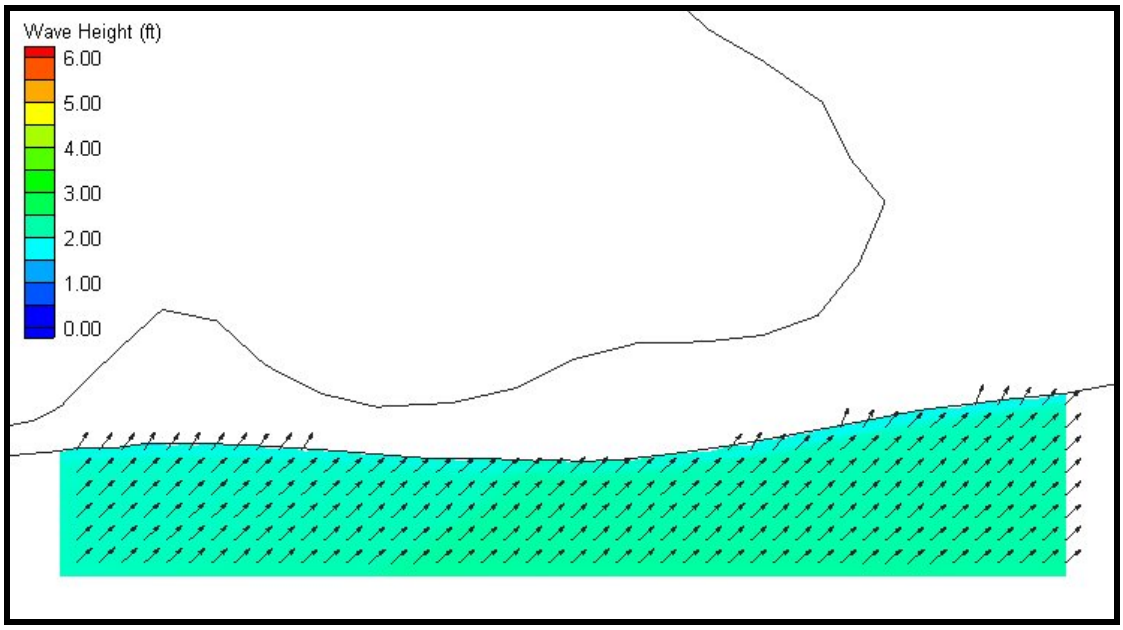

Figure 5-14. Fine grid (25 m x 25 m) wave results for Case 10, Morgan Peninsula. Wave heights are shown by color while wave direction is indicated by the arrow direction.

Longshore Sediment Transport Potential

Overview of Regional Sediment Transport Processes. Nearshore sediment transport is a complex process, which governs erosion and accretion of beaches. Sediment is moved alongshore and cross-shore (on and offshore) by physical coastal processes, such as wind, waves, tides, currents, and sea-level rise. The time scales of sediment transport and shoreline change vary from the initial formation of headlands and coasts on geologic time scales (thousands of years) to severe coastal erosion over a few days or hours during tropical storms and hurricanes.

In addition to physical coastal processes, sediment transport patterns are dependent upon the characteristics and sediment supply. Grain size is the most important characteristic of the sediment. The quantity of sediment moved is inversely proportional to its grain size. Sediment transport rates decrease with increasing grain size, because heavier sediment requires more time and energy to be mobilized and transported. Sediment density, durability, and shape also affect transport rates. In addition, the supply of sediment governs sediment transport rates, because transport rates are reduced where sediment is in short supply (e.g. along armored shorelines).

When waves break at an angle to the beach, alongshore-directed currents are generated, capable of lifting and moving sediment along the coast. For example, waves approaching the Gulf Shores shoreline from the east tend to move sand alongshore from east-to-west towards Mobile Pass. Because wave direction changes frequently, sand is moved back-and-forth along the beach. On an annual basis, however, there typically is a dominant wave direction that occurs most frequently on seasonal time scales.

Determination of Longshore Sediment Transport Potential. To estimate typical values of longshore sediment transport potential along Dauphin Island and Morgan Peninsula, wave modeling results were used to calculate the maximum quantity of sand transport possible based on a sediment-rich environment. Results from the spectral wave modeling formed the basis for quantifying changes in sediment transport rates along the beach because wave-induced transport is a function of wave breaker height, wave period, and wave direction. Longshore transport depends on long-term fluctuations in incident wave energy and the resulting longshore current. Therefore, annual transport rates were calculated from long-term wave statistics.

In general, the longshore sediment transport rate is proportional to longshore wave energy flux at the breaker line, which is dependent on wave height and direction.

Because the transport equation was calibrated in sediment-rich environments, it is typically considered an upper bound for sediment transport rates. However, it provides a useful technique for comparing erosion/accretion trends along a shoreline of interest and for comparing relative magnitudes along different sections of the shoreline.

Longshore Sediment Transport Calculations. The volumetric longshore sand-transport rate, Q_ℓ, past a point on a shoreline is computed using the relationship:

$$Q_\ell = \frac{I_\ell}{(s-1)\rho g a'} \qquad 5.10$$

where I_ℓ is the immersed-weight longshore sand-transport rate, s is the specific gravity of the sediment, a' is the void ratio of sediment, g is the acceleration of gravity, and ρ is the density of seawater.

This study estimates the value of I_ℓ as described by Kamphuis (1990). This approach includes a dependency on median grain diameter of beach sand (d_{50}) and the surf similarity parameter (Irabarren number), ξ_b, which is expressed as

$$\xi_b = \frac{m}{\left(H_b / L_0\right)^{0.5}} \qquad 5.11$$

where m is the bottom slope, H_b is the wave-breaker height, and L_o is the incident deep-water wave length. The complete expression from Kamphuis (1990) is given by

$$I_\ell = K^* \rho g \left(\frac{g}{2\pi}\right)^{0.75} \xi_b T^{0.5} \left(m d_{50}\right)^{-0.25} H_s^{2.5} \sin^{0.6}\left(2\theta_b\right) \qquad 5.12$$

where the coefficient K^* = 0.0013, T is the wave period, H_s is the significant wave height, and θ_b is the wave angle of approach to the shoreline at breaking.

Sediment transport computations were based on wave height, period, and direction at breaking for each grid cell along the modeled coastline. The wave model grids provided the basis for determining shoreline orientation. Computations of sediment transport rates for each of the 10 wave cases listed in Table 5-2 was performed and then weighted by the annual percentage occurrence.

Longshore Sediment Transport Modeling Results. Figure 5-15 illustrates calculated net and gross transport rates predicted for the Dauphin Island and Morgan Peninsula shorelines. Positive values indicate transport from west to east, whereas westerly directed transport is given a negative value. Gross easterly transport is shown as a blue dashed line, gross westerly transport is shown as a red dashed line, and the net transport is a solid black line.

Initial model results for Dauphin Island showed a portion of the island having net easterly directed transport. Although certain storm or even seasonal scale conditions may cause temporary reversals in transport direction, the current analysis shows the composite effect of 20 years. With the morphological data indicating unequivocally that the net direction of transport along Dauphin Island is to the west, a closer look at model results was merited.

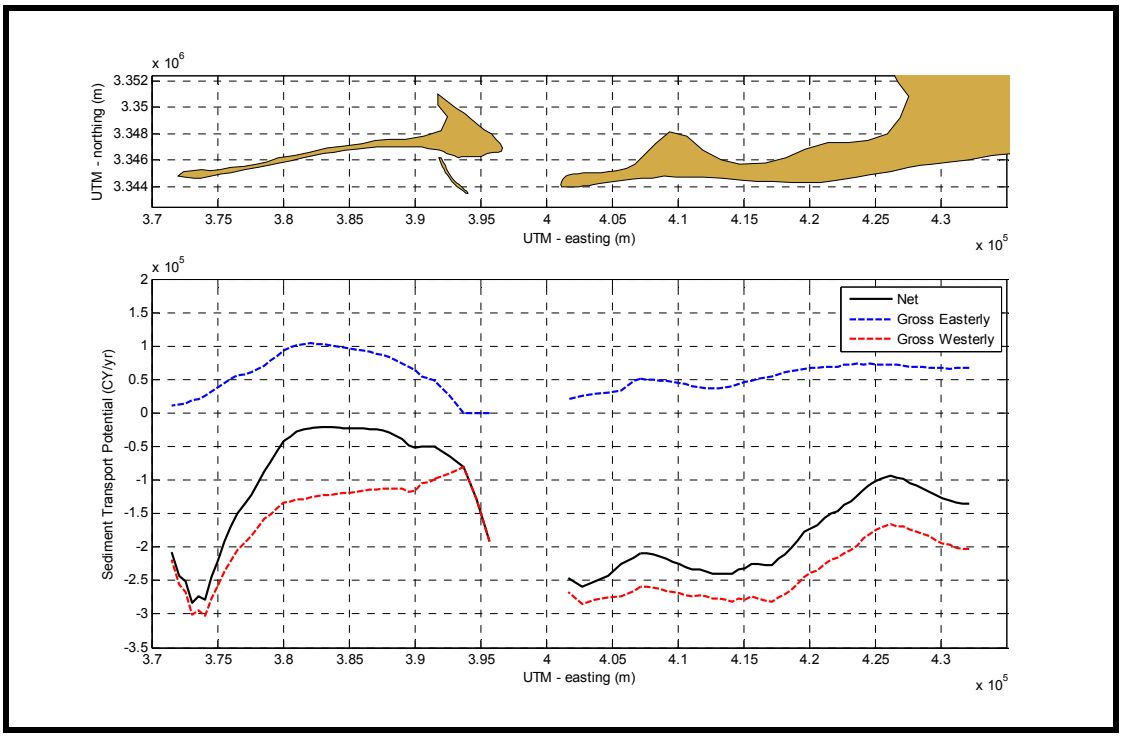

Figure 5-15. Longshore sediment transport potential along Dauphin Island and Morgan Peninsula. Net transport is indicated by a solid black line. Easterly transport is shown as dashed blue, and westerly transport is shown in dashed red.

A sensitivity analysis of model results illustrated that the most influential wave cases from the 20 year composite record (Cases 3, 4, and 5) were essentially shore-normal at breaking along the central portion of Dauphin Island. This is a result of wave refraction caused by nearshore bathymetry and shoreline orientation. As a result, sediment transport calculations were found to be extremely sensitive to wave angle

along this section of the shoreline. Therefore, a minor change in incident wave direction can alter the net direction of transport.

As discussed above, the wave direction reported in the WIS data was found to contain some uncertainty. The analysis discussed in Tracy (1999) revealed that average bounds on the 95% confidence interval were approximately ±8 deg. This uncertainty in the data used to drive the wave model, together with an understanding of the physical processes suggested that an adjustment to the nearshore wave angles may be warranted. Because the evaluation of Dauphin Island morphology indicates relatively strong east-to-west transport along the western two-thirds of the island, wave angles at breaking were adjusted to reflect observations in longshore sediment rates. A rotation of 3 deg to the west was required to reconcile trends in sediment transport prediction with our understanding of net physical processes on Dauphin Island. The 3 deg shift was applied to all wave cases for each of the three model domains. The results discussed below include this alteration of wave angle within the study region.

Overall trends indicate a dominance of west-directed transport. At the eastern edge of the calculation domain, around UTM 426,000 (approximately 15 miles east of Mobile Pass), westerly transport is about twice the rate of easterly transport, and the net value is approximately 125,000 cy/year to the west. The transport rate steadily increases from ~125,000 cy/year at UTM 426,000 to ~240,000 cy/year at UTM 416,000. This increase is due primarily to a gradual change in shoreline orientation, where dominant energy from the southeast arrives with an increasing angle to the shoreline and nearshore bathymetry contours. The western tip of Morgan Peninsula sees a relatively constant transport rate between 200,000 and 250,000 cy/year.

Directly west of Mobile Pass, the net longshore transport rate is approximately 100,000 to 150,000 cy/year to the west. Of note in this section is the absence of easterly transport. This is due to strong wave refraction over the ebb-tidal delta, which results in redirection of waves to the west, regardless of offshore direction. Transport rates decreased in the lee of Pelican Island due to decreased wave heights in this protected area. Central portions of Dauphin Island show transport in both directions to be in the range of 100,000 cy/year, with resulting net transport slightly biased to westerly transport at a rate of ~25,000 cy/year. As discussed earlier, sand transport predictions for this section of island are sensitive to incident wave direction due to shoreline orientation and wave refraction resulting from nearshore bathymetry. At the western end of Dauphin Island (approximately UTM 375,000), incident waves are increasingly directed to the west and the shore-normal angle is gradually shifting from southeast facing (perpendicular to the most energetic wave

conditions) to south facing. Both of these changes result in increased sand transport potential toward the western end of Dauphin Island. Transport rates increased from ~50,000 cy/year at UTM 380,000 to ~270,000 cy/year at UTM 374,000. At the western end of the island, transport rates dropped slightly towards 200,000 cy/year as a result of wave refraction over the shoals of Petit Bois Pass.

Hydrodynamic Modeling

Field Data Collection. Some recorded water levels and flow rates are required to calibrate hydrodynamic modeling. There are existing USACE tide recording stations in the region, each of which has been operational for various periods of time. Unfortunately, there are presently no verified tide recording stations in eastern Mississippi Sound. Together with Mobile Pass, Mississippi Sound serves to transmit water to and from Mobile Bay, and its functioning is important to understanding the hydrodynamics of the region.

Tide Data. To ensure proper data coverage for the modeling effort, a tide gauge was placed in Mississippi Sound in early November 2006. The tide gauge used for this deployment was a Brancker TGR-2050. The instrument was secured to a 10 ft long 2x4 wood beam which was attached to a day marker in the Sound using lag bolts. The instrument was placed as far into the water column as possible. Permission from the U.S. Coast Guard to attach the instrument to the navigational aid had been granted prior to the installation. Data sampling was set for 10-minute intervals, with each 10-minute observation resulting from an average of 16 1-sec pressure measurements. This instrument uses a strain gauge transducer to sense variations in pressure, with resolutions on the order of 1 cm head of water. The gauge was calibrated prior to installation to assure accuracy, and it returned 100% of the desired data.

Once data were downloaded from the instrument, pressure readings were corrected for variations in atmospheric pressure. Hourly atmospheric pressure readings were obtained from the Dauphin Island meteorological station, interpolated to 10-min intervals, and subtracted from the pressure readings. The readings were then converted from pressure units (psi) to head units (for example, feet of water above the tide gauge). After installation, staff from the Irvington Field Office of the USACE, Mobile District, surveyed the elevation of the 2x4 to provide a basis for vertical rectification of the water level. The result from this analysis was a time series record representing variations in water surface elevation in Mississippi Sound relative to NAVD88 (Figure 5-16).

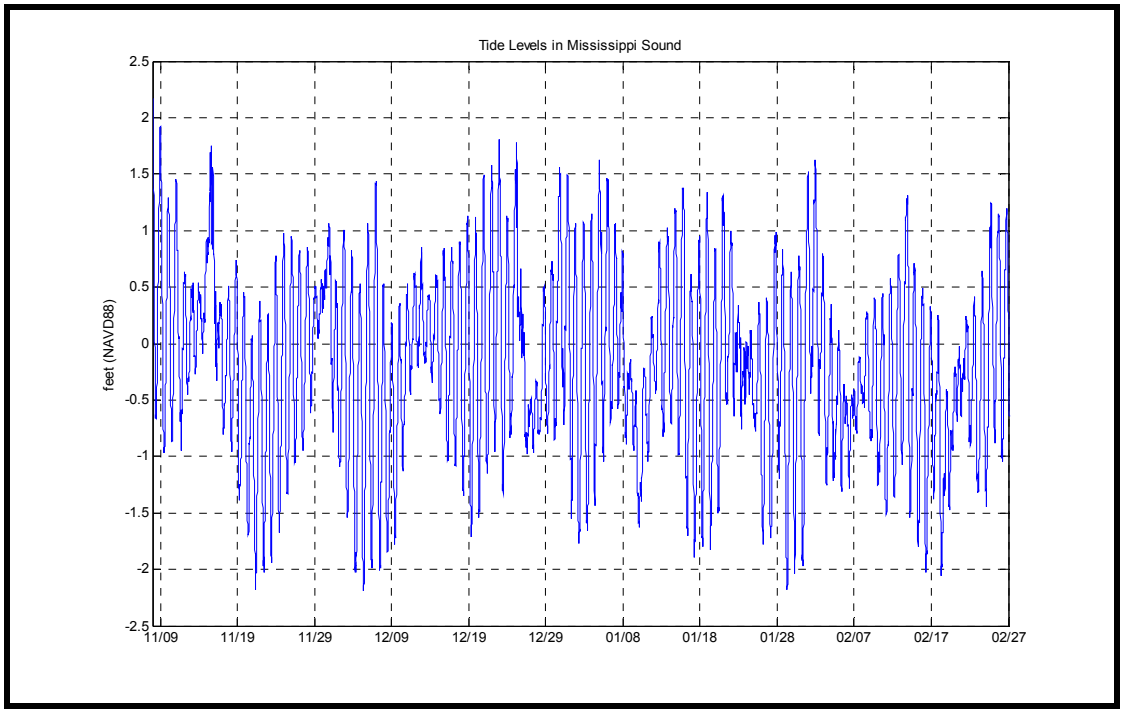

Figure 5-16. Tide data recorded in Mississippi Sound. Elevations are in feet NAVD 88.

Initial plans for field installation called for a 30-day deployment of the tide gauge, followed by a 2-day survey of tidal currents, and then recovery of the instrument. However, due to the pattern of winter weather in the region, the field schedule was delayed for months. The survey and recovery planned for mid-December was not completed until the end of February.

It should be noted that during field deployment of the Mississippi Sound gauge in November 2006, a second tide gauge was installed within Bon Secour Bay. It was also attached to a 2x4 wood beam which was secured to the outside of a day marker along the inter-coastal waterway. Upon arriving at the installation location in February for recovery, neither the 2x4 beam nor the instrument was found.

Tide data from the field deployment in Mississippi Sound, together with data from the Middle Bay Light station and the Exxon Well gauging station, provided excellent tidal information surrounding Mobile Pass. The location of these 3 stations is shown in Figure 5-17.

Figure 5-17. Three tide recording stations used to calibrate the hydrodynamic model. Two ADCP survey lines are shown in yellow.

ADCP Survey. In addition to the time series of water levels in the area, details of flow in and out of Mobile Bay were also integral for developing an understanding of the hydrodynamics in the area. A 2-day survey of tidal currents was undertaken to provide some understanding of flow patterns in the area. Figure 5-17 shows the location of the two survey lines.

Water velocity measurements were obtained with a BroadBand 1200-kHz Acoustic Doppler Current Profiler (ADCP) manufactured by RD Instruments (RDI). The ADCP was mounted to a specially constructed mast, which was rigidly attached to the rail of the survey vessel. The ADCP was oriented to measure downward into the water column, with the sensors located approximately 2 ft below the water surface. The mounting technique assured no flow disturbance due to vessel wake.

Geographic coordinates was recorded with a stand-alone global positioning system (GPS) relative to the 1984 World Geodetic System (WGS-84) datum. The GPS antenna was mounted at the top of the ADCP boom directly over the instrument.

Both ADCP and GPS data were recorded in WinRiver (®RD Instruments), an integrated ADCP and navigation software package running on a PC laptop computer, to provide an accurate position for each backscatter and velocity measurement. Data recording for each survey transect was started, ended, and recorded using the laptop and WinRiver to interface with the ADCP. Because the ADCP uses bottom tracking to correct real-time measurements, several potential error sources affecting the motion-corrected ADCP velocities are eliminated automatically. Fong and Monismith (2004) found this bottom tracking technique to yield a maximum error in measured velocity of less than 6%.

Current surveys of Mobile Pass and Pass aux Herons were performed on 26-27 February 2007, respectively. Because tides in the area are diurnal, a typical survey day of 12-14 hr recorded only a single stage of tide. In this case, both surveys captured the tail end of the ebbing tide, slack water, and then a majority of the flooding tide. The survey line for Mobile Pass ran from the eastern end on Dauphin Island to Mobile Point. The survey line across Pass aux Herons ran parallel to the causeway bridge on its east side. Figures 5-18 and 5-19 illustrate color contour plots of velocities during maximum flood conditions.

Figure 5-18 indicates an enormous volume of water moving through Mobile Pass during flood tide. Velocities of 5 ft/sec are observed to extend from near the surface to depths greater than 25 ft. A majority of flow is sharply contained within the navigational channel. The main channel carries 481,000 cfs which accounts for 76% of the total flow entering the inlet.

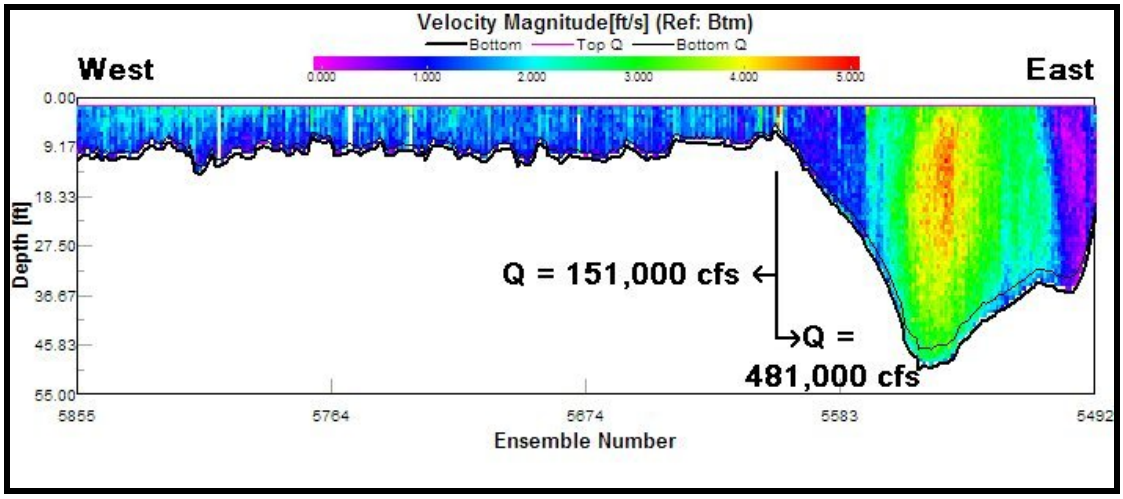

Figure 5-18. Color contour plot of velocities in Mobile Pass during maximum flood tide conditions.

Flows observed in Pass aux Herons (Figure 5-19) are notably smaller. The inter-coastal waterway channel at the right of the figure conveys a majority of the flow. A small unmarked channel approximately 1 mile north of the navigation channel also contributes.

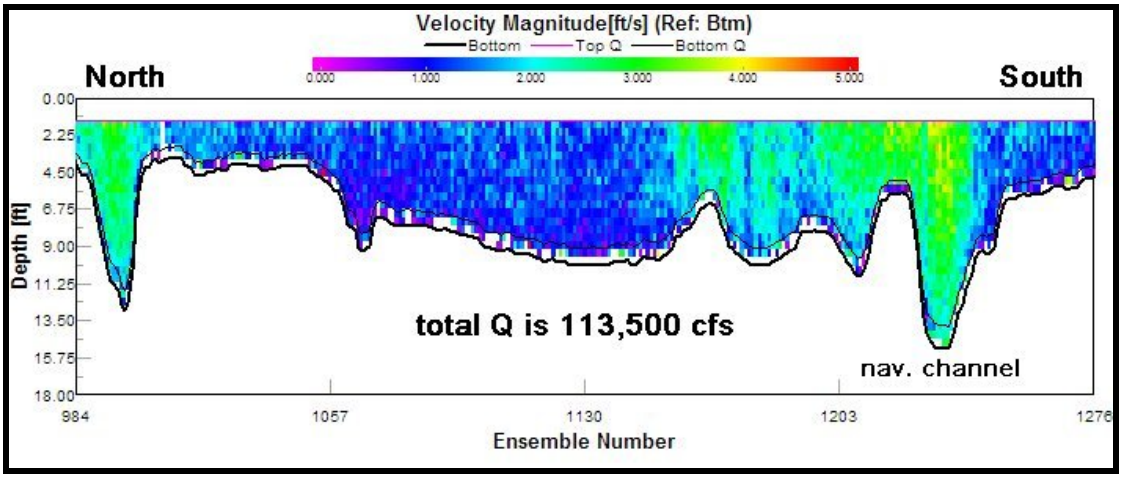

Figure 5-19. Color contour plot of velocities in Pass aux herons during maximum flood tide conditions.

A comparison of the two surveys shows that flow rates entering Mobile Pass on these flood tides was approximately 745,500 cfs, with Mobile Pass contributing 85% of the total and Pass aux Herons accounting for 15%. These quantities are consistent with flow partitioning reported by Isphording et al. (1996).

ADCIRC. A regional hydrodynamic model for the entire Gulf of Mexico was run, using the Advanced Circulation Model for Oceanic Coastal and Estuarine Waters (ADCIRC). ADCIRC is a two-dimensional, depth-integrated circulation model (Westerink et al., 1994). The model domain is described by a collection of finite elements which give the model excellent flexibility to cover both large domains as well as provide the required detail for areas where strong flow variations are expected. Computational features of ADCRIC include variable coriolis forcing, wetting and drying, choice of bottom stress model, and detailed user control over model output.

Model Domain. The ADCIRC model domain for the Gulf of Mexico is illustrated in Figure 5-20. Land boundaries are shown in brown, islands in green, and the open boundaries are in navy blue. The model was forced at 2 open boundaries. The first boundary runs across the Straight of Florida, between the Florida Keys and Cuba. The second open boundary runs from Belize (south of the

Yucatan Peninsula) north to the southern coast of eastern Cuba. The final model grid contained 58,685 nodes and 112,339 elements.

Boundary Conditions. ADCIRC allows various forcing options for driving flow in the model, including a time series of water-surface elevation, tidal constituents, a time series of flow rates, as well as wind stress and atmospheric pressure. For the current study, tidal constituent forcing was applied to the open boundaries, and tidal potential forcing was applied to the interior of the domain. Freshwater inflow at the north end of Mobile Bay was also included.

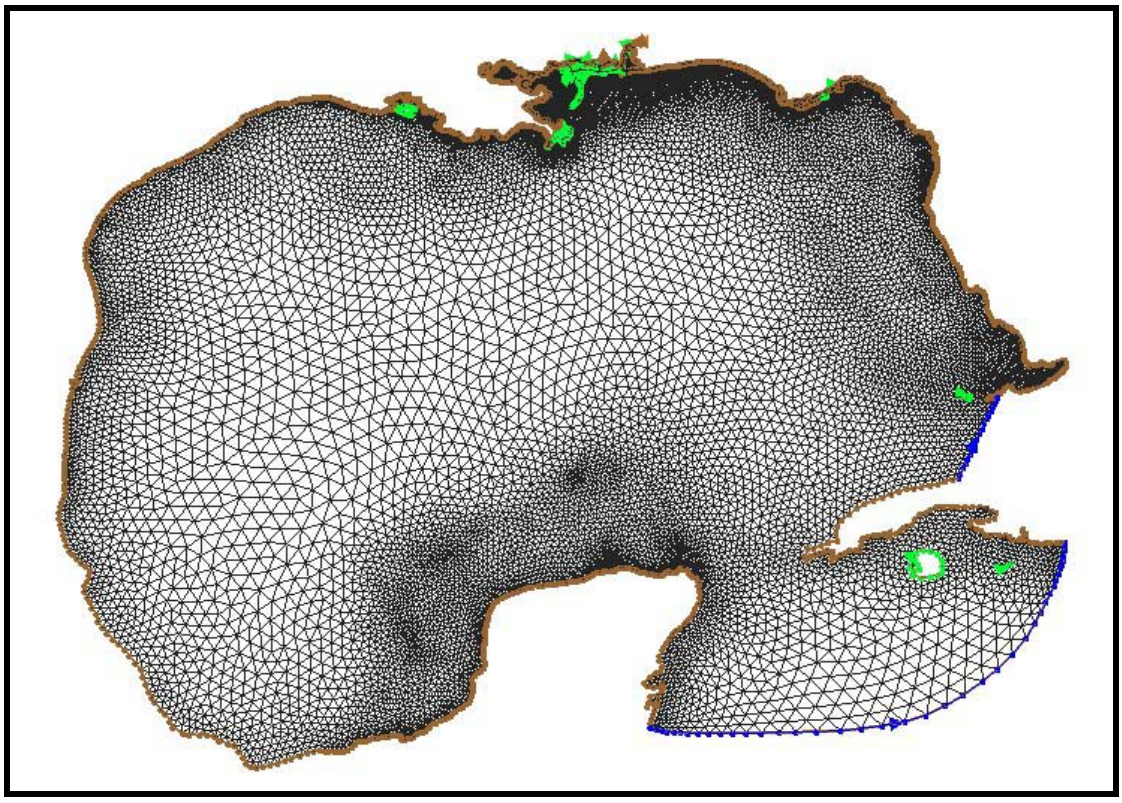

Figure 5-20. ADCIRC model domain for the Gulf of Mexico. The two open boundaries are shown in navy blue, land boundaries are in brown, and islands are in green.

The tidal constituent values for the 2 open boundaries were extracted from the existing Western North Atlantic, Gulf of Mexico, and Caribbean Sea Tidal Database (Mukai et al., 2001). This provided constituent data for the M2, S2, N2, K1, O1, Q1, P1, K2, M4 and M6 components of the tide.

Atmospheric pressure changes and local winds have a significant influence on water levels within the study area. The relatively shallow offshore shelf and shallow water within Mobile Bay suggest that atmospheric forcing can often result in changes in

water level that are similar in magnitude as astronomical tides. However, these atmospheric forcings were not included in the present study. The amount of data required to properly include these aspects into the modeling effort was beyond the scope of work.

Freshwater inflow for the Mobile and Tensaw Rivers was included at the northern extent of Mobile Bay. Flow rate data were taken from the USGS gauging stations for each river (USGS, 2007).

Model Calibration. The primary purpose for running the regional hydrodynamic model was to provide a time series of water surface elevation to serve as a boundary condition for detailed CMS-M2D morphology modeling. Field data used to evaluate model results were taken from the Middle Bay Light gauging station, tidal records from the Exxon Well offshore of Mobile Pass, and the tide gauge deployed in Mississippi Sound in support of this work. Model mesh and bathymetry, as well as the locations of field data stations, are shown in Figure 5-21.

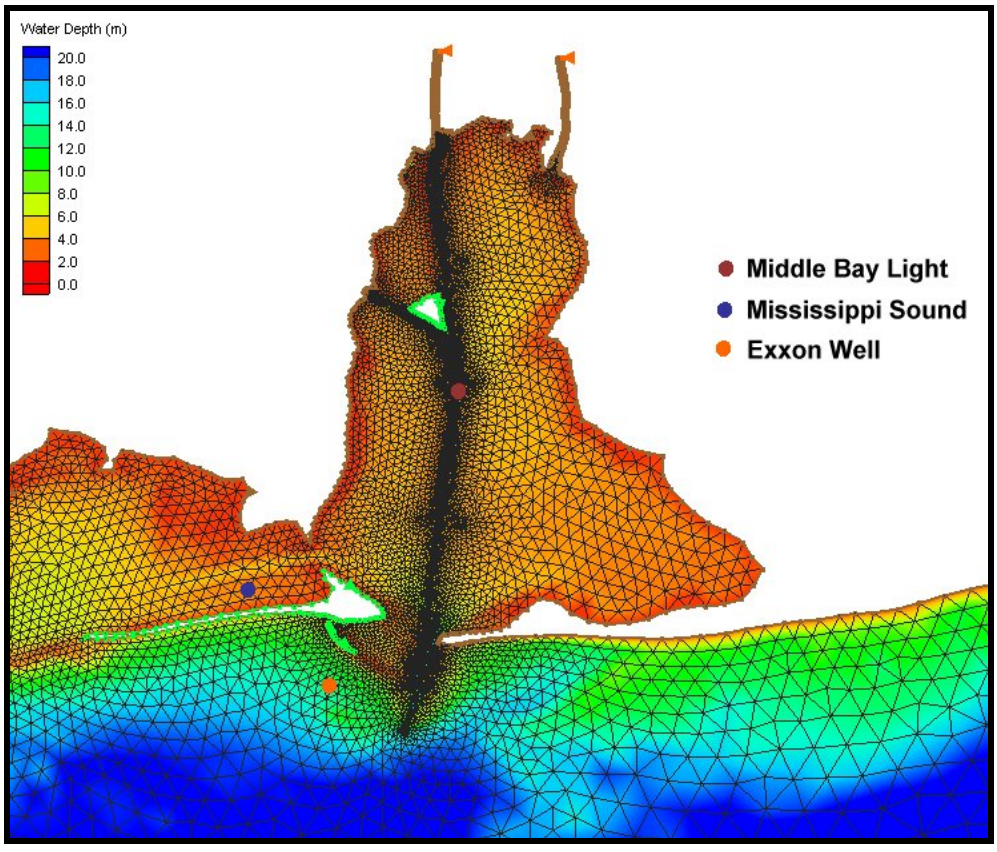

Figure 5-21. Detail of the ADCIRC domain focused on Mobile Bay and Mississippi Sound. Bathymetry contours are shown in color along with the model mesh for this region. Mobile and Tensaw River inflow portions of the mesh can be seen at the north end of Mobile Bay. Three tidal recording stations used to calibrate the model are also shown.

To limit the influence of the atmospheric signal in field data, the tidal record was searched for a period which had no storms and relatively low winds. Seeing as the field deployment was during the winter, such a period of time was difficult to identify. Ultimately the period from December 15 – 22, 2006 was chosen to evaluate the hydrodynamic model.

All runs commenced on December 12, providing 3 days of run time prior to the period of interest. Plots of recorded versus modeled water levels are shown in Figures 5-22, 5-23, and 5-24 for the Exxon Well, Mississippi Sound, and Middle Bay Light, respectively.

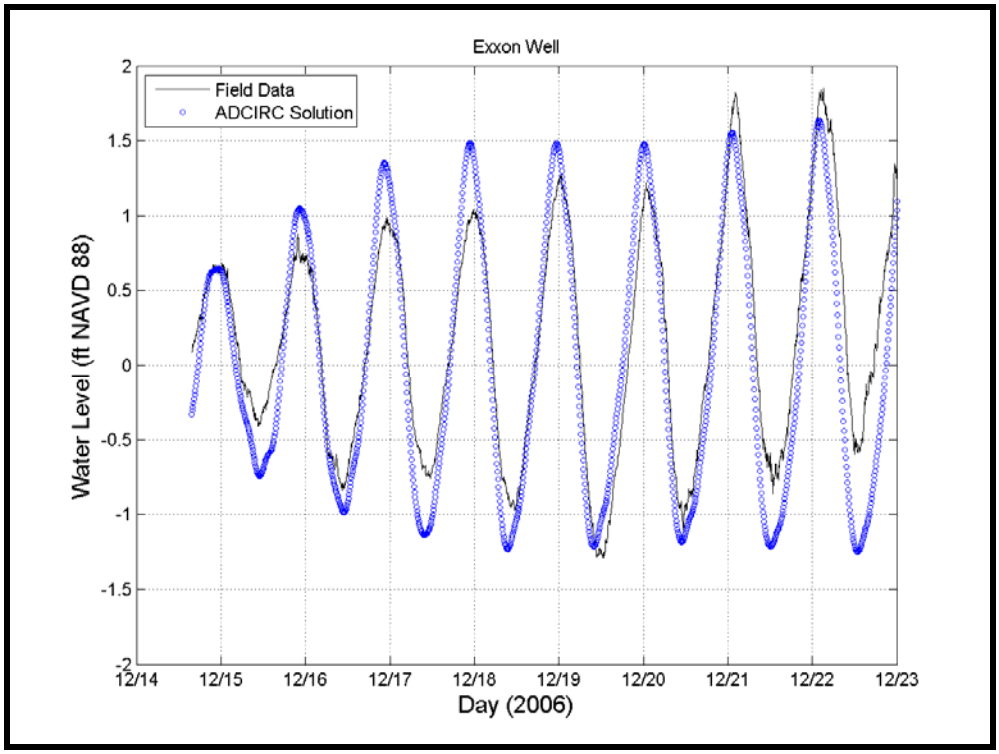

Figure 5-22. Comparison of modeled water levels with measured data for the Exxon Well, December 15, 2006 to December 23, 2006.

Results showed varying degrees of agreement between modeled and measured water levels. Model results offshore Mobile Pass at the Exxon Well (Figure 5-22) tend to show a slightly larger tide range than present in field data. The largest error was 6 inches on the high tide of December 17. Starting mid-day December 21, field data showed a departure from mean tide level of the previous week. This suggested that an atmospheric event was starting to have an influence on measured water levels, bringing them farther out of agreement with model results for those days. In general the phase is reproduced well. Model results lag field data by about 30 minutes.

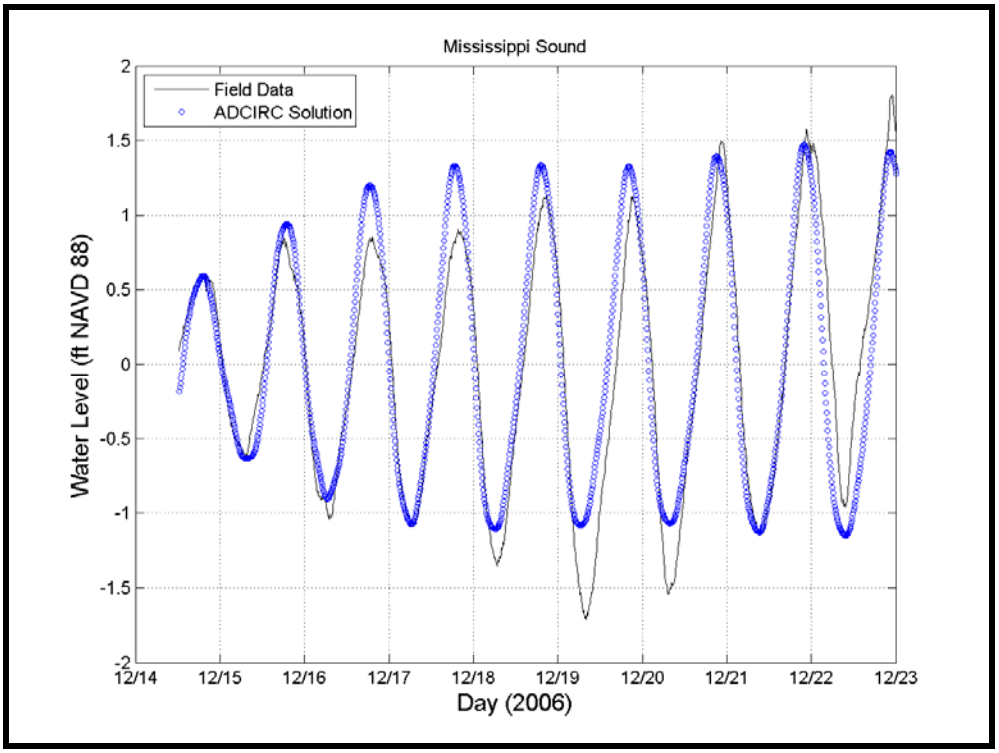

Figure 5-23. Comparison of modeled water levels with measured data for Mississippi Sound, December 15, 2006 to December 23, 2006.

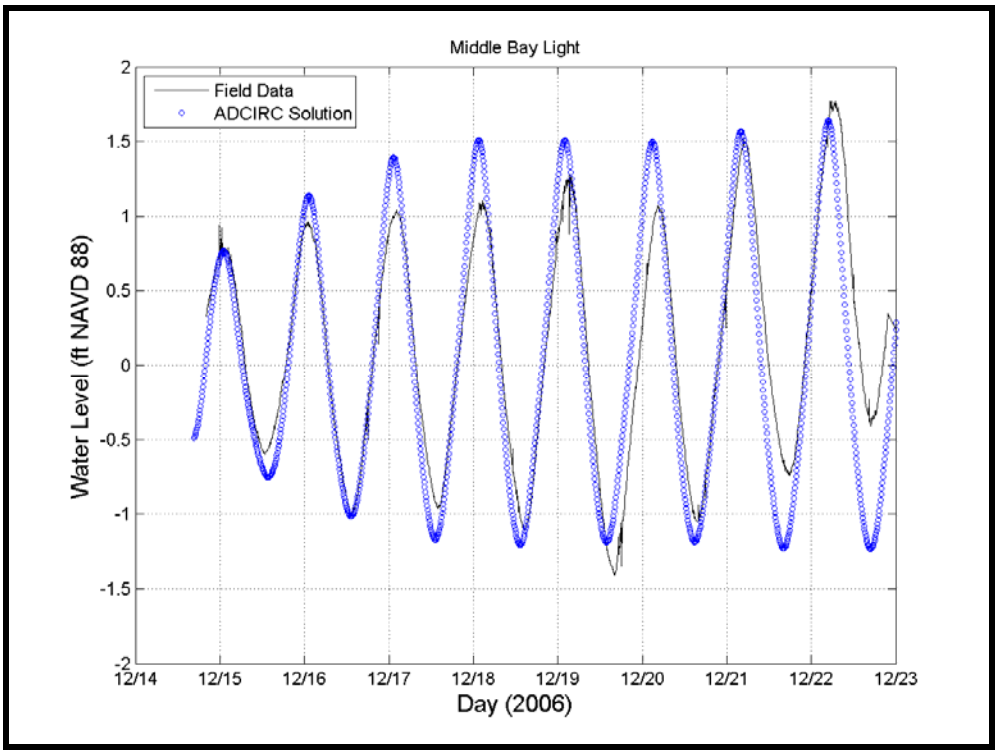

Figure 5-24. Comparison of modeled water levels with measured data for Middle Bay Light, December 15, 2006 to December 23, 2006.

Model results for Mississippi Sound (Figure 5-23) again over-predict high tide level on 17 December by 6 in. In addition, the model under predicts low tide on 19 December by about 1 ft. Tidal phase is again reasonably well predicted in the model solution. A trace of atmospheric influence raising mean water levels in the area is seen in field data for Mississippi Sound as well, although the influence is a bit smaller.

The comparison at Middle Bay Light (Figure 5-24) illustrated the same general trend of the model solution over predicting high tide levels around 17-18 December, with a maximum error of about 6 in. Tidal phase again closely predicted field data. The atmospheric event over the final two days of the record is recognized clearly in this set of data from inside Mobile Bay.

Although the agreement between model and field data is not perfect, trends in field data were reproduced for each recording station. These results are taken from a small portion of a model domain which spans over 600,000 square miles. The primary goal of this part of the modeling effort was to provide a reasonable hydrodynamic boundary condition with which to drive morphological modeling. In that regard, the effort can be considered successful.

General Circulation Patterns. In addition to providing a time series of water surface elevations for the study area, ADCIRC results also provided an understanding of regional flow patterns. To best compare model results with flow data recorded from the ADCP surveys, a separate ADCIRC run was performed to cover the survey days of 26-27 February 2007.

A plot of velocity contours and vectors at Mobile Pass for maximum flood tide during 26 February is shown in Figure 5-25. This result corresponds well with flows measured during this same time period of the ADCP survey (Figure 5-18). A majority of flow is conveyed by the navigation channel, and maximum velocities predicted (~ 5 ft/sec) are similar to those recorded by the ADCP. Velocities predicted by the model between the eastern tip of Dauphin Island and the navigation channel approach 3 ft/sec, while measured velocities for this area were closer to 1.5-2 ft/sec. The navigation channel contains strongest currents well inside Mobile Bay. Pelican Pass is subject to strong eastern flows, with velocities exceeding 3 ft/s. Flows predicted at Pass aux Herons are similar in magnitude to ADCP measurements, both falling around 2.5 ft/sec. ADCP data show the intracoastal waterway carrying much of the flow with low velocities on adjacent shallow channel margins. However, model calculations indicate flow evenly spread across Pass aux Herons. Increased mesh detail may have served to reproduce fine details of flow recorded by the ADCP.

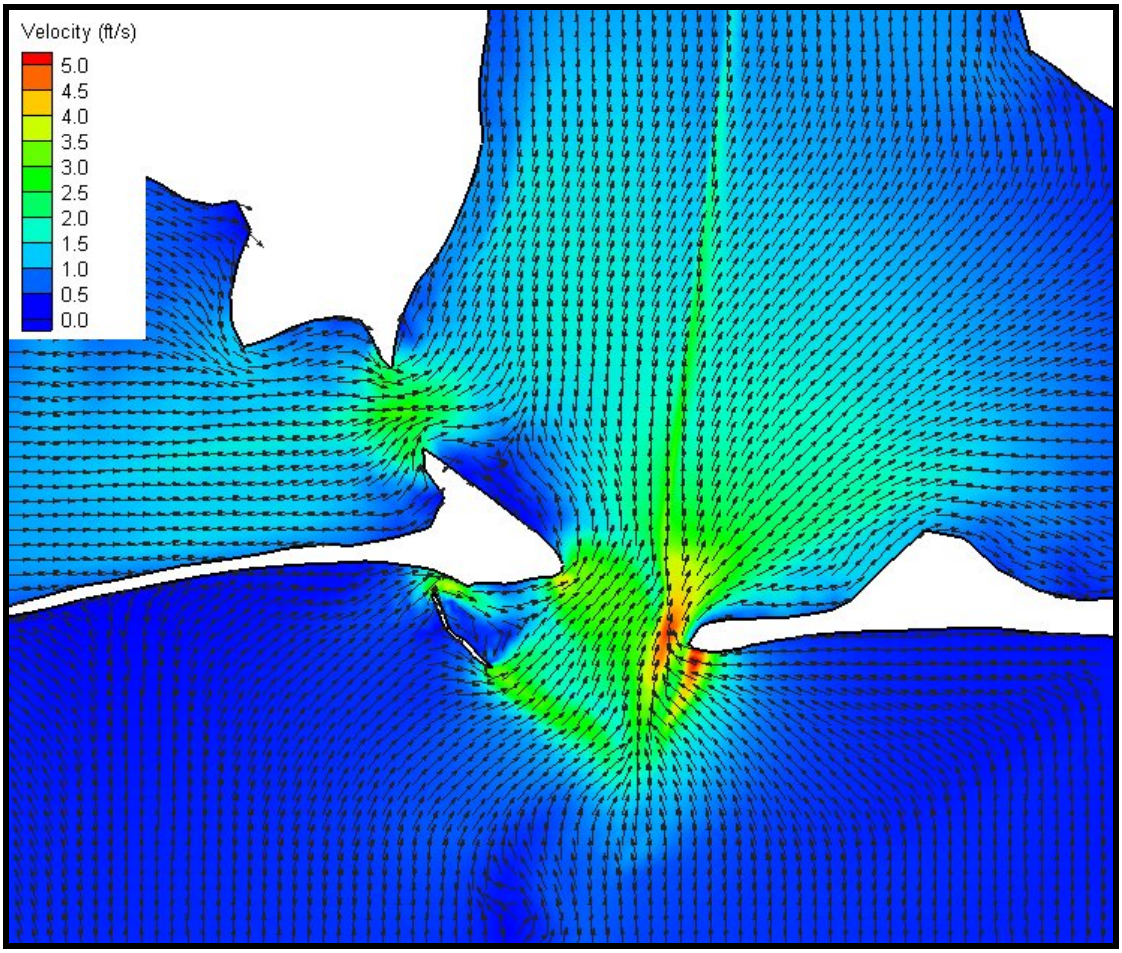

Figure 5-25. Velocity contours and vectors for maximum flooding tide at Mobile Pass February 26, 2007.

Maximum ebb-tidal conditions were not measured during the ADCP survey, so model results provide new insight here. Velocity contours and vectors at Mobile Pass for maximum ebb tide during February 26 are shown in Figure 5-26. A strong ebb-tidal jet is seen to extend offshore of Mobile Pass, with velocities greater than 2 ft/sec persisting more than 5 miles offshore. Pelican Pass carries a portion of the ebbing tide, but velocities are weaker than seen during the flood tide. This is to be expected as a flooding tide gathers water from all directions offshore of the inlet, while an ebbing tide is dominated by the ebb-tidal jet. A counter-clockwise gyre directly east of the navigation channel is seen outside the inlet, which persisted through the 4-5 hr of strongest ebb-tidal flow. Such a feature might serve to facilitate the growth of the eastern lobe of the ebb-tidal delta.

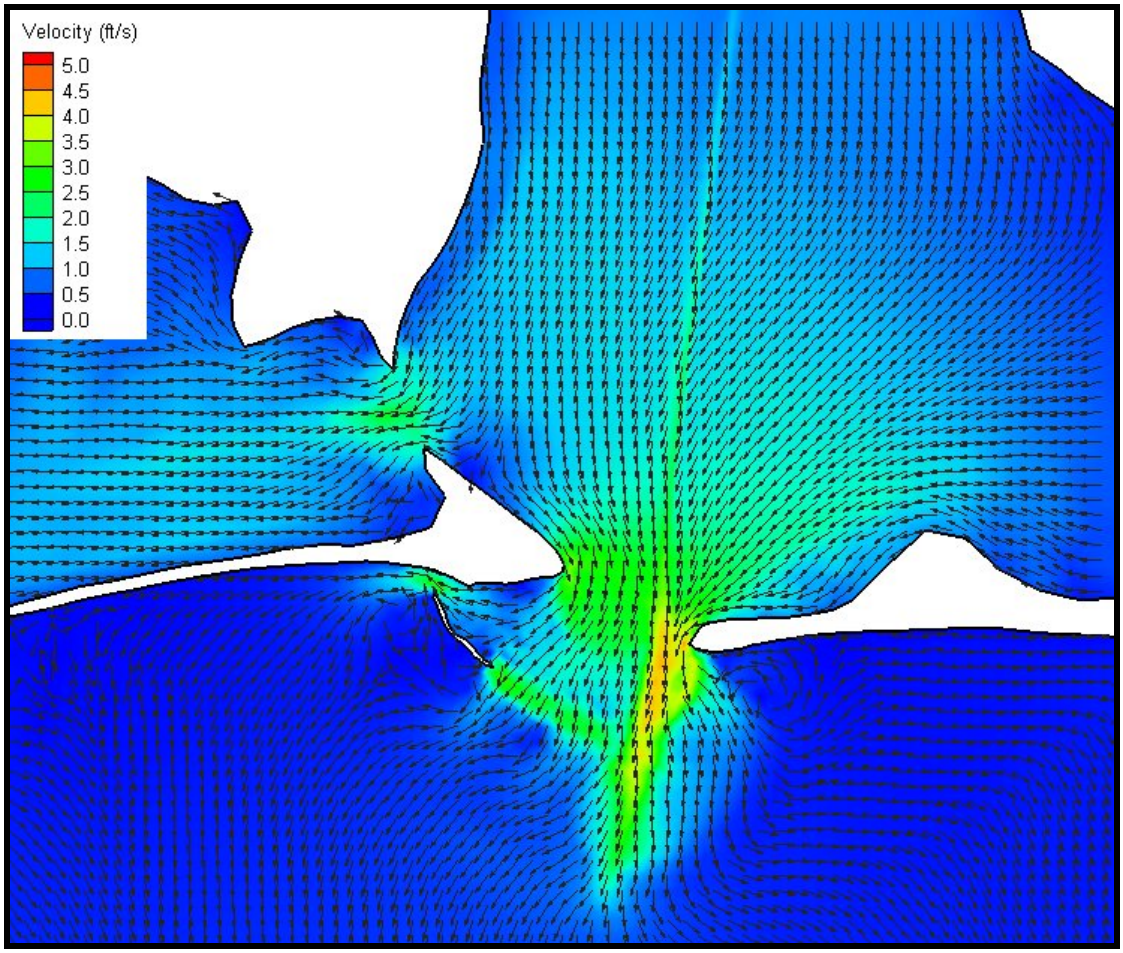

Figure 5-26. Velocity contours and vectors for maximum ebbing tide at Mobile Pass February 26, 2007.

Morphological Modeling

In addition to wave, sediment transport, and hydrodynamic modeling, morphological modeling of the ebb-shoal complex also was completed. Bathymetric change analysis presented in Chapter 4 is the definitive source for analyzing the complexities of the morphology change in and around Mobile Pass. However, it was anticipated that the numerical investigation could shed some light on the most likely pathways for sediment movement, as well as the relative magnitude of change under differing wave conditions.

CMS-M2D. CMS-M2D is a two-dimensional, depth-integrated, finite-difference hydrodynamic model. It also has the option of including morphology change estimates through the use of a sediment continuity equation for updating changes in bathymetry (Buttolph et al., 2006). Full coupling with an external wave model (STWAVE in this case) is possible, with the wave model passing radiation and shear

stresses to CMS-M2D. In return, hydrodynamic and morphology changes are passed back to the wave model.

Model Domain. Limits of the domain were chosen to encompass the ebb shoal and extend into Mobile Bay far enough to provide a well chosen boundary for hydrodynamics. In addition to these concerns, it is best practice for the coupled STWAVE and CMS-M2D runs for the hydrodynamic grid to lie completely within the wave grid. This prevents the need for CMS-M2D to extrapolate radiation and shear stresses past the boundaries of the wave model solution. In this case, the existing fine grid centered on Mobile Pass was used for efficiency. The final CMS-M2D domain is shown in Figure 5-27.

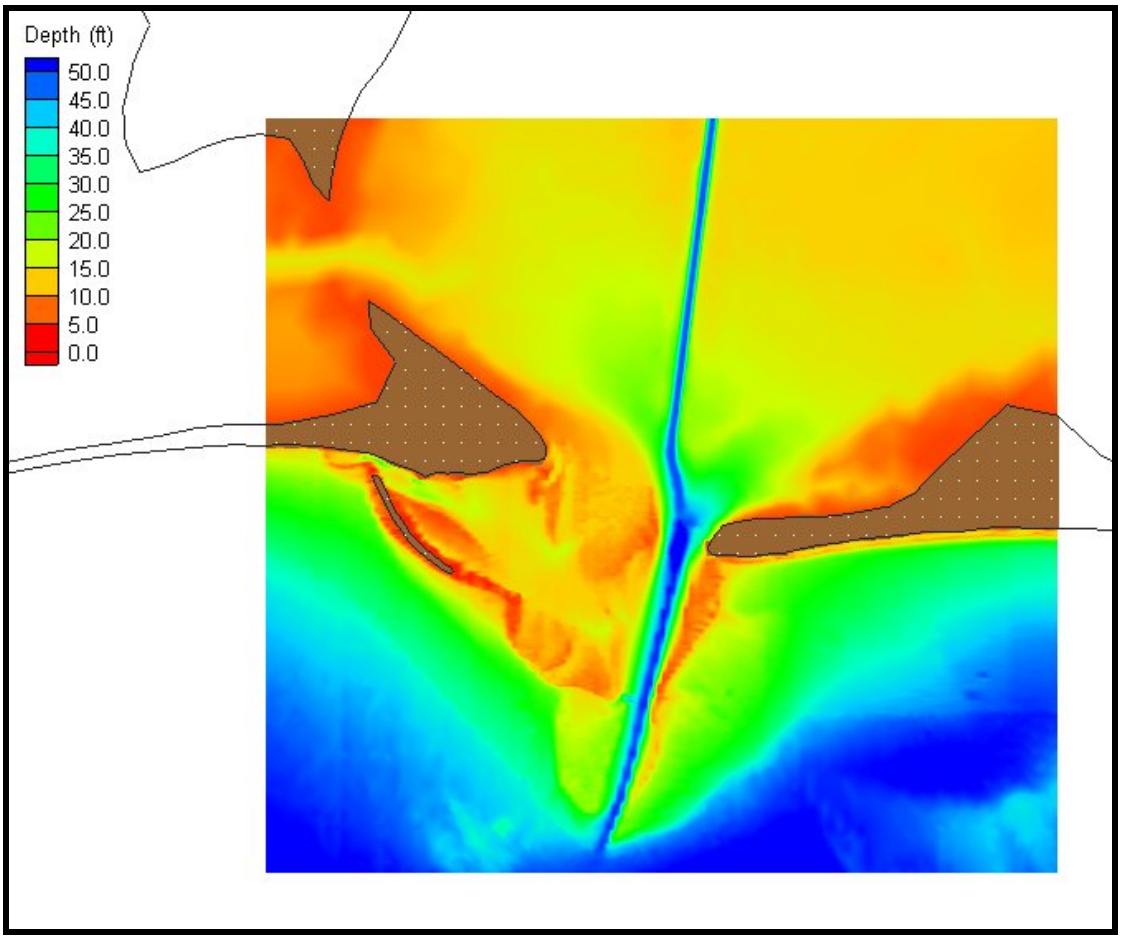

Figure 5-27. CMS-M2D model domain and bathymetry.

Boundary Conditions. The CMS-M2D model domain has three open boundaries. The hydrodynamic solution from ADCIRC was used to provide a time series of water levels along each open boundary. The 3-day period from 15-18 October2006 was used to drive hydrodynamics in the CMS-M2D simulations. This

period was chosen due to the moderate tidal range (1.5-2 ft) and considered representative for an average tidal condition.

Model Setup. With boundary conditions assigned, the remainder of model setup was concerned with properly choosing variables relevant to morphology predictions, as well as the coupling between STWAVE and CMS-M2D. A summary of model variables is shown in Table 5-3.

Table 5-3. Values for CMS-M2D model variables.

Variable	Setting
Hydrodynamic Time Step	3 sec
Transport Rate Time Step	2 min
Morphologic Time Step	30 min
Sediment Transport Formulation	Advection-diffusion
Mean Grain Size	0.25 mm
Interface with STWAVE every	2 hr

Morphological Model Results. It is understood that morphological predictions are useful only to reveal potential pathways for sediment movement and comparison of relative scales of change. Specific locations and values are not considered reliable. As such, results should not be considered quantitative predictions of change, but rather estimates for discussing morphology change on the ebb-tidal delta.

Initial model runs consisted of hydrodynamics only, where 3 days of average tidal conditions were run (Figure 5-28). As expected, there is little change associated with such a short time period and low energy conditions. Largest changes indicate movement of the east lobe of the ebb tidal delta near the shoreline from east-to-west. Deposition falls outside of the navigation channel. Net movement of the east lobe to the west is in keeping with observed morphology change and also with our understanding of nearshore flow regimes in the vicinity of tidal inlets. In addition, scouring of the navigational channel immediately west of Mobile Point is illustrated, an area which has typically not required maintenance dredging. There is also a small

signal of change at the offshore tip of Pelican Island, but no strong indication of transport direction is apparent.

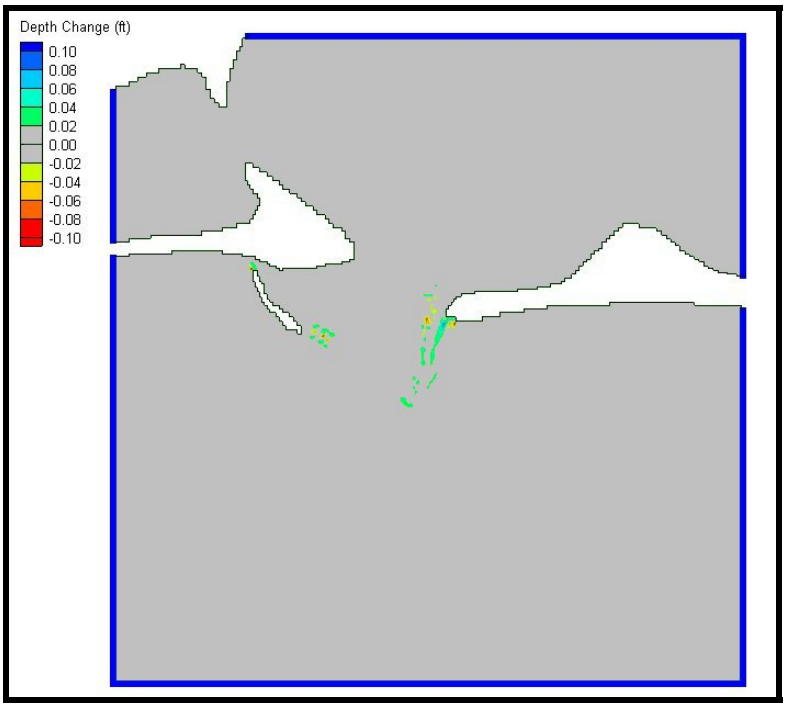

Figure 5-28. Bottom change results for 3 days of average tidal conditions only. Erosion is in yellow/red and accretion is in blue.

Case 2 consisted of the same 3 day tidal hydrodynamics, but with moderate wave energy (H_{mo} = 3.5 ft, T = 6 seconds) incident from the southeast. Results indicate migration of the east channel margin bar to the west (Figure 5-29). Change is much larger relative to the Case 1 results (note the change in scale of the color contours). Strongest change is along the offshore edge of the shoal, where wave breaking is strongest. Again, there is change along the shoal leading into Pelican Island, but these results show a clear trend of the shoal being pushed shoreward.

Figures 5-31 and 5-31 illustrate average transport vectors for Case 2 during maximum flood and ebb conditions, respectively. These plots are snapshots of a single time step extracted from the entire 3 day simulation. Each figure shows magnitude (color) and direction (arrow) of average transport (bed load and suspended load) calculated by CMS-M2D for the time step shown. Figure 5-30 shows clear trends in transport which mirror bottom change observed in Figure 5-29. On a flooding tide, waves and hydrodynamics are working to push material toward the inlet. Southeast of Pelican Island, transport is northward. Along the eastern

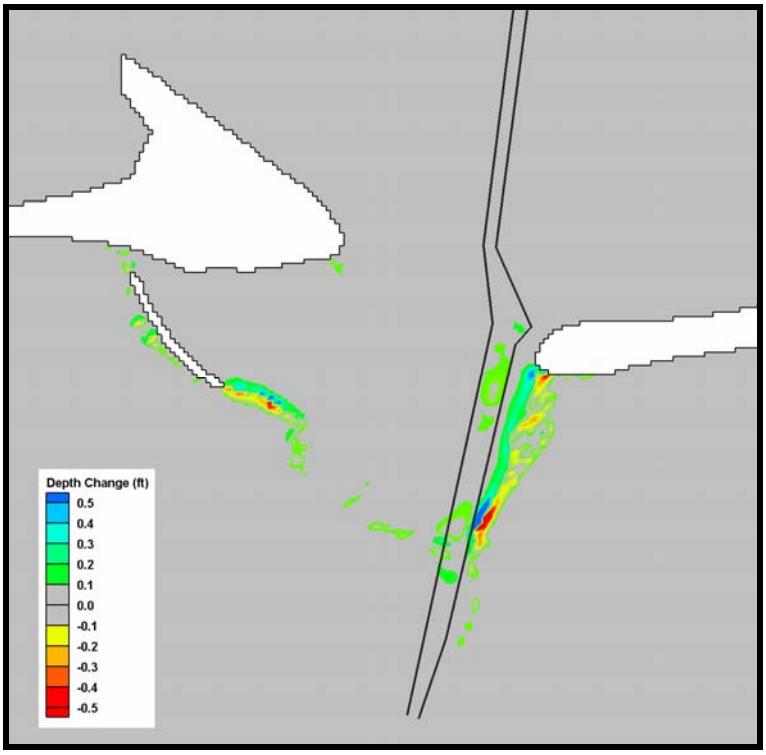

Figure 5-29. CMS-M2D bottom change results for 3 days of average tidal conditions under normal waves. Erosion is in yellow/red and accretion is in blue.

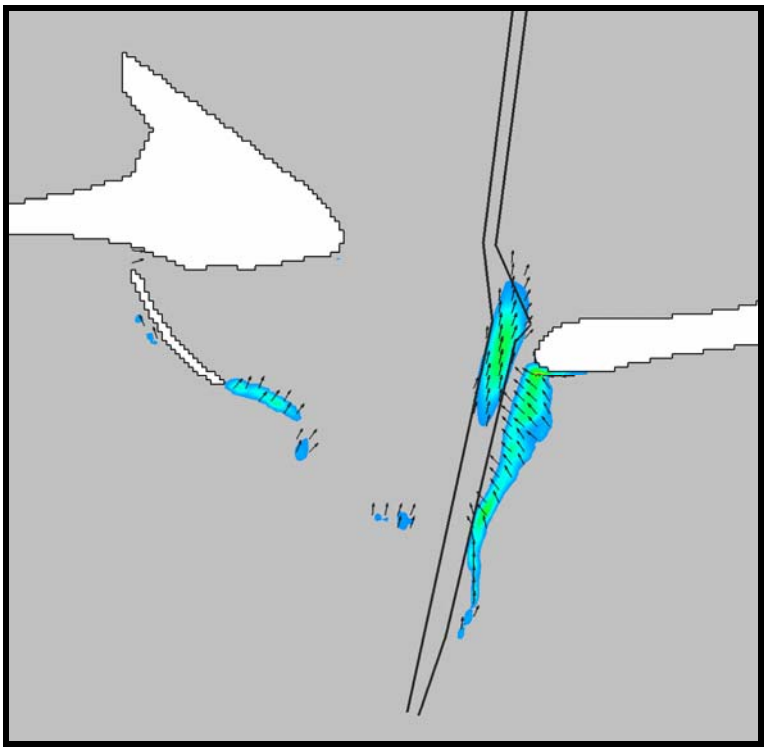

Figure 5-30. CMS-M2D average transport vectors for Case 2 during flood tide.

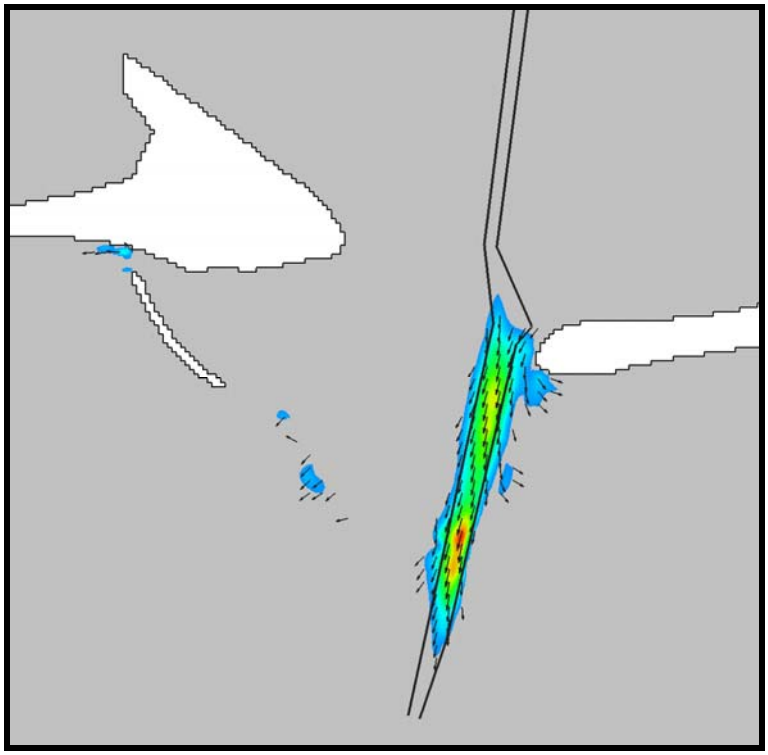

Figure 5-31. CMS-M2D average transport vectors for Case 2 during ebb tide.

channel margin bar, there is a well-defined area of east-directed transport that abruptly dissipates at the channel margin where deposition in bottom morphology is observed (see Figure 5-29). Flood tidal currents moving across the bar under breaking waves push sand from east to west towards the channel.

During ebbing tide (Figure 5-31), hydrodynamic forcing is directed offshore while wave energy is directing transport shoreward. This process results in most transport being confined to the navigation channel, where the currents are strongest, and only minor transport occurs on the shoals. Figure 5-31 illustrates conditions during maximum ebbing currents. Strong transport predicted in the navigation channel is short lived, which may be why only minor bottom change is reflected under these conditions.

Case 3 simulates a 3-day storm condition, with strong wave energy (H_{mo} = 10-15 ft, T = 9-13 sec) incident from the south and southeast. The tide signal is the same as other cases, but with a 3-ft surge added to water levels. As a result of the surge, Pelican Island became submerged during this simulation. Again, the east lobe is seen to migrate from east-to-west, with notable erosion along the outer fringe of the east lobe due to wave breaking farther seaward on the shoal (Figure 5-32). The outer edge of the western lobe is active for the first time, with the model indicating

shoreward migration for this area. Pelican Island shows erosion on the outer beach and deposition along the backshore, suggesting a trend of shoreward migration. There also is evidence of transport along the axis of Pelican Island, where change shows movement from southeast to northwest, towards the attachment area of Pelican Island to Dauphin Island.

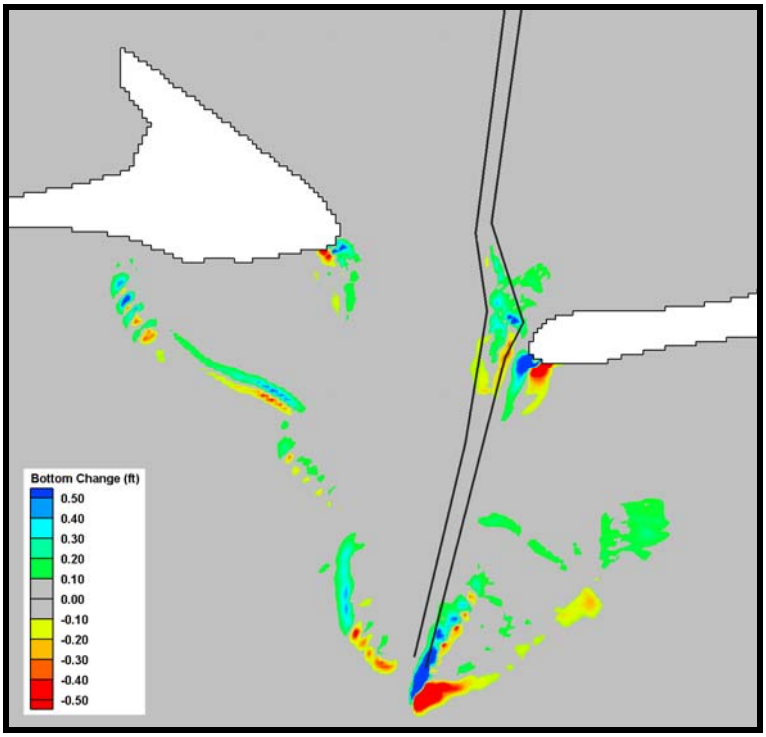

Figure 5-32. Bottom change results for 3 days of storm waves and a3-ft surge. Erosion is in yellow/red and accretion is in blue.

Transport vectors during flood tide (Figure 5-33) illustrate shoreward transport at the outer edges of the east and west lobes of the ebb-tidal delta. At Pelican Point (eastern Dauphin Island) and Mobile Point (western Morgan Peninsula), transport toward the inlet is indicative of changes predicted in the final bottom change plot (Figure 5-32). Both areas have relatively low wave energy, so observed transport can be attributed almost entirely to currents associated with maximum flood tide. Near Pelican Island, shoreward transport in the area immediately southeast of the island is dominant. Furthermore, northwest-directed transport along the seaward margin of Pelican Island indicates a primary direction of transport from the western lobe of the ebb-tidal delta to Dauphin Island. Both transport processes are illustrated in predicted bottom changes shown in Figure 5-32.

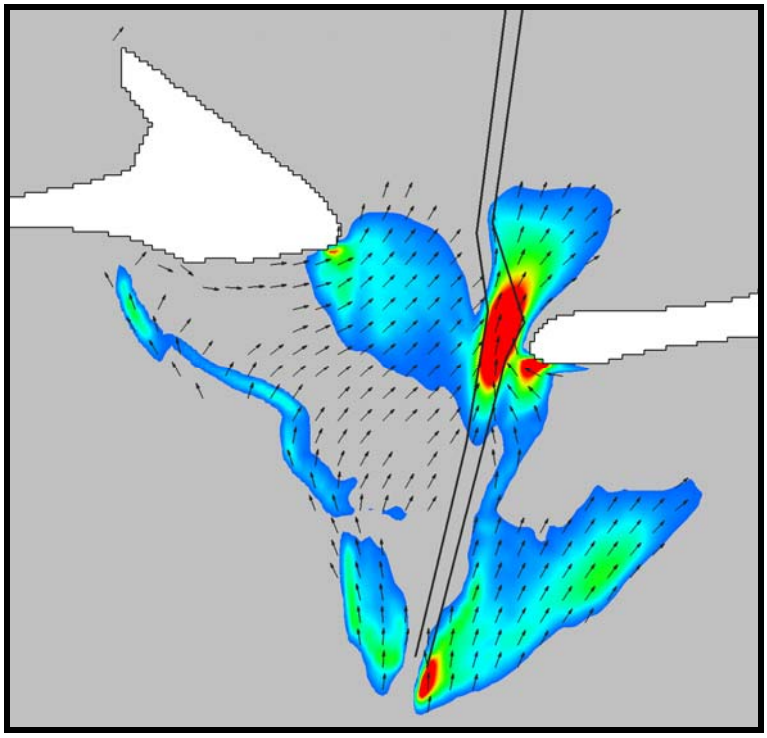

Figure 5-33. CMS-M2D average transport vectors for Case 3 during flood tide.

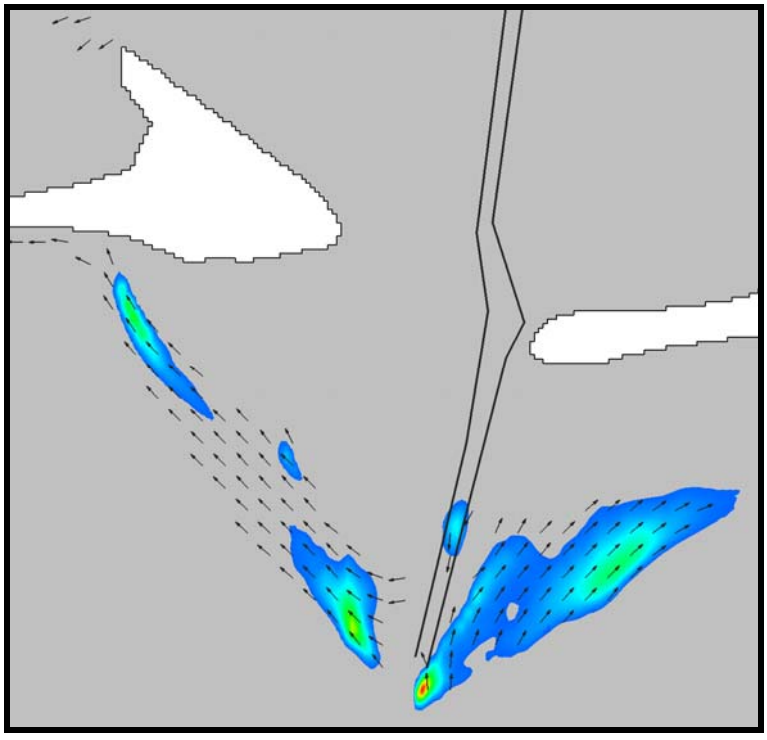

Figure 5-34. CMS-M2D average transport vectors for Case 3 during ebb tide.

During ebbing tide (Figure 5-34), observed transport is largely confined to the outer edges of the shoals on either side of the navigation channel. Ebb flow is confined to the navigation channel, and there is little wave energy across interior portions of the ebb-tidal delta due to wave breaking at the seaward margins. Along the western portion of the ebb shoal, there is a clear transport pathway from southeast to northwest toward Dauphin Island. With ebb currents confined to the navigation channel, waves are the dominant forcing mechanism along the east and west lobes of the shoal.

Summary of Numerical Modeling Results

Through the use of various numerical models, details of wave propagation, sediment transport potential, tidal hydraulics and morphology change in and around Mobile Pass have been analyzed.

Results from STWAVE simulations confirmed that the ebb-tidal delta dominates wave transformation in the area of Mobile Pass. Strong wave breaking and refraction across shoals were seen during energetic events. Pelican Island and surrounding shoals play an integral role in wave refraction and reduction of wave height in the lee of the island. Regardless of the details of the offshore wave conditions, refraction over the shoals southeast of Pelican Island was strong enough that all waves incident at the eastern tip of Dauphin Island were directed to the west.

STWAVE results were employed to calculate longshore sediment transport potential. These results showed a trend of net transport to the west across the entire study area. Transport along Morgan Peninsula increased from about 125,000 cy/year 15 miles east of Mobile Pass to 250,000 cy/year at Mobile Point. Transport along Dauphin Island is again directed to the west. Central portions of the island show significant transport in both directions, with a net transport of 25,000 cy/year directed to the west. For 3 miles of shoreline at the western tip of Dauphin Island, longshore transport showed a dramatic increase. The 25,000 cy/year simulated along the central portion of the island increased steadily to a rate 250,000 cy/year at the western end of the island.

ADCIRC modeling was performed to aid in understanding complex hydrodynamics of the inlet, as well as to provide boundary conditions for morphological modeling. Because of the complexities of tidal propagation in the Gulf of Mexico, and the lack of detailed field measurements outside of Mobile Bay, a regional model of the entire Gulf of Mexico was run. The model was given extra detail around Mobile Pass so that an accurate picture of flow in the area could be developed. Model results showed fair

comparison with tide gauge data in the area and were considered accurate enough to provide reasonable boundary conditions for morphological modeling.

CMS-M2D was used to investigate morphology change on the ebb-tidal delta. Results suggested that wave-driven transport dominated changes in bathymetry offshore Mobile Pass. Under storm conditions, transport from the western lobe of the ebb-tidal delta generally moved from the southeast to the northwest. This was particularly evident during ebbing tide. Although morphology change predictions were considered qualitative in nature, trends revealed from the modeling work closely simulated findings based on analysis of the historical bathymetric change discussed in Chapter 4.

6 Sediment Budget

Sediment budget determination for the coastal zone involves application of the principle of conservation of mass to littoral and offshore sediment (Bowen and Inman, 1966; Rosati and Kraus, 1999; Rosati, 2005). Development of a budget at Mobile Bay entrance and vicinity requires quantitative evaluation of various sediment sources to and losses from the study area, and a comparison of net gains or losses with observed rates of erosion or accretion. The USACE Sediment Budget Analysis System (SBAS; Rosati, 2005) was applied to display transport pathways and analyze sediment volume fluxes.

Originally, sediment erosion and accretion volumes were quantified for the period 1917/20 to 2002 by comparing (differencing) bathymetric survey data. However, the USACE 2002 bathymetry data were determined inadequate for computing a sediment budget because procedures associated with reference datum adjustments could not be verified accurately. This finding was identified during sediment budget formulation when change computations between 1917/20 and 2002 were determined to be abnormally large. Further analysis of the 2002 data set may yield appropriate datum adjustments, but this effort is beyond the scope of the present study.

For the period 1917/20 to 1984/87, twenty zones of erosion and accretion were identified throughout the sediment budget control area based on bathymetric change analysis. Overall, the entire ebb-tidal delta was net depositional. Beach and nearshore environments east of Mobile Pass were net erosional. One exception to this trend was the depositional zone adjacent to the jetties at Perdido Pass. Net west-directed transport deposits sand along the east side of the Pass, and sand dredged from the deposition basin at Perdido Pass was periodically bypassed to downdrift beaches west of the Pass, creating a region of net deposition.

Mobile Pass is an atypical navigation entrance in that jetties were not constructed to control channel shoaling and bar migration, even though a commercial navigation channel is maintained by dredging through the outer bar. The channel has always been a stable feature in that large shifts in shoal and channel geometry have not occurred historically. The modern channel occupies the general course of the ancient Mobile River valley when sea level was much lower than present (Boone, 1973; Smith, 1988; Hummell, 1990; Mars, 1992). Natural depths in the channel gorge are 55 to 60 ft, and flows through the Pass are sufficient to maintain channel depths. In fact, flows are so strong at Mobile Pass that hydrodynamic obstruction of net west-directed longshore currents east of the Pass produces an abrupt change in transport

direction at Mobile Point, forcing littoral sediment primarily south along the channel margin toward the outer part of the ebb-tidal delta. Todd (1968) termed this process dynamic diversion. Under this condition, shoaling through much of the channel is controlled by natural tidal currents. As such, only the seaward portion of the channel, across the outer bar, requires maintenance. Mobile Pass is an ideal entrance for commercial and recreational navigation.

Sediment Sources and Sinks

In recent geologic time, two primary sources of sediment have been available to form shoals on the ebb-tidal delta and beaches west of the Mobile Pass. Hummell (1990) suggested sediment transported out of Mobile Bay when sea level was lower created the foundation upon which the historical ebb-tidal delta has evolved. As sea level flooded the valley of the ancient Mobile River system, supply of sand-sized sediment to the coast diminished. The Mobile River delta was displaced farther inland and fine-grained sedimentation dominated infilling of Mobile Bay. The entrance channel occupied the ancient river valley and sand-sized sediment accumulated on the ebb-tidal delta by interaction of coastal and nearshore currents with cross-shore tidal flow at the entrance. Otvos (1973) suggested that ebb-tidal delta sands at Mobile entrance were derived primarily from Mobile Point and supplemented by sediment emerging from Mobile Bay.

Analysis of historical data from this study indicates that present-day sand supplied to the ebb-tidal delta is derived primarily from beach and nearshore sediment east of Mobile Pass (Stone et al, 2004). Only fine-grained material depositing along the outer margins of the ebb-tidal delta and west on the shelf fronting the Mississippi Sound barrier island system is derived from Mobile Bay. The coast and shelf east of Mobile Pass is sand rich from the 80-ft depth contour north into upland deposits (McBride and Byrnes, 1995); it is the primary source of sand for all beaches and tidal deltas west and into Mississippi.

Mobile Pass ebb-tidal delta also is a source of sediment for the barrier islands fronting Mississippi Sound. Barrier islands in this area historically have been growing and migrating to the west in the dominant direction of littoral transport (Byrnes et al., 1991; Morton, 2007). Inlets and their ebb-tidal deltas act as conduits for sand transport to the west. Islands become local sources of sediment as well, as sand is eroded from their eastern ends and transported to the west to be redeposited. This process is not occurring on Dauphin Island because the eastern end of the island is a relict late Pleistocene barrier ridge (Otvos, 1981). The stable ridge provides an area from which large volumes of littoral sand from the ebb-tidal delta can be

transported west, creating long and narrow sandy shoal platforms and islands off western Alabama and Mississippi (Otvos and Giardino, 2004). As such, Dauphin Island continues to extend to the west (sediment sink) as littoral sand is supplied to the beach via the ebb-tidal delta.

Storm overwash and island breaching have provided large sand volumes to backbarrier environments during landward migration of central Dauphin Island. As sand is transported across the island, the Gulf shoreline migrates to the north, apparently due to beach erosion. However, erosion implies that sand is permanently lost from the beach. Along central Dauphin Island, sand from the front side of the island often is recycled to the backside of the island as the island migrates landward (sand is not lost from the beach). This process is termed barrier rollover because the island migrates in a landward direction in response to storm processes. As such, the Gulf side of Dauphin Island can be considered a local source of sediment for landward island migration and lateral island growth.

Channel Shoaling Rates and Offshore Disposal

History of channel shoaling was discussed in Chapter 1 under Dredging and Placement History. Appendix B contains detailed information on new work and maintenance dredging quantities. Only maintenance dredging quantities can be used for estimating channel shoaling rates. Summarizing maintenance dredging data, one can derive an average shoaling rate for the outer bar channel for the period under which the sediment budget has been developed (1917/20 to 1984/87). Maintenance dredging records indicated that approximately 274,000 cy of sand was extracted from the channel each year between 1917 and 1987 and disposed of offshore. Most of this material was derived from the southern 1 to 2 miles of channel across the outer bar.

Although the exact location for disposal of dredged material from the outer bar is not known, bathymetric changes offshore of the outer bar indicated a large polygon of deposition just seaward and west of the navigation channel (Figure 6-1). This area appears to be the site of offshore dredged material disposal from the Mobile Pass Outer Bar. Prior to analyzing bathymetric changes in this area, it was not known whether dredged material deposited offshore was contributing to net sediment accumulation and transport on the ebb-tidal delta. The direct connection between the offshore disposal area and sand deposition and transport on the southwestern part of the ebb-tidal delta suggests that sediment exchange is active in this area. The mound of deposition to the west of the offshore disposal site is the Mobile Outer

Mound, a berm created by the USACE using about 17 million cy of dredged material from the Mobile Harbor dredging project.

New work and maintenance dredging records provided quantities of sediment dredged from the outer bar that were deposited offshore for the period 1917 to 1987. Summing these data provided an estimate of the quantity of sand dredged from the outer bar that was deposited offshore during this time. The annual maintenance dredging rate was about 274,000 cy, and the annual new work was about 75,000 cy, resulting in net deposition at the offshore site of about 349,000 cy/year. According to bathymetric change results, net sand accumulation at the offshore disposal site was determined to be about 191,000 cy/year. Therefore, the annual quantity of sand from the disposal site contributing to deposition on the western lobe of the outer bar between 1917/20 and 1984/87 was determined to be about 158,000 cy.

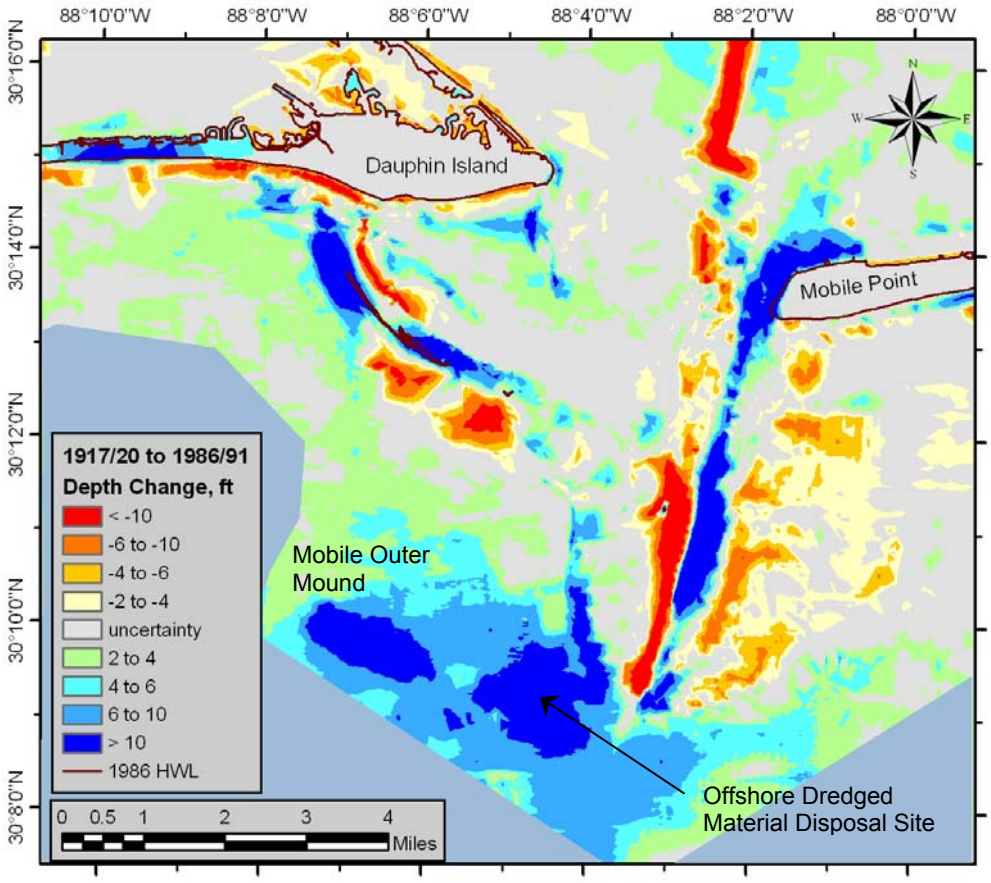

Figure 6-1. Location of offshore dredged material disposal site and the Mobile Outer Mound relative to deposition on the ebb-tidal delta.

Net Longshore Transport

In developing a sediment budget, sources and sinks for open boundaries within the sediment budget control area determine the reliability of the budget. Net littoral transport rates near the eastern boundary of the study area (Perdido Pass) were estimated by Walton (1973) at about 280,000 cy/year to the west. Basillie (1975) computed net west-directed transport at rates between 239,000 cy/year and 334,000 cy/year based upon wave observations for an area west of Pensacola, FL. Douglass (2001) estimated the annual net transport to be about 190,000 cy/year near Perdido Pass. When the USACE constructed two converging jetties at Perdido Pass in 1969, a 400,000 cy capacity deposition basin was built on the eastern side of the channel to capture sand transported over the weir section to limit channel shoaling. Dredging frequency for the basin was every two years, indicating that estimated net littoral drift to the west was about 200,000 cy/yr (Sargent, 1988). Within 2 years of construction, the basin was full and additional material was shoaling the navigation channel. Based on these data, net littoral transport at the eastern boundary of the sediment budget was estimated at 240,000 cy/yr.

Sediment Contribution from Mobile Bay

Fine-grained sediment transport from Mobile Bay to the Gulf has been documented based on photography and Landsat imagery, and discussed by numerous authors (e.g., Chermock, 1974; Hardin et al., 1976; Stumpf and Gelfenbaum, 1990). Using data reported by Hardin et al. (1976) for fine-grained sediment infilling of lower Mobile Bay, sediment transport seaward and to the west of the ebb-tidal delta was estimated at 337,000 cy/yr. Based on more recent discharge values for Mobile Pass, Isphording et al. (1996) estimated that about 420,000 cy of suspended sediment not retained in the lower Bay is transported to the Gulf of Mexico on an annual basis. Fine-grained sediment does not affect the sand budget along the beaches and on the ebb-tidal delta, but it is a component of the regional transport system and was included for completeness.

Net Transport Pathways and Quantities: 1917/20 to 1984/87

Net deposition and erosion throughout coastal Alabama for the period 1917/20 to 1984/87 were determined by differencing the 1917/20 and 1984/87 bathymetric surfaces to isolate polygons of erosion and deposition. This period encompassed a time of significant dredging activity in the outer bar channel. Figure 6-2 illustrates areas of net erosion and deposition (white numbers indicate quantities eroded or deposited in thousands of cubic yards on an annual basis within defined polygons)

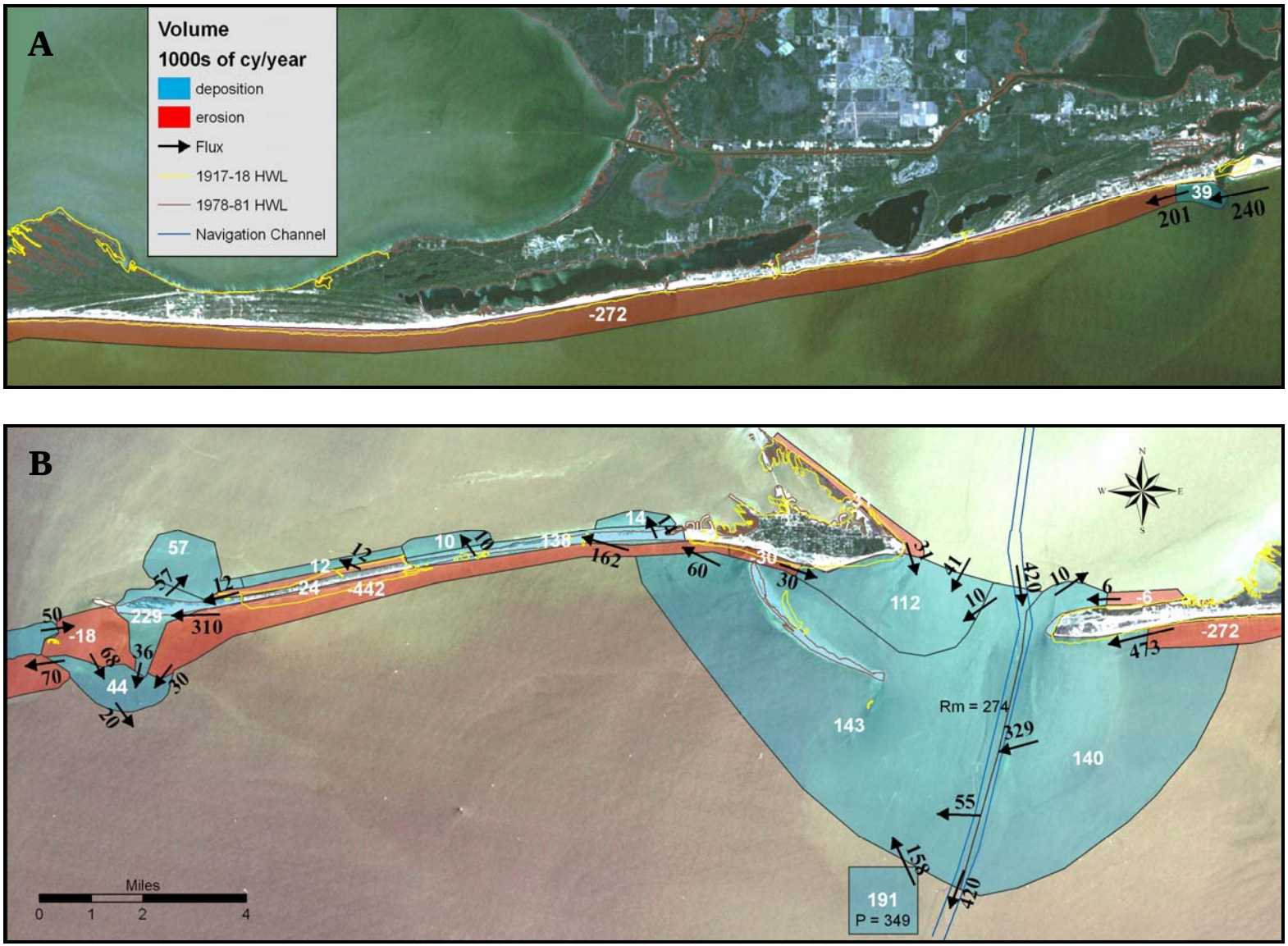

Figure 6-2. Sediment budget for the Alabama outer coast, 1917/20 to 1984/87. A: Alabama coast between Perdido Pass in the east and western Morgan Peninsula; B – Alabama coast between western Morgan Peninsula and eastern Petit Bois Island, MS. White numbers indicate quantities eroded or deposited in thousands of cubic yards on an annual basis within defined polygons, and black numbers associated with black arrows are sediment fluxes in thousands of cubic yards per year.

and associated sediment fluxes (black numbers associated with black arrows in thousands of cubic yards per year) in coastal Alabama.

Starting east of Perdido Pass, net littoral transport at the eastern boundary was estimated by Basillie (1975) to be about 240,000 cy/year. Because net sand deposition was recorded just west of Perdido Pass (39,000 cy/year), the flux of sand from this point west was estimated at 201,000 cy/year (Figure 6-2A). Net erosion along the shoreline, and particularly in the nearshore, was dominant for most of the Gulf shore fronting Morgan Peninsula until encountering Mobile Pass and its ebb-tidal delta. At this point, sand available to the transport system had increased in proportion to net erosion documented via bathymetric change analysis. As such, by the time sand began depositing along Mobile Point and the eastern side of the ebb-tidal delta, sand flux was approximately 473,000 cy/year. The bay side of Mobile Point indicated net erosion as well, which contributed another 6,000 cy/year to the ebb-tidal delta.

Net sediment accumulation dominated sedimentation trends on the eastern lobe of the ebb-tidal delta, adding 140,000 cy/year to shoals on the eastern side of the channel (Figure 6-2B). Bathymetric change results illustrated that most deposition was associated with channel infilling as the channel migrated to the west during this time (Figure 6-1). Sediment deposition at Mobile Point and inside the Bay illustrated the northern extent of channel infilling as the channel margin bar evolved in direct response to strong tidal currents exiting and entering the Bay and their interaction with west-directed sediment transport. Erosion on eastern shoals of the ebb-tidal delta contributed to channel margin sedimentation as well.

Although significant net deposition was computed east of the channel, large quantities of sand were transported to and across the channel to the western lobe of the ebb-tidal delta. Approximately 329,000 cy/year of sand was transported west, 274,000 cy/year of which were dredged from the outer bar channel and deposited at the offshore disposal site (shown as R_m=274 on Figure 6-2B). The remaining 55,000 cy/year bypassed the channel to the west as described in Chapter 4. Disposal of new work and maintenance dredging material from the outer bar at the offshore disposal site was approximately 349,000 cy/year for the period of record (shown as P=349 on Figure 6-2B). Of this quantity, it was estimated that 158,000 cy/year was transported north and west onto the western lobe of the ebb-tidal delta.

Stumpf and Gelfenbaum (1990) and Isphording et al. (1996) indicate that fine-grained material exiting lower Mobile Bay contributes to deposition on the shelf seaward and west of Mobile Pass. Based on discharge values for Mobile Pass, it was

estimated that about 420,000 cy/year of suspended sediment exits the bay and deposits on the shelf outside the study area.

Net deposition west of the channel on the outer portion of the delta amounted to about 143,000 cy/year. Growth of Pelican Island during this time was extensive, and sand bypassing to Dauphin Island provided needed sediment for closing breaches caused by the July 1916 hurricane and expanding the island westward. Approximately 60,000 cy of sand was bypassed to Dauphin Island on an annual basis between 1917/20 and 1984/87, of which 162,000 cy/year was needed to restore the island (138,000 cy/year) and account for washover deposition behind the island (24,000 cy/year). There is evidence in the historical record that flooding currents in Pelican Pass are sufficiently competent to deposit sand along the shoreline and nearshore of Pelican Bay. As such, 30,000 cy/year of sand was directed toward Pelican Bay to account for this process. Hydrodynamic modeling results presented in Chapter 5 confirm that flooding tides to the east through Pelican Pass are stronger than ebbing tides to the west. Another 31,000 cy/year of sand was transported southeast from Little Dauphin Island, predominantly during ebbing tide, and deposited in Pelican Bay as shoals south of eastern Dauphin Island (see Figure 6-1). An additional 41,000 cy of sand was needed on an annual basis from the large shoal fronting Little Dauphin Island to balance net deposition in Pelican Bay of 112,000 cy/year.

Net transport to the west along western Dauphin Island was driven primarily by beach and nearshore erosion along central and western portions of the island that supplied approximately 310,000 cy/year of sand to lengthen Dauphin Island to the west. Of this sediment flux, about 229,000 cy/year was required for island expansion to the west and growth of the ebb-tidal delta at Petit Bois Pass. Approximately 70,000 cy/year was transported to the western side of the pass, where beach erosion and barrier island washover supplied sand to backbarrier shoals and downdrift beaches along Petit Bois Island. Cycling of sand at Petit Bois Pass is complex, but overall net transport pathways and quantities are controlled by recorded patterns of net geomorphic change.

Inlet Reservoir Model

The Inlet Reservoir Model (Kraus, 2000) is a time-dependant model for predicting inlet morphology based on equilibrium volumes and transport rates. With equilibrium volumes and transport rates assigned for an inlet system, the model produces a time-dependant sediment budget based on feature volumes, transport rates, and longshore sediment transport predictions at study area boundaries.

The Reservoir model calls upon five assumptions (Bodge and Rosati, 2003):

- The volume of sand within the study area is conserved.
- Morphological forms and sediment pathways can be identified and preserve their identity while they evolve.
- Changes in morphological forms are relatively smooth.
- Material composing the ebb-tidal shoal is predominately transported to and from the shoal through longshore sediment transport.

Furthermore, to achieve an analytical solution to the sediment balance between morphological features, a linear rate of bypassing for a given feature is assigned such that

$$FlowRateOut = FlowRateIn\left(\frac{CurrentVolume}{EquilibriumVolume}\right)$$

Kraus (2000) and Bodge and Rosati (2003) offer a more thorough discussion of model formulations and theoretical underpinnings.

Inlet Reservoir Model at Mobile Pass. The values from the final sediment budget were applied to a simplified account of Mobile Pass as shown in Figure 6-3. Morphological features included in the model were the east and west lobes of the ebb-tidal delta, an area to represent offshore disposal, and the navigation channel.

Sediment pathways are simplified such that all sediment arriving from the east (Q Left In) is passed into the east lobe of the ebb-tidal delta. The volume not retained by the east lobe is passed into the navigation channel. The navigation channel is represented so no volume remains in the channel. Sediment transported into the navigation channel was either passed into the offshore disposal site (to represent channel dredging) or onto the west lobe of the ebb-tidal delta. The west lobe received material from the navigation channel directly, as well as from the disposal site. The west lobe retains volume as prescribed by model and passes the excess downdrift in the direction of Q Left Out.

Given that a working sediment budget has been established, equilibrium volumes for the east and west lobes of the ebb-tidal delta could be calculated directly and input to the Inlet Reservoir Model. The model was run for the period 1917/20 to 1984/87. Volumes for east and west lobes of the ebb-tidal delta were taken directly from Table 3-5, using the values reported for the 1917/20 year and the 30-ft depth contour. The

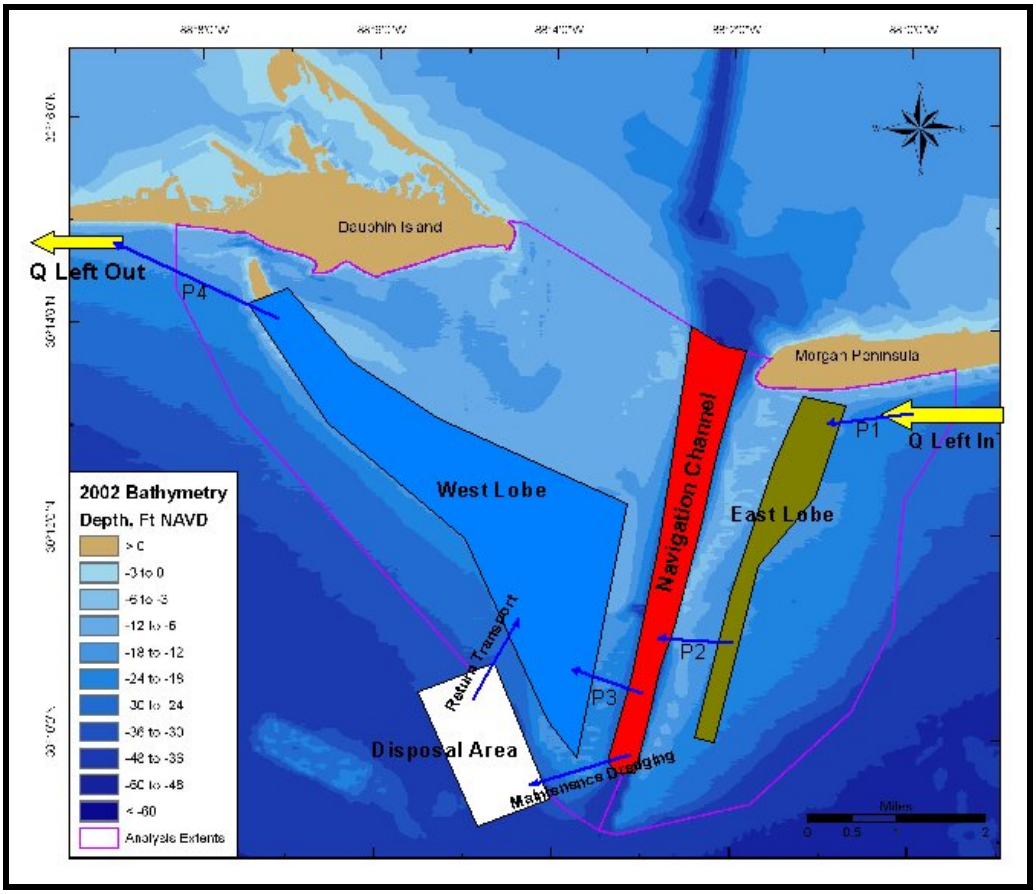

Figure 6-3. The Inlet Reservoir Model domain and component features for Mobile Pass.

Table 6-1. Input variables for the Inlet Reservoir Model.

	Starting Volume (cy)	Equilibrium Volume (cy)	Transport Rate (cy/year)	Coupling Coefficient
East Lobe	112,394,000	151,588,000	--	--
Navigation Channel	100,000	100,000	--	--
Disposal Area	9,500,000	20,984,000	--	--
West Lobe	311,003,000	1,504,606,000	--	--
Q Left In	--	--	473,000	--
P1	--	--	--	1.0
P2	--	--	--	1.0
P3	--	--	--	0.17
Maintenance Dredging	--	--	--	0.83
Return Transport	--	--	--	1.0
P4	--	--	--	1.0

30-ft depth contour was chosen as it better represents the active region of transport on the ebb-tidal delta. Table 6-1 shows input values for the final model run. The coupling coefficient listed for pathways controls the distribution of material leaving a given area.

In general, volumes associated with the navigation channel are irrelevant to the final result, as long as initial and equilibrium volumes are the same so that all material passed into the polygon is passed through pathways P3 and Maintenance Dredging. Similarly, the initial volume chosen for the disposal area is not exact. Instead, the ratio between initial and equilibrium volumes is the critical parameter. This ratio determines the amount of material leaving the disposal area through the return transport pathway.

Figure 6-4 illustrates predicted volumes by time for east and west lobes of the ebb-tidal delta compared with volumes calculated from bathymetry data. In both cases, predicted curves are flat, which is expected because the inlet has been active for thousands of years and these data consider only the past 70 years of evolution. In

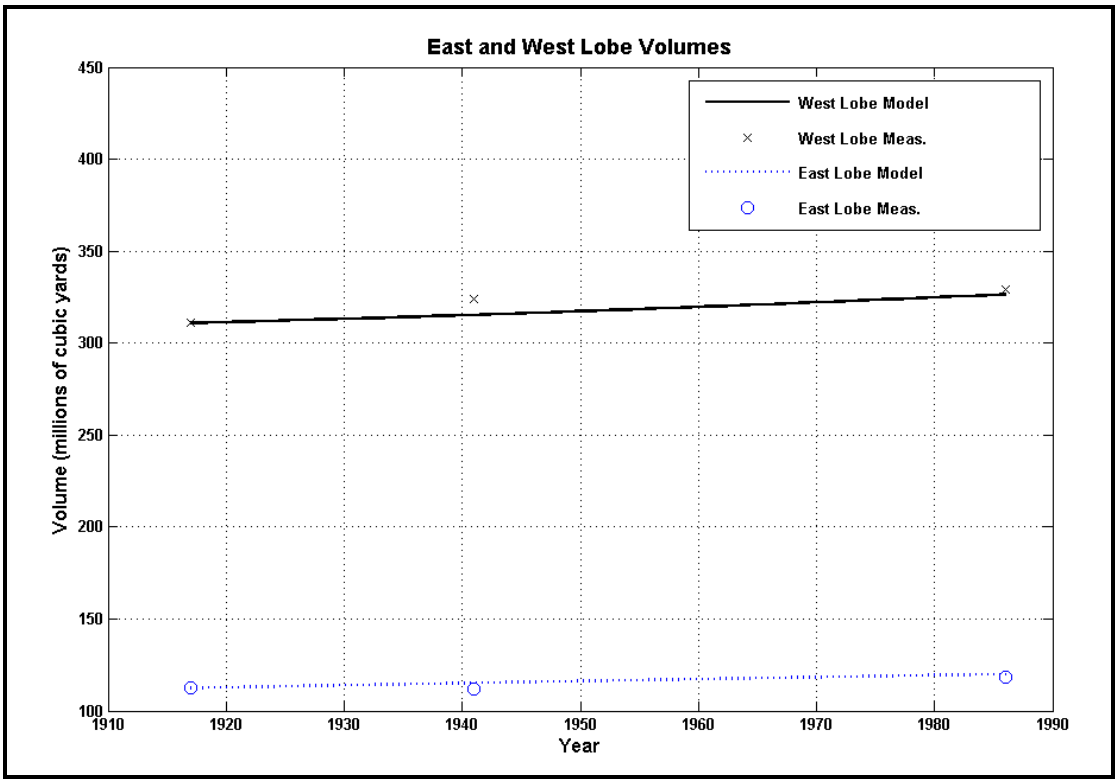

Figure 6-4. Modeled versus measured volume change on the east and west lobes of the ebb-tidal delta, 1917/18 to 1984/87.

addition, the flow rate out of the model, reported as Q Left Out, increased slowly from 40,000 cy/year in 1917 to 77,000 cy/year in 1987, which is in close agreement with the sediment budget estimation of 60,000 cy/year between 1917/20 and 1984/87.

The value of the Inlet Reservoir Model is with establishing bounds on volumes and growth rates for various morphological features for a given inlet. In addition, it can help display the estimated growth of various features during evolution of the inlet. Because Mobile Pass and the ebb-tidal delta are so complex and mature, results from the model are somewhat redundant relative to the sediment budget. The model does provide an estimate of equilibrium shoal volumes, which is something other work does not. However, the change rate, transport rates, and volume changes are all better described within the original sediment budget based on bathymetric change analysis. A further concern with application of the Inlet Reservoir Model is that the role of storms is so dominant, that the model assumption of smooth change to morphological features is violated.

7 Changes Resulting from Channel Dredging

The primary purpose of this study was to evaluate the impact of construction and maintenance dredging for the Federal navigation project in Mobile Outer Bar Channel on shoreline response along Dauphin Island and shoal evolution on the Mobile Pass ebb-tidal delta. A number of previous studies have expressed concern regarding the effect engineering activities may have had on beach changes. Specifically, the USACE Beach Erosion Control and Hurricane Protection report for Mobile County, Alabama (1978) stated

> "The principal causes of shore erosion along the westernmost 11 miles of Dauphin Island are attributable to rise in sea level and maintenance dredging of the Mobile Bay entrance channel."

Douglass (1994) discussed the annual rate of sand removal from the Mobile Outer Bar between 1974 and 1989 and stated

> "Almost all of this sediment has been removed from the littoral system of coastal Alabama to deepwater disposal sites."
>
> "The littoral system of Dauphin Island and Sand Island has probably not received any littoral drift from the east of Mobile Pass in fifty years."
>
> "In essence, because of dredging practices, Mobile Pass has probably functioned as a sink for sand moving along the coast this century. Assuming that all of the sediment dredged from the outer bar came from the littoral system, the efficiency of the sink has been much greater than 100% relative to the flowrate of sand along the coast."

Although neither study relied on a detailed evaluation of historical dredging records for the outer bar channel or a quantitative comparison of historical shoreline and bathymetry surveys for documenting historical sediment transport pathways and net rates of change across the ebb-tidal delta and along the shoreline of Dauphin Island, qualitative connections between channel dredging and beach erosion along Dauphin Island were asserted. Douglass (1994, p. 327) recognized this shortfall when stating "A comprehensive study that conclusively correlates the changes in the shoals and erosional-depositional patterns on Dauphin Island with the dredging history and storm and wave climate record was beyond the scope of this study".

The working hypothesis tested in the present study was that historical construction and channel maintenance dredging in the Mobile Outer Bar Channel have resulted in adverse changes to the western lobe of the ebb-tidal delta and the beach along

Dauphin Island west of Pelican Island. Ebb-shoal changes and shoreline response relative to storm and normal forces, and dredging in the outer bar channel, were evaluated to determine the extent to which beach erosion along Dauphin Island could be attributed to USACE channel construction and maintenance dredging operations.

Minimum Measurable Quantity

Early in the project, one of the tasks requested by the ITRT involved documenting uncertainty related to shoreline position, bathymetry, and numerical simulations of flow and sediment transport to gauge the significance of change rates and transport values for quantifying the potential impact of dredging activities at Mobile Pass on adjacent shorelines. The methods used to document uncertainty with shoreline and bathymetry data were presented in Chapters 2 and 3 and discussed in Byrnes et al. (2002) and Baker and Byrnes (2004). A so-called minimum measurable longshore transport quantity was derived based on our analyses and presented to the ITRT for evaluation in January 2007. The following is a summary of the analysis.

All survey data sets contain some amount of inherent uncertainty associated with data acquisition and compilation procedures. It is important to quantify limitations in survey measurements and document potential systematic errors that can be eliminated during quality control procedures (Byrnes et al., 2002). Substantial effort was spent ensuring that any systematic errors were eliminated from all data sets prior to change analysis. As such, measurement errors associated with present and past surveys are considered random. Because random errors are considered equally distributed, they can be neglected relative to change calculations. This leaves data density as the primary factor for determining the reliability of erosion and accretion quantities associated with change surfaces.

Interpolation between measured points always includes uncertainty associated with terrain irregularity and data density. The density of bathymetry data, survey line orientation, and the magnitude and frequency of terrain irregularities are the most important factors influencing uncertainties in volume change calculations between two bathymetric surfaces (Byrnes et al., 2002; Baker and Byrnes, 2004). Volume uncertainty relative to terrain irregularities and data density can be determined by comparing surface characteristics at adjacent survey lines. Large variations in depth between survey lines (i.e., few data points describing variable bathymetry) will result in large uncertainty calculations between lines. Additionally, surveys with track lines oriented parallel to major geomorphic features can result in large uncertainty calculations between lines. This computation provides the best estimate of

uncertainty for gauging the significance of volume change calculations between two surfaces.

Uncertainty estimates were calculated for the 1917/18, 1960/61, 1982/92, and 2001/2002 bathymetric surfaces using the methods outlined in Byrnes et al. (2002). Multiple sets of line pairs were compared for each time period to represent terrain variability. Line pairs were chosen that would accurately reflect track line spacing for each survey and irregularity of prominent geomorphic features in the region. Lines were established for each time period to overlay survey lines for that year. Bathymetry data were extracted along each line to calculate variations in elevation between line pairs. Depths were extracted at 10-ft intervals, and the absolute value of differences was averaged to calculate potential uncertainty for each line pair.

Results of uncertainty calculations are summarized in Table 7-1. Estimates were generated for each bathymetric surface, with particular emphasis on the ebb–tidal delta of each data set. As expected, areas with greatest uncertainty were associated with channel and ebb shoal features. To identify potential uncertainty related to sediment transport calculations, a separate calculation was made for the channel/ebb-tidal delta area. Potential elevation uncertainty ranged from ±0.54 to ±1.30 ft for calculations made across the entire surface to ±1.88 to ±2.59 ft for the channel/ebb shoal areas. Combining this information to judge the impact of potential uncertainties associated with volume change calculations derived from these surfaces resulted in root-mean-square variations shown in Table 7-2.

Table 7-1. Potential uncertainty for bathymetric surfaces from western Dauphin Island to Perdido Pass, AL.

	Entire Surface (ft)	**Ebb-Tidal Delta/Channel (ft)**
1917/20	±0.84	±1.88
1960/61	±1.02	±2.30
1982/92	±0.54	±1.43
2001/2002	±1.30	±2.59

Table 7-2. Maximum root-mean-square (RMS) potential uncertainty for bathymetric change data from western Dauphin Island to Perdido Pass, AL.

	1960/61	**1982/92**	**2001/2002**
1917/20	±1.32[1] (±2.97[2])	±0.99 (±2.36)	±1.55 (±3.20)
1960/61		±1.15 (±2.71)	±1.65 (±3.46)
1982/92			±1.41 (±2.96)

[1]Entire Surface, [2]Ebb-Tidal Delta/Channel

Applying these limits to the area of sand accumulation along the western end of Dauphin Island as the island expanded to the west in response to dominant westward longshore transport (Figures 7-1 and 7-2), a range in potential uncertainty can be determined relative to the area of accumulation. The sand accumulation rate in Table 7-3 can be directly associated with the net longshore sand transport rate for the ocean fronting portion of Dauphin Island. As such, potential uncertainty calculations can be determined relative to net transport rates, providing an estimate of the minimum measurable quantity for this area. For long-term data comparisons (e.g., 1917/20 to 2001/2002), potential volume uncertainty, calculated using the ebb-tidal delta/channel elevation uncertainty estimates, ranged from ±43,500 to ±70,000 cy/yr (Table 7-4). Using the entire shelf surface elevation uncertainty estimates, potential volume uncertainty ranged from ±18,500 to ±34,000 cy/yr. Because net transport estimates were calculated for an inlet region, the minimum measurable quantity range was estimated at ±43,500 to ±70,000 cy/yr, or about 25 to 30% of calculated net longshore sand transport rates (RMS depth uncertainty in Table 7-2 times the corresponding polygon surface area in Table 7-3).

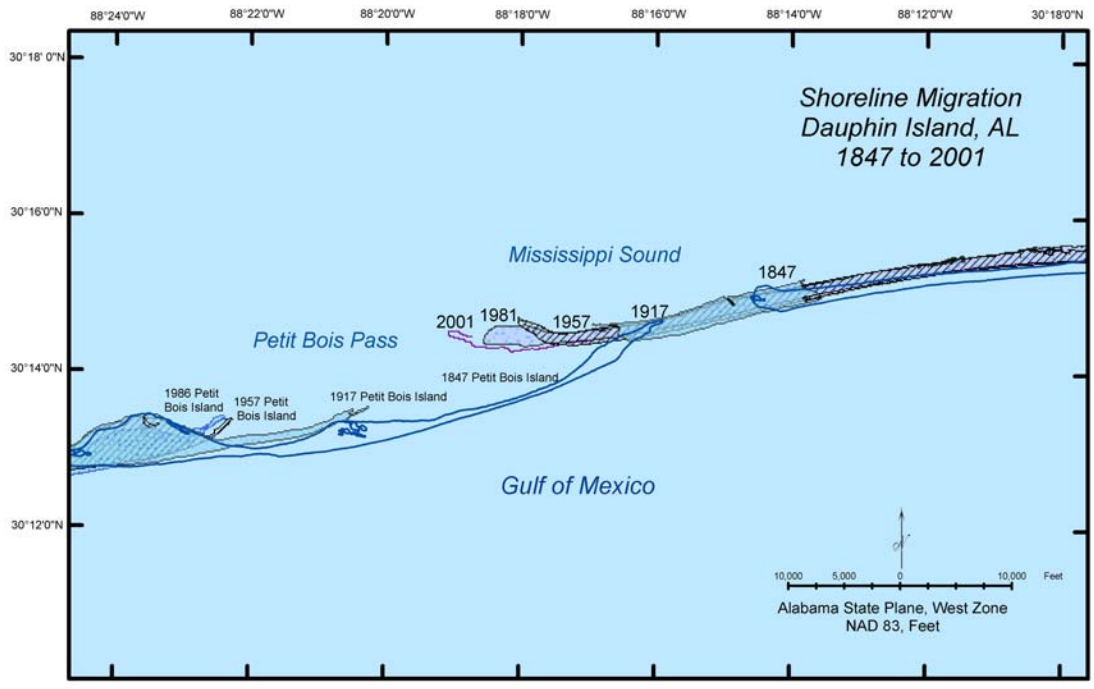

Figure 7-1. Historical shoreline position at the western end of Dauphin Island, 1847/67 to 2001/2002.

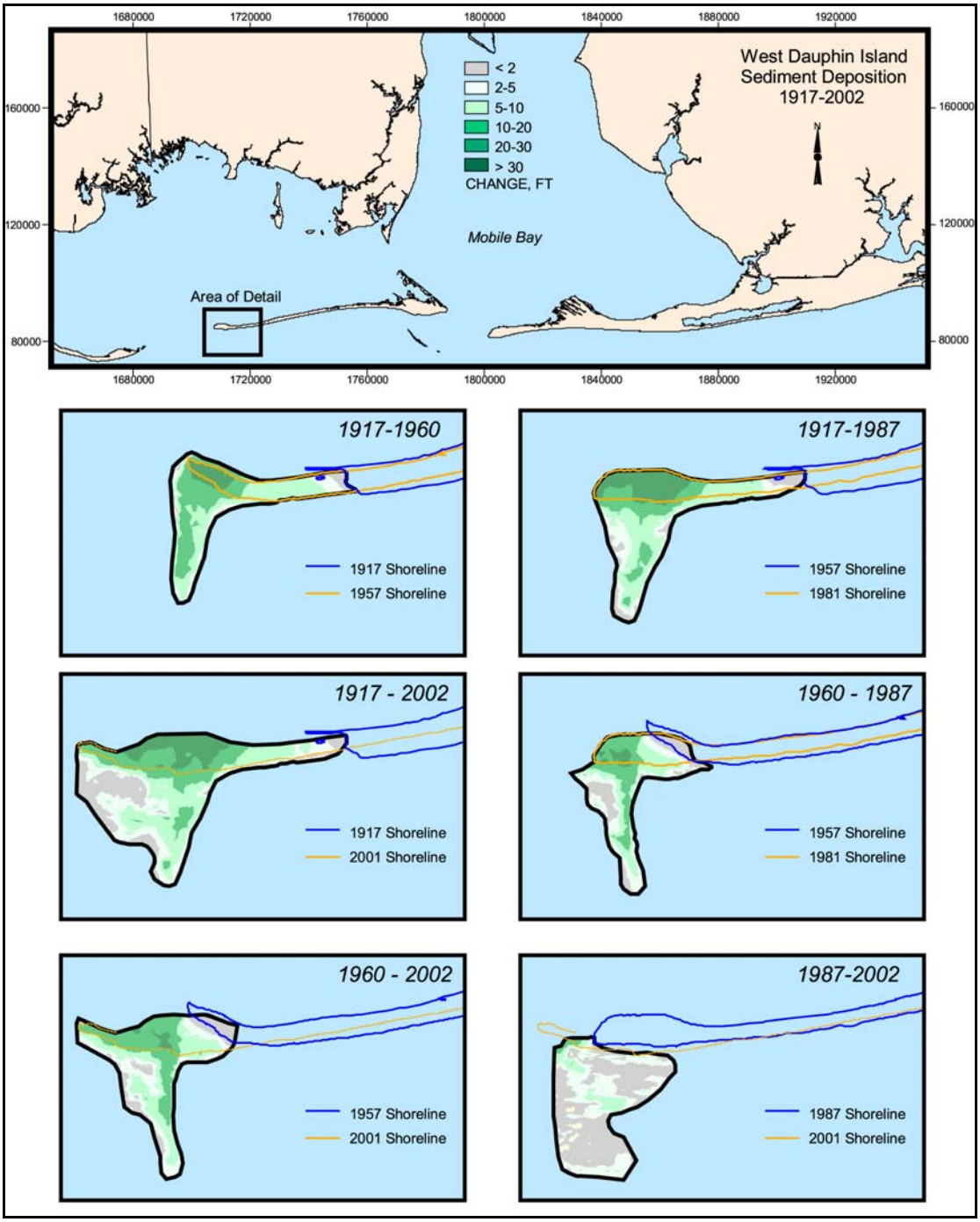

Figure 7-2. Sediment accumulation at the western end of Dauphin Island, 1917/20 to 2001/2002.

Table 7-3. Sediment accumulation at the western end of Dauphin Island in response to net westward longshore sand transport (accumulation polygons illustrated in Figure 7-2).

	1960/61	1982/92	2001/2002
1917/20	230,370[1]	195,704	202,697
	3,042,330[2]	3,853,774	5,580,772
1960/61		268,704	236,802
		2,699,775	3,422,885
1982/92			196,412
			3,321,997

[1] Accumulation Volume (cy/year); [2] Accumulation area (sq yd)

Table 7-4. Maximum potential volume uncertainty for bathymetric change data from western Dauphin Island, AL.

	1960/61	1982/92	2001/2002
1917/20	±30,500 (±68,500)	±18,500 (±43,500)	±34,000 (±70,000)
1960/61		±40,000 (±94,000)	±46,000 (±96,500)
1982/92			±104,000 (±218,000)

[1]Entire Surface, [2]Ebb-Tidal Delta/Channel

Local Changes

After compiling and analyzing at least 50 to 100 historical shoreline and bathymetry data sets, over a century of documentation regarding construction and maintenance dredging history for the channel across the Mobile Outer Bar, detailed histories of tropical cyclones in the northern Gulf of Mexico, and coastal processes data sets in support of numerical modeling, sediment transport and morphology changes at the shoreline and on the Mobile Pass ebb-tidal delta were documented within the context of data coverage and measurement uncertainty. Local changes resulting from navigation channel dredging involved direct removal of sediment from the outer bar to depths at least twice that of the shallowest point across the bar prior to dredging. Channel location has been fixed at its westernmost position since the mid-1800s. Natural westward migration of the channel controlled its current location.

Maintenance dredging captured a substantial quantity of littoral sand from east of the entrance, but a time series of bathymetric changes for the ebb-tidal delta indicated that sand bypassing from east-to-west remained active as channel construction and maintenance occurred. For most of the historical record, sand dredged from the outer bar channel was deposited offshore at a site just west of the navigation channel. Water depths in the area are between 30 and 40 ft, and bathymetric change surfaces indicate that sand from this offshore disposal site is

supplying sediment to the southwestern end of the ebb-tidal delta. Overall, large volumes of sand are being transported onto the western lobe of the inlet shoals, resulting in net deposition in this area and sufficient transport to Dauphin Island to mend storm-related breaches and washover surge channels. This process is supported by numerical modeling results documenting transport pathways and sedimentation patterns consistent with historical trends (see Figures 5-32 through 5-34). Furthermore, sand supply is so robust that island expansion to the west has continued at a relatively consistent rate with or without channel dredging.

Shoal migration and growth on the western lobe of the ebb-tidal delta is controlled by storm frequency and magnitude, and the availability of sand from the eastern side of the channel. Sand transported from east of Mobile Pass has resulted in net deposition on both lobes of the ebb-tidal delta prior to and after dredging commenced. Although storm impacts on sedimentation trends were indicated in a few of the change data sets, recovery to normal depositional patterns was rapid. Overall, there appears to be no measurable negative local impacts to the ebb-tidal delta or Dauphin Island associated with channel dredging.

Regional Changes

Regional changes prior to channel dredging were consistent with those identified after dredging commenced. As stated above, natural channel migration controlled channel location and may have been instrumental in promoting sand bypassing just south of Sand Island Lighthouse where the channel offset formed during westward migration in the early to mid-1900s. The capacity of this inlet system to continue bypassing sand from east-to-west during channel development and maintenance attests to the quantity of material available for transport. Furthermore, because dredged material from the channel appears to have been placed within the active transport system offshore and west of the channel between the 30- and 40-ft depth contours, onshore transport of sand by wave-generated currents during storms is able to supply dredged material to the ebb-tidal delta. Again, transport and bottom change simulations support this finding (see Figures 5-32 through 5-34).

Without the existence of these transport processes, it is difficult to envision how such large quantities of sand could be depositing on both lobes of the ebb-tidal delta, along the shoreline of Dauphin Island to close breaches and add elevation to low-relief washover deposits, and to promote continued growth of Dauphin Island to the west. Similar to local change, there appears to be no measurable negative regional impacts to the ebb-tidal delta or Dauphin Island associated with channel dredging across the Mobile Pass Outer Bar.

8 Conclusions and Recommendations

Sediment erosion, transport, and deposition in coastal Alabama is controlled by storm wave and current processes that produce net littoral transport to the west. The east-to-west gradient in transport is so dominant that minor reversals are not evident in shoreline, bathymetry, or photographic data sets. Effectively, net and gross transport are nearly equal. This bias in transport makes determination of net transport pathways and quantities relatively straightforward.

Historical shoreline and bathymetry data; dredging records; tropical cyclone records; coastal process data sets; and wave, current, and morphologic change modeling results were analyzed to evaluate the potential impact of channel dredging across the Mobile Pass Outer Bar Channel on erosion processes along Dauphin Island and on the ebb-tidal delta west of the navigation channel. In addition, transport pathways and quantities derived during the time of major dredging activities were evaluated in light of natural sand bypassing and shoal development and migration on the Mobile Pass ebb-tidal delta.

Analysis of shoreline position change between 1847/48 and 2006 revealed a common link associated with geomorphic evolution of Dauphin Island. Major changes in island configuration west of Pelican Island were always associated with hurricanes or tropical storms. Every breach recorded along central Dauphin Island (starting in 1853) was connected with a specific storm (or series of storms). Furthermore, all breaches filled within a relatively short post-storm recovery period (decade or so). The breach initiated by Hurricane *Ivan* (2004) and expanded during Hurricane *Katrina* (2005) still exists, but May 2007 photography indicates the breach is gradually closing. The net result of storm overwash and breaching is rapid landward movement (not net erosion) of the Gulf and Sound shorelines. This process, called barrier island rollover, allows the low-profile portion of the barrier island to maintain its integrity at a landward location after major storms.

The primary requirement for breach closure and island recovery is a constant supply of sand updrift of the damaged island. If sufficient sand quantities were not being supplied to the island throughout the historical record, storm breaches along central Dauphin Island would be difficult to fill and beaches would not recover very rapidly. Furthermore, island growth to the west has lengthened the island approximately 5.2 miles since 1847/48, 2.9 miles of which occurred since 1917/20 (the period of major dredging activity in the outer bar channel). Sand transport from Pelican Island and

the west lobe of the ebb-tidal delta had to be maintained throughout the period of channel dredging to repair storm damage and promote island growth.

Analysis of bathymetry data at and adjacent to the Mobile Pass ebb-tidal delta indicated the same response as shoreline data. Pelican and Sand Islands are emergent features that have formed, migrated, and eroded in response to storms and post-storm processes. In addition to creating a 5-mile breach along central Dauphin Island, the July 1916 hurricane degraded most of the shoals and islands on the ebb-tidal delta. Only a small portion of Pelican Island remained above water after the storm. However, shoals and islands on the west lobe of the delta continued to grow and migrate to the northwest between 1917/20 and 1986/2002 (periodically disrupted by hurricanes). By 2002, approximately 85 years after major dredging commenced, Pelican Island had expanded to its greatest extent since 1908. This is the same period under which breach infilling and westward island growth were occurring on Dauphin Island. A simple sand balance evaluation requires that east-to-west sand transport across the channel, on to the ebb-tidal delta, and northwest to Dauphin Island be maintained to produce net deposition on the delta, breach closure, and island expansion along the barrier island west of Pelican Island.

Bathymetric change analysis indicates consistent deposition for the entire ebb-tidal delta prior to and after channel dredging, except for two periods where the end dates were close to major storms. The magnitude of deposition on the delta prior to channel dredging was similar to net deposition recorded during major dredging activities. The observation that net deposition is the trend on the ebb-tidal delta and on Dauphin Island during channel dredging indicates the requirement for an external source of sand and active transport processes to redistribute the sand. If the channel were a long-term total littoral barrier and maintenance dredging and offshore placement were removing sediment from the active transport system, one would expect the rate of sand volume change on the west lobe of the ebb-tidal delta to decrease, not increase. In turn, if sand transport to Dauphin Island were not consistent with pre-dredging quantities, one would not expect storm breaches on the island to recover concomitant with rapid island growth to the west.

Wave, hydrodynamic, and sediment transport modeling were conducted to provide a process link to morphologic response. Wave modeling results illustrated a trend of net transport to the west throughout the study area, consistent with all morphology change analyses. Maximum transport magnitudes occurred near Mobile Point and western Dauphin Island. Morphologic modeling, which includes wave and current modeling, indicated wave-driven transport dominates changes to bathymetry on the Mobile Pass ebb-tidal delta. Under average tide and wave conditions, predicted

bottom changes documented the pattern of channel margin deposition and bypassing to the western lobe of the ebb-tidal delta illustrated in historical bathymetric change results. During storms, sediment from most locations on the ebb-tidal delta, on both sides of the navigation channel, generally moved to the north-northwest.

Patterns of bathymetric change illustrated in Figure 4-10 are well-described by modeling results. Seafloor changes on the outer margins of the ebb-tidal delta reflect sand movement under storm conditions (see Figures 5-32 to 5-34), and depositional patterns near the latitude of Sand Island Lighthouse reflect transport dynamics associated with average tide and wave conditions (see Figures 5-29 to 2-31). The link between historical sand bypassing discussed in Chapter 4 and the dominant processes responsible for patterns of deposition are well-documented when comparing wave-current simulations and bathymetric change results. Although morphology change predictions are qualitative in nature, the trends revealed from modeling are consistent with and confirm findings based on analysis of historical bathymetry data.

A sediment budget was developed to link all data sets analyzed. Shoreline and bathymetry change provided transport volumes along the shore and on the ebb-tidal delta. Dredging data also were incorporated in the analysis. Net transport from east-to-west was dominant in all parts of the system. Net deposition over the entire ebb-tidal delta required substantial transport quantities from the east. The flux of sediment from the Morgan Peninsula Gulf beach and nearshore to the east side of the ebb-tidal delta was estimated at 473,000 cy annually, 55,000 cy/year of which bypass the channel to the west (274,000 cy/year was dredged from the channel). Bathymetric change analysis identified the general location of the offshore disposal site west of the channel mouth, and there appears to be a direct connection between deposition on the western side of the outer bar and the offshore disposal site. Wave and tide simulations indicated that the disposal site was located in the area of north-northwest transport illustrated for storm conditions (see Figure 5-33 and 5-34). After calculating sediment accumulation at the disposal site between 1917/20 and 1986, it was determined that approximately 158,000 cy/year was supplied to the western lobe of the delta. Accounting for net deposition on the western lobe of the delta, approximately 60,000 cy/year was provided to Dauphin Island to nourish and expand the island to the west. These volumes were required to recreate changes recorded between 1917/20 and 1984/87.

Overall, net sediment transport from east-to-west between 1917/20 and 1984/87 has been supplying sand quantities necessary to produce net deposition on the islands and shoals of the ebb-tidal delta, infill and nourish storm breaches and washover

surge channels on Dauphin Island, and promote growth of western end of the island, even though channel dredging has been active. Based on all of this information, there appears to be no measurable negative impacts associated with historical channel dredging across the Mobile Pass Outer Bar.

According to dredging records, disposal procedures in recent years have been to place as much of the sand dredged from the outer bar channel as possible in the SIBUA (beneficial sand disposal area; see Figure 1-23). Because there is no guarantee that sand bypassing and transport from the historical offshore disposal site will continue at rates shown in the sediment budget, it is recommended that procedures followed in recent years for disposal of bar channel sand in the SIBUA be continued for the life of the project.

9 References

Anders, F.J. and M.R. Byrnes, 1991. Accuracy of shoreline change rates as determined from maps and aerial photographs. Shore and Beach, 59(1): 17-26.

ARCE, 1896-1990. Improvement of Rivers and Harbors: Mobile Outer Bar and Mobile Harbor. Annual Reports of the Corps of Engineers, Washington, DC.

Battjes, J.A. and J.P. Janssen, 1978. Energy loss and set-up due to breaking of random waves. Proc. 23rd Int. Conf. Coastal Engineering, ASCE, pp. 569-587.

Baker, J.L. and M.R. Byrnes, 2004. Appendix F: Shoreline and Bathymetry Data. In: Kraus, N.C. and H.T. Arden (editors), North Jetty Performance and Entrance Channel Maintenance, Grays Harbor, Washington. Technical Report ERDC/CHL TR-03-12, US Army Engineer Research and Development Center, Vicksburg, MS.

Balsillie, J.H., 1975. Analysis and Interpretation of Littoral Environment Observation (LEO) and Profile Data Along the Western Panhandle Coast of Florida. USAE Waterways Experiment Station, Coastal Engineering Research Center, Technical Memorandum 49, 104 p.

Bearden, B.L. and R.L. Hummell, 1990. Geomorphology of Coastal Sand Dunes, Morgan Peninsula, Baldwin County, Alabama. Geological Survey of Alabama Circular 150, 71 pp.

Bedford, K.W., and J. Lee, 1994. Near-bottom sediment response to combined wave-current conditions, Mobile Bay, Gulf of Mexico. Journal of Geophysical Research, 16: 161-177.

Bentley, S.J., Y. Furukawa, and W.C. Vaughan, 2000. Record of event sedimentation in Mississippi Sound. Gulf Coast Association of Geological Societies Transactions, 50: 715-723.

Bentley, S.J., T.R. Keen, C.A. Blain, and W.C. Vaughan, 2002. The origin and preservation of a major hurricane event bed in the northern Gulf of Mexico: Hurricane Camille, 1969. Marine Geology, 186: 423-446.

Blake, E.S., E.N. Rappaport, and C.W. Landsea, 2007. The Deadliest, Costliest, and Most Intense United States Tropical Cyclones from 1851 to 2006 (and Other Frequently Requested Hurricane Facts). NOAA Technical Memorandum NWS TPC-5, National Hurricane Center, Miami, FL, 45 p.

Blanton, J.O., 1994. U.S. Southeast Continental Shelf Inner Shelf Processes Relevant to the Northeast Gulf of Mexico Inner Shelf. Proceedings of the Northeast Gulf of Mexico Physical Oceanography Workshop, U.S. Department of the Interior, Minerals Management Service, OCS Study 94-0044.

Bodge, K.R. and J.D. Rosati, 2003. Sediment Management at Inlets. In: Donald L. Ward (Ed.), Coastal Engineering Manual, Part V, Coastal Project Planning and Design, Chapter V-6, Engineer Manual 1110-2-1100, U.S. Army Corps of Engineers, Washington, DC.

Boone, P., 1973. Depositional systems of the Alabama, Mississippi, and western Florida coastal zone. Gulf Coast Association of Geological Societies Transactions, 23: 266-277.

Bossak, B.H., 2003. Early 19th Century U.S. Hurricanes: A GIS Tool and Climate Analysis. PhD Dissertation, Florida State University, Tallahassee, FL, 100 p.

Bossak, B.H. and J.B. Elsner, 2004. Plotting early nineteenth-century hurricane information. EOS, 85(20): 199.

Bowen, A. J. and D.L. Inman, 1966. Budget of Littoral Sands in the Vicinity of Port Arguello, California. Technical Memorandum No. 19, U.S. Army Engineer Waterways Experiment Station, Coastal Engineering Research Center, Vicksburg, MS.

Bruun, P., 1962. Sea level rise as a cause of shore erosion. American Society of Civil Engineers Proceedings, Journal Waterways and Harbors Division, 88: 33-74.

Bruun, P., 1983. Review of conditions for uses of the Bruun Rule of erosion. Coastal Engineering, 7: 77-89.

Bruun, P., 1988. The Bruun Rule of erosion by sea-level rise: a discussion of large-scale two- and three-dimensional usages. Journal of Coastal Research, 4(4): 627-648.

Buttolph, A. M., C.W. Reed, N.C. Kraus, N. Ono, M. Larson, B. Camenen, H. Hanson, T. Wamsley, and A.K. Zundel, 2006. Two-Dimensional Depth-Averaged Circulation Model CMS-M2D: Version 3.0, Report 2, Sediment Transport and Morphology Change. Technical Report ERDC/CHL-TR-06-7, US Army Engineer Research and Development Center, Coastal and Hydraulics Laboratory, Vicksburg, Mississippi.

Byrnes, M.R. and K.J. Gingerich, 1987. Cross-island profile response to Hurricane Gloria. In: N.C. Kraus (editor), Proceedings Coastal Sediments '87, American Society of Civil Engineers, New York, NY, p. 1486-1502.

Byrnes, M.R. and M.W. Hiland, 1995. Large-scale sediment transport patterns on the continental shelf and influence on shoreline response: St. Andrew Sound, Georgia to Nassau Sound, Florida, U.S.A. In: J.H. List and J.H.J. Terwindt (editors), Large-Scale Coastal Behavior. Marine Geology, 126: 19-43.

Byrnes, M.R. and R.A. McBride, 1996. Northeast Gulf of Mexico hard mineral resources study. Proceeding of the 15th Annual Information Transfer Meeting, U.S. Department of the Interior, Minerals Management Service, New Orleans, LA, pp. 481-486.

Byrnes, M.R. and J.L. Baker, 2003. Chapter 3: Inlet and Nearshore Morphodynamics. In: Kraus, N.C. and H.T. Arden (Editors), North Jetty Performance and Entrance Navigation Channel Maintenance, Grays Harbor, Washington, Volume I: Main Text. ERDC/CHL TR-03-12, Coastal and Hydraulics Laboratory, U.S. Army Engineer Research and Development Center, Vicksburg, MS, pp. 67-136.

Byrnes, M.R., J.L. Baker, and F. Li, 2002. Quantifying potential measurement errors and uncertainties associated with bathymetric change analysis. ERDC/CHL CHETN-IV-50, Coastal and Hydraulics Laboratory, U.S. Army Engineer Research and Development Center, Vicksburg, MS, 17 p.

Byrnes, M.R., S.F. Griffee, and H.R. Moritz, 2007. Engineering activities influencing historical sediment transport pathways at the Columbia River Mouth, WA/OR. In: N.C. Kraus and J.D. Rosati (editors), Proceedings Coastal Sediments '07, American Society of Civil Engineers, Reston, VA, pp. 1754-1767.

Byrnes, M.R., R.A. McBride, S. Penland, M.W. Hiland, and K.A. Westphal, 1991. Historical changes in shoreline position along the Mississippi Sound barrier islands. In: Coastal Depositional Systems in the Gulf of Mexico: Quaternary Framework and Environmental Issues, GCS-SEPM 12th Annual Research Conference, pp. 43-55.

Byrnes, M.R., R.M. Hammer, B.A. Vittor, J.S. Ramsey, D.B. Snyder, K.F. Bosma, J.D. Wood, T.D. Thibaut, and N.W. Phillips, 1999. Environmental Study of Identified Sand Resource Areas Offshore Alabama: Volume I: Main Text, Volume II: Appendices. U.S. Department of the Interior, Minerals Management Service, International Activities and Marine Minerals Division (INTERMAR), Herndon, VA. OCS Report MMS 99-0052, 326 pp. + 132 pp. appendices.

Chermock, R.L., P.A. Boone, and R.L. Lipp, 1974. The Environment of Offshore and Estuarine Alabama. Geological Survey of Alabama Information Series 51, 135 pp.

Cipriani, L.E. and G.W. Stone, 2001. Net longshore sediment transport and textural changes in beach sediments along the southwest Alabama and Mississippi barrier islands, USA. Journal of Coastal Research, 17(2):443-458.

Clarke, A.J., 1994. Overview of the Physical Oceanography of the Florida Shelf in the Study Region. Proceedings of the Northeast Gulf of Mexico Physical Oceanography Workshop, U.S. Department of the Interior, Minerals Management Service, OCS Study 94-0044.

Crowell, M., S.P. Leatherman, and M.K. Buckley, 1991. Historical shoreline change: error analysis and mapping accuracy. Journal of Coastal Research, 7(3): 839-852.

Davies, D.J. and R.L. Hummell, 1994. Lithofacies evolution from transgressive to highstand systems tracts, Holocene of the Alabama coastal zone. Gulf Coast Association of Geological Societies Transactions, 44: 145-153.

Dean, R.G. and M. Perlin, 1977. Coastal engineering study of Ocean City Inlet, Maryland. Proceedings Coastal Sediment '77, Charleston, South Carolina, p. 520-542.

Dolan, R.B. and P.J. Godfrey, 1973. Effects of Hurricane Ginger on the barrier islands of North Carolina. Bulletin Geological Society America, 84: 1329-1334.

Douglass, S.L., 1991. Summary of Existing Coastal Engineering Data for Dauphin Island, Alabama. College of Engineering Report No. 91-1, University of South Alabama, Mobile, AL, 39 pp.

Douglass, S.L., 1994. Beach erosion and deposition on Dauphin Island, Alabama, U.S.A. Journal of Coastal Research, 10(2): 306-328.

Douglass, S.L., 2001. "State-of-the-beaches" of Alabama: 2001. Report to Alabama Department of Economic and Community Affairs, 27 pp.

Douglass, S.L. and D.R. Haubner, 1992. Coastal Processes of Dauphin Island, Alabama. College of Engineering Report No. 92-1, University of South Alabama, Mobile, AL, 90 p. plus Appendices.

Douglass, S.L., D.T. Resio, and E.B. Hands, 1995. Impact of Near-Bottom Currents on Dredged Material Mounds Near Mobile Bay. Technical Report DRP-95-6, U.S. Army Engineers Waterways Experiment Station, Dredged Material Research Program, Vicksburg, MS.

Douglass, S.L. and A.E. Browder, 2005. Hurricane Ivan's impacts on the Alabama coast. Shore and Beach, 73(2/3): 71-78.

Doyle, L.J. and T.N. Sparks, 1980. Sediments of the Mississippi, Alabama, and Florida (MAFLA) Continental Shelf. Journal of Sedimentary Petrology, 50(3): 905-915.

Dunn, G.E. and B.I. Miller, 1964. Atlantic Hurricanes. Louisiana State University Press, Baton Rouge, LA, 377 p.

Ellis, M.Y., 1978. Coastal Mapping Handbook. U.S. Department of the Interior, Geological Survey, U.S. Department of Commerce, National Ocean Service, U.S. Government Printing Office, Washington, D.C., 199 pp.

Escoffier, F.F., 1958. Harrison County (Mississippi) artificial beach. American Society of Civil Engineers Transactions, 123: 817-823.

Fisher J.S. and D.K. Stauble, 1977. Impact of Hurricane Belle on Assateague Island washover. Geology, 5: 765-768.

Fong, D.A. and S.G. Monismith, 2004. Evaluation of the accuracy of a ship-mounted, bottom-tracking ADCP in a near-shore coastal flow. Journal of Atmospheric and Oceanic Technology, **21**: 1121–1128.

Foxgrover, A.C., S.A. Higgins, M.K. Ingraca, B.E. Jaffe, and R.E. Smith, 2004. Deposition, Erosion, and Bathymetric Changes in South San Francisco Bay: 1858-1983. USGS Open-File Report 2004-1192, U.S. Geological Survey, Reston, VA.

Froede, C.R., Jr., 2006a. A Hurricane Fredric-generated storm-surge deposit exposed along a surf-zone foredune scarp on Dauphin Island, Alabama, USA. Journal of Coastal Research, 22(2): 371-376.

Froede, C.R., Jr., 2006b. The impact of Hurricane Ivan (September 16, 2004) made across Dauphin Island, Alabama. Journal of Coastal Research, 22(3): 561-573.

Garcia, A. W., 1977. Dauphin Island Littoral Transport Calculations. U.S. Army Engineer Waterways Experiment Station, Hydraulics Laboratory, Vicksburg, MS, Miscellaneous Paper H-77-11, 12 pp.

Gelfenbaum, G. and R.P Stumpf, 1993. Observations of currents and density structure across a buoyant plume front. Estuaries, 16(1): 40-52.

Goda, Y., 1985. Random Seas and Design of Maritime Structures. University of Tokyo Press, Tokyo, Japan.

Graumann, A., T. Houston, J. Lawrimore, D. Levinson, N. Lott, S. McCown, S. Stephens, and D. Wuertz, 2005. *Hurricane Katrina – A Climatological Perspective*. NOAA National Climate Data Center, U.S. Department of Commerce, Asheville, NC, 27 p.

Guidroz, W.S., K.R. Poole, G.W. Stone, D. Dartez, and L.G. Pong, 2007. Contrasting sediment transport along the southwestern Louisiana and upper Texas shorelines: Impacts from Hurricane Rita, 2005. Shore and Beach, 75(1): 57-64.

Hands, E.B., 1991. Wide-area monitoring of Alabama berms. Marine Technology Society Conference, New Orleans, LA, p. 98-105.

Hands, E.B., 1992. Monitoring of Alabama Berms. Technical Note DRP-1-08, UASE Waterways Experiment Station, Dredging Research Program, Vicksburg, MS, 14 p.

Hands, E.B., 1994. Shoreward Movement and Other 5-yr Changes at the Sand Island Berms, Alabama. In: Proceeding of the 15th Western Dredging Association Conference, College Station, TX, pp. 223-235.

Hands, E.B. and M.C. Allison, 1991. Mound migration in deeper water and methods of categorizing active and stable depths. In: N.C. Kraus, K.J. Gingerich, and D.L. Kriebel (editors), Coastal Sediments '91, American Society of Civil Engineers, New York, NY, pp. 1985-1999.

Hardin, J.D., C.D. Sapp, J.L. Emplaincourt, and K.E. Richter, 1976. Shoreline and Bathymetric Changes in the Coastal Area of Alabama: A Remote Sensing Approach. Geological Survey of Alabama Information Series 50, 125 pp.

Harris, D.L., 1981. Tides and Tidal Datums in the United States. Special Report No. 7, U.S. Army Coastal Engineering Research Center, Fort Belvoir, VA, 382 p.

Hayes, M.O., 1967. Hurricanes as Geologic Agents: Case Studies of Hurricane Carla, 1961, and Cindy, 1963. Texas Bureau of Economic Geology, Report of Investigation 61, 54 p.

Hess, K.W., 2004. Tidal datums and tidal coordination. In: Byrnes, M.R., M. Crowell, and C. Fowler (editors), Shoreline Mapping and Change Analysis: Technical Considerations and Management Implications. Journal of Coastal Research, Special Issue 38, pp. 33-43.

Hicks, S.D., 1981. Tidal datums and their uses – A summary. Shore and Beach, 53(1): 27-32.

Hubbard, D.K., G.F. Oertel, and D. Nummedal, 1979. The role of waves and tidal currents in the development of tidal-inlet sedimentary structures and sand body geometry examples from North Carolina, South Carolina, and Georgia. Journal of Sedimentary Petrology, 49(4): 1073-1092.

Hubertz, J.M., R.M. Brooks, W.A. Brandon, and B.A. Tracy, 1993. Hindcast Wave Information for the U.S. Atlantic Coast. WIS Report 30, U.S. Army Engineer Waterways

Experiment Station, Coastal Engineering Research Center, Wave Information Study, Vicksburg, MS.

Hummell, R.L., 1990. Main Pass and the Ebb-Tidal Delta of Mobile Bay, Alabama. Geological Survey of Alabama Circular 146, 45 pp.

Hummell, R.L., 1996. Holocene Geologic History of the West Alabama Inner Continental Shelf, Alabama. Geological Survey of Alabama Circular 189, 131 pp.

Hummell, R.L. and S.J. Parker, 1995. Holocene Geologic History of Mobile Bay, Alabama. Geological Survey of Alabama Circular 186, 96 pp.

Hummell, R.L. and W.E. Smith, 1995. Geologic and Environmental Characterization and Near-term Lease Potential of an Offshore Sand Resource Site for Use in Beach Nourishment Projects on Dauphin Island, Alabama. Final Report, Prepared by the Geological Survey of Alabama in fulfillment of U.S. Department of the Interior, Minerals Management Service Cooperative Agreement No. 14-35-0001-30725, 165 pp.

Hummell, R.L. and W.E. Smith, 1996. Geologic Resource Delineation and Hydrographic Characterization of an Offshore Sand Resource Site for Use in Beach Nourishment Projects on Dauphin Island, Alabama. Final Report, Prepared by the Geological Survey of Alabama in cooperation with the Department of Geology, University of Alabama in fulfillment of U.S. Department of the Interior, Minerals Management Service Cooperative Agreement No. 14-35-0001-30781, 169 pp.

Isphording, W.C. and G.C. Flowers, 1987. Mobile Bay: The right estuary in the wrong place. In: T.A. Lowrey (editor), Symposium on the Natural Resources of the Mobile Bay Estuary, Mississippi-Alabama Sea Grant Consortium, MASGP-87-007, p. 165-174.

Isphording, W.C. and F.D. Imsand, 1991. Cyclonic events and sedimentation in the Gulf of Mexico. In: N.C. Kraus, K.J. Gingerich, and D.L. Kriebel (editors), Coastal Sediments '91, American Society of Civil Engineers, New York, NY, pp. 1122-1136.

Isphording, W.C., F.D. Imsand, and R.B. Jackson, 1996. Fluvial sediment characteristics of the Mobile River delta. Gulf Coast Association of Geological Societies Transactions, 46: 185-191.

Jarrell, J.D., P.J. Hebert, and B.M. Mayfield, 1992. Hurricane Experience Levels of Coastal County Populations - Texas to Maine. NOAA Technical Memorandum NWS-NHC-46, 152 p.

Jarvinen, B.R., C.J. Neumann, and A.S. Davis, 1984. A Tropical Cyclone Data Tape for the North Atlantic Basin, 1886-1983: Contents, Limitations, and Uses. NOAA Technical Memorandum NWS-NHC-22, 21 p.

Kamphuis, J.W., 1990. Alongshore sediment transport rate. Proceedings 22nd Coastal Engineering Conference, ASCE, New York.

Kinoshita, K. and M. Noble, 1995. Current Data from the Northern Gulf of Mexico. Open File Report 95-633, U.S. Department of the Interior, U.S. Geological Survey.

Kraus, N.C., 2000. Reservoir model of ebb-tidal shoal evolution and sand bypassing. Journal of Waterway, Port, Coastal, and Ocean Engineering, 126(3): 305-313.

Kraus, N.C., C.C. Ebbesmeyer, and O.P. Smith., 1991. Introduction to the Mobile, Alabama, Field Data Collection Project. In N.C. Kraus (editor), Mobile, Alabama, Field Data Collection Project, 18 August – 2 September 1989: Report 1, Technical Report DRP-91-3, USAE Waterways Experiment Station, CERC, Vicksburg, MS, p. 7-52.

Lamb, G.M., 1987. Erosion downdrift from tidal passes in Alabama and the Florida Panhandle. Bulletin of the Association of Engineering Geologists, 24: 359-362.

Larson, M. and N.C. Kraus, 1995. Prediction of cross-shore sediment transport at different temporal and spatial scales. In: J.H. List and J.H.J. Terwindt (editors), Large-Scale Coastal Behavior. Marine Geology, 126: 111-127.

Lee, W., 1998. Sand Island Lighthouse Chronicles. Beacon Publishing, Theodore, AL, 89 p.

Lewis, J.K. and R.O. Reid, 1985. Local wind forcing of a coastal sea at subinertial frequencies. Journal of Geophysical Research, 90: 934-944.

Ludlum, D.M., 1963. Early American Hurricanes: 1492 to 1870. American Meteorological Society, 198 p.

Ludwick, J.C., 1964. Sediments in Northeastern Gulf of Mexico. In: R.L. Miller (ed.), Papers in Marine Geology, Macmillan Co., New York, NY, pp. 204-238.

Marmer, H.A., 1951. Tidal Datum Planes. Special Publication No. 135, NOAA National Ocean Service, U.S. Coast and Geodetic Survey, U.S. Government Printing Office, Washington, D.C., 142 p.

Mars, J.C., A.W. Shultz, and W.W. Schroeder, 1992. Stratigraphy and Holocene evolution of Mobile Bay in southwestern Alabama. Gulf Coast Association of Geological Societies Transactions, 42: 529-542.

McBride, R.A., 1997. Synthesis of Hard Mineral Resources of the Florida Panhandle Shelf: Spatial Distribution and Subsurface Evaluation. Final Report, U.S. Department of the Interior, Minerals Management Service, Contract No. 1435-01-96-CT-30812, 5 p. + 727 p. appendix.

McBride, R.A. and M.R. Byrnes, 1995. Surficial sediments and morphology of the southwestern Alabama/western Florida panhandle coast and shelf. Gulf Coast Association of Geological Societies Transactions, 45: 393-404.

McBride, R.A., L.C. Anderson, A. Tudoran, and H.H. Roberts, 1999. Holocene stratigraphic architecture of a sand-rich shelf and the origin of linear shoals: northeastern Gulf of Mexico. In: Bergman, K.M. and Snedden, J.W. (editors), Isolated Shallow Marine Sand Bodies; Sequences, Stratigraphic Analysis, and Sedimentologic Interpretation. SEPM Special Publication 64, p. 95-126.

McBride, R.A., M.R. Byrnes, S. Penland, D.L. Pope, and J.L. Kindinger, 1991. Geomorphic History, Geologic Framework, and Hard Mineral Resources of the Petit Bois Pass Area, Mississippi-Alabama. In: Coastal Depositional Systems in the Gulf of Mexico: Quaternary Framework and Environmental Issues, GCS-SEPM 12th Annual Research Conference, pp. 116-127.

McGehee D., J.P. McKinney, W.E. Grogg, and E.B. Hands, 1994. Monitoring of Waves and Currents at the Dredged Material Mounds Offshore of Mobile Bay, Alabama. Technical Report DRP-94-4, U.S. Army Engineer Waterways Experiment Station, Dredged Material Research Program, Vicksburg, MS.

Meyer, T.H., D.R. Roman, and D.B. Zilkoski, 2004. What does height really mean? Part I: Introduction. Surveying and Land Information Science, 64(4): 223-233.

Morang, A. and L. Parson, 2002. Coastal Morphodynamics. In: A. Morang (editor), Part IV, Coastal Geology, Chapter IV-3. Engineer Manual 1110-2-1100, U.S. Army Engineer Research and Development Center, Vicksburg, MS.

Morton, R.A., 2007. Historical Changes in the Mississippi-Alabama Barrier Islands and the Roles of Extreme Storms, Seal Level, and Human Activities. U.S. Geological Survey Open File Report 2007-1161, Coastal and Marine Geology Program, St. Petersburg, FL, 38 p.

Mukai, A. Y., J.J. Westerink, R.A. Luettich, and D.J. Mark, 2001. East Coast 2001, A Tidal Constituent Database for the Western North Atlantic, Gulf of Mexico and Caribbean Sea. U.S. Army Engineer Research and Development Center, Vicksburg, MS.

Murray, S.P., 1970. Bottom currents near the coast during hurricane Camille. Journal of Geophysical Research, 75(24): 4579-4582.

Nichols R.L. and A.F. Marston, 1939. Shoreline changes in Rhode Island produced by hurricane of September 21, 1938. Bulletin Geological Society America, 50: 241-246.

NOAA, 2001. Tidal Datums and Their Applications. NOAA Special Publication NOS CO-OPS 1, U.S. Department of Commerce, National Oceanic and Atmospheric Administration, Silver Spring, MD, 112 p.

NOAA, 2003. Computational Techniques for Tidal Datums Handbook. NOAA Special Publication NOS CO-OPS 2, U.S. Department of Commerce, National Oceanic and Atmospheric Administration, Silver Spring, MD, 98 p.

Nummedal, D., S. Penland, R. Gerdes, W. Schramm, J. Kahn, and H. Roberts, 1980. Geologic response to hurricane impact on low-profile Gulf Coast barriers. Gulf Coast Association of Geological Societies Transactions, 30: 183-195.

Otvos, E.G., 1973. Sedimentology. In: J.Y. Christmas (editor), Cooperative Gulf of Mexico Estuarine Inventory Study, Mississippi. Gulf Coast Research Laboratory, Ocean Springs, MS, Project 2-25-R, p. 123-139.

Otvos, E.G, 1979. Barrier island evolution and history of migration, north-central Gulf Coast. In: S.P. Leatherman (ed.), Barrier Islands, Academic Press, New York, NY, pp. 291-319.

Otvos, E.G., 1981. Barrier island formation through nearshore aggradation – stratigraphic and field evidence. Marine Geology, 43: 195-243.

Otvos, E.G., 2006. Discussion of : Froede, C.R., Jr., 2006. The impact the Hurricane Ivan (September 16, 2006) made across Dauphin Island, Alabama. *Journal of Coastal Research*, 22(2), 561-573. Journal of Coastal Research, 22(6): 1585-1588.

Otvos, E.G. and Giardino, M.J., 2004. Interlinked barrier chain and delta lobe development, northern Gulf of Mexico. Sedimentary Geology, 169: 47-73.

Parker, S.J., 1990. Assessment of Nonhydrocarbon Mineral Resources in the Exclusive Economic Zone Offshore Alabama. Geological Survey of Alabama Circular 147, 73 pp.

Parker, S.J., A.W. Shultz, and W.W. Schroeder, 1992. Sediment Characteristics and Seafloor Topography of a Palimset Shelf, Mississippi-Alabama Continental Shelf. In: Quaternary Coasts of the United States: Lacustrine and Marine Systems. SEPM Special Publication 48, pp. 243-251.

Parker, S.J., D.J. Davies, and W.E. Smith, 1997. Geologic, Economic, and Environmental Characterization of Selected Near-term Leasable Offshore Sand Deposits and Competing Onshore Sources for Beach Nourishment. Geologic Survey of Alabama, Environmental Geology Division, Tuscaloosa, AL. Circular 190, 173 pp. + app.

Parker, S.J., D.J. Davies, W.E. Smith, T.G. Crawford, and R. Kelly, 1993. Geological, Economic, and Environmental Characterization of Selected Near-term Leasable Offshore Sand Deposits and Competing Onshore Sources for Beach Nourishment. Final Report. Prepared by the Geological Survey of Alabama in fulfillment of U.S. Department of the Interior, Minerals Management Service Cooperative Agreement No. 14-35-0001-30630, 223 pp.

Petrie, G., 1991. Modelling, interpolation and contouring procedures. In: Petrie, G. and Kennie, T.J.M. (editors), Terrain Modelling in Surveying and Civil Engineering, McGraw-Hill, Inc., New York, NY, p. 112-127.

Pilkey, O.H., R.S. Young, S.R. Riggs, A.W. Smith, H. Wu, and W.D. Pilkey, 1993. The concept of shoreface profile of equilibrium: a critical review. Journal of Coastal Research, 9: 255-278.

Reid, R.O., 1994. Preliminary Results of LATEX Relevant to the Proposed Study. Proceedings of the Northeast Gulf of Mexico Physical Oceanography Workshop, U.S. Department of the Interior, Minerals Management Service OCS Study 94-0044.

Resio, D.T., and B.A. Tracy, 1983. A Numerical Model for Wind-Wave Prediction in Deepwater. WIS Report 12, U.S. Army Engineer Waterways Experiment Station, Coastal Engineering Research Center, Wave Information Study, Vicksburg, MS.

Rosati, J.D., 2005. Concepts in sediment budgets. Journal of Coastal Research, 21(2): 307-322.

Rosati, J. D. and N.C. Kraus, 1999. Formulation of Sediment Budgets at Inlets. Coastal Engineering Technical Note CETN-IV-15 (Revised August 1999), U.S. Army Engineer Research and Development Center, Vicksburg, MS.

Sallenger, A.H., C.W. Wright, and J. Lillycrop, 2005. Coastal impacts of the 2004 hurricanes measured with airborne Lidar: initial results. Shore and Beach, 73(2/3): 10-15.

Sanchez, T.A. and S.L. Douglass, 1994. Alabama Shoreline Change Rates: 1970 – 1993. Final Report for the Coastal Programs Office, Alabama Department of Economic and community Affairs, Montgomery, AL, 16 p. plus Appendices.

Sapp, C.D., J.G. Emplaincourt, and J.D. Hardin, 1975. Remote sensing of shoreline dynamics, Mobile Bay area, 1900-1975. Gulf Coast Association of Geological Societies Transactions, 25: 153-167.

Sargent, F.E., 1988. Case Histories of Corps Breakwater and Jetty Structures, Report 2, South Atlantic Division, Perdido Pass Jetties. Technical Report REMR-CO-3, USAE Waterways Experiment Station, Coastal Engineering Research Center, Vicksburg, MS, p. 100-104.

Sawyer, W.B., C. Vaughan, D. Lavoie, Y. Furukawa, N. Carnaggio, J. Maclean, and E. Populis, 2001. Northern Gulf Littoral Initiative (NGLI), Geology and Physical Properties of Marine Sediments in the N.E. Gulf of Mexico: Data Repoort. Naval Oceanographic Office, Stennis Space Center, MS, 12 p.

Schramm, W.E., S. Penland, R.G. Gerdes, and D. Nummedal, 1980. Effects of Hurricane Fredric on Dauphin Island, Alabama. Shore and Beach, 48(3): 20-25.

Schroeder, W.W. and W. Wiseman, 1985. An analysis of the winds *1974-1984) and sea level elevations (1973-1983) in coastal Alabama. Mississippi-Alabama Sea Grant Publication MASGP-84-024.

Schroeder, W.W., S.P Dinnel, F.J. Kelly, W.J. Wiseman, 1994. Overview of the Physical Oceanography of the Louisiana-Mississippi-Alabama Continental Shelf. Proceedings of the Northeast Gulf of Mexico Physical Oceanography Workshop, U.S. Department of the Interior, Minerals Management Service OCS Study 94-0044.

Scott, A.J., R.A. Hoover, and J.H. McGowen, 1969. Effects of Hurricane Beulah, 1967 on Texas coastal lagoons and barriers. In: A.A Castanaras and F.B. Phleger (editors), Lagunas Costeras, un Simposio, pp. 221-236.

Seim, H. E., B. Kjerfve, and J.E. Sneed, 1987. Tides of Mississippi Sound and the adjacent continental shelf. Estuarine, Coastal and Shelf Science, 25: 143-156.

Shalowitz, A.L., 1964. Shoreline and Sea Boundaries, Volume 2. U.S. Department of Commerce Publication 10-1, U.S. Coast and Geodetic Survey, U.S. Government Printing Office, Washington, DC, 420 pp.

Sherrill, C.O., 1913. Mobile Harbor, AL. Professional Memoirs, Corps of Engineers, United States Army and Engineer Department at Large, Washington, DC, Vol. V, No. 19, p. 1-27.

Smith, J.M., D.T. Resio, and A.K. Zundel, 1999. STWAVE: Steady-State Spectral Wave Model. Instructional Report CHL-99-1, U.S. Army Engineering Waterways Experiment Station, Vicksburg, MS.

Smith, W.E., 1981. Geologic Features and Erosion Control in Alabama Gulf Coastal Area. Geological Survey of Alabama Information Series 57, 57 pp.

Smith, W.E., 1988. Geomorphology of the Mobile Delta. Alabama Geological Survey Bulletin 132, 133 p.

Smith, W.E., 1990. Regimes contributory to progressive loss of Alabama coastal shoreline and wetlands. Gulf Coast Association of Geological Societies Transactions, 40: 793-796.

Stone, G.W. and P. Wang, 1999. The importance of cyclogenesis on the short-term evolution of Gulf Coast barriers. Gulf Coast Association of Geological Societies Transactions, 49: 478-486.

Stone, G.W., F.W. Stapor, J.P. May, and J.P. Morgan, 1992. Multiple sediment sources and a cellular, non-integrated, longshore drift system: northwest Florida and southeast Alabama coast, USA. Marine Geology, 105: 141-154.

Stone, G.W., B. Liu, D.A. Pepper, and P. Wang, 2004. The importance of extratropical and tropical cyclones on the short-term evolution of barrier islands along the northern Gulf of Mexico, USA. Marine Geology, 210: 63-78.

Stumpf, R.P., and G. Gelfenbaum, 1990. Effects of high river discharge on suspended sediments in Mobile Bay, Alabama. EOS, 71: 1,406-1,407.

Stumpf, R.P., G. Gelfenbaum, J.R. Pennock, 1993. Wind and tidal forcing of a buoyant plume, Mobile Bay, Alabama. Continental Shelf Research, 13(11): 1281-1301.

Swift, D.J.P. and A.W. Niedoroda, 1985. Fluid and Sediment Dynamics on Continental Shelves. In: Tillman, R.W., D.J.P. Swift, and R.G. Walker (editors), Shelf Sands and Sandstone Reservoirs, SEPM Short Course No. 13, Tulsa, OK, pp. 47-133.

Tannehill, I.R., 1956. Hurricanes, their nature and history. Princeton University Press, 308 p.

Todd, T.W., 1968. Dynamic diversion: influence of longshore current-tidal flow interaction on chenier and barrier island plains. Journal of Sedimentary Petrology, 38: 734-746.

Tracy, B. A., 1999. Directional Characteristics of the 1990-1999 Wave Information Studies. Gulf of Mexico Hindcast. Ft. Belvoir, Defense Technical Information Center. http://handle.dtic.mil/100.2/ADA423403.

Tracy, B.A. and A. Cialone, 2004. Comparison Of Gulf Of Mexico Wave Information Studies (WIS) 2-G Hindcast With 3-G Hindcasting. Engineer Research and Development Center, Coastal and Hydraulics Laboratory, Waterways Experiment Station, Vicksburg, Mississippi, USA.

USACE, 1955. Perdido Pass (Alabama Point) Alabama Beach Erosion Control Study. U.S. Army Corps of Engineers, Mobile District, Mobile, AL.

USACE, 1978. Feasibility Report for Beach Erosion Control and Hurricane Protection, Mobile County, Alabama (Including Dauphin Island). U.S. Army Corps of Engineers, Mobile District, Mobile, AL, 142 pp. plus Attachments.

USACE, 1984. Exploration and Production of Hydrocarbon Resources in Coastal Alabama and Mississippi. U.S. Army Corps of Engineers, Mobile District, Mobile, AL, 615 pp.

USGS, 2007. Real-Time Water Data for the Nation. US Geological Survey Station 02471019, Tensaw River near Mount Vernon, AL and USGS Station 02470629, Mobile River at River Mile 31 at Bucks, AL. http://waterdata.usgs.gov/usa/nwis/uv?

Walton, T. L., 1974. Calculation of Littoral Drift Roses for the Alabama and Mississippi Gulf Coastline. Coastal and Oceanographic Engineering Department, University of Florida, Gainesville, FL, UFL/COEL-74-023, 26 p.

Westerink, J.J., C.A. Blain, R.A. Luettich, and N.W. Scheffner, 1994. ADCIRC: An Advanced Three-Dimensional Circulation Model for Shelves, Coasts and Estuaries; Report 2: Users Manual for ADCIRC-2DDI. Dredging Research Program Technical Report, U.S. Army Engineers Waterways Experiment Station, Vicksburg, MS., 156 pp.

Wilson, W.K., 1951. Beach erosion problems in the Mobile District. Shore and Beach, 19(2): 8-10.

Wiseman, W.J., W.W. Schroeder, and S.P. Dinnel, 1988. Shelf-estuarine water exchanges between the Gulf of Mexico and Mobile Bay, Alabama. American Fisheries Society Symposium, 3: 1-8.

Report Appendices

Appendix A

Gulf and Atlantic Hurricane Tracks: 1851 to 2005; Category 3 or Stronger

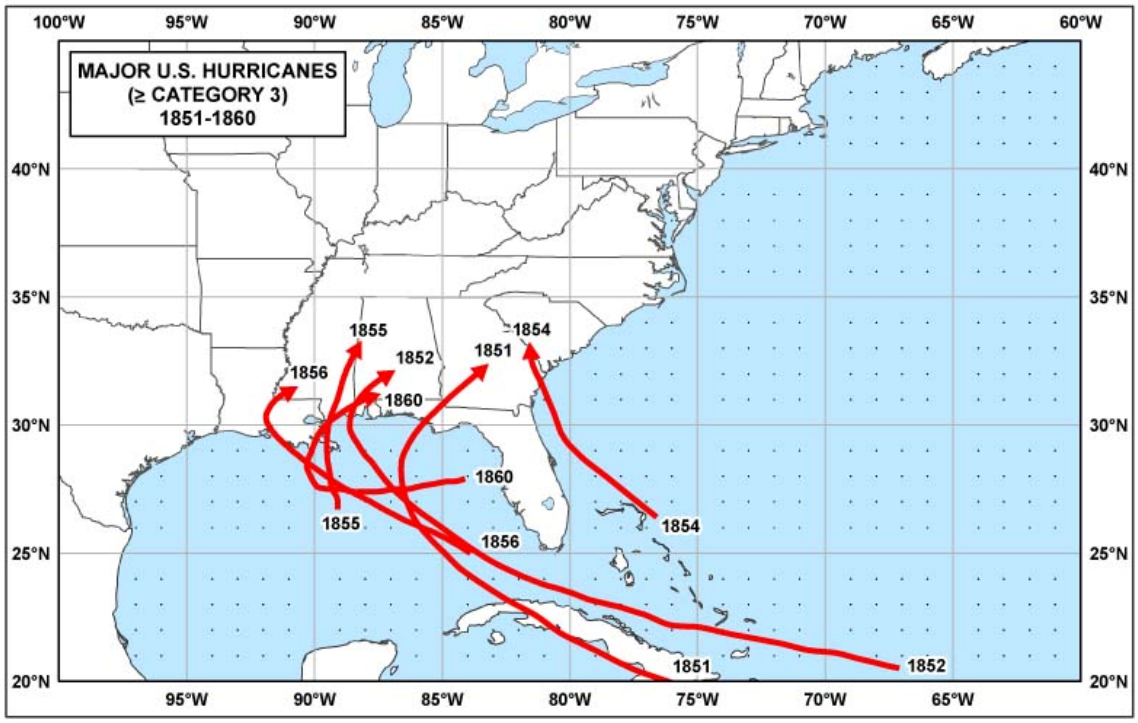

Figure A1. Hurricanes stronger than or equal to category 3 for the Gulf and Atlantic coasts – 1851 to 1860 (Blake et al., 2005).

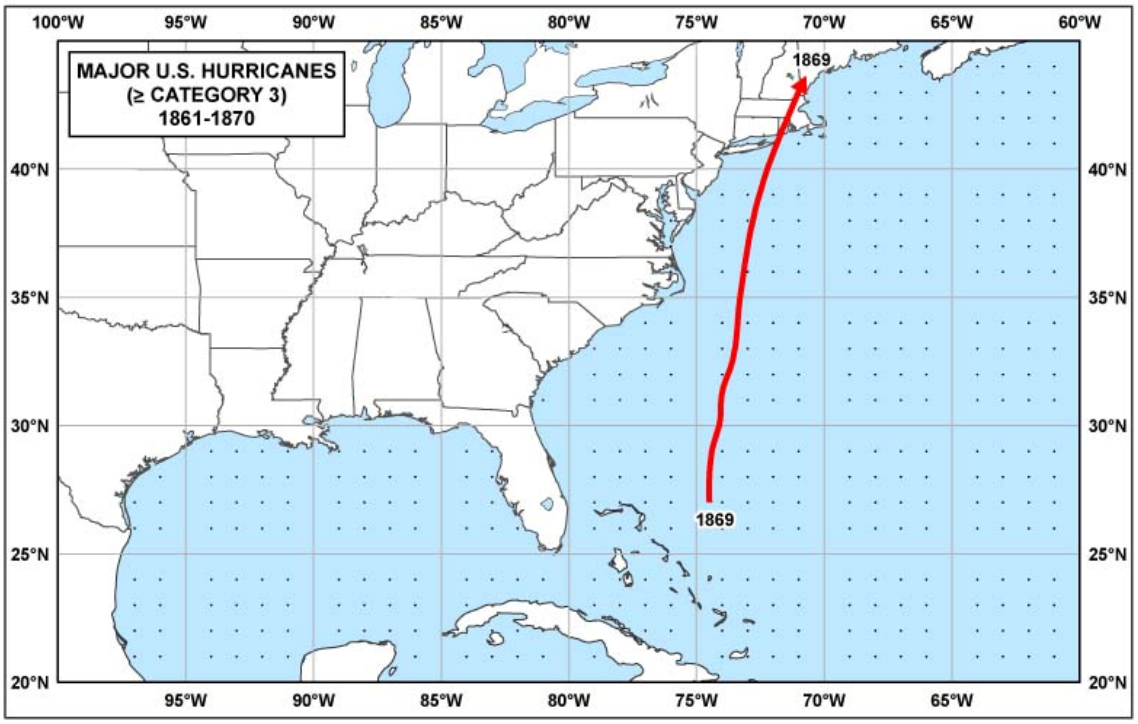

Figure A2. Hurricanes stronger than or equal to category 3 for the Gulf and Atlantic coasts – 1861 to 1870 (Blake et al., 2005).

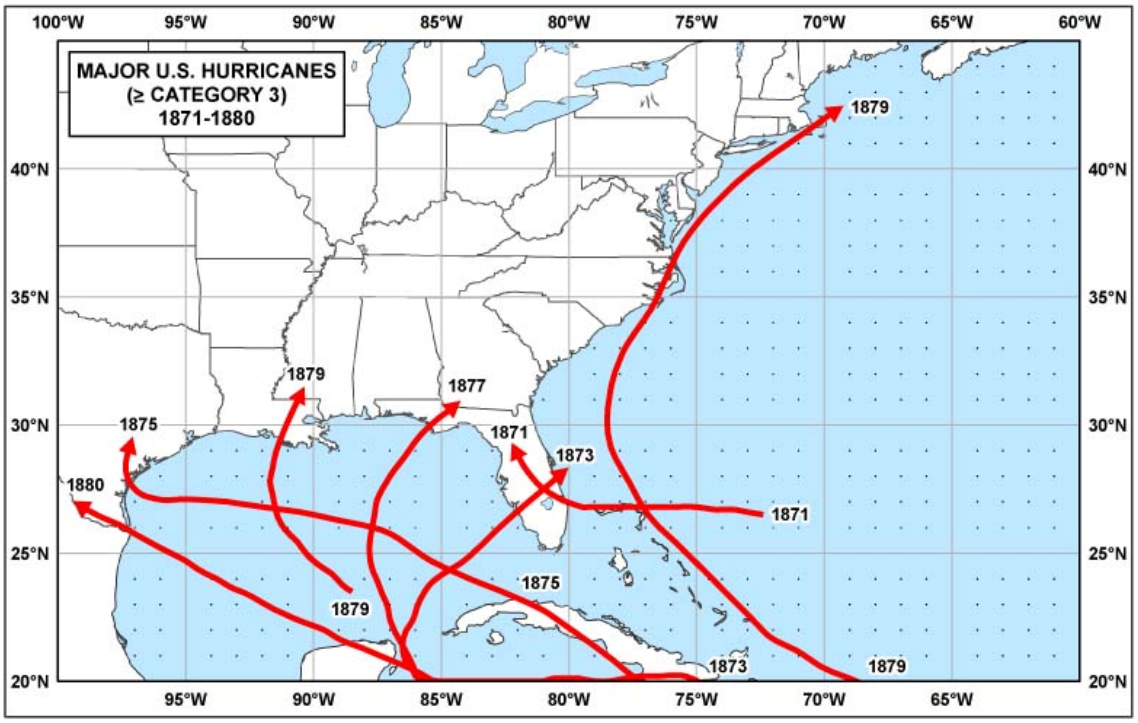

Figure A3. Hurricanes stronger than or equal to category 3 for the Gulf and Atlantic coasts – 1871 to 1880 (Blake et al., 2005).

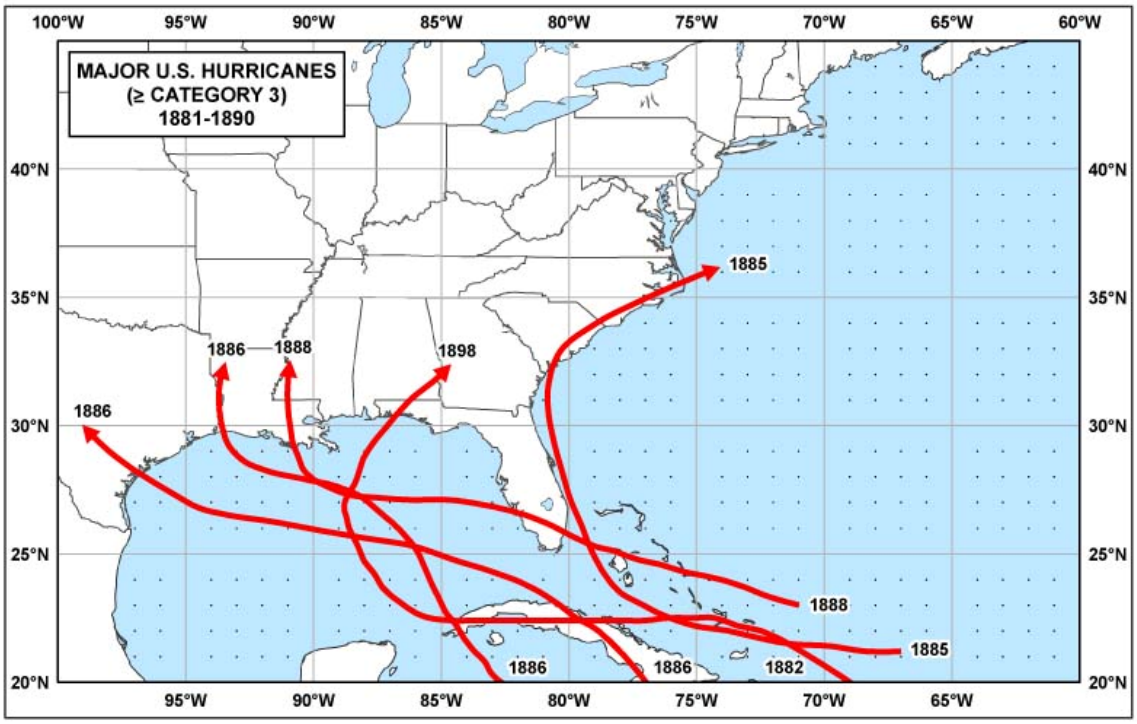

Figure A4. Hurricanes stronger than or equal to category 3 for the Gulf and Atlantic coasts – 1881 to 1890 (Blake et al., 2005).

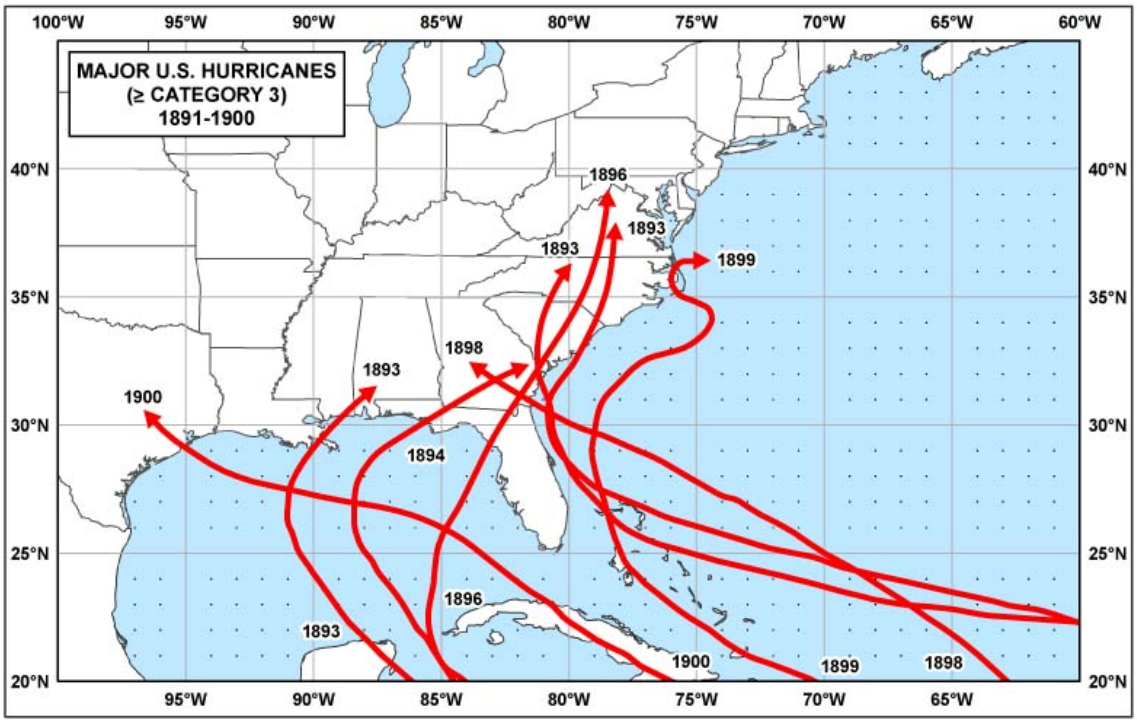

Figure A5. Hurricanes stronger than or equal to category 3 for the Gulf and Atlantic coasts – 1891 to 1900 (Blake et al., 2005).

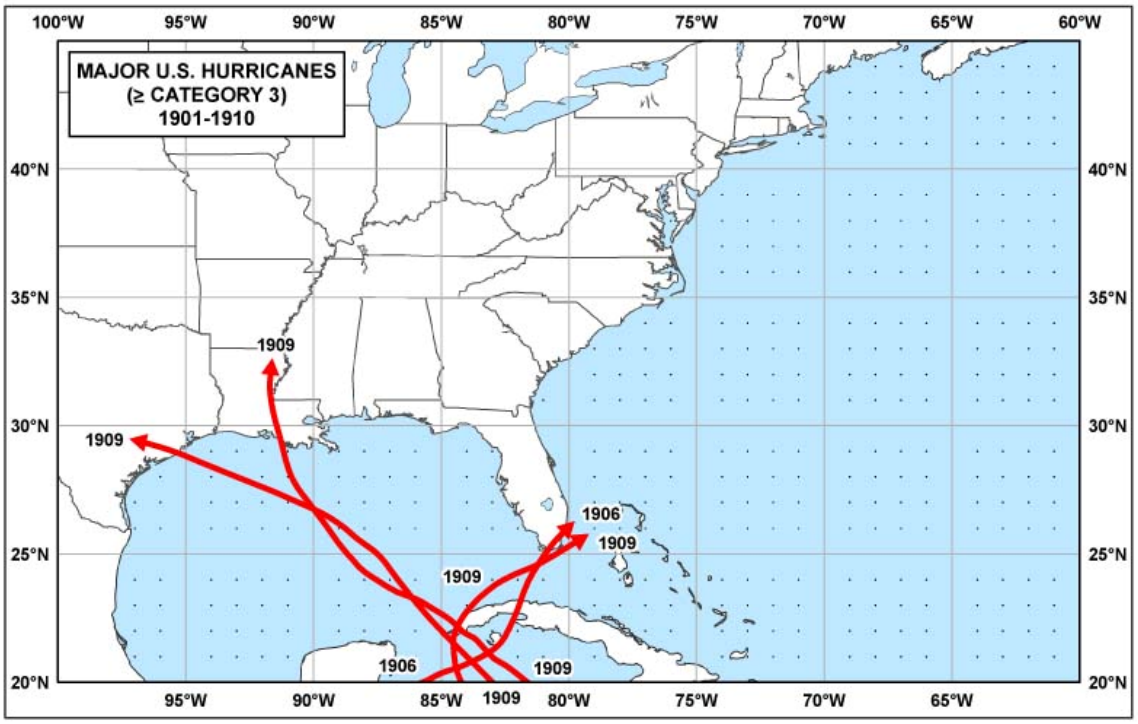

Figure A6. Hurricanes stronger than or equal to category 3 for the Gulf and Atlantic coasts – 1901 to 1910 (Blake et al., 2005).

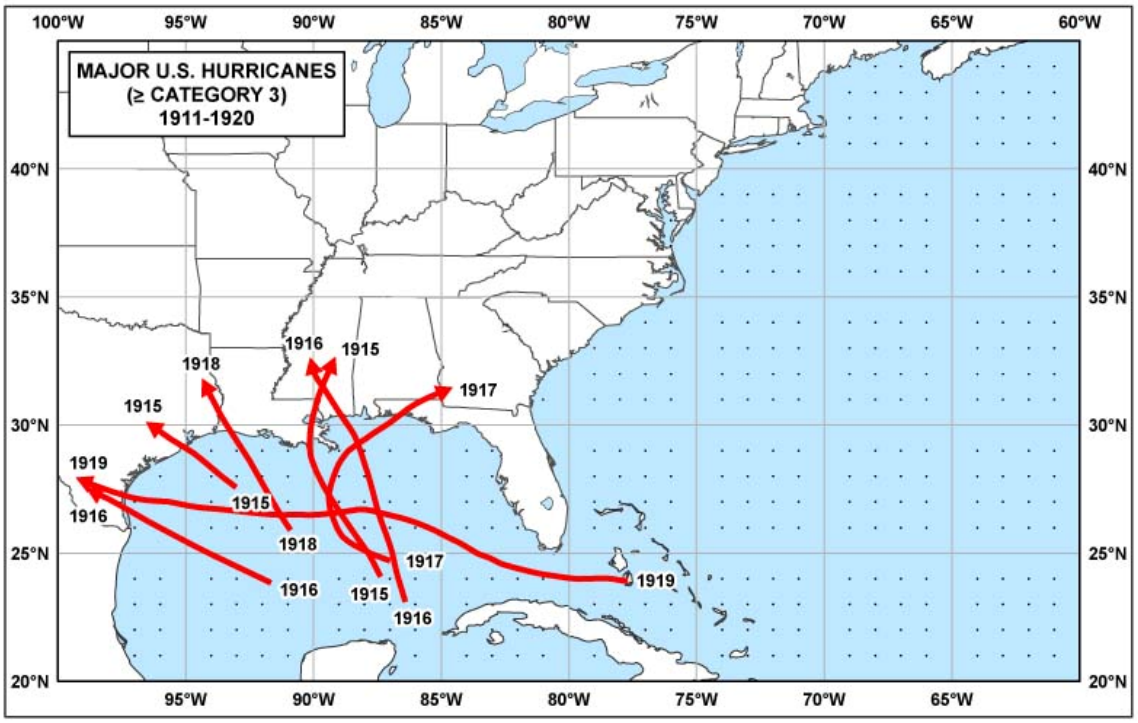

Figure A7. Hurricanes stronger than or equal to category 3 for the Gulf and Atlantic coasts – 1911 to 1920 (Blake et al., 2005).

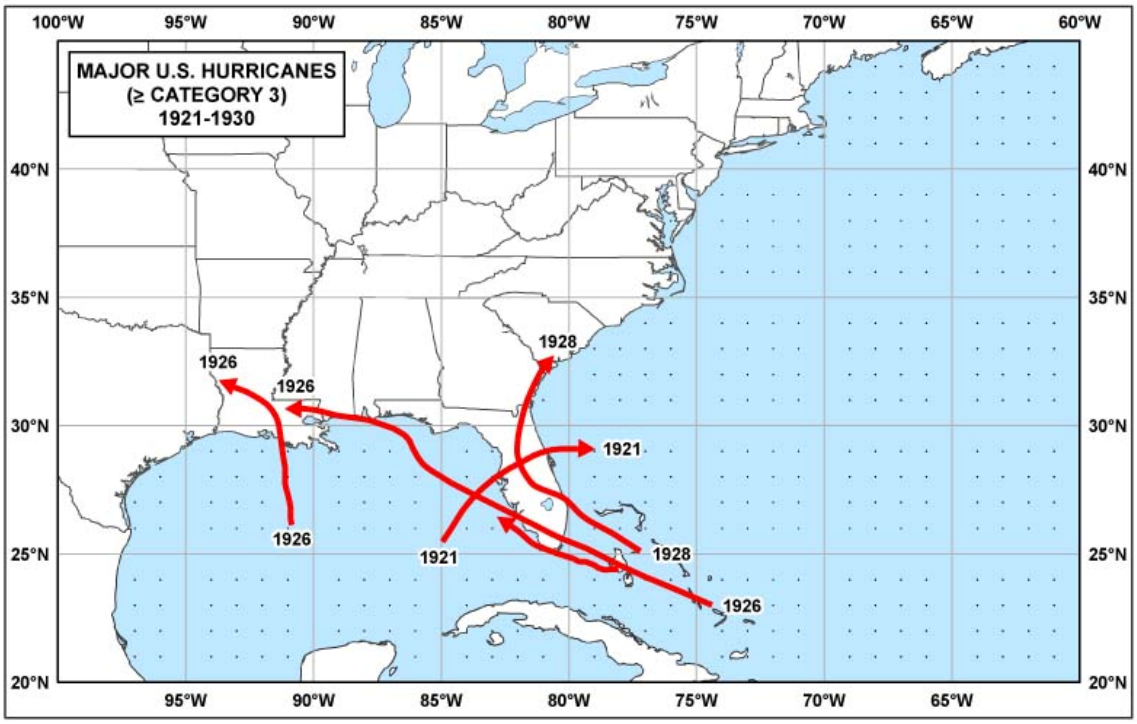

Figure A8. Hurricanes stronger than or equal to category 3 for the Gulf and Atlantic coasts – 1921 to 1930 (Blake et al., 2005).

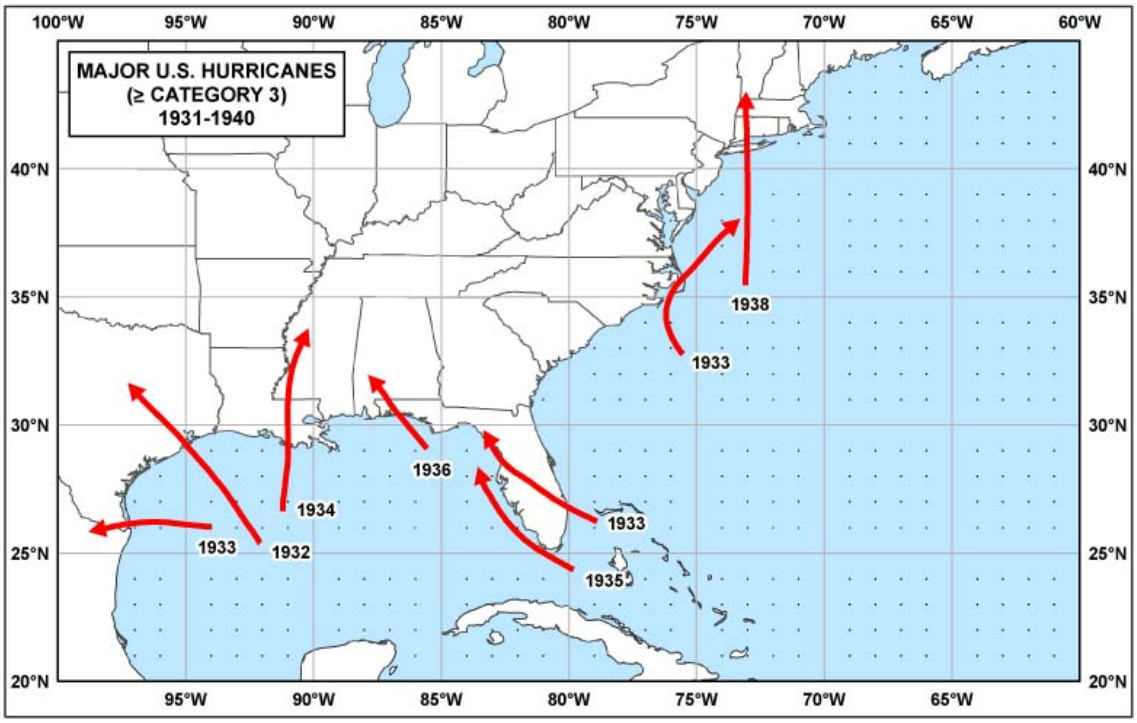

Figure A9. Hurricanes stronger than or equal to category 3 for the Gulf and Atlantic coasts – 1931 to 1940 (Blake et al., 2005).

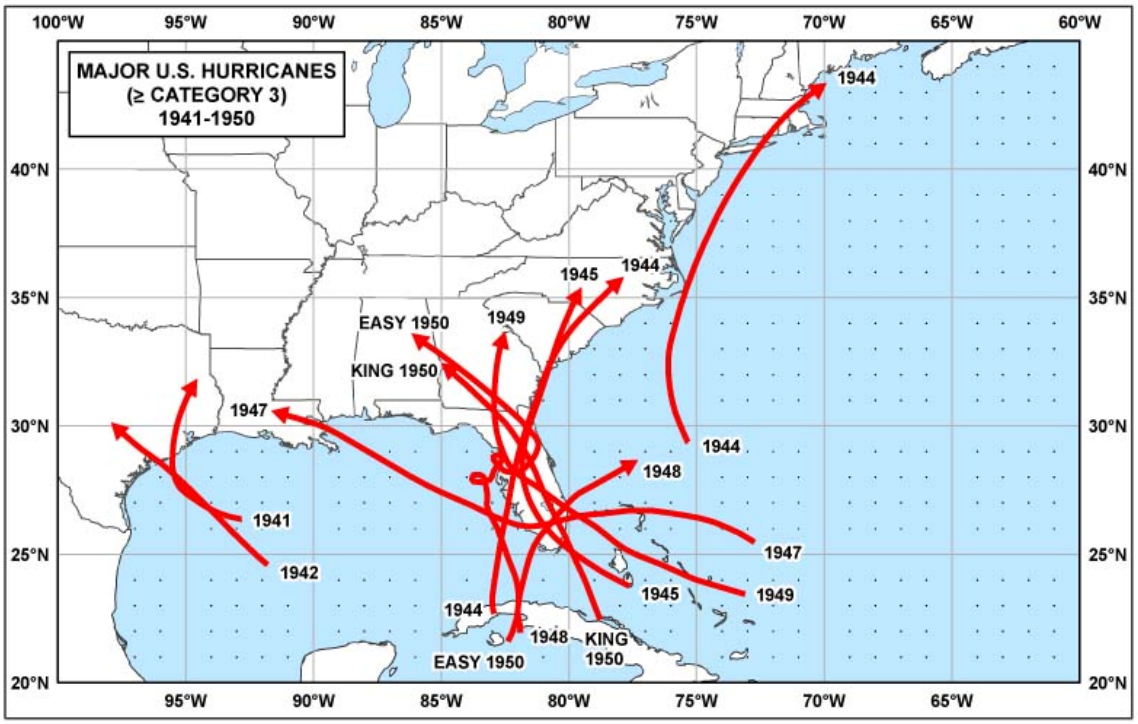

Figure A10. Hurricanes stronger than or equal to category 3 for the Gulf and Atlantic coasts – 1941 to 1950 (Blake et al., 2005).

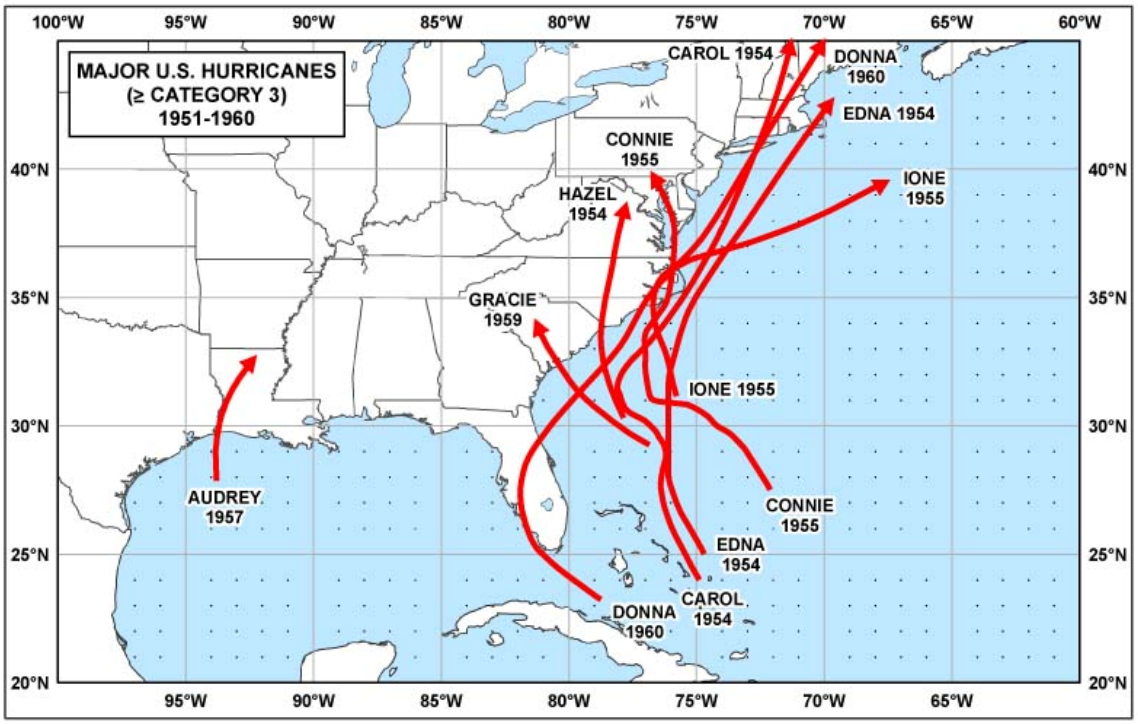

Figure A11. Hurricanes stronger than or equal to category 3 for the Gulf and Atlantic coasts – 1951 to 1960 (Blake et al., 2005).

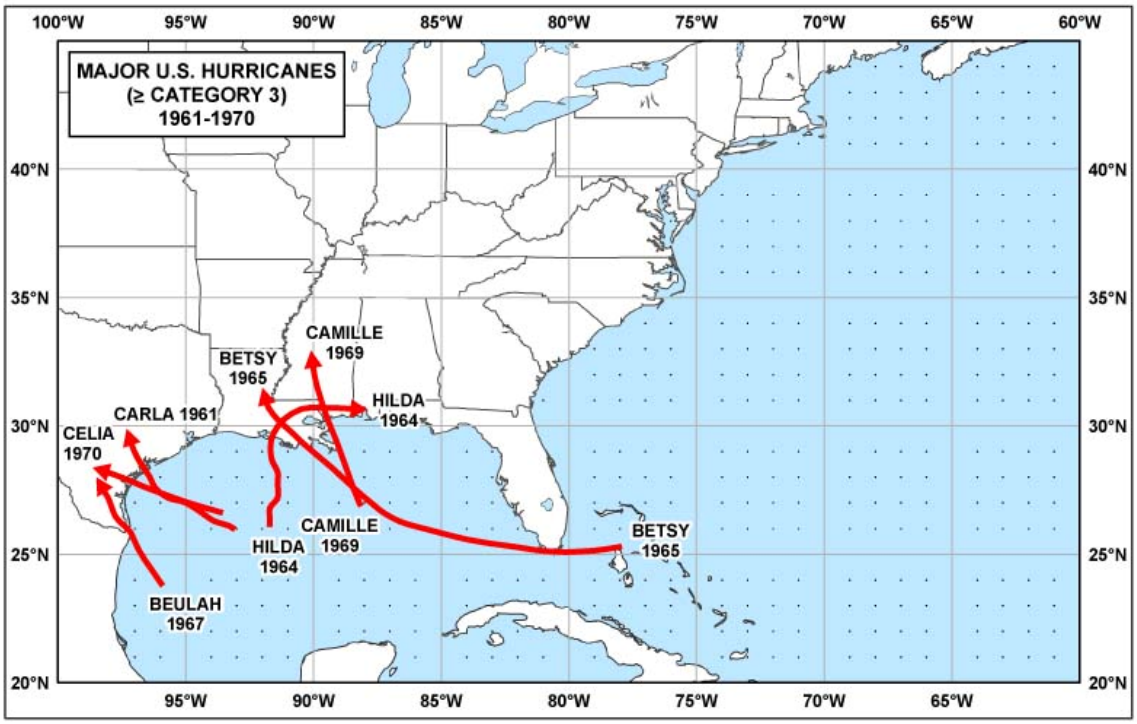

Figure A12.Hurricanes stronger than or equal to category 3 for the Gulf and Atlantic coasts – 1961 to 1970 (Blake et al., 2005).

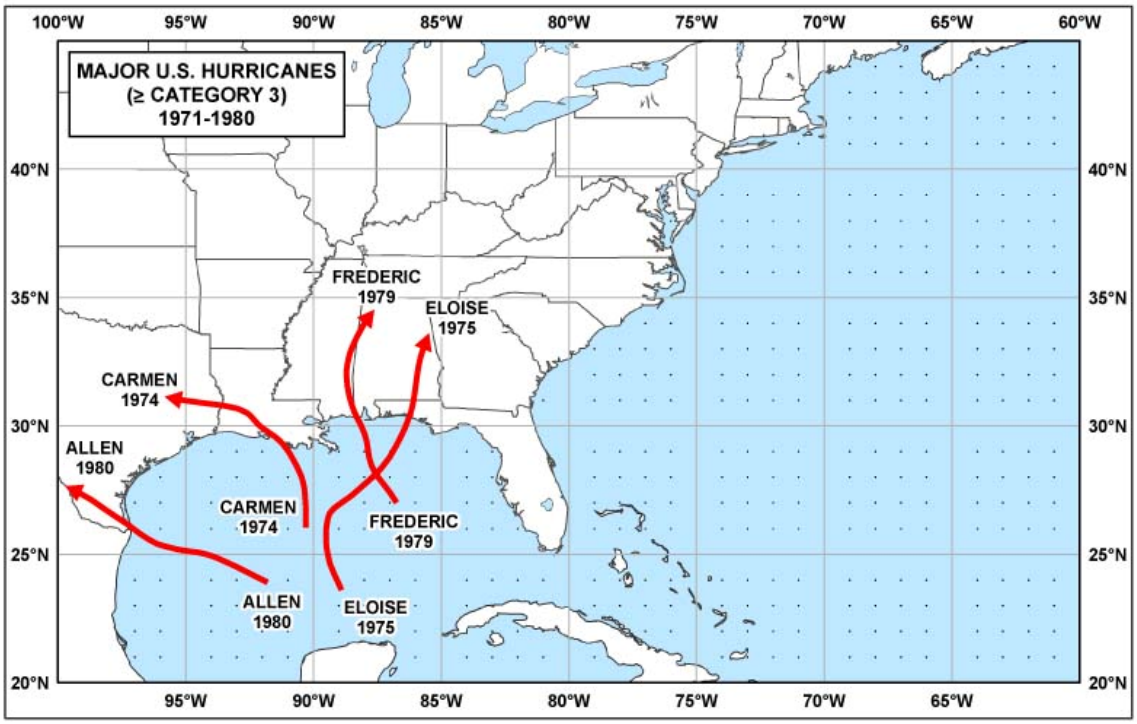

Figure A13.Hurricanes stronger than or equal to category 3 for the Gulf and Atlantic coasts – 1971 to 1980 (Blake et al., 2005).

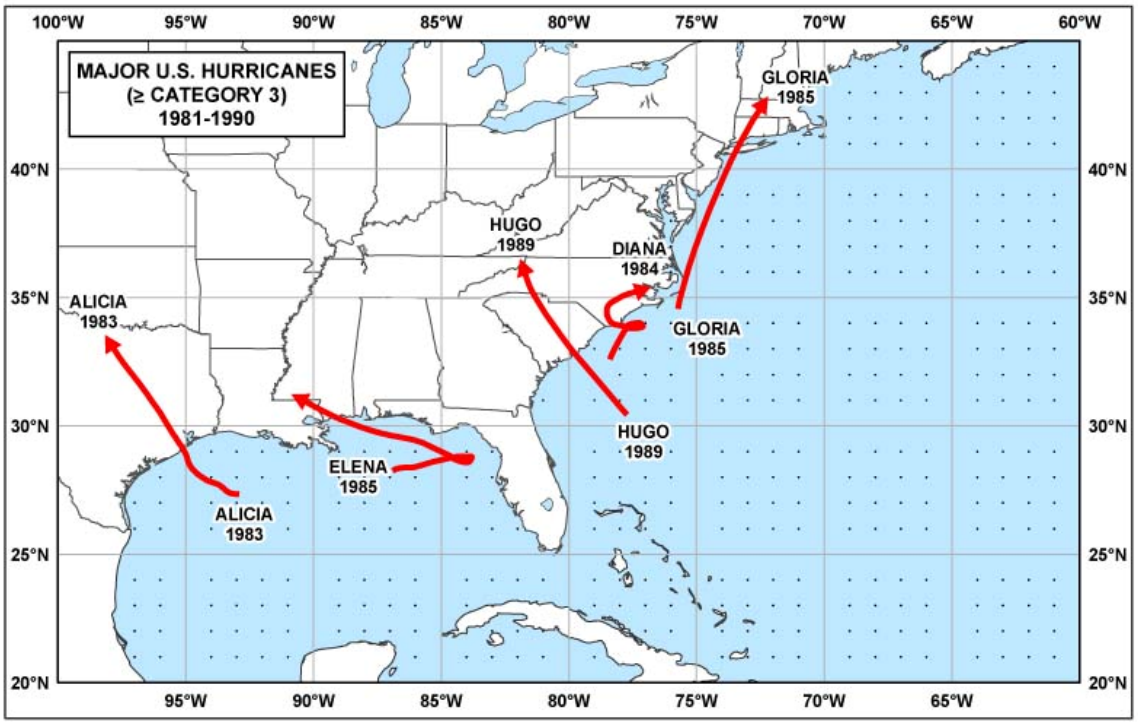

Figure A14. Hurricanes stronger than or equal to category 3 for the Gulf and Atlantic coasts – 1981 to 1990 (Blake et al., 2005).

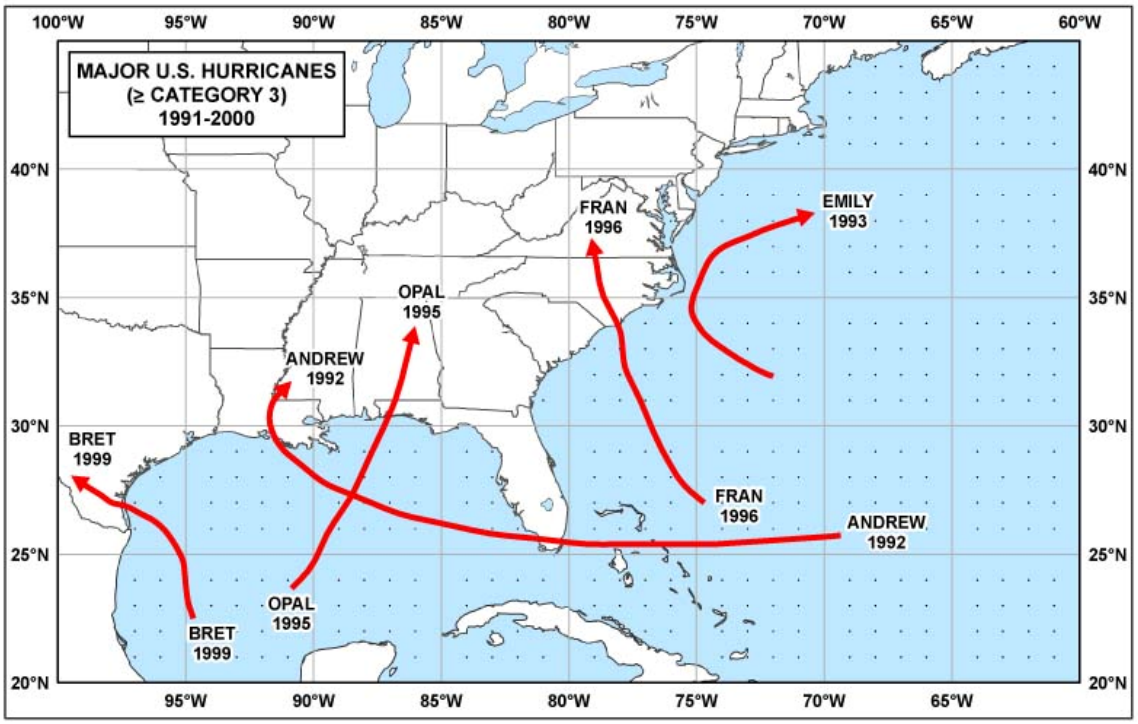

Figure A15.Hurricanes stronger than or equal to category 3 for the Gulf and Atlantic coasts – 1991 to 2000 (Blake et al., 2005).

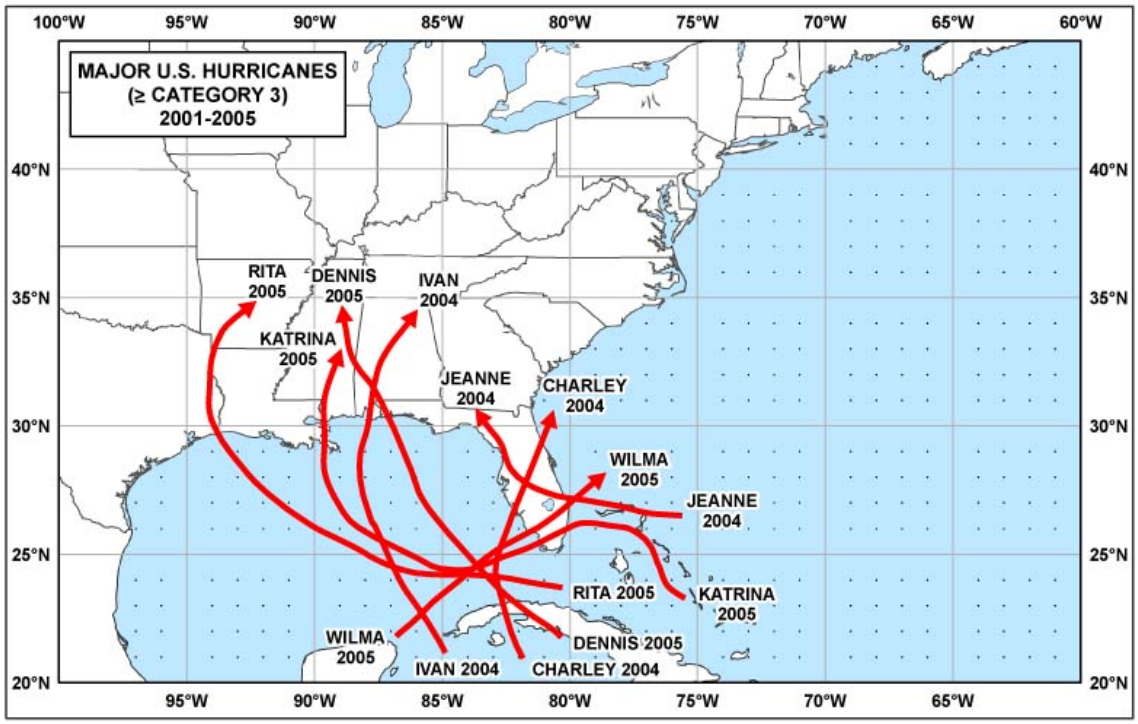

Figure A16. Hurricanes stronger than or equal to category 3 for the Gulf and Atlantic coasts – 2000 to 2005 (Blake et al., 2005).

Appendix B

Dredging History for the Mobile Outer Bar: 1902 to 2006

Dredging History for the Mobile Outer Bar: 1902 to 2006					
Date	**Authority**	**Description**	**New Work (cy)**	**Maintenance (cy)**	**Source**
June 30, 1896		"… in Pickett's History of Alabama it is stated that on February 18, 1702, Iberville found 20 feet over the outer bar."			ARCE, 1896; p. 1426
April 1902		"… detailed survey, including triangulation, to determine the present condition of the ship channel within the limits of the project …"			ARCE, 1902; p. 1282
June 13, 1902	River and Harbor Act	"… the Secretary of War may, in his discretion, expend a sum not to exceed fifty thousand dollars in deepening and widening the channel through the outer bar near Fort Morgan." The original condition of the channel was a minimum usable depth of 23 ft MLW over a distance of about 0.5 mile across the bar.			ARCE, 1902; p. 1282
June 30, 1903		"The work of widening and deepening the channel through the outer bar near Fort Morgan … has not yet commenced as suitable plant for this work could not be obtained."			ARCE, 1903; p. 1238
August 22, 1903		Contract signed between Mr. Rittenhouse Moore (Mobile, AL; the only bidder) and the District to dredge the outer bar channel near Fort Morgan at a rate of 30 cents per cubic yard bin measurement.			ARCE, 1904; p. 1805
October 2, 1903		Work commenced on deepening and widening the channel through the outer bar near Fort Morgan.			ARCE, 1904; p. 1805
November 10, 1903		Contractor's dredge *Jumbo* sank and proved a total loss.			ARCE, 1904; p. 1805
May 16 to June 30, 1904		Dredging commenced and by June 30, a minimum depth on the lighthouse range through the channel to be improved was 25 ft; dredged material was placed in deep water in the Gulf of Mexico.	100,433		ARCE, 1904; p. 1805
July 1 to 20, 1904		Dredging continued through the Mobile bar channel which resulted in a 225- to 250-ft wide channel with a minimum depth of 27 ft.	43,697		ARCE, 1905; p. 1399
March 3, 1905	River and Harbor Act	Made a separate project of the Mobile bar work.			ARCE, 1905; p. 1399
June 15, 1905		Proposals for deepening and widening the existing channel through the Mobile Outer Bar to 30 ft deep and 300 ft wide were opened; awarded to Southern Dredging Company.			ARCE, 1905; p. 1399
August 23, 1905 to May 12, 1906		Dredging operations continued when weather would permit, securing a channel 27- to 30-ft deep with a width 250 to 275 ft.	144,412		ARCE, 1906; p. 1271
July 1, 1906 to June 30, 1907		No dredging work was completed during this fiscal year. "The storm of September, 1906, changed the configuration of the bottom at the entrance to Mobile Bay, but seems not to have affected materially the depth of the dredged channel.			ARCE, 1907; p. 1371
July 1, 1907 to June 30, 1908		The U.S. dredge *Charleston* was dredging the channel most of the year. Most of the bar channel was deepened to 30 ft or more.	185,683		ARCE, 1908; p. 1427
July 1, 1908 to June 30, 1909		Maximum channel depth at the beginning of the year was about 27.5 ft – shoals were in the channel. The dredge *Charleston* removed shoals from the channel and increased the depth to between 30 and 35 ft. Dredged volume missing from Annual Report; value derived from dredged totals listed in the table on page 5 of Professional Memoirs, Corps of Engineers, v. 5, no. 19, January-February, 1913.		198,279	ARCE, 1909; p. 1412
July, 1909 and January 25 to April 20, 1910		The dredge *Charleston* removed shoals that formed in the dredged channel to maintain a project channel depth of 30 ft.		121,640	ARCE, 1910; p. 1559
August 9 to 24, 1910		The dredge *Charleston* worked in the outer bar channel removing shoals from the previously dredge channel and deepening unfinished parts.		32,184	ARCE, 1911; p. 1701
April 22 to June 30, 1912		The dredge *Charleston* worked in the outer bar channel removing shoals from the previously dredge channel.		63,852	ARCE, 1912; p. 1921
July 1, 1912 to June 30, 1913		The U.S. dredge *Charleston* worked on the Mobile Bar Channel during the entire fiscal year when weather permitted. Maintenance work accounted for about 34% of total dredging.		113,772	ARCE, 1913; p. 2142
July 1, 1912 to June 30, 1913		The total amount of sand removed from the channel was 332,190 cy, which involved 218,418 cy of new work to relocate the channel 700 ft west of its previous location. "This change was necessitated by the fact that the channel was naturally shifting in this direction and shoals were forming from the east more rapidly than the dredge could remove them."	218,418		ARCE, 1913; p. 2142
July 10 to October 31, 1913		Dredging work resulted in the completion of the channel through the Mobile Outer Bar to its full project dimensions (30 ft deep and 300 ft wide).	94,661		ARCE, 1914; p. 2187
May 16, 1904 to October 13, 1913	**1905 River and Harbor Act**	**Total dredging upon completion of a channel through the Mobile Outer Bar to a depth of 30 ft MLW and a width of 300 ft.**	**787,304**	**529,727**	
December 31, 1914 to January 30, 1915		The U.S. dredge *Caucus* (rented from the Montgomery, AL District) work on the Mobile Bar to remove all shoals from the channel.		58,418	ARCE, 1915; p. 2530

Dredging History for the Mobile Outer Bar: 1902 to 2006					
Date	**Authority**	**Description**	**New Work (cy)**	**Maintenance (cy)**	**Source**
July 1, 1915 to June 30, 1916		No dredging was done in the Mobile Outer Bar channel during the fiscal year.			ARCE, 1916; p. 2381
July 1, 1916 to June 30, 1917		The channel across the bar was maintained by dredging between the 30-ft contours at the outer and inner end of the bar. Under ordinary conditions, mean tide range over the bar was 1.1 ft; extreme tide rage was 3.4 ft.		144,099	ARCE, 1917; p. 833
August 8, 1917	River and Harbor Act	New project dimension approved for the Mobile Outer Bar channel include 33 ft deep at MLW and 450 ft wide for a length of about 1 mile, connecting the 33-ft contours south and north of the bar.			ARCE, 1917; p. 833
July 1, 1917 to June 30, 1918		All work was for maintenance of dimensions of the previous project (30-ft deep by 300-ft wide channel). "The channel across the bar was maintained by dredging between the 30-ft contours at the outer and inner end of the bar."		177,925	ARCE, 1918; p. 866
July 1, 1918 to June 30, 1919		All work was for maintenance of dimensions of the previous project (30-ft deep by 300-ft wide channel). "No new work has been done on Mobile Bar under the existing project …"		143,746	ARCE, 1919; p. 913
September 29, 1919 to June 30, 1920		The U.S. dredge *Charleston* was used for new and maintenance work in the bar channel. Work on the new outer bar project dimension was initiated on October 13, 1919.	201,368	4,521	ARCE, 1920; p. 2356
December 4, 1919		New Mobile Outer Bar channel location approved.			ARCE, 1921; p. 883
July 1, 1920 to June 30 1921		New work consisted of relocating the existing bar channel.	188,971		ARCE, 1921; p. 882
July 1, 1921 to June 30, 1922		Maintenance work along the Mobile Outer Bar Channel focused on maintaining a channel depth of 30 ft MLW.		60,041	ARCE, 1922; p. 908
July 1, 1922 to June 30, 1923		For new work in the Outer Bar Channel, "… an average depth of 32 feet has been obtained over the project width of 450 feet and the project depth of 33 feet over about one-half the project width along the center line of the channel."	310,989	62,486	ARCE, 1923; p. 785-786
July 1, 1923 to June 30, 1924		New work in the Outer Bar Channel resulted in completion of the channel to project dimensions (33-ft MLW depth and 450-ft wide). Work completed by the U.S. dredge *Charleston*.	377,098		ARCE, 1924; p. 780-781
July 1, 1924 to June 30, 1925		"In the Outer Bar Channel the project dimensions have been obtained." No dredging was done in the Mobile Outer Bar channel during the fiscal year.			ARCE, 1925; p. 762-763
May 16, 1904 to June 30, 1925	**1917 River and Harbor Act**	**Total dredging upon completion of a channel through the Mobile Outer Bar to a depth of 33 ft MLW and a width of 450 ft.**	**1,865,730**	**1,180,963**	
July 1, 1925 to June 30, 1926		The seagoing dredge *Benyaurd* was operated 1¼ months in the Mobile Outer Bar Channel to restore project depth and width.		398,680	ARCE, 1926; p. 769
July 1, 1926 to June 30, 1927		No dredging was done in the Mobile Outer Bar channel during the fiscal year.			ARCE, 1927; p. 798
July 1, 1927 to June 30, 1928		No distinction was made between total maintenance dredging for the entire channel and dredging in the Outer Bar Channel. As such, the reported maintenance dredging quantity for the Outer Bar Channel was estimated based on the previous quantity (for a 2 year period) reported in 1926.		199,340	ARCE, 1928; p. 833
July 1, 1928 to June 30, 1929		No dredging was done in the Mobile Outer Bar channel during the fiscal year.			ARCE, 1929; p. 835
July 1, 1929 to June 30, 1930		No dredging was done in the Mobile Outer Bar channel during the fiscal year.			ARCE, 1930; p. 903
July 3, 1930	River and Harbor Act	New project "… provides for a channel across the Mobile Bar 36 feet deep at mean low water and 450 feet wide, and about 1 mile long, connecting the 36-foot contours south and north of the bar …"			ARCE, 1931; p. 900
July 1, 1930 to June 30, 1931		Dredging was completed in the channel to maintain existing project dimensions (33-ft deep channel, 450-ft wide) and begin work on the new project. No distinction was made between maintenance dredging and new work; however, the statement "work remaining to be done to complete the project is the dredging of the Outer Bar Channel to a width of 450 feet and depth of 36 feet" suggests that new work was started. As such, previous maintenance dredging quantities were used to estimate new versus maintenance dredging volumes for FY1931. Dredging was completed by the U.S. hopper dredge *Benyuard*.	347,741	598,020	ARCE, 1931; p. 901-902
July 1, 1931 to June 30, 1932		No dredging was done in the Mobile Outer Bar channel during the fiscal year.			ARCE, 1932; p. 802-803
July 1, 1932 to June 30, 1933		No dredging was done in the Mobile Outer Bar channel during the fiscal year.			ARCE, 1933; p. 482-483
May 7 to June 30, 1934		The U.S hopper dredge *Benyuard* dredged the Outer Bar Channel to a controlling depth of 34 ft. No distinction between new work and maintenance dredging was made,		816,571	ARCE, 1934; p. 565

Dredging History for the Mobile Outer Bar: 1902 to 2006					
Date	**Authority**	**Description**	**New Work (cy)**	**Maintenance (cy)**	**Source**
		except to state that the channel is now 1 ft deeper than the previous project depth. As such, all dredged sediment was considered maintenance, although some of it would have been new work. Work remaining to complete the project consisted of dredging the Outer Bar Channel to a width of 450 ft and a depth of 36 ft MLW.			
July 16 to August 3, 1934		The U.S hopper dredge *Benyuard* dredged the Outer Bar Channel to a depth of 36 ft MLW and a width of 450 ft. All dredging was new work. The 1930 River and Harbor Act Outer Bar Channel project dimensions were completed. As of June 30, 1935, the channel controlling depth was 36 ft MLW.	337,430		ARCE, 1935; p. 657
May 16, 1904 to June 30, 1935	**1930 River and Harbor Act**	**Total dredging upon completion of a channel through the Mobile Outer Bar to a depth of 36 ft MLW and a width of 450 ft.**	**2,550,901**	**3,193,574**	
October 21 to December 6, 1935		The U.S hopper dredge *Benyuard* dredged the Outer Bar Channel to maintain a controlling depth of 36 ft MLW and a width of 450 ft. All dredging was maintenance work.		690,196	ARCE, 1936; p. 637
July 1, 1936 to June 30, 1937		No dredging was done in the Mobile Outer Bar channel during the fiscal year.			ARCE, 1937; p. 678
August 5-13, September 18-29, October 1-13, 1937		The U.S hopper dredge *Benyuard* dredged the Outer Bar Channel to maintain a controlling depth of 36 ft MLW and a width of 450 ft. All dredging was maintenance work.		451,085	ARCE, 1938; p. 720
May 27 to June 27, 1939		The U.S hopper dredge *Manhattan* dredged the Outer Bar Channel to maintain a controlling depth of 36 ft MLW and a width of 450 ft. All dredging was maintenance work.		455,062	ARCE, 1939; p. 797
August 10 to September 8, 1939		The U.S hopper dredge *Benyuard* dredged the Outer Bar Channel to maintain a controlling depth of 36 ft MLW and a width of 450 ft. All dredging was maintenance work.		335,816	ARCE, 1940; p. 790
August 23 to October 15, 1940		The U.S hopper dredge *Benyuard* dredged the Outer Bar Channel to maintain a controlling depth of 36 ft MLW and a width of 450 ft. All dredging was maintenance work.		600,656	ARCE, 1941; p. 754
August 7 to September 7, 1941		The U.S hopper dredge *Benyuard* dredged the Outer Bar Channel to maintain a controlling depth of 36 ft MLW and a width of 450 ft. All dredging was maintenance work.		350,067	ARCE, 1942; p. 667
May 29 to June 30, 1943		The U.S hopper dredge *Benyuard* dredged the Outer Bar Channel to maintain a controlling depth of 36 ft MLW and a width of 450 ft. All dredging was maintenance work.		386,634	ARCE, 1943; p. 599
July 1, 1943 to June 30, 1944		No dredging was done in the Mobile Outer Bar Channel during the fiscal year.			ARCE, 1944; p. 586
December 27, 1944 to January 28, 1945		The U.S hopper dredge *Benyuard* dredged the Outer Bar Channel to maintain a controlling depth of 36 ft MLW and a width of 450 ft. All dredging was maintenance work.		226,000	ARCE, 1945; p. 826
July 1, 1945 to June 30, 1946		No dredging was done in the Mobile Outer Bar Channel during the fiscal year.			ARCE, 1946; p. 891
July 1, 1946 to June 30, 1947		No dredging was done in the Mobile Outer Bar Channel during the fiscal year.			ARCE, 1947; p. 874
December 26, 1947 to February 7, 1948		The U.S hopper dredge *Lyman* dredged the Outer Bar Channel to maintain a controlling depth of 36 ft MLW and a width of 450 ft. All dredging was maintenance work.		385,200	ARCE, 1948; p. 969-970
June 16-19, 1949		The U.S hopper dredge *Langfitt* dredged a small portion of the Outer Bar Channel. The controlling depth throughout the channel as of June 1949 was 35 ft MLW. All dredging was maintenance work.		78,361	ARCE, 1949; p. 872
April 30 to June 10, 1950		The U.S hopper dredge *Hyde* dredged the Outer Bar Channel to maintain a controlling depth of 36 ft MLW and a width of 450 ft. The controlling depth throughout the channel as of May 1950 was 36 ft MLW. All dredging was maintenance work.		475,004	ARCE, 1950; p. 880-881
July 1, 1950 to June 30, 1951		No dredging was done in the Mobile Outer Bar Channel during the fiscal year.			ARCE, 1951; p. 713
May 16-29, 1952		The U.S hopper dredge *Gerig* dredged the Outer Bar Channel to maintain a controlling depth of 36 ft MLW and a width of 450 ft. As of June 1952, only the controlling depth on the east side of the channel was shallower than 36 ft MLW. All dredging was maintenance work.		345,773	ARCE, 1952; p. 671-672
July 31, 1952		Chief of Engineers recommended modification of the existing project to enlarge the Mobile Bar Channel to a depth of 42 ft MLW and a width of 600 ft.			ARCE, 1953; p. 628
July 1, 1952 to June 30, 1953		No dredging was done in the Mobile Outer Bar Channel during the fiscal year. By June 1953, all parts of the channel had controlling depths of between 35- and 36-ft MLW, except the eastern section of the outer channel, which had a controlling depth of 29 ft.			ARCE, 1953; p. 628-629
July 1, 1953 to June 30, 1954		No dredging was completed for the Mobile Outer Bar Channel during the fiscal year.			ARCE, 1954; p. 430

Dredging History for the Mobile Outer Bar: 1902 to 2006					
Date	**Authority**	**Description**	**New Work (cy)**	**Maintenance (cy)**	**Source**
September 3, 1954	River and Harbor Act	Authorized deepening of the project to 42-ft MLW and widening the channel to 600 ft.			ARCE, 1955; p. 423
July 1, 1954 to June 30, 1955		No dredging was completed for the Mobile Outer Bar Channel during the fiscal year. Channel controlling depths reported in March 1955 indicated a shoaled channel that was 31 ft deep in the southwestern quarter, 26-ft deep in the southeaster quarter, 34-ft deep in the northwestern quarter , and 35.5-ft deep in the northeastern quarter.			ARCE, 1955; p. 423-424
September 26 – October 13, 1955		The U.S hopper dredge *Langfitt* dredged the Outer Bar Channel for a relatively short period of time. As of October 1955, the controlling depth in the channel was 36 ft MLW. All dredging was maintenance work.		495,452	ARCE, 1956; p. 547
July 15-18, 1956		The U.S hopper dredge *Langfitt* dredged the Outer Bar Channel to previous project dimensions (36-ft deep, 450-ft wide). All dredging was maintenance work.		135,606	ARCE, 1957; p. 545
July 5 – September 15, 1956		The U.S hopper dredge *Langfitt* dredged the Outer Bar Channel to a controlling depth of 38 ft MLW. This was the initial phase of development for the 42-ft deep by 600-ft wide authorized project.	1,204,526		ARCE, 1957; p. 545
July 1, 1957 to June 30, 1958		No dredging was completed for the Mobile Outer Bar Channel during the fiscal year.			ARCE, 1958; p. 495
July 1, 1958 to June 30, 1959		No dredging was completed for the Mobile Outer Bar Channel during the fiscal year.			ARCE, 1959; p. 522
July 1, 1959 to June 30, 1960		No dredging was completed for the Mobile Outer Bar Channel during the fiscal year.			ARCE, 1960; p. 509
July 1, 1960 to June 30, 1961		No dredging was completed for the Mobile Outer Bar Channel during the fiscal year.			ARCE, 1961; p. 558
April 21 – May 10, 1962		The U.S hopper dredge *Gerig* dredged the Outer Bar Channel to a controlling depth of 38 ft MLW. No new work was done on the 42-ft deep by 600-ft wide authorized project.		533,875	ARCE, 1962; p. 569-570
July 1, 1962 to June 30, 1963		No dredging was completed for the Mobile Outer Bar Channel during the fiscal year.			ARCE, 1963; p. 505
July 1, 1963 to June 30, 1964		No dredging was completed for the Mobile Outer Bar Channel during the fiscal year.			ARCE, 1964; p. 469
October 24 – December 10, 1964		The U.S hopper dredge *Harding* dredged the Outer Bar Channel toward completion of the authorized 42-ft deep by 600-ft wide channel.	1,381,500		ARCE, 1965; p. 460
June 30, 1965		The U.S hopper dredge *Gerig* operated in the Outer Bar Channel toward completion of the authorized project.	13,271		ARCE, 1965; p. 460
July 1-30, 1965		The U.S hopper dredge *Gerig* operated in the Outer Bar Channel completing the authorized project to a depth of 42 ft and a width of 600 ft.	911,581		ARCE, 1966; p. 497
May 16, 1904 to July 30, 1965	**1954 River and Harbor Act**	**Total dredging upon completion of a channel through the Mobile Outer Bar to a depth of 42 ft MLW and a width of 600 ft.**	**6,061,779**	**9,138,361**	
November 18 - December 1, 1966		The U.S hopper dredge *Gerig* operated in the Mobile Outer Bar Channel maintaining the authorized project to a depth of 42 ft and a width of 600 ft.		272,439	ARCE, 1967; p. 487
April 1-10, 1968		The U.S hopper dredge *Langfitt* operated in the Mobile Outer Bar Channel maintaining the authorized project to a depth of 42 ft and a width of 600 ft.		192,857	ARCE, 1968; p. 373
December 28, 1968 – January 4, 1969		The U.S hopper dredge *Langfitt* operated in the Mobile Outer Bar Channel maintaining the authorized project to a depth of 42 ft and a width of 600 ft.		174,953	ARCE, 1969; p. 356
January 13 – February 4, 1970		The U.S hopper dredge *Langfitt* operated in the Mobile Outer Bar Channel maintaining the authorized project to a depth of 42 ft and a width of 600 ft.		361,815	ARCE, 1970; p. 341
October 19 – November 2, 1970 and January 23 – February 10, 1971		The U.S hopper dredge *Langfitt* operated in the Mobile Outer Bar Channel maintaining the authorized project to a depth of 42 ft and a width of 600 ft.		827,388	ARCE, 1971; p. 10-11
June 14 - 30, 1972		The U.S hopper dredge *McFarland* operated in the Mobile Outer Bar Channel maintaining the authorized project to a depth of 42 ft and a width of 600 ft.		262,450	ARCE, 1972; p. 10-11
July 1, 1972 to June 30, 1973		No dredging was completed for the Mobile Outer Bar Channel during the fiscal year.			ARCE, 1973; p.10-11
July 1, 1973 to June 30, 1974		No dredging was completed for the Mobile Outer Bar Channel during the fiscal year.			ARCE, 1974; p. 10-9
July 16-31, 1974		The U.S hopper dredge *Gerig* operated in the Mobile Outer Bar Channel maintaining the authorized project to a depth of 42 ft and a width of 600 ft.		349,260	Mobile District O&M

Dredging History for the Mobile Outer Bar: 1902 to 2006					
Date	**Authority**	**Description**	**New Work (cy)**	**Maintenance (cy)**	**Source**
February 16-28, 1975		The U.S hopper dredge *Gerig* operated in the Mobile Outer Bar Channel maintaining the authorized project to a depth of 42 ft and a width of 600 ft.		982,829	Mobile District O&M
May 3 - June 14, 1976		The U.S hopper dredge *Gerig* operated in the Mobile Outer Bar Channel maintaining the authorized project to a depth of 42 ft and a width of 600 ft.		1,364,113	Mobile District O&M
May 17 to June 14, 1977		The U.S hopper dredge *McFarland* dredged sediment from the Mobile Outer and Inner Bar Channel maintaining the authorized project to a depth of 42 ft and a width of 600 ft.		1,272,432	ARCE, 1977; p. 10-11; Mobile District O&M
July 1, 1977 to June 30, 1978		No dredging was completed for the Mobile Outer Bar Channel during the fiscal year.			ARCE, 1978; p. 10-11
July 1, 1978 to June 30, 1979		No dredging was completed for the Mobile Outer Bar Channel during the fiscal year.			ARCE, 1979; p. 10-12
October 15-27, 1979		The U.S hopper dredge *Langfitt* operated in the Mobile Outer Bar Channel maintaining the authorized project to a depth of 42 ft and a width of 600 ft.		707,142	Mobile District O&M
March 10-24, 1980		U.S. hopper dredges *Essayons* and *Goethals* operated in the Mobile Outer Bar Channel maintaining the authorized project to a depth of 42 ft and a width of 600 ft.		190,300	Mobile District O&M
October 15 – December 17, 1980		Contractor's hopper dredge *Buster Bean* operated in the Mobile Outer Bar Channel maintaining the authorized project to a depth of 42 ft and a width of 600 ft.		939,037	ARCE, 1981; p. 10-11
January 26 to February 8, 1981		The U.S hopper dredge *Langfitt* operated in the Mobile Outer Bar Channel maintaining the authorized project to a depth of 42 ft and a width of 600 ft.		610,623	Mobile District O&M
December 11, 1982 to January 7, 1983		Contractor's dredge *Mermentau* operated in the Mobile Outer Bar Channel maintaining the authorized project to a depth of 42 ft and a width of 600 ft.		312,408	Mobile District O&M
January 1-23, 1984		Contractor's dredge *Atchafalaya* operated in the Mobile Outer Bar Channel maintaining the authorized project to a depth of 42 ft and a width of 600 ft.		218,672	Mobile District O&M
October 22-November 1, 1984		Contractor's dredge *Eagle* operated in the Mobile Outer Bar Channel maintaining the authorized project to a depth of 42 ft and a width of 600 ft.		340,935	Mobile District O&M
August 15, 1985	Supplemental Appropriations Act	Deepen and widen Mobile Outer Bar Channel to 57 feet deep and 700 feet wide for a distance of approximately 7.4 miles. A General Design Memorandum was approved at Division level modifying for project dimensions.			ARCE, 1985; Table 10-B and p. 10-9
August 20 to October 8, 1985		Contractor's dredge *Sugar Island* operated in the Mobile Outer Bar Channel maintaining the authorized project to a depth of 42 ft and a width of 600 ft. Hurricane *Elena* caused significant channel shoaling on Mobile Outer Bar that was handled through emergency procurement.		1,386,536	Mobile District O&M
January 6 – February 24, 1987		Contractor's dredges *Atchafalaya* and *Mermentau* operated in the Mobile Outer Bar Channel maintaining the authorized project to a depth of 46 ft and a width of 600 ft. **All material disposed on the nearshore feeder berm.**		656,089	Mobile District O&M
October 1, 1987 to September 30, 1988		Although the authorized project is for construction of a 57-ft deep x 700-ft wide channel across the outer bar, the plan for improvement consists of deepening the channel from 42 feet to 47 feet for a distance of about 6.1 miles from the Gulf of Mexico to Mobile Bay.			ARCE, 1988; p.10-10
February 7, 1989 to May 8, 1990		Contractor's dredges *Sugar Island* operated in the Mobile Outer Bar Channel creating new authorized project dimensions of 47 ft deep by 600 ft wide of a distance of about 1.5 miles across Mobile Outer Bar.	1,911,284		ARCE, 1990; p. 10-10; Mobile District O&M
February 23, 1989 to April 16, 1990		Contractor's dredges *Manhattan Island* operated in the Mobile Outer Bar Channel creating new authorized project dimensions of 47 ft deep by 600 ft wide of a distance of about 1.5 miles across Mobile Outer Bar.	4,844,068		Mobile District O&M
May 16, 1904 to April 16, 1990		**Total dredging upon completion of a channel through the Mobile Outer Bar to a depth of 47 ft MLW and a width of 600 ft.**	**12,817,131**	**20,560,639**	
October 1, 1990 to September 30, 1991		No dredging was completed for the Mobile Outer Bar Channel during the fiscal year.			Mobile District O&M
August 13 - September 2, 1992		Contractor's dredges *Ouachita* operated in the Mobile Outer Bar Channel maintaining the authorized project dimensions of 47 ft deep by 600 ft wide.		466,607	Mobile District O&M
October 1, 1992 to September 30, 1993		No dredging was completed for the Mobile Outer Bar Channel during the fiscal year.			Mobile District O&M

Dredging History for the Mobile Outer Bar: 1902 to 2006					
Date	**Authority**	**Description**	**New Work (cy)**	**Maintenance (cy)**	**Source**
October 1, 1993 to September 30, 1994		No dredging was completed for the Mobile Outer Bar Channel during the fiscal year.			Mobile District O&M
October 1, 1995 to September 30, 1995		No dredging was completed for the Mobile Outer Bar Channel during the fiscal year.			Mobile District O&M
November 17 to December 16, 1995		Contractor's dredges *Eagle I* operated in the Mobile Outer Bar Channel maintaining the authorized project dimensions of 47 ft deep by 600 ft wide.		621,172	Mobile District O&M
August 8 – 20, 1997		Contractor's dredges *Padre Island* operated in the Mobile Outer Bar Channel maintaining the authorized project dimensions of 47 ft deep by 600 ft wide.		238,256	Mobile District O&M
September 4 – October 2, 1997		Contractor's dredges *Eagle I* operated in the Mobile Outer Bar Channel maintaining the authorized project dimensions of 47 ft deep by 600 ft wide.		292,200	Mobile District O&M
December 16 – 25, 1997		Contractor's dredges *Columbus* operated in the Mobile Outer Bar Channel maintaining the authorized project dimensions of 47 ft deep by 600 ft wide.		180,540	Mobile District O&M
September 21 – October 9, 1998		Contractor's dredges *Eagle* operated in the Mobile Outer Bar Channel maintaining the authorized project dimensions of 47 ft deep by 600 ft wide.		443,761	Mobile District O&M
October 9 – 28, 1998		The U.S hopper dredge *Wheeler* dredged sediment on an emergency basis from the Mobile Outer and Inner Bar Channel to maintain the authorized project to a depth of 47 ft and a width of 600 ft. Hurricane *Georges* caused significant channel shoaling on the Mobile Outer Bar.		836,054	Mobile District O&M
August 26 to September 22, 1999		Contractor's dredges *Columbus and Atchafalaya* operated in the Mobile Outer Bar Channel maintaining the authorized project dimensions of 47 ft deep by 600 ft wide. **54,600 cy placed in the nearshore disposal area.**		125,580	Mobile District O&M
May 3 to September 29, 1999		Contractor's dredge *Newport* operated in the Mobile Outer Bar Channel creating new authorized project dimensions of 49 ft deep by 600 ft wide. **Placed in the Sand Island Beneficial Use Area.**	3,061,598		Mobile District O&M
May 16, 1904 to September 29, 1999		**Total dredging upon completion of a channel through the Mobile Outer Bar to a depth of 49 ft MLW and a width of 600 ft.**	**15,878,729**	**23,764,809**	
July 13-26, 2000		Contractor's dredge *Stuyvesant* operated in the Mobile Outer Bar Channel maintaining the authorized project dimensions of 49-ft deep by 600-ft wide.		758,280	Mobile District O&M
March 27 - May 10, 2002		Contractor's dredge *Atchafalaya* operated in the Mobile Outer Bar Channel maintaining the authorized project dimensions of 49-ft deep by 600-ft wide. **Placed in the Sand Island Beneficial Use Area (SIBUA).**		92,820	Mobile District O&M
June 1-24, 2004		Contractor's dredge *Atchafalaya* operated in the Mobile Outer Bar Channel maintaining the authorized project dimensions of 49-ft deep by 600-ft wide. **Placed in SIBUA.**		230,110	Mobile District O&M
October 2 - November 14, 2004		Contractor's dredge *Dodge Island* operated in the Mobile Outer Bar Channel maintaining the authorized project dimensions of 49-ft deep by 600-ft wide. **Placed in SIBUA.**		1,184,817	Mobile District O&M
October 26, 2004 - January 13, 2005		Contractor's dredge *Padre Island* operated in the Mobile Outer Bar Channel maintaining the authorized project dimensions of 49-ft deep by 600-ft wide. **Placed in SIBUA and Sand Island Lighthouse disposal area.**		1,808,765	Mobile District O&M
April 28 to June 11, 2006		Contractor's dredge *Atchafalaya* operated in the Mobile Outer Bar Channel maintaining the authorized project dimensions of 49-ft deep by 600-ft wide. **Placed in SIBUA.**		487,975	Mobile District O&M
1904 to 2006		**Total dredging in the Mobile Outer Bar Channel**	**15,878,729**	**28,327,576 (277,721 cy/yr)**	
1904 to 2006		**Dredged Material placed in nearshore disposal areas.**	**3,061,598**	**4,515,176**	
1904 to 2006		**Dredged Material placed offshore.**	**12,817,131**	**23,812,400**	

Appendix C

Historical Shoreline Position Change for Dauphin Island: 1847 to 2006

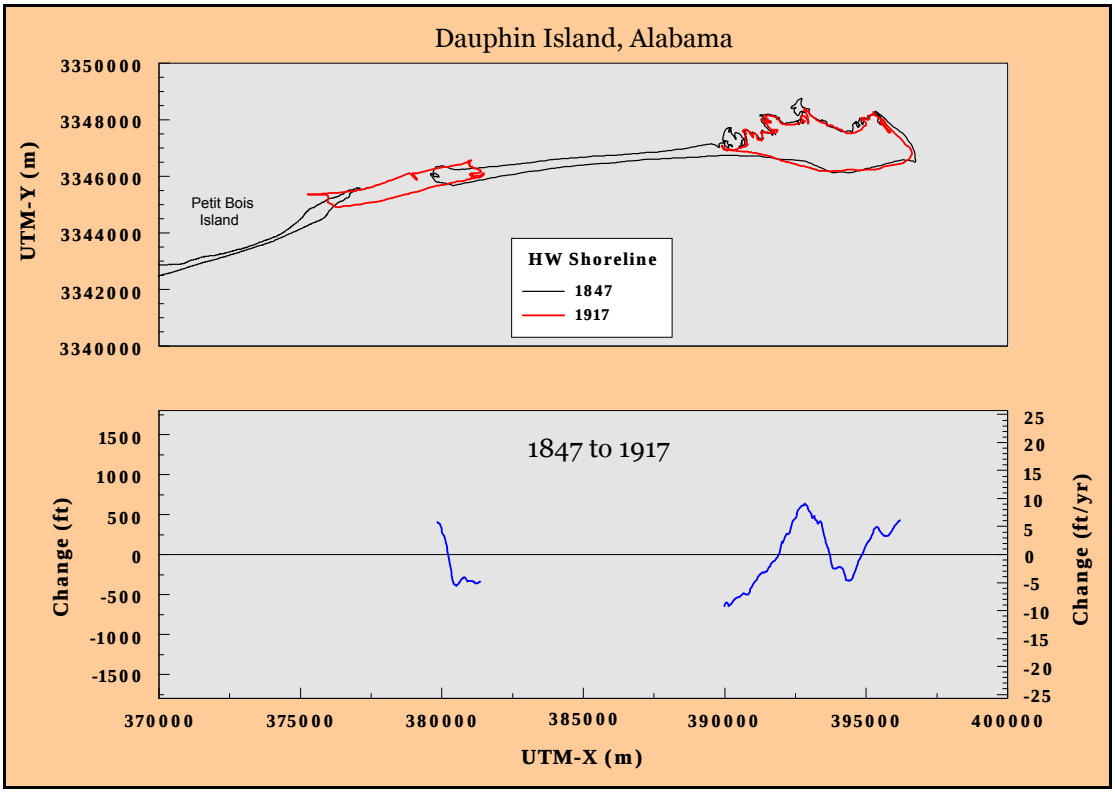

Figure C1. Historical shoreline position change, Dauphin Island, Alabama: 1847 to 1917.

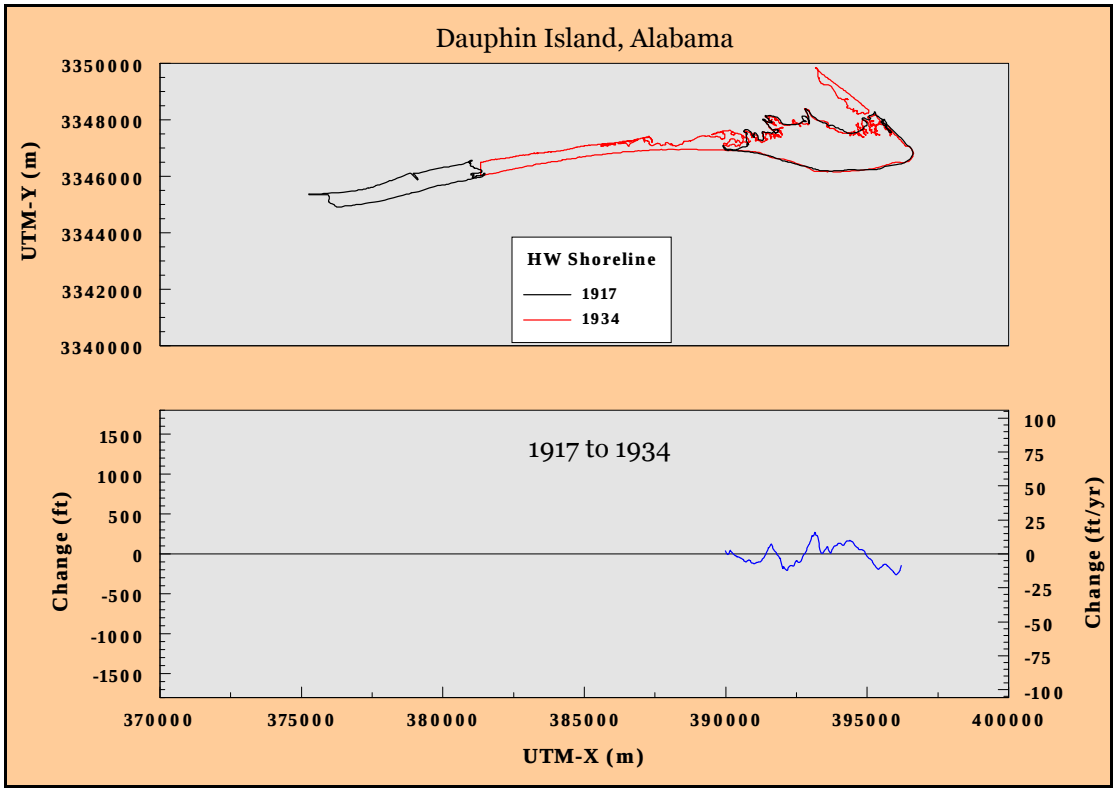

Figure C2. Historical shoreline position change, Dauphin Island, Alabama: 1917 to 1934.

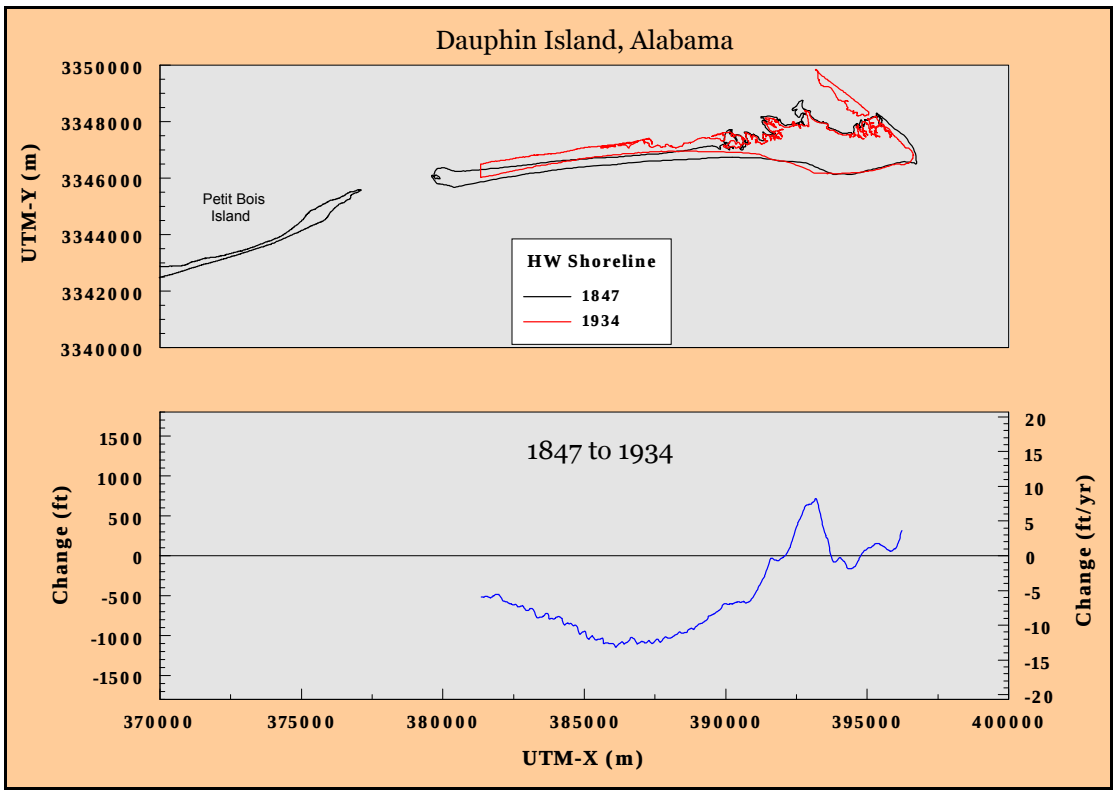

Figure C3. Historical shoreline position change, Dauphin Island, Alabama: 1847 to 1934.

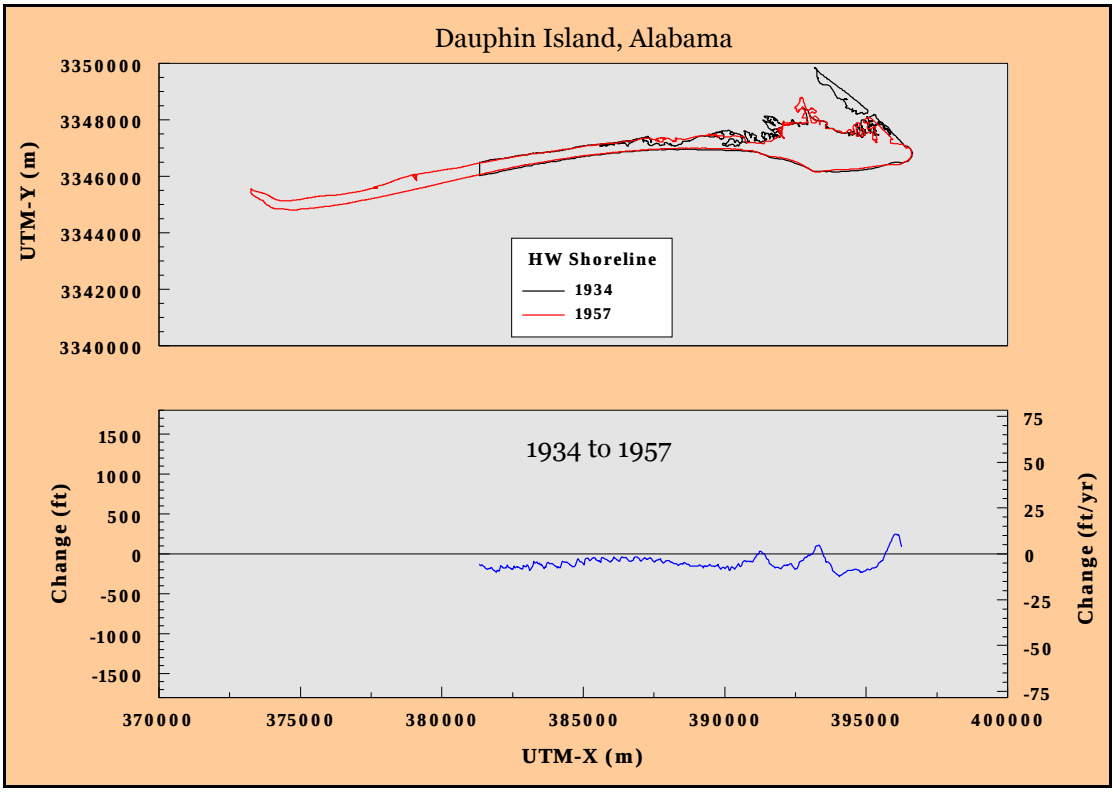

Figure C4. Historical shoreline position change, Dauphin Island, Alabama: 1934 to 1957.

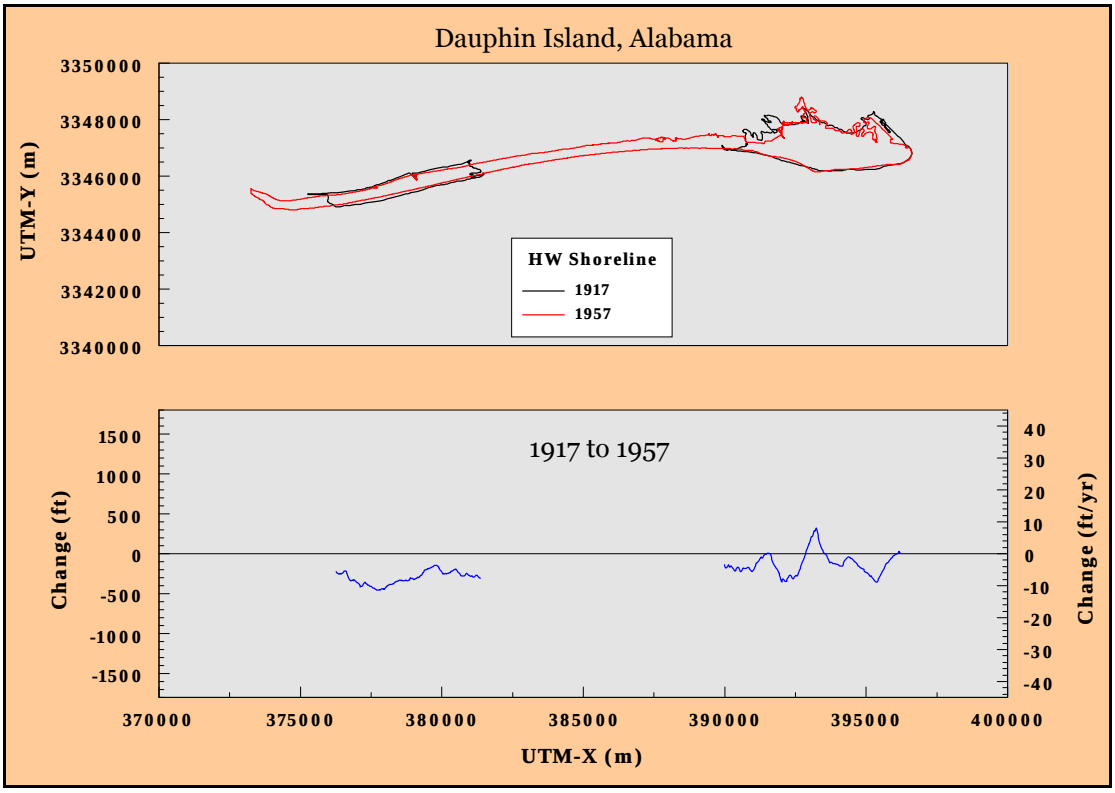

Figure C5. Historical shoreline position change, Dauphin Island, Alabama: 1917 to 1957.

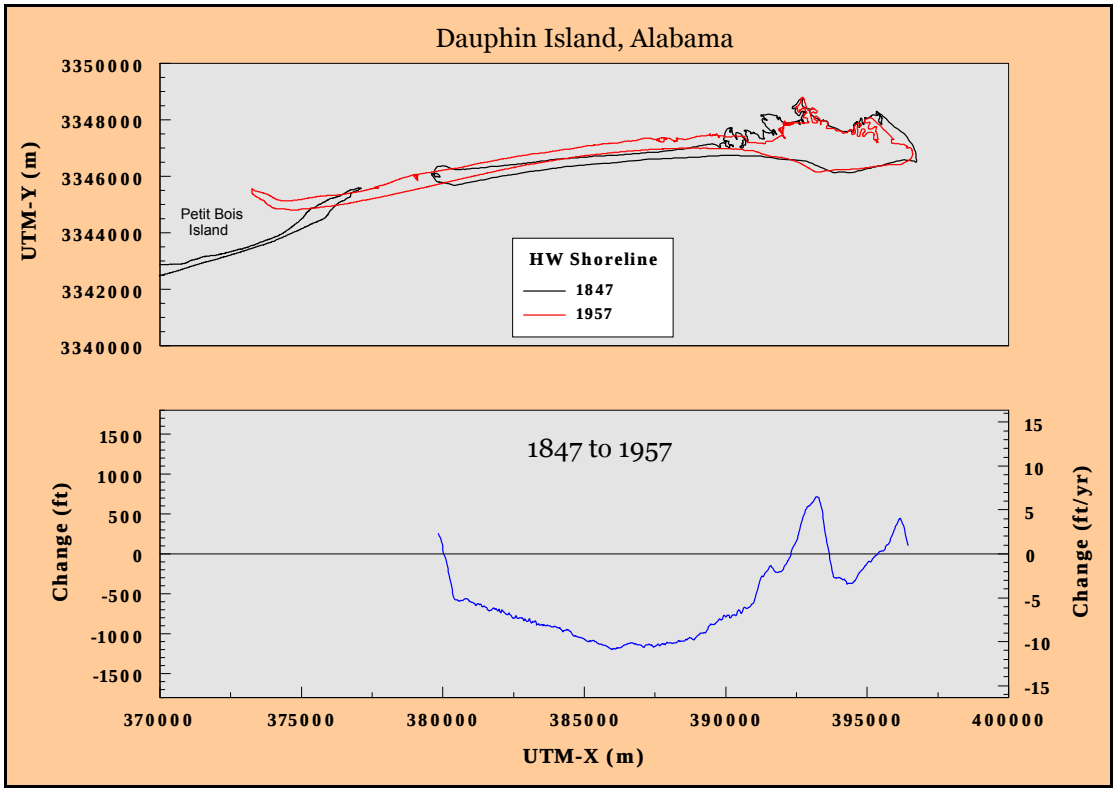

Figure C6. Historical shoreline position change, Dauphin Island, Alabama: 1847 to 1957.

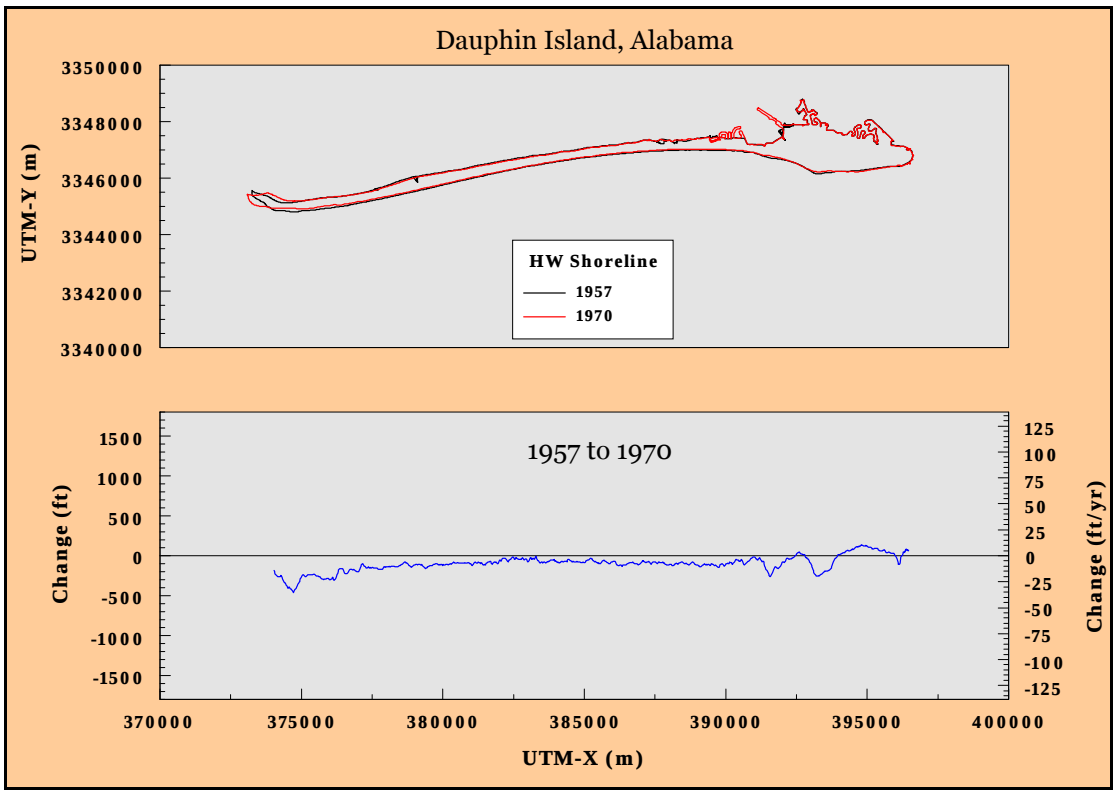

Figure C7. Historical shoreline position change, Dauphin Island, Alabama: 1957 to 1970.

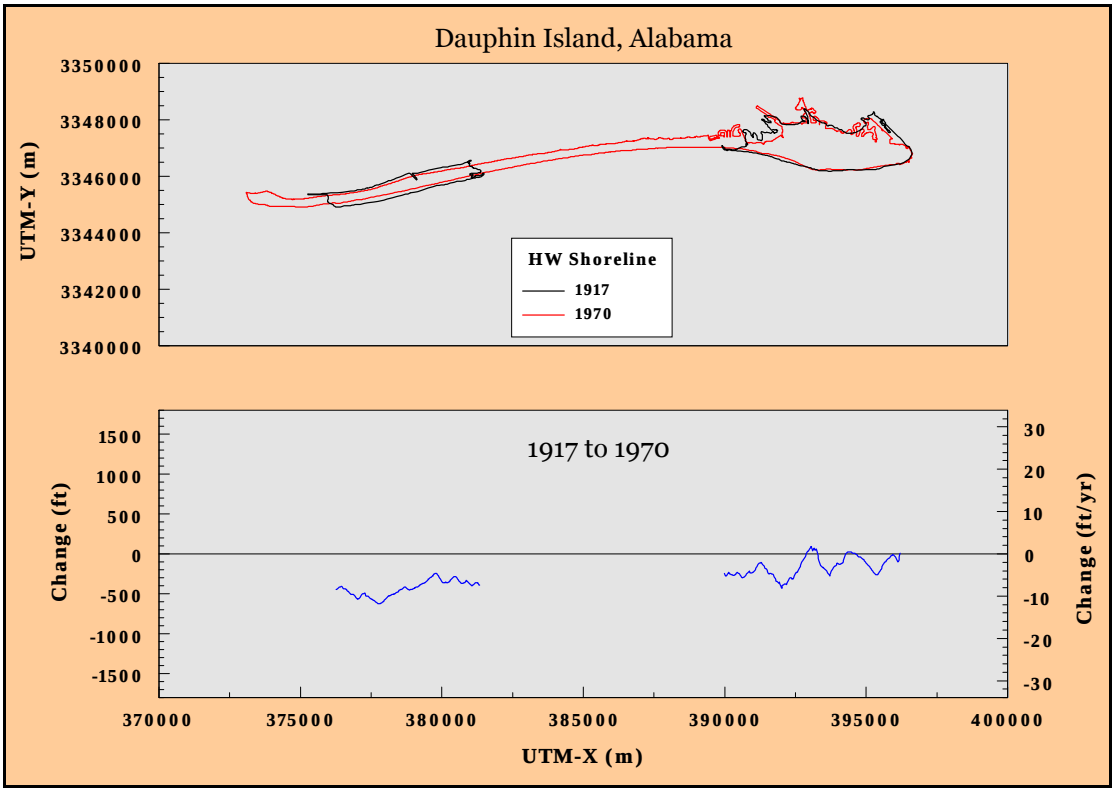

Figure C8. Historical shoreline position change, Dauphin Island, Alabama: 1917 to 1970.

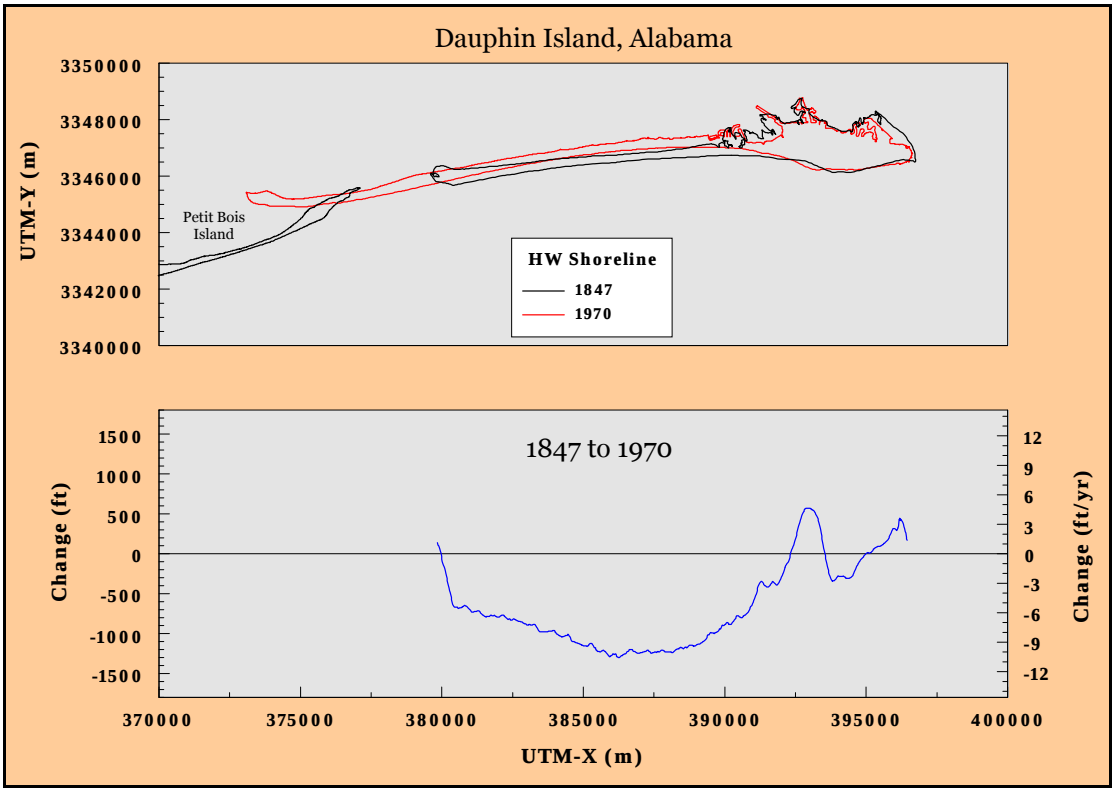

Figure C9. Historical shoreline position change, Dauphin Island, Alabama: 1847 to 1970.

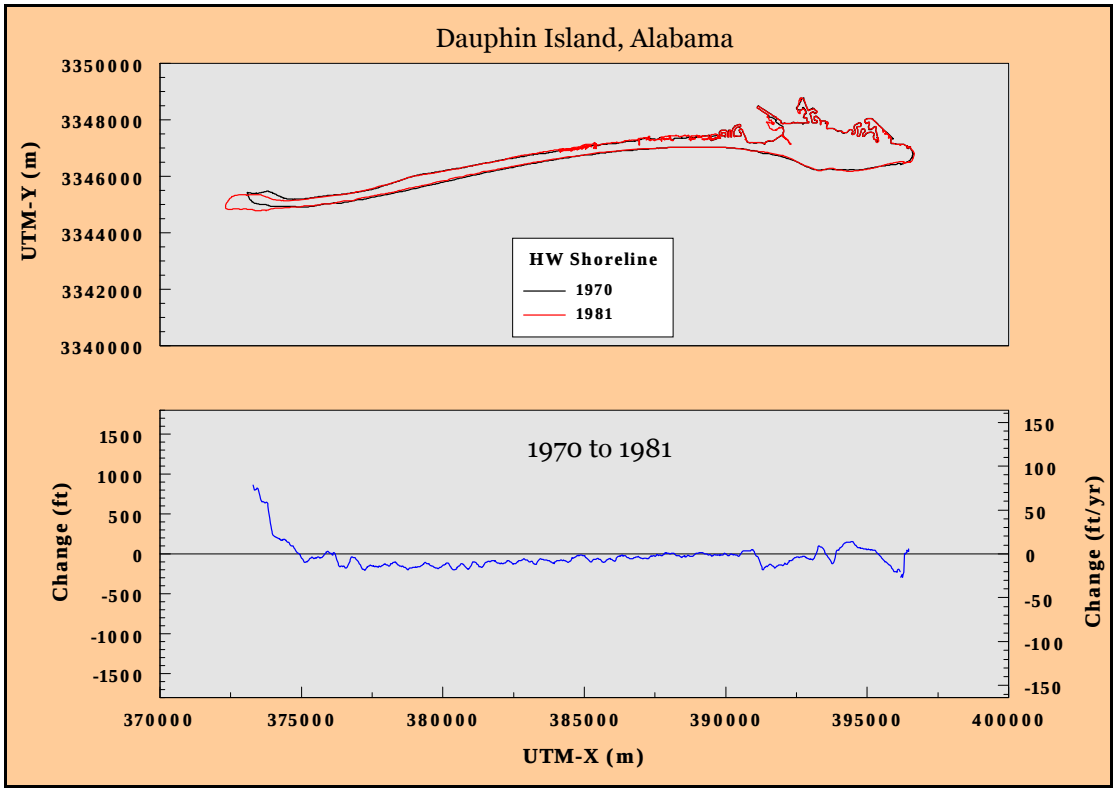

Figure C10. Historical shoreline position change, Dauphin Island, Alabama: 1970 to 1981.

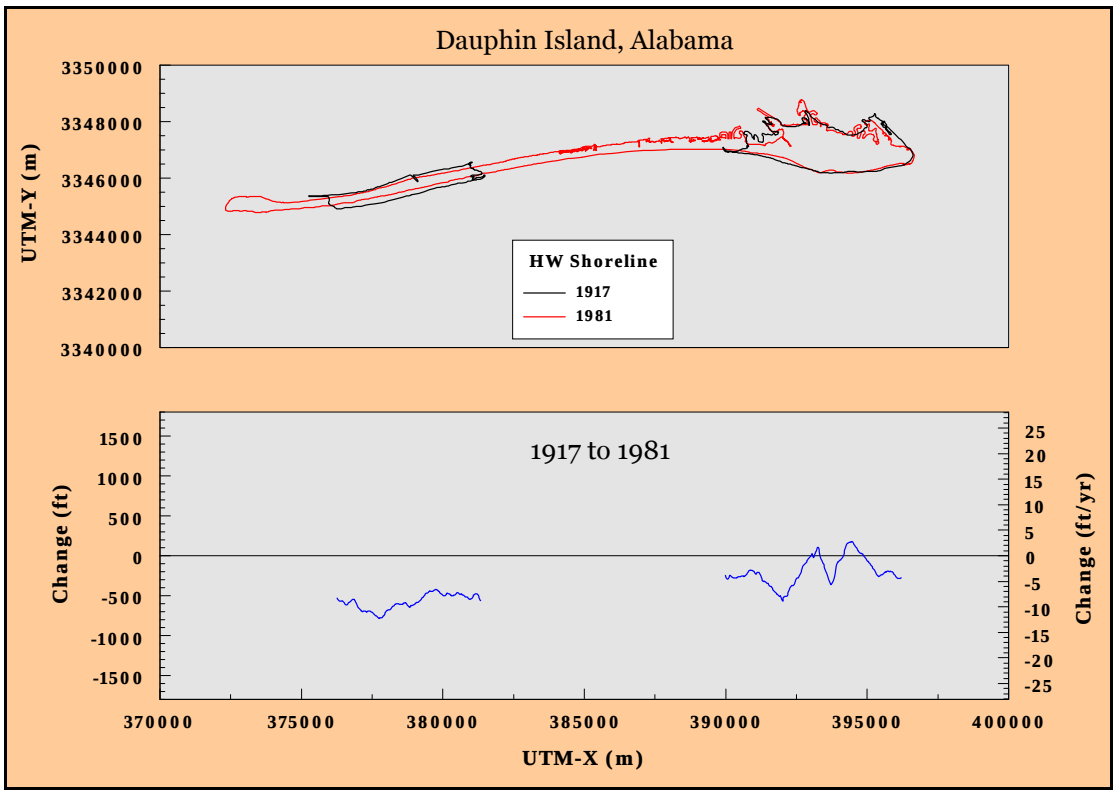

Figure C11. Historical shoreline position change, Dauphin Island, Alabama: 1917 to 1981.

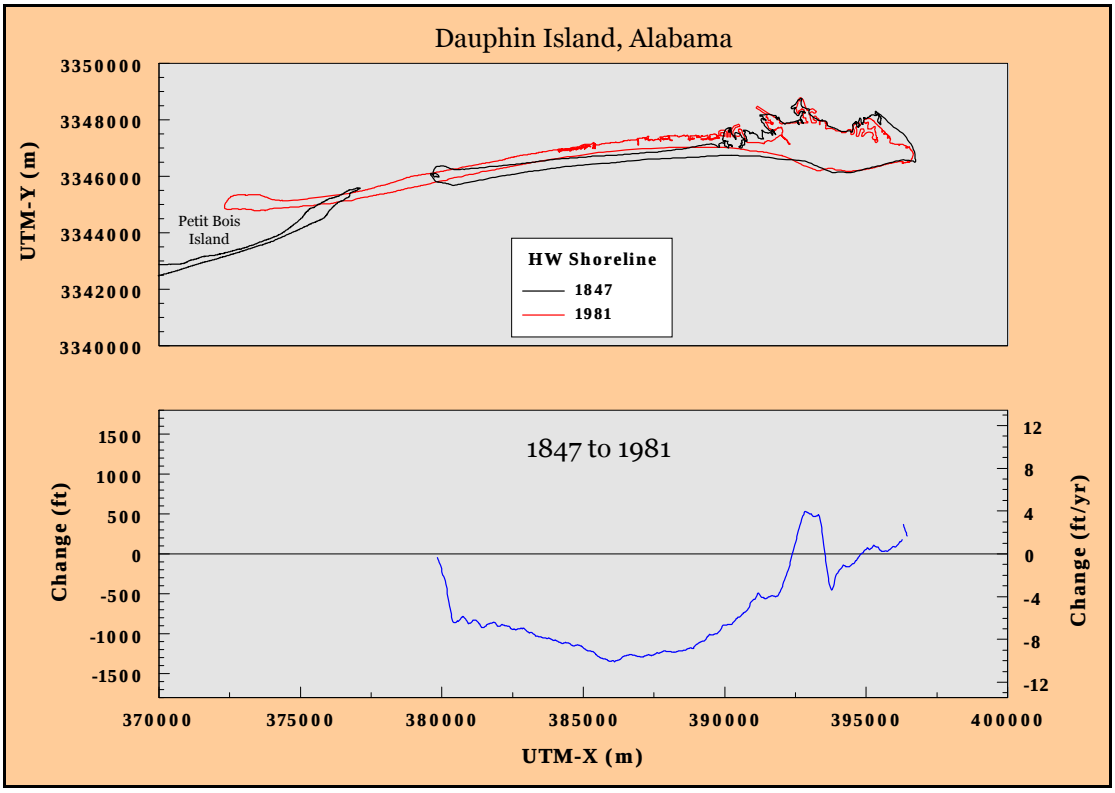

Figure C12.Historical shoreline position change, Dauphin Island, Alabama: 1847 to 1981.

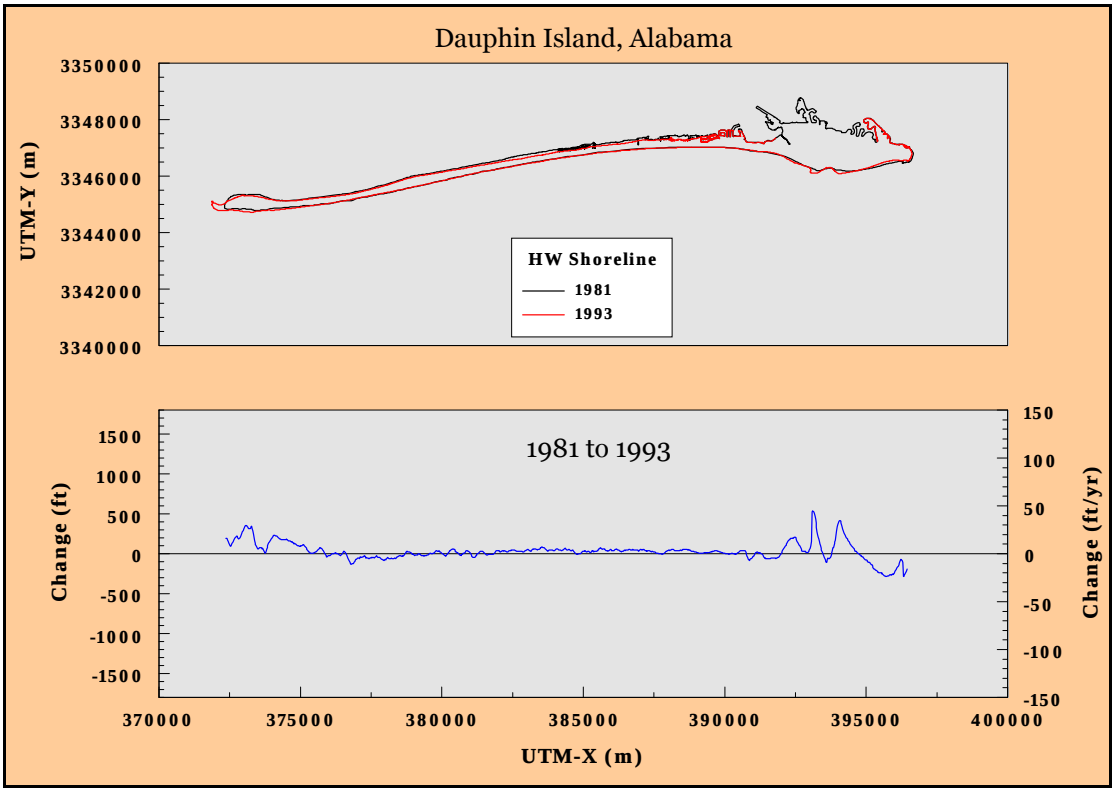

Figure C13.Historical shoreline position change, Dauphin Island, Alabama: 1981 to 1993.

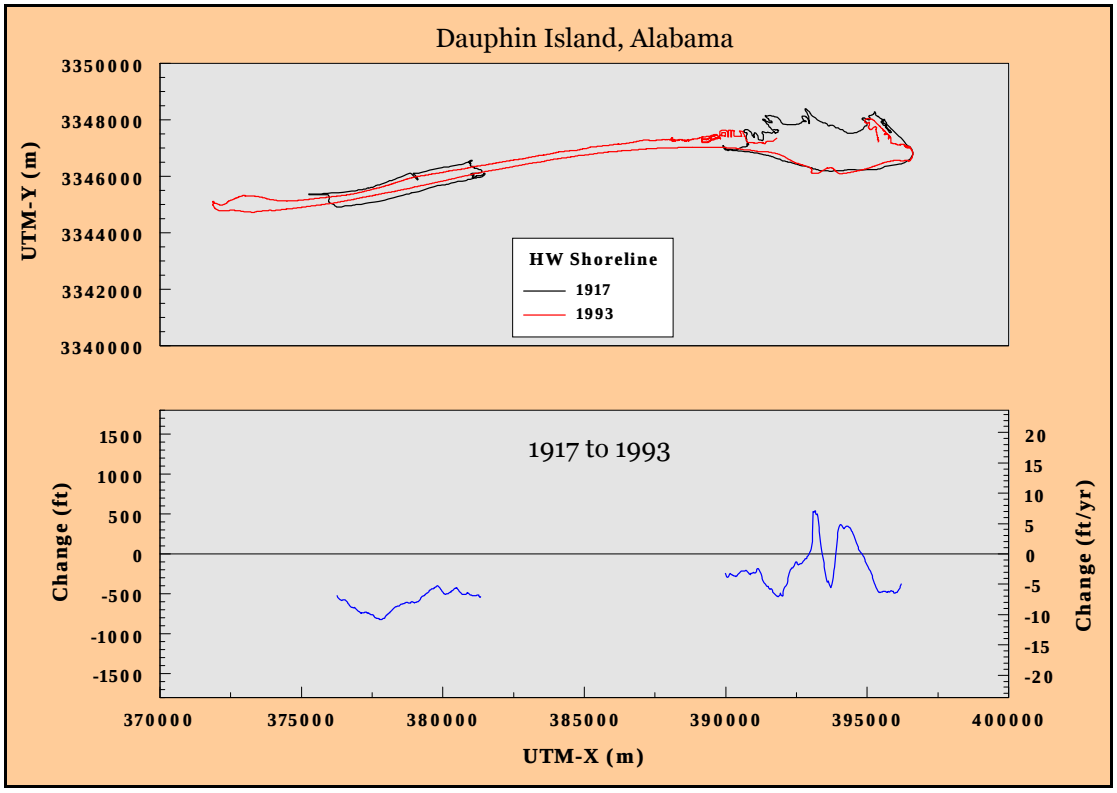

Figure C14. Historical shoreline position change, Dauphin Island, Alabama: 1917 to 1993.

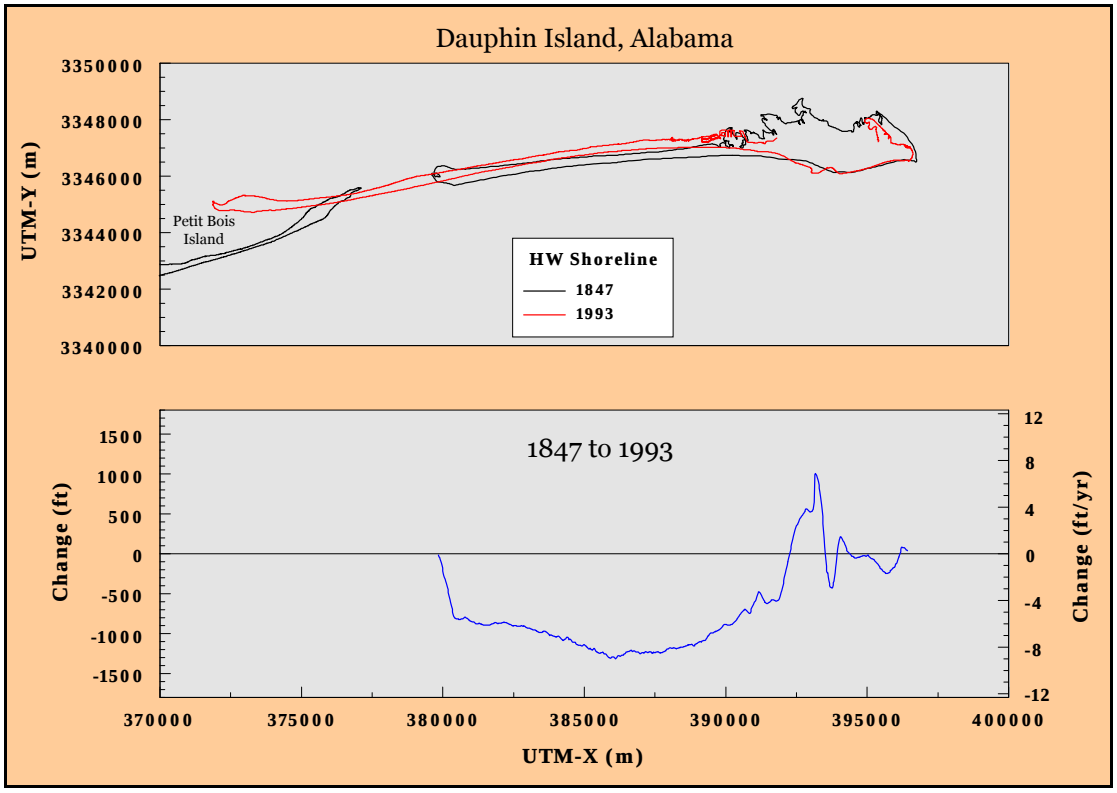

Figure C15. Historical shoreline position change, Dauphin Island, Alabama: 1847 to 1993.

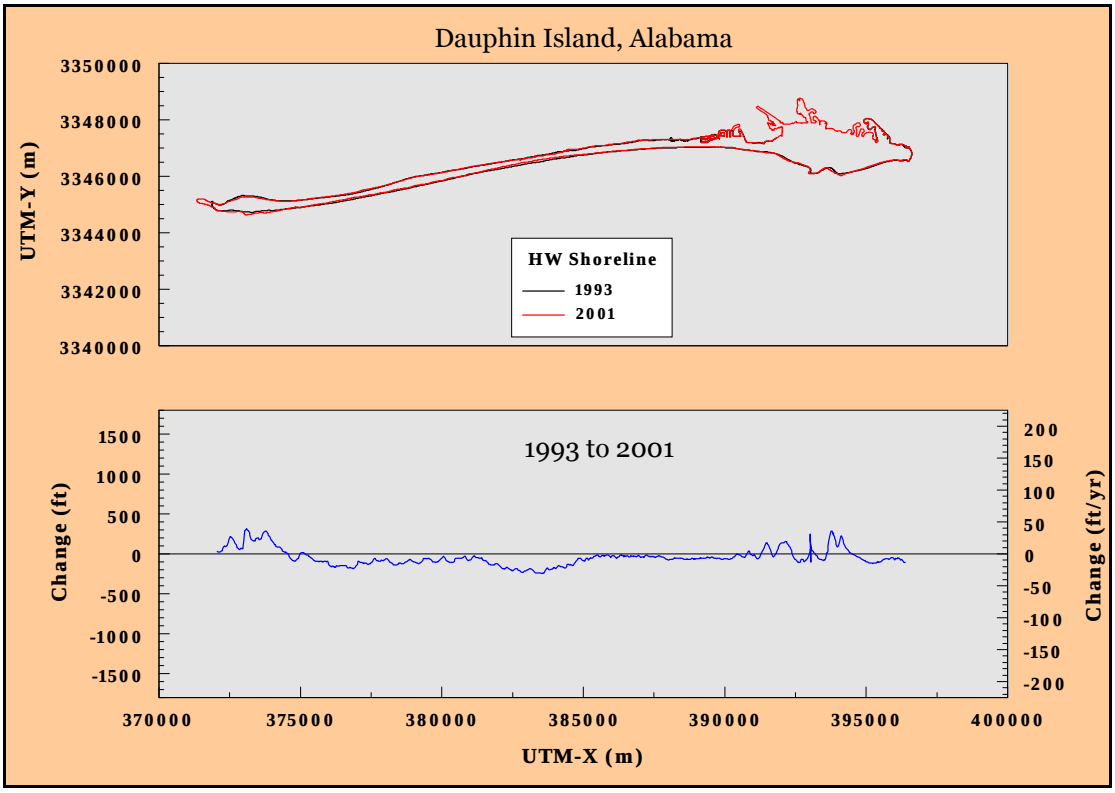

Figure C16. Historical shoreline position change, Dauphin Island, Alabama: 1993 to 2001.

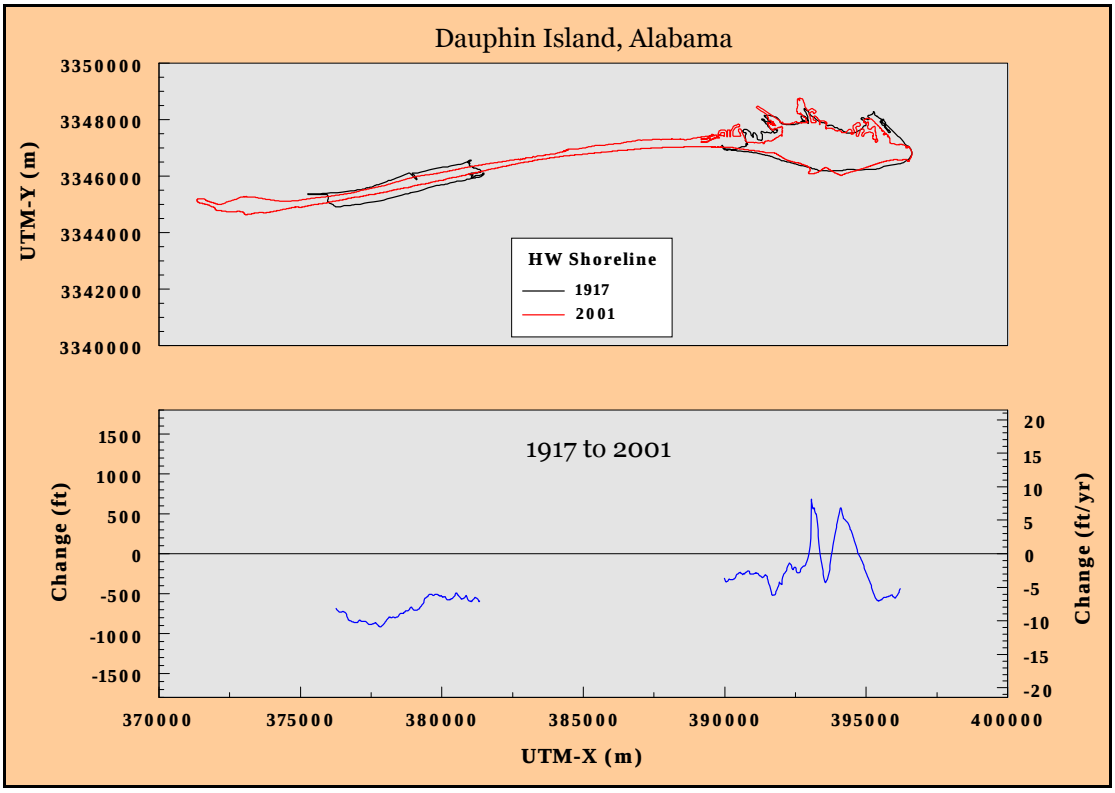

Figure C17. Historical shoreline position change, Dauphin Island, Alabama: 1917 to 2001.

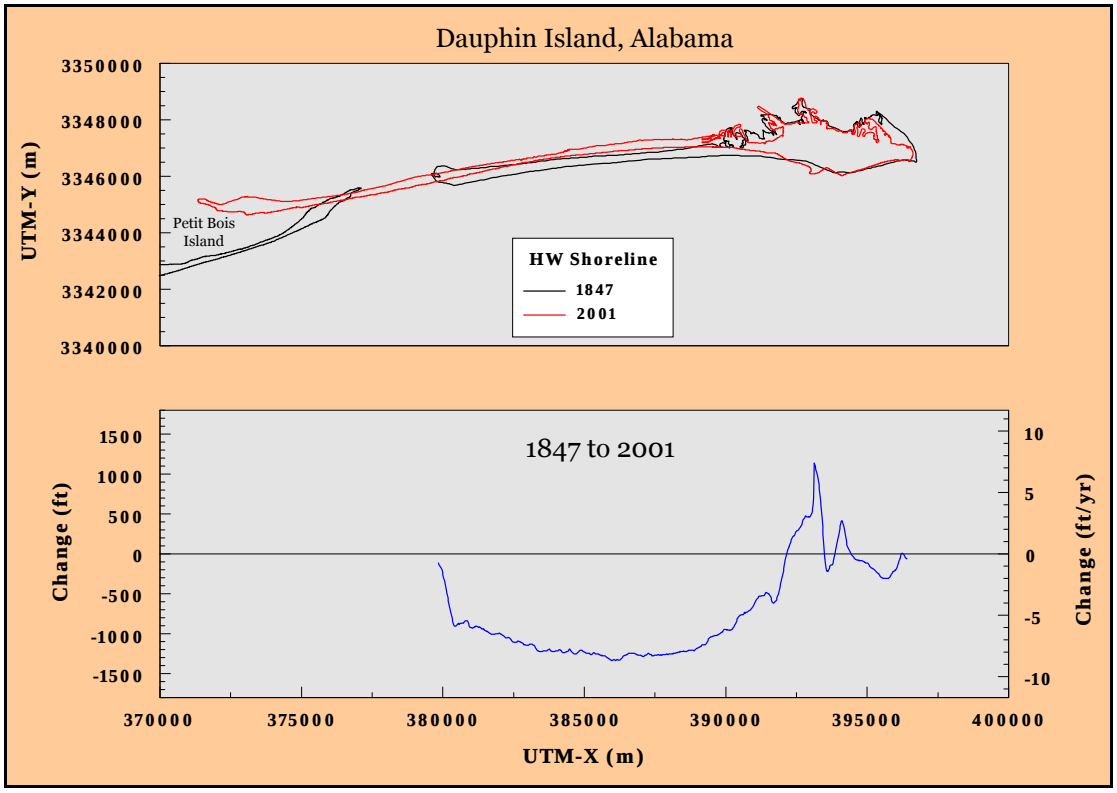

Figure C18. Historical shoreline position change, Dauphin Island, Alabama: 1847 to 2001.

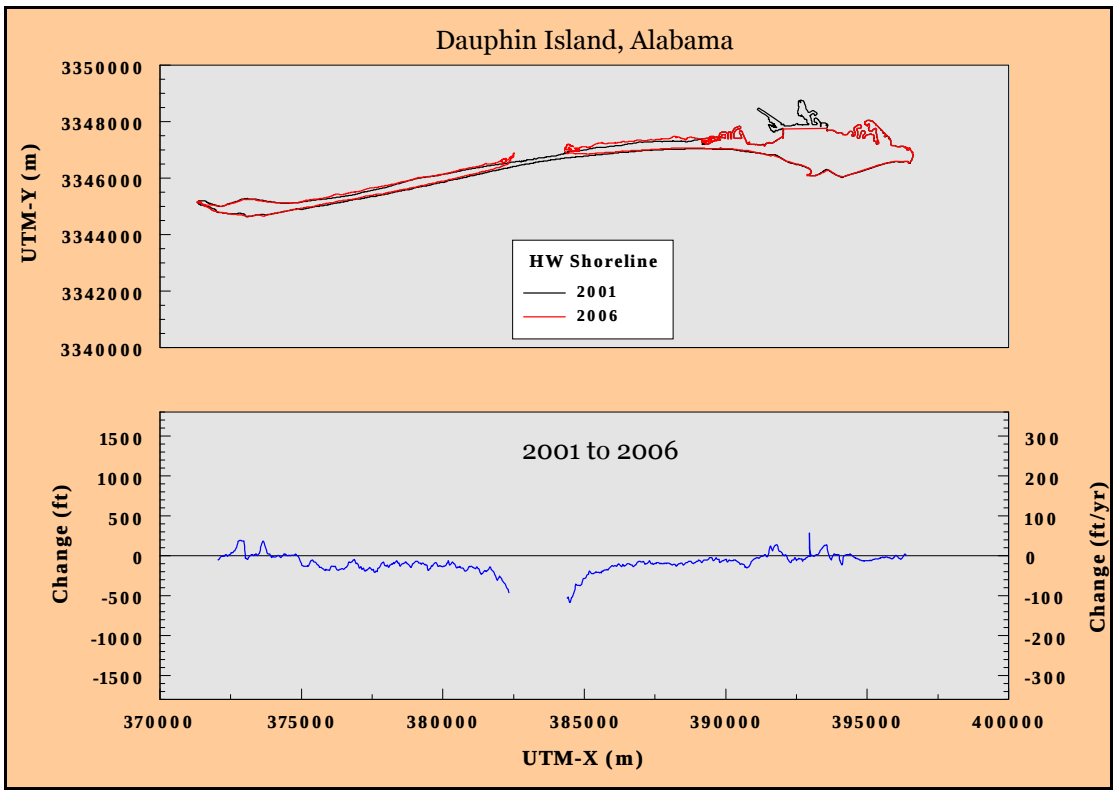

Figure C19.Historical shoreline position change, Dauphin Island, Alabama: 2001 to 2006.

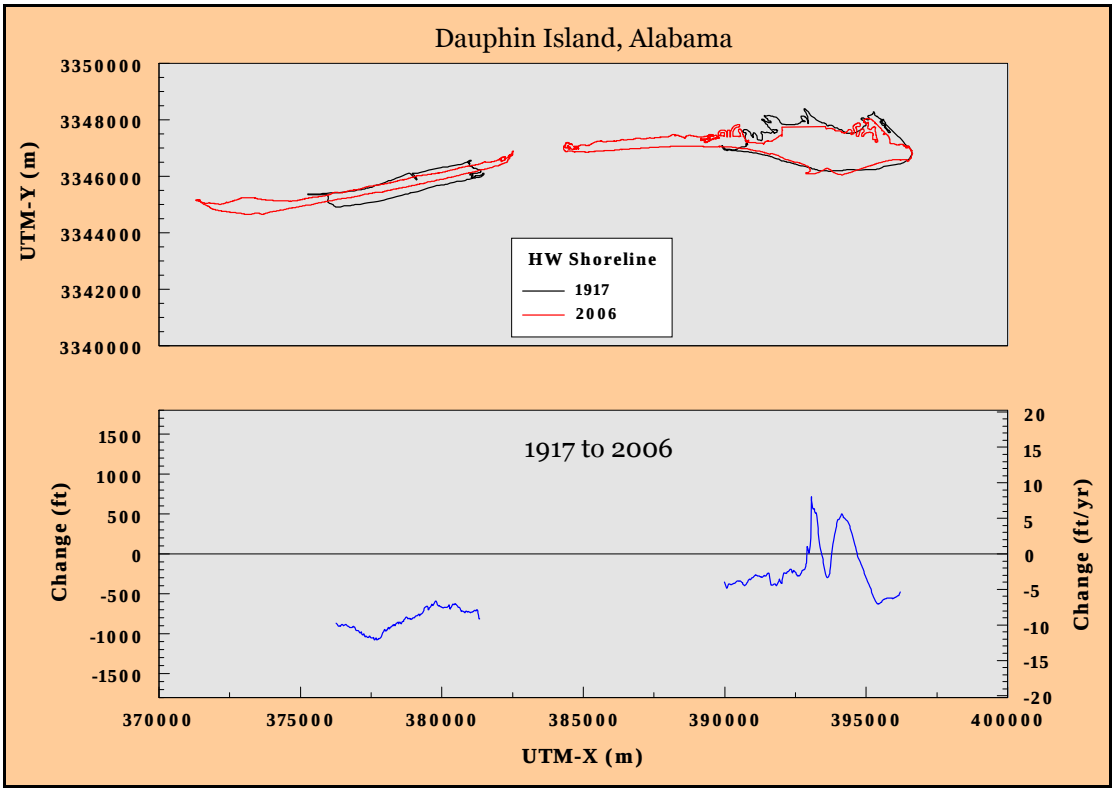

Figure C20. Historical shoreline position change, Dauphin Island, Alabama: 1917 to 2006.

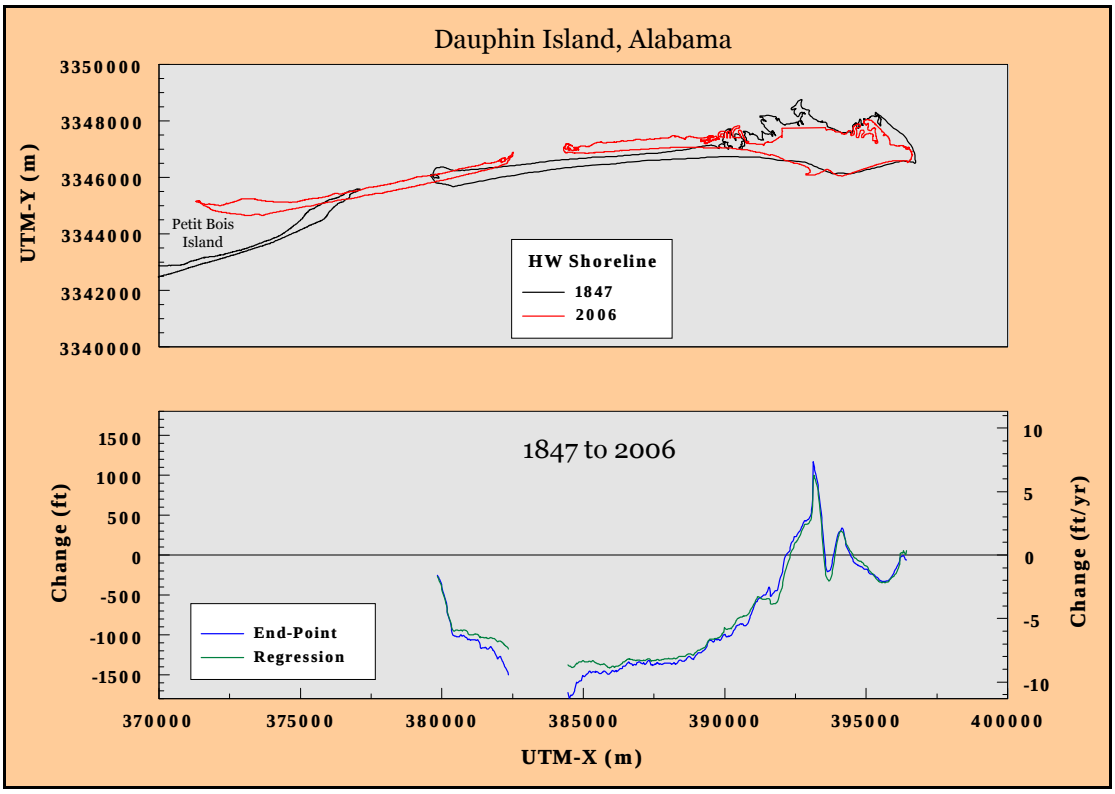

Figure C21.Historical shoreline position change, Dauphin Island, Alabama: 1847 to 2006.

Appendix D

Historical Shoreline Position Change Perdido Pass to Mobile Point: 1847 to 2006

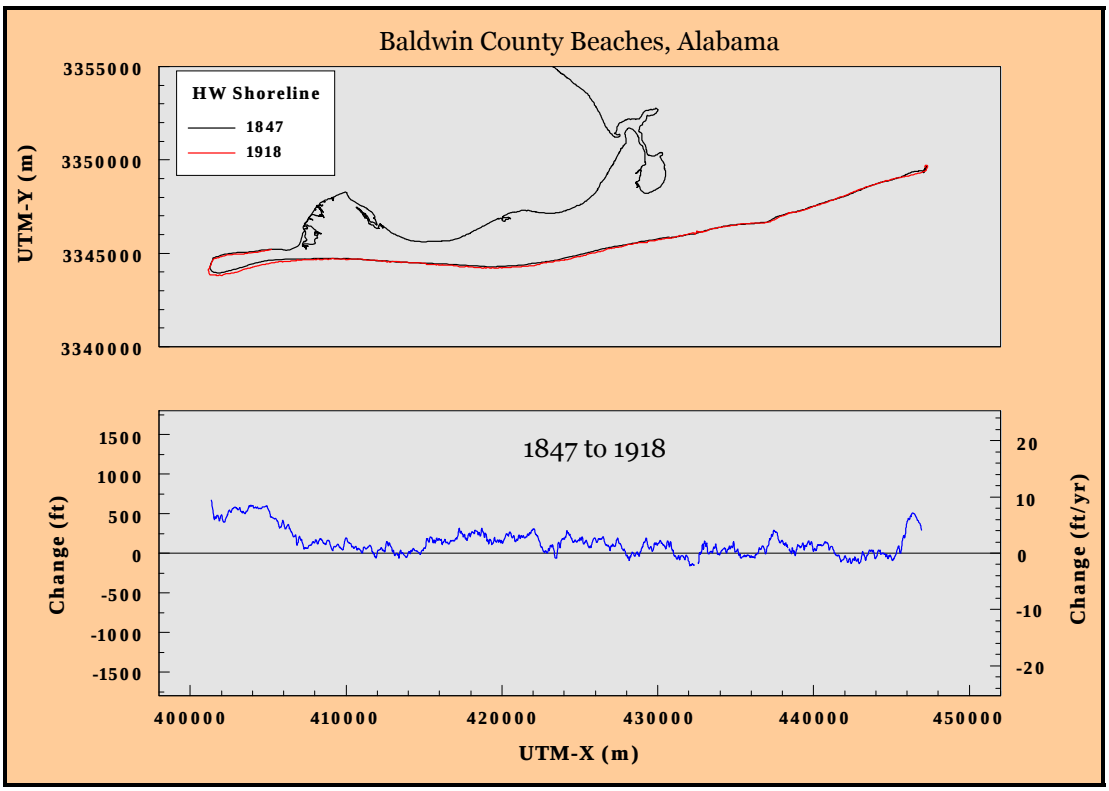

Figure D1. Historical shoreline position change, Perdido Pass to Mobile Point, Alabama: 1847 to 1918.

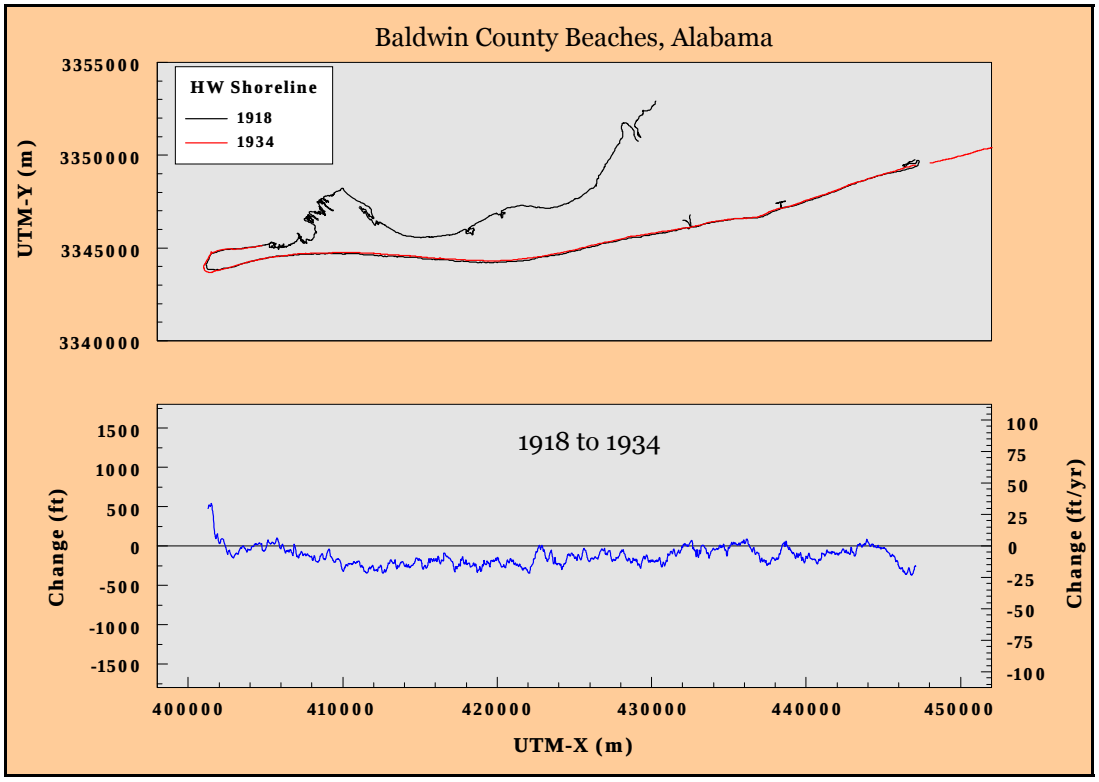

Figure D2. Historical shoreline position change, Perdido Pass to Mobile Point, Alabama: 1918 to 1934.

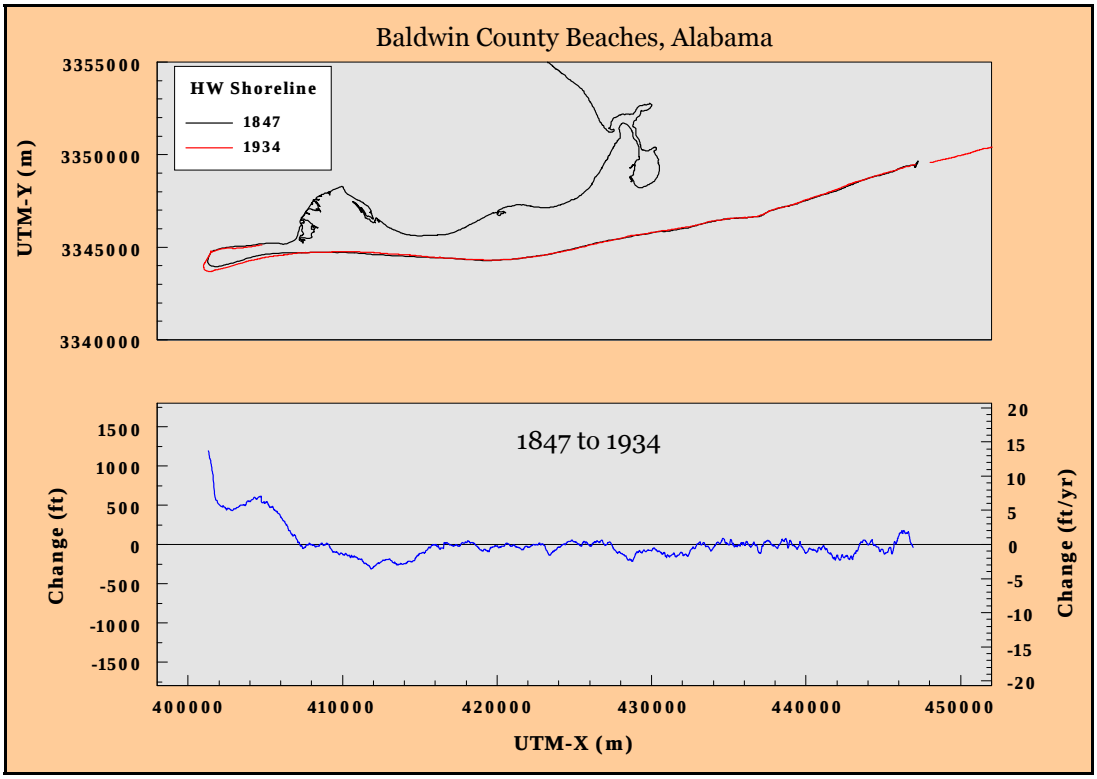

Figure D3. Historical shoreline position change, Perdido Pass to Mobile Point, Alabama: 1847 to 1934.

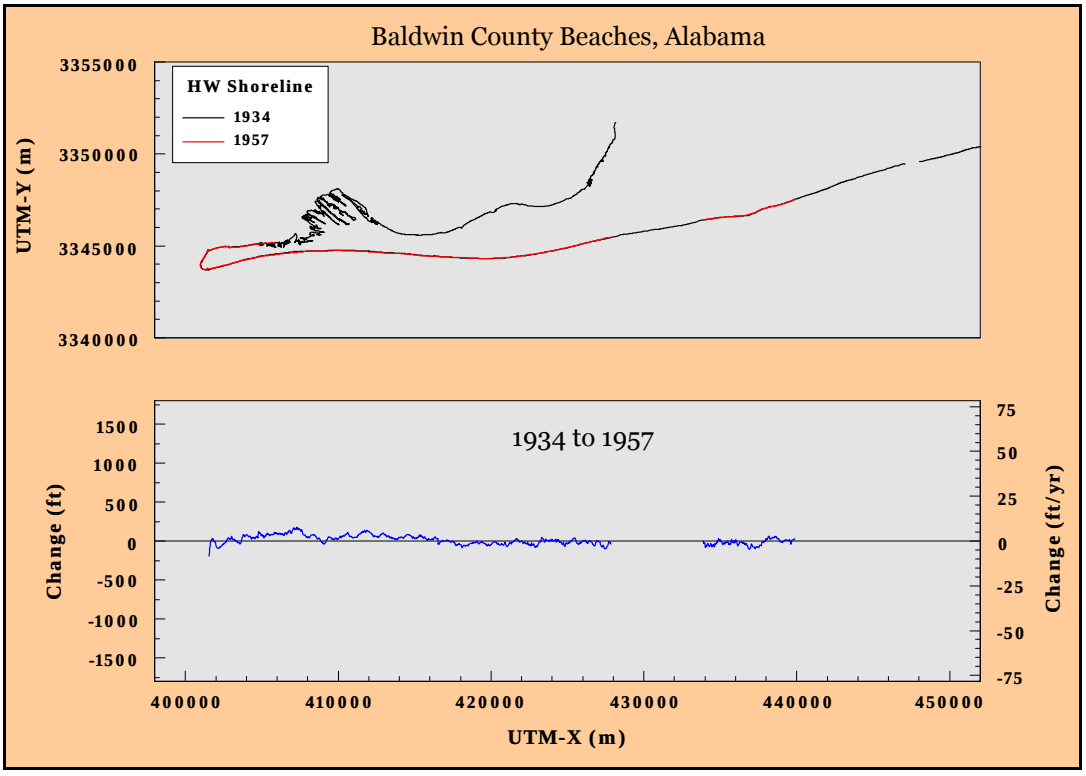

Figure D4. Historical shoreline position change, Perdido Pass to Mobile Point, Alabama: 1934 to 1957.

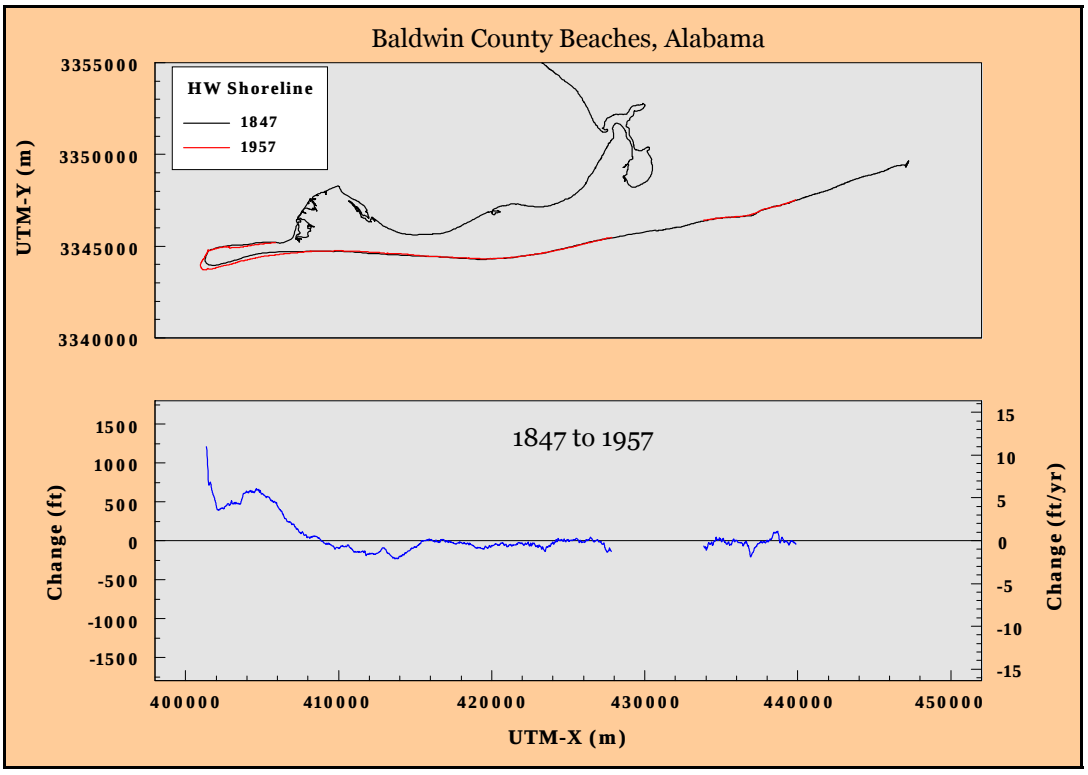

Figure D5. Historical shoreline position change, Perdido Pass to Mobile Point, Alabama: 1847 to 1957.

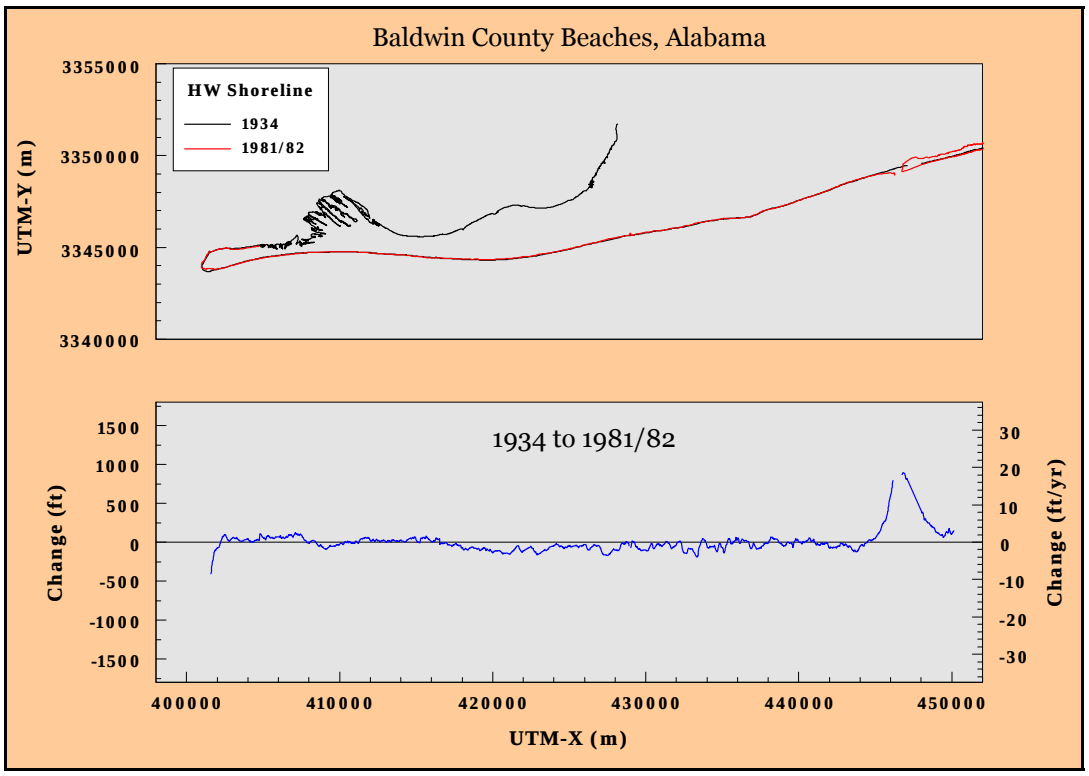

Figure D6. Historical shoreline position change, Perdido Pass to Mobile Point, Alabama: 1934 to 1981/82.

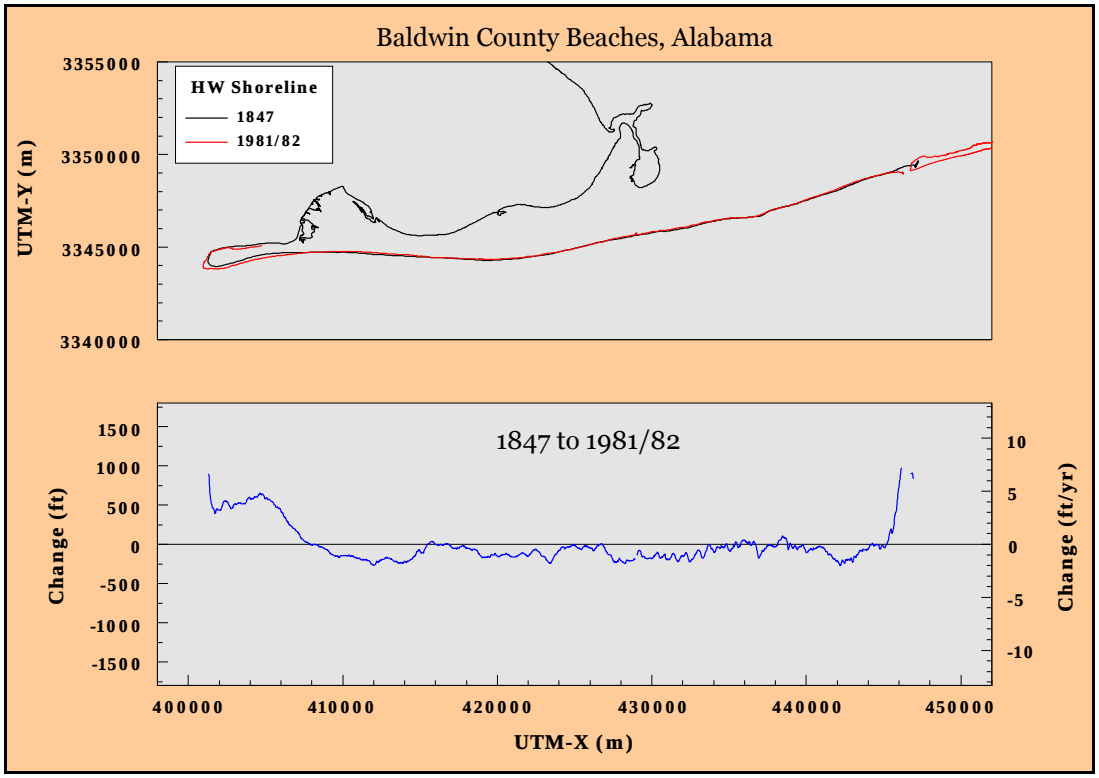

Figure D7. Historical shoreline position change, Perdido Pass to Mobile Point, Alabama: 1847 to 1981/82.

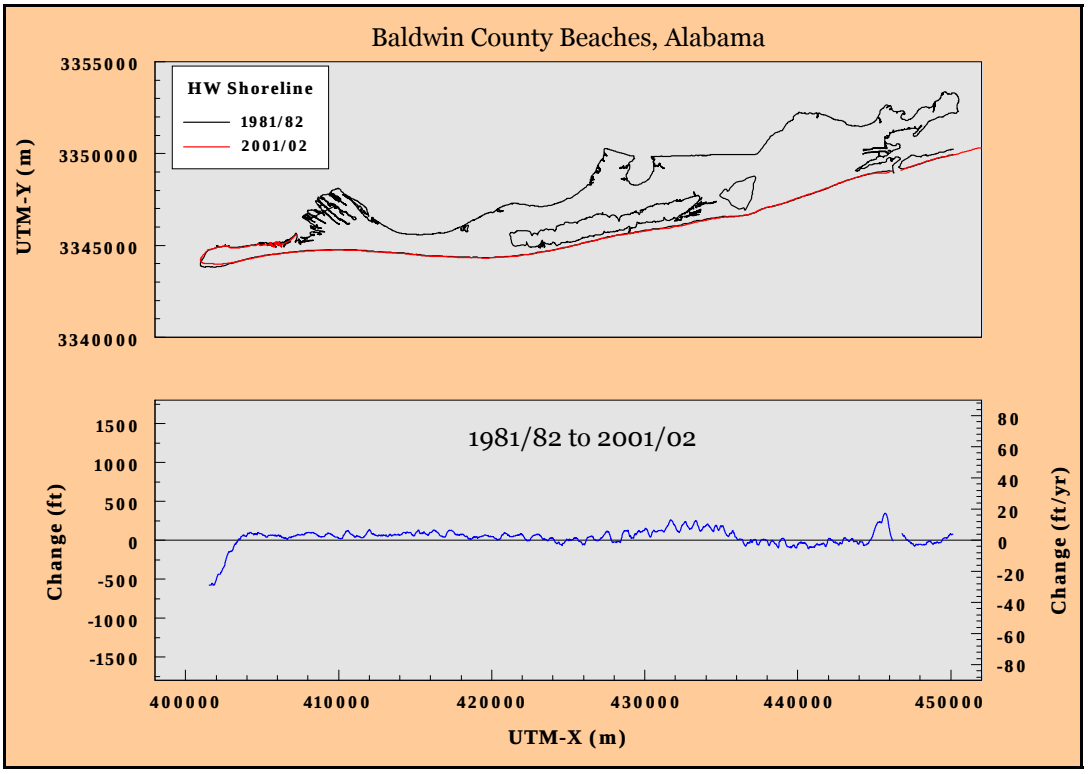

Figure D8. Historical shoreline position change, Perdido Pass to Mobile Point, Alabama: 1981/82 to 2001/02.

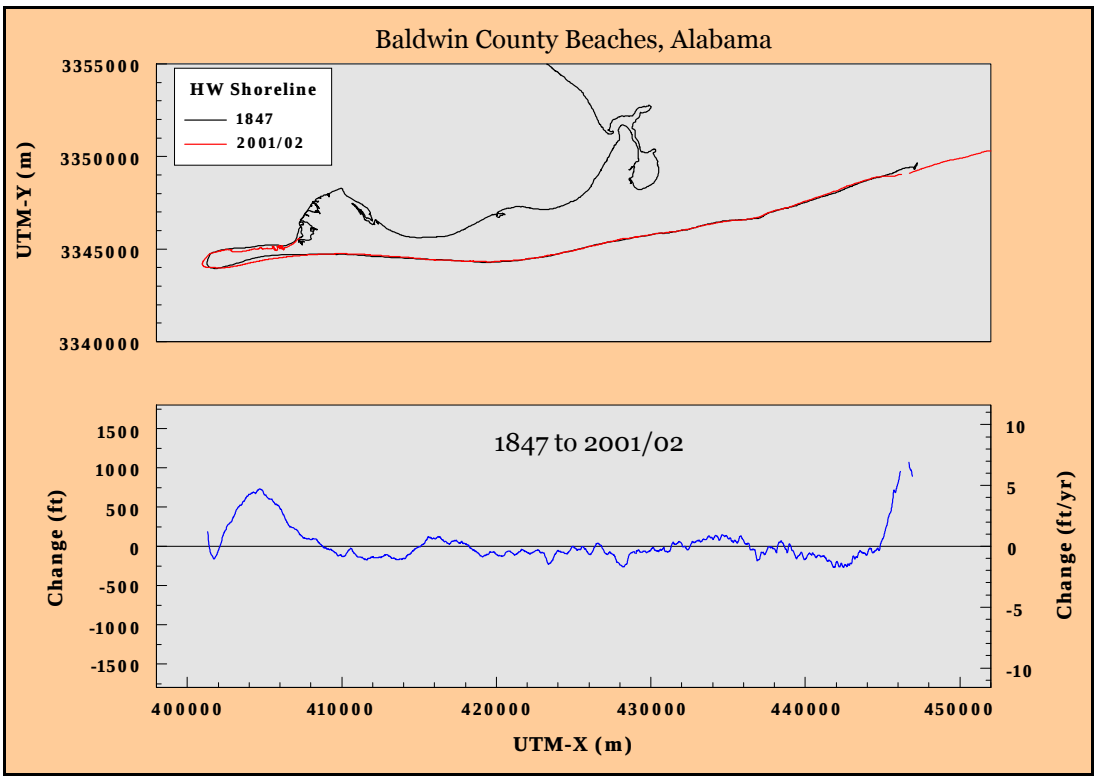

Figure D9. Historical shoreline position change, Perdido Pass to Mobile Point, Alabama: 1847 to 2001/02.

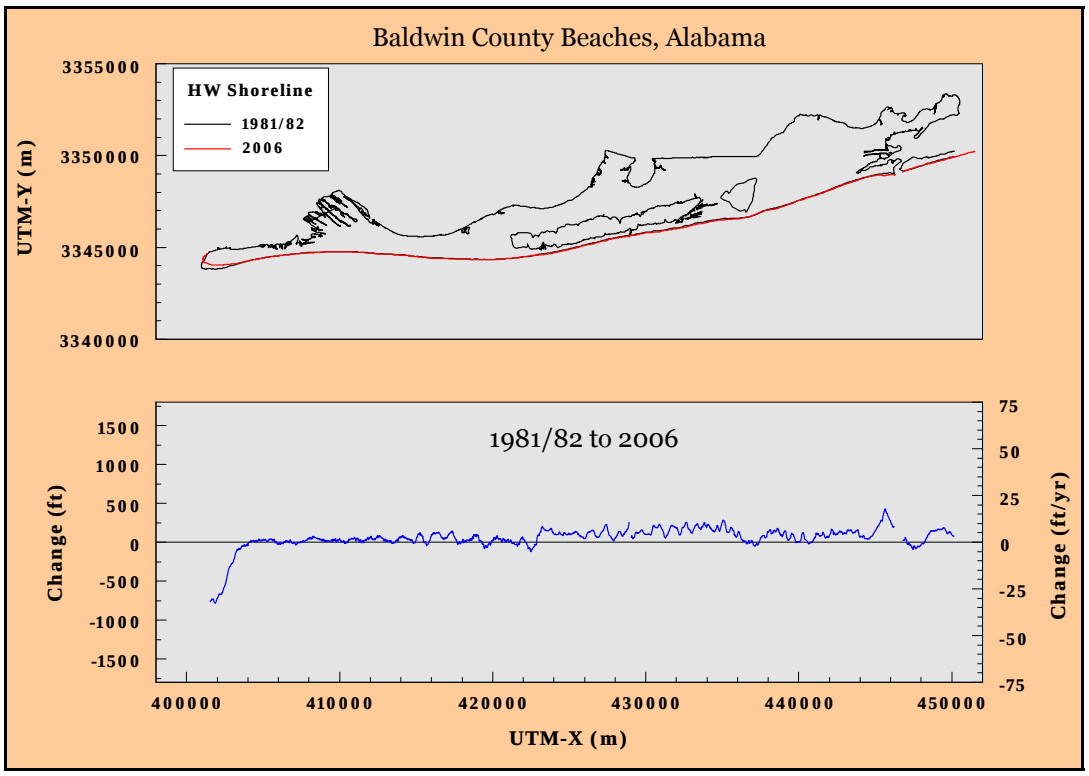

Figure D10. Historical shoreline position change, Perdido Pass to Mobile Point, Alabama: 1981/82 to 2006.

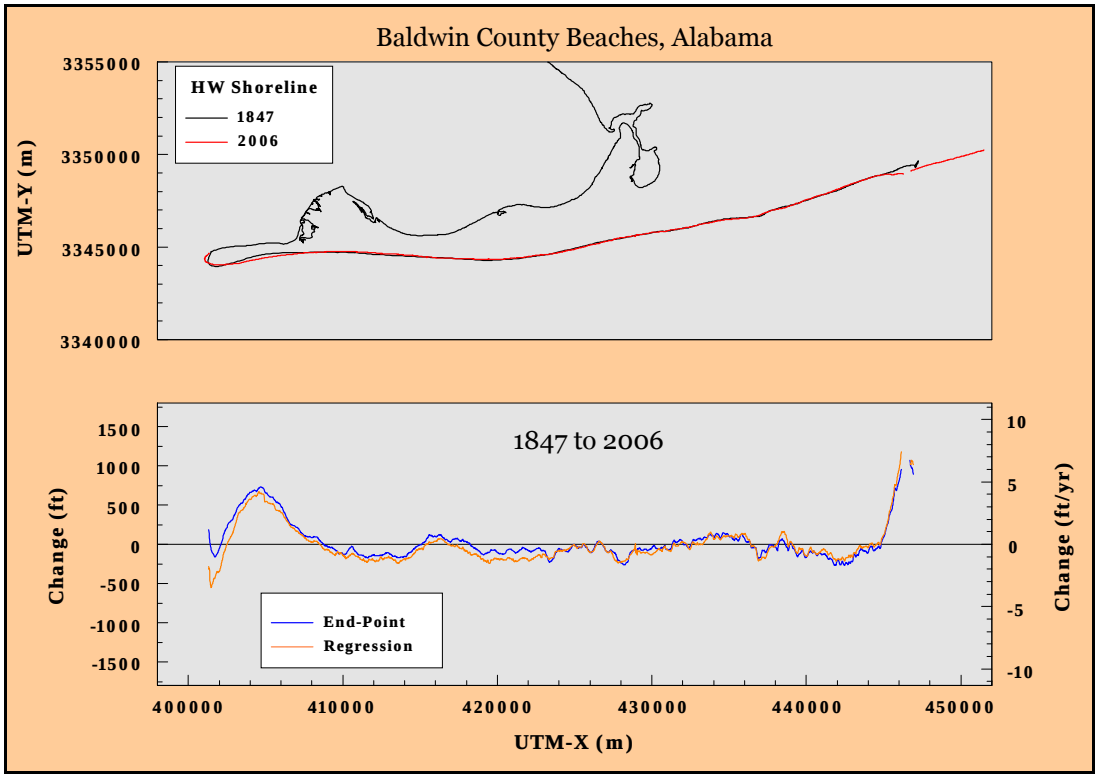

Figure D11. Historical shoreline position change, Perdido Pass to Mobile Point, Alabama: 1847 to 2006.

Appendix E

Shoreline and Bathymetry Data Extents

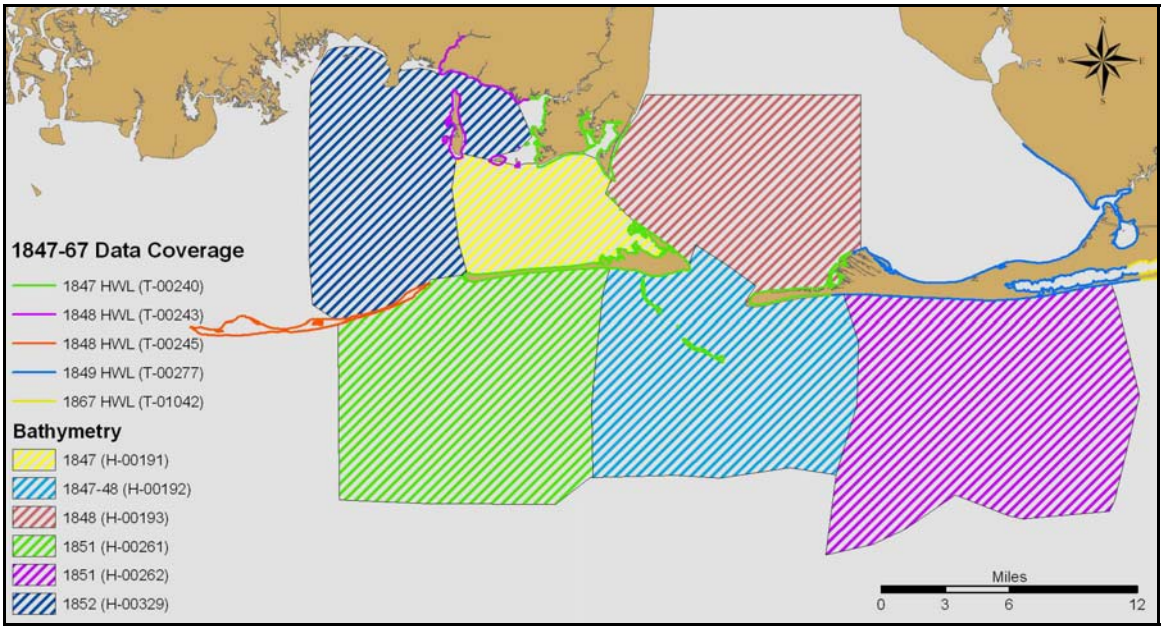

Figure E1. Bathymetry and high-water shoreline data coverage – 1847/52.

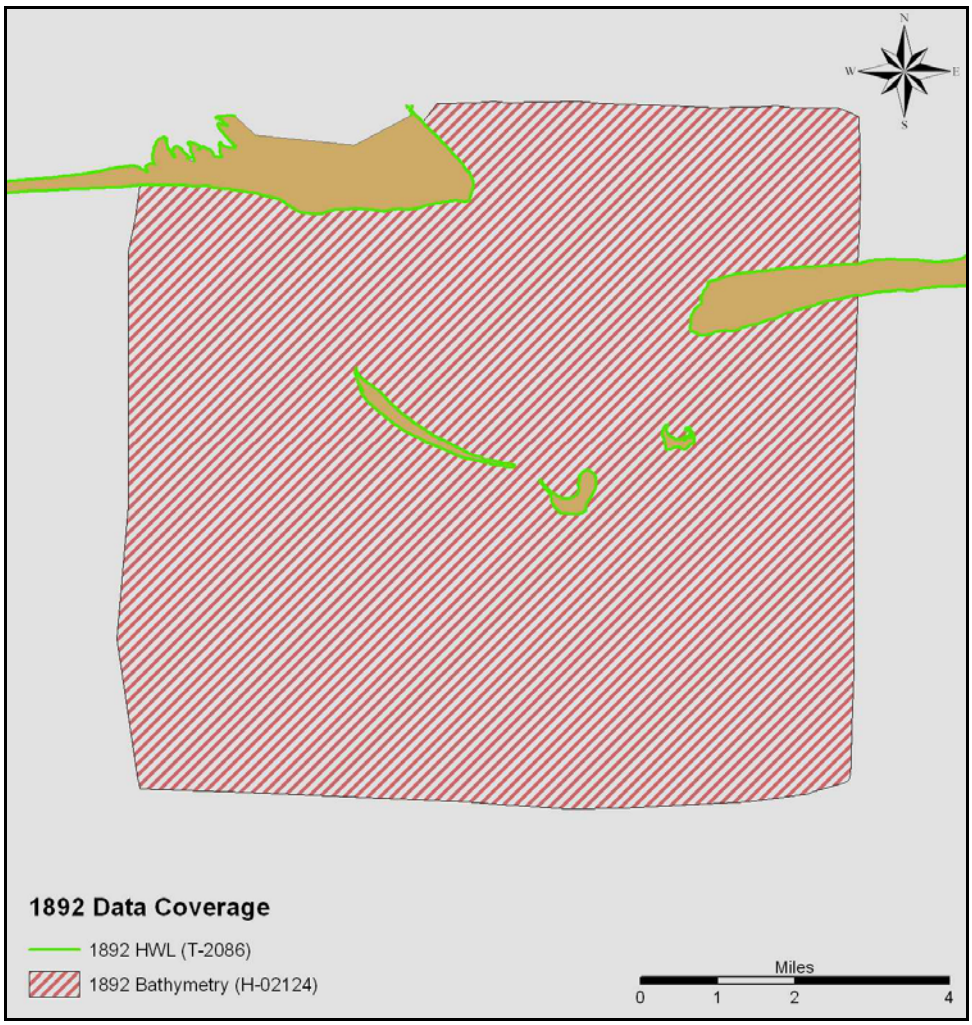

Figure E2. Bathymetry and high-water shoreline data coverage – 1892.

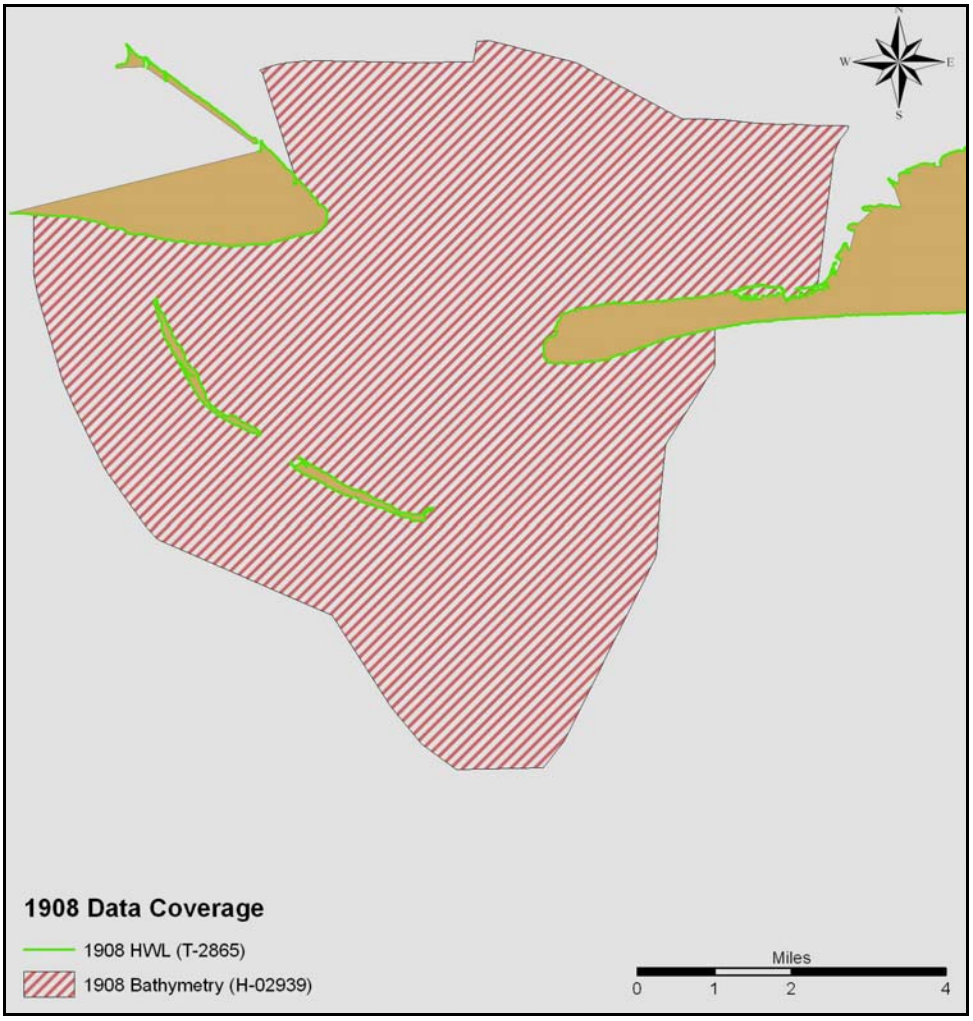

Figure E3. Bathymetry and high-water shoreline data coverage – 1908.

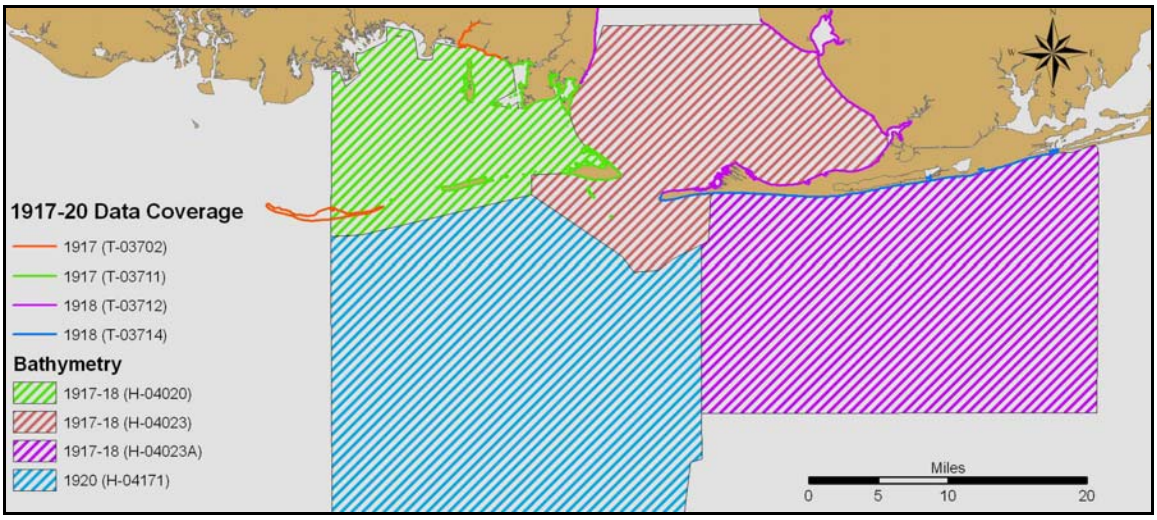

Figure E4. Bathymetry and high-water shoreline data coverage – 1917/20.

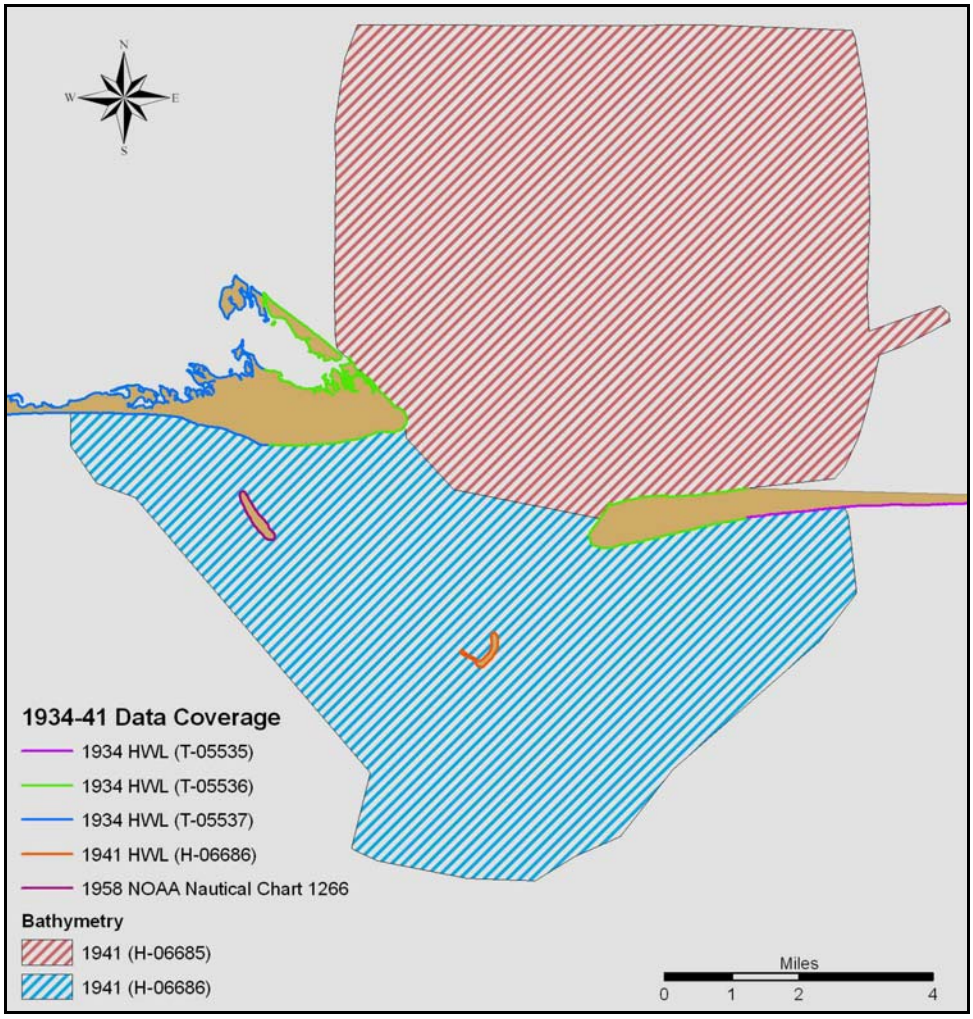

Figure E5. Bathymetry and high-water shoreline data coverage – 1941.

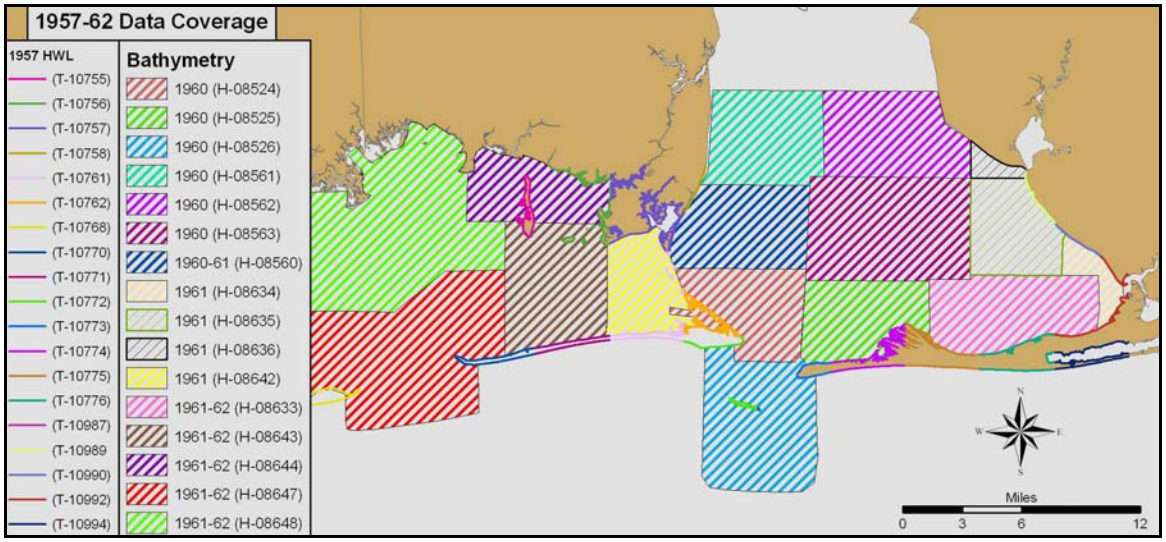

Figure E6. Bathymetry and high-water shoreline data coverage – 1957/62.

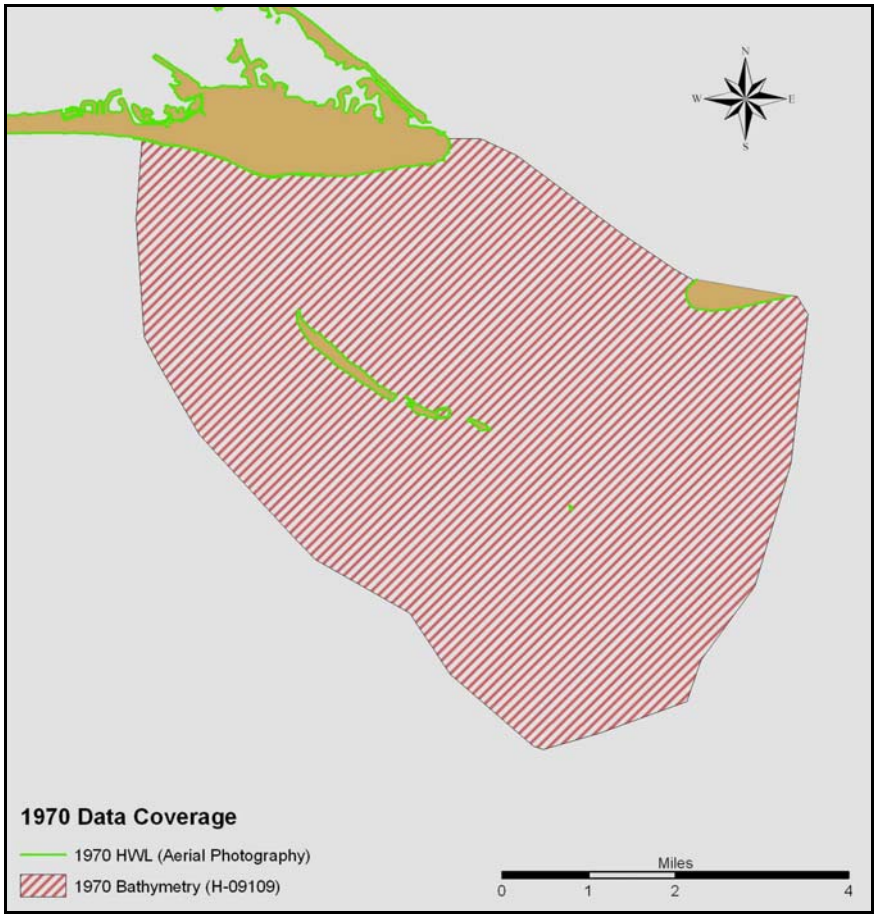

Figure E7. Bathymetry and high-water shoreline data coverage – 1970.

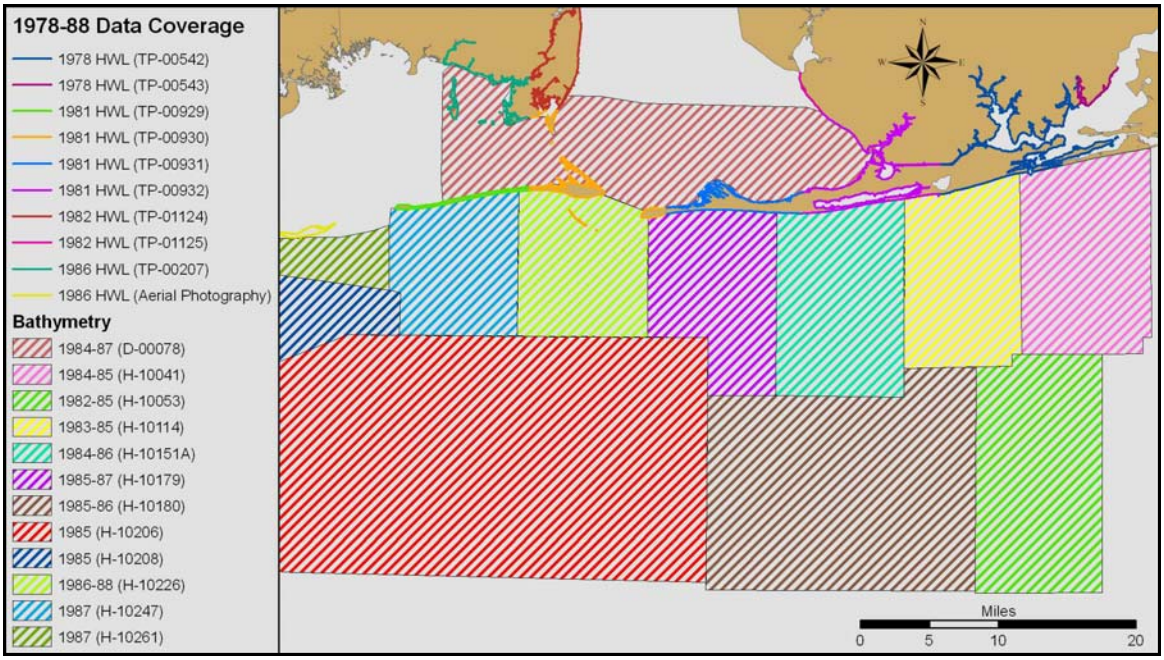

Figure E8. Bathymetry and high-water shoreline data coverage – 1978/88.

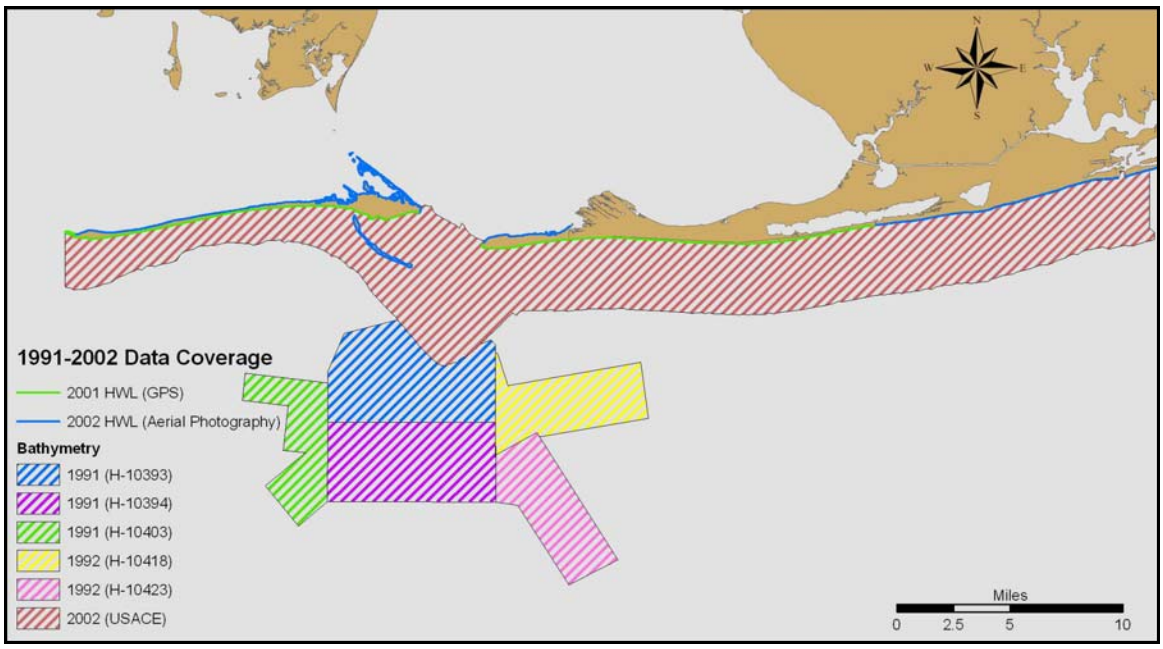

Figure E9. Bathymetry and high-water shoreline data coverage – 1991/2002.

Appendix F

Ebb-Tidal Delta Volume Calculation Extents

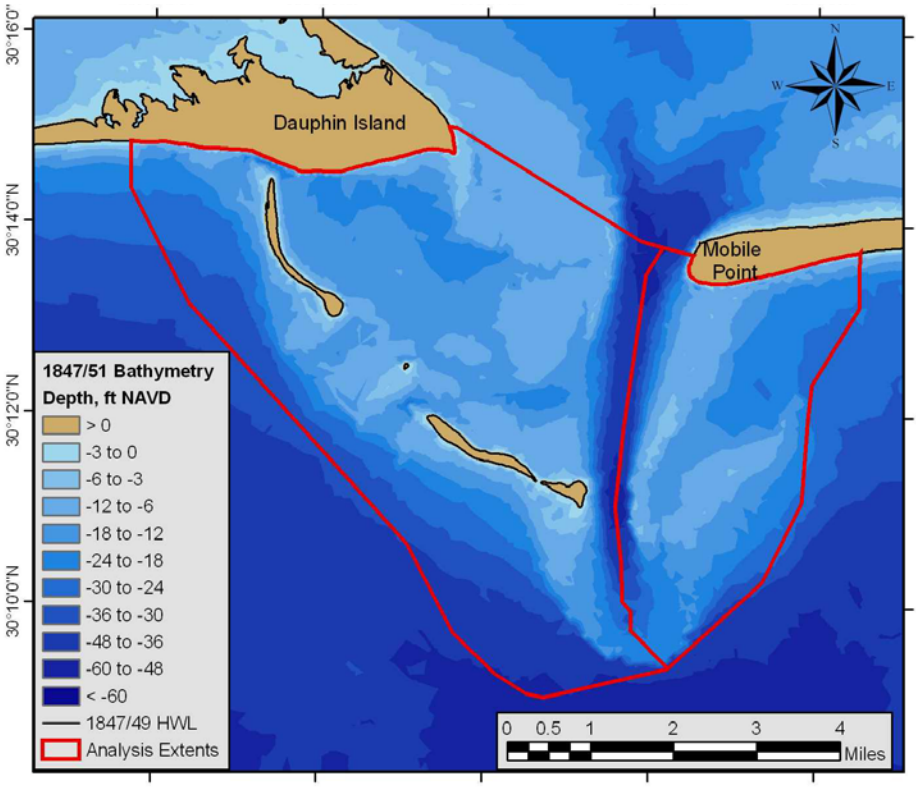

Figure F1. Analysis extent for calculating sand volume above the 30-ft depth contour – 1847/48.

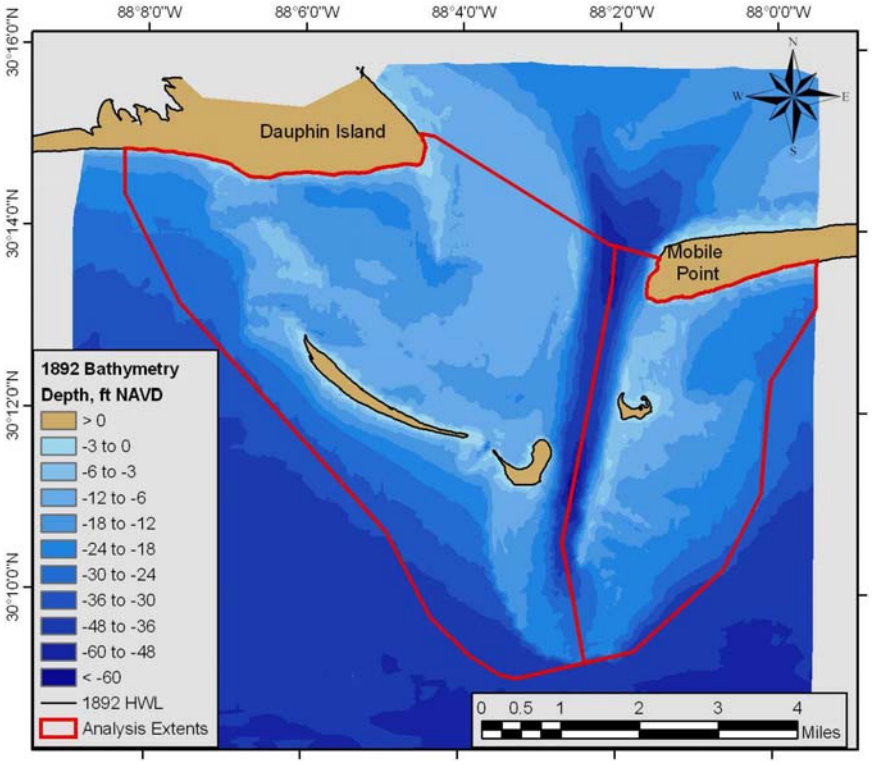

Figure F2. Analysis extent for calculating sand volume above the 30-ft depth contour – 1892.

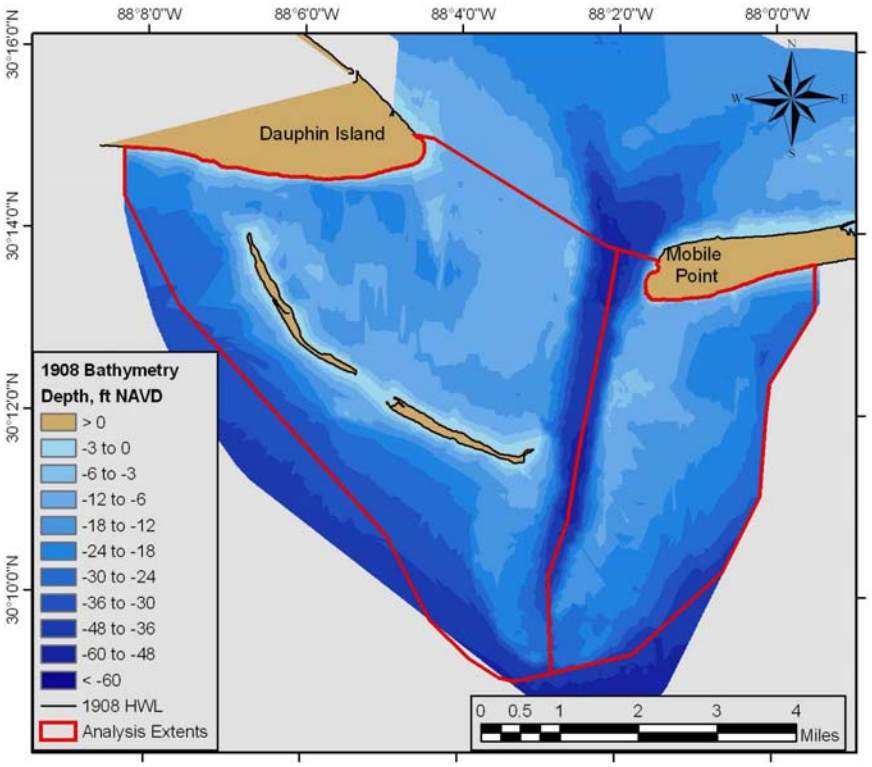

Figure F3. Analysis extent for calculating sand volume above the 30-ft depth contour – 1908.

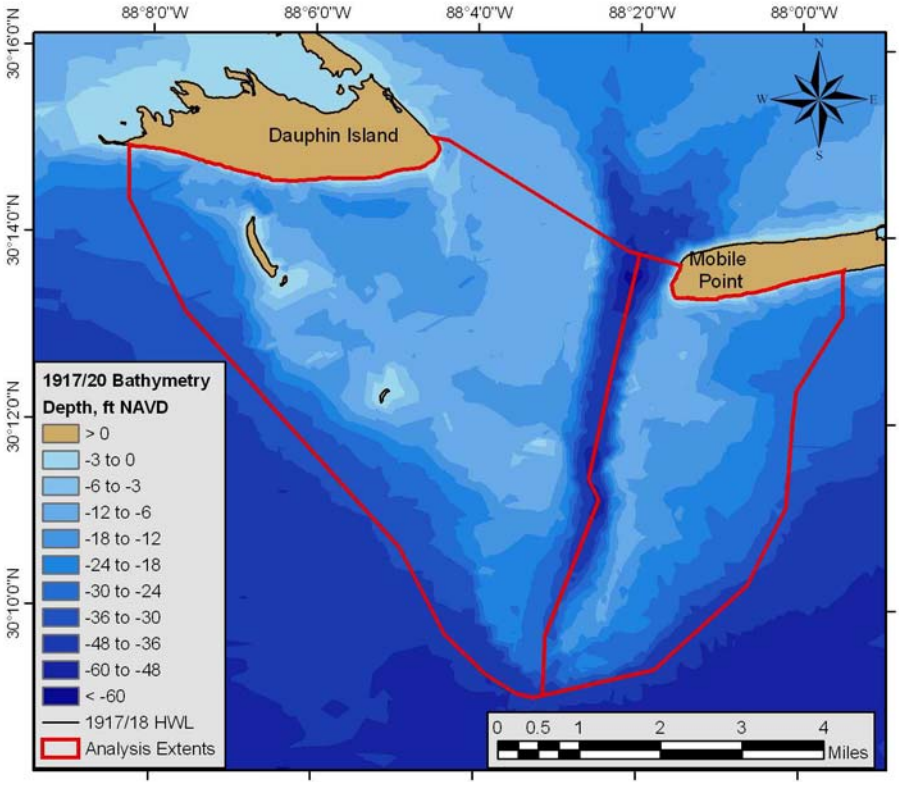

Figure F4. Analysis extent for calculating sand volume above the 30-ft depth contour – 1917/20.

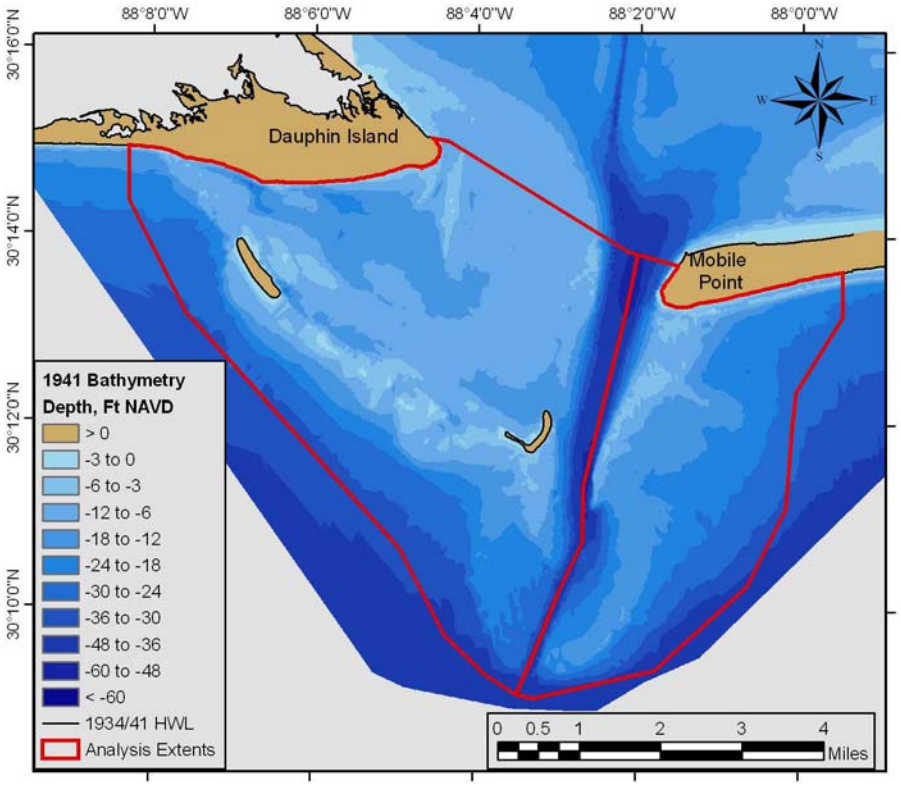

Figure F5. Analysis extent for calculating sand volume above the 30-ft depth contour – 1941.

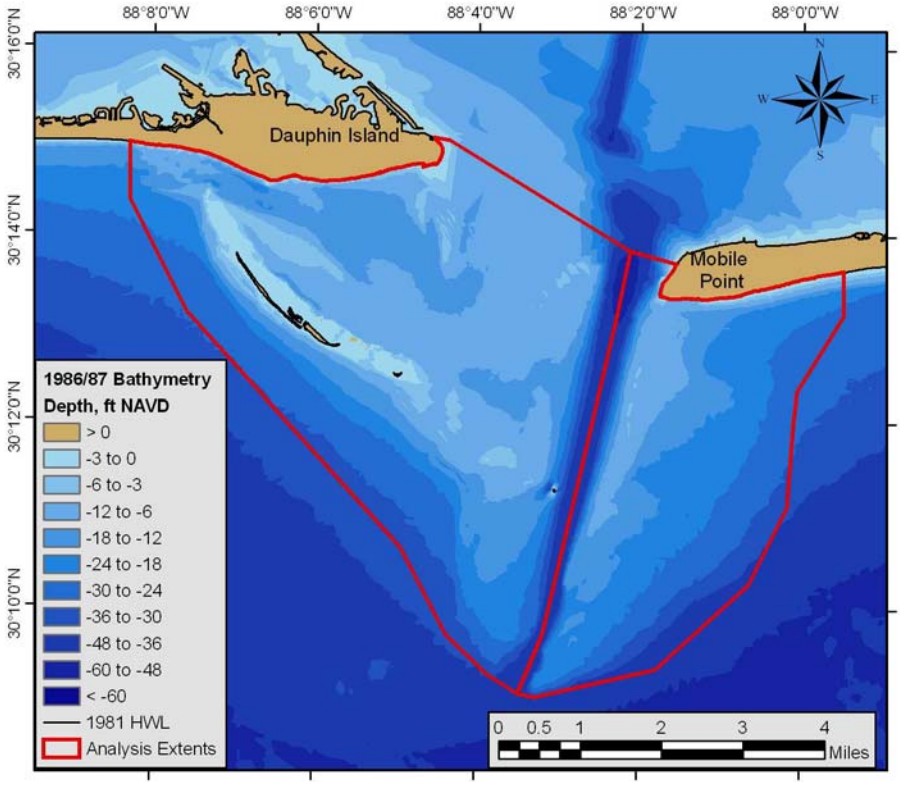

Figure F6. Analysis extent for calculating sand volume above the 30-ft depth contour – 1986/87.

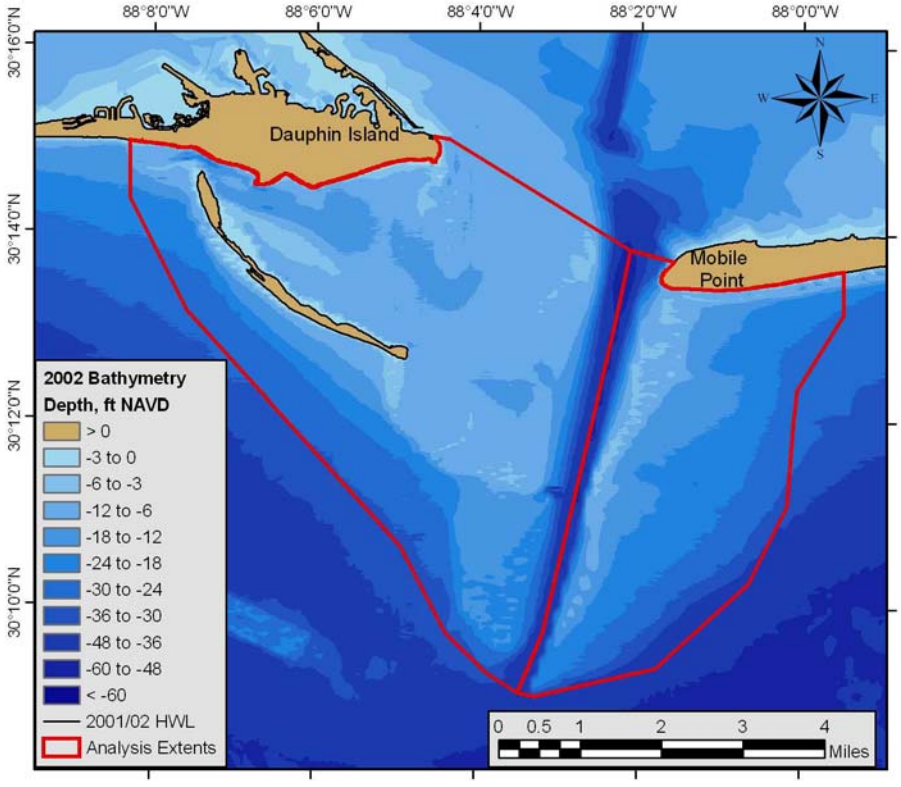

Figure F7. Analysis extent for calculating sand volume above the 30-ft depth contour – 2002.

Appendix G

Bathymetric Change Volume Calculation Extents for Mobile Ebb-Tidal Delta

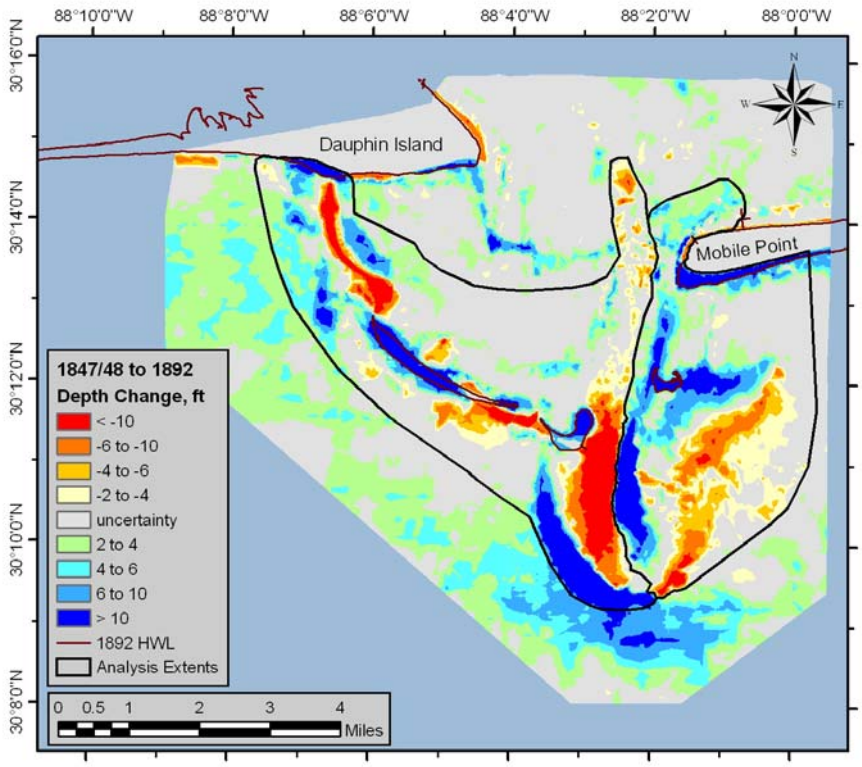

Figure G1. Analysis extent for calculating sand volume change – 1847/48 to 1892.

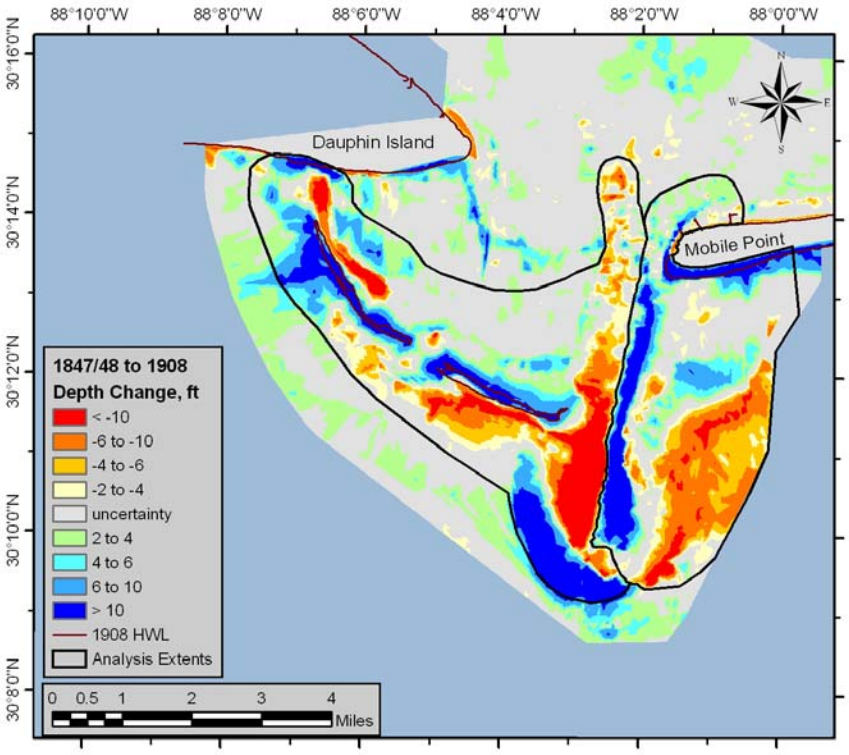

Figure G2. Analysis extent for calculating sand volume change – 1847/48 to 1908.

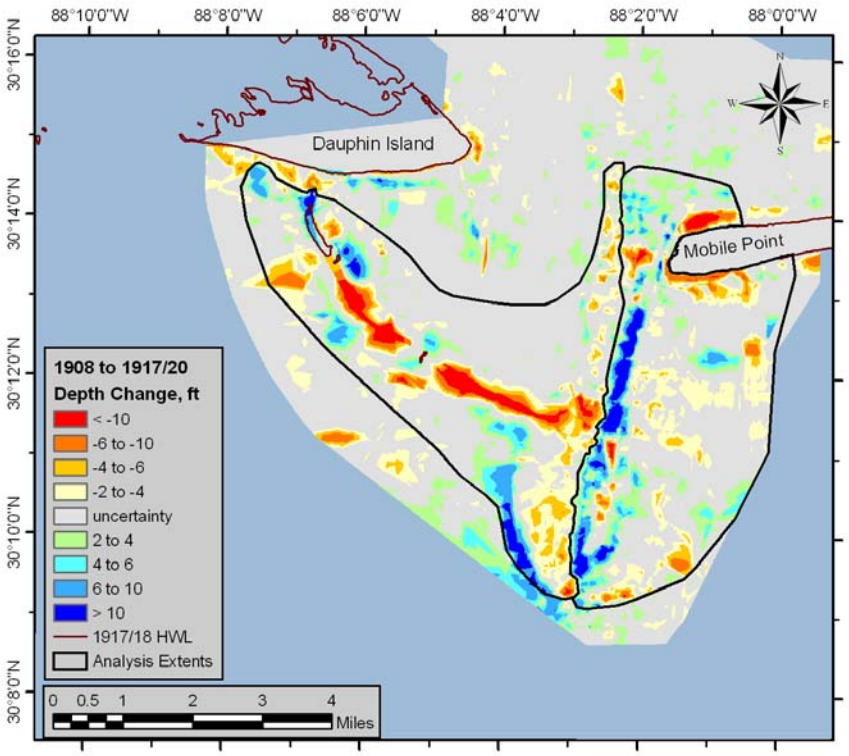

Figure G3. Analysis extent for calculating sand volume change – 1908 to 1917/20.

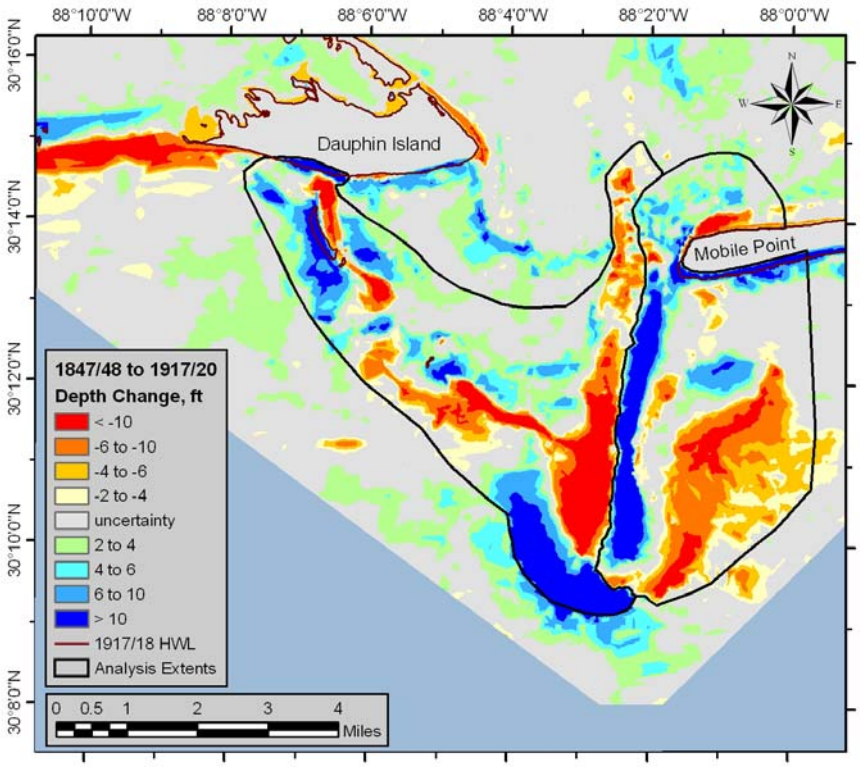

Figure G4. Analysis extent for calculating sand volume change – 1847/48 to 1917/20.

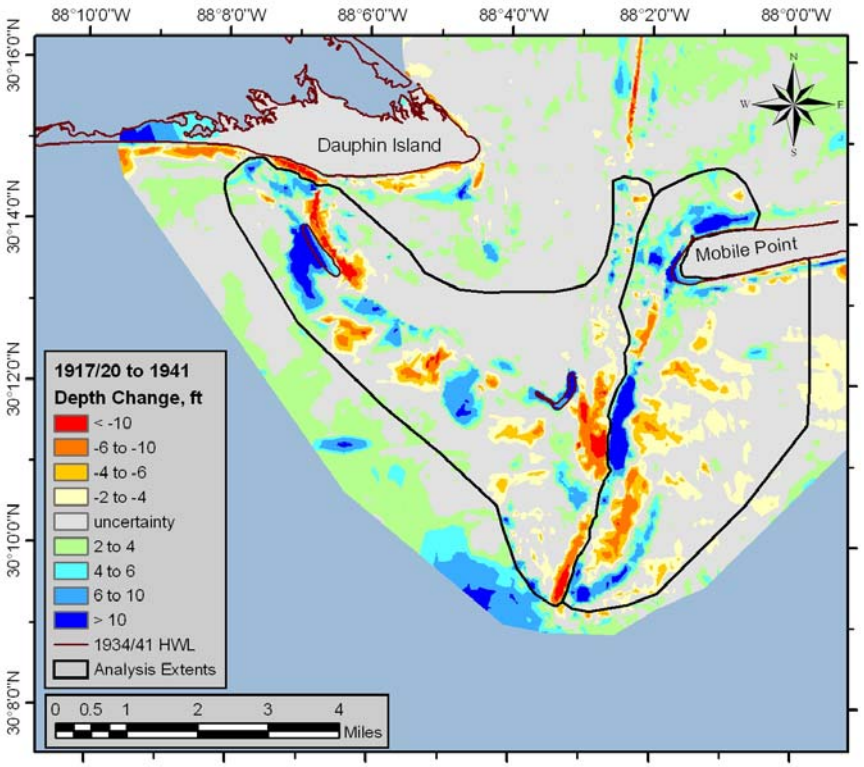

Figure G5. Analysis extent for calculating sand volume change – 1917/20 to 1941.

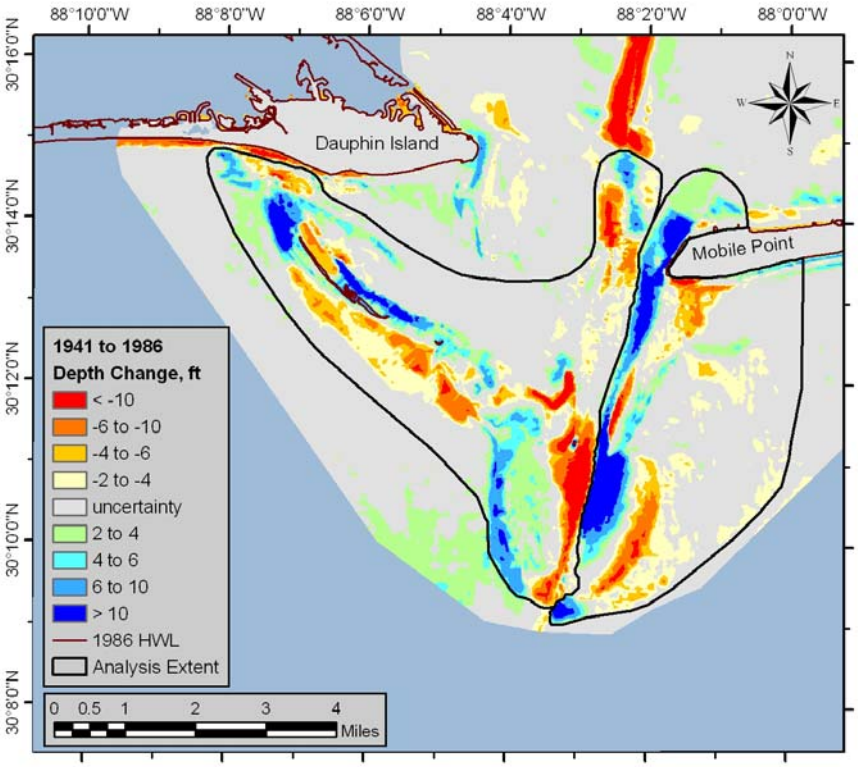

Figure G6. Analysis extent for calculating sand volume change – 1941 to 1986.

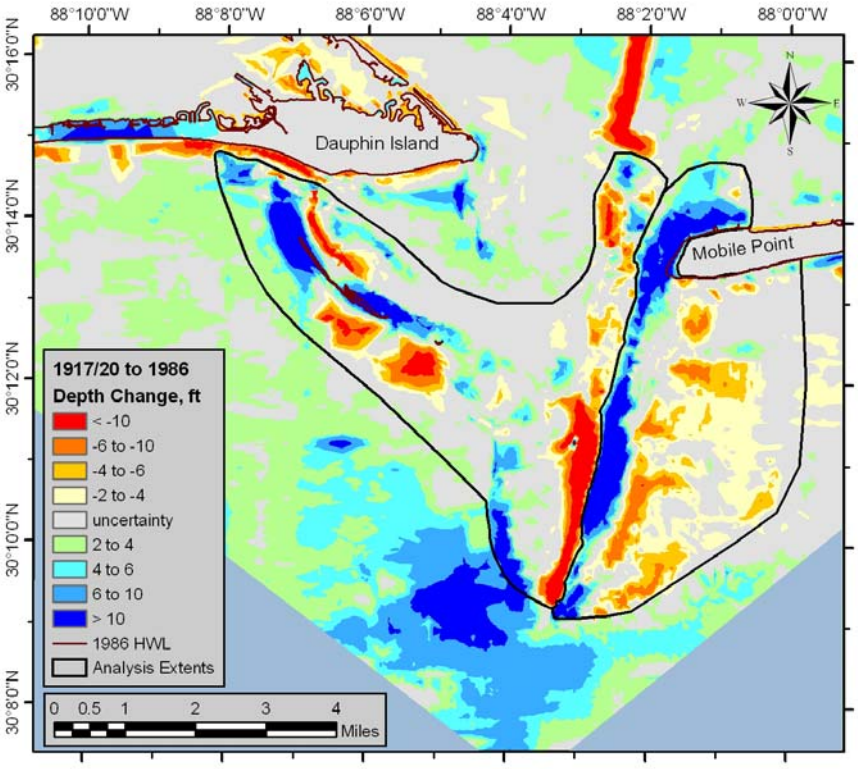

Figure G7. Analysis extent for calculating sand volume change – 1917/20 to 1986.

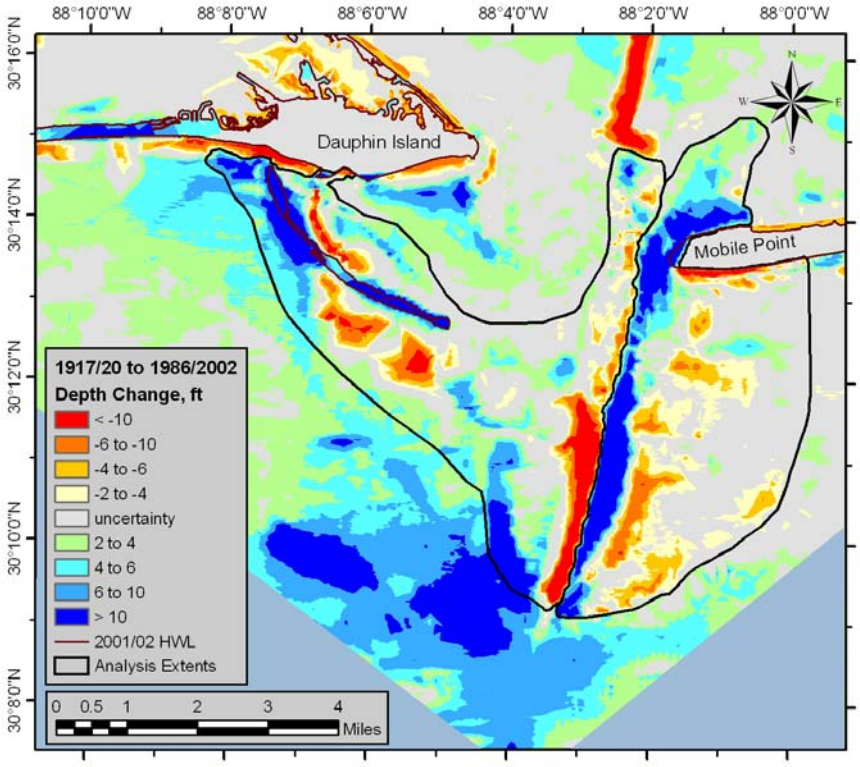

Figure G8. Analysis extent for calculating sand volume change – 1917/20 to 2002.

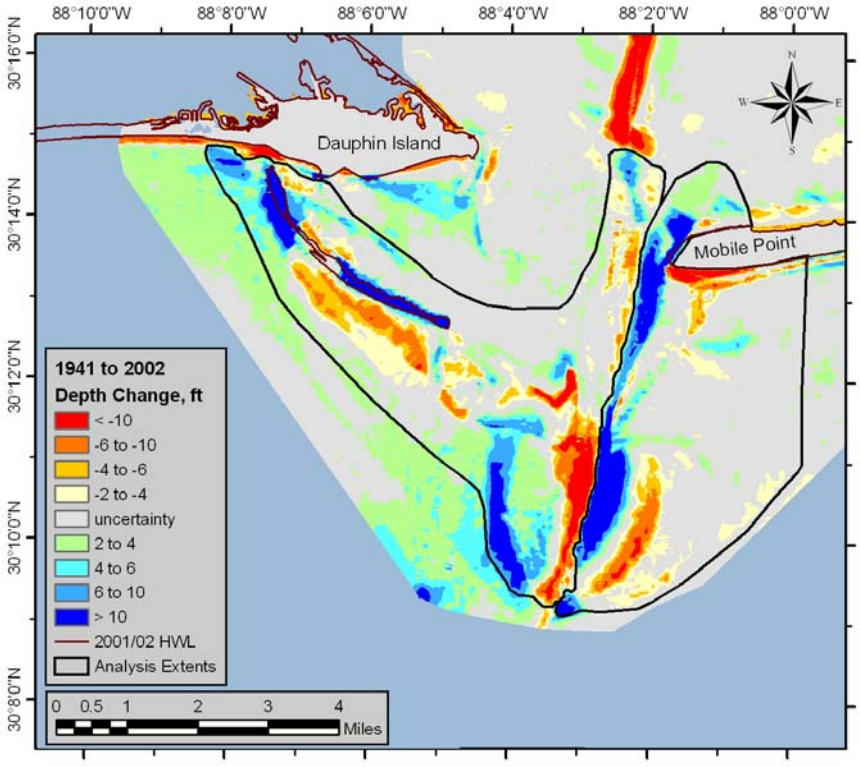

Figure G9. Analysis extent for calculating sand volume change – 1941 to 2002.

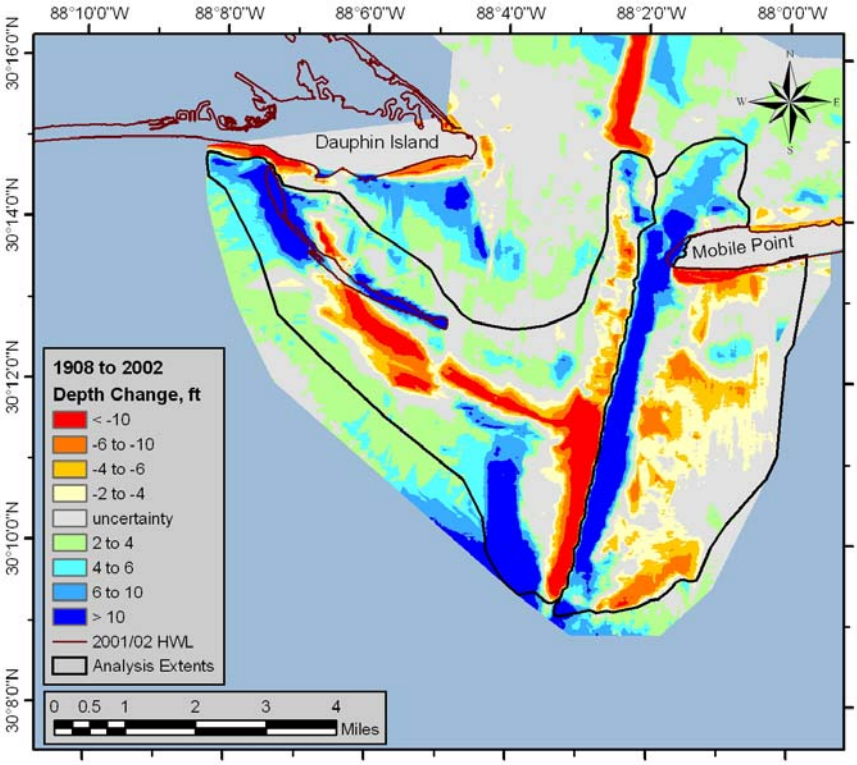

Figure G10. Analysis extent for calculating sand volume change – 1908 to 2002.

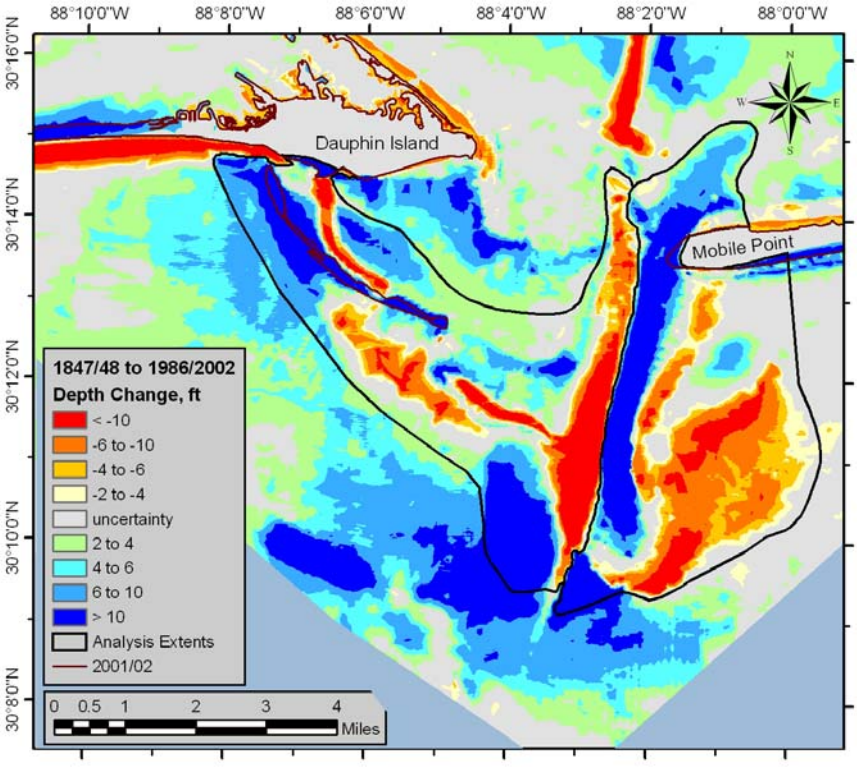

Figure G11. Analysis extent for calculating sand volume change – 1847/48 to 2002.

Appendix H

STWAVE Modeling Results

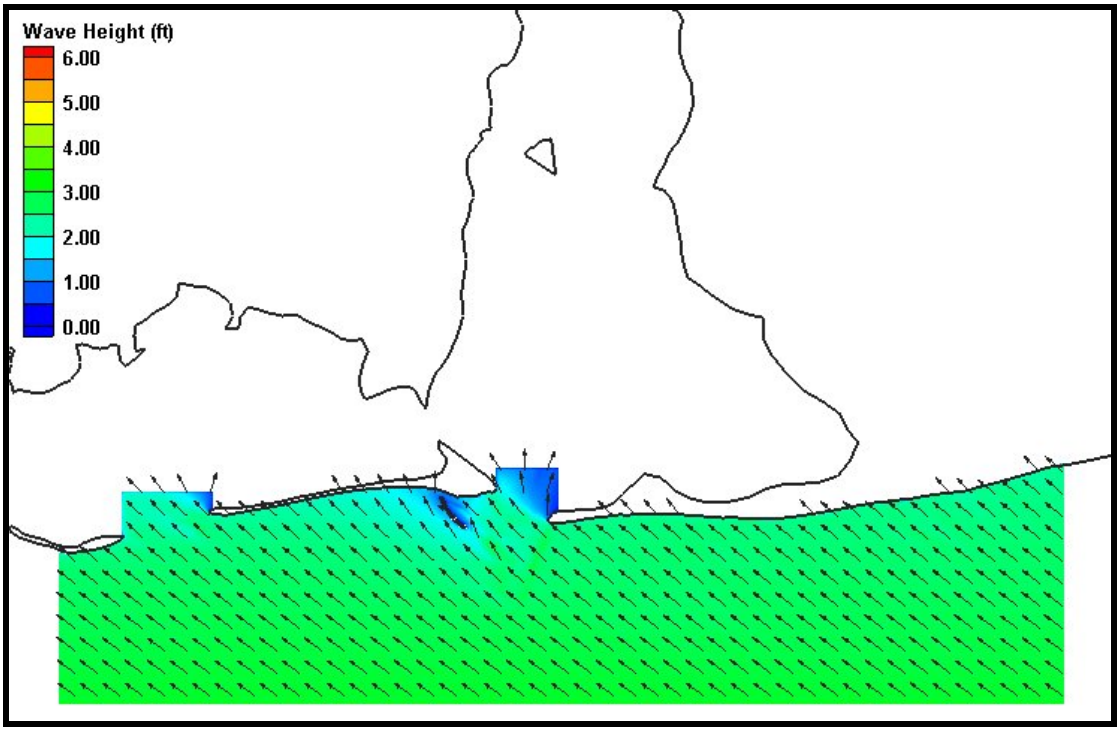

Figure H1. Coarse grid (200m x 200m) wave results for Case 1. Wave heights are shown by color while wave direction is indicated by the arrow direction.

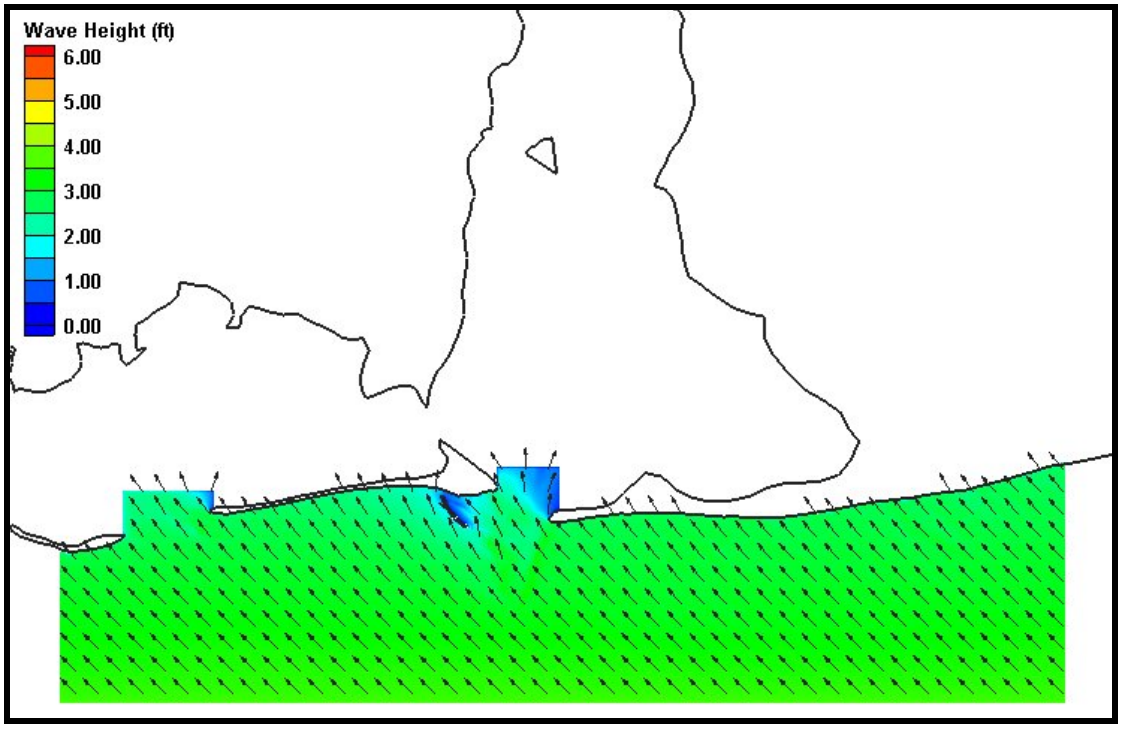

Figure H2. Coarse grid (200m x 200m) wave results for Case 2. Wave heights are shown by color while wave direction is indicated by the arrow direction.

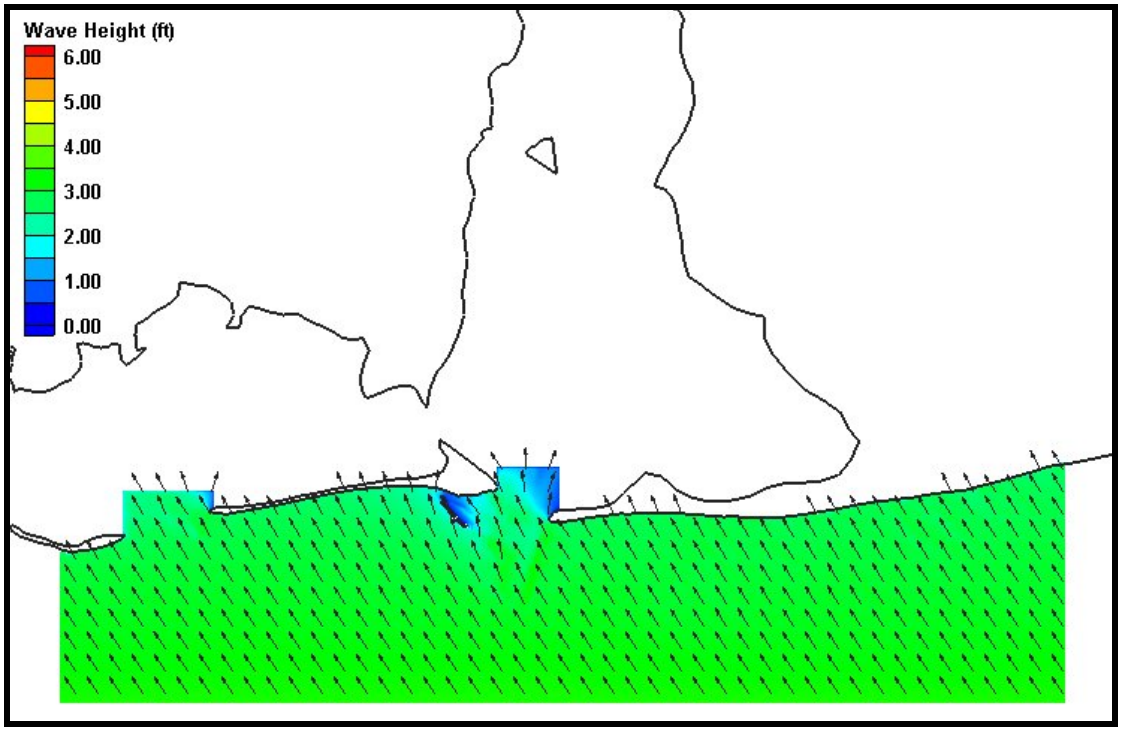

Figure H3. Coarse grid (200m x 200m) wave results for Case 3. Wave heights are shown by color while wave direction is indicated by the arrow direction.

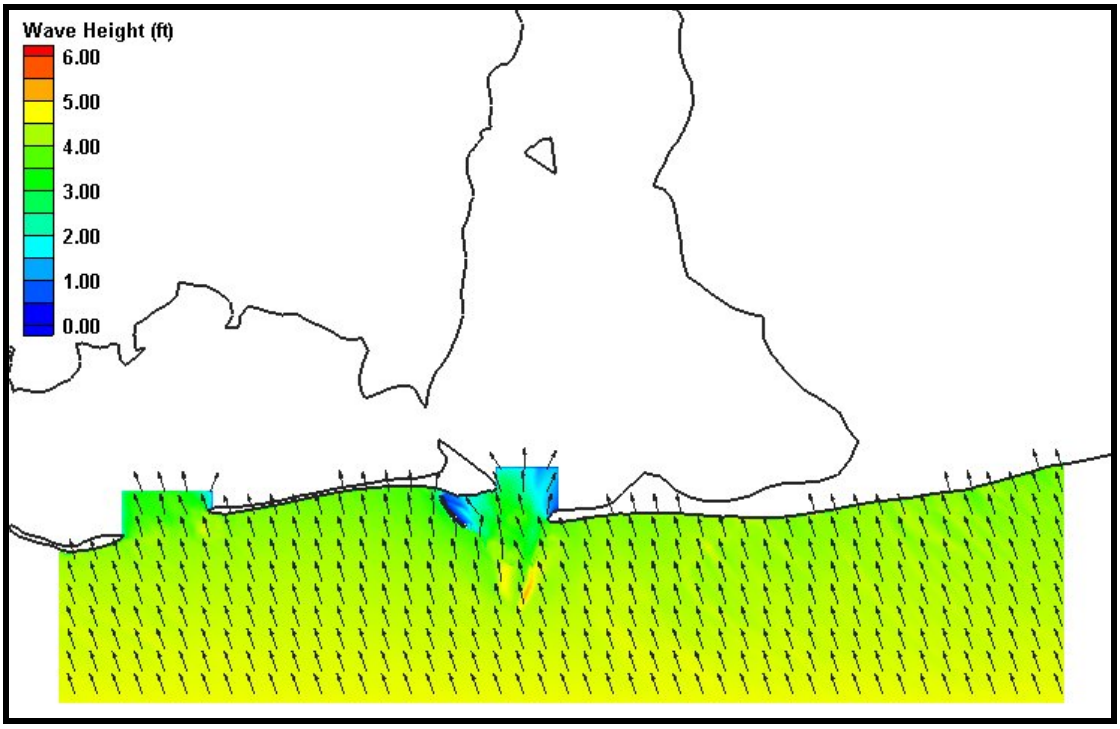

Figure H4. Coarse grid (200m x 200m) wave results for Case 4. Wave heights are shown by color while wave direction is indicated by the arrow direction.

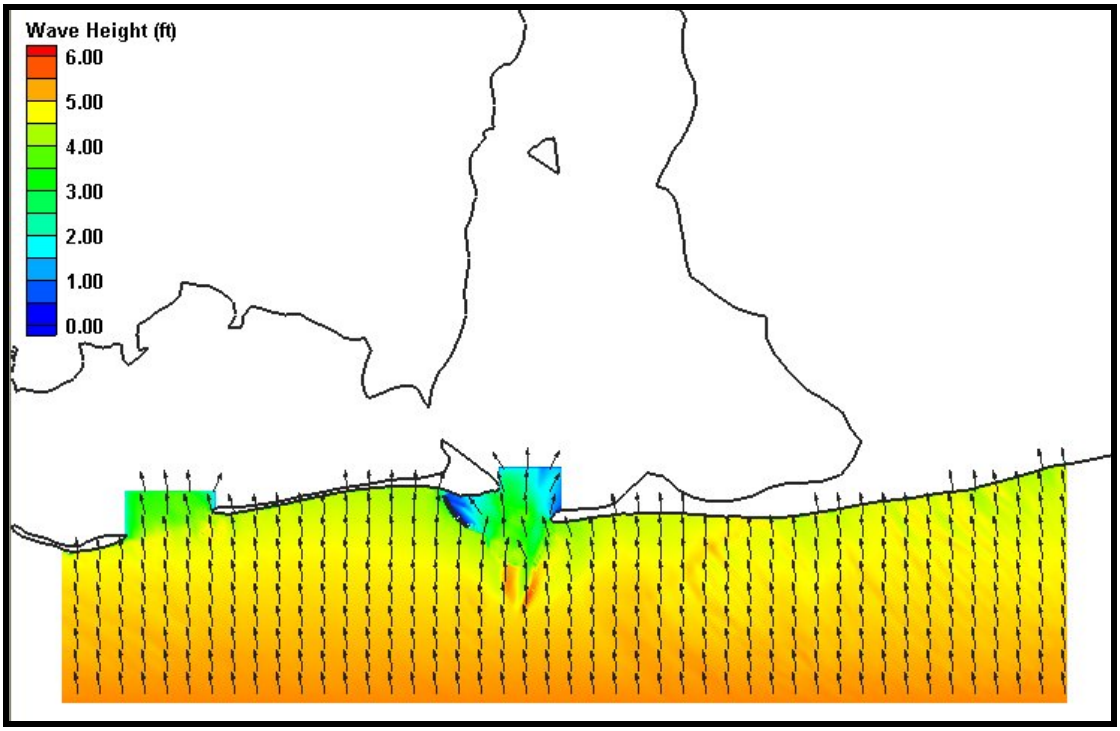

Figure H5. Coarse grid (200m x 200m) wave results for Case 5. Wave heights are shown by color while wave direction is indicated by the arrow direction.

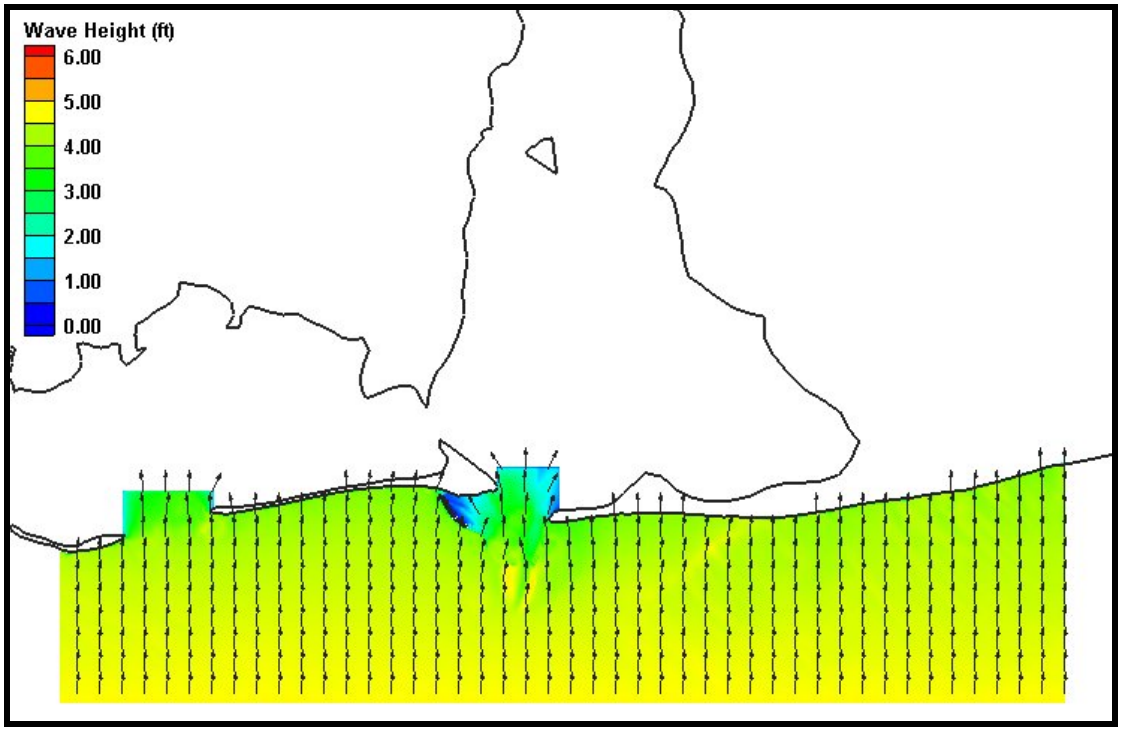

Figure H6. Coarse grid (200m x 200m) wave results for Case 6. Wave heights are shown by color while wave direction is indicated by the arrow direction.

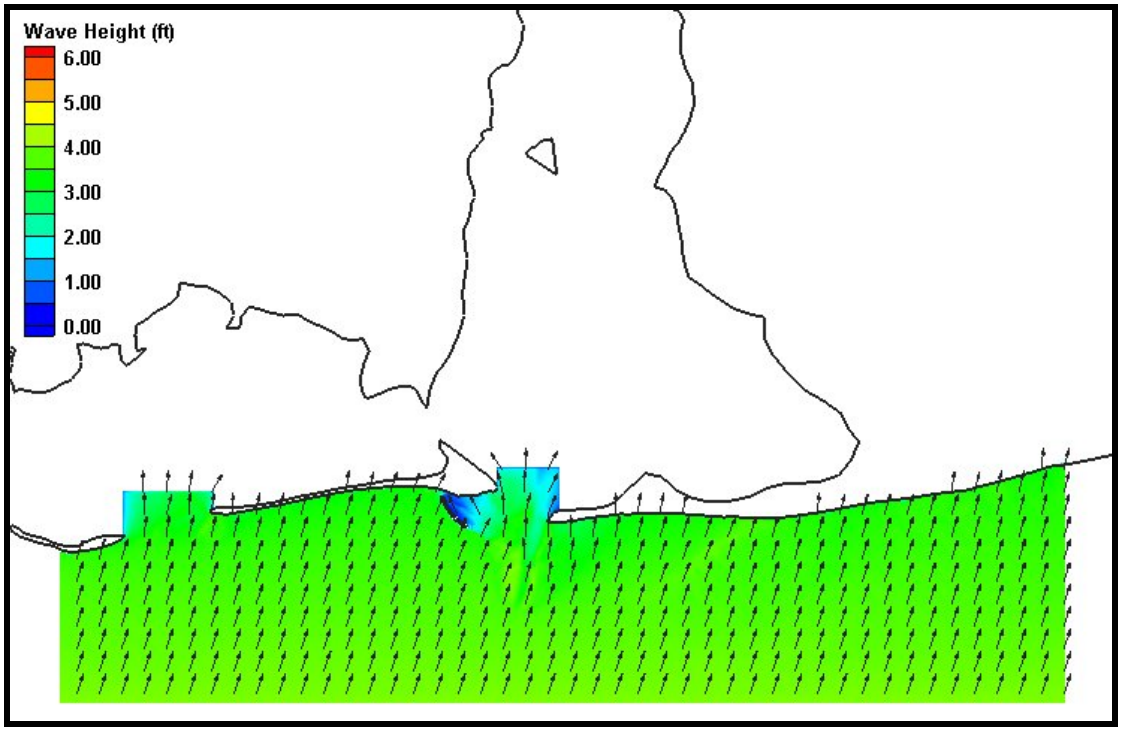

Figure H7. Coarse grid (200m x 200m) wave results for Case 7. Wave heights are shown by color while wave direction is indicated by the arrow direction.

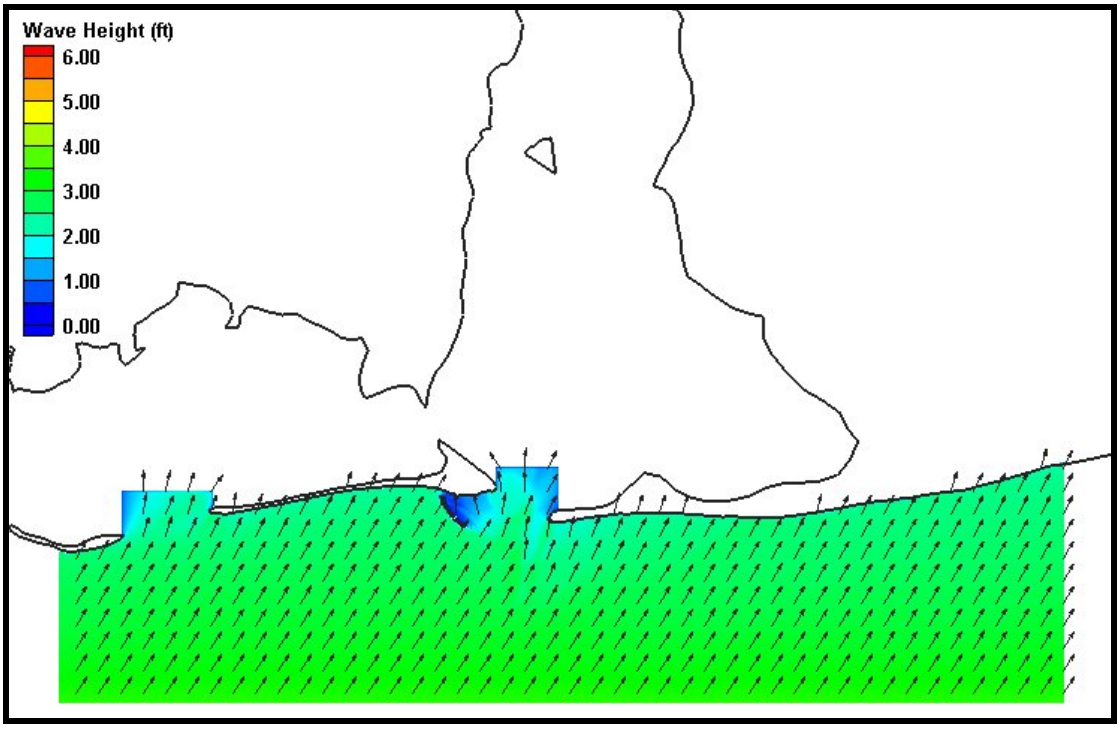

Figure H8. Coarse grid (200m x 200m) wave results for Case 8. Wave heights are shown by color while wave direction is indicated by the arrow direction.

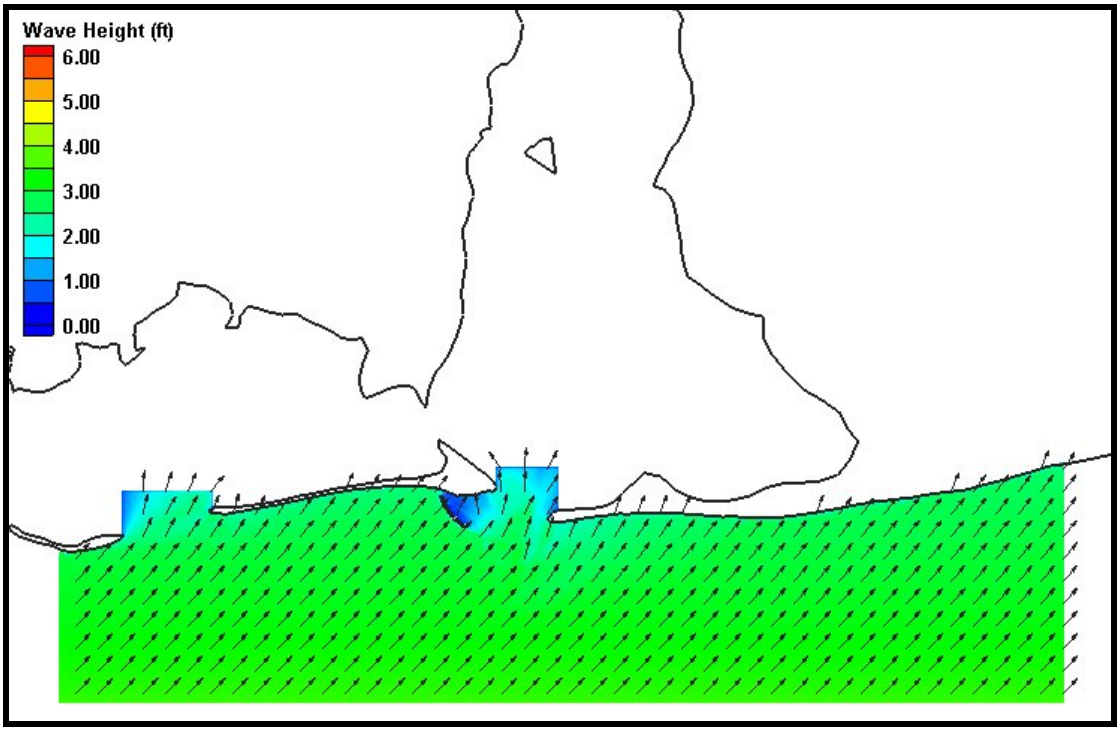

Figure H9. Coarse grid (200m x 200m) wave results for Case 9. Wave heights are shown by color while wave direction is indicated by the arrow direction.

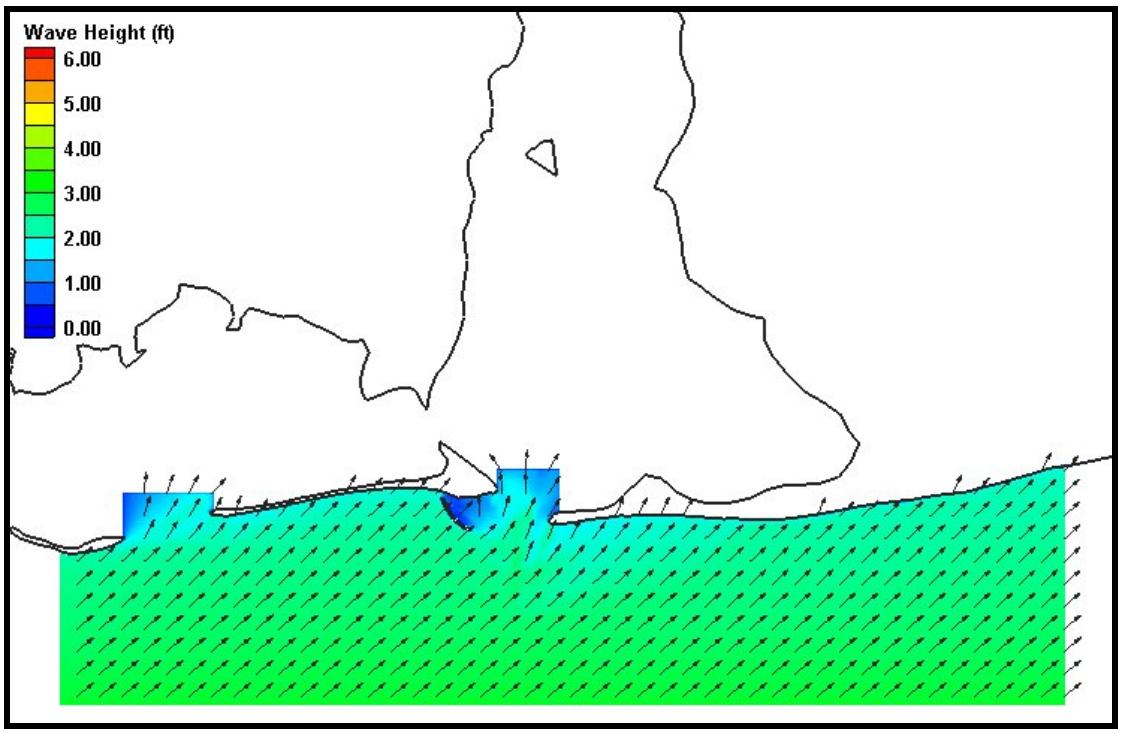

Figure H10. Coarse grid (200m x 200m) wave results for Case 10. Wave heights are shown by color while wave direction is indicated by the arrow direction.

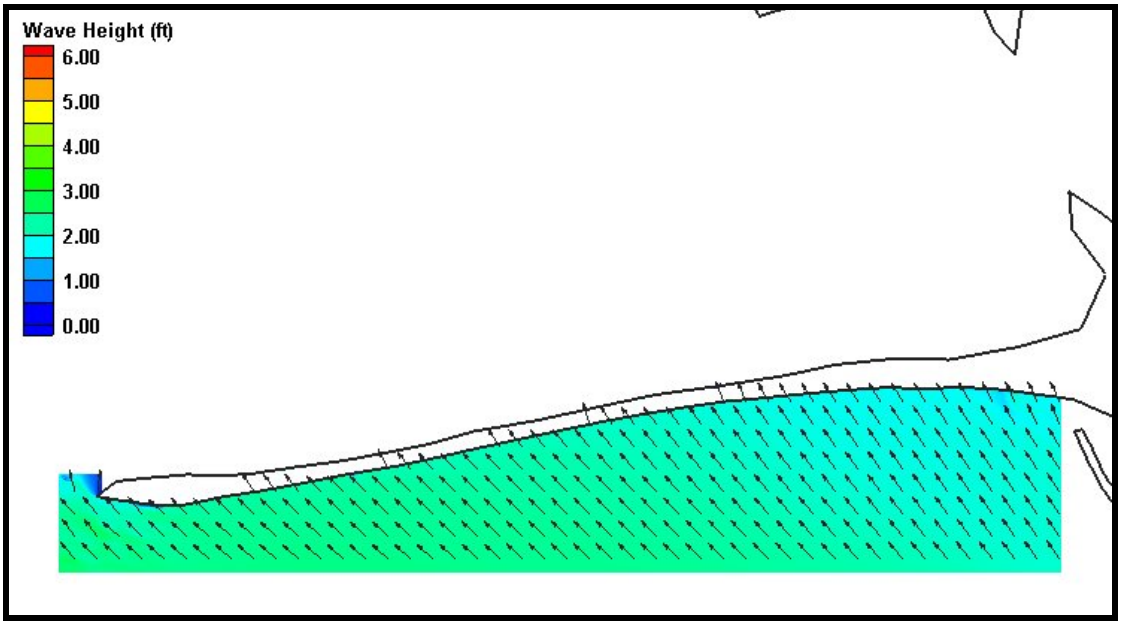

Figure H11. Fine grid (25m x 25m) wave results for Case 1, Dauphin Island. Wave heights are shown by color while wave direction is indicated by the arrow direction.

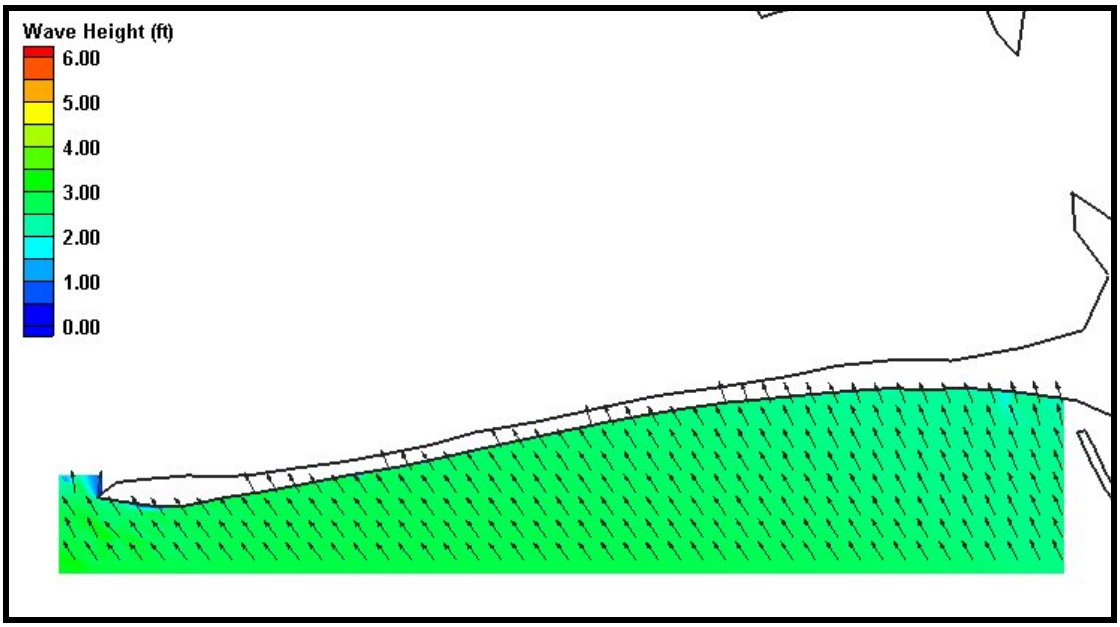

Figure H12. Fine grid (25m x 25m) wave results for Case 2, Dauphin Island. Wave heights are shown by color while wave direction is indicated by the arrow direction.

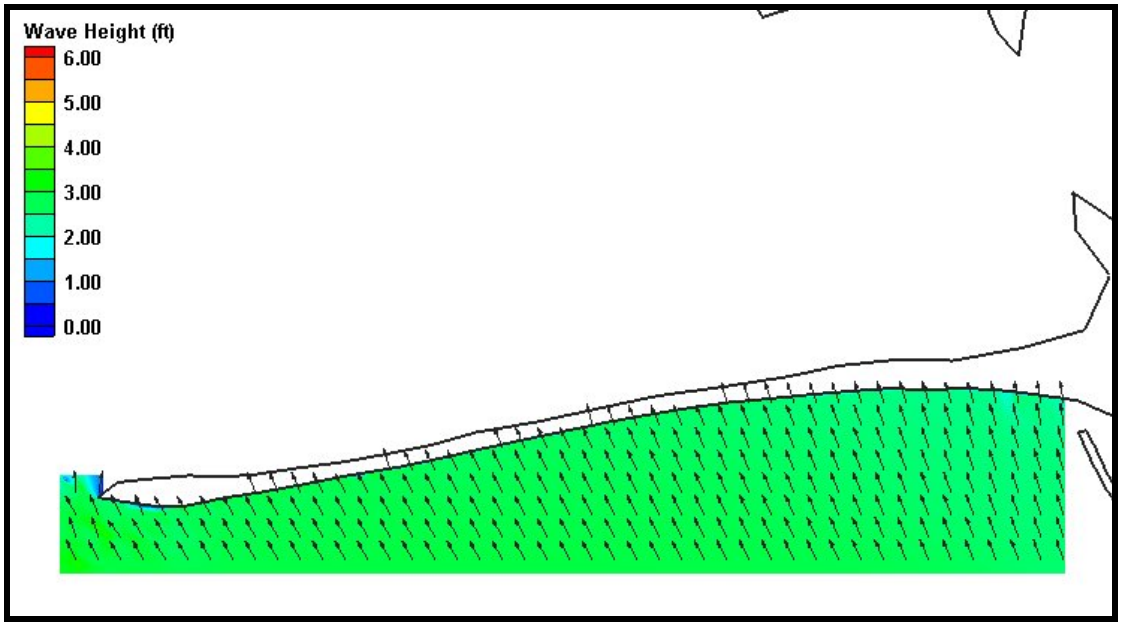

Figure H13. Fine grid (25m x 25m) wave results for Case 3, Dauphin Island. Wave heights are shown by color while wave direction is indicated by the arrow direction.

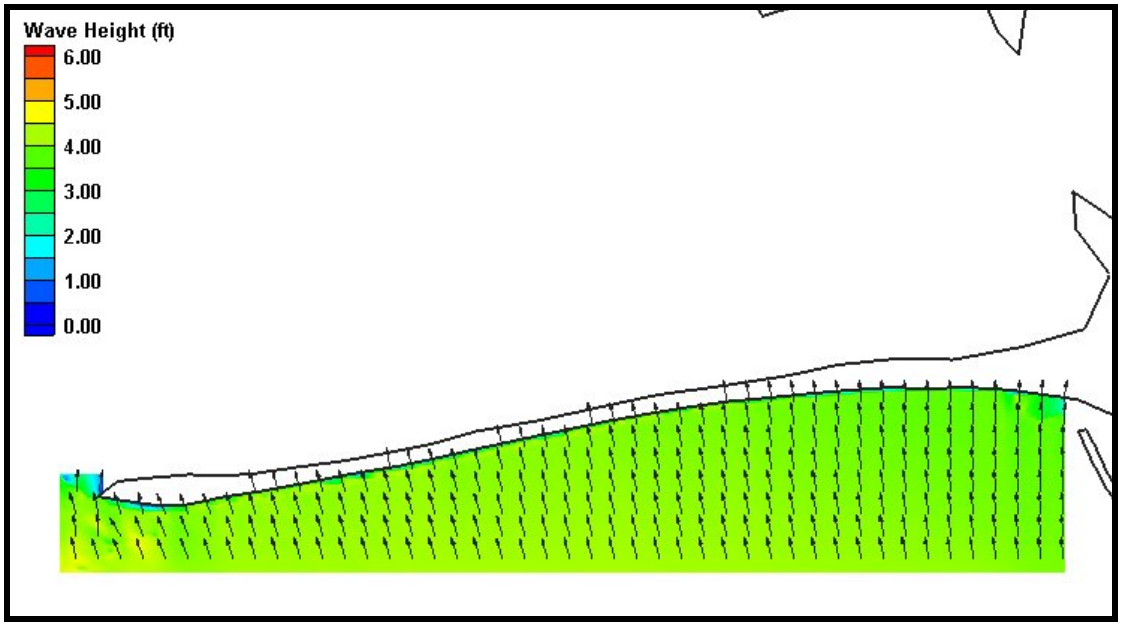

Figure H14. Fine grid (25m x 25m) wave results for Case 4, Dauphin Island. Wave heights are shown by color while wave direction is indicated by the arrow direction.

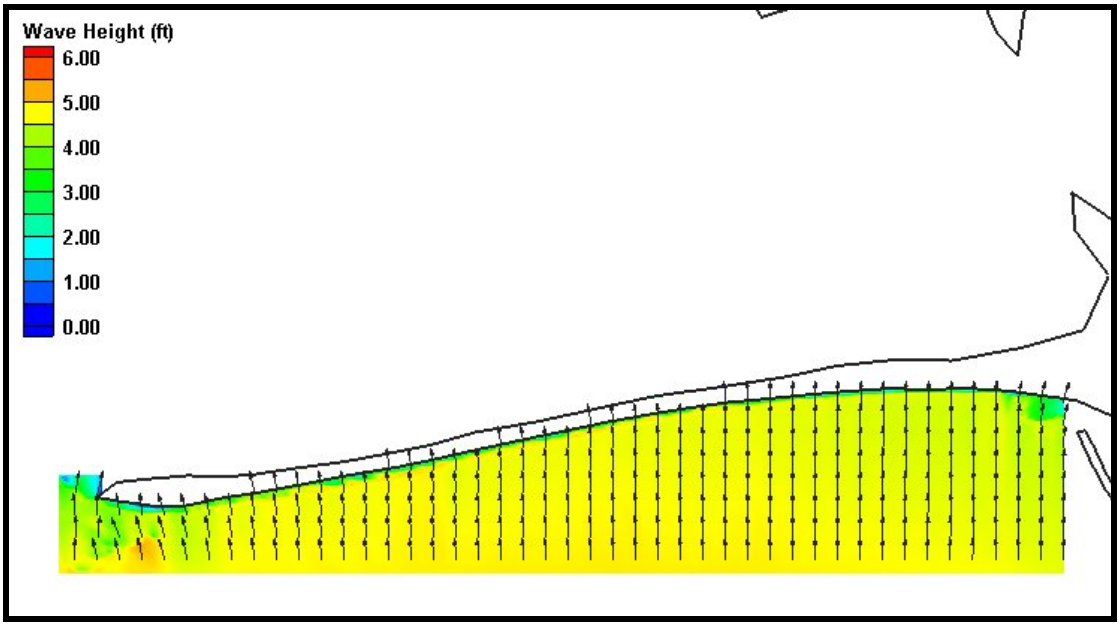

Figure H15. Fine grid (25m x 25m) wave results for Case 5, Dauphin Island. Wave heights are shown by color while wave direction is indicated by the arrow direction.

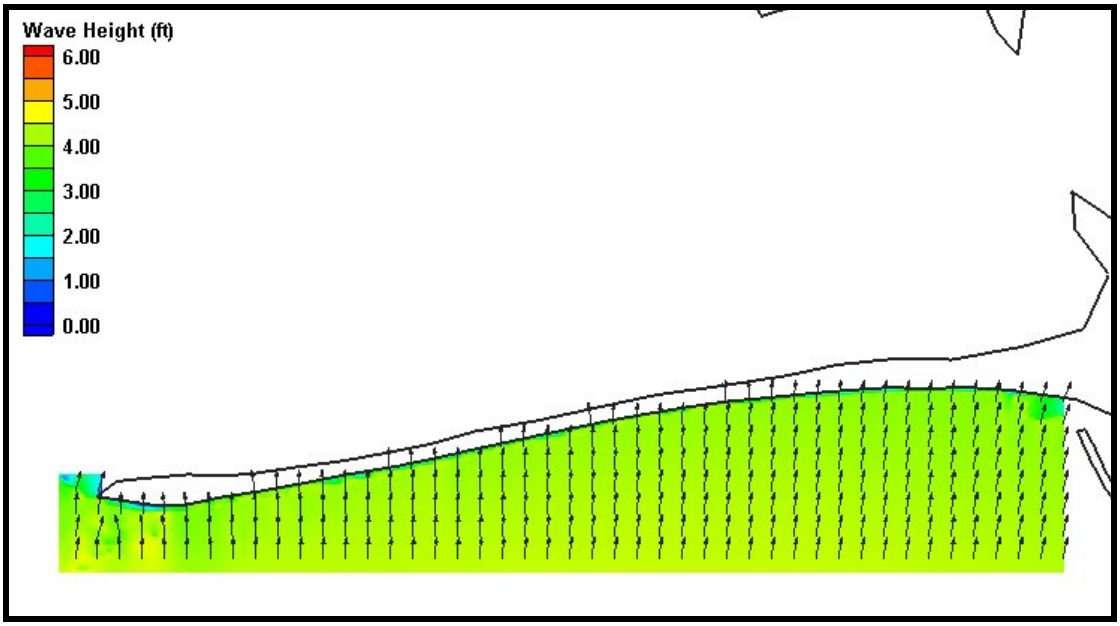

Figure H16. Fine grid (25m x 25m) wave results for Case 6, Dauphin Island. Wave heights are shown by color while wave direction is indicated by the arrow direction.

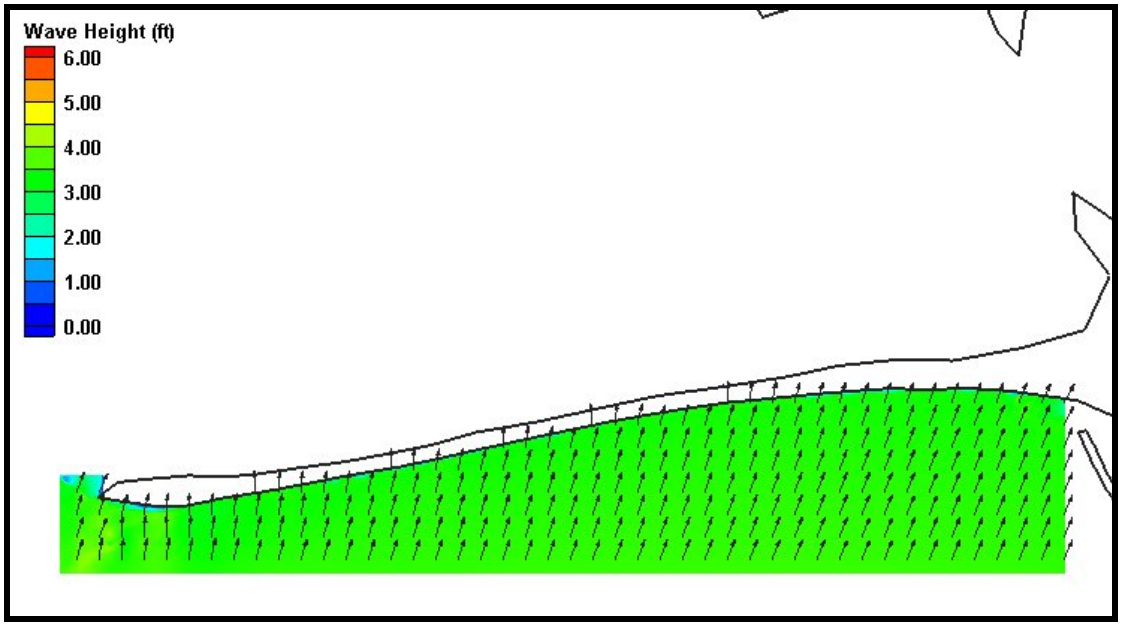

Figure H17. Fine grid (25m x 25m) wave results for Case 7, Dauphin Island. Wave heights are shown by color while wave direction is indicated by the arrow direction.

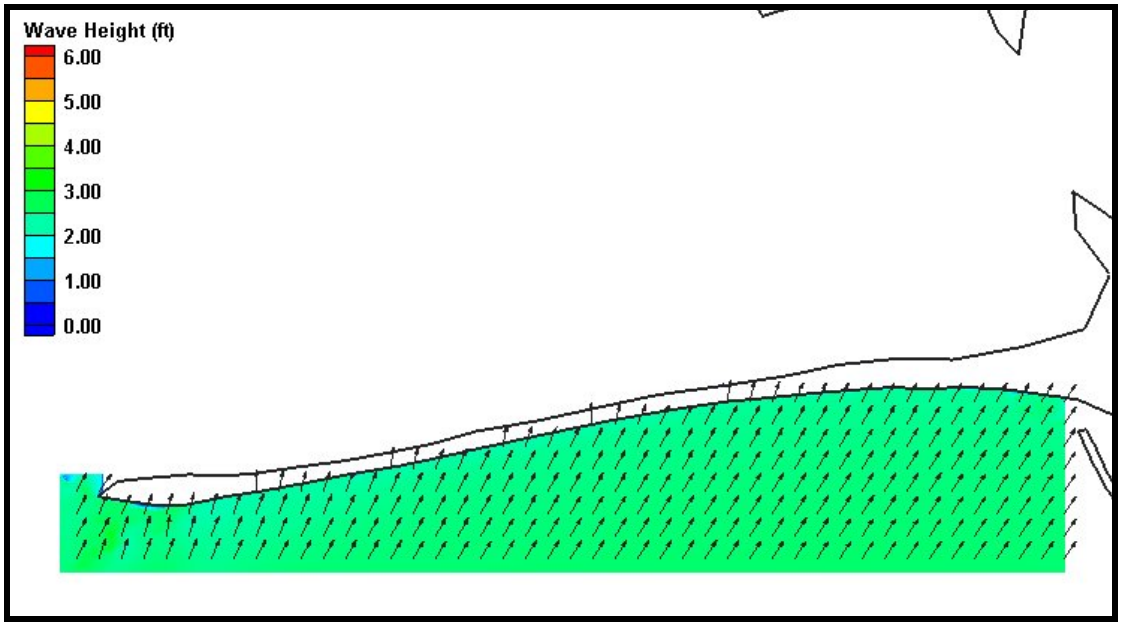

Figure H18. Fine grid (25m x 25m) wave results for Case 8, Dauphin Island. Wave heights are shown by color while wave direction is indicated by the arrow direction.

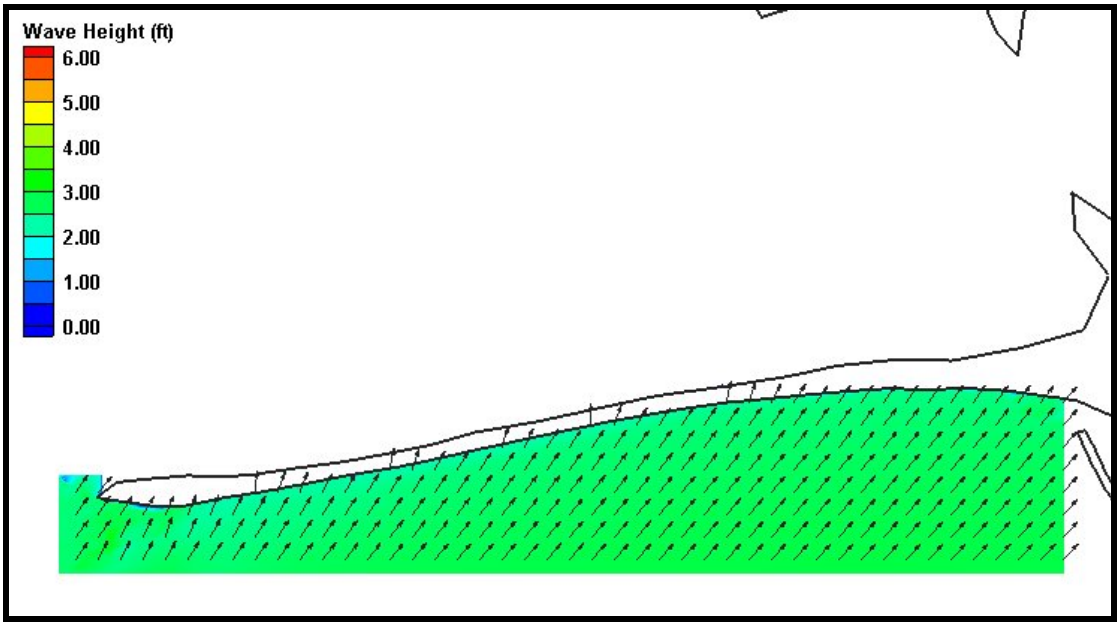

Figure H19. Fine grid (25m x 25m) wave results for Case 9, Dauphin Island. Wave heights are shown by color while wave direction is indicated by the arrow direction.

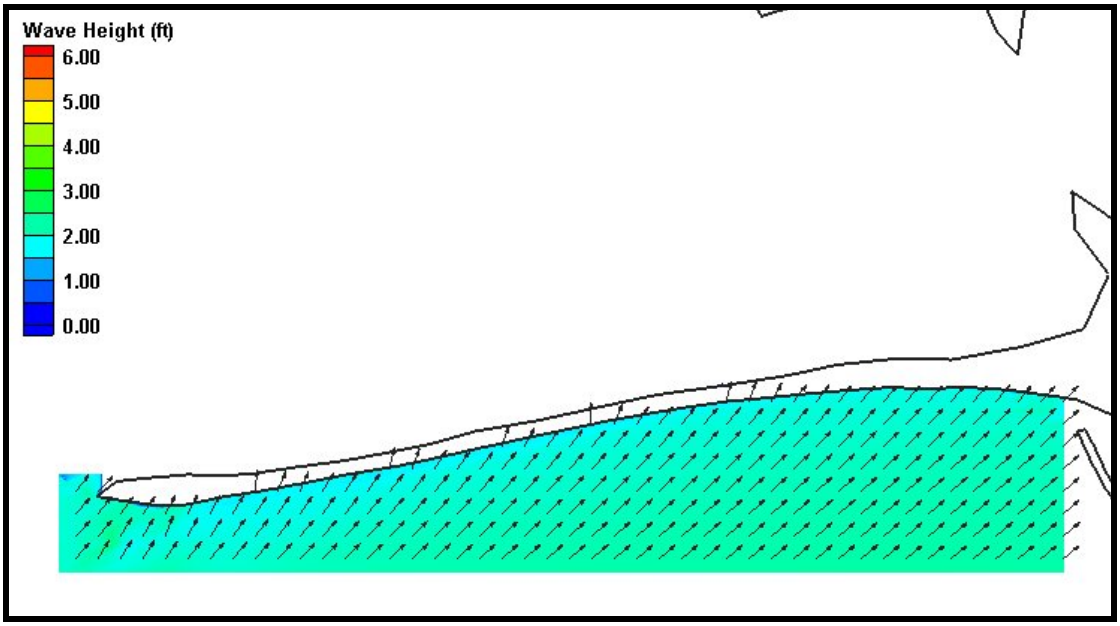

Figure H20. Fine grid (25m x 25m) wave results for Case 10, Dauphin Island. Wave heights are shown by color while wave direction is indicated by the arrow direction.

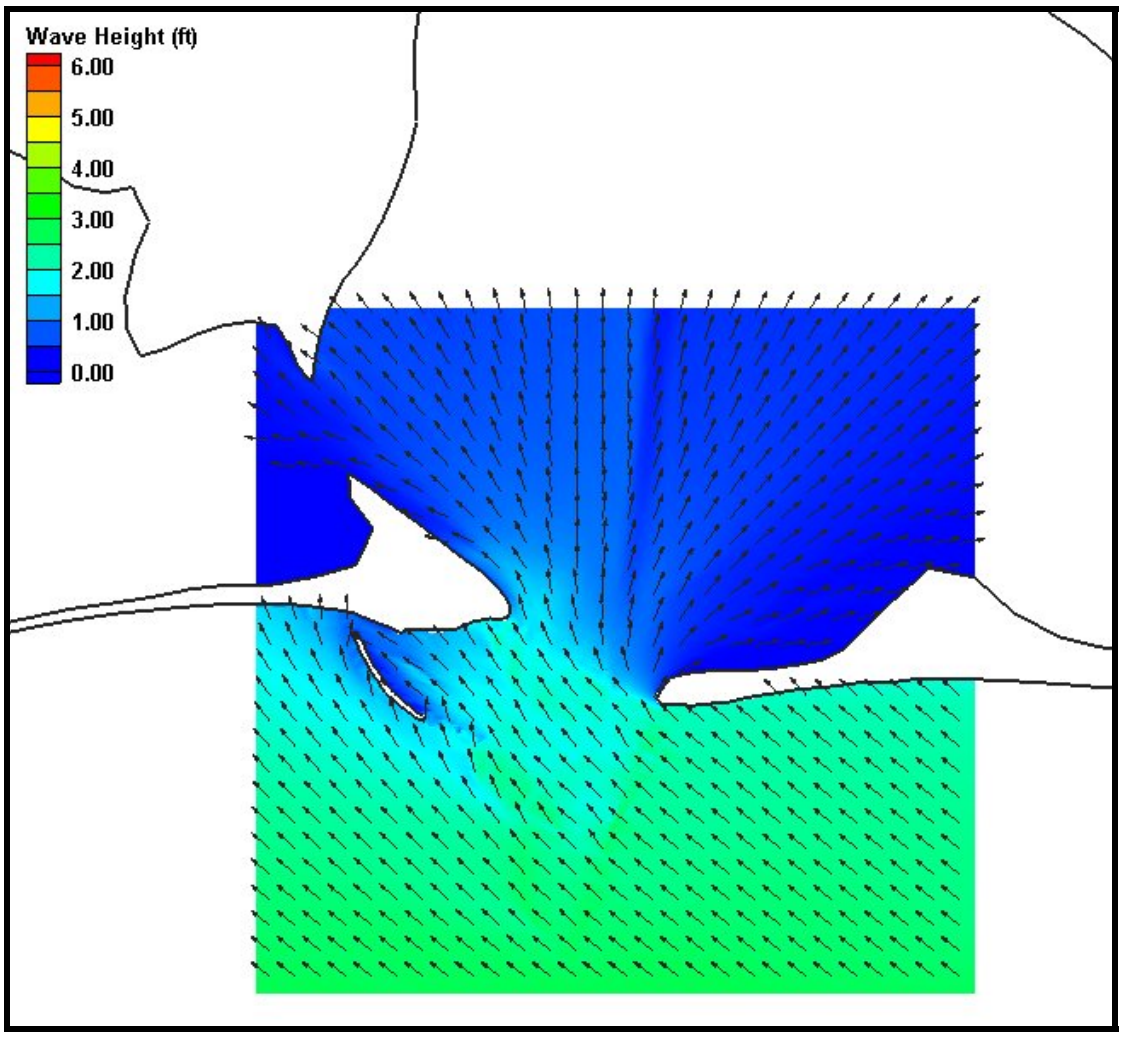

Figure H21. Fine grid (50m x 50m) wave results for Case 1, Mobile Pass. Wave heights are shown by color while wave direction is indicated by the arrow direction.

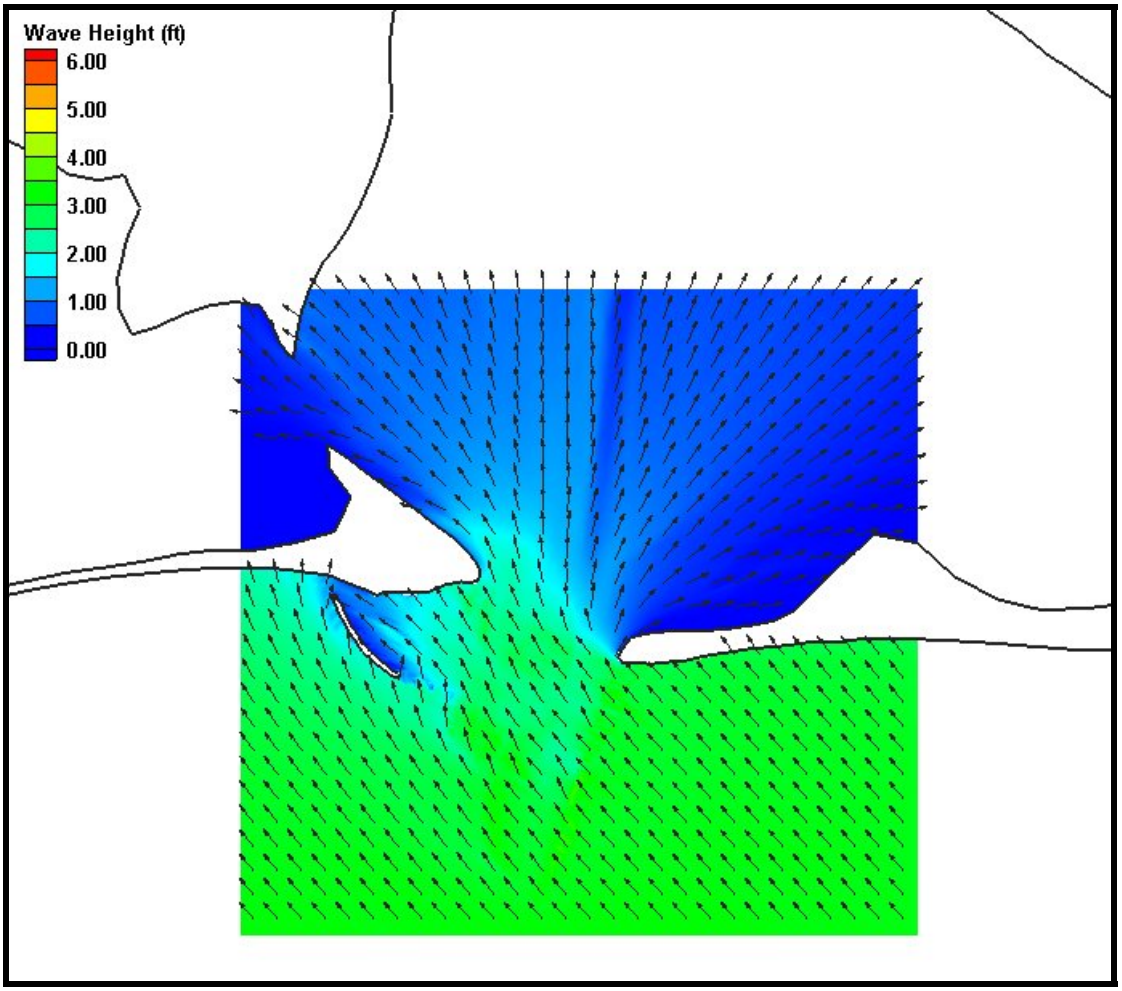

Figure H22. Fine grid (50m x 50m) wave results for Case 2, Mobile Pass. Wave heights are shown by color while wave direction is indicated by the arrow direction.

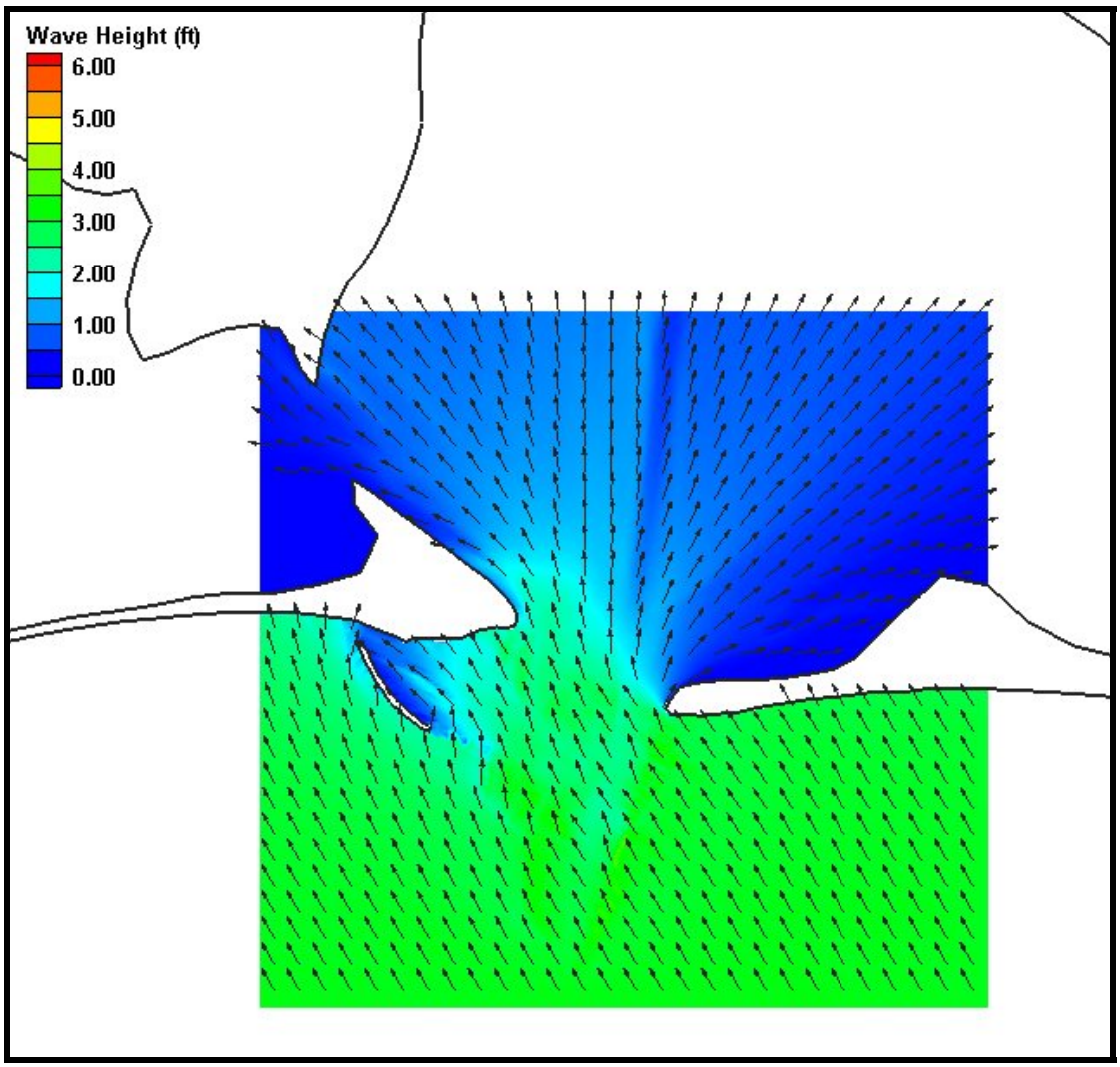

Figure H23. Fine grid (50m x 50m) wave results for Case 3, Mobile Pass. Wave heights are shown by color while wave direction is indicated by the arrow direction.

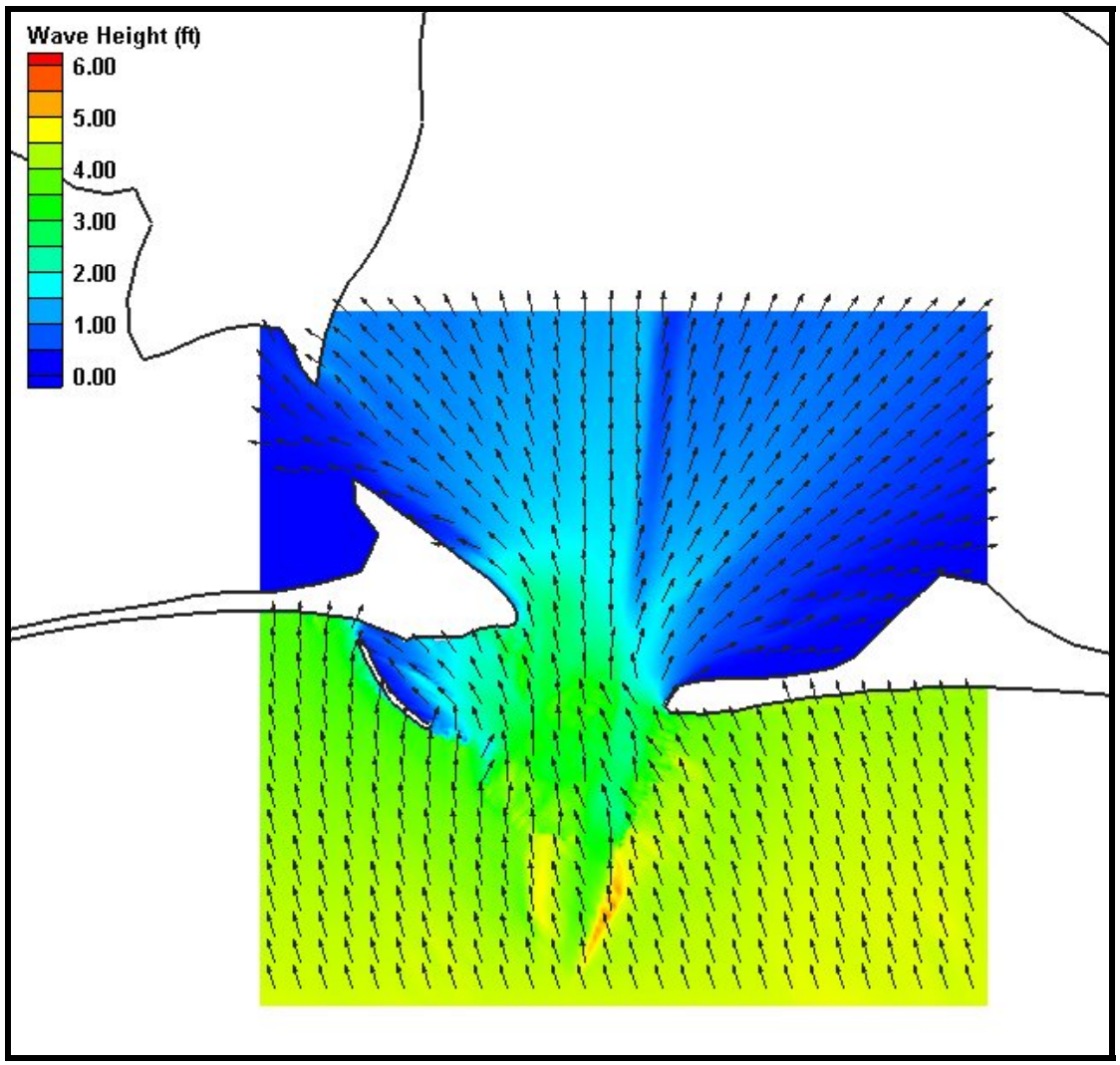

Figure H24. Fine grid (50m x 50m) wave results for Case 4, Mobile Pass. Wave heights are shown by color while wave direction is indicated by the arrow direction.

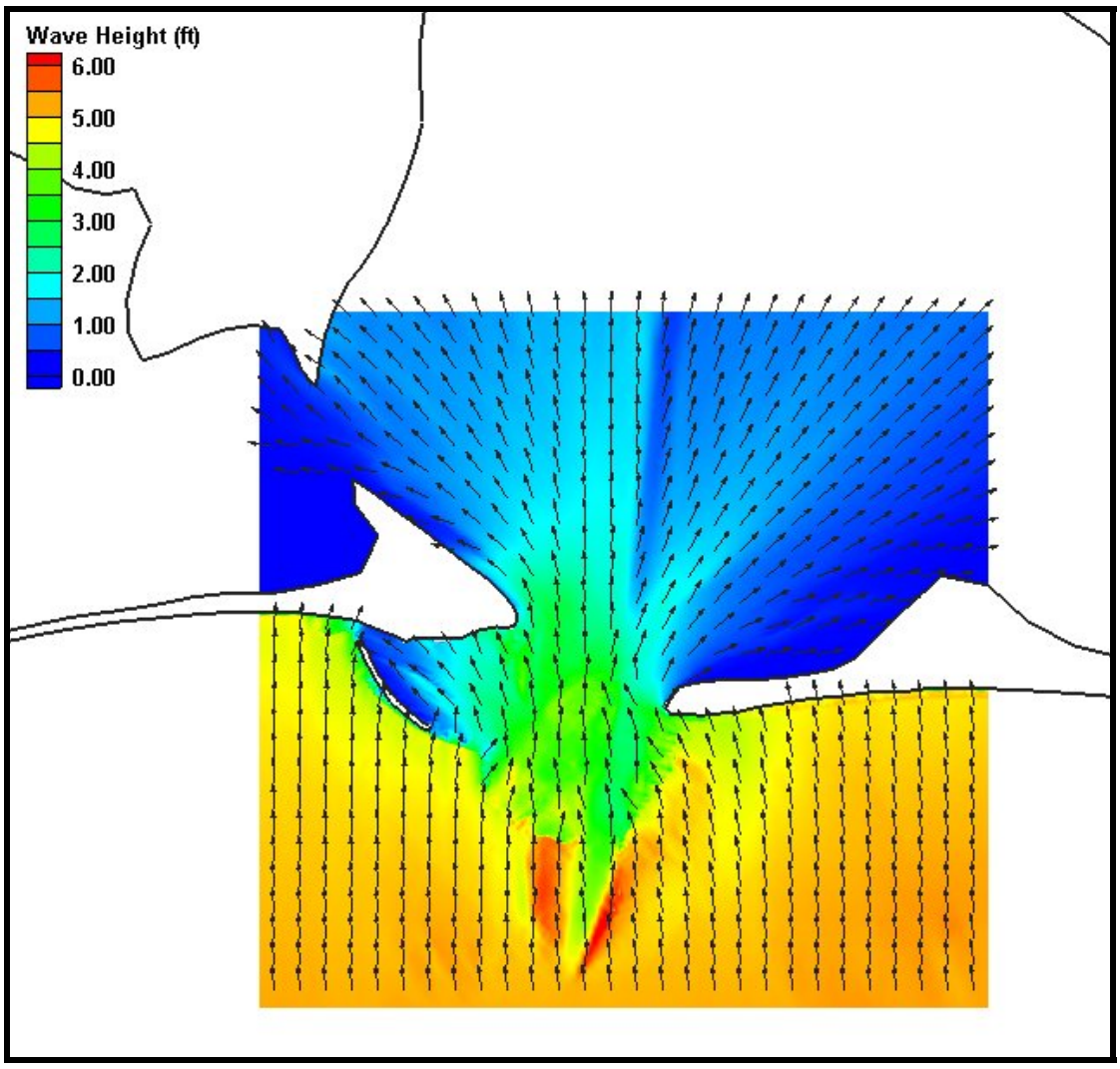

Figure H25. Fine grid (50m x 50m) wave results for Case 5, Mobile Pass. Wave heights are shown by color while wave direction is indicated by the arrow direction.

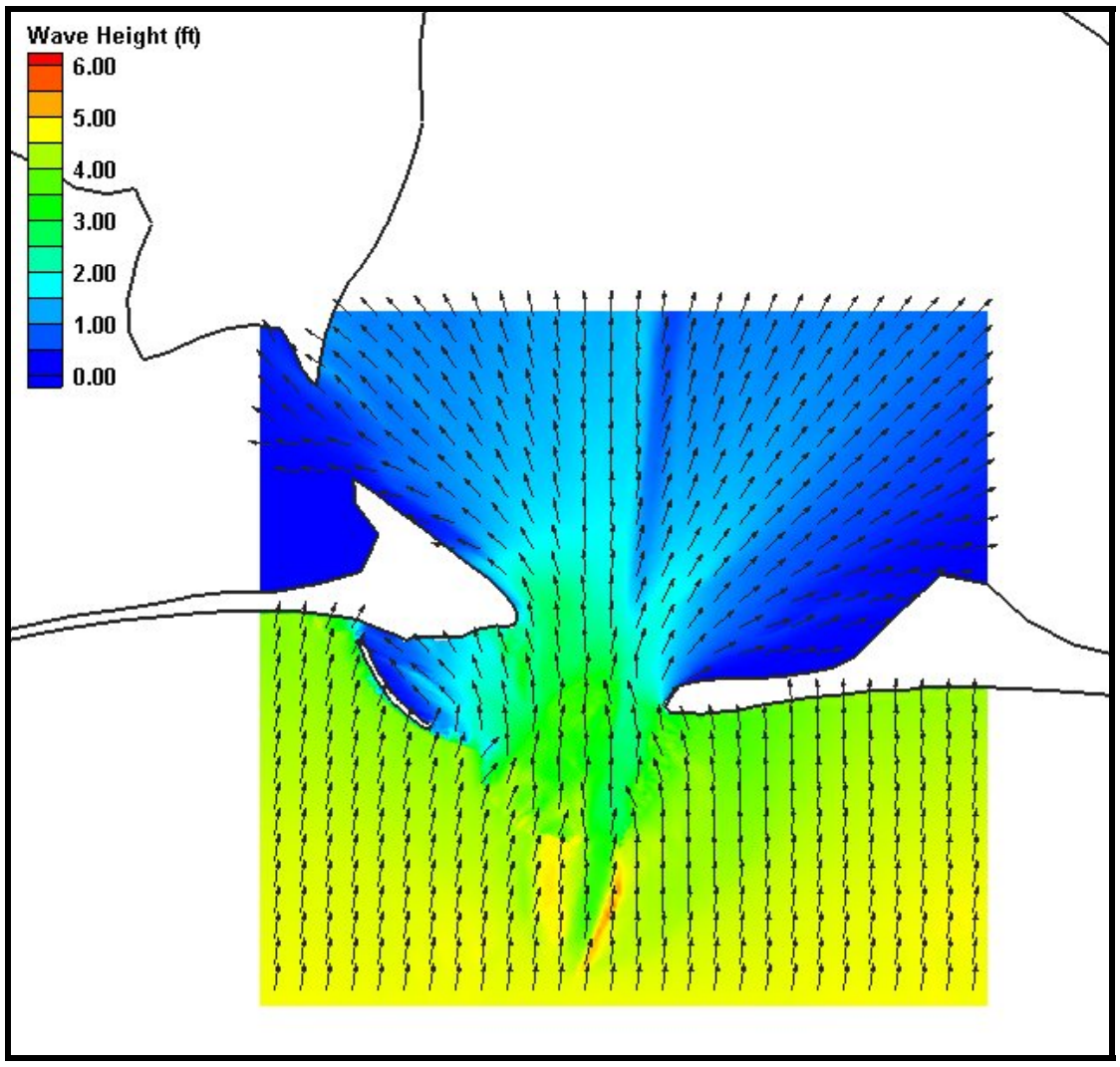

Figure H26. Fine grid (50m x 50m) wave results for Case 6, Mobile Pass. Wave heights are shown by color while wave direction is indicated by the arrow direction.

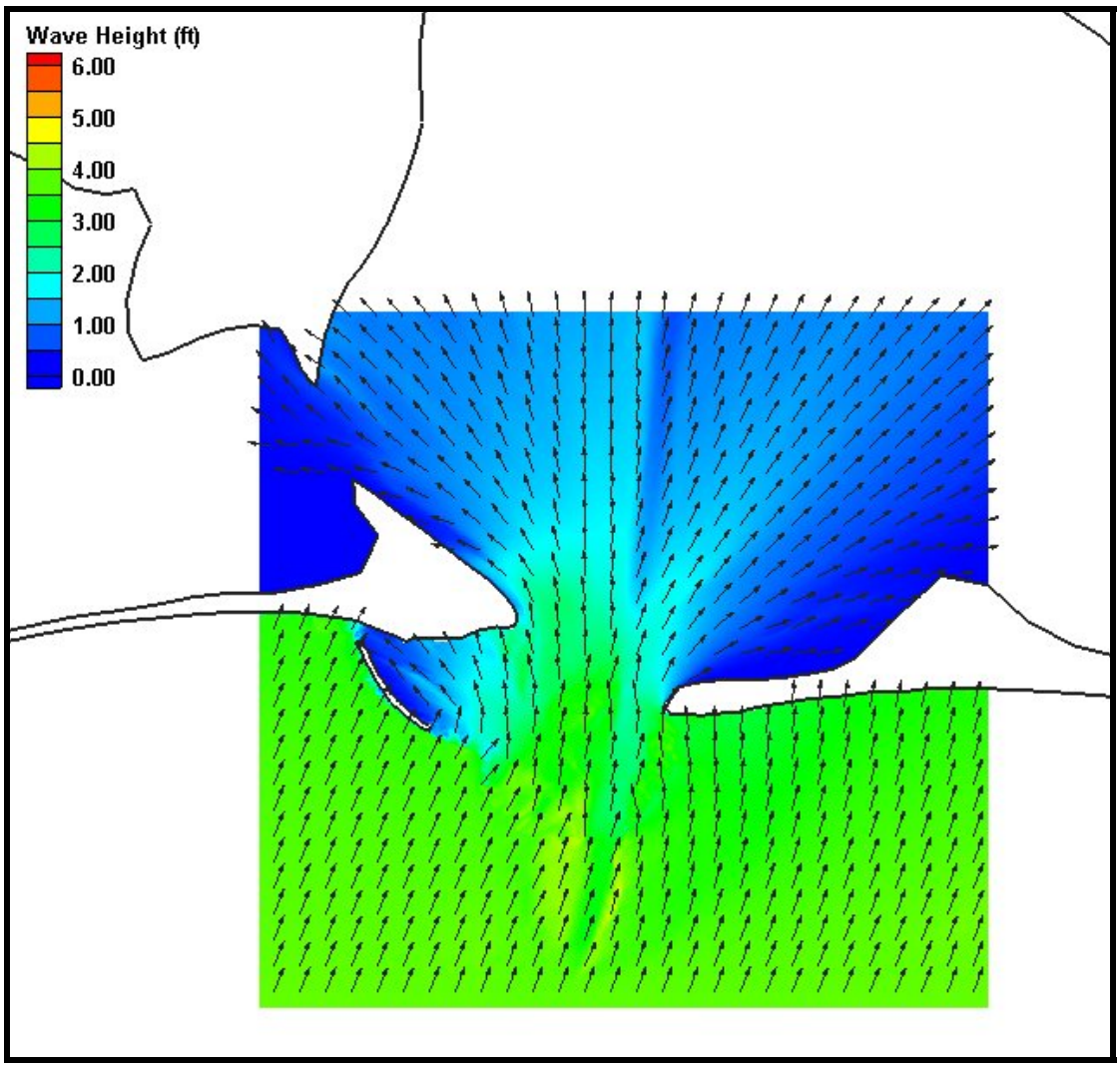

Figure H27. Fine grid (50m x 50m) wave results for Case 7, Mobile Pass. Wave heights are shown by color while wave direction is indicated by the arrow direction.

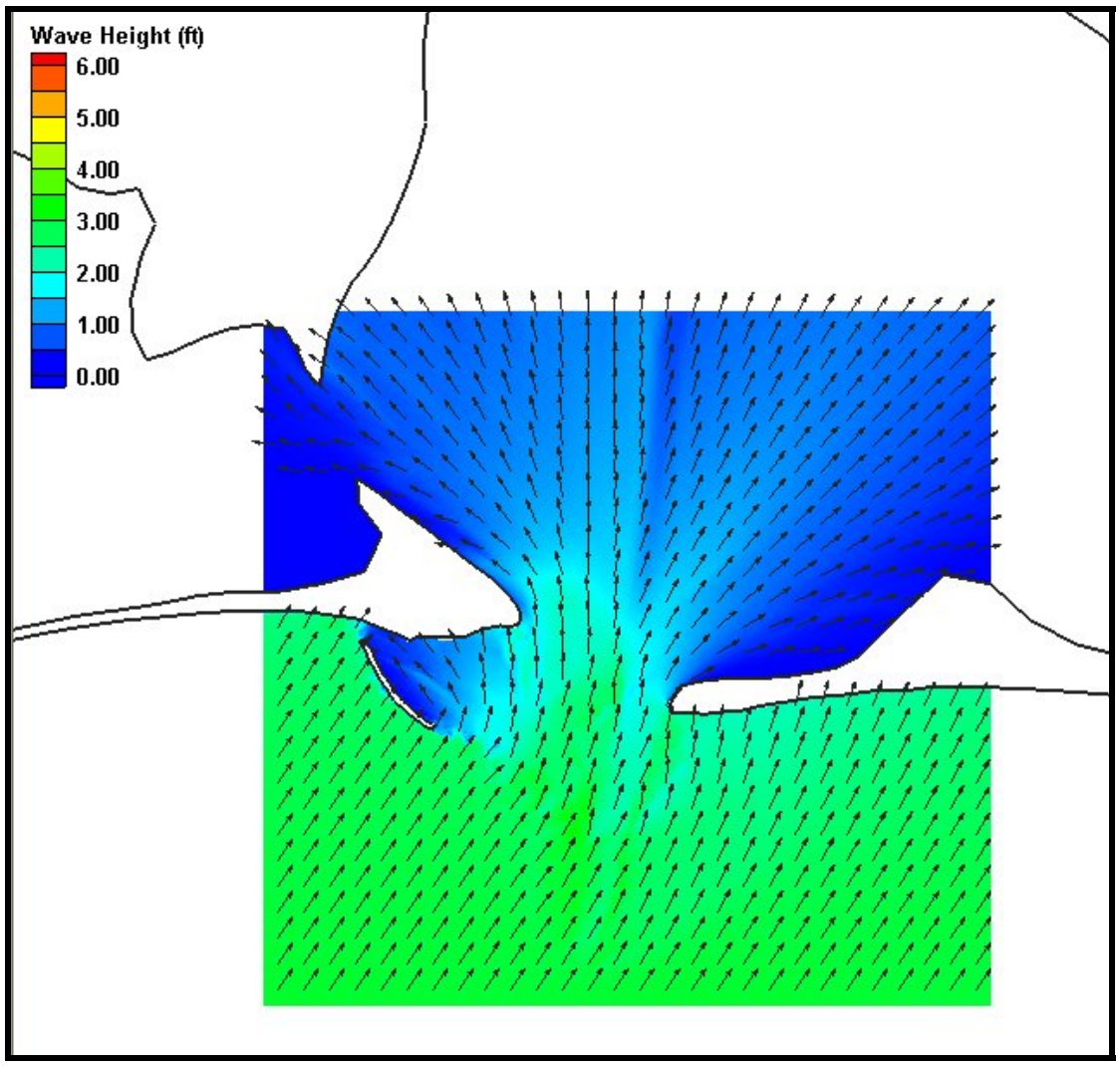

Figure H28. Fine grid (50m x 50m) wave results for Case 8, Mobile Pass. Wave heights are shown by color while wave direction is indicated by the arrow direction.

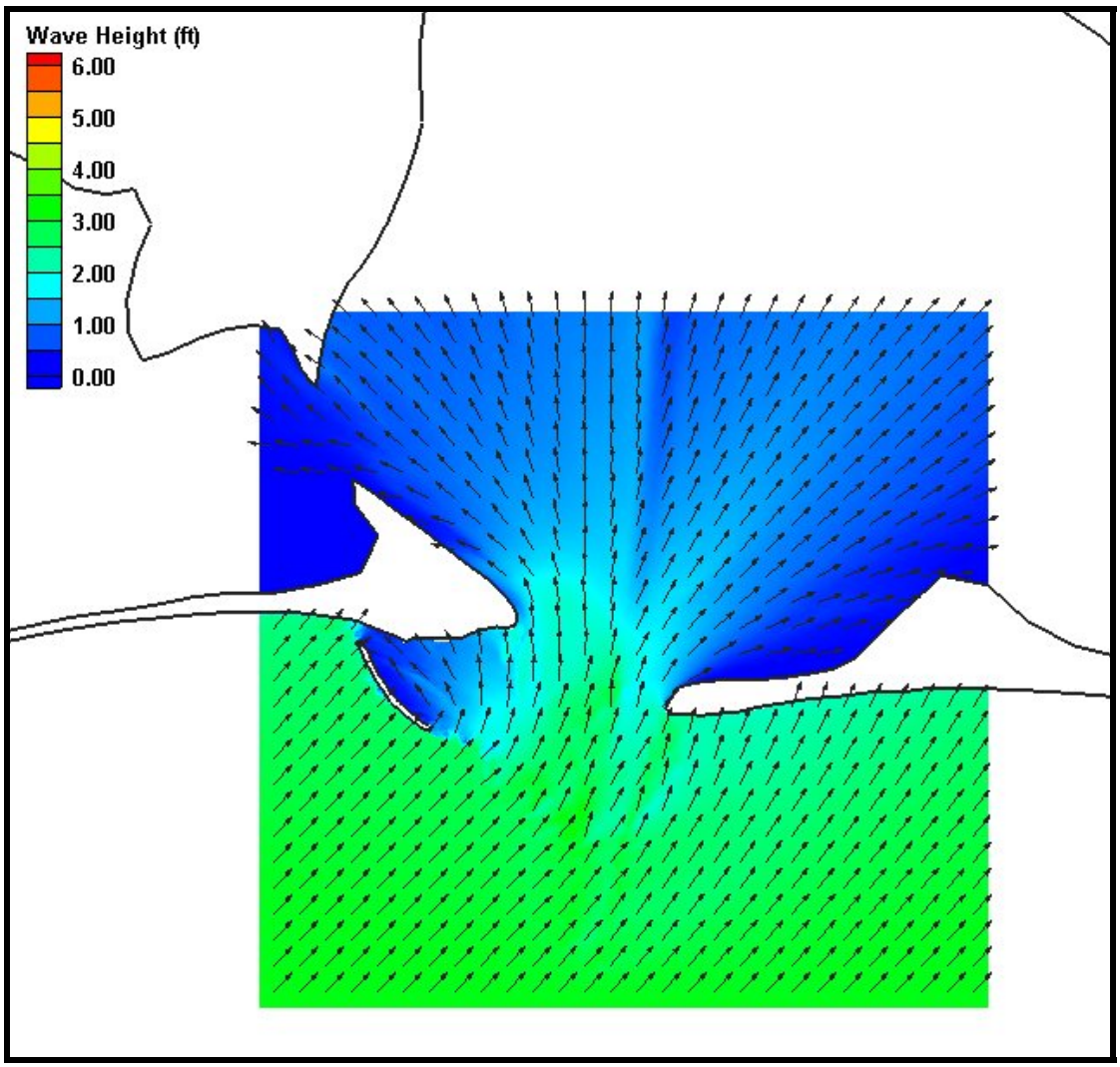

Figure H29. Fine grid (50m x 50m) wave results for Case 9, Mobile Pass. Wave heights are shown by color while wave direction is indicated by the arrow direction.

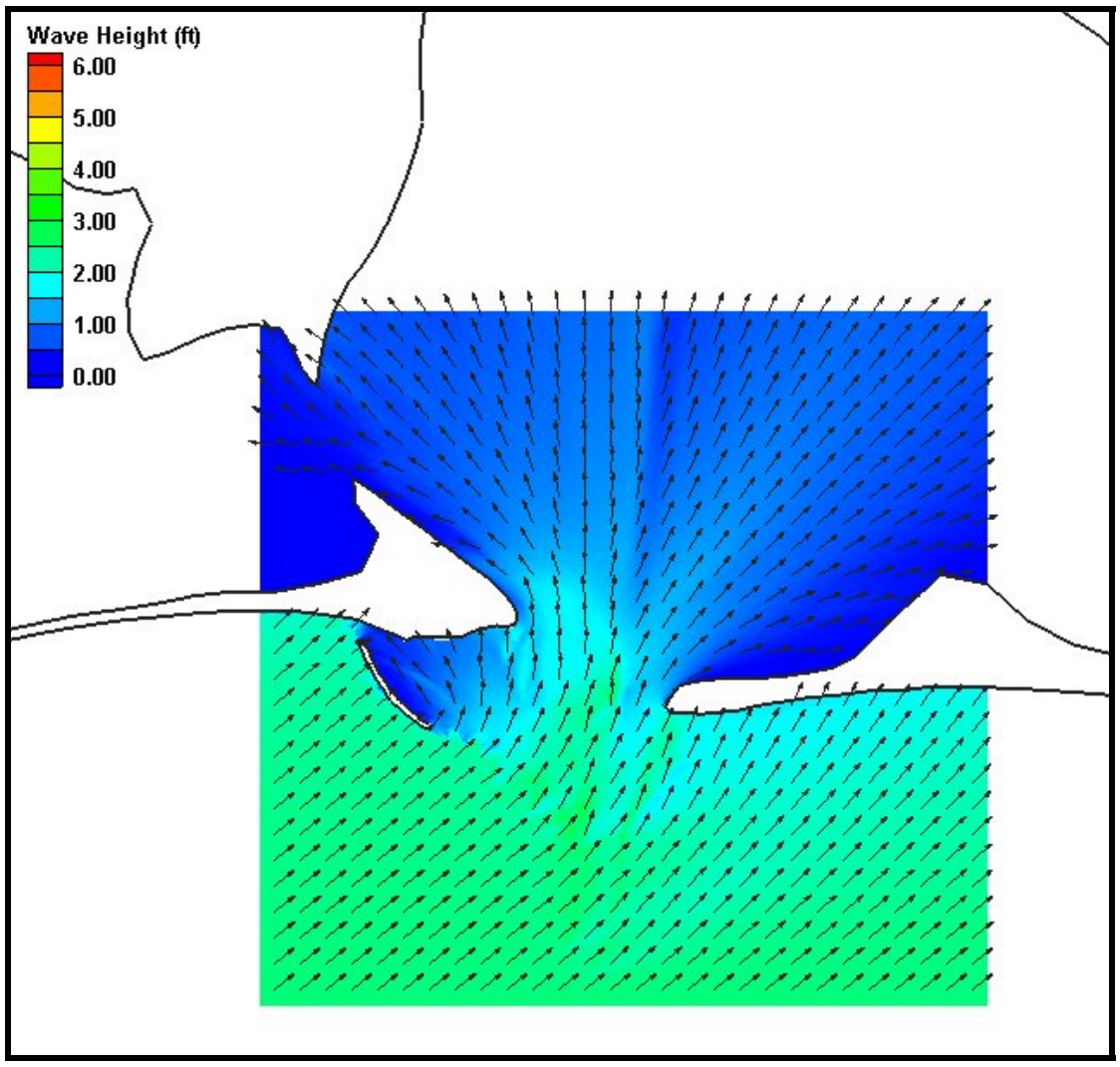

Figure H30. Fine grid (50m x 50m) wave results for Case 10, Mobile Pass. Wave heights are shown by color while wave direction is indicated by the arrow direction.

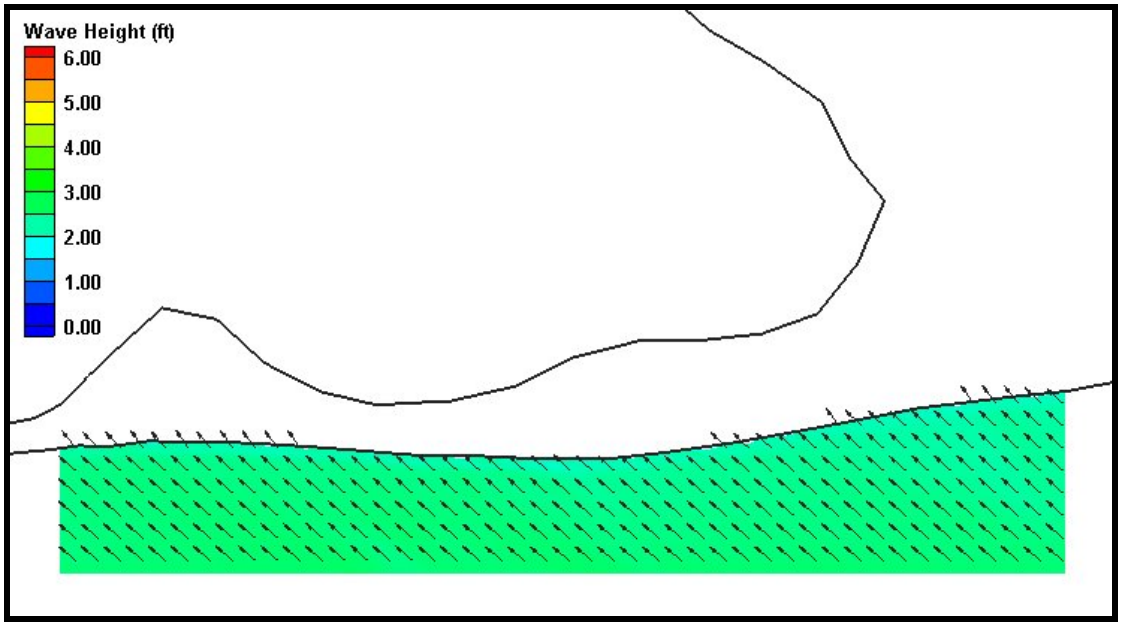

Figure H31. Fine grid (25m x 25m) wave results for Case 1, Morgan Peninsula. Wave heights are shown by color while wave direction is indicated by the arrow direction.

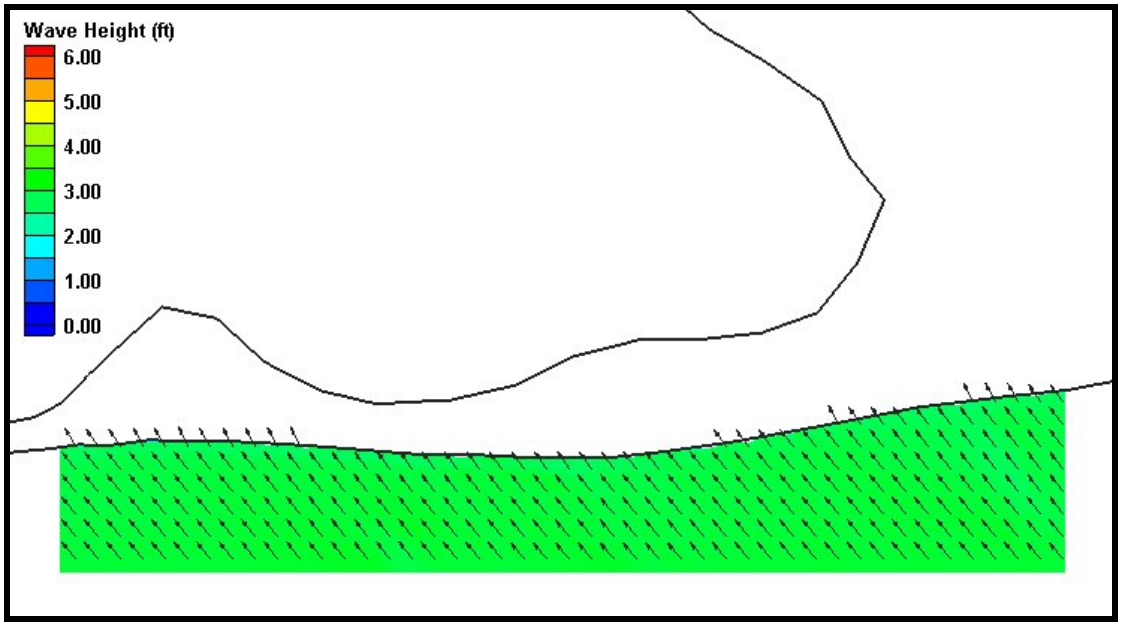

Figure H32. Fine grid (25m x 25m) wave results for Case 2, Morgan Peninsula. Wave heights are shown by color while wave direction is indicated by the arrow direction.

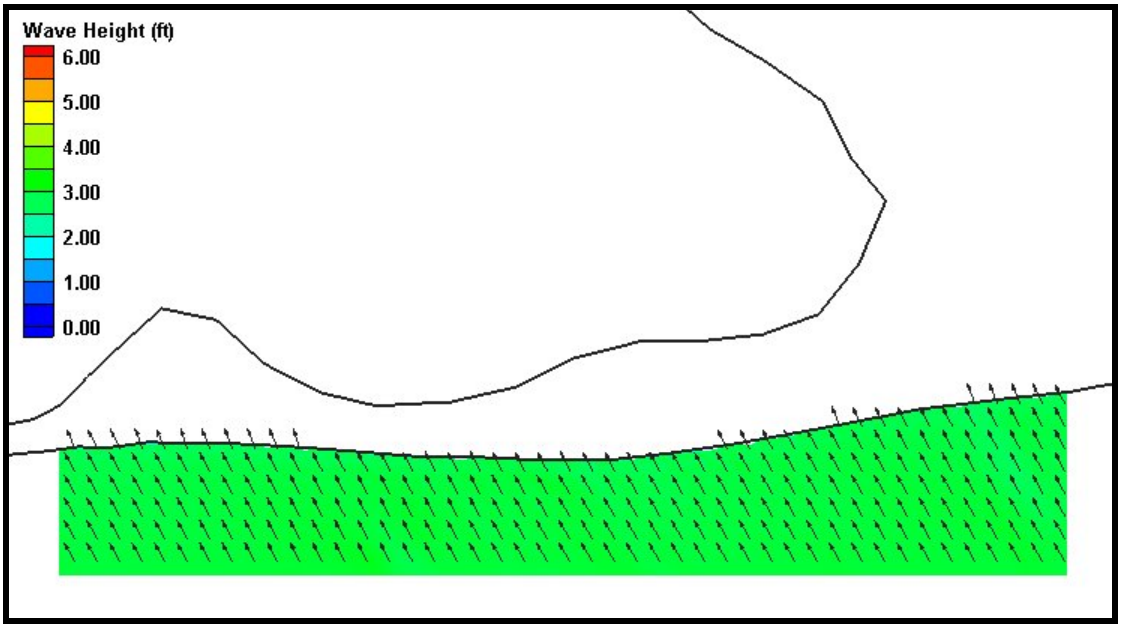

Figure H33. Fine grid (25m x 25m) wave results for Case 3, Morgan Peninsula. Wave heights are shown by color while wave direction is indicated by the arrow direction.

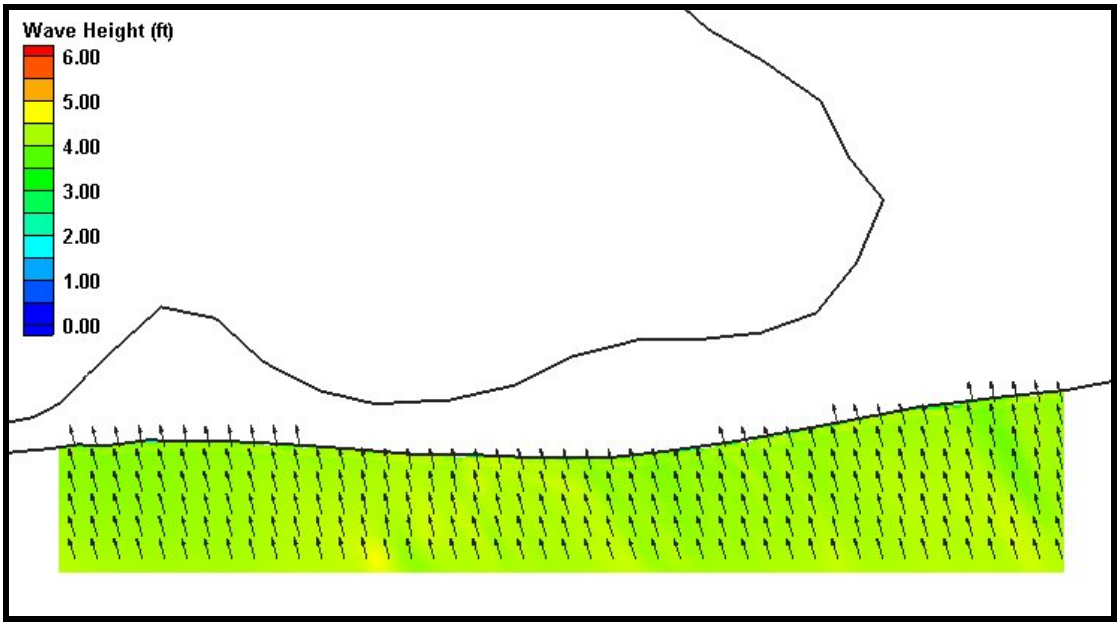

Figure H34. Fine grid (25m x 25m) wave results for Case 4, Morgan Peninsula. Wave heights are shown by color while wave direction is indicated by the arrow direction.

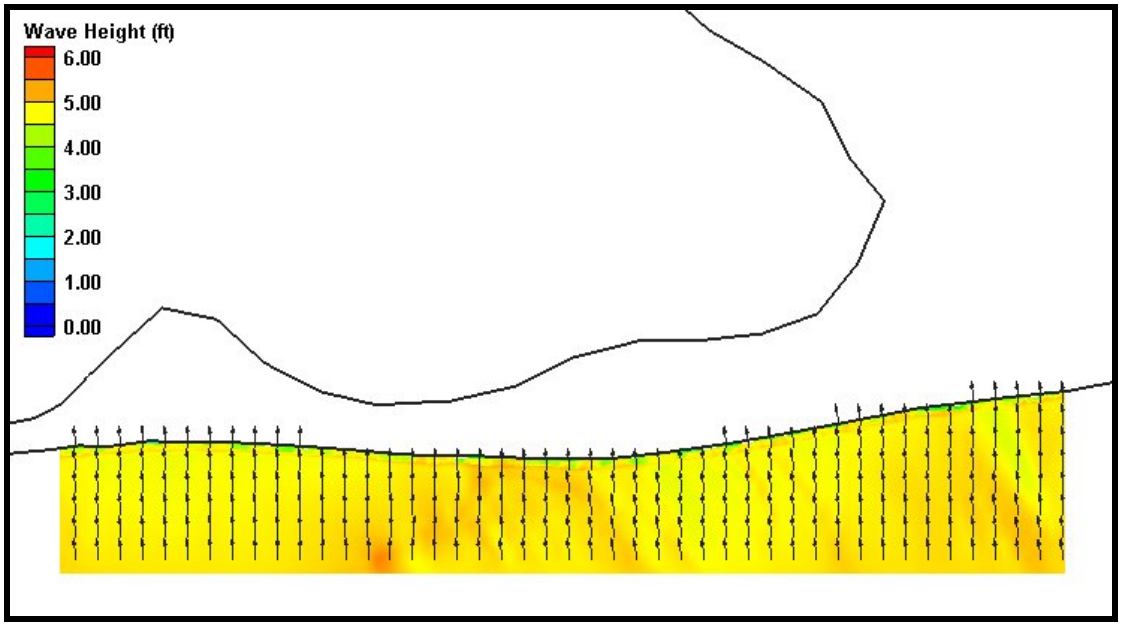

Figure H35. Fine grid (25m x 25m) wave results for Case 5, Morgan Peninsula. Wave heights are shown by color while wave direction is indicated by the arrow direction.

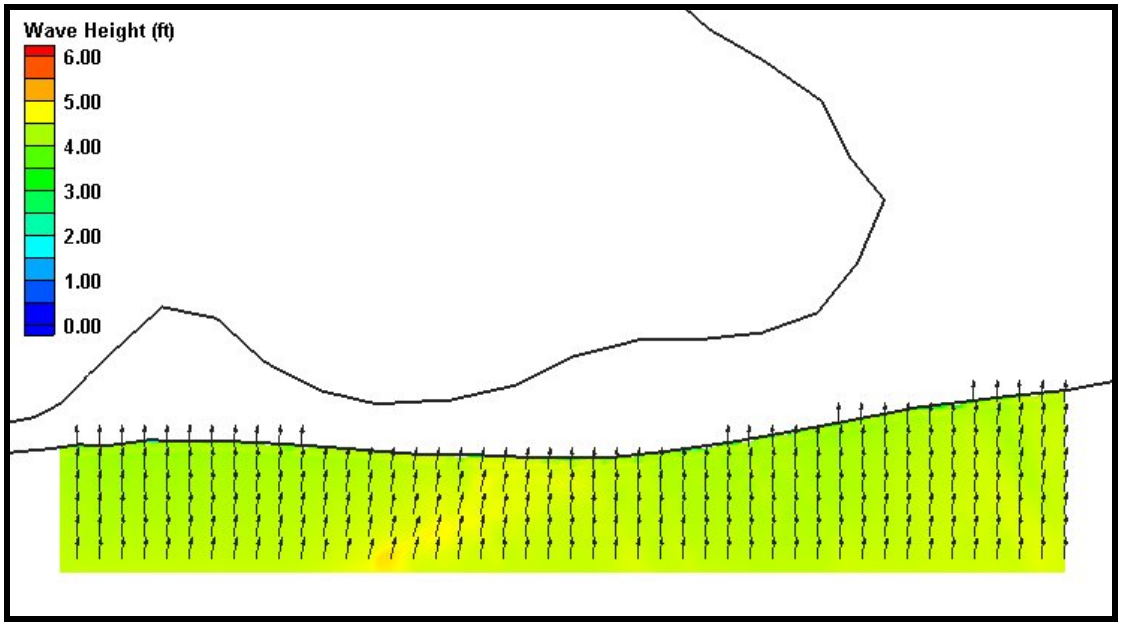

Figure H36. Fine grid (25m x 25m) wave results for Case 6, Morgan Peninsula. Wave heights are shown by color while wave direction is indicated by the arrow direction.

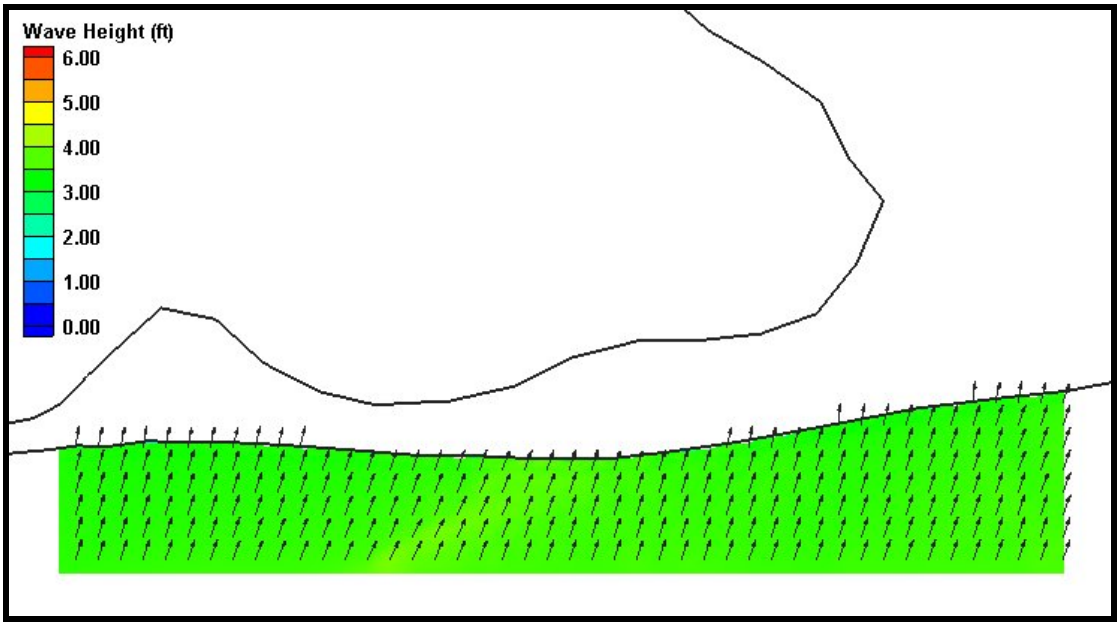

Figure H37. Fine grid (25m x 25m) wave results for Case 7, Morgan Peninsula. Wave heights are shown by color while wave direction is indicated by the arrow direction.

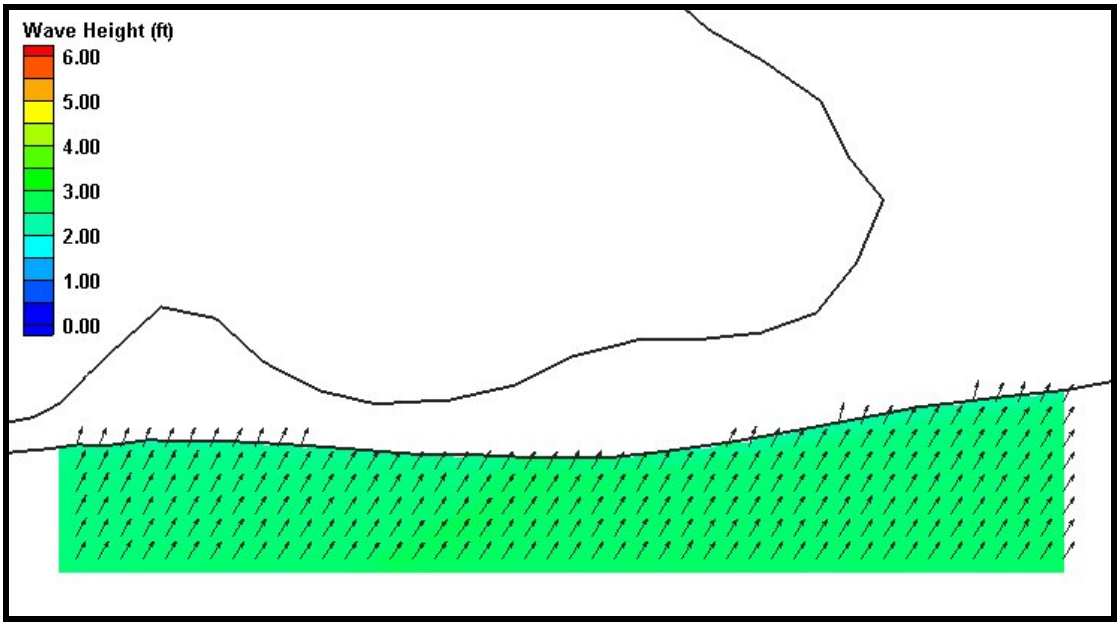

Figure H38. Fine grid (25m x 25m) wave results for Case 8, Morgan Peninsula. Wave heights are shown by color while wave direction is indicated by the arrow direction.

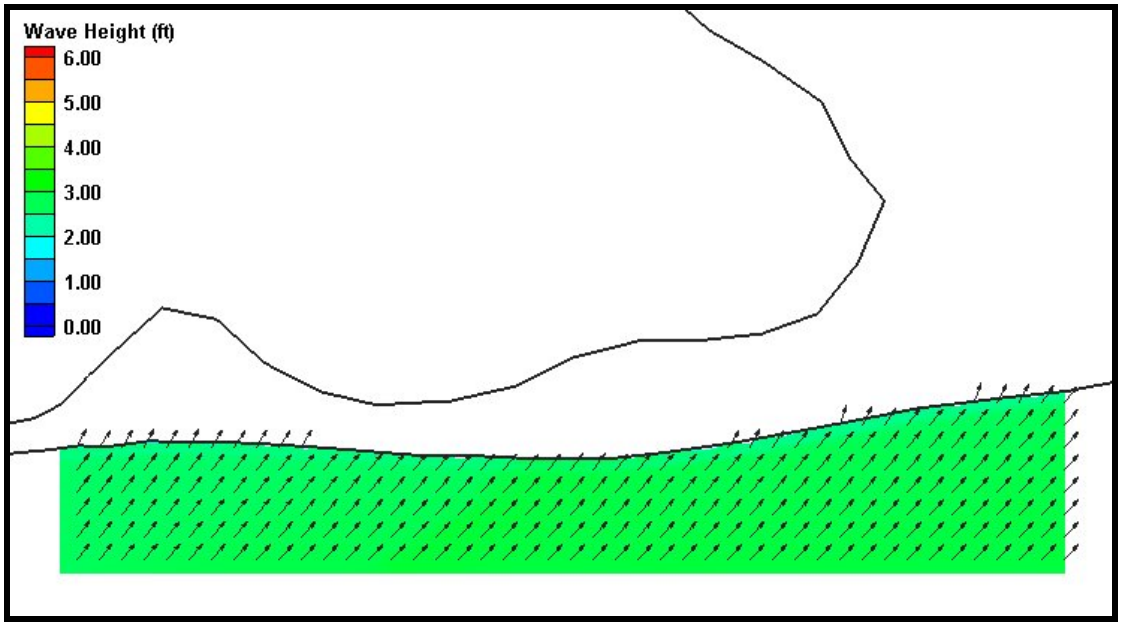

Figure H39. Fine grid (25m x 25m) wave results for Case 9, Morgan Peninsula. Wave heights are shown by color while wave direction is indicated by the arrow direction.

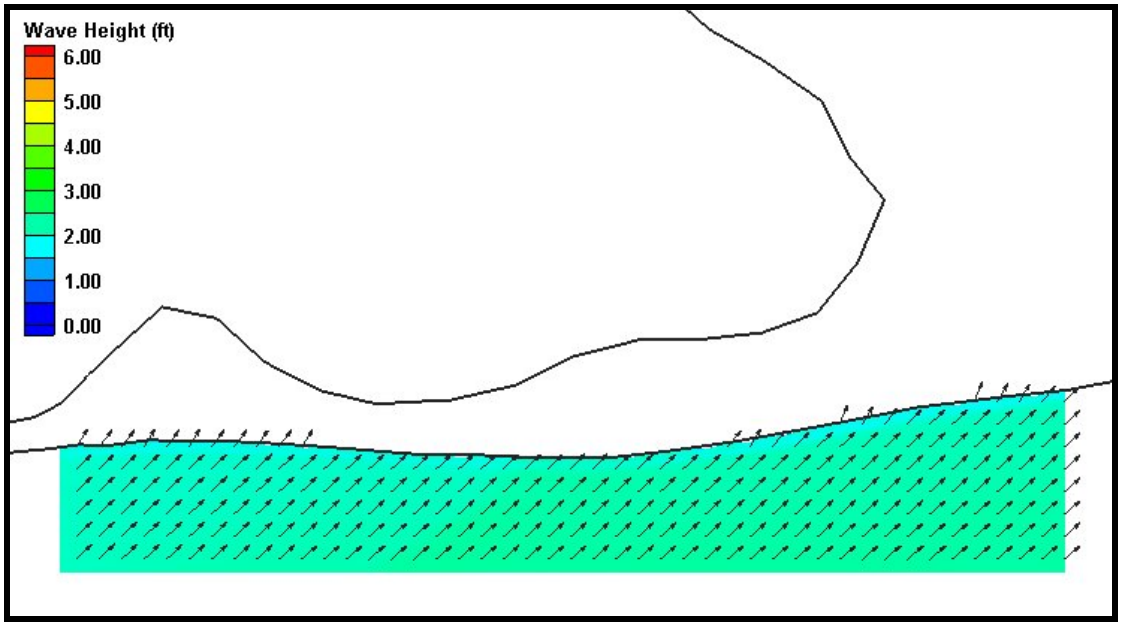

Figure H40. Fine grid (25m x 25m) wave results for Case 10, Morgan Peninsula. Wave heights are shown by color while wave direction is indicated by the arrow direction.